

Supersymmetric Scattering Amplitudes and Algebraic Aspects of Holography from the Projective Line

Thesis by
Matthew Thomas Edwin Heydeman

In Partial Fulfillment of the Requirements for the
Degree of
Doctor of Philosophy in Physics

The logo for the California Institute of Technology, featuring the word "Caltech" in a bold, orange, sans-serif font.

CALIFORNIA INSTITUTE OF TECHNOLOGY
Pasadena, California

2019
Defended May 9, 2019

© 2019

Matthew Thomas Edwin Heydeman

ORCID: 0000-0001-7033-9075

All rights reserved

To my parents.

ACKNOWLEDGEMENTS

Throughout my time as a graduate student at Caltech, I have enjoyed the company, support, and mentorship of many amazing people. While this thesis represents a personal milestone in scientific achievement for me, it would not have been possible without the support of my advisors, colleagues, friends, and family. My experiences, my work, and my life have been shaped by these people in small ways and large, and I would like to thank them, including those not explicitly mentioned, for the magnitude of all their contributions.

As a graduate student, I have been very fortunate to be advised by not one, but two, great thinkers. My two advisors, John Schwarz and Matilde Marcolli, have had a profound impact on my research interests and practices, and I have learned a great deal from both. Both were willing to work with and support me at a time when I knew very little about how to do research, and I sincerely appreciate their patience and advice. I also benefited enormously from their tendencies to pursue challenging and ambitious projects, while still allowing me room to learn and grow more broadly. John has an ever-present energy for doing physics, and I found his enthusiasm infectious. Working with John provided me with a great opportunity to learn from his physical intuition and approach to problem solving; he encouraged me to attempt hard problems but still be grounded in concrete and explicit calculation. Matilde showed me many amazing connections between different branches of mathematics and physics; it takes an extraordinary thinker and advisor to be able to guide one to success using such beautiful ideas at the interface of multiple disciplines. Matilde was willing to work with me as a physics student even though mathematics was not my background, and I was very fortunate to have her help in bridging the gap between math and physics. I thank them both for all their advice and support over these past five years; it has been a great honor and privilege to work with them!

In addition to my advisors, I have had many excellent coauthors whose work is directly represented in this thesis. I would like to thank Freddy Cachazo, Steve Gubser, Alfredo Guevara, Christian Jepsen, Sebastian Mizera, Sarthak Parikh, Ingmar Saberi, Bogdan Stoica, Brian Trundy, Congkao Wen, and Shun-Qing Zhang for their collaborations, advice, and friendship. This thesis would not exist without their contributions, and I hope we get the opportunity to col-

laborate in the future. I would especially like to thank Freddy, Steve, Ingmar, and Congkao for being exceptional mentors when I was less experienced at research.

The high energy theory group gave me many opportunities to meet and learn from fantastic scientists. I would like to thank first my candidacy committee, which included John, Matilde, Sean Carroll, and Clifford Cheung. A special thanks goes to Mark Wise for his friendly banter, jokes, stories, and most importantly, his work to help fund me, which was complicated by me having two advisors. I would also like to thank the faculty in our group more generally for facilitating helpful interactions in classes, seminars, and informal discussions. These faculty include Sergei Gukov, Anton Kapustin, Hirosi Ooguri, and David Simmons-Duffin. The Burke Institute has been an excellent environment to work in, and I would like to thank Carol Silberstein for working tirelessly to administer the group.

I am happy to have received funding and financial support for basic research. This has come to me in the form of various grants and fellowships and, in particular, I would like to acknowledge the Department of Energy for Award No: DE-SC0011632 and Grant No. DE-FG02-91ER40671, and the Simons Foundation for Grant 511167 (SSG). In addition to these funding sources, I would like to thank Perimeter Institute and Princeton University for their warm hospitality during my stays during the winter months. A special thanks goes to Steve Gubser for providing an invitation and support while at Princeton.

Throughout these past years at Caltech, I have had many wonderful interactions with peers, colleagues, and friends. I would like to thank all of them for making my life in graduate school better through our friendly interactions around the physics department. Many thanks to those other students who remained friends with me despite all my bad jokes: Arian Jadbabaie, Peter Kravchuk, Murat Kologlu, Julio Parra-Martinez, Lev Spodyneiko, Alex Turzillo, Ke Ye, and Minyoung You, as well as all the other students on the fourth floor over the years. While I didn't often work in my office, I was happy to have two great office mates to chat with, Nick Hunter-Jones and Ashmeet Singh. Thanks also to all my friends in the math department and Matilde's group for tolerating my physics explanations despite a lack of rigor. I would also like to thank those students at Perimeter and Princeton for welcoming me and showing me friendship as a visitor.

In addition to other graduate students, I learned from and had a great time interacting with several postdocs at Caltech and elsewhere. I would like to thank Mykola Dedushenko, Martin Fluder, Yvonne Geyer, Ying-Hsuan Lin, Natalie Paquette, and Eric Perlmutter for fun times around the office, advice, and some collaborations. I hope to have opportunities to work with them all in the future.

Caltech was an interesting experience for me as a graduate student, but many of the choices that led me to this point came about from my experiences at Caltech as an undergraduate. The Caltech undergraduate culture and experience is a totally unique part of my life; I simply cannot begin to explain why this place is so special. I would like to thank all of my friends throughout undergrad who made Caltech a magical place. This includes everyone in Blacker Hovse who supported my crazy antics and theoretical physics. Blacker also produced two theoretical physicists who served as a great inspiration for me. I would like to thank Kip Thorne for being a friendly and enthusiastic mentor for undergraduates and also for inspiring me to want to work on general relativity. Unfortunately, my other great inspiration, Joseph Polchinski, passed away during the time of this thesis. I would like to thank him for his fantastic contributions to string theory as well as to the Caltech undergraduate culture. He will be missed. I sincerely hope that, in the future, Caltech maintains the unique undergraduate experience that has helped to foster amazing creative and independent scientists like Kip, Joe, and many others.

Many thanks to my friends from undergraduate and beyond who kept close contact with me throughout my time in graduate school. My experiences with these longer term friends have been a fun and healthy distraction from the busy life of graduate school, and many of my friends supported me through some stressful and difficult times. A special thanks goes to Darcy Caldwell, Ilya Nepomnyashchii, Jeff Odell, Samuel Savitz, and Kirby Sikes, and also to Oliver Banham and Jerry Politzer, all of whom have been incredible friends and companions!

Finally, I would like to thank my family who supported my interest in science as I was growing up. Most importantly, I would like to thank my parents, Helen and Tom Heydeman, for their love, encouragement, and support, without which my PhD would not have been possible. For this, I dedicate this thesis to them.

ABSTRACT

In this thesis, we consider two topics in string theory and quantum field theory which are related by the common appearance of one-dimensional projective geometry. In the first half of the thesis, we study *six-dimensional* (6D) supersymmetric quantum field theories and supergravity at the leading (tree) approximation and compute the complete S-matrix for these theories as world-sheet integrals over the punctured Riemann sphere. This exploits the analytic structure of tree amplitudes which are rational and holomorphic in the kinematics and naturally related to the geometry of points on the complex projective line. The 6D n -particle S-matrix makes many symmetries and hidden properties manifest and generalizes the well-studied formulas for four-dimensional amplitudes in the form of twistor string theory and the rational curves formalism. While the systems we study are all field theories, they are in essence *low-energy effective field theory* limits of string theory and M-theory backgrounds. This includes theories such as those with 6D $(2, 0)$ supersymmetry which contain $U(1)$ self-dual tensor fields which are difficult to treat from a Lagrangian point of view. Our formulas circumvent this difficulty and allow a generalization and unification of a large class of 6D scattering amplitudes which permit a sensible classical limit, including the abelian world-volume of the M-theory Five-brane. Dimensional reduction to four dimensions is also possible, leading to new formulas for 4D physics from 6D.

In the second half of the thesis, we discuss the projective algebraic and geometric structure of the $\text{AdS}_3/\text{CFT}_2$ correspondence. In the usual statement of this correspondence, two-dimensional conformal field theory (CFT) on the Riemann sphere or a higher-genus surface is holographically dual to features of topological gravity in three dimensions with negative curvature. Since every compact Riemann surface is a projective algebraic curve, many constructions of interest in physics (which *a priori* depend on the analytic structure of the spacetime) can be formulated in purely algebraic language. We generalize the AdS (anti-de Sitter space)/CFT correspondence according to this principle using projective geometry over the p -adic numbers, \mathbb{Q}_p . The result is a formulation of holography in which the bulk geometry is discrete—the Bruhat–Tits tree for $\text{PGL}(2, \mathbb{Q}_p)$ —but the group of bulk isometries nonetheless agrees with that of boundary conformal transformations and is not broken by discretiza-

tion. Parallel to the usual holographic correspondence, semi-classical dynamics of fields in the bulk compute the correlation functions of local operators on the boundary. Beyond correlators on the p -adic line, we propose a tensor network model in which the patterns of entanglement on the boundary are computed by discrete geometries in the bulk. We suggest that this forms the natural geometric setting for tensor networks that have been proposed as models of bulk reconstruction via quantum error correcting codes. The model is built from tensors based on projective geometry over finite fields, \mathbb{F}_p , and correctly computes the Ryu-Takayanagi formula, holographic entanglement and black hole entropy, and multiple interval entanglement inequalities.

In Chapter 2, we present tree-level n -particle on-shell scattering amplitudes of various brane theories with 16 conserved supercharges which are generalizations of Dirac–Born–Infeld theory. These include the world-volume theory of a probe D3-brane or D5-brane in 10D Minkowski spacetime as well as a probe M5-brane in 11D Minkowski spacetime, which describes self interactions of an abelian tensor supermultiplet with 6D $(2, 0)$ supersymmetry. We propose twistor-string-like formulas for tree-level scattering amplitudes of all multiplicities for each of these theories, and the amplitudes are written as integrals over the moduli space of certain rational maps localized on the $(n - 3)!$ solutions of the scattering equations. The R symmetry of the D3-brane theory is shown to be $SU(4) \times U(1)$, and the $U(1)$ factor implies that its amplitudes are helicity conserving. Each of 6D theories (D5-brane and M5-brane) reduces to the D3-brane theory by dimensional reduction. As special cases of the general M5-brane amplitudes, we present compact formulas for examples involving only the self-dual B field with $n = 4, 6, 8$.

In Chapter 3, we extend this formalism to n -particle tree-level scattering amplitudes of six-dimensional $\mathcal{N} = (1, 1)$ super Yang–Mills (SYM) and $\mathcal{N} = (2, 2)$ supergravity (SUGRA). The SYM theory arises on the world volume of coincident D5-branes, and the supergravity is the result of toroidal compactification of string theory. These theories have non-abelian interactions which allow for both even and odd-point amplitudes, unlike the branes of Chapter 2. Due to the properties of spinor-helicity variables in six dimensions, the even- n and odd- n formulas are quite different and have to be treated separately. We first propose a manifestly supersymmetric expression for the even- n amplitudes of $\mathcal{N} = (1, 1)$ SYM theory and perform various consistency checks. By consid-

ering soft-gluon limits of the even- n amplitudes, we deduce the form of the rational maps and the integrand for n odd. The odd- n formulas obtained in this way have a new redundancy that is intertwined with the usual $\text{SL}(2, \mathbb{C})$ invariance on the Riemann sphere. We also propose an alternative form of the formulas, analogous to the Witten–RSV (Roiban, Spradlin, and Volovich) formulation, and explore its relationship with the symplectic (or Lagrangian) Grassmannian. Since the amplitudes are formulated in a way that manifests double-copy properties, formulas for the six-dimensional $\mathcal{N} = (2, 2)$ SUGRA amplitudes follow. These six-dimensional results allow us to deduce new formulas for five-dimensional SYM and SUGRA amplitudes, as well as massive amplitudes of four-dimensional $\mathcal{N} = 4$ SYM on the Coulomb branch.

In Chapter 4, we consider half-maximal supergravity and present a twistor-like formula for the complete tree-level S matrix of chiral 6D $(2, 0)$ supergravity coupled to 21 abelian tensor multiplets. This is the low-energy effective theory that corresponds to Type IIB superstring theory compactified on a K3 surface. As in previous chapters, the formula is expressed as an integral over the moduli space of certain rational maps of the punctured Riemann sphere; the new ingredient is an integrand which successfully incorporates both gravitons and multiple flavors of tensors. By studying soft limits of the formula, we are able to explore the local moduli space of this theory, $\frac{SO(5, 21)}{SO(5) \times SO(21)}$. Finally, by dimensional reduction, we also obtain a new formula for the tree-level S-matrix of 4D $\mathcal{N} = 4$ Einstein–Maxwell theory.

In Chapter 5, we introduce p -adic AdS/CFT and discuss several physical and mathematical features of the holographic correspondence between conformal field theories on $\mathbb{P}^1(\mathbb{Q}_p)$ and lattice models on the Bruhat–Tits tree of $\text{PGL}(2, \mathbb{Q}_p)$, an infinite tree of $p + 1$ valence which has the p -adic projective line as its boundary. We review the p -adic numbers, the Bruhat–Tits tree, and some of their applications to physics including p -adic CFT. A key feature of these constructions is the discrete and hierarchical nature of the tree and the corresponding field theories, which serve as a toy model of holography in which there are no gravitons and no conformal descendants. Standard holographic results for massive free scalar fields in a fixed background carry over to the tree; semi-classical dynamics in the bulk compute correlation functions in the dual field theory and we obtain a precise relationship between the bulk mass and the scaling dimensions of local operators. It is also possible to interpret

the vertical direction in the tree a renormalization-group scale for modes in the boundary CFT. Higher-genus bulk geometries (the BTZ black hole and its generalizations) can be understood straightforwardly in our setting and their construction parallels the story in AdS₃ topological gravity.

In Chapter 6, we consider a class of holographic quantum error-correcting codes, built from perfect tensors in network configurations dual to Bruhat–Tits trees and their quotients by Schottky groups corresponding to BTZ black holes. The resulting holographic states can be constructed in the limit of infinite network size. We obtain a p -adic version of entropy which obeys a Ryu–Takayanagi like formula for bipartite entanglement of connected or disconnected regions, in both genus-zero and genus-one p -adic backgrounds, along with a Bekenstein–Hawking-type formula for black hole entropy. We prove entropy inequalities obeyed by such tensor networks, such as subadditivity, strong subadditivity, and monogamy of mutual information (which is always saturated). In addition, we construct infinite classes of perfect tensors directly from semi-classical states in phase spaces over finite fields, generalizing the CRSS algorithm. These codes and the resulting networks provide a natural bulk geometric interpretation of non-Archimedean notions of entanglement in holographic boundary states.

PUBLISHED CONTENT AND CONTRIBUTIONS

The work in this thesis is adapted from original research papers. Chapters 2, 3, 4, 5, and 6 are based on [1, 2, 3, 4, 5], respectively, with some modification. All are available as arXiv preprints; where appropriate, the published version also has a DOI available. These works are a collaborative process and all authors have contributed equally.

- [1] Matthew Heydeman, John H. Schwarz, and Congkao Wen. “M5-Brane and D-Brane Scattering Amplitudes”. In: *JHEP* 12 (2017), p. 003. DOI: [10.1007/JHEP12\(2017\)003](https://doi.org/10.1007/JHEP12(2017)003). arXiv: [1710.02170](https://arxiv.org/abs/1710.02170) [[hep-th](#)].
- [2] Freddy Cachazo, Alfredo Guevara, Matthew Heydeman, Sebastian Mizera, John H. Schwarz, and Congkao Wen. “The S Matrix of 6D Super Yang-Mills and Maximal Supergravity from Rational Maps”. In: *JHEP* 09 (2018), p. 125. DOI: [10.1007/JHEP09\(2018\)125](https://doi.org/10.1007/JHEP09(2018)125). arXiv: [1805.11111](https://arxiv.org/abs/1805.11111) [[hep-th](#)].
- [3] Matthew Heydeman, John H. Schwarz, Congkao Wen, and Shun-Qing Zhang. “All Tree Amplitudes of 6D (2, 0) Supergravity: Interacting Tensor Multiplets and the $K3$ Moduli Space”. In: *Phys. Rev. Lett.* 122.11 (2019), p. 111604. DOI: [10.1103/PhysRevLett.122.111604](https://doi.org/10.1103/PhysRevLett.122.111604). arXiv: [1812.06111](https://arxiv.org/abs/1812.06111) [[hep-th](#)].
- [4] Matthew Heydeman, Matilde Marcolli, Ingmar Saberi, and Bogdan Stoica. “Tensor networks, p -adic fields, and algebraic curves: arithmetic and the $\text{AdS}_3/\text{CFT}_2$ correspondence”. In: *Adv. Theor. Math. Phys.* 22 (2018), pp. 93–176. DOI: [10.4310/ATMP.2018.v22.n1.a4](https://doi.org/10.4310/ATMP.2018.v22.n1.a4). arXiv: [1605.07639](https://arxiv.org/abs/1605.07639) [[hep-th](#)].
- [5] Matthew Heydeman, Matilde Marcolli, Sarthak Parikh, and Ingmar Saberi. “Nonarchimedean Holographic Entropy from Networks of Perfect Tensors”. In: (2018). arXiv: [1812.04057](https://arxiv.org/abs/1812.04057) [[hep-th](#)].

TABLE OF CONTENTS

Acknowledgements	iv
Abstract	vii
Published Content and Contributions	xi
Table of Contents	xii
List of Illustrations	xiv
Chapter I: Introduction	1
1.1 Overview and Motivation	1
1.2 Review of Perturbative String Theory and D-Branes	6
1.3 Yang–Mills Amplitudes in 4D and Twistor String Theory	13
1.4 Holography, AdS/CFT, and p -Adic Algebraic Curves	24
Chapter II: Amplitudes on the World Volume of M5 and D-Branes	30
2.1 Introduction	30
2.2 Symmetries, Conserved Charges, and Supermultiplets	34
2.3 Four-Particle Amplitudes	43
2.4 n -Particle Amplitudes of the D3 Theory	48
2.5 n -Particle Amplitudes of the M5 Theory	52
2.6 n -Particle Amplitudes of the D5 Theory	72
2.7 Conclusion	75
Chapter III: The S -Matrix of 6D Super Yang–Mills and Supergravity	77
3.1 Introduction	77
3.2 Rational Maps and Connected Formulas	81
3.3 $\mathcal{N} = (1, 1)$ Super Yang–Mills: Even Multiplicity	91
3.4 $\mathcal{N} = (1, 1)$ Super Yang–Mills: Odd Multiplicity	100
3.5 Linear Form of the Maps	120
3.6 Various Theories in $D \leq 6$ and $\mathcal{N} = 4$ SYM on the Coulomb Branch	130
3.7 Conclusion and Discussion	148
Chapter IV: Half Maximal Chiral Supergravity: 6D $(2, 0)$ Supergravity and the K3 Moduli Space	157
4.1 Introduction	157
4.2 6D $(2, 0)$ Supergravity	163
4.3 The K3 Moduli Space from Soft Limits	166
4.4 4D $\mathcal{N} = 4$ Einstein–Maxwell Theory	169
4.5 Discussion and Conclusion	170
Chapter V: Projective curves and p -adic AdS/CFT	172
5.1 Introduction	172
5.2 Review of Necessary Ideas	174
5.3 p -adic CFT and Holography for Scalar Fields	189
5.4 Entanglement Entropy	205

5.5	p -adic Bulk Geometry: Schottky Uniformization and Non-Archimedean Black Holes	211
5.6	Conclusion	218
Chapter VI: Non-Archimedean Holographic Entropy and Tensor Networks		221
6.1	Introduction	221
6.2	Background	228
6.3	Entanglement in p -adic AdS/CFT	241
6.4	p -adic BTZ Black Hole	256
6.5	Von Neumann Entropy and Inequalities	269
6.6	Geometric Properties of the Tensor Networks	305
6.7	Outlook	309
Bibliography		312
Appendix A: Appendices for Chapter 2		335
A.1	Further Technical Details	335
A.2	R-Symmetry	339
Appendix B: Appendices for Chapter 3		343
B.1	Symmetry Algebra	343
B.2	Details of the Soft-Limit Calculations	346
Appendix C: Appendices for Chapter 5		363
C.1	p -adic Integration	363
C.2	p -adic Differentiation	364
Appendix D: Appendices for Chapter 6		367
D.1	The Three-Qutrit Code	367

LIST OF ILLUSTRATIONS

<i>Number</i>	<i>Page</i>
1.1 A rough figure of the twistor string for four dimensions. An abstract internal space representing a D1 brane with coordinate $z \in \mathbb{CP}^1$ wraps a holomorphic curve in \mathbb{CP}^3 . The holomorphic maps are schematically of the form $\lambda^\alpha(z) = \sum_{k=0}^d \rho_k^\alpha z^k$ and $\tilde{\lambda}^{\dot{\alpha}}(z) = \sum_{k=0}^{\tilde{d}} \tilde{\rho}_k^{\dot{\alpha}} z^k$. Punctures correspond to insertions of on-shell fields in the form of $U(N)$ open B-strings, and for n particles the degree of the maps and amount of helicity violation are given by $d + \tilde{d} = n - 2$ and $d - \tilde{d} = \Delta h$, respectively. The amplitude is obtained by integrating the correlator of these punctures over the moduli of positions z_i and maps $\rho, \tilde{\rho}$ into the target. This integral is totally localized and is equivalent to an expression obtained in field theory using Feynman diagrams. A very similar picture holds true for the six-dimensional versions of the twistor string discussed in this work, and the kinematics of 6D scattering amount to a correct choice of target space and parametrization of the curves.	22
1.2 Euclidean AdS_3 and a Euclidean BTZ black hole obtained as a quotient. The interior metric has constant negative curvature and the boundary is a torus.	26
1.3 A p -adic BTZ black hole obtained by a quotient of an infinite tree. This parallels the construction in 3D topological gravity, but now the bulk is discrete. The boundary is a genus-one curve over \mathbb{Q}_p . Certain simple features of AdS/CFT still hold for this kind of geometry. (There exists a black hole like this for every prime p — as pictured, $p = 3$).	27

2.1 Exchange diagrams contributing to the 6 B_{++} amplitude. The internal line may be any of the three states, and we sum over all the factorization channels as well. It is important to note that these diagrams do not come directly from Feynman rules as there is no covariant action available for the M5 theory; instead, they represent the factorization of the amplitude at the poles where $s_{ijk} \rightarrow 0$ 69

2.2 Diagrammatic expression of the local term for a six-particle amplitude. In the example where all external particles are B_{ab} , this local term vanishes, and the exchange diagrams are the only contribution to the total amplitude. 70

4.1 On-shell diagrams contributing to the 2-supergraviton, 2-tensor supermultiplet amplitude in Eq. (4.8). Wavy lines denote a propagating $(2, 0)$ supergravity multiplet, and straight lines denote tensor supermultiplets with $SO(21)$ flavor symmetry. Vertices represent the 3-point amplitudes, and *not* the 3-point couplings in the Lagrangian. At tree level, the amplitude is fixed by these pole diagrams. 160

5.1 The standard representation of the Bruhat–Tits tree. The point at infinity and the center are arbitrary as the tree is homogeneous. Geodesics such as the highlighted one are infinite paths through the tree from ∞ to the boundary which uniquely specify elements of \mathbb{Q}_p . This path as a series specifies the digits of the decimal expansion of $x \in \mathbb{Q}_2$ in this example. At the n th vertex, we choose either 0 or 1 corresponding to the value of x_n in the p^n th term of x . Negative powers of p correspond to larger p -adic norms as we move towards the point ∞ 176

- 5.2 An alternative representation of the Bruhat–Tits Tree (for $p = 3$) in which we have unfolded the tree along the 0 geodesic. The action of elements of $\mathrm{PGL}(2, \mathbb{Q}_p)$ acts by translating the entire tree along different possible geodesics. In this example we translate along the 0 geodesic, which can be thought of as multiplication of each term in a p -adic decimal expansion by p . This map has two fixed points at 0 and ∞ . In this “unfolded” form, a point in $\mathbb{P}^1(\mathbb{Q}_p)$ is specified by a geodesic that runs from ∞ and follows the 0 geodesic until some level in the tree where it leaves the 0 geodesic towards the boundary. The p -adic norm is simply p to the inverse power of the point where it leaves the 0 geodesic (so leaving “sooner” leads to a larger norm, and later to a smaller norm. 180
- 5.3 A helpful figure reproduced from 1.4. The Fundamental domain and quotient for the Euclidean BTZ black hole. Compare with the p -adic BTZ geometry, shown in Figure 5.7. 184
- 5.4 Fundamental domains for the action of Γ on \mathbf{H}^3 186
- 5.5 A drawing of \mathbb{Z}_p ($p = 2$ for simplicity). Here $k = p^{-4}$. The marked fractions at vertices indicate contributions to $\{kx\}$, which are summed along the geodesic ending at x 203

- 5.6 Boundary-anchored geodesics in T_p have a natural interpretation in terms of the p -adic norm. Once the arbitrary position of the center C is fixed, the norm of open sets in \mathbb{Q}_p is given by p^{-d} , where d is the integer number of steps from C required before the path to the endpoints splits. In this example, $|x - y|_p$ is described by the red geodesic and the value is p^{-2} . The set corresponding to the green geodesic has a smaller norm by a factor of p because the vertex is 1 step further down the tree. As in the case of real AdS, the length of the geodesic is formally infinite because an infinite number of steps is required to reach the boundary. One may introduce a cutoff corresponding to truncation of the tree at a fixed distance, then take the limit as this cutoff goes to zero. It should be apparent that the (formally infinite) red geodesic is longer than the green one by two steps. Up to constant factors, the length of any boundary-anchored geodesic is an infinite term minus d . This explains the logarithmically divergent scaling of geodesic length with p -adic norm. 210
- 5.7 The p -adic BTZ black hole, reproduced from 1.4. (As pictured, $p = 3$). 214
- 5.8 Drinfeld's p -adic upper half plane and the Bruhat–Tits tree. 216
- 5.9 The action of a rank-one Schottky group (translation by ℓ along a fixed geodesic) on the Bruhat–Tits tree. As pictured, $n = h = 2$. 217
- 6.1 A finite part of the infinite Bruhat–Tits tree is shown in red, with the nodes labeled v_i . The graphical representation of the dual graph for the finite red subgraph is shown in black. The Bruhat–Tits tree in (b) is obtained by acting on the Bruhat–Tits tree in (a) with a $\text{PGL}(2, \mathbb{Q}_p)$ transformation fixing the vertex v_0 . Equivalently, the dual graphs in (a) and (b) correspond to two different choices of incidence relations for bonds on the dual graph, subject to the two requirements mentioned in definition 3. In the infinite graph limit, the geometry of the Bruhat–Tits tree is represented by the Schläfli symbol $\{\infty, p + 1\}$, while the dual graph is given by the Schläfli symbol $\{p + 1, \infty\}$ 243

6.2	The construction of the holographic tensor network for the cutoff Bruhat–Tits tree. In this example, we have used perfect tensors of rank eight. The construction shown here corresponds to the parameters $p = 3$, $\Lambda = 2$, and $r = 7$. Hereafter we will suppress showing the free uncontracted/dangling legs displayed in (b).	245
6.3	Two pictures of the Bruhat–Tits tree for $P^1(\mathbb{Q}_2)$, emphasizing either the action of the multiplicative group \mathbb{Q}_2^\times or the Patterson–Sullivan measure.	247
6.4	The region at the boundary of the dual graph “in between” boundary points v_8 and v_7 for two choices of planar embedding for the dual graph, depicted in blue.	250
6.5	(a) The set of vertices on the dual graph marked in blue form a “connected region”. (b) The set of blue vertices form a “disconnected region” which can be specified by a set of four boundary points. Note that for the given set of boundary points and a chosen planar embedding, another choice of disconnected regions, shown in black circles, is possible.	252
6.6	The p -adic BTZ black hole, obtained here for $p = 3$ by a quotient of the Bruhat–Tits tree by a Schottky generator with $\log_p q _p^{-1} = 6$. The geometry is locally indistinguishable from the Bruhat–Tits tree, but the presence of the horizon signifies the boundary interpretation will be very different. In the tensor network analysis we will find the boundary state of this geometry will have a thermal entropy proportional to $6 \log p$	262
6.7	The quotient construction of the dual graph tensor network (in black). As pictured, $p = 3$ and $\text{ord}_p(q) = 5$	263
6.8	The genus 1 tensor network after tracing out the vertex behind the horizon. One should imagine the two sides corresponding to $ \psi\rangle$ and $\langle\psi $, and the total state being the mixed density matrix which has von Neumann entropy proportional to the number of shared bonds. We postpone the explanation of the graphical rules and the computation of the entropy until Section 6.5, but the reader might be reminded of the 2-sided BTZ black hole.	265
6.9	Geodesics in the BTZ black hole geometry. Moving y to y' leads to a “jump” of the minimal geodesic to a path wrapping the other side of the horizon.	267

6.10	Computation of $\langle \psi \psi \rangle$	279
6.11	A schematic representation of the bipartite entanglement entropy calculation for the cases shown in figures 6.12 and 6.13b, here (a) and (b) respectively, to emphasize the parallel with the usual story over the reals. The disconnected region $A = A_1 \cup A_2$ is shown in black, while the minimal geodesics homologous to A is shown in blue.	289
6.12	The setup for the bipartite entanglement calculation for a disconnected region, in the case when the cross-ratio $u(x_1, x_2, x_3, x_4)$ defined in (6.99) is strictly less than one. Left: The holographic state with the region marked in blue. Right: Computation of the reduced density matrix, and the depiction of the minimal surface homologous to the boundary region. See the main text for the detailed explanation of the figure.	290
6.13	The case of a disconnected region with cross-ratio $u(x_1, x_2, x_3, x_4)$ defined in (6.99) greater than or equal to 1.	292
6.14	Boundary anchored bulk geodesics on the Bruhat–Tits tree and the boundary point configuration such that $u(x_1, x_2, x_3, x_4) \leq 1$	295
6.15	Boundary anchored bulk geodesics on the Bruhat–Tits tree and the boundary point configuration such that $u(x_1, x_2, x_4, x_5) \leq 1$ and $u(x_3, x_4, x_1, x_5) \leq 1$. Up to relabelling, this is the most general configuration of five boundary points at the terminus of the Bruhat–Tits tree.	299
6.16	The density matrix associated to the thermal state on the boundary of a BTZ black hole tensor network.	302
6.17	A schematic depiction of the three topologically distinct cases of minimal geodesics for a connected region A	305

Chapter 1

INTRODUCTION

1.1 Overview and Motivation

The last quarter century of theoretical high energy physics has been a time of great unification of seemingly disparate physical and mathematical concepts. Much of this interplay has come about both from a better understanding of quantum field theory, which describes all known elementary particles and forces, as well as the emergence of superstring theory and M-theory as a consistent theory of quantum gravity which seems to unify the laws of nature. Quantum fields and strings not only imply, but in fact require, a dramatic departure from our familiar notions of matter, space, time, and even observables; the laws of modern physics appear at times subtle and geometrical with a great deal of hidden structure and interconnectedness. Additionally, mathematical concepts and disciplines which were once thought to be disjoint from the physical world now play an essential role in how we describe these theories quantitatively.

These patterns and structures in the laws of nature appear again and again, and often great progress can be made by utilizing these connections. In my opinion, it is both pragmatic and fascinating to maintain broad theoretical interests; one never knows what tools or ideas might be powerful when viewed in a new light, or what “coincidences” might hint at a deeper, more general truth.

In the spirit of these ideals, this thesis is about several distinct but ultimately related ideas involving quantum field theory, string theory, and the mathematical tools with which we can make sense of these theories. It represents the culmination of my graduate work and the publications [1, 2, 3, 4, 5, 6, 7], many of which have been adapted more or less directly for this dissertation. Because the available topics are varied, I have chosen a loose and admittedly somewhat artificial theme of “one-dimensional projective geometry”, a classical branch of mathematics which is both general and powerful enough to be very useful for the physical theories we describe. While the mathematics is very beautiful, my ultimate emphasis in this work is how these structures inform our understand-

ing of physics, therefore some of the original works have been adapted to fit this theme. Beyond this introductory chapter, the thesis splits into two main parts. Chapters 2, 3, and 4 discuss how we can use symmetry principles and the geometry of the Riemann sphere to understand scattering amplitudes in six-dimensional supersymmetric quantum field theories and gravity. In some cases, these theories have resisted a concise description before the introduction of our techniques. Chapters 5 and 6 focus on holographic duality, p -adic projective geometry, conformal field theory (CFT), and the emergence of spacetime from quantum entanglement.

We now briefly introduce the important physical concepts which are central to the thesis.

Perturbative Quantum Field Theory (QFT) is the physical and mathematical framework which appears to describe all elementary particles and their interactions. This celebrated framework unifies two of the most important ideas of the early 20th century— the Special Theory of Relativity and Quantum Mechanics. In the standard path integral approach, one begins with a classical field theory Lagrangian which is local and invariant under the Lorentz transformations of relativity as well as other global and gauge (spacetime dependent) symmetries. To promote this classical theory to a quantum theory, it is necessary to identify the elementary field excitations as particles and then account for the interactions of these particles order by order in a perturbative expansion using the Feynman rules. This procedure is not always possible for some quantum field theories, including a large class of *conformal field theories* (CFT) which have conformal transformations as an enhanced spacetime symmetry. CFT's do not necessarily have particles, but they will play a major role later in the thesis. For now we focus on perturbative QFT in a setting where we can talk about scattering of particles.

In a QFT as we have described, there are no longer definite trajectories and outcomes for individual particles, but observables such as transition probabilities between initial and final states may be computed to fantastic accuracy in theories for which the standard framework applies. The transition probability amplitude (the complex distribution whose square is the probability) is a basic observable which we call the *scattering amplitude* A associated to the *S-matrix* between initial and final states. By construction, this object depends only on gauge invariant information in which all asymptotic particles are physi-

cal and satisfy the mass-shell relation $p^2 = -m^2$. This makes sense in Lorentz invariant local field theories with a weakly coupled limit, where asymptotic states can be taken to be products of one-particle states which satisfy their appropriate free equation of motion. Additionally, local symmetries such as the gauge symmetries of the electromagnetic, weak, and strong forces as well as the diffeomorphisms of Einstein's General Relativity must still satisfy some fixed boundary conditions at spacetime infinity (though they are redundancies of the description in the interior of spacetime). For this reason, amplitudes can detect the elementary short distance dynamics of a quantum theory while still only depending on physical asymptotic data.

For a given theory with a choice of external particles and boundary conditions, the amplitude is gauge invariant and annihilated by all global charges. However, the individual Feynman diagrams (built out of manifestly local information) are typically not gauge invariant on their own. Only the sum is, and this fact represents a general rule of quantum mechanics; unitary evolution is not usually associated with a specific semi-classical process or diagram.

In the case of perturbative scattering amplitudes, this strategy of composing elementary interactions between particles and then summing over all histories à la Feynman is often very successful though technically difficult, and it can also hide important physical and mathematical structures present in the final answers. Much of the modern program of amplitudes is to find alternative formulations of QFT which expose these structures. Perhaps an even bigger reason to find an alternative to perturbative QFT comes from the fact that it is difficult to address Einstein's theory of general relativity as quantum corrections lead to a breakdown of the theory at short distances. Beyond scattering amplitudes, non-perturbative objects such as black holes naively violate the unitary evolution of quantum mechanics; the resolution seems to require holographic features of quantum gravity in which information is not quite local. This all suggests that an even deeper structure is necessary.

One possibility for a deeper structure is string theory and M-theory, which has emerged as a framework in which it is possible to unify particles, forces, and gravity in a unique and consistent way. This is a vast and complex topic, but simply stated, in string theory we replace the point-like particles of quantum field theory with extended one-dimensional objects called strings. It is outside the scope of this thesis to explain all the implications of this simple sounding

idea, but string theory has led to many remarkable insights in both high energy theoretical physics and mathematics.¹ This has led to a new understanding of gravity at short distances, as well as black holes, supersymmetric particle physics, the holographic and emergent nature of spacetime, and even pure mathematics in geometry, topology, and number theory among many other disciplines. Additionally, string theory has provided new ways to compute the S-Matrix of ordinary QFT and gravity without the use of a Lagrangian, and also makes many hidden properties manifest (this was actually the starting point of the subject, before string theory was shown to imply quantum gravity). It is thus of great theoretical interest to study string theory both as a candidate for a unified theory of nature, but also as a rich mathematical tool to explore other areas of physics. The latter motivation is compelling even if string theory turns out to not be realized in nature.

In the first half of this thesis, we study the interplay between string theory and scattering amplitudes in several interconnected ways. At the basic level, all the scattering amplitudes we present will be those of quantum field theories at the leading (tree) order of approximation. However, the formulas for the amplitudes themselves are not based on the ordinary techniques of perturbative QFT, but instead are more similar to the machinery of perturbative string theory. This allows us to obtain the complete n -particle S-matrix and makes certain properties manifest that were invisible in QFT. Importantly, the field theories we are able to address are in some cases difficult to treat with standard techniques. In fact, M-theory and string theory dualities have predicted the (mathematical) existence of very special kinds of interacting field theories in *six spacetime dimensions*. While we only discuss the tree amplitudes, in principle all the theories we discuss have an ultraviolet completion as systems in M-theory.

So far, we have mostly discussed perturbative quantum field and string theories in which all coupling constants are small and spacetime is approximately flat. This is the situation in which perturbative QFT and strings are most successful, but it clearly cannot be the full story. The real world is rich with non-perturbative physics, such as bound states and black holes. Analogous situations appear in superstring theory, and it is natural to ask what we can learn about physics in the strong coupling or large curvature regimes. Re-

¹See [8, 9, 10, 11] for an introduction to this subject.

markably, in certain cases powerful dualities may relate perturbative and non-perturbative physics. While it is generally hard to do exact computations (of amplitudes, for example) at strong coupling or curvature, sometimes a dual description may lead to a better understanding.

Of these fascinating dualities, perhaps the most striking is the celebrated AdS/CFT correspondence [12], which is the equivalence of string theory in negatively curved anti-de Sitter space (AdS) to a conformal field theory living at the boundary of the space. The details of this correspondence will be discussed later, but here we will say that this correspondence gives a way to translate questions about gravitational physics in AdS into ordinary (though strongly coupled) questions about the dual CFT. Likewise, quantum mechanical properties of the CFT may be translated into properties of semi-classical general relativity. This duality is one of the main triumphs of string theory as a theory of quantum gravity, as it allows us to directly answer questions about quantum gravity in curved backgrounds.

Despite these successes, there remain many mysteries about *how* exactly this duality works in detail. In the “bulk” AdS space, which is higher dimensional, it is hard to give a precise microscopic description in terms of string geometry. Because of this, it is helpful to seek out toy models in which exact computations are possible, while still preserving some essential features. Models of this type can sometimes expose interesting physical and mathematical structures which are essential for understanding more complicated and realistic theories.

The second half of this thesis is devoted to one proposal for a model of AdS/CFT in which the projective and algebraic geometry plays an essential role, but where many subtleties of the full holographic duality are absent. This model is based on the *p-adic numbers*, which is a classical number system in mathematics parallel to the real numbers. The *p*-adics are naturally discrete, but still have a version of conformal symmetry. Perhaps surprisingly, we find that certain physical, algebraic features of AdS/CFT are still captured by quantum field theories over *p*-adic geometries. We give a more complete introduction to this proposal in Section 1.4.

In Section 1.2 we review perturbative string theory and some of the background of world-sheet techniques for amplitudes. We also discuss some non-perturbative features of string theory including D-branes, dualities, and the interesting case of six-dimensional field theory. In Section 1.3 we discuss mass-

less scattering in four dimensions and the twistor string theory. In Section 1.4, we introduce AdS/CFT and the proposal for a p -adic version of this duality. Subsequent chapters are based on the original papers and are a presentation of our results.

1.2 Review of Perturbative String Theory and D-Branes

The early days of QFT saw the success of the theory of Quantum Electrodynamics, which describes the interaction of fundamental electrons and photons. However, in the 1960s many new strongly interacting particles dubbed hadrons were discovered; these massive particles had high spin and did not appear to be fundamental. The tools of perturbative QFT which were highly successful in the theory of Quantum Electrodynamics seemed inapplicable to these strongly coupled particles, and in principle the scattering amplitudes with exchanged higher-spin hadrons has bad high energy behavior. Lacking the microscopic explanation in terms of Yang–Mills theory in which hadrons are not fundamental, but instead strongly interacting bound states, an early approach at the time were the so-called “dual models” of hadrons (see the introduction of [8] for a historical overview).

The spirit of dual model school of thought was to de-emphasize the role of the apparent higher spin “fundamental particles” which could be exchanged in interactions, and instead try to directly construct an amplitude with the correct properties. The goal would be to determine the scattering matrix of asymptotic states from consistency conditions; symmetries such as the Lorentz invariance of special relativity, the unitarity of quantum mechanics, and the apparently local nature of fundamental interactions. This S-Matrix or *bootstrap* approach promised to constrain or potentially even solve the general problem of hadron scattering. While this approach was eventually replaced by Yang–Mills theory, many ideas developed during this time were essential to the discovery of string theory. We will only review some essential technical highlights which serve as motivation for this thesis.

One of the most striking and unique examples of a scattering amplitude produced by the S-matrix program is the now famous *Veneziano Amplitude* [13]. This describes the scattering of four external particles (2 incoming \rightarrow 2 outgoing), and with ‘Regge type’ exchanges involving infinite towers of higher-spin particles. These infinite towers of particles were suggested by the pattern of

hadronic resonances. It was only later discovered that the Veneziano Amplitude describes the scattering of not point-like particles, but strings, and in fact four tachyons in open string theory [14, 15]. The infinite tower of particles is interpreted as the infinite set of string modes which can be exchanged and regulate the amplitude at high energies. The tree-level amplitude which is leading in perturbation theory is given (depending on convention) by:

$$A_4(s, t) = g^2 \frac{\Gamma(-\alpha's - 1)\Gamma(-\alpha't - 1)}{\Gamma(-\alpha'(s + t) - 2)} = g^2 \int_0^1 d\sigma \sigma^{-\alpha's-2} (1 - \sigma)^{-\alpha't-2}, \quad (1.1)$$

Here g is the coupling constant, α' is the Regge slope which is the inverse tension of the string, s, t, u are the usual Mandelstam variables which serve as Lorentz-invariant combinations of the external momenta,

$$s = -(p_1 + p_2)^2, \quad t = -(p_2 + p_3)^2, \quad u = -(p_1 + p_3)^2, \quad (1.2)$$

and $\Gamma(x)$ is the usual Euler Gamma Function. The last inequality in which the amplitude is written as the integral over a coordinate σ is a key idea in this work. This is in fact a gauge-fixed integral over the moduli space of four punctures $\sigma_i, i = 1, \dots, 4$ on $\mathbb{P}^1(\mathbb{R})$, the boundary of a disk world-sheet. This punctured disk is equivalent via a conformal transformation to a spacetime process involving two open strings combining and then again splitting into two open strings. Once we pick a given cyclic ordering for the strings on the disk, the boundary conformal group $SL(2, \mathbb{R})$ is used to fix the positions of three punctures to $\sigma_1, \sigma_3, \sigma_4 = 0, 1, \infty$. This $SL(2, \mathbb{R})$ symmetry is the group of real unit determinant 2×2 matrices which act on coordinates as

$$\begin{pmatrix} a & b \\ c & d \end{pmatrix} : \quad \sigma \rightarrow \frac{a\sigma + b}{c\sigma + d}, \quad ad - bc = 1. \quad (1.3)$$

This is the familiar *fractional linear transformation*, which is the symmetry group of the projective line. It plays a critical role in virtually every aspect of this thesis, and in general we refer to this kind of transformation as $SL(2, \mathbb{K})$ for some field \mathbb{K} .

This interpretation of the four-particle amplitude as scattering on the disk has a generalization to n -particle/string scattering in the form of the Koba-Nielsen formula for open string tachyons [16, 17]. Unlike the usual method of computing scattering amplitudes using Feynman diagrams, which rapidly grow in complexity as the number n of particles increases, the string amplitude

has a single general expression as an integral over the gauge fixed moduli of the disk:

$$A_n = g^{n-2} \int_{0 < \sigma_2 < \dots < \sigma_{n-2} < 1} d\sigma_2 \dots d\sigma_{n-2} \prod_{i=2}^{n-2} |\sigma_i|^{\alpha'(p_1 \cdot p_i)} |1 - \sigma_i|^{\alpha'(p_i \cdot p_{n-1})} \prod_{2 \leq j < k \leq n-2} |\sigma_j - \sigma_k|^{\alpha'(p_j \cdot p_k)}. \quad (1.4)$$

For 4-particles, this reduces to the Veneziano amplitude after using the tachyon mass squared $m_i^2 = -\frac{1}{\alpha'}$.

The abstract form of this amplitude is shared by virtually all formulas which are found later in this thesis, and will be repeatedly emphasized:

$$A_n(p_i) = \int d\mu_n(\sigma_i) \mathcal{I}_n(p_i, \sigma_i). \quad (1.5)$$

As written this formula is somewhat formal, but this generality is by design a virtue. Depending on the precise theory and definition of the *measure* $d\mu$ and *integrand* \mathcal{I}_n , (1.5) may describe the scattering of tachyons, gluons, gravitons, open and closed strings, four-dimensional $\mathcal{N} = 4$ supersymmetric Yang–Mills, and (as we will uncover over the course of this thesis), exotic self-dual gauge fields which arise in M-theory and appear difficult to treat using standard perturbative QFT techniques such as path integrals and Feynman diagrams.

In string theory and superstring theory, the measure is typically taken to be a functional integral over the target space coordinates $X^\mu(\sigma, \bar{\sigma})$ describing the embedding of the string with complex coordinate σ in spacetime. External states which carry definite spacetime momentum p_i are inserted at positions σ_i on the world-sheet traced out by the string, and we integrate over the positions of these σ_i in the measure as well. We also integrate over all metrics g_{ab} of the two-dimensional internal space traced out by the strings up to diffeomorphisms. The topology of the internal space and domain of the coordinates σ_i may be a disk, a sphere, or higher-genus surface possibly with boundary, depending on the choice of open/closed strings and order in perturbation theory. This choice also effects whether σ_i are real or complex, and also if the amplitude potentially depends only holomorphically on the positions of the punctures. We must additionally fix the global conformal symmetry of the string world-sheet, which amounts to fixing a $SL(2, \mathbb{R})$ or $SL(2, \mathbb{C})$ redundancy acting on the coordinates σ_i .

Another interesting feature of (1.1) and (1.4) is the relationship to special automorphic functions such as the Gamma function. In the spirit of what will come later in Chapter 5, one could imagine evaluating this integral not over marked points on $\mathbb{P}^1(\mathbb{R})$, but instead over the p -adic projective line, $\mathbb{P}^1(\mathbb{Q}_p)$, where p is any prime. Readers not familiar with p -adic numbers will find a review in that chapter, but we comment that this number system is an alternate way to metrically complete the rational numbers with respect to an ultrametric norm. The Veneziano and Koba-Nielsen amplitudes make sense in this more exotic setting, and in fact have some remarkable number theoretic properties; this is the subject of *p -adic string theory* [18, 19].

Returning to (1.5), besides the measure, the other important object is the integrand. In the two-dimensional CFT of the string world-sheet, the integrand is the quantum correlation function of vertex operators $\mathcal{V}_i(\sigma_i)$ representing the emission or absorption of external physical string states,

$$\mathcal{I}_n(p_i, \sigma_i) \sim \langle \mathcal{V}_1(\sigma_1) \mathcal{V}_2(\sigma_2) \dots \mathcal{V}_n(\sigma_n) \rangle \quad (1.6)$$

In the case of tachyons, a local insertion of a vertex operator

$$\mathcal{V}(\sigma) =: \exp(ip \cdot X(\sigma)) : \quad (1.7)$$

corresponds to the emission of a tachyon with spacetime momentum p_i which satisfies a wrong sign mass-shell relation. The $::$ notation means the operators inside are normal ordered [9]. Evaluation of this correlation function leads to (1.4).

Fortunately, more physical particles do appear in string theory with the local vertex operators essentially being dressed versions of these tachyon operators. The identification of external (coherent) states with local operator insertions follows from the famous state operator correspondence of conformal field theory. One family of operators corresponds to deformations of the spacetime metric, and this plays an important role in string perturbation theory which may describe the consistent interaction of gravitons. With the extension of supersymmetry, the tachyon may be removed from the theory. This along with many other insights such as high energy consistency of the S-matrix has led to the compelling proposal that superstring theory is a candidate for a consistent theory of quantum gravity [20].² However, at the time of writing it

²An incomplete selection of classic papers on the development of string theory is [21, 22, 23, 24, 25, 26, 27].

is not known if string theory is truly realized in nature.

String amplitudes such as the Veneziano Amplitude have a characteristic mass scale α' for the stringy effects to become important. These degrees of freedom are important for the UV consistency of the theory, but should essentially be absent at distances long compared to the string scale. In the limit $\alpha' \rightarrow 0$, the scattering amplitudes computed in string theory must reproduce the known results for point-like particles. As an example, the scattering of three gluons with momenta p_i and polarizations e_i in D spacetime dimensions is computed in string theory as

$$A_3^{\text{YM}} = ig(2\pi)^D \delta^D \left(\sum_i p_i \right) \left(e_1 \cdot (p_2 - p_3) e_2 \cdot e_3 + e_2 \cdot (p_3 - p_1) e_3 \cdot e_1 + e_3 \cdot (p_1 - p_2) e_1 \cdot e_2 + \frac{\alpha'}{2} e_1 \cdot (p_2 - p_3) e_2 \cdot (p_3 - p_1) e_3 \cdot (p_1 - p_2) \right). \quad (1.8)$$

Here, we have picked a cyclic ordering and have omitted the gauge theory color factors which label the adjoint representation element of the gauge group G carried by the external gluons. This omission is common in the amplitudes literature and are known as color-stripped amplitudes. In the $\alpha' \rightarrow 0$ limit, this and higher-point amplitudes would be produced by the standard Yang–Mills action,

$$S = -\frac{1}{4g^2} \int d^D x \text{Tr} (F_{\mu\nu} F^{\mu\nu}), \quad (1.9)$$

where $F = dA + A \wedge A$ is the Yang–Mills field strength tensor associated to the connection A of a G -principal bundle. This theory has a supersymmetric extension [28] which we will later study as a QFT in Chapter 3. However, at linear order in α' this action is deformed by a cubic term $\sim \alpha' \text{Tr}(F^3)$ which is responsible for the additional term in the scattering amplitude. Higher-point amplitudes will reveal more string scale corrections, even in the case of a $U(1)$ gauge theory. The complete string corrected effective action in the abelian case will be of considerable interest in Chapter 2, where we construct the complete classical S-matrix of the supersymmetric completion; this is an extension of the so called Dirac–Born–Infeld theory (DBI). The DBI theory describes the fluctuations of extended objects in string theory called D-branes.

This is our first encounter with D-branes, but they play a central role both in our study of amplitudes and in the original derivation of the AdS/CFT correspondence. D-branes are extended non-perturbative objects in string

theory on which open strings may end. These solitonic objects were shown by Polchinski [29, 10] to be stable objects which are required for the consistency of string theory. A D p -brane traces out a $p + 1$ dimensional world-volume in spacetime and also carries a $U(1)$ world-volume gauge field. The flat space effective action may be derived from open string theory (see a review in [30]), and has the (diffeomorphism fixed) bosonic part

$$S_p = -T_p \int d^{p+1}x \sqrt{-\det(\eta_{\mu\nu} + \partial_\mu \phi^i \partial_\nu \phi^i + 2\pi\alpha' F_{\mu\nu})}. \quad (1.10)$$

Here $\mu = 0, \dots, p$ is a world-volume Lorentz index with standard metric $\eta_{\mu\nu}$. ϕ^i are a number of scalar fields corresponding to the transverse position of the brane, and T_p is the tension whose precise form is unimportant, but contains a factor of the string coupling g . This action should also be supplemented by fermions as dictated by supersymmetry.³ The six dimensional version of this brane theory is studied from an amplitudes point of view in Chapter 2.

We have already observed that open string amplitudes are described by an effective field theory involving gauge fields. When multiple D-branes coincide, new massless string states appear corresponding to open strings stretched between different branes. In the simplest situation with N parallel coincident branes, these new massless states fill out precisely what is required for a $U(N)$ (supersymmetric) Yang–Mills theory. We study the scattering amplitudes of this theory in 6D language in Chapter 3. Coincident branes also provide the physical mechanism for the AdS/CFT correspondence, and in the case of the D3 brane, the CFT side is precisely the 4D $U(N)$ $\mathcal{N} = 4$ SYM theory; this is outlined in 1.4.

One final comment about D-branes involves the lift to M-theory, which we discuss in much greater detail in Chapter 2. M-theory is the conjectural non-perturbative completion of string theory introduced by Witten [36, 37], combining the results of many authors about string theory dualities up to that point. The low-energy effective field theory is eleven-dimensional supergravity [38], but the full quantum theory is unknown because of the lack of any expansion parameter or coupling constant g . There is strong evidence that the various strings and D-branes of string theory all arise from what are called M2 and M5 branes in M-theory. Analogous to D-branes and Yang–Mills, multiple

³The supersymmetric action is what we study in this thesis, but the form is somewhat complicated. See [31, 32, 33, 34, 35].

coincident M5-branes lead to a strongly coupled superconformal field theory with 6D (2, 0) supersymmetry [39]. This theory is not believed to have any Lagrangian at all, and thus no classical limit or scattering amplitudes (see 3.7 for a discussion.) Even a single M5 brane is difficult to describe in perturbation theory due to the existence of a chiral self-dual $U(1)$ *three-form* gauge field $H = dB$ on the world-volume. The free equation of motion is $H = \star H$, and the analog of 1.10 would involve higher powers of H which are difficult to write a Lagrangian for. We discuss these difficulties in Chapter 2 and proposing a resolution for the scattering amplitudes by bypassing the Lagrangian entirely.

So far, we have mostly discussed the scattering of open strings via amplitudes on the disk with our related digression into D-branes. Much of the above reasoning also applies to closed string amplitudes which include the scattering of gravitons. Instead of the disk boundary, we integrate the vertex operators over the coordinates σ_i of the Riemann sphere up to the global conformal group $SL(2, \mathbb{C})$. A surprising fact about the closed string spectrum and tree amplitudes is that they can be written as the square of an open string amplitude at tree level. The intuition is that a pair of open string disk amplitudes may be glued together to give a closed string amplitude on the sphere. This is made precise in what is known as the *KLT copy* after the authors of [40]. The simplest example (which holds more generally at tree level) is:

$$A_3^{\text{gravity}} = A_3^{\text{YM}} \times A_3^{\text{YM}}. \quad (1.11)$$

(This is not a group-theoretic product, but an ordinary product of the two amplitudes with pairs of polarization vectors replaced by symmetric traceless tensors.) The leading terms in α' of these amplitudes reproduce the expectation from general relativity, and corrections correspond to specific higher curvature terms which modify Einstein's theory at short distances. As with the corrections to Yang–Mills, it is unlikely that the existence or absence of these stringy effects will be determined by experiment any time soon. Nevertheless, the general formalism of string amplitudes and KLT copies has been fruitful even in the study of ordinary QFT. For us, the KLT copy will play an essential role in Chapters 3 and 4 where gravity amplitudes will be obtained by combining simpler ingredients.

1.3 Yang–Mills Amplitudes in 4D and Twistor String Theory

We have already presented a basic result for the tree-level scattering of three gluons. This and other simple processes such as $2 \rightarrow 2$ gluon scattering may be straightforwardly computed by summing diagrams, but the computation for more general processes involving more particles requires a rapidly growing number of diagrams. For instance, the six-gluon amplitude in Yang–Mills theory famously requires over 200 diagrams!

While we will not have much to say about this, amplitudes such as these are phenomenologically relevant in colliders due to the asymptotic freedom of quantum chromodynamics. Thus in principle and in practice, there is great theoretical interest in understanding the general structure of amplitudes. This includes not just efficient techniques for computation beyond Feynman rules, but also a global understanding of how symmetry principles constrain the form of the general final answer. By now, a wide range of vibrant techniques and approaches has been developed with applications ranging from phenomenology to combinatorics. For a review of some of these developments, see [41].

In order to describe the scattering of massless particles with spin, it is useful to introduce spinor-helicity variables which algebraically solve the on-shell constraint $p_i^2 = 0$ using spacetime spinor variables. An important consequence of this is that massless particles may only travel on *null* trajectories in Minkowski space. Spinor-helicity and also twistor variables [42] are tools for parametrizing the space of these null trajectories. For the most part we will be concerned with six-dimensional spinor helicity [43], but we begin with a brief review of this construction for massless particles in four spacetime dimensions.

The four-dimensional Lorentz group will be taken to be $Spin(3,1)$ with the standard isomorphism $Spin(3,1) \sim SU(2) \times SU(2)$. For the tree-level amplitudes considered in this work, the amplitudes are holomorphic functions of the external kinematics. This means we can be somewhat flexible with our metric signature, and generally we will complexify all kinematics for technical reasons. This complexified Lorentz group is $SL(2, \mathbb{C}) \times SL(2, \mathbb{C})$ ⁴, and the finite-dimensional representations are pairs of half integers for the usual spin under each $SL(2)$. For example, a generic four-vector transforms as the bi-spinor $(\mathbf{2}, \bar{\mathbf{2}})$ representation.

⁴Alternatively, the Lorentz group will depend on the metric signature and the reality properties; a “split” signature metric with independent real spinors would give $SL(2, \mathbb{R}) \times SL(2, \mathbb{R})$, and a Euclidean metric would give $SU(2) \times SU(2)$ with pseudoreal spinors.

For a massless particle with four-momentum p_μ obeying the on-shell condition $p^2 = 0$, it is possible to algebraically solve this constraint by introducing spinor-helicity variables. (For an n -particle process we will typically label particles with the subscript $i = 1, \dots, n$.) By explicitly mapping the momentum four-vector to a bi-spinor using the appropriate Dirac matrices σ_μ , one may recast the mass-shell condition as

$$p_i^{\alpha\dot{\alpha}} = \sigma_\mu^{\alpha\dot{\alpha}} p_i^\mu, \quad p_i^2 = 0 \rightarrow \det(p_i^{\alpha\dot{\alpha}}) = 0, \quad \alpha, \dot{\alpha} = 1, 2. \quad (1.12)$$

In this representation, the momentum can be seen to be a 2×2 rank 1 matrix. This rank 1 condition implies that any null vector is not just a bi-spinor, but actually a product of two spinors of opposite chirality. Therefore, we introduce λ^α and $\tilde{\lambda}^{\dot{\alpha}}$, which transform as $\mathbf{2}$ and $\bar{\mathbf{2}}$ representations of the $Spin(3, 1)$ Lorentz group and give the null momentum of any massless particle as:

$$p_i^{\alpha\dot{\alpha}} = \lambda_i^\alpha \tilde{\lambda}_i^{\dot{\alpha}}. \quad (1.13)$$

The above formula shows that a given null momentum can only determine the spinors up to a scaling, and this redundancy is corroborated by the counting of degrees of freedom, which should properly be 3 on both sides for a null ray in four dimensions. Explicitly, a null vector is invariant under a transformation of the form $\lambda \rightarrow t\lambda$, $\tilde{\lambda} \rightarrow t^{-1}\tilde{\lambda}$. This action is the essential *little group* of Wigner, $SO(D-2)$. The little group is the stabilizer of a given null ray, which means it acts as rotations on the transverse polarization vectors. In four dimensions, the group we will use is typically $SO(2) \sim U(1)$, though sometimes it will be convenient to extend this to $GL(1)$. If we restrict to real momenta in Minkowski signature, this redundancy can be fixed by requiring the λ and $\tilde{\lambda}$ to be complex conjugates of each other. Therefore, it is conventional to call the negative chirality λ^α the holomorphic spinor, and the $\tilde{\lambda}^{\dot{\alpha}}$ is the positive chirality anti-holomorphic spinor. These carry $h = \mp 1/2$ units of helicity under the $U(1)$ little group, respectively.

In addition to the massless momenta, the spinor variables also naturally carry information about the on-shell spin state of each external particle. An example is an unnormalized plane-wave solution of the massless four-dimensional Dirac equation for a particle of spin $(1/2, 0)$ under $SU(2) \times SU(2)$:

$$\psi^\alpha(x^\mu) \sim \lambda^\alpha \exp\left(ix_{\alpha\dot{\alpha}} \lambda^\alpha \tilde{\lambda}^{\dot{\alpha}}\right). \quad (1.14)$$

This may be generalized for particles of arbitrary spin. An on-shell particle of a given helicity is generally characterized by the number of positive and negative spinors. This includes the important example of the $h = \mp 1$ helicity self-dual and anti-self-dual gluon field strengths $F^{\alpha\beta} \sim \lambda^\alpha \lambda^\beta$ and $F^{\dot{\alpha}\dot{\beta}} \sim \tilde{\lambda}^{\dot{\alpha}} \tilde{\lambda}^{\dot{\beta}}$.

We remark that in the six-dimensional version of this construction, we may still use ordinary spinors of the larger Lorentz group, but the little group becomes non-abelian in an interesting way which will allow for surprising chiral theories. However, this also introduces new complications for constructing amplitudes which had to be overcome over the course of this thesis work.

As usual in 4D, we may raise and lower the two-dimensional spinor indices using the anti-symmetric Levi-Civita tensor. This allows us to construct the Lorentz-invariants:

$$\langle \lambda_i \lambda_j \rangle = \epsilon_{\alpha\beta} \lambda_i^\alpha \lambda_j^\beta, \quad [\tilde{\lambda}_i \tilde{\lambda}_j] = \epsilon_{\dot{\alpha}\dot{\beta}} \tilde{\lambda}_i^{\dot{\alpha}} \tilde{\lambda}_j^{\dot{\beta}}. \quad (1.15)$$

Note that these are anti-symmetric in their arguments and depend on a contraction between two different spinors. One of the great virtues of the spinor-helicity formalism is that amplitudes may typically be written in a very compact way in terms of these kinds of Lorentz invariants.

So, with the kinematics in hand, we may now seek to construct amplitudes in terms of these convenient variables. We first focus on the case of gluon amplitudes in Yang–Mills theory, which already turn out to have surprising properties. These may be generalized to supersymmetric Yang–Mills, and in particular the maximally supersymmetric $\mathcal{N} = 4$ SYM theory which has already appeared in our discussion of D-branes and AdS/CFT.

Since all the on-shell information is contained in the momenta and helicities of external particles, we can write the scattering amplitude for $i = 1, \dots, n$ particles abstractly as a function (with the convention that all momenta are incoming unless otherwise specified):

$$A_n = A(\lambda_1, \tilde{\lambda}_1, h_1, \dots, \lambda_n, \tilde{\lambda}_n, h_n) \equiv (2\pi)^4 \delta^4 \left(\sum_i \lambda_i \tilde{\lambda}_i \right) A(\lambda_i, \tilde{\lambda}_i, h_i). \quad (1.16)$$

Depending on the context, we often omit normalizing factors and powers of the coupling constant. Above, we have explicitly displayed the momentum conserving delta function, which sometimes we will also omit. In the six-dimensional models we study later, the amplitudes will have additional conserved quantities such as supersymmetries and R symmetries. These may

appear explicitly as the appropriate delta functions and are thus manifest symmetries. However, generally it is impossible to make all such symmetries manifest.

The simplest and most famous example of the utility of the spinor-helicity formalism is the case of an n -gluon amplitude with 2 negative helicity gluons and the rest positive (we take $n > 3$ as cubic amplitudes are a special case due to degenerate kinematics). As with the open string amplitudes discussed in Section 1.2, tree-level Yang–Mills amplitudes depend on a cyclic ordering and carry group theory factors $\text{Tr}(T_1 T_2 \dots T_n)$ which we will usually omit. The color-stripped amplitude should thus depend on a particular cyclic choice of the kinematics.

Amplitudes with 0 or 1 gluon of a given helicity can be shown to vanish, and those amplitudes with only 2 negative (positive) helicity gluons and $(n - 2)$ positive (negative) gluons are known as *Maximally Helicity Violating*, or MHV (anti-MHV). For the MHV amplitude, the remarkably simple result is the famous Parke–Taylor formula [44, 45]:

$$A_n^{\text{PT}}(-, -, +, \dots, +) = \delta^4 \left(\sum_i p_i \right) \frac{\langle 12 \rangle^4}{\langle 12 \rangle \langle 23 \rangle \dots \langle n1 \rangle}. \quad (1.17)$$

Here we have used a further shorthand $\langle \lambda_i \lambda_j \rangle \equiv \langle ij \rangle$. The Parke–Taylor formula was found by the difficult direct computation of Feynman diagrams, but the final form is simple and general enough that it suggests hidden properties of n -particle amplitudes which are not obvious from the Lagrangian point of view, (1.9). This amplitude has the correct homogeneity in the spinors, and also depends only on the λ , so it is holomorphic in the sense mentioned above. Finally, the anti-MHV amplitude $A_n^{\text{PT}}(+, +, -, \dots, -)$ may be obtained from (1.17) by replacing all angle brackets with square brackets. These two expressions agree for $n = 4$ upon using momentum conservation; the four-point amplitude is both MHV, anti-MHV, and in the *middle helicity sector*. We sometimes speak of MHV^k sectors to denote the amount of helicity violation.

Given the MHV formula (1.17), there is no obvious generalization to amplitudes with other helicities. However, in a landmark paper [46], Witten introduced a *twistor string theory* which generalizes the Parke–Taylor formula (and its supersymmetric extension) to arbitrary helicity sectors using world-sheet techniques similar to those in Section 1.2. These string theories are appropriate for QFT because the only propagating states are massless— i.e., there are

no α' corrections. These results serve as a major motivation for work in this thesis.⁵

Supersymmetric Yang–Mills [28] theories contain additional global fermionic symmetries which relate particles of different spin to the gluons. Equation (1.17) applies to gluons, but these can be seen as the vector component of a supersymmetric vector multiplet with extended supersymmetry. Gauge invariance of the pure gluon amplitudes greatly restricts their form, and the supersymmetric completion of these amplitudes leads to a nearly unique expression in the case of $\mathcal{N} = 4$ supersymmetry, the maximal supermultiplet in four dimensions with spins ≤ 1 . We assume the reader is familiar with supersymmetry in 4D, and later basic properties of 6D supersymmetry. An introduction to these topics can be found in most standard texts, such as [48].

In light of the above discussion, an $\mathcal{N} = 4$ supersymmetric extension of the Parke–Taylor Formula turns out to be [49]:

$$A_n^{\mathcal{N}=4}(\lambda_i, \tilde{\lambda}_i, \eta_i^I) = \delta^4\left(\sum_i p_i\right) \frac{\delta^8(\sum_i \lambda_i^\alpha \eta_i^I)}{\langle 12 \rangle \langle 23 \rangle \cdots \langle n1 \rangle}. \quad (1.18)$$

Here we introduced Grassmann numbers η_i^I for each particle to organize the $\mathcal{N} = 4$ on-shell states. The index $I = 1, \dots, 4$ denotes the fundamental representation of the global $SU(4)$ R symmetry of the theory. The combination $Q_i^{\alpha I} = \lambda_i^\alpha \eta_i^I$ is the on shell supercharge carried by each particle, and the fermionic delta function implies the conservation

$$A_n^{\mathcal{N}=4} \sim \delta^8\left(\sum_i Q_i\right) \rightarrow \left(\sum_i Q_i\right) A_n^{\mathcal{N}=4} = 0. \quad (1.19)$$

Like the momentum conserving delta functions, their fermionic counterparts imply the conservation of 8 the total 16 super-Poincaré symmetries. (This theory also has conformal and superconformal symmetries; we provide more details of the superspace formalism in Chapter 2). Here it suffices to say that various component amplitudes involving specific choices of external particles may be obtained from Eq. (1.18) by performing a chosen number of Grassmann integrations over each η_i^I . In this superspace formalism, to recover the Parke–Taylor formula we may select two particles in the bottom component of the multiplet and the rest from the top component; these turn out to be the on-shell photon helicity states A_+ and A_- .

⁵A review of twistor strings and perturbative Yang–Mills may be found in [47].

The twistor string theory generalizes Eq. (1.18) to arbitrary MHV^k helicity sectors. This drew on the inspiration that the supersymmetric Parke–Taylor formula can be written as the correlation function of a certain two-dimensional current algebra [49] on the Riemann sphere, and the situation becomes surprisingly similar to the holomorphic closed string amplitudes discussed in Section 1.2. We see that scattering in four dimensions can be understood in terms of the geometry of the complex projective line with $SL(2, \mathbb{C})$ symmetry.

An intermediate step which we briefly explain is the observation that the MHV amplitudes may also be written as an integral over the *moduli space of degree-1 curves in twistor space*. Twistor space was introduced by Penrose [42, 46, 50], which is essentially the three complex dimensional projective space \mathbb{CP}^3 . This space is useful for describing conformally invariant particle wavefunctions because the 4D conformal group, $SO(4, 2) \sim SU(2, 2)$ acts linearly on this space. The complex coordinates are four component spinors:

$$Z^A = (\lambda^\alpha, \mu_{\dot{\alpha}}). \quad (1.20)$$

As explained below, the $\mu_{\dot{\alpha}}$ are related to the $\tilde{\lambda}^{\dot{\alpha}}$ by Fourier transform in split signature (other signatures are possible). In the complex case, the action of the $U(1)$ little group is $Z \sim tZ$ for $t \in \mathbb{C}^*$, so we see that the kinematic information is equivalent to points in \mathbb{CP}^3 . Z^A itself transforms as a **4** under the complexified conformal group $SL(4, \mathbb{C})$. We remark here that this structure is echoed in six spacetime dimensions, since the Euclidean 4D conformal group $SO(5, 1) \sim SU^*(4)$ is equivalent to the Lorentzian 6D Poincaré group.

The abstract idea here is that 4D conformal wavefunctions of external gluons are best represented as points in twistor space representing their null trajectories and helicities in spacetime. Given these external kinematics, the MHV scattering amplitudes are localized integrals of the current algebra correlator over curves in twistor space. The ultimate result of this procedure is still the Parke–Taylor amplitude, but the interpretation in terms of curves will allow a generalization. We will start by rewriting Eq. (1.17) in the schematic form,

$$A(\lambda_i, \tilde{\lambda}_i, h_i) = \delta^4 \left(\sum_i \lambda_i \tilde{\lambda}_i \right) f(\lambda_i), \quad (1.21)$$

We may rewrite the momentum conserving delta functions as a position space integral over the variable $x_{\alpha\dot{\alpha}}$ which we will identify with the moduli of the

curve in twistor space. The transformation to twistor space is simplest to describe in $++--$ signature with real $\tilde{\lambda}$, because it then becomes an ordinary Fourier transform,

$$\tilde{\lambda}_{\dot{\alpha}} \rightarrow i \frac{\partial}{\partial \mu^{\dot{\alpha}}}, \quad (1.22)$$

$$\frac{\partial}{\partial \tilde{\lambda}^{\dot{\alpha}}} \rightarrow i \mu_{\dot{\alpha}}. \quad (1.23)$$

This series of transformations is straightforward to implement for the MHV amplitudes due to the holomorphic dependence on λ only. The result is

$$A(\lambda_i, \mu_i) = \int d^4 x_{\alpha\dot{\alpha}} \prod_{j=1}^n \delta^2(\mu_{j\dot{\alpha}} + x_{\alpha\dot{\alpha}} \lambda_j^\alpha) f(\lambda_i). \quad (1.24)$$

This implies that the amplitude may be written as a localized integral supported on the solutions to the delta functions,

$$\mu_{i\dot{\alpha}} + x_{\alpha\dot{\alpha}} \lambda_i^\alpha = 0, \quad (1.25)$$

The linear form of these implies that this is a degree 1 curve, and by solving for $\mu_{\dot{\alpha}}$ in terms of λ^α we may see this curve is a copy of \mathbb{CP}^1 with (λ^1, λ^2) as the homogeneous coordinate. For each choice of $x_{\alpha\dot{\alpha}}$, we get a map from this Riemann sphere to the twistor space \mathbb{CP}^3 with the projective coordinate $Z^A = (\lambda^\alpha, \mu_{\dot{\alpha}})$, and all such degree one genus-zero curves in \mathbb{CP}^3 are of this type. The amplitude evidently vanishes unless all points lie on this degree one genus-zero curve, which contains in it the statement of momentum conservation back in ordinary space. Later, we will discuss different versions of these constraints which imply and reformulate the on-shell information in different ways.

A critical observation of [46], is that the $\mathcal{N} = 4$ extension of the above analysis involves the Calabi-Yau supermanifold $\mathbb{CP}^{3|4}$, which has both bosonic and fermionic coordinates. The fermi coordinates with the $SU(4)$ R symmetry action now describe which on-shell state to scatter, and this leads us to conclude that the on-shell field theory states are described by points

$$(Z^A, \eta^I), \quad \text{with} \quad (Z^A, \eta^I) \sim (tZ^A, t\eta^I), \quad t \in \mathbb{C}^*, \quad (1.26)$$

This has the scale-invariant Calabi-Yau measure

$$\Omega = \frac{1}{4!^2} \epsilon_{ABCD} \epsilon_{IJKL} Z^A dZ^B dZ^C dZ^D d\eta^I d\eta^J d\eta^K d\eta^L. \quad (1.27)$$

Being a Calabi-Yau manifold (of a somewhat unusual type due to the fermi coordinates), $\mathbb{CP}^{3|4}$, is an anomaly free target space of the Topological B-model, which is a topologically twisted $\mathcal{N} = 2$ two-dimensional world-sheet theory. Topological string theory is a vast and fascinating subject which is outside the scope of this thesis. An interested reader is encouraged to read some of the original papers [51, 52] as well as reviews [53, 54].

For our purposes, we describe a few important conclusions. For definiteness, Witten considers the B-model with open string boundary conditions and $U(N)$ gauge group on the $\mathbb{CP}^{3|4}$ target space. The boundary conditions correspond to filling the target with N space filling branes (topological string versions of the ones discussed previously). These topological branes enforce the holomorphic B-model boundary conditions and must wrap holomorphic curves in the target space. The physical states of the open B-model with super-twistor target turn out to be exactly the 1-particle on-shell superfields of $\mathcal{N} = 4$ super Yang–Mills. The degree one genus-zero holomorphic curves which support the MHV amplitudes are interpreted as D1-branes wrapping holomorphic curves in the twistor space. These real co-dimension four curves (sometimes called D-instantons or instanton strings) may be generalized to higher degree and genus so long as the embedding is holomorphic. The conjecture is that the tree-level perturbative expansion of $\mathcal{N} = 4$ SYM is computed by the D-instanton expansion of the B-model, with the MHV^k sectors appearing as different degrees of D-instanton.

There is much more that can be said about this B-model construction, but in the interest of producing explicit formulas for a more general class of theories and amplitudes, we focus on the work of Roiban, Spradlin, and Volovich (RSV) who studied concrete versions of the twistor string formula and provided a useful alternative formulation.

In the Witten–RSV formula, the moduli space to be integrated over contains components characterized by the degree of the maps and by the number of disconnected curves in the target space. (RSV) conjectured and gave evidence that by integrating over only maps to *connected* curves the complete tree-level S-matrix could be recovered [55]. The Witten–RSV formula then expresses n -particle amplitudes as integrals over the moduli space of maps from n -punctured spheres into connected curves in twistor space. The formula can then be translated into momentum space. Unlike string amplitudes such

as Eq. (1.4), the Witten–RSV formula is not a true integral as it is totally localized on rational curves. The result of such an integral will always be a rational function of the kinematics, which is expected for consistent tree amplitudes due to unitarity arguments involving complex kinematics.

As a final comment, we will present a version of the Witten-RSV formula which is somewhat different than the original paper. This form was first found in [56] and is equivalent to what was discussed above, but is more convenient for 6D kinematics. Instead of using twistors directly, the key ingredients of the formula are rational maps from \mathbb{CP}^1 into the null cone in spinor coordinates:

$$z \rightarrow \lambda_\alpha(z)\tilde{\lambda}_{\dot{\alpha}}(z), \quad (1.28)$$

with $\lambda_\alpha(z)$ and $\tilde{\lambda}_{\dot{\alpha}}(z)$ polynomials of degree d and \tilde{d} , respectively, such that $d + \tilde{d} = n - 2$. These have the explicit parametrization,

$$\lambda^\alpha(z) = \sum_{k=0}^d \rho_k^\alpha z^k, \quad \tilde{\lambda}^{\dot{\alpha}}(z) = \sum_{k=0}^{\tilde{d}} \tilde{\rho}_k^{\dot{\alpha}} z^k. \quad (1.29)$$

In addition to the moduli of the curve, we must also integrate over the positions of the punctures σ_i . The combined integral of bosonic moduli is totally localized, and we will soon introduce the equations satisfied by the punctures. We also introduce the notation $\sigma_{ij} \equiv \sigma_i - \sigma_j$ which will be convenient; products of these factors often appear in denominators similar to fermion correlators in 2D CFT.

To incorporate supersymmetry into the formula, we may integrate over fermionic maps $\chi^I(z)$, $\tilde{\chi}^I(z)$ which impose target space supersymmetry. These fermionic integrals are Grassmann integrals, and their constraints are fermionic delta functions similar to the one in Eq. (1.18). These delta functions constitute part of the integrand discussed in Eq. (1.5).

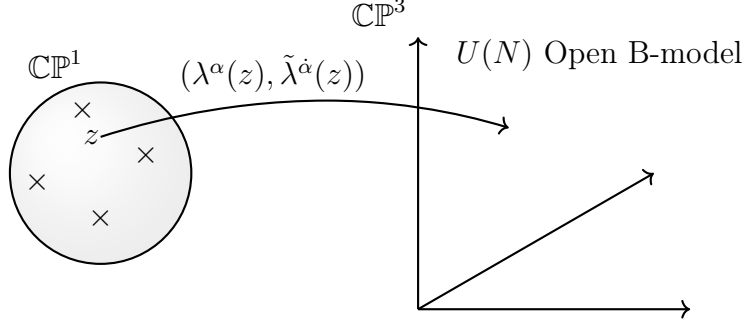


Figure 1.1: A rough figure of the twistor string for four dimensions. An abstract internal space representing a D1 brane with coordinate $z \in \mathbb{CP}^1$ wraps a holomorphic curve in \mathbb{CP}^3 . The holomorphic maps are schematically of the form $\lambda^\alpha(z) = \sum_{k=0}^d \rho_k^\alpha z^k$ and $\tilde{\lambda}^{\dot{\alpha}}(z) = \sum_{k=0}^{\tilde{d}} \tilde{\rho}_k^{\dot{\alpha}} z^k$. Punctures correspond to insertions of on-shell fields in the form of $U(N)$ open B-strings, and for n particles the degree of the maps and amount of helicity violation are given by $d + \tilde{d} = n - 2$ and $d - \tilde{d} = \Delta h$, respectively. The amplitude is obtained by integrating the correlator of these punctures over the moduli of positions z_i and maps $\rho, \tilde{\rho}$ into the target. This integral is totally localized and is equivalent to an expression obtained in field theory using Feynman diagrams. A very similar picture holds true for the six-dimensional versions of the twistor string discussed in this work, and the kinematics of 6D scattering amount to a correct choice of target space and parametrization of the curves.

The amplitude is at first sight somewhat formidable. For completeness, we display the formula here, but it is our task of Chapters 2 and 3 is to explain it in much greater detail. For an amplitude involving n particles in the r th helicity sector, with $d = r - 1$, the amplitude is:

$$\boxed{A_{n,d}^{\mathcal{N}=4 \text{ SYM}}(\alpha) = \int d\mu_{n,d}^{4\text{D}} \text{PT}(\alpha) \int d\Omega_{F,d}^{(4)}} \quad (1.30)$$

with the measure,

$$\int d\mu_{n,d}^{4\text{D}} = \int \frac{\prod_{i=1}^n d\sigma_i \prod_{k=0}^d d^2 \rho_k \prod_{k=0}^{n-d-2} d^2 \tilde{\rho}_k}{\text{vol SL}(2, \mathbb{C}) \times \text{GL}(1, \mathbb{C})} \prod_{i=1}^n \delta^4 \left(p_i^{\alpha\dot{\alpha}} - \frac{\lambda^\alpha(\sigma_i) \tilde{\lambda}^{\dot{\alpha}}(\sigma_i)}{\prod_{j \neq i} \sigma_{ij}} \right). \quad (1.31)$$

The fermionic integrand $d\Omega_{F,d}^{(4)}$ is given by

$$\left(\prod_{k=0}^{d,\tilde{d}} d^2 \chi_k d^2 \tilde{\chi}_k \right) \prod_{i=1}^n \delta^4 \left(q_i^{\alpha I} - \frac{\rho^\alpha(\sigma_i) \chi^I(\sigma_i)}{\prod_{j \neq i} \sigma_{ij}} \right) \delta^4 \left(\tilde{q}_i^{\dot{\alpha} I} - \frac{\tilde{\rho}^{\dot{\alpha}}(\sigma_i) \tilde{\chi}^I(\sigma_i)}{\prod_{j \neq i} \sigma_{ij}} \right) \quad (1.32)$$

while the *Parke–Taylor factor* depends on the choice of cyclic ordering and is given by

$$\text{PT}(12 \cdots n) = \frac{1}{\sigma_{12}\sigma_{23} \cdots \sigma_{n1}}. \quad (1.33)$$

It is possible to analytically show that this is equivalent to the Witten–RSV formula and the curves in twistor space. However, practical evaluation of higher-point amplitudes outside of the MHV sector is essentially not possible by hand. However, this formula has all the correct symmetry properties, can be checked numerically to high point amplitudes, and in principle gives a complete solution to the classical scattering problem.

Motivated by the success of twistor string constructions in 4D, Cachazo, He, and Yuan (CHY) looked for alternative formulations, leading to what is now known as the *scattering equations* and the CHY formulation [57, 58, 59]. This formulation opened up world-sheet-like constructions for a large variety of theories in any number of dimensions at the expense of giving up on fermions and hence supersymmetry. The search for a CFT that reproduced the CHY formulas led to the discovery of ambitwistor strings [60, 61, 62] whose development allowed computations beyond tree-level [63, 64, 65, 66, 67] (for a recent review see [68]).

In the simplest setting for the CHY formalism, the rational maps $\lambda(z)$, $\tilde{\lambda}(z)$ are integrated out, leaving only the $d^n\sigma$ moduli integral. Since the spinor-helicity variables are also tied to supersymmetry, the CHY formalism also requires a specific choice of component amplitudes and the corresponding integrands. The result are formulas which are applicable for tree level amplitudes in any dimension.

As with the Witten–RSV formula, the moduli integral over the punctures σ_i on \mathbb{CP}^1 is not a true integral; after gauge fixing, the number of integrations is equal to the number of constraints. Therefore, it is a totally localized integral, and CHY found the key equations which the punctures must solve, the scattering equations:

$$E_i = \sum_{j \neq i} \frac{s_{ij}}{\sigma_{ij}} = 0, \quad (1.34)$$

where s_{ij} are the Mandelstam invariants. Due to the fractional linear symmetry, only $n - 3$ of these equations are linearly independent. It can also be shown that there are $(n - 3)!$ solutions. Virtually all amplitudes considered

in this thesis are localized on the support of the scattering equations in some way.

The general CHY formula is the prototypical example of Eq. (1.5) and can be written as [58]:

$$\mathcal{A}_n^{\text{theory}} = \int \delta^D(\sum_{i=1}^n p_i^\mu) \left(\prod_{i=1}^n \delta(p_i^2) \right) \frac{\prod_{i=1}^n d\sigma_i}{\text{vol SL}(2, \mathbb{C})} \prod_i' \delta(E_i) \mathcal{I}^{\text{theory}}. \quad (1.35)$$

where the primed delta function indicates that we must fix three scattering equations, giving a Jacobian. Also, $\mathcal{I}^{\text{theory}}$ is the theory-dependent integrand (which may contain information such as polarization vectors or color factors). Many integrands are possible, but they must have weight -2 under an $\text{SL}(2, \mathbb{C})$ transformation for each puncture for the integral to be well defined. It is sometimes convenient, but not required, to write the integrand as a product of ‘left’ and ‘right’ factors for use with the KLT copy construction. By now a large catalog of such CHY integrands is known, and we will introduce them throughout this thesis. The simplest integrand which has already appeared in the twistor string amplitudes is the Parke–Taylor factor, and the simplest CHY amplitude is a product of two such factors. This describes the tree-level scattering of a scalar ϕ^3 theory in which the scalar transforms in the *bi-adjoint* representation of two gauge groups. The bi-adjoint scalar amplitude is given by 1.35 with $\mathcal{I}^{\text{theory}}$ being the product of two Parke–Taylor factors.

We go into many more details of the CHY formalism in Chapter 3 where it is useful to define notation and generalize the 4D Witten–RSV formula.

1.4 Holography, AdS/CFT, and p -Adic Algebraic Curves

This section of the introduction discusses the second major line of research in this thesis, which involves *holographic dualities*. While we will use somewhat similar mathematical tools to those employed for amplitudes in 6D, Chapters 2, 3, and 4 are logically distinct from Chapters 5 and 6. In these latter chapters, we will introduce lattice models which utilize number theoretic, algebro-geometric, and information theoretic ideas from mathematics in order to study dual pairs of theories. Once again, one-dimensional projective geometry plays a critical role, as we will soon explain.

AdS/CFT is a concrete realization of holography in quantum gravity first proposed by Maldacena in the landmark paper [12], and the construction there

involved N coincident D3-branes in flat space Type IIB string theory. The low-energy effective theory of open strings on these branes is the 4D $U(N)$ $\mathcal{N} = 4$ SYM theory, which we have so far discussed in the context of scattering amplitudes. However, in Type IIB string theory, these branes act as sources for the closed string fields such as the graviton. In the large N near horizon limit, the gravitational backreaction curves the flat 10D geometry to $\text{AdS}_5 \times S^5$, an effect that is clear from classical general relativity but not obvious in perturbation theory. By adjusting the parameters, it is possible to continuously interpolate between a description in which the field theory is valid and a description in which the supergravity background is valid. This leads to the now well-established conjecture that $\mathcal{N} = 4$ SYM at large N and strong coupling is equivalent to supergravity on $\text{AdS}_5 \times S^5$ with stringy corrections being subleading. Soon after, [69, 70] performed a semi-classical analysis of AdS bulk perturbation theory which is found to be equivalent to correlation functions in boundary strongly coupled gauge theory.

A surprising feature about this duality is that it is holographic—the gravity theory in the interior of AdS is equivalent to a field theory at the boundary, essentially living in one lower dimension, aka $\text{AdS}_5/\text{CFT}_4$. This has led many to conclude that AdS/CFT allows gravitational dynamics and perhaps even spacetime itself to ‘emerge’ from an underlying quantum theory.

By now there are a vast number of generalizations and extensions of this correspondence, and it has passed many checks. A review of the literature is far outside the scope of this thesis, but we comment that many quantities can be matched on both sides of the duality, and this has led to new insights into topics such as black hole thermodynamics, non-perturbative effects, stringy and $1/N$ corrections, and even applications in condensed matter physics and pure mathematics. Many examples of holographically dual theories have also been found (see [71] for a review of these developments). For instance, the mysterious 6D $(2, 0)$ large N M5-brane theory is believed to be dual to M-Theory on $\text{AdS}_7 \times S^4$, and this was one motivation for studying the amplitudes of a single M5-brane in this thesis. A much more tractable example is the case of $\text{AdS}_3/\text{CFT}_2$. This is because there are no propagating gravitons in three dimensions, and additionally there are many tools to do exact computations in 2D CFT (we have already discussed correlation functions in the context of string amplitudes, which use identical machinery).

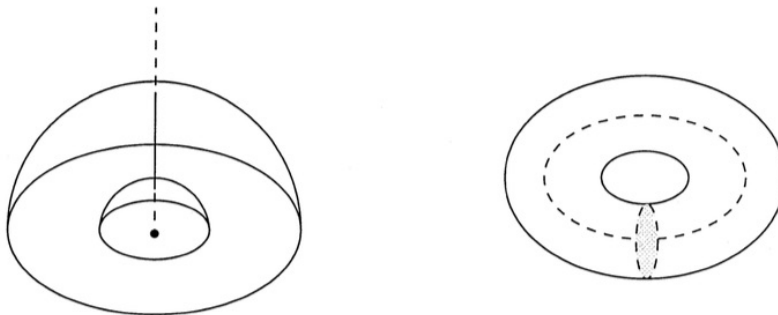


Figure 1.2: Euclidean AdS_3 and a Euclidean BTZ black hole obtained as a quotient. The interior metric has constant negative curvature and the boundary is a torus.

In $\text{AdS}_3/\text{CFT}_2$, one often realizes the boundary conformal field theory as living on the genus zero Riemann surface $\mathbb{P}^1(\mathbb{C})$ with the hyperbolic bulk AdS space as a coset space. Higher-genus bulk and boundary spaces can be seen as generalizations of the (Euclidean) BTZ black hole [72]. The original BTZ black hole [73] corresponds to the genus one case, see Figure 1.2. As curves and cosets, the construction of these spaces is entirely algebraic, and one may find other spaces by *changing the underlying field*.⁶ For instance, one might use \mathbb{R} , a finite field \mathbb{F}_p , or the p -adics \mathbb{Q}_p , where p is any prime. Since some of these ingredients may be unfamiliar, a review is found at the beginning of Chapter 5.

In [74] it was suggested that certain p -adic algebraic curves coming from the replacement $\mathbb{C} \rightarrow \mathbb{Q}_p$ such as $\mathbb{P}^1(\mathbb{Q}_p)$ and the higher genus Mumford curves of [75], are suitable boundary spaces for holography where the analog of a 2D CFT might live. Since some of the objects that exist on the p -adic side have a discrete, combinatorial nature, one can take advantage of this structure to carry out computations in a more convenient discretized setting. An attractive feature of this proposal is that the bulk space is still a coset, but now becomes the Bruhat–Tits tree [76] (an infinite tree of uniform valence) at genus zero. This opens up the possibility of studying certain features of AdS/CFT by passing to a p -adic setting where the bulk and boundary geometry are relatively simple.

There has been a considerable amount of work over the years concerned with

⁶Here we mean “field” in the sense of mathematics, an unfortunate collision of nomenclature with the physical notion of a field.

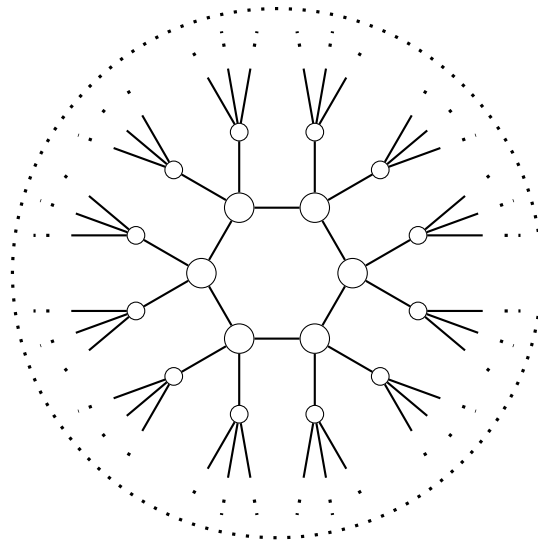


Figure 1.3: A p -adic BTZ black hole obtained by a quotient of an infinite tree. This parallels the construction in 3D topological gravity, but now the bulk is discrete. The boundary is a genus-one curve over \mathbb{Q}_p . Certain simple features of AdS/CFT still hold for this kind of geometry. (There exists a black hole like this for every prime p — as pictured, $p = 3$).

developing various aspects of physics in a p -adic setting, see for instance the reviews [77, 78, 79, 80]. In particular, the Bruhat–Tits tree of \mathbb{Q}_p (the p -adic numbers) and its boundary $\mathbb{P}^1(\mathbb{Q}_p)$ were used in the setting of p -adic string theory [18, 19, 81, 82, 83]. A major result of this thesis was the introduction of these p -adic techniques to AdS/CFT in an explicit way, expanding the early proposals to a more modern understanding of holography. Appropriate boundary and bulk field theories for p -adic holography were developed independently in [84, 4], where certain essential features such as the holographic computation of correlation functions in p -adic conformal field theories were established. Chapter 5 of this thesis explains this correspondence in detail, following the original paper.

Beyond the discussion included in this thesis, many additional lines of inquiry were found which parallel the situation in real AdS/CFT, but the discrete p -adic geometry often makes these models much more solvable. These models have been explored further in a series of subsequent papers, such as [7, 85, 86, 87, 6, 88, 89, 90, 91]. Much of this work has focused on exploring analogies between p -adic models and ordinary AdS/CFT, and searching for structures familiar from the traditional holographic correspondence in the discretized or p -adic world.

Beyond holographic correlators, one may look for structures associated to the bulk geometry directly. One of the current main challenges of ordinary AdS/CFT and holography is to explain how exactly this bulk space can *emerge* from the conformal field theory. Arguments from black hole entropy and the Ryu–Takayanagi (RT) formula [92, 93] and its quantum and covariant generalizations [94, 95, 96] suggest that the emergence of semi-classical bulk spacetime is related to quantum statistical mechanics of the boundary theory. In particular it is the CFT entanglement entropy which appears to compute the areas of minimal surfaces and horizons in AdS. These entropic quantities are difficult to compute on the boundary, and difficult to make microscopic sense of in the bulk. One can also ask about other basic properties of the boundary entropy, such as the strong subadditivity property [97] or other entropy inequalities.

The critical role played by quantum information suggests that any holographic model which captures features of AdS/CFT should at least have the right pattern of entanglement. The simplest many-body systems in which non-trivial entanglement can be studied are finite-dimensional systems of quantum mechanical bits, or qubits. Toy models of these qubits and quantum circuits built from self-similar tensors or gates are a natural setting to study long range entanglement. The density matrix in these systems is well defined and may often be computed exactly. There are by now many tensor network models which may capture some of the entanglement features of empty AdS spacetime. Part of the motivation for seeking these models comes from the proposal made in [98], which pointed out that bulk reconstruction and bulk locality in the AdS/CFT correspondence bear strong similarities to the properties of quantum error-correcting codes and tensor networks. This intuition was used in [99] to construct a family of “holographic” quantum codes, associated to hyperbolic tilings. In these codes, bulk qubits are thought of as the logical inputs, the boundary qubits at the periphery of the tiling constitute the encoded state, and the error-correcting properties of the code mimic features of holography such as the Ryu–Takayanagi formula.

In Chapter 6, we propose a new kind of tensor network where the elementary tensors come from algebro-geometric quantum codes based on the geometry of projective lines over finite fields. These basic building blocks are glued together according to rules set by the Bruhat–Tits tree and significantly generalize the toy model of [99] to a p -adic version which can compute a large class of

entanglement quantities analytically. We find p -adic or ultrametric versions of the Ryu–Takayanagi formula, the BTZ black hole entropy, multi-interval entropy inequalities, and several additional quantities previous networks have failed to compute. In the limit of an infinite network, these quantities can be shown to exactly match what is expected of p -adic field theory, and there is a natural geometric interpretation in the bulk of the network.

AMPLITUDES ON THE WORLD VOLUME OF M5 AND D-BRANES

2.1 Introduction

This chapter proposes explicit formulas for on-shell n -particle scattering amplitudes in the tree approximation for three massless field theories, each of which is a maximally supersymmetric matter theory with 16 unbroken supersymmetries and 16 additional spontaneously broken supersymmetries. The fermions in these theories are Goldstone particles (or Goldstinos) of the type first considered by Volkov and Akulov [100] [101]. These three theories arise naturally in string theory as the world-volume theories of branes, as we have described in Sec. (1.2). The first theory is the world-volume theory of a probe D3-brane (of type IIB superstring theory) in a 10D Minkowski-space background. The second theory is the world-volume theory of a probe D5-brane (of type IIB superstring theory) in a 10D Minkowski-space background. The third theory is the world-volume theory of a probe M5-brane (of M theory) in an 11D Minkowski-space background. We will refer to these theories as the D3 theory, the D5 theory, and the M5 theory. These three theories are closely related. Specifically, both of the 6D theories (D5 and M5) can be truncated (by a procedure called dimensional reduction) to give rise to the 4D theory (D3). These relationships, which are predicted by string theory, will provide powerful checks of the results, as well as a role in their derivation. Another important feature that all three of these theories have in common is that non-vanishing on-shell scattering amplitudes require an even number of particles, *i.e.*, n must be even. The generalization of these formulas to odd n for theories such as super Yang-Mills and Supergravity turns out to be considerably more challenging, and this is the subject of Chapter 3.

The D3 theory is a 4D Dirac–Born–Infeld (DBI) theory, with $\mathcal{N} = 4$ supersymmetry, which some authors call sDBI theory. It is a self-interacting theory of a massless abelian $\mathcal{N} = 4$ vector supermultiplet, which consists of a vector, four spinors, and six scalars. Its R-symmetry group is $SU(4) \times U(1)$. Although the helicity-conservation property of scattering amplitudes of the D3 theory

has also been understood previously [102] using the electric magnetic duality of D3-brane action [103], the additional $U(1)$ enlargement in the R-symmetry group at tree level has not been noted previously.¹ The action for the D3 theory was derived in [31] by dimensional reduction of the action for the D9-brane, which was constructed using string-theoretic techniques. (See [32][33][34][35] for related work.) The D3 theory has been examined in some detail recently in [104]. There has been a recent proposal for the tree amplitudes of this theory in [105][106]. Our formulas will take a different form based on techniques described in Sec. (1.3) of the Introduction.

The action for the D5 theory also can be obtained by dimensional reduction of the D9-brane action. This theory is a self-interacting theory of a single vector supermultiplet with $(1, 1)$ supersymmetry in 6D. The vector supermultiplet consists of a vector, four spinors, and four scalars. The R-symmetry group of the D5 theory is $SU(2) \times SU(2)$.

The M5 theory is a self-interacting theory of a single tensor supermultiplet with $(2, 0)$ supersymmetry in 6D. This multiplet contains a two-form field B with a self-dual field strength ($H = dB = \star H$) as well as four spinors and five scalars. There is an analog of the Born–Infeld action that describes self interactions of the B field, which was constructed in [107]. This theory has 6D Lorentz invariance, though the action only has manifest 5D Lorentz invariance. The five additional Lorentz transformations that involve a particular (arbitrarily chosen) direction are not obvious symmetries. These transformations of the Lagrangian give a total derivative. Dimensional reduction of this theory to five dimensions gives pure Born–Infeld theory. The action for the supersymmetric extension of the 6D theory that incorporates the complete $(2, 0)$ supermultiplet, *i.e.*, the M5 theory, was constructed in [108]. (See [109][110][111][112] for related work.) The R-symmetry group of this theory is $USp(4)$. Certain lower-point amplitudes for the M5 theory have been discussed previously, for example, in [113][114][115][116][117]. The requirement that they give D3 amplitudes after dimensional reduction to 4D will play an important role in our analysis.

Another feature that these three theories have in common is that they inherit their symmetries from those of the parent theories, *i.e.*, M-theory in flat space

¹We will explain later why the D3 theory has a larger R-symmetry group than $\mathcal{N} = 4$ super Yang–Mills theory. Of course, there are many other differences. For example, the D3 theory is not conformal.

and Type IIB superstring theory in flat space. By positioning the probe branes in the ambient space, some of the symmetries of the parent theory are spontaneously broken. Broken symmetries include translations perpendicular to the branes and half of the supersymmetries. These symmetries are realized nonlinearly in the brane theories. Thus, the scalars and spinors in these theories are Goldstone particles. As a result, the amplitudes of these theories satisfy various soft theorems. The vector and tensor gauge symmetries are inherited from the background NS-NS 2-form of Type IIB and the M-theory 3-form, respectively [118].

One of the challenges in formulating on-shell scattering amplitudes for these theories is to make their various required symmetries manifest. As has become conventional for massless particles, we use twistor-like spinor-helicity coordinates to represent momenta and supercharges. These introduce a little-group symmetry for each of the scattered particles. As we will explain, this group is $SU(2) \times SU(2)$ for the D5 theory, $SU(2)$ for the M5 theory, and $U(1)$ for the D3 theory. The use of spinor-helicity variables allows us to construct on-shell amplitudes with manifest Lorentz invariance even for chiral theories, such as the M5 theory, which has well-known obstructions to constructing a useful Lorentz-invariant action. In addition to super-Poincaré symmetry, each of these theories has an R-symmetry group: $SU(2) \times SU(2)$ for the D5 theory, $USp(4)$ for the M5 theory, and $SU(4) \times U(1)$ for the D3 theory.

Our formulas for scattering amplitudes in each of the three theories take forms that are similar to the twistor-string formulation of 4D $\mathcal{N} = 4$ super Yang–Mills amplitudes (SYM) in Witten’s classic twistor-string paper [46]. This formula and related discussions were reviewed in Sec. 1.3, and we continue the discussion here. The twistor-string formulation of 4D $\mathcal{N} = 4$ SYM is given by the Witten-RSV formula, which was studied in detail in [119, 120, 55]. In particular, we associate a coordinate σ_i on the Riemann sphere to the i th particle in an n -particle scattering amplitude. The formula for the amplitude is required to be invariant under a simultaneous $SL(2, \mathbb{C})$ transformation of these coordinates. Following Cachazo et al. [56], in the twistor-string-like formalism that we use, certain rational functions of σ_i are associated to the i th particle. These functions are restricted by delta-function constraints in such a way that the number of bosonic delta functions is equal to the number of bosonic integrations. Thus, the formulas are actually algebraic, as they should

be for tree amplitudes. Furthermore, the delta-function constraints imply the scattering equations [57], which are $\sum_j p_i \cdot p_j / \sigma_{ij} = 0$, where $\sigma_{ij} = \sigma_i - \sigma_j$. We have already discussed the scattering equations in Sec. 1.3, and they will appear throughout this work. This approach allows us to formulate all of the amplitudes for the three theories in a uniform way. It also is convenient for verifying some of their essential properties.

Our main results are general formulas for the n -particle on-shell tree amplitudes for each of the three theories. These formulas make most of the required symmetries manifest, or at least easy to understand. The exception is the R symmetry, where only a subgroup is manifest. The supermultiplets are incorporated by associating four Grassmann coordinates, with specified transformation properties, to each external particle. The key to making the full R-symmetry group manifest is to carry out a Fourier transformation for half of the Grassmann coordinates – two per particle. The price that one pays for making R symmetry manifest is that the formulas become somewhat more complicated for the 6D theories.

This chapter is organized as follows: We begin in Section 2.2 with a discussion of general properties, such as symmetries, conserved charges, and on-shell states, for each of the three theories considered in this chapter. We utilize the 4D spinor-helicity formalism for the D3 theory and the 6D one for the M5 theory and the D5 theory. To illustrate the structures and ideas, Section 2.3 examines the four-particle amplitudes for these theories. Section 2.4 presents a general formula for the n -particle amplitudes of the D3 theory. As mentioned previously, our formulas for scattering amplitudes in each of the three theories take forms that are similar to the twistor-string formulation of 4D $\mathcal{N} = 4$ super Yang–Mills amplitudes [46]. This formulation of the D3 theory is somewhat different from those in the literature. It is more suitable for the generalization to 6D, which is required for the M5 and D5 theories.

In Section 2.5 we propose a new formula, given in Eq. (2.100), which gives all of the tree amplitudes of the M5 theory and generalizes the D3 formula in a way that is consistent with dimensional reduction of $\mathcal{N} = (2, 0)$ in 6D to $\mathcal{N} = 4$ in 4D. This is our most novel result, providing a mathematical formula for the complete tree-level S-matrix for a theory whose Lagrangian description has well-known issues mentioned earlier. This section also describes various checks of the formula, including symmetries, soft theorems, and factorization.

Using knowledge of the lower-point amplitudes and factorization, we obtain compact analytic expressions for certain amplitudes of the self-dual B fields for $n = 6$ and $n = 8$. These agree perfectly with the general integral formula and give explicit consistency checks. Despite the apparent differences between the M5 and D5 theories, in Section 2.6 we present a similar integral formula for the D5-brane amplitudes, which reproduces what one obtains from the D5-brane action. Finally, our conclusions and remarks concerning future directions are presented in Section 2.7. Further technical details and an analysis of the R symmetries are presented in Appendix A.1.

2.2 Symmetries, Conserved Charges, and Supermultiplets

The three theories that we are considering have three types of conserved charges, which form a nice superalgebra in each case. These charges, are the momenta p_i , supersymmetry charges q_i , and R-symmetry charges R_i , where the index $i = 1, 2, \dots, n$ labels the n particles participating in an n -particle on-shell scattering amplitude A_n . By treating all of the particles symmetrically as ingoing, conservation of these charges is simply the statement that

$$\sum_{i=1}^n p_i = 0, \quad \sum_{i=1}^n q_i = 0, \quad \sum_{i=1}^n R_i = 0. \quad (2.1)$$

In practice, some of these conservation laws are implemented by including appropriate delta functions in the formula for A_n . The other charges are represented by differential operators and their conservation is achieved by requiring that A_n is annihilated by the appropriate sums of these differential operators. Lorentz invariance will be manifest in all formulas.

M5 theory

The world-volume theory of a probe M5 in an 11D Minkowski space background has $(2, 0)$ 6D supersymmetry. This theory describes a single massless self-interacting tensor supermultiplet. This supermultiplet contains a two-form field $B_{\mu\nu}$, with a three-form field strength $H = dB$, which is self-dual in the free-theory limit. Such a field gives rise to three on-shell degrees of freedom. The tensor supermultiplet also contains four fermions and five scalars. Altogether, there are eight bosonic and eight fermionic on-shell degrees of freedom. The three multiplicities $(1, 4, 5)$ correspond to representations of the $USp(4) = Spin(5)$ R-symmetry group, which is an unbroken global symmetry of the M5 theory. This symmetry can be thought of as arising from rota-

tions in the five spatial dimensions that are orthogonal to a flat M5 in 11D Minkowski spacetime. The little group for massless particles in d dimensions is $Spin(d-2)$. Thus, in 6D it is $SU(2) \times SU(2)$. However, in the special case of the tensor multiplet all of the on-shell particles are singlets of one of the two $SU(2)$ factors. Specifically, the self-dual tensor transforms as $(3,1)$, the spinors, which are also chiral, transform as $(2,1)$ and the scalars transform as $(1,1)$. Therefore, we shall ignore the trivial $SU(2)$ and refer to the non-trivial $SU(2)$ as the little group of this theory. In the case of the D5 theory, considered in the next subsection, both $SU(2)$ factors will be required.

It is convenient to introduce four Grassmann coordinates, such that the entire on-shell supermultiplet can be described by a single scalar expression. There are various ways to do this. One obvious choice is to introduce four Grassmann coordinates η^I , which transform as the fundamental four-dimensional representation of the $USp(4)$ R-symmetry group. In this way, one can make the R symmetry manifest, and we first discuss this formulation. However, because amplitudes for massless particles are labeled by incoming momenta and little-group indices, in most formulas we will make use of a second description of the supermultiplet that makes little group symmetry manifest.

For theories involving massless particles, it is also convenient to introduce eight bosonic spinor-helicity coordinates λ_a^A , where $A = 1, 2, 3, 4$ labels a spinor representation of the 6D Lorentz group $Spin(5,1)$ and $a = \pm$ labels a doublet of the chiral little group discussed above. These coordinates belong to a real representation of the product group, because the spinor representation of the Lorentz group and the doublet little-group representation are both pseudoreal. In terms of these coordinates the momentum of an on-shell massless particle is written [43],

$$p^{AB} = \varepsilon^{ab} \lambda_a^A \lambda_b^B = \lambda_a^A \lambda^{Ba} = \lambda_+^A \lambda_-^B - \lambda_-^A \lambda_+^B. \quad (2.2)$$

This formula is invariant under the $SU(2)$ little group, and therefore three of the eight λ coordinates are redundant, leaving five non-trivial degrees of freedom, as appropriate for the momentum of a massless particle in 6D. Note also that $p^{AB} = -p^{BA}$ is a six-vector of the Lorentz group. p^2 , which gives the square of the mass, is proportional to the Pfaffian of p^{AB} . This vanishes because the 4×4 matrix p^{AB} has rank two. When we describe n -particle scattering amplitudes we attach labels i, j, \dots , which take the values $1, 2, \dots, n$, to the coordinates. Thus, the i th particle is associated to λ_{i+}^A , λ_{i-}^A , and η_i^I .

The 16 supersymmetry charges of the M5 theory can be represented by²

$$q^{AI} = \lambda_+^A \eta^I - \Omega^{IJ} \lambda_-^A \frac{\partial}{\partial \eta^J}, \quad (2.3)$$

where the antisymmetric matrix Ω^{IJ} is the symplectic metric. We will find it convenient later to choose $\Omega^{13} = \Omega^{24} = 1$. This formula can be recast as

$$q^{AI} = \varepsilon^{ab} \lambda_a^A \eta_b^I = \lambda_a^A \eta^{Ia}, \quad (2.4)$$

where $\eta_-^I = \eta^I$ and $\eta_+^I = \Omega^{IJ} \partial / \partial \eta^J$. Then

$$\{\eta_a^I, \eta_b^J\} = \varepsilon_{ab} \Omega^{IJ}. \quad (2.5)$$

This makes the little-group invariance of the supercharges manifest. Note that the supercharges belong to a chiral representation of the Lorentz group, and the opposite chirality representation does not appear. This is what is meant by saying that the theory has $(2, 0)$ supersymmetry. As usual, the supercharges anticommute to give the momenta

$$\{q^{AI}, q^{BJ}\} = \Omega^{IJ} p^{AB}. \quad (2.6)$$

The ten R charges, $R^{IJ} = R^{JI}$, are represented by

$$R^{IJ} = \varepsilon^{ab} \eta_a^I \eta_b^J = \eta_a^I \eta^{Ja} = \eta^I \Omega^{JK} \frac{\partial}{\partial \eta^K} + \eta^J \Omega^{IK} \frac{\partial}{\partial \eta^K}. \quad (2.7)$$

These charges generate $USp(4)$ and they transform the supercharges appropriately

$$[R^{IJ}, q^{AK}] = \Omega^{IK} q^{AJ} + \Omega^{JK} q^{AI}. \quad (2.8)$$

The on-shell supermultiplet consists of three kinds of particles: a helicity triplet $B^{ab} = B^{ba}$, which is an R-symmetry singlet, a helicity doublet ψ_I^a , which is an R-symmetry quartet, and a helicity singlet $\phi_{IJ} = -\phi_{JI}$, $\Omega^{IJ} \phi_{IJ} = 0$, which is an R-symmetry quintet. These can be combined into a single R-symmetry invariant expression:

$$\Phi(\eta) = B^{++} + \eta^I \psi_I^+ + \frac{1}{2} \eta^I \eta^J \phi_{IJ} + \frac{1}{2} (\eta \cdot \eta) B^{+-} + (\eta \cdot \eta) \eta^I \psi_I^- + \frac{1}{2} (\eta \cdot \eta)^2 B^{--}, \quad (2.9)$$

where we have defined

$$\eta \cdot \eta = \frac{1}{2} \Omega_{IJ} \eta^I \eta^J = \eta^1 \eta^3 + \eta^2 \eta^4. \quad (2.10)$$

²6D $\mathcal{N} = (2, 0)$ on-shell superspace was first discussed in [113].

Note that each $+$ or $-$ superscript correspond to half a unit of H_3 , the third component of the little group $SU(2)$ algebra. Each term in Φ , and hence Φ itself, carries a total of one unit of H_3 if we assign a half unit of H_3 to each factor of η . This was to be expected because η^I was introduced as a renaming of $\eta_-^I = \eta^{I+}$.

This description of the supermultiplet has two deficiencies: first, it is not invariant under the little group; second, little-group multiplets are split up among different terms in the expansion. As noted already, both of these deficiencies can be overcome by using a different formulation of the supermultiplet. The price to be paid will be that only an $SU(2)$ subgroup of the $USp(4)$ R-symmetry group will be manifest.

The $SU(2)$ little group is not a global symmetry of the M5 theory. Rather, it is a redundancy in the formalism, analogous to a local symmetry, which is not manifest in the preceding equations. It can be made manifest by Fourier transforming half of the η coordinates. A Fourier transform replaces a Grassmann coordinate by a Grassmann derivative and vice versa. As before, we choose $\Omega^{13} = -\Omega^{31} = \Omega^{24} = -\Omega^{42} = 1$, while all other components of Ω^{IJ} vanish. Then we replace η^3 and η^4 by derivatives with respect to $\tilde{\eta}^1$ and $\tilde{\eta}^2$ and rename $(\eta^I, \tilde{\eta}^I)$ as (η_-^I, η_+^I) . Altogether, the four coordinates η^I are replaced by four coordinates η_a^I , which now transform as a doublet of the little group and as a doublet of an $SU(2)$ subgroup of the R symmetry group. The formulas for the 16 supercharges become

$$q^{AI} = \lambda_a^A \eta^{Ia} \quad \text{and} \quad \tilde{q}_I^A = \lambda_a^A \frac{\partial}{\partial \eta_a^I} \quad I = 1, 2. \quad (2.11)$$

As promised, we have traded manifest $USp(4)$ R symmetry for little group $SU(2)$ symmetry. This is also the case for the on-shell supermultiplet formula, which is a Grassmann Fourier transform of the one in Eq. (2.9). It now takes the form

$$\tilde{\Phi}(\eta) = \phi + \eta_a^I \psi_I^a + \varepsilon_{IJ} \eta_a^I \eta_b^J B^{ab} + \eta_a^I \eta^{Ja} \phi_{IJ} + (\eta^3)_a^I \tilde{\psi}_I^a + (\eta^4) \phi', \quad (2.12)$$

where $(\eta^3)_a^I = \varepsilon_{JK} \eta_b^I \eta^{Jb} \eta_a^K$ and $(\eta^4) = \varepsilon_{IJKL} \eta_a^I \eta_b^J \eta^{Ka} \eta^{Lb}$. Recall that in $\Phi(\eta)$ the index I takes four values, whereas in $\tilde{\Phi}(\eta)$ it takes two values. (We prefer not to introduce another symbol.) The five scalars are split $1 + 3 + 1$ and the four spinors are split $2 + 2$ even though they form irreducible R-symmetry multiplets. To summarize, the Φ representation has manifest R symmetry,

whereas the $\tilde{\Phi}$ representation has manifest little-group symmetry. The latter representation will turn out to be the easier one to deal with, and our main formulas for scattering amplitudes will use this superfield description.

D5 theory

The world-volume theory of a probe D5 in a 10D Minkowski space background has (1, 1) 6D supersymmetry. On-shell superspace with (1, 1) 6D supersymmetry has been used for studying 6D super Yang–Mills theory, see, e.g., [121, 122, 123]. This theory, which is nonchiral, *i.e.*, parity invariant, describes a single massless self-interacting vector supermultiplet. This supermultiplet contains a one-form field A_μ , with a two-form field strength $F = dA$. Such a field gives rise to four on-shell degrees of freedom. The vector supermultiplet also contains four fermions and four scalars. Altogether, there are eight bosonic and eight fermionic on-shell degrees of freedom. The three multiplicities (1, 4, 4) correspond to representations of the $SU(2) \times SU(2) = Spin(4)$ R-symmetry group, which is an unbroken global symmetry of the D5 theory. The representations are (1, 1) for the vector, (2, 2) for the scalars and (1, 2) + (2, 1) for the fermions. This symmetry can be thought of as arising from rotations in the four spatial dimensions that are orthogonal to a flat D5 in 10D Minkowski spacetime.

As discussed earlier, the little group in 6D is also $SU(2) \times SU(2)$. Altogether, in terms of four $SU(2)$ factors, with the first two referring to the little group and the second two to the R-symmetry group, the vector supermultiplet contains the following representations:

$$(2, 2; 1, 1) + (1, 1; 2, 2) + (2, 1; 1, 2) + (1, 2; 2, 1). \quad (2.13)$$

Note that, unlike the M5 theory, the D5 theory involves nontrivial representations of both $SU(2)$ factors of the little group. In terms of on-shell fields, these representations correspond to $A^{a\hat{a}}$, $\phi^{I\hat{I}}$, $\psi^{a\hat{I}}$, and $\psi^{\hat{a}I}$, in a notation that should be self-explanatory.

As before, we can introduce eight bosonic expressions λ_a^A , where $A = 1, 2, 3, 4$ labels a spinor representation of the 6D Lorentz group $Spin(5, 1)$ and $a = \pm$ labels a doublet of the first $SU(2)$ factor in the little group. In terms of these coordinates the momentum of an on-shell massless particle can be written in the form

$$p^{AB} = \varepsilon^{ab} \lambda_a^A \lambda_b^B = \lambda_a^A \lambda^{Ba}. \quad (2.14)$$

Three of the eight λ coordinates are redundant, leaving five nontrivial degrees of freedom, as appropriate for a massless particle in 6D. Unlike the case of the M5 theory, this is not sufficient. The Lorentz group has a second four-dimensional spinor representation, corresponding to the opposite chirality, and the little group has a second $SU(2)$ factor, both of which are utilized (on an equal footing) in the D5 theory. Therefore, it is natural to introduce an alternative formula for the momentum utilizing them

$$\hat{p}_{AB} = \varepsilon^{\hat{a}\hat{b}} \hat{\lambda}_{A\hat{a}} \hat{\lambda}_{B\hat{b}} = \hat{\lambda}_{A\hat{a}} \hat{\lambda}_{B\hat{a}}. \quad (2.15)$$

The two sets of spinor-helicity variables are orthogonal in the sense that

$$\lambda_a^A \hat{\lambda}_{A\hat{b}} = 0. \quad (2.16)$$

This combination must vanish in order that $p^2 \sim p^{AB} \hat{p}_{AB} = 0$.

Since the momentum six-vector p_i^μ is given by $\frac{1}{2} \sigma_{AB}^\mu p_i^{AB} = \frac{1}{2} \hat{\sigma}^{\mu AB} \hat{p}_{iAB}$, where σ and $\hat{\sigma}$ are the appropriate Lorentz-invariant tensors, the information encoded in λ and $\hat{\lambda}$, modulo little-group transformations, is the same. In fact, if one of them is given, the other is determined up to a little-group transformation. The two four-dimensional representations of the 6D Lorentz group, labeled by the upper and lower indices A and B , are inequivalent. If the group were $SU(4)$ they would be complex conjugates of another, but for Lorentzian signature the group is $Spin(5, 1)$ and each of these representations is pseudoreal. Nonetheless, for either signature it is a fact that the Kronecker product of these two representations gives the adjoint plus a singlet. It will be important in the analysis of the M5 theory that λ determines $\hat{\lambda}$ up to a little-group transformation and that the Lorentz invariant combination of λ and $\hat{\lambda}$ in Eq. (2.16) vanishes.

In the notation introduced above the 16 supercharges are given by q^{AI} and $\hat{q}_A^{\hat{I}}$. Then the (1, 1) supersymmetry algebra is

$$\{q^{AI}, q^{BJ}\} = p^{AB} \varepsilon^{IJ}, \quad \{\hat{q}_A^{\hat{I}}, \hat{q}_B^{\hat{J}}\} = \hat{p}_{AB} \varepsilon^{\hat{I}\hat{J}}, \quad \{q^{AI}, \hat{q}_B^{\hat{J}}\} = 0. \quad (2.17)$$

These are conveniently represented by

$$q^{AI} = \varepsilon^{ab} \lambda_a^A \eta_b^I = \lambda_a^A \eta^{Ia}, \quad \hat{q}_A^{\hat{I}} = \varepsilon^{\hat{a}\hat{b}} \hat{\lambda}_{A\hat{a}} \hat{\eta}_{\hat{b}}^{\hat{I}} = \hat{\lambda}_{A\hat{a}} \hat{\eta}^{\hat{I}\hat{a}}, \quad (2.18)$$

where the Grassmann coordinates satisfy

$$\{\eta_a^I, \eta_b^J\} = \varepsilon_{ab} \varepsilon^{IJ}, \quad \{\hat{\eta}_{\hat{a}}^{\hat{I}}, \hat{\eta}_{\hat{b}}^{\hat{J}}\} = \varepsilon_{\hat{a}\hat{b}} \varepsilon^{\hat{I}\hat{J}}, \quad \{\eta_a^I, \hat{\eta}_{\hat{b}}^{\hat{J}}\} = 0. \quad (2.19)$$

Now, there are again two alternative representations of the on-shell superfield distinguished by whether the R symmetry or the little-group symmetry is manifest. The formula with manifest R symmetry utilizes the four anticommuting Grassmann coordinates η_-^I and $\hat{\eta}_-^{\hat{I}}$, which we simplify to η^I and $\hat{\eta}^{\hat{I}}$. In terms of these, the expansion is

$$\Phi(\eta) = A^{+\hat{+}} + \eta_I \psi^{+\hat{I}} + \hat{\eta}_{\hat{I}} \psi^{+I} + \eta_I \hat{\eta}_{\hat{I}} \phi^{I\hat{I}} + \eta^2 A^{-\hat{+}} + \hat{\eta}^2 A^{+\hat{-}} + \dots + \eta^2 \hat{\eta}^2 A^{-\hat{-}}, \quad (2.20)$$

where $\eta^2 = \frac{1}{2} \varepsilon_{IJ} \eta^I \eta^J$ and similarly for $\hat{\eta}^2$

The alternative representation with manifest little-group symmetry utilizes the $I = 1$ components of η_a^I , now denoted η_a , and the $\hat{I} = 1$ components of $\hat{\eta}_{\hat{a}}^{\hat{I}}$, now denoted $\hat{\eta}_{\hat{a}}$. The on-shell superfield in this representation is

$$\tilde{\Phi}(\eta) = \phi^{1\hat{1}} + \eta_a \psi^{a\hat{1}} + \hat{\eta}_{\hat{a}} \psi^{\hat{a}1} + \eta_a \hat{\eta}_{\hat{a}} A^{a\hat{a}} + \eta^2 \phi^{2\hat{1}} + \hat{\eta}^2 \phi^{1\hat{2}} + \dots + \eta^2 \hat{\eta}^2 \phi^{2\hat{2}}. \quad (2.21)$$

As before, the two representations are related by a Grassmann Fourier transform. Since the little group and the R symmetry are both $SU(2) \times SU(2)$ for the D5 theory the two superfield formulas have the same structure with the role of the R-symmetry and little-group symmetry interchanged.

D3 theory

Since the D3 theory can be obtained by dimensional reduction of the M5 theory or the D5 theory, let us consider what happens when all of the momenta are restricted to a 4D Minkowski subspace. The Lorentz group then becomes $SL(2, \mathbb{C})$ and the $\mathbf{4}$ of $Spin(5, 1)$ decomposes as $\mathbf{2} + \bar{\mathbf{2}}$. In fact, this is correct for both of the four-dimensional spinor representations of the 6D Lorentz group, and it is appropriate and consistent to require that λ_a^A and $\hat{\lambda}_{A\hat{a}}$ become identical when restricted to 4D. In standard notation, the spinor index $A \rightarrow (\alpha, \hat{\alpha})$. In terms of λ_a^A the restriction to 4D is achieved by setting $\lambda_-^\alpha = 0$ and $\lambda_+^{\hat{\alpha}} = 0$. This then gives $p^{\alpha\beta} = p^{\hat{\alpha}\hat{\beta}} = 0$ leaving the familiar 4D formula for an on-shell massless particle in helicity variables:

$$p^{\alpha\hat{\alpha}} = \lambda_+^\alpha \lambda_-^{\hat{\alpha}}. \quad (2.22)$$

Now p^2 is proportional to the determinant of $p^{\alpha\hat{\alpha}}$, which vanishes because this matrix has rank one.

Let us now focus on reduction of the M5 theory. The case of the D5 theory is very similar. The restrictions on the momenta imply that the supercharges in

Eq. (2.3) reduce to

$$q^{\alpha I} = \lambda^\alpha \eta^I \quad \text{and} \quad q_I^{\dot{\alpha}} = \tilde{\lambda}^{\dot{\alpha}} \frac{\partial}{\partial \eta^I} \quad I = 1, 2, 3, 4, \quad (2.23)$$

where we have set $\lambda_+^\alpha = \lambda^\alpha$ and $\lambda_-^{\dot{\alpha}} = \tilde{\lambda}^{\dot{\alpha}}$, which is the standard notation. Also, an unnecessary constant factor has been removed in the formula for $q_I^{\dot{\alpha}}$. Then $q^{\alpha I}$ and $q_{\dot{\alpha} I}$ form complex-conjugate representations.

The R symmetry can now be extended to $SU(4)$, with generators given by the traceless expression

$$R^I{}_J = \eta^I \frac{\partial}{\partial \eta^J} - \frac{1}{4} \delta_J^I \eta^K \frac{\partial}{\partial \eta^K}. \quad (2.24)$$

The $SU(4)$ symmetry is manifest in the on-shell supermultiplet expression derived from Eq. (2.9)

$$\Phi(\eta) = A^{--} + \eta^I \psi_I^- + \eta^I \eta^J \phi_{IJ} + \frac{1}{6} \varepsilon_{IJKL} \eta^I \eta^J \eta^K \psi^{L+} + \eta^1 \eta^2 \eta^3 \eta^4 A^{++}. \quad (2.25)$$

The middle term now describes six scalars, one of which descends from B^{+-} . The amplitudes of the D3 theory have an additional $U(1)$ symmetry that can be interpreted as conservation of helicity. Its generator is

$$H = \frac{1}{4} \left[\eta^I, \frac{\partial}{\partial \eta^I} \right] = \frac{1}{2} \eta^I \frac{\partial}{\partial \eta^I} - 1. \quad (2.26)$$

This is the operator that reads off the helicity of a particle, and therefore its conservation, $HA_n = (\sum_i H_i)A_n = 0$, implies that the total helicity of the particles participating in a nonvanishing n -particle scattering amplitude must be zero. Conservation of this charge implies that the amplitude is homogeneous of degree $2n$ in these η coordinates. Moreover, $SU(4)$ R symmetry requires that the total number of η 's must be a multiple of four. Together these statements imply that n must be even for the D3 theory. In fact, we claim that n must also be even for the M5 and D5 theories even though this reasoning is not applicable in those cases.

The $U(1)$ symmetry generated by H does not commute with the supercharges. Therefore, by definition, it is an additional R symmetry, extending the R-symmetry group to $SU(4) \times U(1)$. Let us now explain how the appearance of this symmetry could have been anticipated. Since the D3 theory can be obtained by dimensional reduction of the D9-brane theory, the $SU(4)$ subgroup

can be regarded as arising from rotations in the six dimensions transverse to the D3. So where does the additional $U(1)$ R symmetry come from? Having posed the question, the answer becomes clear. The D3 theory can also be obtained by dimensional reduction of the M5 theory, so the $U(1)$ can be interpreted as rotations in the two extra dimensions of this construction.

In the case of $\mathcal{N} = 4$ super Yang–Mills (SYM) theory the $SU(4)$ R symmetry can also be understood by dimensional reduction starting from SYM in ten dimensions. In fact, like the D3 theory, that is how this theory was originally obtained. However, $\mathcal{N} = 4$ SYM cannot be obtained by dimensional reduction of a *perturbative* theory in 6D with $(2, 0)$ supersymmetry. There are nonperturbative $(2, 0)$ theories in 6D that reduce to $\mathcal{N} = 4$ SYM when placed on a torus. In such a reduction, the 4D coupling constant is determined by the ratio of the radii of two cycles of the torus, and different choices are related by dualities. This is not the kind of dimensional reduction that would give rise to an extra $U(1)$ symmetry. Even when Kaluza–Klein excitations are omitted, such a reduction does not retain the transverse rotational symmetry that is needed to give an additional $U(1)$ R symmetry. Therefore, in the case of $\mathcal{N} = 4$ SYM, helicity is not conserved and n does not need to be even.

As in the previous examples, there is an alternative form of the supercharges and the on-shell superfield that exhibits manifest little-group symmetry. As a consequence, only an $SU(2) \times SU(2)$ subgroup of the $SU(4)$ R symmetry remains manifest. As before, this representation is related to the previous one by Fourier transforming two of the four Grassmann coordinates. In this new basis the 16 supercharges take the form

$$q^{\alpha I} = \lambda^\alpha \eta_-^I \quad \text{and} \quad \hat{q}_I^{\dot{\alpha}} = \tilde{\lambda}^{\dot{\alpha}} \frac{\partial}{\partial \eta_-^I} \quad I = 1, 2, \quad (2.27)$$

$$\hat{q}_I^\alpha = \lambda^\alpha \frac{\partial}{\partial \eta_+^{\hat{I}}} \quad \text{and} \quad \hat{q}^{\dot{\alpha} \hat{I}} = \tilde{\lambda}^{\dot{\alpha}} \eta_+^{\hat{I}} \quad \hat{I} = 1, 2. \quad (2.28)$$

The indices I and \hat{I} label doublets of distinct $SU(2)$ subgroups of the R symmetry group. The indices \pm keep track of $U(1)$ little-group representations, which corresponds to helicity. In this formulation the on-shell superfield becomes

$$\begin{aligned} \tilde{\Phi}(\eta) = & \phi + \eta_-^I \psi_I^- + \eta_+^{\hat{I}} \psi_{\hat{I}}^+ + \eta_+^{\hat{I}} \eta_-^J \phi_{\hat{I}J} + (\eta_+)^2 A^+ + (\eta_-)^2 A^- \\ & + (\eta_+)^2 \eta_-^I \psi_I^+ + (\eta_-)^2 \eta_+^{\hat{I}} \psi_{\hat{I}}^- + (\eta_+)^2 (\eta_-)^2 \bar{\phi}, \end{aligned} \quad (2.29)$$

where $(\eta_+)^2 = \frac{1}{2}\varepsilon_{IJ}\eta_+^I\eta_+^J$ and $(\eta_-)^2 = \frac{1}{2}\varepsilon_{IJ}\eta_-^I\eta_-^J$.

2.3 Four-Particle Amplitudes

M5 theory

Before discussing the general case, let us consider four-particle amplitudes, starting with the M5 theory. The plan is to first propose a formula for the result that corresponds to supermultiplets written in the form given in Eq. (2.12). This representation has a manifest $SU(2)$ little-group symmetry for each external particle. Up to normalization, the four-particle amplitude with four derivatives for an abelian tensor supermultiplet with 6D (2, 0) supersymmetry is uniquely given by

$$A_4 = \delta^6 \left(\sum_{i=1}^4 p_i^{AB} \right) \delta^8 \left(\sum_{i=1}^4 q_i^{AI} \right). \quad (2.30)$$

As discussed in Sect. 2.2, $p_i^{AB} = \lambda_{i+}^A \lambda_{i-}^B - \lambda_{i-}^A \lambda_{i+}^B$ and $q_i^{AI} = \lambda_{i+}^A \eta_{i-}^I - \lambda_{i-}^A \eta_{i+}^I$, where $A, B = 1, 2, 3, 4$ and $I = 1, 2$. The fermionic delta functions are defined for instance in [121]. It will be useful later to write the momentum-conservation condition in matrix notation as

$$\lambda_+ \lambda_-^T = \lambda_- \lambda_+^T. \quad (2.31)$$

In other words, the matrix $(\lambda_+ \lambda_-^T)^{AB}$ is symmetric. This is valid for any number of particles n . In the special case of $n = 4$, λ_+ and λ_- are square matrices. If $n = 4$ and λ_- is invertible, which is generically the case, this implies that $(\lambda_-^{-1} \lambda_+)^{ij}$ is symmetric. This fact will be useful later.

The formula for A_4 manifestly satisfies several requirements: total symmetry in the four particles, Lorentz invariance, conservation of momentum and half of the supercharges, and little-group symmetry. Also, the second factor scales as λ^8 or p^4 , as expected. Conservation of the other half of the supersymmetries is easy to verify. What one needs to show is that

$$\left(\sum_{i=1}^4 \tilde{q}_{iI}^A \right) A_4 = 0. \quad (2.32)$$

This fact is an immediate consequence of $\{\tilde{q}_{iI}^A, q_j^{BJ}\} = p_i^{AB} \delta_{ij} \delta_J^I$ and conservation of momentum.

In order to appreciate Eq. (2.30), let us examine what it implies for the scattering of four B particles. They are R-symmetry singlets whose on-shell degrees

of freedom are described by a symmetric tensor $B_{ab} = B_{ba}$ of the $SU(2)$ little group. Eq. (2.30) implies that their four-particle amplitudes are given by

$$\langle B_{a_1 a_2} B_{b_1 b_2} B_{c_1 c_2} B_{d_1 d_2} \rangle = \langle 1_{a_1} 2_{b_1} 3_{c_1} 4_{d_1} \rangle \langle 1_{a_2} 2_{b_2} 3_{c_2} 4_{d_2} \rangle + \mathcal{P}_4, \quad (2.33)$$

where \mathcal{P}_4 denotes the symmetrization over little group indices. Here and throughout, we make use of a Lorentz-invariant bracket:

$$\langle 1_a 2_b 3_c 4_d \rangle := \varepsilon_{ABCD} \lambda_{1a}^A \lambda_{2b}^B \lambda_{3c}^C \lambda_{4d}^D. \quad (2.34)$$

It is interesting to note that any four B particles have a nonzero amplitude. For example,

$$\langle B_{++} B_{++} B_{++} B_{++} \rangle \propto \langle 1_+ 2_+ 3_+ 4_+ \rangle^2 = (\det \lambda_+)^2, \quad (2.35)$$

Similarly, the amplitude for four B_{--} particles is given by $(\det \lambda_-)^2$. On reduction to the D3 theory, B_{++} becomes a positive-helicity photon, and this amplitude vanishes. Indeed, Eq. (2.33) gives all the four-photon amplitudes correctly, with the only nonzero ones involving two positive-helicity and two negative-helicity photons. It also describes amplitudes involving additional scalars that arises from reduction of $B_{+-} = B_{-+}$.

Let us now turn to the more difficult issue: verifying $USp(4)$ R symmetry of an arbitrary four-particle amplitude. We have learned earlier that this symmetry should be manifest in the representation of the supermultiplet given in Eq. (2.9). To get to this representation, we rename η_{i-}^I as η_i^I and η_{i+}^I as $\tilde{\eta}_i^I$. Then we Fourier transform the latter coordinates to conjugate Grassmann coordinates denoted ζ_{iI} . Thus, we consider

$$A_4 = \int d^8 \tilde{\eta}_i^I e^{\sum_{iI} \tilde{\eta}_i^I \zeta_{iI}} \delta^8 \left(\sum_{i=1}^4 q_i^{AI} \right). \quad (2.36)$$

Substituting an integral representation of the delta functions and carrying out the $\tilde{\eta}$ integrations gives

$$A_4 = \int d^8 \theta_{AI} \delta^8(\zeta_{iI} + \sum_A \theta_{AI} \lambda_{i-}^A) e^{\sum_{AI} \theta_{AI} \lambda_{i+}^A \eta_i^I}. \quad (2.37)$$

If we now assume that the 4×4 matrix λ_{i-}^A is nonsingular, which is generically the case, then

$$\delta^8(\zeta_{iI} + \sum_A \theta_{AI} \lambda_{i-}^A) = (\det \lambda_-)^2 \delta^8((\zeta \lambda_-^{-1})_{IA} + \theta_{AI}) \quad (2.38)$$

and thus

$$A_4 = (\det \lambda_-)^2 \exp(-\text{tr}(\zeta \lambda_-^{-1} \lambda_+ \eta)) \quad (2.39)$$

More explicitly, the exponent is

$$-\text{tr}(\zeta \lambda_-^{-1} \lambda_+ \eta) = \text{tr}(\lambda_-^{-1} \lambda_+ \eta \zeta) = \sum_{ij} (\lambda_-^{-1} \lambda_+)_{ij} (\eta \zeta)_{ji} \quad (2.40)$$

As was explained earlier, momentum conservation implies that $(\lambda_-^{-1} \lambda_+)_{ij}$ is a symmetric matrix. Therefore only the symmetric part of $(\eta \zeta)_{ji}$ contributes, which can therefore be replaced by half of

$$E_{ij} = \sum_{I=1}^2 (\eta_i^I \zeta_{Ij} + \eta_j^I \zeta_{Ii}). \quad (2.41)$$

We now claim that E (and hence A_4) can be rewritten in a form that has manifest $USp(4)$ symmetry

$$E_{ij} = \sum_{I,J=1}^4 \Omega_{IJ} \eta_i^I \eta_j^J, \quad (2.42)$$

where the only nonzero elements above the diagonal of the symplectic metric are $\Omega_{13} = \Omega_{24} = 1$. Note that we have renamed $\zeta_{Ii} = \eta_i^{I+2}$. Then η_i^I belongs to the fundamental representation of the $USp(4)$ R-symmetry group. The same idea discussed here applies to more general n -particle amplitudes, as we show in Appendix A.2.

Note that the amplitude for four B_{--} particles is given by the first term in the expansion of the exponential, whereas the amplitude for four B_{++} particles is given by the last (eighth) term in the series expansion of the exponential. All other four-particle amplitudes are contained in the intermediate powers. Clearly, this representation (with manifest R symmetry) is more complicated than the previous one with manifest little group $SU(2)$ symmetries for each of the scattered particles, that amplitudes are no longer homogenous polynomials in terms of fermionic variables η 's.

D5 theory

The four-particle amplitude for this theory is quite similar to the one for the M5 theory. In the representation with manifest little-group symmetry the four Grassmann coordinates that are used in the superfield $\tilde{\Phi}(\eta)$ are η_a and

$\hat{\eta}_{\hat{a}}$. They transform as (2, 1) and (1, 2) with respect to the $SU(2) \times SU(2)$ little group. In terms of these we can define eight anticommuting supercharges

$$q^A = \varepsilon^{ab} \lambda_a^A \eta_b = \lambda_a^A \eta^a \quad \text{and} \quad \hat{q}_A = \varepsilon^{\hat{a}\hat{b}} \hat{\lambda}_{A\hat{a}} \eta_{\hat{b}} = \hat{\lambda}_{A\hat{a}} \eta^{\hat{a}}. \quad (2.43)$$

Then the desired amplitude is

$$A_4 = \delta^6 \left(\sum_{i=1}^4 p_i^\mu \right) \delta^4 \left(\sum_{i=1}^4 q_i^A \right) \delta^4 \left(\sum_{i=1}^4 \hat{q}_{iA} \right). \quad (2.44)$$

In particular, we can read off the amplitude for scattering four vector particles

$$\langle A_{a\hat{a}} A_{b\hat{b}} A_{c\hat{c}} A_{d\hat{d}} \rangle = \langle 1_a 2_b 3_c 4_d \rangle \langle 1_{\hat{a}} 2_{\hat{b}} 3_{\hat{c}} 4_{\hat{d}} \rangle \quad (2.45)$$

where

$$\langle 1_a 2_b 3_c 4_d \rangle \equiv \varepsilon_{ABCD} \lambda_{1a}^A \lambda_{2b}^B \lambda_{3c}^C \lambda_{4d}^D, \quad \langle 1_{\hat{a}} 2_{\hat{b}} 3_{\hat{c}} 4_{\hat{d}} \rangle \equiv \varepsilon^{ABCD} \hat{\lambda}_{1A\hat{a}} \hat{\lambda}_{2B\hat{b}} \hat{\lambda}_{3C\hat{c}} \hat{\lambda}_{4D\hat{d}} \quad (2.46)$$

For example,

$$\langle A_{+\hat{+}} A_{+\hat{+}} A_{+\hat{+}} A_{+\hat{+}} \rangle \propto \det \lambda_+ \det \hat{\lambda}_{\hat{+}}. \quad (2.47)$$

As in the case of the M5 theory, the R symmetry of the D5 amplitudes can be verified by carrying out a Grassmann Fourier transform to the representation in which that symmetry becomes manifest.

D3 theory

Since the D3 theory can be obtained by dimensional reduction of the M5 theory, its four-particle amplitude can be deduced from the preceding results. Specifically, Eq. (2.30) reduces to

$$A_4 = \delta^4 \left(\sum_{i=1}^4 p_i^{\alpha\dot{\alpha}} \right) \delta^4 \left(\sum_{i=1}^4 q_i^{\alpha I} \right) \delta^4 \left(\sum_{i=1}^4 \hat{q}_i^{\dot{\alpha} \hat{I}} \right), \quad (2.48)$$

where $p_i^{\alpha\dot{\alpha}} = \lambda_i^\alpha \tilde{\lambda}_i^{\dot{\alpha}}$, $q_i^{\alpha I} = \lambda_i^\alpha \eta_{i-}^I$, and $\hat{q}_i^{\dot{\alpha} \hat{I}} = \tilde{\lambda}_i^{\dot{\alpha}} \eta_{i+}^{\hat{I}}$. As before, this is easily seen to have all of the required properties aside from R symmetry. Alternatively, the same result can be obtained by dimensional reduction of the D5 theory, whose four-particle amplitude is given in Eq. (2.44). In this case, dimensional reduction of q^A gives $q^{\alpha 1}$ and $q^{\dot{\alpha} 1}$, while dimensional reduction of \hat{q}_A gives $q^{\alpha 2}$ and $q^{\dot{\alpha} 2}$.

R symmetry can be investigated, as before, by Fourier transforming the $\eta_{i+}^{\hat{I}}$ coordinates. (Recall that $I = 1, 2$ and $\hat{I} = 1, 2$ label doublets of the two

$SU(2)$ factors of an $SU(2) \times SU(2)$ subgroup of the $SU(4)$ R symmetry group.) However, the analysis requires some modification, since the matrix λ_- , which was previously assumed to be nonsingular, is now singular. In fact, two of its four columns are identically zero.

Since η_+ only occurs in the last delta-function factor, let us consider its Fourier transform

$$I_4 = \int d^8 \eta_{i+}^{\hat{I}} e^{\sum_{i\hat{I}} \eta_{i+}^{\hat{I}} \zeta_{i\hat{I}}} \delta^4 \left(\sum_{i=1}^4 \hat{q}_i^{\hat{I}} \right) = \int d^4 \theta_{\hat{\alpha}\hat{I}} \delta^8 \left(\zeta_{i\hat{I}} + \sum_{\hat{\alpha}} \tilde{\lambda}_i^{\hat{\alpha}} \theta_{\hat{\alpha}\hat{I}} \right). \quad (2.49)$$

Momentum conservation can be written as the matrix equation $(\lambda^T \tilde{\lambda})^{\alpha\hat{\alpha}} = 0$. Therefore the eight delta functions imply the four relations $\sum_i \lambda_i^\alpha \zeta_{i\hat{I}} = 0$. From this it follows that

$$I_4 = J \delta^4 \left(\sum_{i=1}^4 \lambda_i^\alpha \zeta_{i\hat{I}} \right), \quad (2.50)$$

where J is a Jacobian factor. It is straightforward to see that the Jacobian is

$$J = \left(\frac{[12]}{\langle 34 \rangle} \right)^2. \quad (2.51)$$

Here we are using the standard notation of 4D spinor helicity formalism, $\langle ij \rangle = \varepsilon_{\alpha\beta} \lambda_i^\alpha \lambda_j^\beta$ and $[ij] = \varepsilon_{\hat{\alpha}\hat{\beta}} \tilde{\lambda}_i^{\hat{\alpha}} \tilde{\lambda}_j^{\hat{\beta}}$. It is important that J should have total symmetry in the four particles. The proof that $[12]/\langle 34 \rangle$ has total antisymmetry, and hence that J has total symmetry, is straightforward using momentum conservation.

To complete the analysis, we define $\zeta_{\hat{1}} = \eta^3$ and $\zeta_{\hat{2}} = \eta^4$, as before. Then, assembling the results above, the Fourier-transformed scattering amplitude becomes

$$A_4 = \left(\frac{[12]}{\langle 34 \rangle} \right)^2 \delta^4 \left(\sum_{i=1}^4 p_i^{\alpha\hat{\alpha}} \right) \delta^8 \left(\sum_{i=1}^4 q_i^{\alpha I} \right), \quad (2.52)$$

where the index I on $q_i^{\alpha I} = \lambda_i^\alpha \eta_i^I$ now takes four values. This version of four-particle superamplitude has appeared before, for instance in [116]. It now has manifest $SU(4)$ R symmetry, because the Grassmann delta functions contain two factors of $\varepsilon_{IJKL} \eta_i^I \eta_j^J \eta_k^K \eta_l^L$, which is $SU(4)$ invariant. The amplitude has an additional $U(1)$ R symmetry, because it contains $2n = 8$ factors of η , as explained earlier.

2.4 n -Particle Amplitudes of the D3 Theory

This section briefly reviews the n -particle amplitudes for the tree-level S-matrix of the D3 theory. A nice formula with manifest $SU(4)$ R symmetry appeared recently in [105][106]. However, for the purpose of generalizing to the M5 theory, it is more convenient to break the $SU(4)$ R-symmetry $SU(4) \rightarrow SU(2)_L \times SU(2)_R$ and make the little-group symmetry manifest. A formula of the required type has appeared previously for 4D $\mathcal{N} = 4$ SYM and $\mathcal{N} = 8$ supergravity [56]. It contains complex coordinates σ_i (on the Riemann sphere) associated to the n particles. The formula is required to be invariant under simultaneous $SL(2, \mathbb{C})$ transformations of these coordinates. This implies that only $n - 3$ of them are integrated, while the other three can be set to arbitrarily chosen distinct values.

The on-shell n -particle amplitude formula takes the form

$$\mathcal{A}_n = \int \frac{d^n \sigma d\mathcal{M}}{\text{Vol}(G)} \Delta_B(p, \rho) \Delta_F(q, \rho, \chi) \mathcal{I}, \quad (2.53)$$

where Δ_B is a product of bosonic delta functions

$$\Delta_B(p, \rho) = \prod_{i=1}^n \delta^4 \left(p_i^{\alpha\dot{\alpha}} - \frac{\rho^\alpha(\sigma_i) \tilde{\rho}^{\dot{\alpha}}(\sigma_i)}{P_i(\sigma)} \right), \quad (2.54)$$

and Δ_F is a product of fermionic (or Grassmann) delta functions

$$\Delta_F(q, \rho, \chi) = \prod_{i=1}^n \delta^4 \left(q_i^{\alpha I} - \frac{\rho^\alpha(\sigma_i) \chi_-^I(\sigma_i)}{P_i(\sigma)} \right) \delta^4 \left(\hat{q}_i^{\dot{\alpha} \hat{I}} - \frac{\tilde{\rho}^{\dot{\alpha}}(\sigma_i) \chi_+^{\hat{I}}(\sigma_i)}{P_i(\sigma)} \right). \quad (2.55)$$

Here $\rho^\alpha(\sigma)$ and $\chi_+^{\hat{I}}(\sigma)$ are degree- d polynomials, while $\tilde{\rho}^{\dot{\alpha}}(\sigma)$ and $\chi_-^I(\sigma)$ are degree- \tilde{d} polynomials, with

$$d + \tilde{d} = n - 2. \quad (2.56)$$

Thus, $\rho^\alpha(\sigma)$ (bosonic) and $\chi_-^I(\sigma)$ (fermionic) take the form

$$\rho^\alpha(\sigma) = \sum_{m=0}^d \rho_m^\alpha \sigma^m, \quad \chi_-^I(\sigma) = \sum_{m=0}^{\tilde{d}} \chi_{m,-}^I \sigma^m, \quad (2.57)$$

and

$$\tilde{\rho}^{\dot{\alpha}}(\sigma) = \sum_{m=0}^{\tilde{d}} \tilde{\rho}_m^{\dot{\alpha}} \sigma^m, \quad \chi_+^{\hat{I}}(\sigma) = \sum_{m=0}^d \chi_{m,+}^{\hat{I}} \sigma^m. \quad (2.58)$$

Also,

$$P_i(\sigma) = \prod_{j \neq i} \sigma_{ji} \quad i, j = 1, 2, \dots, n, \quad (2.59)$$

where $\sigma_{ij} = \sigma_i - \sigma_j$. Note that $P_i(\sigma)$ depends on all n of the σ coordinates, but σ_i has a distinguished role. The integral is taken over the space of punctures and polynomials, the measure for which contains the following $2n$ bosonic and $2n$ fermionic integrations:

$$d\mathcal{M} = \prod_{m=0}^d \prod_{\tilde{m}=0}^{\tilde{d}} d^2 \rho_m^\alpha d^2 \tilde{\rho}_{\tilde{m}}^{\dot{\alpha}} d^2 \chi_{\tilde{m},-}^I d^2 \chi_{m,+}^{\dot{I}}. \quad (2.60)$$

The integral has a gauge redundancy from the modular and little-group symmetries, so we must divide by the volume of

$$G = SL(2, \mathbb{C}) \times GL(1, \mathbb{C}), \quad (2.61)$$

where the modular group $SL(2, \mathbb{C})$ acts on the σ_i 's and $GL(1, \mathbb{C})$, the complexified little group, acts on the ρ 's and $\tilde{\rho}$'s.

Eq. (2.53) describes maximally supersymmetric theories with the on-shell states organized according to Eq. (2.29). It gives the usual scattering amplitude supplemented by additional delta functions, namely

$$\mathcal{A}_n = \left(\prod_{i=1}^n \delta(p_i^2) \delta^2(\langle \lambda_i q_i^I \rangle) \delta^2([\tilde{\lambda}_i \hat{q}_i^{\dot{I}}]) \right) A_n, \quad (2.62)$$

where A_n is the usual scattering amplitude including the four momentum-conservation delta functions and eight supercharge-conservation delta functions. (When the momentum-conservation delta function is also omitted, the amplitude is denoted T_n). The bracket notation is the same as described following Eq. (2.51). The extra delta functions in Eq. (2.62) impose the conditions that allow us to introduce the usual on-shell relations of the schematic form $p = \lambda \tilde{\lambda}$ and $q = \lambda \eta$. So, in practice, to extract the scattering amplitudes A_n from Eq. (2.53), one should use these relations and remove the extra delta functions. Appendix A.1 contains the proof that the $4n$ bosonic delta functions Δ_B account for the n mass-shell conditions, four momentum conservation equations, and the $n - 3$ scattering equations. These are precisely the $2n + 1$ delta functions that survive after carrying out the $(2n - 1)$ -dimensional ρ integration.

The choice of the factor \mathcal{I} in the integrand depends on the theory. For example, the color-ordered $\mathcal{N} = 4$ SYM amplitudes, discussed in [56], are given by the Parke–Taylor-like factor

$$\mathcal{I}^{\text{YM}} = \frac{1}{\sigma_{12}\sigma_{23} \cdots \sigma_{n-1n}\sigma_{n1}}. \quad (2.63)$$

In the case of YM and SYM theories in 4D, the solutions of the scattering equations can be separated into $n-3$ sectors characterized by the total helicity (or “helicity violation”) of the n particles participating in the reaction. The sectors, labeled by $d = 1, 2, \dots, n-3$, have $\tilde{d} - d = n - 2(d+1)$ units of helicity violation. In particular, the $d = 1$ sector, which has $n - 4$ units of helicity violation, is usually referred to as having “maximal helicity violation” (MHV). If n is even, the sector with $d = \tilde{d} = \frac{n}{2} - 1$ is helicity conserving. As was first conjectured in [124] and later proven in [56], the number of solutions of the scattering equations that contribute to the (d, \tilde{d}) sector, denoted $N_{d, \tilde{d}}$, is given by an Eulerian number. These numbers satisfy $N_{d, \tilde{d}} = N_{\tilde{d}, d}$ and $N_{d, 1} = 1$. They are fully determined by these relations and the recursion relation [56]

$$N_{d, \tilde{d}} = \tilde{d}N_{d-1, \tilde{d}} + dN_{d, \tilde{d}-1}. \quad (2.64)$$

Furthermore,

$$\sum_{d=1}^{n-3} N_{d, \tilde{d}} = (n-3)! \quad (2.65)$$

which accounts for all the solutions of the scattering equations.

Due to the recent progress in understanding CHY representations of scattering amplitudes [58, 59, 125], it is known that one can pass from YM theories to DBI theories by simply replacing \mathcal{I}^{YM} by

$$\mathcal{I}^{\text{DBI}} = \det' S_n, \quad (2.66)$$

where S_n is an $n \times n$ anti-symmetric matrix with

$$(S_n)_{ij} = \frac{s_{ij}}{\sigma_{ij}}, \quad i, j = 1, 2, \dots, n, \quad (2.67)$$

where $s_{ij} = (p_i + p_j)^2 = 2p_i \cdot p_j$ are the familiar Mandelstam invariants. Also,

$$\text{Pf}' S_n = \frac{(-1)^{i+j}}{\sigma_{ij}} \text{Pf} S_{i,j}^{i,j}, \quad \det' S_n = (\text{Pf}' S_n)^2. \quad (2.68)$$

Here $S_{i,j}^{i,j}$ means that the i -th and j -th rows and columns of the matrix S_n are removed before computing the Pfaffian or determinant. This is required because S_n has rank $n-2$ if n is even. Then $\det' S_n$ is independent of the choice of i and j and transforms with weight two under $SL(2, \mathbb{C})$ transformations of the σ coordinates. If n is odd, there is no satisfactory nonzero definition. Therefore all nonzero amplitudes of all DBI-like theories must have n even. This includes all three brane theories (D3, D5, M5) that are the main emphasis of this chapter. We will later consider other theories which do have odd point amplitudes which require additional developments.

However, if one examines the actions in the literature for these theories, it is only obvious that n must be even for the bosonic truncation, in each case, but it is not at all obvious when fermions are involved. These actions, which were derived using various string theory considerations, contain vertices involving an odd number of bosons when fermions are also present. Since we claim that on-shell amplitudes with an odd number of bosons always vanish, it must be possible to eliminate all terms in the action that have an odd number of boson fields by field redefinitions. At the leading nontrivial order, the analysis in Sect. 2.1 of [104] implies that this is the case for the D3 theory. Otherwise, this issue does not seem to have been explored.

In the case of the D3 theory, the extra $U(1)$ R symmetry, discussed earlier, implies that only the helicity-conserving sector, with

$$d = \tilde{d} = \frac{n}{2} - 1, \quad (2.69)$$

is nonvanishing. The number of solutions of the scattering equations that contribute to this sector is $N_{1,1} = 1$ for $n = 4$, $N_{2,2} = 4$ for $n = 6$, $N_{3,3} = 66$ for $n = 8$, $N_{4,4} = 2416$ for $n = 10$ and so forth. These numbers are a significant fraction of $(n-3)!$.

As indicated in Eq. (2.53), one should mod out the volume of $G = SL(2, \mathbb{C}) \times GL(1, \mathbb{C})$, where $SL(2, \mathbb{C})$ acts on the σ_i 's and $GL(1, \mathbb{C})$ acts on the ρ 's and χ 's. In practice, we may fix any three σ_i 's (for instance $\sigma_1, \sigma_2, \sigma_3$) and one ρ (for instance ρ_0^1) to arbitrary values, with the compensating Jacobian

$$J_{SL(2,\mathbb{C}) \times GL(1,\mathbb{C})} = \rho_0^1 (\sigma_1 - \sigma_2)(\sigma_2 - \sigma_3)(\sigma_3 - \sigma_1). \quad (2.70)$$

We note that the integral formula is not a “true integral”, in the sense that the number of bosonic delta-functions is equal to the number of integration

variables (after taking account of the G symmetry). This is not a surprise, of course, since we know that tree amplitudes are entirely algebraic.

As mentioned earlier, the counting of bosonic delta functions is as follows: the $4n$ bosonic delta-functions in Δ_B give rise to n delta functions for mass-shell conditions in the coefficient of A_n in Eq. (2.62) and four more for momentum conservation, $\delta^4(\sum_1^n p_i^\mu)$, which are included in A_n . The remaining $3n - 4$ delta functions determine the $(n - 3)$ σ 's and $(2n - 1)$ ρ 's that survive after modding out by the volume of G . The Jacobian that arises from these evaluations is computed explicitly in Appendix A.1. Also, there are $8n$ fermionic delta functions in Δ_F and $2n$ fermionic integrations in $d\mathcal{M}$, leaving an expression of order $6n$ in fermionic coordinates. $4n$ of these appear in the coefficient of A_n in Eq. (2.62). Therefore the remaining $2n$ η 's must be in A_n . In fact, half of them are η_+ 's and half are η_- 's. This is the number that we argued earlier are required (in this representation) by the $U(1)$ factor in the R symmetry group of this theory.

The powers of momenta that appear in \mathcal{A}_n can also be checked. In theories of Born–Infeld type, such as we are considering, one expects that $T_n \sim p^n$. In four dimensions this implies that $A_n \sim p^{n-4}$ and $\mathcal{A}_n \sim p^{3n-4}$. The latter, given for the D3 theory in Eq. (2.53), contains p^n from the measure, p^{-4n} from Δ_B , p^{4n} from Δ_F , and p^{2n-4} from $\det' S_n$. These combine to give p^{3n-4} , as desired.

Appendix A.1 describes the Jacobian factor generated by pulling out the “wave functions” and the momentum conservation delta function. Using these results for the Jacobian, we have checked explicitly that Eq. (2.53), with $\mathcal{I} = \det' S_n$, reproduces the four-point amplitude of the D3 theory given in Eq. (2.48) as well as the six-point super amplitudes, which may be found in [116]. The appendix also contains the proof that the amplitudes have $SU(4)$ R symmetry (in addition to the $U(1)$ already demonstrated).

2.5 n -Particle Amplitudes of the M5 Theory

The proposed formula

This section generalizes the twistor-string-like formula of the D3 theory in Eq. (2.53) to the M5 theory with $(2, 0)$ supersymmetry in 6D. The n -particle tree-level scattering amplitude for this theory takes the form

$$\mathcal{A}_n = \int \frac{d^n \sigma d\mathcal{M}}{\text{Vol}(G)} \Delta_B(p, \rho) \Delta_F(q, \rho, \chi) \det' S_n U(\rho, \sigma), \quad (2.71)$$

where

$$\Delta_B(p, \rho) = \prod_{i=1}^n \delta^6 \left(p_i^{AB} - \frac{\rho_a^A(\sigma_i) \rho^{Ba}(\sigma_i)}{P_i(\sigma)} \right) \quad (2.72)$$

and

$$\Delta_F(q, \rho, \chi) = \prod_{i=1}^n \delta^8 \left(q_i^{AI} - \frac{\rho_a^A(\sigma_i) \chi^{Ia}(\sigma_i)}{P_i(\sigma)} \right). \quad (2.73)$$

These delta functions are the natural (2, 0) generalization of the corresponding D3 formulas. The factor $\det' S_n$ is unchanged from the D3 case, since it is a sensible function of the invariants s_{ij} for any space-time dimension. A crucial requirement for the M5 theory amplitudes is that they reproduce the D3 amplitudes under dimensional reduction. The additional factor $U(\rho, \sigma)$ will be determined by this requirement and 6D Lorentz invariance later in this section.

The M5 analog of the D3 formula in Eq. (2.62) is

$$\mathcal{A}_n = \left(\prod_{i=1}^n \delta(p_i^2) \delta^4 \left(\hat{\lambda}_{iA\hat{a}} q_i^{AI} \right) \right) A_n. \quad (2.74)$$

The logic here is as follows. The bosonic delta functions Δ_B imply that the n particles are massless, and therefore they allow us to introduce spinor-helicity variables λ_a^A and $\hat{\lambda}_{A\hat{a}}$ for each of the momenta that are unique up to little-group transformations, as explained in Sect. 2.3. The fermionic delta functions Δ_F imply that $\hat{\lambda}_{A\hat{a}} q^{AI}$ should vanish, which accounts for the delta functions given above. The vanishing of $\hat{\lambda}_{A\hat{a}} q^{AI}$ also implies that q^{AI} can be expressed as $q^{AI} = \lambda_a^A \eta^{Ia}$ due to Eq. (2.16). On reduction to 4D these fermionic delta functions account for the fermionic delta functions that appear in Eq. (2.62).

Also by analogy with the D3 theory, $\rho_a^A(\sigma)$ and $\chi_a^I(\sigma)$ are bosonic and fermionic polynomials of degree d

$$\rho_a^A(\sigma) = \sum_{m=0}^d \rho_{m,a}^A \sigma^m, \quad \chi_a^I(\sigma) = \sum_{m=0}^d \chi_{m,a}^I \sigma^m, \quad (2.75)$$

and the measure $d\mathcal{M}$ for the M5 case is given by

$$d\mathcal{M} = \prod_{m=0}^d d^8 \rho_{m,a}^A d^4 \chi_{m,b}^I, \quad (2.76)$$

where $d = \frac{n}{2} - 1$, just as in the D3 theory. The symmetry that needs to be gauge fixed is now

$$G = SL(2, \mathbb{C}) \times SL(2, \mathbb{C}). \quad (2.77)$$

The first $SL(2, \mathbb{C})$ factor, which concerns the usual modular symmetry transformations of the σ coordinates, removes the integration over three σ_i 's. This symmetry will be verified later. The second $SL(2, \mathbb{C})$ factor, which is the complexification of the $SU(2)$ little group of the M5 theory, removes three ρ integrations.

The bosonic delta functions completely fix the integration variables, as in the 4D case, leaving a sum over the solutions of the scattering equations. Specifically, the $6n$ bosonic delta functions give rise to n on-shell conditions $p_i^2 = 0$ and 6D momentum conservation leaving $(5n-6)$ bosonic delta functions. Since the σ_i 's and $\rho_{m,a}^A$'s are constrained by $G = SL(2, \mathbb{C}) \times SL(2, \mathbb{C})$, there are $(n-3)$ σ_i 's and $(4n-3)$ $\rho_{m,a}^A$'s to be integrated, which is the right number to be fixed by the remaining $(5n-6)$ delta functions. The proof of momentum conservation and the scattering equations is essentially the same as described for the D3 theory in Appendix A.1.

The gauge-fixing Jacobian for the first $SL(2, \mathbb{C})$ factor is $(\sigma_1 - \sigma_2)(\sigma_2 - \sigma_3)(\sigma_3 - \sigma_1)$ as usual. The one for the second $SL(2, \mathbb{C})$ factor will be discussed later. These symmetries, as well as other properties, will be verified after we have made a specific proposal for $U(\rho, \sigma)$. It will be determined by considering dimensional reduction to 4D, with the final result shown in Eq. (2.100) or equivalently Eq. (2.103).

In contrast to the 4D case, the polynomials $\rho^{Aa}(\sigma)$ and $\chi_a^I(\sigma)$ are required to have degree $d = \frac{n}{2} - 1$ due to the $SU(2)$ little-group symmetry. Thus, the solutions of the scattering equations, which are implied by $\Delta_B(p, \rho) = 0$, cannot be subdivided into sectors. There is only one sector, which we find interestingly already contains all $(n-3)!$ solutions of the scattering equations. (This assertion has been checked explicitly for $n = 4, 6, 8$.) When reduced to 4D massless kinematics and for the D3 theory, only a subset of the $(n-3)!$ solutions contributes, namely those $N_{d,d}$ helicity-conserving solutions.

We have checked explicitly that Eq. (2.100) correctly reproduces the amplitudes with lower multiplicities, such as the four-particle amplitude that was discussed previously. As we discussed, to extract the amplitudes, one should

take out the “wave functions” from Δ_B and Δ_F defined in Eq. (2.72) and Eq. (2.73)

$$\mathcal{A}_4 = \left(\prod_{i=1}^4 \delta(p_i^2) \delta^4 \left(\hat{\lambda}_{iA\hat{a}} q_i^{AI} \right) \right) A_4, \quad (2.78)$$

and one can further extract the momentum and (half of the) supercharge conservation delta functions, namely,

$$A_4 = \delta^6 \left(\sum_{i=1}^4 p_i^{AB} \right) \delta^8 \left(\sum_{i=1}^4 q_i^{AI} \right) \times J_{4,B} J_{4,F} \times I_4. \quad (2.79)$$

The factors $J_{4,B}$ and $J_{4,F}$ are Jacobians, generated in this process, which can be found in Appendix A.1. Finally, I_4 is an integral over the remaining delta functions,

$$\begin{aligned} I_4 &= \int \frac{d^4\sigma d\mathcal{M}_4}{\text{Vol}(G)} \prod_{i=1}^2 \delta^5 \left(p_i^{AB} - \frac{\rho_a^A(\sigma_i) \rho^{Ba}(\sigma_i)}{P_i(\sigma)} \right) \delta^4 \left(p_4^{AB} - \frac{\rho_a^A(\sigma_4) \rho^{Ba}(\sigma_4)}{P_4(\sigma)} \right) \\ &\times \prod_{i=1}^2 \delta^2 \left(q_i^{1I} - \frac{\rho_a^1(\sigma_i) \chi^{Ia}(\sigma_i)}{P_i(\sigma)} \right) \delta^2 \left(q_i^{3I} - \frac{\rho_a^3(\sigma_i) \chi^{Ia}(\sigma_i)}{P_i(\sigma)} \right) \det' S_4 U(\rho, \sigma) \end{aligned}$$

with $\{A, B\} \neq \{3, 4\}$ for the five-dimensional delta-functions, and the four-dimensional one has $\{A, B\} \neq \{3, 4\}, \{1, 3\}$. The result is, of course, independent of the choice of $\{A, B\}$ which are singled out to be special here. Performing the integral,³ and using the formula for $U(\rho, \sigma)$ that will be determined later (Eqs. (2.98) and (2.101) or equivalently Eq. (2.104)), we find that I_4 precisely cancels the Jacobian factors $J_{4,B} J_{4,F}$, leaving

$$A_4 = \delta^6 \left(\sum_{i=1}^4 p_i^{AB} \right) \delta^8 \left(\sum_{i=1}^4 q_i^{AI} \right), \quad (2.80)$$

which is the result that was obtained in the previous section.

Higher-point amplitudes in the M5 theory have not appeared in the literature to our knowledge. However, amplitudes with scalars are constrained by soft theorems (as we will describe in a later subsection), and some of them are completely determined by recursion relations [126]. For instance, pure-scalar amplitudes are fixed in terms of the four-point ones. We have tested

³This means solving for the σ 's and ρ 's using the bosonic delta functions, together with gauge fixing the symmetry G , and integrating over the eight fermionic variables $\chi_{m,a}^I$ using the eight fermionic delta functions.

numerically that Eq. (2.100) indeed reproduces such amplitudes correctly for $n = 6, 8$. Those results, combined with supersymmetry and R symmetry, which we have explicitly checked for six and eight particles in Appendix A.2, imply that Eq. (2.100) should be valid for the entire supermultiplet for $n = 6, 8$. It seems very likely that they are correct for all n , as we find evidence supporting this in the following sections.

Reduction to four dimensions

This subsection will determine the constraint on $U(\rho, \sigma)$ in Eq. (2.71) that arises from requiring that its reduction to 4D cancels the Jacobian that is generated by the dimensional reduction of the M5 amplitude to 4D. So the key step is to evaluate the relevant Jacobian. What dimensional reduction does is to set two components of the six-component momenta equal to zero. In our conventions this means $p_i^{12} \rightarrow 0$ and $p_i^{34} \rightarrow 0$. This can be implemented by inserting

$$\int dp_n^{12} dp_n^{34} \prod_{i=1}^{n-1} dp_i^{12} dp_i^{34} \delta(p_i^{12}) \delta(p_i^{34}) \quad (2.81)$$

into the formula for the n -particle amplitude of the M5 theory in Eq. (2.71). Note that $\delta(p_i^{12})\delta(p_i^{34})$ is only inserted for $n - 1$ particles, even though the integration is over all n particles, because momentum conservation in 6D ensures that $p_n^{12} = p_n^{34} = 0$ as well, if $p_i^{12} = p_i^{34} = 0$ for $i = 1, 2, \dots, n-1$. Since dimensional reduction requires setting $\lambda_{i,-}^1 = \lambda_{i,-}^2 = 0$ and $\lambda_{i,+}^3 = \lambda_{i,+}^4 = 0$, therefore we should integrate out the corresponding $\rho_{m,-}^1, \rho_{m,-}^2$ and $\rho_{m,+}^3, \rho_{m,+}^4$. Due to the fact that only the middle sector contributes to the scattering amplitudes of the D3 theory, we will focus on that sector only in the following computations. Explicitly, we have that the M5 amplitudes given in Eq. (2.71) reduce to 4D amplitudes of the form given in Eq. (2.53), where the factor \mathcal{I} is given by

$$\begin{aligned} \mathcal{I}_R &= \int \frac{\prod_{m=0}^d d\rho_{m,-}^1 d\rho_{m,-}^2 d\rho_{m,+}^3 d\rho_{m,+}^4}{\text{Vol}(SL(2, \mathbb{C}))} dp_n^{12} dp_n^{34} \prod_{i=1}^{n-1} dp_i^{12} dp_i^{34} \delta(p_i^{12}) \delta(p_i^{34}) \\ &\times \prod_{i=1}^n \delta\left(p_i^{12} - \frac{\rho_a^1(\sigma_i) \rho^{2a}(\sigma_i)}{P_i(\sigma)}\right) \delta\left(p_i^{34} - \frac{\rho_a^3(\sigma_i) \rho^{4a}(\sigma_i)}{P_i(\sigma)}\right) \det' S_n U(\rho, \sigma). \end{aligned} \quad (2.82)$$

The goal here is to determine the condition on $U(\rho, \sigma)$ that will ensure that $\mathcal{I}_R = \mathcal{I}^{\text{DBI}} = \det' S_n$. Here the $SL(2, \mathbb{C})$ group is the one that acts on the little-group indices that will be reduced to $U(1)$ after the dimensional reduction.

The trivial $n - 1$ integrations over p_i^{12} and p_i^{34} give

$$\begin{aligned} \mathcal{I}_R &= \int \frac{\prod_{m=0}^d d\rho_{m,-}^1 d\rho_{m,-}^2 d\rho_{m,+}^3 d\rho_{m,+}^4 dp_n^{12} dp_n^{34} \prod_{i=1}^{n-1} \delta\left(\frac{\rho_a^1(\sigma_i)\rho^{2a}(\sigma_i)}{P_i(\sigma)}\right) \delta\left(\frac{\rho_a^3(\sigma_i)\rho^{4a}(\sigma_i)}{P_i(\sigma)}\right)}{\text{Vol}(SL(2, \mathbb{C}))} \\ &\times \delta\left(p_n^{12} - \frac{\rho_a^1(\sigma_n)\rho^{2a}(\sigma_n)}{P_n(\sigma)}\right) \delta\left(p_n^{34} - \frac{\rho_a^3(\sigma_n)\rho^{4a}(\sigma_n)}{P_n(\sigma)}\right) \det' S_n U(\rho, \sigma). \end{aligned} \quad (2.83)$$

The delta functions force $\rho_a^1(\sigma_i)\rho^{2a}(\sigma_i)$ and $\rho_a^3(\sigma_i)\rho^{4a}(\sigma_i)$ to vanish for $i = 1, 2, \dots, n-1$. However, $\rho_a^1(\sigma)\rho^{2a}(\sigma)$ and $\rho_a^3(\sigma)\rho^{4a}(\sigma)$ are polynomials of degree $2d = n-2$

$$\rho_a^1(\sigma)\rho^{2a}(\sigma) = \sum_{m=0}^{2d} c_m^{12} \sigma^m, \quad \rho_a^3(\sigma)\rho^{4a}(\sigma) = \sum_{m=0}^{2d} c_m^{34} \sigma^m, \quad (2.84)$$

where

$$c_m^{12} = \sum_{m'=0}^m \rho_{m',a}^1 \rho_{m-m'}^{2,a}, \quad c_m^{34} = \sum_{m'=0}^m \rho_{m',a}^3 \rho_{m-m'}^{4,a}, \quad m = 0, 1, \dots, 2d. \quad (2.85)$$

Because the degree of these polynomials is less than the $n - 1$ required roots, we conclude that all of the coefficients c_m^{12} and c_m^{34} should vanish. Since this also implies that $\rho_a^1(\sigma_n)\rho^{2a}(\sigma_n) = 0$ and $\rho_a^3(\sigma_n)\rho^{4a}(\sigma_n) = 0$, the integrations over p_n^{12} and p_n^{34} in Eq. (2.83) are trivial.

The formula for \mathcal{I}_R now contains $2n - 2$ delta functions, but there are $2n$ integrations, so we should use $SL(2, \mathbb{C})$ to fix two of them. This leaves a $U(1)$ unfixed, as expected. Let us now perform the integrations over $\rho_{m,-}^1$ and $\rho_{m,-}^2$ as well as $\rho_{m,+}^3$ and $\rho_{m,+}^4$ explicitly. A convenient method is to change the integration variables to the coefficients c_m^{12} defined previously,

$$\begin{aligned} &\frac{\prod_{m=0}^d d\rho_{m,-}^1 d\rho_{m,-}^2 d\rho_{m,+}^3 d\rho_{m,+}^4 \prod_{i=1}^{n-1} \left\{ [P_i(\sigma)]^2 \delta\left(\sum_{m=0}^{n-2} c_m^{12} \sigma_i^m\right) \delta\left(\sum_{m=0}^{n-2} c_m^{34} \sigma_i^m\right) \right\}}{\text{Vol}(SL(2, \mathbb{C}))} \\ &= V^2(\sigma) \frac{\prod_{m=0}^d d\rho_{m,-}^1 d\rho_{m,-}^2 d\rho_{m,+}^3 d\rho_{m,+}^4}{\text{Vol}(SL(2, \mathbb{C}))} \prod_{m=0}^{n-2} \delta(c_m^{12}) \delta(c_m^{34}) \\ &= J_C J_{SL(2, \mathbb{C})} V^2(\sigma) d\rho_{d,-}^2 d\rho_{d,+}^4 \prod_{m=0}^{n-2} dc_m^{12} dc_m^{34} \prod_{m=0}^{n-2} \delta(c_m^{12}) \delta(c_m^{34}), \end{aligned} \quad (2.86)$$

where

$$V(\sigma) = \prod_{i>j} \sigma_{ij} = \prod_{i=2}^n \prod_{j=1}^{i-1} \sigma_{ij} \quad (2.87)$$

is the Vandermonde determinant. It arose from the following combination of factors:

$$V(\sigma) = \frac{1}{V_n(\sigma)} \prod_{i=1}^{n-1} P_i(\sigma), \quad (2.88)$$

where

$$V_n(\sigma) = \det \sigma_i^m = V(\sigma)/P_n(\sigma), \quad (2.89)$$

and

$$V^2(\sigma) = \prod_{i=1}^n P_i(\sigma). \quad (2.90)$$

There are no minus sign issues, since n is even.

The factor $J_{SL(2,\mathbb{C})}$ is due to gauge-fixing the $SL(2, \mathbb{C})$ symmetry of the complexified little-group symmetry. We have chosen to gauge fix $\rho_{d,-}^2, \rho_{d,+}^4$ and $\rho_{d,+}^2$, and thus, the Jacobian due to the gauge-fixing of the complexified $SU(2)$ symmetry is given by

$$J_{SL(2,\mathbb{C})} = \rho_{d,-}^4 (\rho_{d,+}^2 \rho_{d,-}^4 - \rho_{d,-}^2 \rho_{d,+}^4). \quad (2.91)$$

The factor J_C is the Jacobian that arises due to the change of variables from ρ coordinates to c coordinates. It contains a product of two resultants, and it is given by

$$J_C^{-1} = \rho_{d,+}^2 \rho_{d,-}^4 R(\rho_+^1, \rho_+^2) R(\rho_-^3, \rho_-^4). \quad (2.92)$$

The resultant has appeared previously in a twistor-string-like formulation of scattering amplitudes in various theories [127][56], and include the D3 theory [106]. Its crucial property is that it vanishes if and only if the two polynomials $\rho_a^A(\sigma)$ and $\rho_a^B(\sigma)$ have a root in common.

A resultant of the form $R(\rho_a^A, \rho_a^B)$, where ρ_a^A and ρ_a^B are both polynomials of degree d , is given by the determinant of a Sylvester matrix $M_a^{(2d)}(A, B)$,

$$R(\rho_a^A, \rho_a^B) = \det M_a^{(2d)}(A, B). \quad (2.93)$$

In particular, $R(\rho_+^1, \rho_+^2) = \det M_+^{(2d)}(1, 2)$ is the resultant of the pair of degree $d = \frac{n}{2} - 1$ polynomials

$$\rho_+^1(\sigma) = \sum_{m=0}^d \rho_{m,+}^1 \sigma^m, \quad \rho_+^2(\sigma) = \sum_{m=0}^d \rho_{m,+}^2 \sigma^m. \quad (2.94)$$

Explicitly, the Sylvester matrix $M_a^{(2d)}(A, B)$ is given by

$$M_a^{(2d)}(A, B) = \begin{pmatrix} \rho_{0,a}^A & \rho_{1,a}^A & \rho_{2,a}^A & \cdots & \cdots & \rho_{d,a}^A & 0 & \cdots & 0 \\ 0 & \rho_{0,a}^A & \rho_{1,a}^A & \cdots & \cdots & \rho_{d-1,a}^A & \rho_{d,a}^A & \cdots & 0 \\ \vdots & \vdots & \cdots & \cdots & \vdots & \vdots & \vdots & \cdots & \vdots \\ 0 & 0 & \cdots & \rho_{0,a}^A & \rho_{1,a}^A & \cdots & \cdots & \rho_{d-1,a}^A & \rho_{d,a}^A \\ \rho_{0,a}^B & \rho_{1,a}^B & \rho_{2,a}^B & \cdots & \cdots & \rho_{d,a}^B & 0 & \cdots & 0 \\ 0 & \rho_{0,a}^B & \rho_{1,a}^B & \cdots & \cdots & \rho_{d-1,a}^B & \rho_{d,a}^B & \cdots & 0 \\ \vdots & \vdots & \cdots & \cdots & \vdots & \vdots & \vdots & \cdots & \vdots \\ 0 & 0 & \cdots & \rho_{0,a}^B & \rho_{1,a}^B & \cdots & \cdots & \rho_{d-1,a}^B & \rho_{d,a}^B \end{pmatrix} \quad (2.95)$$

For instance, for $n = 6$ or $d = 2$, the Sylvester matrices are 4×4 ,

$$M_a^{(4)}(A, B) = \begin{pmatrix} \rho_{0,a}^A & \rho_{1,a}^A & \rho_{2,a}^A & 0 \\ 0 & \rho_{0,a}^A & \rho_{1,a}^A & \rho_{2,a}^A \\ \rho_{0,a}^B & \rho_{1,a}^B & \rho_{2,a}^B & 0 \\ 0 & \rho_{0,a}^B & \rho_{1,a}^B & \rho_{2,a}^B \end{pmatrix}. \quad (2.96)$$

To exhibit the residual $U(1)$ little-group symmetry in 4D, we may set $\rho_{d,-}^2 = \rho_{d,+}^4 = 0$ using partly the complexified 6D little-group symmetry $SL(2, \mathbb{C})$. Now we see that all the factors are exactly canceled, except for $\rho_{d,-}^4$, which is precisely the Jacobian for the gauge-fixing of the left-over $U(1)$ symmetry of the 4D theory. Furthermore, the fermionic delta functions of $(2, 0)$ supersymmetry also reduce to the 4D ones, without any complications. Thus, the proposed formula for the M5 amplitude in Eq. (2.71) reduces to the D3 amplitude in Eq. (2.62) under dimensional reduction provided that the factor $U(\rho, \sigma)$ reduces according to

$$U(\rho, \sigma) \rightarrow V^{-2}(\sigma)R(\rho_+^1, \rho_+^2)R(\rho_-^3, \rho_-^4) \quad (2.97)$$

in 4D.

The extra factor $U(\rho, \sigma)$

To complete the construction of the M5 amplitudes, we need to determine the extra factor (relative to the D3 formula) $U(\rho, \sigma)$. We have just learned what it should give when reduced to 4D. This goes a long way towards determining it. We claim that the σ and ρ dependence factorizes already in 6D, so that

$$U(\rho, \sigma) = V^{-2}(\sigma)R(\rho). \quad (2.98)$$

Note that V^{-2} has total symmetry in the n σ_i 's. As will be verified later, V^{-2} transforms under $SL(2, \mathbb{C})$ in the way required to compensate for the additional bosonic coordinates in the M5 theory. The factor $R(\rho)$ should scale like p^{2d} or ρ^{4d} and on reduction to 4D it should give the product of resultants $R(\rho_+^1, \rho_+^2)R(\rho_-^3, \rho_-^4)$. This expression does not have 6D Lorentz invariance or little-group symmetry, so it must be embellished by additional pieces that vanish upon dimensional reduction.

The crucial observation is that the product of resultants $R(\rho_+^1, \rho_+^2)R(\rho_-^3, \rho_-^4)$ can be expressed in terms of $\text{Pf}'S_n$ and the Vandermonde determinant $V(\sigma)$ [106],

$$R(\rho_+^1, \rho_+^2)R(\rho_-^3, \rho_-^4) = \text{Pf}'S_n V(\sigma). \quad (2.99)$$

The above relation is valid for ρ and σ under the constraints of the helicity-conserving sector, Eq. (2.69), which is the case here. As functions of s_{ij} and σ_i , now both $\text{Pf}'S_n$ and $V(\sigma)$ can be lifted to 6D straightforwardly without violating Lorentz invariance.

This leads to our proposal for all tree-level scattering amplitudes of the M5 theory,

$$\mathcal{A}_n = \int \frac{d^n \sigma d\mathcal{M}}{\text{Vol}(G)} \Delta_B(p, \rho) \Delta_F(q, \rho, \chi) \frac{(\text{Pf}'S_n)^3}{V(\sigma)}, \quad (2.100)$$

which is the main result of the chapter. This formula reduces to the D3 amplitude in Eq. (2.62) correctly, and it also has many other correct properties that we will discuss shortly. Importantly, Eq. (2.100) produces known amplitudes as we mentioned.

Alternatively, one can use the definition of the resultant in terms of Sylvester matrix in Eq. (2.95). With that, a different possible uplift to 6D is realized by a natural generalization of the resultant and Sylvester matrix. They are given by,

$$R(\rho) = \det M^{(4d)}, \quad (2.101)$$

where $M^{(4d)}$ is the following $4d \times 4d$ matrix, a generalization of Sylvester matrix,

$$M^{(4d)} = \begin{pmatrix} M_+^{(2d)}(1, 2) & M_-^{(2d)}(1, 2) \\ M_+^{(2d)}(3, 4) & M_-^{(2d)}(3, 4) \end{pmatrix}. \quad (2.102)$$

The subscripts $+$ and $-$ are little-group indices, whereas $SU(4)$ Lorentz indices, $A = 1, 2, 3, 4$, are shown in parentheses. The four submatrices in $M^{(4d)}$ are $2d \times 2d$ matrices, which take the form of Sylvester matrices. Upon dimension reduction, the off-diagonal matrices of $M^{(4d)}$ vanish, and thus $R(\rho)$ also has the required reduction to 4D. So in terms of $R(\rho)$, the scattering amplitudes of M5 theory then take an alternative form,

$$\mathcal{A}_n = \int \frac{d^n \sigma d\mathcal{M}}{\text{Vol}(G)} \Delta_B(p, \rho) \Delta_F(q, \rho, \chi) \det' S_n \frac{R(\rho)}{V^2(\sigma)}. \quad (2.103)$$

In fact, like the case of 4D where the resultant is related to $\text{Pf}' S_n$ and the Vandermonde determinant $V(\sigma)$, we find that, under the support of delta function constraint Δ_B , $R(\rho)$ defined in Eq. (2.101) is related to $\text{Pf}' S_n$ and $V(\sigma)$ in the same way, namely,

$$R(\rho) = \text{Pf}' S_n V(\sigma). \quad (2.104)$$

Plugging this result into Eq. (2.103) reproduces Eq. (2.100). Therefore, these two different approaches actually lead to the same result.

Although the quantity $R(\rho)$ can be re-expressed in terms of $\text{Pf}' S_n$ and $V(\sigma)$ on the support of delta-function constraints, it may still be of interest on its own right. Let us make a few comments on it here before closing this subsection. It is straightforward to show that $R(\rho)$ is invariant under little-group and Lorentz-group transformations, which together act on $R(\rho)$ as $SL(2, \mathbb{C}) \times SL(4, \mathbb{C})$. A natural generalization would be invariant under $SL(k, \mathbb{C}) \times SL(2k, \mathbb{C})$, and it would relate $2k^2$ polynomials of degree d , which transform as bifundamentals. The generalization to $k > 2$ may be relevant for scattering amplitudes of the D-brane theories in dimension greater than six. We will leave this for the future study. The usual resultant, which corresponds to $k = 1$, vanishes whenever the two polynomials have a common zero. It would be interesting to know the generalization of this statement when $k > 1$. In any case, these remarks suggest introducing the alternative notation $R_d^{(k)}(\rho) = \det M_d^{(k)}$, where the matrix $M_d^{(k)}$ has $2kd$ rows and columns. However, we will not utilize that notation in this manuscript.

$SL(2, \mathbb{C})$ symmetry

Let us examine whether Eq. (2.100) has the correct $SL(2, \mathbb{C})$ symmetry which we have emphasized in this thesis. The punctures transform as

$$\sigma'_i = \frac{a \sigma_i + b}{c \sigma_i + d} \quad \text{with} \quad ad - bc = 1. \quad (2.105)$$

Let us begin with the rescaling symmetry, $\sigma_i \rightarrow a \sigma_i$, where a is a nonzero complex number (the square of the preceding a with $b = c = 0$). To maintain the same delta functions, $\Delta_B(p, \rho)$ and $\Delta_F(q, \rho, \chi)$ in Eqs. (2.72) and (2.73), we rescale

$$\rho_m^{Aa} \rightarrow a^{\frac{n-1}{2}-m} \rho_m^{Aa}, \quad \chi_m^{Ia} \rightarrow a^{\frac{n-1}{2}-m} \chi_m^{Ia}. \quad (2.106)$$

With this rescaling

$$V^{-1}(\sigma) \rightarrow a^{-\frac{n}{2}+\frac{n}{2}} V^{-1}(\sigma), \quad (2.107)$$

$$\text{Pf}' S_n \rightarrow a^{-\frac{n}{2}} \text{Pf}' S_n, \quad (2.108)$$

$$\prod_{i=1}^n d\sigma_i \rightarrow a^n \prod_{i=1}^n d\sigma_i, \quad (2.109)$$

$$\prod_{m=0}^d d^8 \rho_m^{Aa} d^4 \chi_m^{Ia} \rightarrow a^{\frac{n^2}{2}} \prod_{m=0}^d d^8 \rho_m^{Aa} d^4 \chi_m^{Ia}. \quad (2.110)$$

Thus all the factors of a cancel out, and scale invariance is verified.

Next let us consider inversion, $\sigma_i \rightarrow -1/\sigma_i$.⁴ First we note that

$$P_i(\sigma) \rightarrow \left(\prod_{j=1}^n \sigma_j^{-1} \right) \sigma_i^{2-n} P_i(\sigma). \quad (2.111)$$

Therefore, we rescale ρ_m^{Aa} and χ_m^{Ia} to keep the delta functions unchanged by

$$\rho_m^{Aa} \rightarrow (-1)^m \left(\prod_{j=1}^n \sigma_j^{-1/2} \right) \rho_{d-m}^{Aa}, \quad \chi_m^{Ia} \rightarrow (-1)^m \left(\prod_{j=1}^n \sigma_j^{-1/2} \right) \chi_{d-m}^{Ia}. \quad (2.112)$$

Under such rescalings, we have,

$$V(\sigma) \rightarrow \left(\prod_{j=1}^n \sigma_j^{1-n} \right) V(\sigma) \quad (2.113)$$

and

$$\text{Pf}' S_n \rightarrow \left(\prod_{j=1}^n \sigma_j \right) \text{Pf}' S_n, \quad (2.114)$$

⁴The minus sign is unnecessary, because we could set $a = -1$ in the preceding scaling symmetry, but it reduces the need to keep track of minus signs.

while the measure behaves as

$$\prod_{i=1}^n d\sigma_i \prod_{m=0}^d d^8 \rho_m^{Aa} d^4 \chi_m^{Ia} \rightarrow \left(\prod_{j=1}^n \sigma_j^{-n-2} \right) \prod_{i=1}^n d\sigma_i \prod_{m=0}^d d^8 \rho_m^{Aa} d^4 \chi_m^{Ia}. \quad (2.115)$$

Combine all the contributions, the invariance under inversion becomes clear.

Finally, let us consider translation, $\sigma_i \rightarrow \sigma_i + b$. This leaves $V(\sigma)$, $P_i(\sigma)$, and $\text{Pf}'S_n$ invariant. So we let $\rho \rightarrow \rho'$ and $\chi \rightarrow \chi'$ such that

$$\sum_{m=0}^d \rho_m^{Aa} (\sigma_i + b)^m = \sum_{m=0}^d \rho_m'^{Aa} \sigma_i^m, \quad \sum_{m=0}^d \chi_m^{Ia} (\sigma_i + b)^m = \sum_{m=0}^d \chi_m'^{Ia} \sigma_i^m. \quad (2.116)$$

It is easy to see that the integration measures are also invariant under this transformation, since the Jacobian is the determinant of a triangular matrix with 1's on the diagonal.

Factorization

The formula for the amplitude \mathcal{A}_n in Eq. (2.100) is an integral over sets of polynomials $\rho_a^A(\sigma)$ and $\chi_a^I(\sigma)$ of degree $d = \frac{n}{2} - 1$. To study the multi-particle factorization behavior of the amplitudes, one may take a limit on the moduli space such that the higher-degree polynomials degenerate into products of lower-degree ones [128, 129, 130]. Specifically, there is a ‘‘left’’ factor containing polynomials of degree $d_L = \frac{n_L}{2} - 1$ and a ‘‘right’’ factor containing polynomials of degree $d_R = \frac{n_R}{2} - 1$, where $d_L + d_R = d$ or $n_L + n_R = n + 2$. To achieve this goal, we introduce a parameter s that approaches zero in the desired limit and perform the following rescaling of the ρ_m 's⁵

$$\begin{aligned} \rho_m &\rightarrow t_L s^{d_L - m} \rho_{L, d_L - m}, & \text{for } m = 0, 1, \dots, d_L \\ \rho_m &\rightarrow t_R s^{m - d_L} \rho_{R, m - d_L}, & \text{for } m = d_L, d_L + 1, \dots, d, \end{aligned} \quad (2.117)$$

with

$$t_L^2 = (-1)^{n-1} s^{-2d_R - 1} \frac{\prod_{i \in R} \sigma_i}{\prod_{i \in L} \sigma_i} \quad (2.118)$$

and

$$t_R^2 = s^{-2d_R - 1}, \quad (2.119)$$

where L or R denotes the set of particles on the left- or right-hand side of a factorization channel.

⁵We thank Ellis Yuan for a discussion about the factorization limit.

We will show that the left-hand side of the factorization channel has polynomials of degree d_L and the right-hand side has polynomials of degree d_R . Accordingly, we rename the ρ 's as either ρ_L or ρ_R . Note ρ_{d_L} appears on both sides, but we separate it into two coordinates by setting $\rho_{d_L} = \rho_{L,0}$ and $\rho_{d_L} = \rho_{R,0}$, and introducing $\int d\rho_{L,0}\delta(\rho_{L,0} - \rho_{R,0})$. Now for the σ_i 's, we make the replacements

$$\begin{aligned} \sigma_i &\rightarrow \frac{s}{\sigma_i}, & \text{for } i \in L \\ \sigma_i &\rightarrow \frac{\sigma_i}{s}, & \text{for } i \in R \end{aligned} \quad (2.120)$$

In the limit $s \rightarrow 0$, a degree- d polynomial degenerates into a product of degree d_L or d_R polynomials, depending on whether the particle is on the left- or the right-hand side, namely

$$\begin{aligned} \rho_a^A(\sigma_i) &= \sum_{m=0}^d \rho_m^{Aa} \sigma_i^m \rightarrow \rho_{L,a}^A(\sigma_i) = \sum_{m=0}^{d_L} \rho_{L,m}^{Aa} \sigma_i^m & \text{for } i \in L, \\ \rho_a^A(\sigma_i) &= \sum_{m=0}^d \rho_m^{Aa} \sigma_i^m \rightarrow \rho_{R,a}^A(\sigma_i) = \sum_{m=0}^{d_R} \rho_{R,m}^{Aa} \sigma_i^m & \text{for } i \in R. \end{aligned} \quad (2.121)$$

It is also straightforward to see that the delta functions reduce to the corresponding lower-point delta functions, namely,

$$p_i^{AB} - \frac{\rho_a^A(\sigma_i)\rho^{Ba}(\sigma_i)}{P_i(\sigma)} = 0 \rightarrow p_i^{AB} - \frac{\rho_{L,a}^A(\sigma_i)\rho_L^{Ba}(\sigma_i)}{P_{L,i}(\sigma)} = 0, \quad \text{or} \quad p_i^{AB} - \frac{\rho_{R,a}^A(\sigma_i)\rho_R^{Ba}(\sigma_i)}{P_{R,i}(\sigma)} = 0 \quad (2.122)$$

depending on whether σ_i is on the left or the right. If $i \in L$, $P_{L,i}(\sigma) = (0 - \sigma_i) \prod_{j \neq i}^{n_L} (\sigma_{ji})$, where “0” is the value of the σ coordinate associated to the internal line in the factorization, and similarly for $i \in R$.

It is important that the integrand and the integration measure factorize correctly, and this is straightforward to see for the measure. On the other hand, the building blocks of the integrand, the Vandermonde determinant $V(\sigma)$ and $\text{Pf}'S_n$, have already appeared in literature in the construction of scattering amplitudes in other theories; they are also known to factorize correctly. Alternatively for the proposal Eq. (2.103), we find the new mathematical object we constructed, $R_n(\rho)$, also factorizes properly in the $s \rightarrow 0$ limit,

$$\begin{aligned} R_n(\rho_0, \rho_1, \dots, \rho_d) &\rightarrow t_L^{Ad_L} t_R^{Ad_R} s^{2(d_L^2 + d_R^2)} R_{n_L}(\rho_{L,0}, \rho_{L,1}, \dots, \rho_{L,d_L}) \\ &\quad \times R_{n_R}(\rho_{R,0}, \rho_{R,1}, \dots, \rho_{R,d_R}). \end{aligned} \quad (2.123)$$

Here the subscript of ρ_m denotes the index m of $\rho_m^{A,a}$, and we have suppressed Lorentz and little-group indices A and a

Finally, because $P_L^2 \sim s^2$ in the limit $s \rightarrow 0$ at a factorization pole $1/P_L^2$, the amplitude should go as ds^2/s^2 [130]. By collecting all of the s factors arising from the integration measure and the various factors in the integrand, we have verified that this is indeed the case. Thus, the general formula Eq. (2.100) has the required factorization properties for a tree-level scattering amplitude.

Soft theorems

As we discussed previously, the five scalars of the M5 theory are Goldstone bosons arising from spontaneous breaking of 11D Poincaré symmetry. More specifically, the relevant broken symmetries are translations in the five spatial directions that are orthogonal to the M5-brane. Let us now study how the scattering amplitudes of the M5 theory behave in soft limits, *i.e.*, in the limit where the momentum p^{AB} of a Goldstone boson vanishes. As shown in [131], amplitudes involving such scalars have enhanced soft behavior [132], specifically

$$A(p_1, \dots, p_{n-1}, \tau p_n) \sim \mathcal{O}(\tau^2), \quad (2.124)$$

where particle n is a scalar, with momentum τp_n , and the soft limit is realized by $\tau \rightarrow 0$. Of course, some of the other momenta should also depend on τ , so as to maintain momentum conservation and masslessness.

We claim that the amplitudes obtained from general formula in Eq. (2.100) indeed have this enhanced soft behavior. In particular, if we rescale $\lambda_n^{A,a} = \tau^{1/2} \lambda_n^{A,a}$, so that the momentum p_n is replaced by τp_n , we find that the various pieces that contribute to the amplitude scale as follows

$$(\text{Pf}' S)^3 \sim \tau^3, \quad J_B \sim \tau^{-1}, \quad J_F \sim \tau^0, \quad (2.125)$$

and the rest, including the Vandermonde determinant $V(\sigma)$, scales as τ^0 in the soft limit. As discussed in Appendix A.1, J_B and J_F are Jacobians that arise from extracting various “wave functions” and momentum-conservation delta functions, and from performing integrations over σ 's, ρ 's, and χ 's. J_F also depends on the fact that we are considering a scalar component of the supermultiplet. Altogether, we obtain the expected $\mathcal{O}(\tau^2)$ behavior of the amplitudes in the M5 theory.

Just for the comparison, in the case of the D3 theory, in the soft limit each piece in Eq. (2.53) behaves as

$$\det' S \sim \tau^2, \quad J_B \sim \tau^0, \quad J_F \sim \tau^0. \quad (2.126)$$

In total, the amplitudes again scale correctly, namely as $\mathcal{O}(\tau^2)$.

We can also study how the amplitudes behave in the double-soft limit, where we let two momenta approach zero simultaneously, say, $p_{n+1} \rightarrow \tau p_{n+1}$ and $p_{n+2} \rightarrow \tau p_{n+2}$ with $\tau \rightarrow 0$. For simplicity, here we only consider the leading soft theorems. The result of the double-soft limit depends on the species of particles involved as shown here

$$\begin{aligned} A_{n+2}(\phi, \bar{\phi}) &= \sum_{i=1}^n \frac{(s_{n+1i} - s_{n+2i})^2}{(s_{n+1i} + s_{n+2i})} A_n + \dots, \quad (2.127) \\ A_{n+2}(\psi_a, \tilde{\psi}_b) &= \sum_{i=1}^n \langle (n+1)_a (n+2)_b i_+ i_- \rangle \frac{(s_{n+1i} - s_{n+2i})}{(s_{n+1i} + s_{n+2i})} A_n + \dots, \\ A_{n+2}(B_{a_1 b_1}, B_{a_2 b_2}) &= \sum_{i=1}^n \frac{\langle (n+1)_{a_1} (n+2)_{a_2} i_+ i_- \rangle \langle (n+1)_{b_1} (n+2)_{b_2} i_+ i_- \rangle}{(s_{n+1i} + s_{n+2i})} A_n + \dots. \end{aligned}$$

The soft particles $\phi, \bar{\phi}$ (and $\psi, \tilde{\psi}$) are conjugate to each other to form an R-symmetry singlet. The ellipsis denotes higher-order terms in the soft limit, and the lower-point amplitude A_n is the amplitude with the two soft particles removed. In the case of soft theorems for B fields, on the right-hand side one should symmetrize the little-group indices a_1, b_1 and a_2, b_2 .

The double-soft theorems for the scalars and fermions agree with the known result [131] derived from the Ward identity for scalars that are Goldstone bosons of spontaneously broken higher-dimensional Poincaré symmetry, while the fermions are Goldstinos of broken supersymmetries. The double-soft theorems for B fields are new; it would be of interest to study the corresponding symmetries. If we choose both of the soft B fields to be B_{+-} and reduce to 4D, we obtain the double-soft result for scalars as in the first line of Eq. (2.127). If, instead, we take the two soft B fields to be B_{--} and B_{++} , and reduce to 4D, we obtain the double-soft theorem for photons in Born–Infeld theory, namely

$$A_{n+2}(\gamma_+, \gamma_-) = \sum_{i=1}^n \frac{[n+1i]^2 \langle n+2i \rangle^2}{(s_{n+1i} + s_{n+2i})} A_n + \dots, \quad (2.128)$$

which agrees with what was found in [105]. Similarly, the double-soft theorem for fermions reproduces that of Volkov–Akulov theory upon reduction to 4D

[133]. To obtain these results we have applied the following identities for the dimensional reduction $6D \rightarrow 4D$, according to our convention,

$$\begin{aligned} \langle k_+ l_+ i_- j_- \rangle &\rightarrow -\langle kl \rangle [ij], & [k_+ l_+ i_- j_-] &\rightarrow -\langle kl \rangle [ij], \\ \langle i_- j_- k_- l_\pm \rangle &\rightarrow 0, & \langle i_+ j_+ k_+ l_\pm \rangle &\rightarrow 0, \\ [i_- j_- k_- l_\pm] &\rightarrow 0, & [i_+ j_+ k_+ l_\pm] &\rightarrow 0. \end{aligned} \quad (2.129)$$

Six- and eight-particle amplitudes of the M5 theory

As an application of the n -particle amplitude in Eq. (2.100), this section presents analytic results for some specific amplitudes of the M5 theory, namely six- and eight-particle amplitudes of self-dual B fields. To our knowledge, these amplitudes have not been presented in the literature before. The use of spinor-helicity variables circumvents the usual difficulties associated to the lack of a manifestly covariant formulation of the M5-brane action. Still, it is not easy to directly compute any higher-point amplitudes analytically, especially due to the fact that the scattering-equation constraints are high-degree polynomial equations whose solutions are rather complicated. The approach that we have used to obtain analytic results is to write down an ansatz with unknown coefficients for the amplitude of interest, and then to fix the coefficients by comparing the ansatz with the result obtained from the general formula in Eq. (2.100).

Let us begin with the six-particle amplitude of B_{++} . Recall that the B particles form a triplet of the $SU(2)$ helicity group. B_{++} corresponds to the $J_3 = 1$ component of this triplet. (The other two components are $B_{+-} = B_{-+}$ and B_{--} .) The ansatz clearly should have correct factorization properties. Specifically, the amplitude should contain poles at which the residue factorizes as a product of two four-point amplitudes,

$$\begin{aligned} &A(B_{++}, B_{++}, B_{++}, B_{++}, B_{++}, B_{++}) \\ &\rightarrow \sum_{a,b} \frac{A_L(B_{++}, B_{++}, B_{++}, B_{ab}) A_R(\bar{B}_{ab}, B_{++}, B_{++}, B_{++})}{P_L^2}. \end{aligned} \quad (2.130)$$

The summation over a, b denotes the fact that the internal B_{ab} can be B_{++} , B_{--} and B_{+-} , whereas \bar{B}_{ab} is the conjugate. Here we have used the fact that $A(B_{++}, B_{++}, B_{++}, B_{ab})$ are the only non-vanishing four-point amplitudes involving three B_{++} 's allowed by R symmetry. Recall the known result of

$A(B_{++}, B_{++}, B_{++}, B_{ab})$, given in Sect. 2.2,

$$A(B_{++}, B_{++}, B_{++}, B_{ab}) = \langle 1_+ 2_+ 3_+ 4_a \rangle \langle 1_+ 2_+ 3_+ 4_b \rangle. \quad (2.131)$$

where we have used the bracket notation defined in Eq. (2.34). Using the results of Eq. (2.130) and Eq. (2.131), it is straightforward to write an ansatz that has the correct factorization properties,

$$A(B_{++}, B_{++}, B_{++}, B_{++}, B_{++}, B_{++}) = \frac{1}{s_{123}} \left(\sum_{i=1}^3 \langle 1_+ 2_+ 3_+ i_a \rangle \langle i^a 4_+ 5_+ 6_+ \rangle \right)^2 + \mathcal{P}_6 \quad (2.132)$$

here \mathcal{P}_6 means summing over all ten factorization channels (nine in addition to the one that is shown).

The ansatz in Eq. (2.132) is the simplest guess that has the correct factorization and little-group properties, and it ends up being correct. It is instructive to see how one arrives at this conclusion using Feynman diagrams without recourse to an action. At the poles we can represent the six-point amplitude in Eq. (2.132) as a sum of exchange diagrams that are the product of four-point amplitudes and an internal propagator. These diagrams are shown in Fig. (2.1).

In evaluating these diagrams, one must sum over all exchange channels as well as all fields allowed to propagate on the internal lines. As we have explained, only B_{++}, B_{--} , or $B_{+-} = B_{-+}$ can be exchanged. The pure positive and negative helicity states are conjugates of each other, and as with chiral fermions we use an arrow to distinguish them from the neutral helicity.

The sum of such diagrams must be invariant under the little group of the internal particle, and this ends up being the case due to a subtlety in the spinor-helicity formalism. This “glitch” in the spinor-helicity formalism as discussed for 6d SYM in [122] is that the spinors cannot distinguish particles and antiparticles, which causes issues for diagrams with fermions. A new feature of 6d chiral self-dual tensors is that the tensor field itself has this issue with the B_{++} and B_{--} polarizations. The resolution, as outlined in [122], is to add extra factors of i to the spinor-helicity variables when we flip the sign of the momentum for either of these fields:

$$\lambda_a^A(-p) = i\lambda_a^A(p) \quad (2.133)$$

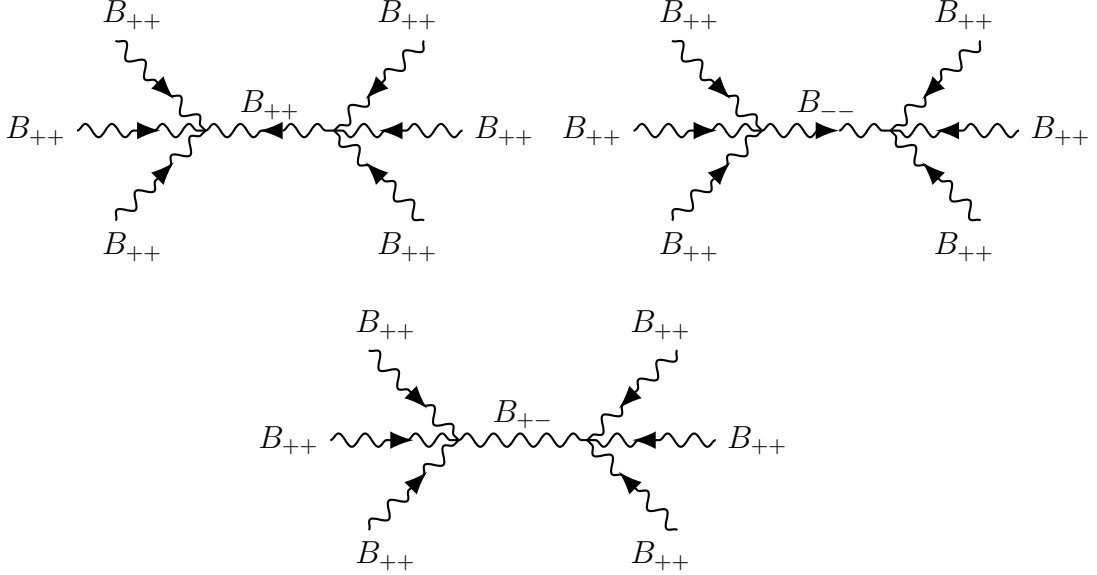


Figure 2.1: Exchange diagrams contributing to the 6 B_{++} amplitude. The internal line may be any of the three states, and we sum over all the factorization channels as well. It is important to note that these diagrams do not come directly from Feynman rules as there is no covariant action available for the M5 theory; instead, they represent the factorization of the amplitude at the poles where $s_{ijk} \rightarrow 0$.

so that the momentum is properly

$$\lambda_a^A(-p)\lambda^{Ba}(-p) = -p^{AB}. \quad (2.134)$$

This introduces additional minus signs for a four-particle amplitude of the form

$$A(B_{++}(+p_1), B_{++}(+p_2), B_{++}(+p_3), B_{\pm\pm}(-p)) = \langle 1_+ 2_+ 3_+ i\lambda_{\pm} \rangle \langle 1_+ 2_+ 3_+ i\lambda_{\pm} \rangle. \quad (2.135)$$

Applying this recipe to the exchange diagrams of Fig. (2.1), one is led directly to Eq. (2.132), which does not depend on the little-group structure of the internal line, as it should be.

Of course, Eq. (2.132) might not be the final result, since it could differ from the correct answer by terms that have no poles (thought of as a 6-particle contact interaction, depicted in Fig. 2.2). The only local term allowed by power counting and little-group constraints is

$$\langle 1_+ 2_+ 3_+ 4_+ \rangle \langle 1_+ 2_+ 5_+ 6_+ \rangle \langle 3_+ 4_+ 5_+ 6_+ \rangle + \mathcal{P}_6. \quad (2.136)$$

It turns out that this local term vanishes identically after summing over the permutations. Thus, we claim that Eq. (2.132) is the complete result for the amplitude of six B_{++} 's. Indeed, we find perfect agreement by comparing Eq. (2.132) numerically with the general integral formula Eq. (2.100).

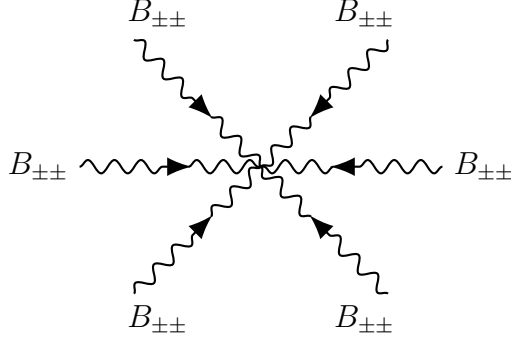


Figure 2.2: Diagrammatic expression of the local term for a six-particle amplitude. In the example where all external particles are B_{ab} , this local term vanishes, and the exchange diagrams are the only contribution to the total amplitude.

One can perform a similar analysis for more general amplitudes of self-dual B fields. In all cases we find that the result takes a form similar to Eq. (2.132),

$$A(B_{a_1 b_1}, B_{a_2 b_2}, B_{a_3 b_3}, B_{a_4 b_4}, B_{a_5 b_5}, B_{a_6 b_6}) \quad (2.137)$$

$$= \frac{1}{s_{123}} \left(\sum_{i=1}^3 \langle 1_{a_1} 2_{a_2} 3_{a_3} i_a \rangle \langle i^a 4_{a_4} 5_{a_5} 6_{a_6} \rangle \right) \left(\sum_{j=1}^3 \langle 1_{b_1} 2_{b_2} 3_{b_3} j_b \rangle \langle j^b 4_{b_4} 5_{b_5} 6_{b_6} \rangle \right) + \mathcal{P}_6.$$

The symbol \mathcal{P}_6 represents the symmetrization of the little-group indices a_i, b_i for all $i = 1, 2, \dots, 6$, and the summation over all other factorization channels.

It is instructive to consider the reduction of these results to the D3 theory. B_{++} and B_{--} reduce to positive- and negative-helicity photons γ_+ and γ_- in 4D, while B_{+-} reduces to a scalar. If we restrict to external B_{++} and B_{--} only, then $A(B_{++}, B_{++}, B_{++}, B_{--}, B_{--}, B_{--})$ is the only amplitude that is non-vanishing after dimensional reduction to 4D. This is consistent with the claim that the amplitudes of the D3 theory are helicity conserving. The helicity-conserving amplitude obtained in this way is

$$A(\gamma_+, \gamma_+, \gamma_+, \gamma_-, \gamma_-, \gamma_-) = \frac{1}{s_{124}} [12]^2 \langle 56 \rangle^2 \langle 4|1+2|3 \rangle^2 + \mathcal{P}_6, \quad (2.138)$$

where $\langle 4|1+2|3 \rangle := \langle 41 \rangle [13] + \langle 42 \rangle [23]$, and the permutations \mathcal{P}_6 sum over γ_+ 's and γ_- 's, respectively. The amplitude in Eq. (2.138) obtained by dimensional

reduction agrees with the amplitude for six photons in the D3 theory computed for instance in [134]. We also find that Eq. (2.137) for the case of six B_{+-} 's reduces correctly to the amplitude for six identical scalars,

$$\left(\frac{(s_{12}^2 + s_{13}^2 + s_{23}^2)(s_{45}^2 + s_{46}^2 + s_{56}^2)}{s_{123}} + \dots \right) - \frac{1}{2} (s_{123}^3 + \dots), \quad (2.139)$$

where the ellipsis in the parentheses denote summation over all factorization channels, as well as all other independent s_{ijk} 's for six-particle kinematics. It is straightforward to verify that this is the unique amplitude for identical scalars determined by the soft theorem.

One can also consider amplitudes of other particles. For instance, we find that the six-particle amplitude of ϕ_{IJ} in the spectrum Eq. (2.12) agrees with the result in Eq. (2.139). Also, the amplitude for six fermions can be expressed as

$$A(\psi_+^I, \psi_+, \psi_+^I, \tilde{\psi}_-^I, \tilde{\psi}_-, \tilde{\psi}_-^I) = A_f^{(6)} - \frac{1}{12} A_c^{(6)}, \quad (2.140)$$

where the factorization term $A_f^{(6)}$ and the local term $A_c^{(6)}$ are given by

$$\begin{aligned} A_f^{(6)} &= \frac{1}{s_{124}} \left(\sum_{i=1,2,4} \langle 1_+ 4_+ 4_- i_a \rangle \langle i^a 5_- 6_+ 6_- \rangle \right) \left(\sum_{j=1,2,4} \langle 2_+ 4_- j_+ j_- \rangle \langle 3_+ 6_- 5_+ 5_- \rangle \right) + \mathcal{P}_6 \\ A_c^{(6)} &= \langle 1_+ 2_+ 3_+ 4_- \rangle \langle 5_- 6_- 4_+ 4_- \rangle \langle 5_+ 5_- 6_+ 6_- \rangle + \mathcal{P}_6, \end{aligned} \quad (2.141)$$

where \mathcal{P}_6 denotes summing over anti-symmetrizations among all ψ and $\tilde{\psi}$ particles separately. Reduced to 4D, the six-fermion amplitude gives that of Volkov-Akulov theory computed in [135].

Let us now consider the amplitudes with eight B particles. For simplicity, we only consider the amplitude with eight B_{++} 's and the amplitude with seven B_{++} 's and one B_{--} . As we will see, they take a very similar form. The strategy is the same as in the case of six-particle amplitudes. We write down an ansatz that includes factorization parts and local terms, and then compare the ansatz against the general formula to determine the unknown coefficients. As before, one can arrive at the ansatz for exchange diagrams by summing diagrams that are products of amplitudes with fewer particles. Unlike the case of six B particles, we find that in general there are contributions from local terms. Explicitly, we find

$$A(B_{++}, B_{++}, B_{++}, B_{++}, B_{++}, B_{++}, B_{++}, B_{aa}) = A_f^{(8)} - 2A_c^{(8)}, \quad (2.142)$$

where the little-group index a can be $+$ or $-$ depending on whether B_{aa} is B_{++} or B_{--} , and $A_f^{(8)}, A_c^{(8)}$ are the factorization part and the local term, respectively. $A_f^{(8)}$ and $A_c^{(8)}$ are given by

$$\begin{aligned} A_f^{(8)} &= \frac{1}{s_{123} s_{678}} \left(\sum_{i=1}^3 \sum_{j=6}^8 \langle 1_+ 2_+ 3_+ i_b \rangle \langle i^b 4_+ 5_+ j_c \rangle \langle j^c 6_+ 7_+ 8_a \rangle \right)^2 \\ &+ \frac{1}{s_{123} s_{567}} \left(\sum_{i=1}^3 \sum_{j=5}^7 \langle 1_+ 2_+ 3_+ i_b \rangle \langle i^b 4_+ 8_a j_c \rangle \langle j^c 5_+ 6_+ 7_+ \rangle \right)^2 + \mathcal{P}_8, \\ A_c^{(8)} &= (\langle 1_+ 2_+ 3_+ 4_+ \rangle \langle 5_+ 6_+ 7_+ 8_a \rangle)^2 + \mathcal{P}_8, \end{aligned} \quad (2.143)$$

where \mathcal{P}_8 denotes the summation over independent permutations.

As mentioned previously, the amplitudes involving scalars in the M5 theory should satisfy soft theorems. Some such amplitudes are completely fixed by the soft theorems. Therefore they can also be computed in a completely different way via on-shell recursion relations [126]. We have verified that the results agree perfectly with what is obtained from the proposed formula, Eq. (2.100), for such amplitudes containing up to eight particles.

2.6 n -Particle Amplitudes of the D5 Theory

This section describes the tree-level S matrix for the theory of a single probe D5-brane with 6D $\mathcal{N} = (1, 1)$ supersymmetry. The general formula we propose for the D5 theory takes a form similar to that of the M5 theory, which we discussed in the previous section. In particular, the formula contains the same factors of $\det' S_n$ and $U(\rho, \sigma)$,

$$\mathcal{A}_n = \int \frac{d^n \sigma d\mathcal{M}}{\text{Vol}(G)} \Delta_B(p, \rho) \Delta_F(q, \rho, \chi) \hat{\Delta}_F(\hat{q}, \hat{\rho}, \hat{\chi}) \det' S_n \frac{R(\rho)}{V^2(\sigma)}, \quad (2.144)$$

or equivalently

$$\mathcal{A}_n = \int \frac{d^n \sigma d\mathcal{M}}{\text{Vol}(G)} \Delta_B(p, \rho) \Delta_F(q, \rho, \chi) \hat{\Delta}_F(\hat{q}, \hat{\rho}, \hat{\chi}) \frac{(\text{Pf}' S_n)^3}{V(\sigma)}. \quad (2.145)$$

The bosonic delta functions are the same as those in the M5 theory

$$\Delta_B(p, \rho) = \prod_{i=1}^n \delta^6 \left(p_i^{AB} - \frac{\rho_a^A(\sigma_i) \rho^{Ba}(\sigma_i)}{P_i(\sigma)} \right), \quad (2.146)$$

but now there are two kinds of fermionic delta functions due to (1, 1) supersymmetry,

$$\begin{aligned}\Delta_F(q, \rho, \chi) &= \prod_{i=1}^n \delta^4 \left(q_i^A - \frac{\rho_a^A(\sigma_i) \chi^a(\sigma_i)}{P_i(\sigma)} \right), \\ \hat{\Delta}_F(\hat{q}, \hat{\rho}, \hat{\chi}) &= \prod_{i=1}^n \delta^4 \left(\hat{q}_{iA} - \frac{\hat{\rho}_{A\hat{a}}(\sigma_i) \hat{\chi}^{\hat{a}}(\sigma_i)}{P_i(\sigma)} \right).\end{aligned}\quad (2.147)$$

The measure is given by

$$d\mathcal{M} = \prod_{m=0}^d d^8 \rho_m^{Aa} d^2 \chi_m^b d^2 \hat{\chi}_m^{\hat{b}}. \quad (2.148)$$

As before, $d = \frac{n}{2} - 1$. Note that this integration measure does not include $d^8 \hat{\rho}_{mA\hat{a}}$, even though $\hat{\rho}_{mA\hat{a}}$ do appear explicitly in the formula. The prescription is that the $\hat{\rho}_{mA\hat{a}}$ are fixed by the constraint of the conjugate of Δ_B in Eq. (2.146), namely,

$$\hat{p}_{iAB} - \frac{\hat{\rho}_{A\hat{a}}(\sigma_i) \hat{\rho}_{B\hat{a}}(\sigma_i)}{P_i(\sigma)} = 0, \quad \text{for } i = 1, 2, \dots, n. \quad (2.149)$$

This constraint does not appear explicitly in the general formula Eq.(2.145), but we impose it implicitly. To fully fix $\hat{\rho}_{mA\hat{a}}$, we also use the second $SU(2)$ factor of the little-group symmetry to fix three of the $\hat{\rho}_{mA\hat{a}}$ coordinates. Since Eq. (2.145) takes a form that is very similar to Eq. (2.100) for the M5 theory, with a simple change to half of the fermionic delta functions due to the change of chirality for half of the supersymmetry, it is straightforward to show that Eq. (2.145) also has all of the required properties, such as correct factorizations, soft theorems, and reduction to the D3 theory. Thus, we will not repeat the analysis and discussion here.

For computing scattering amplitudes from Eq. (2.145), as in the case of the D3 theory and M5 theory, we again should pull out the bosonic and fermionic “wave functions” first. For the D5 theory, they are given by

$$\mathcal{A}_n = \left(\prod_{i=1}^n \delta(p_i^2) \delta^2 \left(\hat{\lambda}_{iA\hat{a}} q_i^A \right) \delta^2 \left(\lambda_{i\hat{b}}^B \hat{q}_{iB} \right) \right) A_n. \quad (2.150)$$

The same as in the case of M5 brane, here the constraints $\hat{\lambda}_{iA\hat{a}} q_i^A = 0$ and $\lambda_{i\hat{b}}^B \hat{q}_{iB} = 0$ allow us to express the supercharges in the amplitude A_n as $q_i^A = \lambda_a^A \eta^a$ and $\hat{q}_i^A = \hat{\lambda}_{\hat{a}}^A \hat{\eta}^{\hat{a}}$. We have checked explicitly that A_n , as defined here,

produces the correct fully supersymmetric four-particle amplitudes, as well as many examples of six- and eight-particle amplitudes in the D5 theory. Here we list the analytical results for some of these amplitudes.

The amplitude for six photons with the same helicity, given by $A_{1\hat{1}}$, is

$$\begin{aligned} & A(A_{1\hat{1}}, A_{1\hat{1}}, A_{1\hat{1}}, A_{1\hat{1}}, A_{1\hat{1}}, A_{1\hat{1}}) \quad (2.151) \\ &= \frac{1}{s_{123}} \left(\sum_{i=1}^3 \langle 1_{\hat{1}} 2_{\hat{1}} 3_{\hat{1}} i_a \rangle \langle i^a 4_{\hat{1}} 5_{\hat{1}} 6_{\hat{1}} \rangle \right) \left(\sum_{j=1}^3 [1_{\hat{1}} 2_{\hat{1}} 3_{\hat{1}} \hat{j}_a] [\hat{j}^a 4_{\hat{1}} 5_{\hat{1}} 6_{\hat{1}}] \right) + \mathcal{P}_6. \end{aligned}$$

There are similar expressions for other choices of helicities of $A_{a\hat{a}}$. We have verified that these results agree with the amplitudes obtained directly from the Born–Infeld action. One can also consider the amplitude of eight $A_{1\hat{1}}$'s, which takes the form

$$A(A_{1\hat{1}}, A_{1\hat{1}}, A_{1\hat{1}}, A_{1\hat{1}}, A_{1\hat{1}}, A_{1\hat{1}}, A_{1\hat{1}}, A_{1\hat{1}}) = A_f - 2A_c. \quad (2.152)$$

The factorization term A_f and the local term A_c are given by

$$\begin{aligned} A_f &= \frac{1}{s_{123} s_{678}} \left(\sum_{i=1}^3 \sum_{j=6}^8 \langle 1_{\hat{1}} 2_{\hat{1}} 3_{\hat{1}} i_a \rangle \langle i^a 4_{\hat{1}} 5_{\hat{1}} j_b \rangle \langle j^b 6_{\hat{1}} 7_{\hat{1}} 8_{\hat{1}} \rangle \right) \quad (2.153) \\ &\quad \times \left(\sum_{i=1}^3 \sum_{j=6}^8 [1_{\hat{1}} 2_{\hat{1}} 3_{\hat{1}} \hat{i}_a] [\hat{i}^a 4_{\hat{1}} 5_{\hat{1}} \hat{j}_b] [\hat{j}^b 6_{\hat{1}} 7_{\hat{1}} 8_{\hat{1}}] \right) + \mathcal{P}_8, \\ A_c &= (\langle 1_{\hat{1}} 2_{\hat{1}} 3_{\hat{1}} 4_{\hat{1}} \rangle \langle 5_{\hat{1}} 6_{\hat{1}} 7_{\hat{1}} 8_{\hat{1}} \rangle) ([1_{\hat{1}} 2_{\hat{1}} 3_{\hat{1}} 4_{\hat{1}}] [5_{\hat{1}} 6_{\hat{1}} 7_{\hat{1}} 8_{\hat{1}}]) + \mathcal{P}_8. \quad (2.154) \end{aligned}$$

These results for photon amplitudes in the D5 theory take a form that is very similar to the amplitudes of B_{ab} particles in the M5 theory. They are related to each other by replacing the anti-chiral $\hat{\lambda}_{\hat{a}}$ by the chiral one λ_a .

The similarity between D5 and M5 amplitudes in the above explicit examples, and more generally the formulas Eq. (2.145) and Eq. (2.100), may be surprising, especially given the fact that the classical action for the M5 theory is more subtle to write down than the one for the D5 theory. However, one should note that the entire difference between the four-particle amplitudes, which are completely fixed by the symmetries and power counting in the D5 theory and the M5 theory, is just a simple modification of the fermionic delta functions. Since both theories reduce to the same 4D amplitudes, the similarity is really not so surprising. The complication of writing the classical M5 action caused by the self-duality of B field is avoided by considering only the on-shell degrees of freedom for the S matrix using the spinor-helicity formalism.

2.7 Conclusion

This chapter has proposed general formulas for n -particle on-shell tree-level scattering amplitudes for three theories: the D3 and D5 theories of type IIB superstring theory and, especially, the M5 theory of 11D M-theory. The scattering amplitudes of the M5 theory— even its bosonic truncation — have been studied little in the previous literature. In each of these theories n is required to be even, and the amplitudes take similar forms, expressed as integrals over rational constraints, built from degree $d = \frac{n}{2} - 1$ polynomials. The integrand contains a new mathematical ingredient, a generalization of resultant (denoted $R(\rho)$ in the text), which is equal to the product of $\text{Pf}' S_n$ and the Vandermonde determinant $V(\sigma)$ on the support of the rational constraints.

The three theories are related to one another in various ways. For instance, dimensional reduction of each of the 6D n -particle amplitudes, which pertain to the D5 and M5 theories, reduces to the same 4D n -particle amplitude, which pertains to the D3 theory. The function $U(\rho, \sigma)$ in the 6D integrands cancels the Jacobian factors arising from the dimensional reduction. As we explained, one consequence is that the R symmetry of the D3 theory is $SU(4) \times U(1)$. The $U(1)$ factor implies that the D3 amplitudes are helicity conserving. Interestingly, the formulas for the M5 and D5 amplitudes only differ by a simple modification of the fermionic delta functions that accounts for the chirality difference between $(2, 0)$ supersymmetry and $(1, 1)$ supersymmetry.

We have also checked various general properties such as $SL(2, \mathbb{C})$ modular symmetry, R symmetries, factorization properties, and soft limits. We have further tested the formulas by explicitly computing amplitudes that are fixed by the soft theorems, up to 8 particles. Using the general formulas, compact analytic expressions for six- and eight-particle amplitudes of self-dual B particles of the M5 theory for certain choices of the little-group indices were obtained.

Our formulas for scattering amplitudes are similar to those for the twistor-string formulation of 4D $\mathcal{N} = 4$ super Yang–Mills amplitudes in Witten’s twistor-string paper [46]. Those amplitudes, and their generalizations, see e.g. [136][60], are understood in terms of two-dimensional world-sheet twistor-string theories. It would be interesting to explore whether there exists a similar twistor-string theory for the M5 theory. Such an underlying theory ought to generate the M5 amplitudes in Eq. (2.100) directly. The fact that a twistor-

string-like formulation of the tree-level S-matrix of the M5 theory does exist already points to some deep structures of the theory.

Finally, we note that the rational constraints in 6D consist of a single sector of solutions to the scattering equations, which utilizes all $(n-3)!$ solutions of the arbitrary-dimensional scattering equations. We do not have a general proof of these assertions, but they have been checked explicitly for the cases $n = 4, 6, 8$. It would be nice to prove (or disprove) them and to understand better this general feature of the 6D rational constraints. Upon dimensional reduction to the D3 theory, many of these solutions vanish leaving only contributions from those that correspond to the middle (helicity conserving) sector in 4D. We address the unification of helicity sectors in Chapter 3 of this thesis when we consider 6D SYM. It would also be interesting to study the rational constraints in dimensions greater than six, such as 10D or 11D, and to apply them to the D9-brane theory, as well as the various gauge and gravity theories in those dimensions. Some progress on this problem using a different variation of our formalism was proposed in [137], and it would be interesting to see what theories may be addressed in this way.

THE S -MATRIX OF 6D SUPER YANG–MILLS AND SUPERGRAVITY

3.1 Introduction

So far in Chapter 2, we have discussed scattering amplitudes in various brane theories. These theories are relatively simple, having only even point amplitudes and contact interactions. Our task of this chapter is to search for more interesting 6D amplitudes. Effective theories in 6D are very interesting for a variety of reasons. On a practical side, besides the interest in their own right, computing 6D SYM formulas would allow, for instance, via dimensional reduction, for a unification of 4D helicity sectors for massless amplitudes [138] as well as for obtaining amplitudes along the Coulomb branch of $\mathcal{N} = 4$ SYM, which contains massive particles such as W bosons [122]. Unifying different helicity sectors of 4D $\mathcal{N} = 4$ SYM into a generalization of the Witten–RSV formula in 6D proved to be a difficult problem resisting a solution. This was partially addressed in Chapter 2, but the lack of odd point amplitudes means these brane theories do not provide any 4D helicity information beyond the middle sector. As we have discussed, these 6D D5 and M5 brane theories have $\mathcal{N} = (1, 1)$ and $(2, 0)$ supersymmetry, respectively, and the former is the supersymmetric version of Born–Infeld theory, while the latter describes analogous interactions for a supermultiplet containing an abelian self-dual tensor.

The vanishing of all odd-multiplicity amplitudes in these brane theories describing spontaneously broken symmetries was a great convenience in the previous chapter, and allowed the introduction of polynomial maps:

$$z \rightarrow \rho_a^A(z)\rho_b^B(z)\epsilon^{ab}, \quad (3.1)$$

with $\deg \rho_a^A(z) = n/2 - 1$, such that the total degree of the maps is $n - 2$. Here A is a 6D spinor index while a is a “global” little-group index transforming in $\text{SL}(2, \mathbb{C})$ (“global” meaning that it does not refer to a specific particle.)

It is well known that scattering amplitudes can make symmetries manifest that the corresponding Lagrangian does not. A striking and unexpected example is dual superconformal invariance of $\mathcal{N} = 4$ SYM, which combines with the

standard superconformal invariance to generate an infinite-dimensional structure known as the Yangian of $\text{PSU}(2, 2|4)$ [139]. As discussed previously, the M5-brane theory provides an even more fundamental example. The self-dual condition on the three-form field strength causes difficulties in writing down a manifestly Lorentz invariant action for the two-form gauge field [107, 108]. In contrast, the formulas found in Chapter 2 for the complete tree-level S matrix are manifestly Lorentz invariant. These examples highlight the importance of finding explicit formulas for the complete tree-level S matrix, as they can provide new insights into known symmetries of theories or even the discovery of unexpected ones.

The 6D formulas presented in Chapter 2 are built using two half-integrands, usually called *left* and *right* integrands, $\mathcal{I}_{L/R}$, in the sense of the CHY formulation. In the case of the D5- and M5-brane theories, the right integrand carries the supersymmetric information while the left one is purely bosonic. Amusingly, the only difference in the choice of right integrands is $\mathcal{N} = (1, 1)$ or $\mathcal{N} = (2, 0)$ supersymmetry, and the left half-integrands agree in both theories:

$$\mathcal{I}_L^{\text{D5}} = \mathcal{I}_L^{\text{M5}} = (\text{Pf}' A_n)^2. \quad (3.2)$$

Here A_n is an antisymmetric $n \times n$ matrix whose reduced Pfaffian has made an appearance in CHY formulas for the non-linear sigma model, special Galileon and Born–Infeld theories [125, 106]. The entries of A_n are given by:

$$[A_n]_{ij} = \begin{cases} \frac{p_i \cdot p_j}{\sigma_i - \sigma_j} & \text{if } i \neq j, \\ 0 & \text{if } i = j, \end{cases} \quad \text{for } i, j = 1, 2, \dots, n. \quad (3.3)$$

Here the puncture associated to the i th particle is located at $z = \sigma_i$. The right integrands in both theories also contain a single power of the reduced Pfaffian of A_n in addition to the supersymmetry information.

In this chapter we continue the exploration of worldsheet formulas in 6D and provide explicit such formulas for the complete tree-level S matrix of $\mathcal{N} = (1, 1)$ SYM with $U(N)$ gauge group, the effective theory on N coincident D5-branes as described in Sec. 1.2. The S matrix of this theory has been studied previously in [121, 122, 113, 140, 123, 114, 141].

A proposal for amplitudes with an even number of particles is naturally obtained [142] by noticing that the CHY formulation for Yang–Mills partial am-

plitudes of gluons can be obtained from that of the Born–Infeld theory by the replacement

$$\mathcal{I}_L^{\text{BI}} = (\text{Pf } A_n)^2 \quad \longrightarrow \quad \mathcal{I}_L^{\text{YM}} = \text{PT}(12 \cdots n), \quad (3.4)$$

where $\text{PT}(12 \cdots n)$ is the famous Parke–Taylor factor [44, 49, 46]. Applying the same substitution to the D5-brane formula we get a formula for $\mathcal{N} = (1, 1)$ SYM amplitudes with even multiplicity, and we provide strong evidence for its validity.

The formula for odd-point amplitudes proves to be a more difficult task, since the maps given in (3.1) do not have an obvious generalization to odd multiplicity. In all previously known formulations of Yang–Mills amplitudes, soft limits have provided a way of generating $(n-1)$ -particle amplitudes from n -particle ones since the leading singular behavior is controlled by Weinberg’s soft theorem [143]. However, in all such cases the measure over the moduli space of maps has had the same structure for $n-1$ and n particles.

In 6D the soft limit needs additional technical considerations, in part due to the $\text{SL}(2, \mathbb{C})$ redundancy of the maps, inherited from the little group. (In 4D the redundancy was only $\text{GL}(1, \mathbb{C})$.) The $\text{SL}(2, \mathbb{C})$ structure introduces new degrees of freedom in the computation of the soft limit. In contrast to the 4D case, these degrees of freedom in 6D turn out to be inherently intertwined with the Möbius group $\text{SL}(2, \mathbb{C})$ acting on \mathbb{CP}^1 .

One of the main results of this chapter is to uncover a fascinating structure that appears in the definition of the maps for an odd number of particles. In a nutshell, we find that the maps for n odd can be defined by

$$\rho_a^A(z) = \sum_{k=0}^{(n-3)/2} \rho_{k,a}^A z^k + w^A \xi_a z^{(n-1)/2}, \quad (3.5)$$

while the moduli space is obtained by modding out by a novel redundancy, which we call T-shift invariance. It acts on the maps in addition to the two $\text{SL}(2, \mathbb{C})$ s. In fact, the new T-shift action emerges due to the non-commutativity between such groups. This fact becomes apparent already from the soft-limit perspective as mentioned above. We start the exploration of the corresponding algebra and find that when the coefficients of the maps are partially fixed, the remaining redundancies take a form of a semi-direct product $\text{SL}(2, \mathbb{C}) \ltimes \mathbb{C}^2$. We introduce a formula for the integration measure for the space of maps of

odd multiplicity as well as its supersymmetric extension. It can be used both for super Yang–Mills and supergravity theories.

Finally, we derive an explicit integrand for the $\mathcal{N} = (1, 1)$ SYM odd-multiplicity amplitudes. The ingredients are a Parke–Taylor factor for the left-integrand and a generalization of the A_n matrix whose reduced Pfaffian enters in the right-integrand together with the supersymmetric part of the measure. The new matrix and its reduced Pfaffian behave as quarter-integrands, again in standard CHY terminology. This means that it provides a new building block that can be used to construct potentially consistent theories by mixing it with other quarter-integrands. The new matrix \widehat{A}_n is given by

$$[\widehat{A}_n]_{ij} = \begin{cases} \frac{p_i \cdot p_j}{\sigma_i - \sigma_j} & \text{if } i \neq j, \\ 0 & \text{if } i = j, \end{cases} \quad \text{for } i, j = 1, 2, \dots, n, \star, \quad (3.6)$$

where the final column and row feature a new null vector p_\star of the form:

$$p_\star^{AB} = \frac{2 q^{[A} \langle \rho^{B]}(\sigma_\star) \rho^C(\sigma_\star) \tilde{q}_C}{q^D [\tilde{\rho}_D(\sigma_\star) \tilde{\xi}] \langle \rho^E(\sigma_\star) \xi \rangle \tilde{q}_E}, \quad (3.7)$$

where q and \tilde{q} are reference spinors and σ_\star is a reference puncture that can take an arbitrary value.

The connected formula for odd multiplicity is derived using the soft limit of the corresponding even-multiplicity result. We also obtain it by assuming the supersymmetric quarter-integrand and matching the rest by comparing to the CHY formula for $n - 1$ scalars and one gluon. The same strategy of examining component amplitudes can also be used for even multiplicity using the same assumptions.

In addition to constraints which connect the external momenta to the product of maps as in (3.1), we also find a linear form of the constraints which leads to an alternative expression for the amplitudes. This form is the direct analog of the original Witten–RSV formula and connects the maps directly to the external 6D spinor-helicity variables. We further recast the linearized form of maps in the form of the so-called Veronese maps, and explore their relations to the symplectic (or Lagrangian) Grassmannian.

Having explicit integrands for the complete 6D $\mathcal{N} = (1, 1)$ SYM tree amplitudes allows the construction of the 6D $\mathcal{N} = (2, 2)$ SUGRA integrand by the

standard replacement of the left-integrand Parke–Taylor factor by a copy of the right integrand, which contains the necessary new supersymmetric information.

We end with various applications to other theories in four, five, and six dimensions. These include mixed superamplitudes of 6D $\mathcal{N} = (1, 1)$ SYM coupled to a single D5-brane, 5D SYM and SUGRA, and also 4D scattering amplitudes involving massive particles of $\mathcal{N} = 4$ SYM on the Coulomb branch of its moduli space. The formulas for 5D theories take forms very similar to those of 6D, but with additional constraints on the rational maps to incorporate 5D massless kinematics. In order to describe the massive amplitudes of $\mathcal{N} = 4$ SYM on the Coulomb branch, we utilize the spinor-helicity formalism recently developed for massive particles in 4D [144], which in fact can naturally be viewed as a dimensional reduction of 6D massless helicity spinors. We also would like to emphasize that, although it is a straightforward reduction of our 6D formula, this is the first time that a connected formula has been proposed for 4D $\mathcal{N} = 4$ SYM away from the massless point of the moduli space.

This chapter is organized as follows. In Section 3.2, we review the general construction of rational maps from \mathbb{CP}^1 to the null cone in general spacetime dimensions. We also review 4D constructions and then 6D maps for an even number of particles. Sections 3.3 and 3.4 are devoted to $\mathcal{N} = (1, 1)$ SYM amplitudes in 6D. Section 3.3 deals with an even number of particles while Section 3.4 contains the main results of this work by presenting formulas and consistency checks for odd multiplicity. In Section 3.5 we discuss a linear form of the scattering maps in 6D and its relationship to the symplectic Grassmannian. Extensions and applications are presented in Section 3.6. We conclude and give a discussion of future directions in Section 3.7. In Appendix B.1 we present the algebra of the new T-shift, and in Appendix B.2 we give details of the soft-limit calculations.

3.2 Rational Maps and Connected Formulas

This section begins by reviewing rational maps and the CHY formulas for an arbitrary space-time dimension. Some of this was already discussed in Sec. 1.3, but we recall it here as some details and notation will be needed later on. Next, it discusses the specialization to 4D and the Witten–RSV formulas. Finally, it gives an overview of the form of the even- n rational maps in 6D, whose

generalizations will be the subject of later sections.

Arbitrary Dimension

Let us consider scattering of n massless particles in an arbitrary space-time dimension. To each particle, labeled by the index i , we associate a puncture at $z = \sigma_i$ on the Riemann sphere, \mathbb{CP}^1 , whose local coordinate is z . We then introduce polynomial maps, $p^\mu(z)$, of degree $n - 2$. They are constructed such that the momentum p_i^μ associated to the i th particle is given by:

$$p_i^\mu = \frac{1}{2\pi i} \oint_{|z-\sigma_i|=\varepsilon} \frac{p^\mu(z)}{\prod_{j=1}^n (z - \sigma_j)} dz, \quad (3.8)$$

which means that $p^\mu(z)$ can be written as a polynomial in z :

$$p^\mu(z) = \sum_{i=1}^n p_i^\mu \prod_{j \neq i} (z - \sigma_j). \quad (3.9)$$

Here we take all momenta to be incoming, so that momentum conservation is given by $\sum_{i=1}^n p_i^\mu = 0$. In this chapter we sometimes call $p^\mu(z)$ the *scattering map*.

In order to relate the positions of the punctures σ_i to the kinematics, the additional condition that the scattering map is null, i.e., $p^2(z) = 0$ for all z , is imposed. Since $p^2(z)$ is of degree $2n - 4$ and it is already required to vanish at n points, σ_i , requiring $p^\mu(z)$ to be null gives $n - 3$ additional constraints. Using (3.9) these constraints can be identified by considering the combination

$$\frac{p^2(z)}{\prod_{i=1}^n (z - \sigma_i)^2} = \sum_{i,j=1}^n \frac{p_i \cdot p_j}{(z - \sigma_i)(z - \sigma_j)} = 0. \quad (3.10)$$

The expression (3.10) does not have any double poles, since the punctures are distinct and all of the momenta are null, $p_i^2 = 0$. Requiring that residues on all the poles vanish implies:

$$E_i := \sum_{j \neq i} \frac{p_i \cdot p_j}{\sigma_{ij}} = 0 \quad \text{for all } i, \quad (3.11)$$

where $\sigma_{ij} = \sigma_i - \sigma_j$. These are the scattering equations [57] which were introduced in Sec. 1.3 and used extensively in Chapter 2. Due to the above counting, only $n - 3$ of them are independent. In fact, $\sum_i \sigma_i^\ell E_i$ automatically vanishes for $\ell = 0, 1, 2$ as a consequence of the mass-shell and momentum-conservation conditions. Using the $\text{SL}(2, \mathbb{C})$ symmetry of the scattering equations to fix three

of the σ_i coordinates, there are $(n-3)!$ solutions of the scattering equations for the remaining σ_i 's for generic kinematics [57].

The scattering equations connect the moduli space of n -punctured Riemann spheres to the external kinematic data. Tree-level n -particle scattering amplitudes of massless theories can be computed using the Cachazo–He–Yuan (CHY) formula, which takes the form [58]:

$$\mathcal{A}_n^{\text{theory}} = \int d\mu_n \mathcal{I}_L^{\text{theory}} \mathcal{I}_R^{\text{theory}}. \quad (3.12)$$

$\mathcal{I}_L^{\text{theory}}$ and $\mathcal{I}_R^{\text{theory}}$ are left- and right-integrand factors, respectively, and they depend on the theory under consideration. Their precise form is not important for now, other than that they carry weight -2 under an $\text{SL}(2, \mathbb{C})$ transformation for each puncture, i.e., $\mathcal{I}_{L/R}^{\text{theory}} \rightarrow \prod_{i=1}^n (C\sigma_i + D)^2 \mathcal{I}_{L/R}^{\text{theory}}$ when $\sigma_i \rightarrow (A\sigma_i + B)/(C\sigma_i + D)$ and $AD - BC = 1$. Correctly identifying the separation into left- and right-integrands is important for making the double-copy properties of amplitudes manifest.

Let us now review the CHY measure from (1.35):

$$d\mu_n = \delta^D(\sum_{i=1}^n p_i^\mu) \left(\prod_{i=1}^n \delta(p_i^2) \right) \frac{\prod_{i=1}^n d\sigma_i}{\text{vol SL}(2, \mathbb{C})} \prod'_i \delta(E_i). \quad (3.13)$$

This is a distribution involving momentum conservation and null conditions for the external momenta. The factor $\text{vol SL}(2, \mathbb{C})$ denotes the fact that it is necessary to quotient by the $\text{SL}(2, \mathbb{C})$ redundancy on the Riemann surface by fixing the positions of three of the punctures, specifically $i = p, q, r$. Similarly, the prime means that the corresponding three scattering equations are redundant and should be removed. Fixing these redundancies leads to

$$\begin{aligned} \int d\mu_n &= \delta^D(\sum_{i=1}^n p_i^\mu) \left(\prod_{i=1}^n \delta(p_i^2) \right) \int (\sigma_{pq}\sigma_{qr}\sigma_{rp})^2 \prod_{i \neq p, q, r} (d\sigma_i \delta(E_i)) \\ &= \delta^D(\sum_{i=1}^n p_i^\mu) \left(\prod_{i=1}^n \delta(p_i^2) \right) \sum_{s=1}^{(n-3)!} \frac{(\sigma_{pq}\sigma_{qr}\sigma_{rp})^2}{\det \left[\frac{\partial E_i}{\partial \sigma_j} \right]} \Big|_{\sigma_i = \sigma_i^{(s)}}, \end{aligned} \quad (3.14)$$

which can be shown to be independent of the choice of labels p, q, r . The delta functions fully localize the measure on the $(n-3)!$ solutions $\{\sigma_i^{(s)}\}$ of the scattering equations. The measure transforms with $\text{SL}(2, \mathbb{C})$ -weight 4 in each puncture, so that the CHY integral (3.12) is $\text{SL}(2, \mathbb{C})$ -invariant.

Finally, one of the advantages of the CHY formulation is that soft limits can be derived from a simple application of the residue theorem [57]. Under the soft limit of an $(n + 1)$ -point amplitude with the last particle soft, i.e., $\tau \rightarrow 0$ where $p_{n+1} = \tau \hat{p}_{n+1}$, the measure behaves as

$$\int d\mu_{n+1} = \delta(p_{n+1}^2) \int d\mu_n \frac{1}{2\pi i} \oint_{|\hat{E}_{n+1}|=\varepsilon} \frac{d\sigma_{n+1}}{E_{n+1}} + O(\tau^0). \quad (3.15)$$

Here we have rewritten the scattering equation $\hat{E}_{n+1} = 0$ as a residue integral. Note that $E_{n+1} = \tau \hat{E}_{n+1}$ is proportional to τ , and thus the displayed term is dominant. Therefore the scattering equation associated to the last particle completely decouples in the limit $\tau \rightarrow 0$. For each of the $(n - 3)!$ solutions of the remaining scattering equations, the contour $\{|\hat{E}_{n+1}| = \varepsilon\}$ localizes on $n - 2$ solutions [57].

Four Dimensions: Unification of Sectors

Since our ultimate goal of this chapter is to find amplitudes for 6D SYM and SUGRA, we start this section with the well-understood case of 4D. Some of this is reviewed in Sec. (1.3), but we go into more detail here since our 6D SYM formula will reduce to 4D $\mathcal{N} = 4$ SYM upon dimensional reduction. Various aspects of specifying CHY formulations to 4D have also been discussed in [105, 145].

We recall the 4D spinor helicity variables. The momentum four-vector of a massless particle in 4D Lorentzian spacetime can be written in terms of a pair of two-component bosonic spinors, λ^α and $\tilde{\lambda}^{\dot{\alpha}}$, which transform as $\mathbf{2}$ and $\bar{\mathbf{2}}$ representations of the $\text{SL}(2, \mathbb{C}) = \text{Spin}(3, 1)$ Lorentz group

$$p^{\alpha\dot{\alpha}} = \sigma_\mu^{\alpha\dot{\alpha}} p^\mu = \lambda^\alpha \tilde{\lambda}^{\dot{\alpha}} \quad \alpha = 1, 2, \quad \dot{\alpha} = \dot{1}, \dot{2}. \quad (3.16)$$

For physical momenta, λ and $\pm\tilde{\lambda}$ are complex conjugates. However, when considering analytic continuations, it is convenient to treat them as independent. The little group for a massless particle¹ in 4D is $\text{U}(1)$. Its complexification is $\text{GL}(1, \mathbb{C})$. λ and $\tilde{\lambda}$ transform oppositely under this group so that the momentum is invariant. In discussing n -particle scattering amplitudes, we label the particles by an index $i = 1, 2, \dots, n$. It is important to understand that there is a distinct little group associated to each of the n particles. Thus, the little group $\text{GL}(1, \mathbb{C})$ transforms the spinors as $\lambda_i \rightarrow t_i \lambda_i$ and

¹In this work we only consider massless particles that transform trivially under translations of the full little group of Euclidean motions in $D - 2$ dimensions.

$\tilde{\lambda}_i \rightarrow t_i^{-1} \tilde{\lambda}_i$, leaving only three independent degrees of freedom for the momentum. Lorentz-invariant spinor products are given by: $\langle \lambda_i \lambda_j \rangle = \varepsilon_{\alpha\beta} \lambda_i^\alpha \lambda_j^\beta$ and $[\tilde{\lambda}_i \tilde{\lambda}_j] = \varepsilon_{\dot{\alpha}\dot{\beta}} \tilde{\lambda}_i^{\dot{\alpha}} \tilde{\lambda}_j^{\dot{\beta}}$. It is sometimes convenient to simplify further and write $\langle ij \rangle$ or $[ij]$. Given a scattering amplitude, expressed in terms of spinor-helicity variables, one can deduce the helicity of the i th particle by determining the power of t_i by which the amplitude transforms. For example, the most general Parke–Taylor (PT) formula, Eq. (1.17), for MHV amplitudes in 4D YM theory is as follows [44]: if gluons i and j have negative helicity, while the other $n - 2$ gluons have positive helicity, then the (color-stripped) amplitude is

$$A_n^{\text{YM}}(1^+ 2^+ \dots i^- \dots j^- \dots n^+) = \frac{\langle ij \rangle^4}{\langle 12 \rangle \langle 23 \rangle \dots \langle n1 \rangle}. \quad (3.17)$$

Since the scattering map $p^\mu(z)$ in (3.9) is required to be null for all z , it can also be expressed in a factorized form in terms of spinors:

$$p^{\alpha\dot{\alpha}}(z) = \rho^\alpha(z) \tilde{\rho}^{\dot{\alpha}}(z). \quad (3.18)$$

The roots of $p^{\alpha\dot{\alpha}}(z)$ can be distributed among the polynomials $\rho(z)$, $\tilde{\rho}(z)$ in different ways, such that their degrees add up to $n - 2$. When $\deg \rho(z) = d$ and $\deg \tilde{\rho}(z) = \tilde{d} = n - d - 2$, the maps are said to belong to the d th sector. As before for 4D, we parametrize the polynomials as:

$$\rho^\alpha(z) = \sum_{k=0}^d \rho_k^\alpha z^k, \quad \tilde{\rho}^{\dot{\alpha}}(z) = \sum_{k=0}^{\tilde{d}} \tilde{\rho}_k^{\dot{\alpha}} z^k. \quad (3.19)$$

The spinorial maps (3.18) carry the same information as the scattering equations, and therefore they can be used to redefine the measure. Here it is natural to introduce a measure for each sector as:

$$\int d\mu_{n,d}^{\text{4D}} = \int \frac{\prod_{i=1}^n d\sigma_i \prod_{k=0}^d d^2 \rho_k \prod_{k=0}^{\tilde{d}} d^2 \tilde{\rho}_k}{\text{vol SL}(2, \mathbb{C}) \times \text{GL}(1, \mathbb{C})} \frac{1}{R(\rho)R(\tilde{\rho})} \prod_{i=1}^n \delta^4 \left(p_i^{\alpha\dot{\alpha}} - \frac{\rho^\alpha(\sigma_i) \tilde{\rho}^{\dot{\alpha}}(\sigma_i)}{\prod_{j \neq i} \sigma_{ij}} \right). \quad (3.20)$$

These measures contain an extra $\text{GL}(1, \mathbb{C})$ redundancy, analogous to the little group symmetries of the momenta, which allows fixing one coefficient of $\rho(z)$ or $\tilde{\rho}(z)$. $R(\rho)$ denotes the resultant $R(\rho^1(z), \rho^2(z), z)$ and similarly for $R(\tilde{\rho})$ [146, 127]. The physical reason resultants appear in the denominator can be understood by finding the points in the moduli space of maps where they vanish. A resultant of any two polynomials, say $\rho_1(z)$ and $\rho_2(z)$, vanishes if and only if the two polynomials have a common root z^* . If such a z^* exists then

the map takes it to the tip of the momentum-space null cone, i.e., to the strict soft-momentum region. This is a reflection of the fact that in four (and lower) dimensions IR divergences are important in theories of massless particles. The measure is giving the baseline for the IR behavior while integrands can change it depending on the theory. As reviewed below, the gauge theory and gravity integrands contain $(R(\rho)R(\tilde{\rho}))^{\mathbf{s}}$, where $\mathbf{s} = 1$ for YM and $\mathbf{s} = 2$ for gravity, which coincides with the spins of the particles. Combined with the factor in the measure one has $(R(\rho)R(\tilde{\rho}))^{\mathbf{s}-1}$, which indicates that the IR behavior improves as one goes from a scalar theory, with $\mathbf{s} = 0$, to gravity [147].

Summing over all sectors gives the original CHY measure:

$$\int d\mu_n = \sum_{d=1}^{n-3} \int d\mu_{n,d}^{4D}. \quad (3.21)$$

This separation works straightforwardly for theories where the integrand only depends on σ_i 's and not on the maps. One such theory is the bi-adjoint scalar whose amplitudes are given by

$$m(\alpha|\beta) = \int d\mu_n \text{PT}(\alpha) \text{PT}(\beta) = \sum_{d=1}^{n-3} m_{n,d}(\alpha|\beta), \quad (3.22)$$

where $\text{PT}(\alpha)$ is the Parke–Taylor factor. The definition for the identity permutation is

$$\text{PT}(12 \cdots n) = \frac{1}{\sigma_{12}\sigma_{23} \cdots \sigma_{n1}}. \quad (3.23)$$

In general, α denotes a permutation of the indices $1, 2, \dots, n$. The quantities $m_{n,d}(\alpha|\beta)$ are the “scalar blocks” defined in [147]. In the d th sector the number of solutions is given by the Eulerian number $\langle \frac{n-3}{d-1} \rangle$, as conjectured in [124] and proved in [56]. Upon summation (3.21) gives all $\sum_{d=1}^{n-3} \langle \frac{n-3}{d-1} \rangle = (n-3)!$ solutions of the scattering equations. Note that momentum conservation and the factorization conditions that ensure masslessness are built into the measure (3.20).

An alternative version of the above constraints, which is closer to the original Witten–RSV formulas, can be obtained by integrating-in auxiliary variables t_i and \tilde{t}_i

$$\delta^4 \left(p_i^{\alpha\dot{\alpha}} - \frac{\rho^\alpha(\sigma_i)\tilde{\rho}^{\dot{\alpha}}(\sigma_i)}{\prod_{j \neq i} \sigma_{ij}} \right) = \delta(p_i^2) \int dt_i d\tilde{t}_i \delta \left(t_i \tilde{t}_i - \frac{1}{\prod_{j \neq i} \sigma_{ij}} \right) \quad (3.24)$$

$$\times \delta^2(\lambda_i^\alpha - t_i \rho^\alpha(\sigma_i)) \delta^2(\tilde{\lambda}_i^{\dot{\alpha}} - \tilde{t}_i \tilde{\rho}^{\dot{\alpha}}(\sigma_i)).$$

This formulation helps to linearize the constraints and make the little-group properties of theories with spin, such as Yang–Mills theory, more manifest.

The on-shell tree amplitudes of $\mathcal{N} = 4$ SYM theory in 4D are usually written as a sum over sectors

$$\mathcal{A}_n^{\mathcal{N}=4 \text{ SYM}} = \sum_{d=1}^{n-3} \mathcal{A}_{n,d}^{\mathcal{N}=4 \text{ SYM}}. \quad (3.25)$$

The d th sector has $n - 2 - 2d$ units of ‘‘helicity violation’’: $d \rightarrow n - 2 - d$ corresponds to reversing the helicities. Partial amplitudes in each sector are given by

$$\mathcal{A}_{n,d}^{\mathcal{N}=4 \text{ SYM}}(\alpha) = \int d\mu_{n,d}^{4\text{D}} \text{PT}(\alpha) \left(R(\rho)R(\tilde{\rho}) \int d\Omega_{\mathbb{F},d}^{(4)} \right), \quad (3.26)$$

where $d\Omega_{\mathbb{F},d}^{(4)}$ denotes integrations over fermionic analogs of the maps $\rho(z)$ and $\tilde{\rho}(z)$ implementing the $\mathcal{N} = 4$ supersymmetry, whose precise form can be found in [56].

Due to the fact that the little group is $\text{Spin}(4)$ in 6D, it is expected that the SYM amplitudes in 6D should not separate into helicity sectors. Dimensional reduction to 4D would naturally lead to a formulation with unification of sectors. This may appear somewhat puzzling as (3.25) and (3.26) seem to combine the measure in a given sector with an integrand that is specific to that sector. This puzzle is resolved by noticing that

$$R(\rho) = \det' \Phi_d, \quad R(\tilde{\rho}) = \det' \tilde{\Phi}_{\tilde{d}}, \quad (3.27)$$

where $[\Phi_d]_{ij} := \langle ij \rangle / (t_i t_j \sigma_{ij})$ and $[\tilde{\Phi}_{\tilde{d}}]_{ij} := [ij] / (\tilde{t}_i \tilde{t}_j \sigma_{ij})$ for $i \neq j$. The diagonal components are more complicated and depend on d and \tilde{d} [148, 127]. The corresponding reduced determinants are computed using submatrices of size $d \times d$ and $\tilde{d} \times \tilde{d}$, respectively. One of the main properties of these reduced determinants is that they vanish when evaluated on solutions in sectors that differ from their defining degree, i.e.,

$$\int d\mu_{n,d}^{4\text{D}} \det' \Phi_{d'} \det' \tilde{\Phi}_{\tilde{d}'} = \delta_{d,d'} \int d\mu_{n,d}^{4\text{D}} \det' \Phi_d \det' \tilde{\Phi}_{\tilde{d}}. \quad (3.28)$$

Using this it is possible to write the complete amplitude in terms of factors that can be uplifted to 6D and unified!

$$\mathcal{A}_n^{\mathcal{N}=4 \text{ SYM}}(\alpha) = \int \left(\sum_{d=1}^{n-3} d\mu_{n,d}^{4\text{D}} \right) \text{PT}(\alpha) \left(\sum_{d'=1}^{n-3} \det' \Phi_{d'} \det' \tilde{\Phi}_{\tilde{d}'} \int d\Omega_{\mathbb{F},d'}^{(4)} \right). \quad (3.29)$$

Finally, it is worth mentioning that (3.28) can be used to write unified 4D $\mathcal{N} = 8$ SUGRA amplitudes, via the double copy, as

$$\mathcal{M}_n^{\mathcal{N}=8 \text{ SUGRA}} = \int \left(\sum_{d=1}^{n-3} d\mu_{n,d}^{4\text{D}} \right) \left(\sum_{d'=1}^{n-3} \det' \Phi_{d'} \det' \tilde{\Phi}_{\tilde{d}'} \int d\Omega_{\mathbb{F},d'}^{(4)} \right) \left(\sum_{d'=1}^{n-3} \det' \Phi_{d'} \det' \tilde{\Phi}_{\tilde{d}'} \int d\hat{\Omega}_{\mathbb{F},d'}^{(4)} \right).$$

Six Dimensions: Even Multiplicity

We now turn to a review of scattering maps in 6D. It turns out that the 6D spinor-helicity formalism requires separate treatments for amplitudes with an even and an odd number of particles. In this subsection we review the construction for an even number of particles, as was introduced in Chapter 2 for M5- and D5-brane scattering amplitudes. (These theories only have non-vanishing amplitudes for n even.) A formula for odd multiplicity, which is required for Yang–Mills theories, is one of the main results of this chapter and it is given in Section 3.4.

The little group for massless particles in 6D is $\text{Spin}(4) \sim \text{SU}(2) \times \text{SU}(2)$. We use indices without hats when referring to representations of the first $\text{SU}(2)$ or its $\text{SL}(2, \mathbb{C})$ complexification and ones with hats when referring to the second $\text{SU}(2)$ or its $\text{SL}(2, \mathbb{C})$ complexification. Momenta of massless particles are parametrized in terms of 6D spinor-helicity variables $\lambda_i^{A,a}$ by [43]:

$$p_i^{AB} = \sigma_\mu^{AB} p_i^\mu = \langle \lambda_i^A \lambda_i^B \rangle, \quad A, B = 1, 2, 3, 4, \quad (3.30)$$

where σ_μ^{AB} are six antisymmetric 4×4 matrices, which form an invariant tensor of $\text{Spin}(5, 1)$. The angle bracket denotes a contraction of the little-group indices:

$$\langle \lambda_i^A \lambda_i^B \rangle = \epsilon_{ab} \lambda_i^{A,a} \lambda_i^{B,b} = \lambda_i^{A+} \lambda_i^{B-} - \lambda_i^{A-} \lambda_i^{B+}, \quad a, b = +, -. \quad (3.31)$$

ϵ_{ab} is an invariant tensor of the $\text{SU}(2)$ little group, as well as its $\text{SL}(2, \mathbb{C})$ complexification. The on-shell condition, $p_i^2 = 0$, is equivalent to the vanishing of the Pfaffian of p_i^{AB} . The little group transforms the spinors as $\lambda_i^{A,a} \rightarrow (L_i)_b^a \lambda_i^{A,b}$, where $L_i \in \text{SL}(2, \mathbb{C})$, leaving only five independent degrees of freedom for the spinors, appropriate for a massless particle in six dimensions. The momenta can be equally well described by conjugate spinors $\tilde{\lambda}_{i,A,\hat{a}}$:

$$p_{i,AB} = \frac{1}{2} \epsilon_{ABCD} p_i^{CD} = [\tilde{\lambda}_{i,A} \tilde{\lambda}_{i,B}], \quad (3.32)$$

where

$$[\tilde{\lambda}_{i,A} \tilde{\lambda}_{i,B}] = \epsilon^{\hat{a}\hat{b}} \tilde{\lambda}_{i,A,\hat{a}} \tilde{\lambda}_{i,B,\hat{b}} = \tilde{\lambda}_{i,A,\hat{+}} \tilde{\lambda}_{i,B,\hat{-}} - \tilde{\lambda}_{i,A,\hat{-}} \tilde{\lambda}_{i,B,\hat{+}}, \quad \hat{a}, \hat{b} = \hat{+}, \hat{-}. \quad (3.33)$$

These conjugate spinors belong to the second (inequivalent) four-dimensional representation of the $\text{Spin}(5, 1) \sim \text{SU}^*(4)$ Lorentz group, and they transform under the right-handed little group. Using the invariant tensors of $\text{SU}^*(4)$, Lorentz invariants can be constructed as follows:

$$\langle \lambda_i^a \lambda_j^b \lambda_k^c \lambda_l^d \rangle = \epsilon_{ABCD} \lambda_i^{A,a} \lambda_j^{B,b} \lambda_k^{C,c} \lambda_l^{D,d}, \quad (3.34)$$

$$[\tilde{\lambda}_{i,\hat{a}} \tilde{\lambda}_{j,\hat{b}} \tilde{\lambda}_{k,\hat{c}} \tilde{\lambda}_{l,\hat{d}}] = \epsilon^{ABCD} \tilde{\lambda}_{i,A,\hat{a}} \tilde{\lambda}_{j,B,\hat{b}} \tilde{\lambda}_{k,C,\hat{c}} \tilde{\lambda}_{l,D,\hat{d}}, \quad (3.35)$$

$$\langle \lambda_i^a | \tilde{\lambda}_{j,\hat{b}} \rangle = \lambda_i^{A,a} \tilde{\lambda}_{j,A,\hat{b}} = [\tilde{\lambda}_{j,\hat{b}} | \lambda_i^a]. \quad (3.36)$$

The λ and $\tilde{\lambda}$ variables are not independent. They are related by the condition

$$\langle \lambda_i^a | \tilde{\lambda}_{i,\hat{a}} \rangle = 0, \quad (3.37)$$

for all a and \hat{a} . We also have

$$\epsilon_{ABCD} p_i^{AB} p_j^{CD} = 2 p_{i,AB} p_j^{AB} = 8 p_i \cdot p_j. \quad (3.38)$$

Using the notation given above, the scattering maps can be written in terms of 6D spinor-helicity variables:

$$p^{AB}(z) = \langle \rho^A(z) \rho^B(z) \rangle. \quad (3.39)$$

In the following we take the spinorial maps $\rho^{A,a}(z)$, for $a \in \{+, -\}$, to be polynomials of the same degree. In contrast to 4D, we can also consider non-polynomial forms of the maps (such that (3.39) is still a polynomial), see discussion at the end of Section 3.4. Note that this choice is consistent with the action of the group denoted $\text{SL}(2, \mathbb{C})_\rho$. This is the same abstract group as the little group, but it does not refer to a specific particle. Let us now focus on the construction for n even. In this case the degree of the polynomials is $m = \frac{n}{2} - 1$. Thus they can be expanded as:

$$\rho^{A,a}(z) = \sum_{k=0}^m \rho_k^{A,a} z^k. \quad (3.40)$$

With these maps the polynomial constructed in (3.39) is null and has the correct degree $n - 2$. By the arguments reviewed in Section 3.2 we conclude that the equations constructed from $\rho^{A,a}(z)$,

$$p_i^{AB} = \frac{\langle \rho^A(\sigma_i) \rho^B(\sigma_i) \rangle}{\prod_{j \neq i} \sigma_{ij}}, \quad (3.41)$$

imply the scattering equations for $\{\sigma_i\}$. However, the converse, i.e., that any solution of the scattering equations is a solution to (3.41) is not guaranteed. This was checked numerically in Chapter 2 for even multiplicity up to $n = 8$ particles. In this work we give an inductive proof of this fact in Appendix B.2, obtained by considering consecutive soft limits of the maps. Using this fact together with the counting of delta functions we then argue that the following measure

$$\int d\mu_n^{6D}{}_{\text{even}} = \int \frac{\prod_{i=1}^n d\sigma_i \prod_{k=0}^m d^8 \rho_k}{\text{vol}(\text{SL}(2, \mathbb{C})_\sigma \times \text{SL}(2, \mathbb{C})_\rho)} \frac{1}{V_n^2} \prod_{i=1}^n \delta^6 \left(p_i^{AB} - \frac{\langle \rho^A(\sigma_i) \rho^B(\sigma_i) \rangle}{\prod_{j \neq i} \sigma_{ij}} \right) \quad (3.42)$$

is equivalent to the CHY measure given in (3.13), after integrating out the ρ moduli. Also, it has momentum conservation and null conditions built-in. The formula contains the Vandermonde factor

$$V_n = \prod_{1 \leq i < j \leq n} \sigma_{ij}. \quad (3.43)$$

which is needed to match the $\text{SL}(2, \mathbb{C})_\sigma$ weight of (3.13). In order to avoid confusion, we use the notation $\text{SL}(2, \mathbb{C})_\sigma$ for the Möbius group acting on the Riemann sphere. Just as the $\text{SL}(2, \mathbb{C})_\sigma$ symmetry can be used to fix three of the σ coordinates, the $\text{SL}(2, \mathbb{C})_\rho$ symmetry can be used to fix three of the coefficients of the polynomial maps $\rho^{A,a}(z)$. This form of the measure imposes $6n$ constraints on $5n - 6$ integration variables, leaving a total of $n + 6$ delta functions which account for the n on-shell conditions and the six momentum conservation conditions. Fixing the values of $\sigma_1, \sigma_2, \sigma_3$ and of $\rho_0^{1,+}, \rho_0^{1,-}, \rho_0^{2,+}$, the gauge-fixed form of the measure becomes:

$$\int d\mu_n^{6D}{}_{\text{even}} = \int \frac{J_\rho J_\sigma}{V_n^2} \left(\prod_{i=4}^n d\sigma_i \right) d\rho_0^{2,-} d^2 \rho_0^3 d^2 \rho_0^4 \left(\prod_{k=1}^m d^8 \rho_k \right) \prod_{i=1}^n \delta^6 \left(p_i^{AB} - \frac{\langle \rho^A(\sigma_i) \rho^B(\sigma_i) \rangle}{\prod_{j \neq i} \sigma_{ij}} \right),$$

where the Jacobians are²

$$J_\sigma = \sigma_{12} \sigma_{23} \sigma_{31}, \quad J_\rho = \rho_0^{1,+} \langle \rho_0^1 \rho_0^2 \rangle. \quad (3.44)$$

It is convenient to use a short-hand notation for the bosonic delta functions:

$$\Delta_B = \prod_{i=1}^n \delta^6 \left(p_i^{AB} - \frac{\langle \rho^A(\sigma_i) \rho^B(\sigma_i) \rangle}{\prod_{j \neq i} \sigma_{ij}} \right) = \delta^6(\sum_{i=1}^n p_i^{AB}) \left(\prod_{i=1}^n \delta(p_i^2) \right) \hat{\Delta}_B, \quad (3.45)$$

²This Jacobian can be derived from the identity $\int d^6 p_0 \delta(p_0^2) = \int J_\rho d\rho_0^{2,-} d\rho_0^{3,+} d\rho_0^{3,-} d\rho_0^{4,+} d\rho_0^{4,-}$, since the map component $p_0^{AB} = \langle \rho_0^A \rho_0^B \rangle$ is a null vector.

where $\hat{\Delta}_B$ is

$$\hat{\Delta}_B = \delta^4 \left(p_n^{AB} - \frac{\langle \rho^A(\sigma_n) \rho^B(\sigma_n) \rangle}{\prod_{i \neq n} \sigma_{ni}} \right) \prod_{i=1}^{n-2} \delta^5 \left(p_i^{AB} - \frac{\langle \rho^A(\sigma_i) \rho^B(\sigma_i) \rangle}{\prod_{j \neq i} \sigma_{ij}} \right) \prod_{i=1}^n p_i^{12} \left(\frac{p_{n-1}^{24}}{p_{n-1}^{12}} - \frac{p_n^{24}}{p_n^{12}} \right). \quad (3.46)$$

Here the five dimensional delta functions are chosen such that $\{A, B\} \neq \{3, 4\}$, whereas $\{A, B\} \neq \{3, 4\}, \{1, 3\}$ for the four-dimensional ones, and the additional factors are the Jacobian of taking out the momentum conservation and on-shell conditions. Alternatively, a covariant extraction of the on-shell delta functions can be obtained by introducing auxiliary variables M_i that linearize the constraints, analogous to the ones given in (3.24), as follows:

$$\delta^6 \left(p_i^{AB} - \frac{\langle \rho^A(\sigma_i) \rho^B(\sigma_i) \rangle}{\prod_{j \neq i} \sigma_{ij}} \right) = \delta(p_i^2) \int d^4 M_i |M_i|^3 \delta \left(|M_i| - \prod_{j \neq i} \sigma_{ij} \right) \times \delta^8 \left(\rho^{A,a}(\sigma_i) - (M_i)_b^a \lambda_i^{A,b} \right), \quad (3.47)$$

where $|M_i|$ denotes the determinant of the matrix M_i , and for some purpose it is more convenient to use this version of constraints. This form connects the maps directly to the external 6D spinors, and is a 6D version of the Witten–RSV constraints, which we explore in Section 3.5.

3.3 $\mathcal{N} = (1, 1)$ Super Yang–Mills: Even Multiplicity

In the following sections, we will propose a formula based on rational maps for the tree amplitudes of 6D maximal SYM theory, which has $\mathcal{N} = (1, 1)$ non-chiral supersymmetry. This theory describes the non-abelian interactions of a vector, four scalars, and four spinors all of which are massless and belong to the adjoint representation of the gauge group. As usual, we will generally consider color-stripped SYM amplitudes. Some properties of these amplitudes have been discussed in [121, 122, 123, 141] using 6D $\mathcal{N} = (1, 1)$ superspace.

In addition to the usual spacetime and gauge symmetries of Yang–Mills theory, the $\mathcal{N} = (1, 1)$ theory has a $\text{Spin}(4) \sim \text{SU}(2) \times \text{SU}(2)$ R symmetry group. The intuitive way to understand this is to note that this theory arises from dimensional reduction of 10D SYM theory, and the R symmetry corresponds to rotations in the four transverse directions. This group happens to be the same as the little group, which is just a peculiarity of this particular theory. From these and other considerations, one may argue that 6D $\mathcal{N} = (1, 1)$ SYM with $U(N)$ gauge symmetry (in the perturbative regime with no theta term)

describes the IR dynamics of N coincident D5-branes in type IIB superstring theory [149]. In contrast to 4D $\mathcal{N} = 4$ SYM, the gauge coupling in six dimensions has inverse mass dimension, so this theory is non-renormalizable and not conformal. This is not an issue for the tree amplitudes that we consider in this work. Further dimensional reduction on a T^2 leads to 4D $\mathcal{N} = 4$ SYM, and this provides a consistency check of the results.

Six-dimensional $\mathcal{N} = (1, 1)$ SYM is a theory with 16 supercharges. Its physical degrees of freedom form a 6D $\mathcal{N} = (1, 1)$ supermultiplet consisting of eight on-shell bosons and eight on-shell fermions. These may be organized according to their quantum numbers under the four $SU(2)$'s of the little group and R symmetry group. For example, the vectors belong to the representation $(\mathbf{2}, \mathbf{2}; \mathbf{1}, \mathbf{1})$, which means that they are doublets of each of the little-group $SU(2)$'s and singlets of each of the R symmetry $SU(2)$'s. In this notation, the fermions belong to the representation $(\mathbf{1}, \mathbf{2}; \mathbf{2}, \mathbf{1}) + (\mathbf{2}, \mathbf{1}; \mathbf{1}, \mathbf{2})$, and the scalars belong to the representation $(\mathbf{1}, \mathbf{1}; \mathbf{2}, \mathbf{2})$. (Whether one writes $(\mathbf{1}, \mathbf{2}; \mathbf{2}, \mathbf{1}) + (\mathbf{2}, \mathbf{1}; \mathbf{1}, \mathbf{2})$ or $(\mathbf{1}, \mathbf{2}; \mathbf{1}, \mathbf{2}) + (\mathbf{2}, \mathbf{1}; \mathbf{2}, \mathbf{1})$ is a matter of convention.)

It is convenient to package all 16 of these particles into a single on-shell ‘‘superparticle’’, by introducing four Grassmann numbers (per superparticle),

$$\Phi(\eta) = \phi^{1\hat{1}} + \eta_a \psi^{a\hat{1}} + \tilde{\eta}_{\hat{a}} \hat{\psi}^{\hat{a}1} + \eta_a \tilde{\eta}_{\hat{a}} A^{a\hat{a}} + (\eta)^2 \phi^{2\hat{1}} + \dots + (\eta)^2 (\tilde{\eta})^2 \phi^{2\hat{2}}. \quad (3.48)$$

Here η_a and $\tilde{\eta}_{\hat{a}}$ are the four Grassmann numbers, and the $SU(2)$ indices a and \hat{a} are little-group indices as before. The explicit 1's and 2's in the spectrum described above are R symmetry indices. Since the superfield transforms as a little-group scalar, this formulation makes the little-group properties manifest, but it obscures the R symmetry. By means of an appropriate Grassmann Fourier transform one could make the R symmetry manifest, but then the little-group properties would be obscured as explained in Chapter 2. The choice that has been made here turns out to be the more convenient one for the study of superamplitudes.

When discussing an n -particle amplitude the Grassmann coordinates carry an additional index i , labeling the n particles, just like the spinor-helicity coordinates. Thus, the complete color-stripped on-shell n -particle tree amplitude will be a cyclically symmetric function of the λ_i 's and the η_i 's. The various component amplitudes correspond to the terms with the appropriate dependence on the Grassmann coordinates. Thus, the superamplitude is like

a generating function in which the Grassmann coordinates play the role of fugacities. This is an on-shell analog of the use of superfields in the construction of Lagrangians. Fortunately, it exists in cases where the latter does not exist.

Often we will refer to the momenta p_i^{AB} and supercharges q_i^A , \tilde{q}_{iA} of the on-shell states. For (1,1) supersymmetry, they can be expressed in terms of the Grassmann coordinates:

$$q_i^A = \epsilon^{ab} \lambda_{ia}^A \eta_{ib} = \langle \lambda_i^A \eta_i \rangle, \quad \tilde{q}_{iA} = \epsilon^{\hat{a}\hat{b}} \tilde{\lambda}_{iA\hat{a}} \tilde{\eta}_{i\hat{b}} = [\tilde{\lambda}_{iA} \tilde{\eta}_i], \quad (3.49)$$

and the superamplitudes should be annihilated by the supercharges $Q^A = \sum_{i=1}^n q_i^A$ and $\tilde{Q}_A = \sum_{i=1}^n \tilde{q}_{iA}$. These symmetries will be manifest in the formulas that follow. However, there are eight more supercharges, involving derivatives with respect to the η coordinates, which should also be conserved. Once one establishes the first eight supersymmetries and the R symmetry, these supersymmetries automatically follow. The explicit form of the derivatively realized supercharges is:

$$\bar{q}_i^A = \lambda_{ia}^A \frac{\partial}{\partial \eta_{ia}}, \quad \tilde{\bar{q}}_{iA} = \tilde{\lambda}_{iA\hat{a}} \frac{\partial}{\partial \tilde{\eta}_{i\hat{a}}}, \quad (3.50)$$

In terms of these Grassmann variables, one may also write the generators of the $SU(2) \times SU(2)$ R symmetry group. One first notes that they obey the anti-commutation relations:

$$\left\{ \eta_a, \frac{\partial}{\partial \eta^b} \right\} = \epsilon_{ab}, \quad \left\{ \tilde{\eta}_{\hat{a}}, \frac{\partial}{\partial \tilde{\eta}^{\hat{b}}} \right\} = \epsilon_{\hat{a}\hat{b}}. \quad (3.51)$$

In terms of these, the six generators of the R symmetry group may be defined as

$$R^+ = \eta_a \eta^a, \quad R^- = \frac{\partial}{\partial \eta^a} \frac{\partial}{\partial \eta_a}, \quad R = \eta_a \frac{\partial}{\partial \eta_a} - 1, \quad (3.52)$$

$$\tilde{R}^+ = \tilde{\eta}_{\hat{a}} \tilde{\eta}^{\hat{a}}, \quad \tilde{R}^- = \frac{\partial}{\partial \tilde{\eta}^{\hat{a}}} \frac{\partial}{\partial \tilde{\eta}_{\hat{a}}}, \quad \tilde{R} = \tilde{\eta}_{\hat{a}} \frac{\partial}{\partial \tilde{\eta}_{\hat{a}}} - 1, \quad (3.53)$$

which have the standard raising and lowering commutation relations. These generate a global symmetry of $\mathcal{N} = (1,1)$ SYM. It is easy to see that linear generators R and \tilde{R} annihilate amplitudes since they are homogeneous polynomials of degree n in both η and $\tilde{\eta}$. The non-linearly realized ones become more transparent in an alternative form of the constraints that we will discuss in Section 3.5. As explained earlier, this is due to the choice of parametrization of the non-chiral on-shell superspace.

As discussed in previous literature for tree-level amplitudes of 6D $\mathcal{N} = (1, 1)$ SYM, the four-particle partial amplitude is particularly simple when expressed in terms of the supercharges:

$$\mathcal{A}_4^{\mathcal{N}=(1,1) \text{ SYM}}(1234) = \delta^6 \left(\sum_{i=1}^4 p_i^{AB} \right) \frac{\delta^4 \left(\sum_{i=1}^4 q_i^A \right) \delta^4 \left(\sum_{i=1}^4 \tilde{q}_{i,A} \right)}{s_{12} s_{23}}. \quad (3.54)$$

Here and throughout this work one should view this expression as a superamplitude; the component amplitudes may be extracted by Grassmann integration. For example, in terms of the Lorentz invariant brackets the four-gluon amplitude is:

$$\mathcal{A}_4(A_{a\hat{a}}A_{b\hat{b}}A_{c\hat{c}}A_{d\hat{d}}) = \delta^6 \left(\sum_{i=1}^4 p_i^{AB} \right) \frac{\langle 1_a 2_b 3_c 4_d \rangle [1_{\hat{a}} 2_{\hat{b}} 3_{\hat{c}} 4_{\hat{d}}]}{s_{12} s_{23}}. \quad (3.55)$$

Using the formalism of rational maps for the 6D spinor-helicity variables, the main technical result of this section is a formula for the n -point generalization of the superamplitude when n is even. The formula for odd n will be given in Section 3.4.

Connected Formula

We propose that the connected formula for even-multiplicity 6D $\mathcal{N} = (1, 1)$ SYM amplitudes is given by

$$\boxed{\mathcal{A}_{n \text{ even}}^{\mathcal{N}=(1,1) \text{ SYM}}(\alpha) = \int d\mu_n^{\text{6D}} \text{PT}(\alpha) \left(\text{Pf}' A_n \int d\Omega_F^{(1,1)} \right)}, \quad (3.56)$$

where $d\mu_n^{\text{6D}}$ is the measure given in (3.42), and we will shortly explain other ingredients that enter this formula. This formula is inspired by the D5-brane effective field theory scattering amplitudes written as a connected formula as in Chapter 2, where the factor of $(\text{Pf}' A_n)^2$ has been replaced with $\text{PT}(\alpha)$ given in (3.23). This is a standard substitution in the CHY formalism for passing from a probe D-brane theory to a Yang–Mills theory. Since the only non-vanishing amplitudes of the D5-brane theory have even n , this only works for the even-point amplitudes of SYM.

As indicated explicitly in the expression (3.56), the integrand of (3.56) factorizes into two half-integrands. Such a factorization of the integrand will be important later when we deduce the formulas for 6D SUGRA with $\mathcal{N} = (2, 2)$ supersymmetry. The left half-integrand $\text{PT}(\alpha)$ is the Parke–Taylor factor, where

α is a permutation that denotes the color ordering of Yang–Mills partial amplitudes. The right half-integrand further splits into two quarter-integrands. The first of these is the reduced Pfaffian of the antisymmetric matrix A_n , whose entries are given by:

$$[A_n]_{ij} = \begin{cases} \frac{p_i \cdot p_j}{\sigma_{ij}} & \text{if } i \neq j, \\ 0 & \text{if } i = j, \end{cases} \quad \text{for } i, j = 1, 2, \dots, n. \quad (3.57)$$

Since this matrix has co-rank 2, its Pfaffian vanishes. Instead, one defines the reduced Pfaffian:

$$\text{Pf}' A_n = \frac{(-1)^{p+q}}{\sigma_{pq}} \text{Pf} A_n^{[pq]}, \quad (3.58)$$

where we have removed two rows and columns labeled by p and q , and denoted the resulting reduced matrix by $A_n^{[pq]}$. The reduced Pfaffian is independent of the choice of p and q [125] and transforms under $\text{SL}(2, \mathbb{C})_\sigma$ in an appropriate way.

The remaining quarter integrand is the fermionic integration measure responsible for implementing the 6D $\mathcal{N} = (1, 1)$ supersymmetry which was found in Chapter 2, but we will review it here. The formula is

$$d\Omega_F^{(1,1)} = V_n \left(\prod_{k=0}^m d^2 \chi_k d^2 \tilde{\chi}_k \right) \Delta_F \tilde{\Delta}_F, \quad (3.59)$$

where $m = \frac{n}{2} - 1$, as before. This measure contains the Vandermonde determinant V_n , as well as a fermionic measure and fermionic delta functions. The integration variables arise as the coefficients of the fermionic rational maps, which are defined by

$$\chi^a(z) = \sum_{k=0}^m \chi_k^a z^k, \quad \tilde{\chi}^{\hat{a}}(z) = \sum_{k=0}^m \tilde{\chi}_k^{\hat{a}} z^k, \quad (3.60)$$

where χ_k^a and $\tilde{\chi}_k^{\hat{a}}$ are Grassmann variables. The fermionic delta functions, Δ_F and $\tilde{\Delta}_F$ are given by:

$$\Delta_F = \prod_{i=1}^n \delta^4 \left(q_i^A - \frac{\langle \rho^A(\sigma_i) \chi(\sigma_i) \rangle}{\prod_{j \neq i} \sigma_{ij}} \right), \quad (3.61)$$

$$\tilde{\Delta}_F = \prod_{i=1}^n \delta^4 \left(\tilde{q}_{i,A} - \frac{[\tilde{\rho}_A(\sigma_i) \tilde{\chi}(\sigma_i)]}{\prod_{j \neq i} \sigma_{ij}} \right). \quad (3.62)$$

These delta functions are built from the external chiral and anti-chiral supercharges of each particle and are responsible for the $(1, 1)$ supersymmetry in this formalism. Conservation of half of the 16 supercharges is made manifest by this expression. As in (3.54), the component amplitudes can be extracted by Grassmann integration of the appropriate η_a 's and $\tilde{\eta}_{\hat{a}}$'s, which enter via the supercharges.

Even though the maps $\tilde{\rho}_{A\hat{a}}(z)$ appear explicitly in $\tilde{\Delta}_F$, just as in the construction of D5-brane amplitudes in Chapter 2, the integration measure does not include additional integrations associated to the maps $\tilde{\rho}_{A\hat{a}}(z)$. If it did, the formula, for instance, would have the wrong mass dimension to describe SYM amplitudes in 6D. Instead, the $\tilde{\rho}$ coefficients are fixed by the conjugate set of rational constraints

$$p_{i,AB} - \frac{[\tilde{\rho}_A(\sigma_i) \tilde{\rho}_B(\sigma_i)]}{\prod_{j \neq i} \sigma_{ij}} = 0, \quad (3.63)$$

for all $i = 1, 2, \dots, n$. These equations are not enough to determine all of the $\tilde{\rho}_{A,k}^{\hat{a}}$'s. One needs to utilize $\text{SL}(2, \mathbb{C})_{\tilde{\rho}}$ to fix the remaining ones. The resulting amplitude is independent of choices that are made for the $\text{SL}(2, \mathbb{C})_{\tilde{\rho}}$ fixing because $\tilde{\rho}_{A,\hat{a}}(\sigma_i) \tilde{\chi}^{\hat{a}}(\sigma_i)$ and the fermionic measure $d^2 \tilde{\chi}_k$ are $\text{SL}(2, \mathbb{C})_{\tilde{\rho}}$ invariant. The usual scattering amplitudes A_n are obtained by removing the bosonic and fermionic on-shell conditions (“wave functions”), which appear as delta functions, namely,

$$\mathcal{A}_n^{\mathcal{N}=(1,1) \text{ SYM}} = \delta^6 \left(\sum_{i=1}^n p_i \right) \left(\prod_{i=1}^n \delta(p_i^2) \delta^2(\tilde{\lambda}_{i,A,\hat{a}} q_i^A) \delta^2(\lambda_{i,b}^B \tilde{q}_{i,B}) \right) A_n^{\mathcal{N}=(1,1) \text{ SYM}}. \quad (3.64)$$

It is straightforward to show that this formula produces the correct four-point superamplitude of 6D $\mathcal{N} = (1, 1)$ SYM, expressed in (3.54). A quick way to see it is to utilize the relation between the D5-brane amplitudes and the amplitudes of 6D $\mathcal{N} = (1, 1)$ SYM. As we discussed previously, they are related by the exchange of $(\text{Pf}' A_n)^2$ with the Parke–Taylor factor $\text{PT}(\alpha)$. We recall the four-point superamplitude for the D5-brane theory is given by

$$A_4^{\text{D5-brane}} = \delta^4 \left(\sum_{i=1}^4 q_i^A \right) \delta^4 \left(\sum_{i=1}^4 \tilde{q}_{i,A} \right). \quad (3.65)$$

From the explicit solution of the four-point scattering equations for the σ_i 's, it is easy to check that the effect of changing from $(\text{Pf}' A_4)^2$ to $\text{PT}(1234)$,

defined in (3.23), is to introduce an additional factor of $1/(s_{12} s_{23})$. Namely, on the support of the scattering equations, we have the following identity for the $\text{SL}(2, \mathbb{C})_\sigma$ -invariant ratio,

$$\frac{\text{PT}(1234)}{(\text{Pf}' A_4)^2} = \frac{1}{s_{12} s_{23}}. \quad (3.66)$$

Thus, combining this identity and the D5-brane formula (3.65), we arrive at the result of the four-point of 6D $\mathcal{N} = (1, 1)$ SYM (3.54). We have further checked numerically that the above formula reproduces the component amplitudes of scalars and gluons for $n = 6, 8$, obtained from Feynman diagram computations.

Comparison with CHY

This section presents a consistency check of the integrand by comparing a special bosonic sector of the theory with a CHY formula of YM amplitudes valid in arbitrary spacetime dimensions. This comparison actually also gives a derivation of the integrand in (3.56). We begin with the general form of the superamplitude,

$$\mathcal{A}_{n \text{ even}}^{\mathcal{N}=(1,1) \text{ SYM}}(\alpha) = \int d\mu_{n \text{ even}}^{6\text{D}} \int d\Omega_F^{(1,1)} \times \mathcal{J}_{n \text{ even}}, \quad (3.67)$$

where the measures $d\mu_{n \text{ even}}^{6\text{D}}$ and $d\Omega_F^{(1,1)}$ take care of 6D massless kinematics and 6D $\mathcal{N} = (1, 1)$ supersymmetry, respectively. The goal is then to determine the integrand $\mathcal{J}_{n \text{ even}}$. The strategy is to consider a particular component amplitude by performing fermionic integrations of the superamplitude $\mathcal{A}_{n \text{ even}}^{\mathcal{N}=(1,1) \text{ SYM}}(\alpha)$ such that our formula can be directly compared to the known CHY integrand, thereby determining $\mathcal{J}_{n \text{ even}}$.

To make the fermionic integration as simple as possible, it is convenient to consider a specific all-scalar amplitude, for instance,

$$\mathcal{A}_n(\phi_1^{1\hat{1}}, \dots, \phi_{\frac{n}{2}}^{1\hat{1}}, \phi_{\frac{n}{2}+1}^{2\hat{2}}, \dots, \phi_n^{2\hat{2}}). \quad (3.68)$$

Half of the particles have been chosen to be the scalar of the top component of the superfield, while the other half are the scalar of the bottom component of the superfield. This equal division is required to obtain a non-zero amplitude, because the superamplitude is homogeneous of degree n both in the η and $\tilde{\eta}$ coordinates. Due to this convenient choice of the component amplitude, the fermionic integral over χ 's and $\tilde{\chi}$'s can be done straightforwardly. Explicitly,

for the component amplitude we are interested in,

$$\int d\Omega_F^{(1,1)} \implies V_n J_w \int \prod_{k=0}^m d^2\chi_k d^2\tilde{\chi}_k \Delta_F^{\text{proj}} \tilde{\Delta}_F^{\text{proj}}, \quad (3.69)$$

where we have taken out the fermionic wave functions as in (3.64), which results in a Jacobian $J_w = \prod_{i=1}^n \frac{1}{(p_i^{13})^2}$ in the above expression. Furthermore, the fermionic delta functions are projected to the component amplitude of interest,

$$\Delta_F^{\text{proj}} = \prod_{i \in Y} \prod_{A=1,3} \delta \left(\frac{\langle \rho^A(\sigma_i) \chi(\sigma_i) \rangle}{\prod_{j \neq i} \sigma_{ij}} \right) \prod_{i \in \bar{Y}} p_i^{13}, \quad (3.70)$$

$$\tilde{\Delta}_F^{\text{proj}} = \prod_{i \in Y} \prod_{A=2,4} \delta \left(\frac{[\tilde{\rho}_A(\sigma_i) \tilde{\chi}(\sigma_i)]}{\prod_{j \neq i} \sigma_{ij}} \right) \prod_{i \in \bar{Y}} p_i^{13}. \quad (3.71)$$

Here Y labels all the scalars $\phi^{1\hat{1}}$, namely $Y := \{1, \dots, \frac{n}{2}\}$, and \bar{Y} labels the other type of scalars $\phi^{2\hat{2}}$, so $\bar{Y} := \{\frac{n}{2} + 1, \dots, n\}$.

Carrying out the integrations over $d^2\chi_k$ and $d^2\tilde{\chi}_k$, we see that the maps $\rho_a^A(\sigma_i)$ combine nicely into $\langle \rho^A(\sigma_i) \rho^B(\sigma_i) \rangle$, which on the support of the rational map constraints becomes $p_i^{AB} \prod_{j \neq i} \sigma_{ij}$. Concretely, we have,

$$\begin{aligned} \int \prod_{k=0}^m d^2\chi_k d^2\tilde{\chi}_k \prod_{i \in Y} \prod_{A=1,3} \delta \left(\frac{\langle \rho^A(\sigma_i) \chi(\sigma_i) \rangle}{\prod_{j \neq i} \sigma_{ij}} \right) \prod_{B=2,4} \delta \left(\frac{[\tilde{\rho}_B(\sigma_i) \tilde{\chi}(\sigma_i)]}{\prod_{j \neq i} \sigma_{ij}} \right) \\ = \prod_{i \in Y} p_i^{13} p_{i,24} \times \prod_{i \in Y} \prod_{J \in \bar{Y}} \frac{1}{\sigma_{iJ}^2}. \end{aligned} \quad (3.72)$$

Collecting terms, we find that the wave-function Jacobian J_w cancels out completely, and we obtain the final result

$$V_n J_w \int \prod_{k=0}^m d^2\chi_k d^2\tilde{\chi}_k \Delta_F^{\text{proj}} \tilde{\Delta}_F^{\text{proj}} = V_n \prod_{i \in Y} \prod_{J \in \bar{Y}} \frac{1}{\sigma_{iJ}^2} := J_F, \quad (3.73)$$

where we have defined the final result to be J_F . Therefore we have,

$$\mathcal{A}_n(\phi_1^{1\hat{1}}, \dots, \phi_{\frac{n}{2}}^{1\hat{1}}, \phi_{\frac{n}{2}+1}^{2\hat{2}}, \dots, \phi_n^{2\hat{2}}) = \int d\mu_n^{\text{6D}} (J_F \times \mathcal{J}_{n \text{ even}}). \quad (3.74)$$

We are now ready to compare this result directly with CHY amplitude, which is given by

$$\mathcal{A}_n(\phi_1^{1\hat{1}}, \dots, \phi_{\frac{n}{2}}^{1\hat{1}}, \phi_{\frac{n}{2}+1}^{2\hat{2}}, \dots, \phi_n^{2\hat{2}}) = \int d\mu_n \text{PT}(\alpha) \text{Pf}' \Psi_n \Big|_{\text{project}}, \quad (3.75)$$

and $d\mu_n = d\mu_n^{\text{6D}}$ if we restrict the CHY formula to 6D.

The notation $\Psi_n|_{\text{project}}$ denotes projection of the matrix Ψ_n of the CHY formulation to the specific scalar component amplitude we want via dimensional reduction. In particular, the ‘‘polarization vectors’’ should satisfy $\varepsilon_i \cdot \varepsilon_I = 1$ if $i \in Y$ and $I \in \bar{Y}$ or vice versa. If they belong to the same set, then we have $\varepsilon_i \cdot \varepsilon_j = \varepsilon_I \cdot \varepsilon_J = 0$. Furthermore, $p_i \cdot \varepsilon_j = 0$ for all i and j , i.e., both sets, since all of the vectors are dimensionally reduced to scalars. Let us now recall the definition of the matrix Ψ_n that enters the CHY construction of YM amplitudes. It can be expressed as

$$\Psi_n = \begin{pmatrix} A_n & -C_n^\top \\ C_n & B_n \end{pmatrix}, \quad (3.76)$$

where A_n is given in (3.57), and B_n and C_n are $n \times n$ matrices defined as

$$[B_n]_{ij} = \begin{cases} \frac{\varepsilon_i \cdot \varepsilon_j}{\sigma_{ij}} & \text{if } i \neq j, \\ 0 & \text{if } i = j. \end{cases} \quad [C_n]_{ij} = \begin{cases} \frac{p_j \cdot \varepsilon_i}{\sigma_{ij}} & \text{if } i \neq j, \\ -\sum_{l \neq i} \frac{p_l \cdot \varepsilon_i}{\sigma_{il}} & \text{if } i = j. \end{cases} \quad (3.77)$$

Like A_n , the matrix Ψ_n is also an antisymmetric matrix of co-rank 2. Its non-vanishing reduced Pfaffian is defined as

$$\text{Pf}'\Psi_n = \frac{(-1)^{p+q}}{\sigma_{pq}} \text{Pf}\Psi_n^{[pq]}, \quad (3.78)$$

where $\Psi_n^{[pq]}$ denotes the matrix Ψ_n with rows p, q and columns p, q removed. These should be chosen from the first n rows and columns. Otherwise, the result is independent of the choice of p, q .

For the specific choice of the component amplitude described above, $C_n = 0$ and the reduced Pfaffian $\text{Pf}'\Psi_n$ becomes

$$\text{Pf}'\Psi_n|_{\text{project}} = \text{Pf}'A_n \times \text{Pf}B_n|_{\text{scalar}}, \quad (3.79)$$

where the ‘‘projected’’ matrix B_n is

$$[B_n|_{\text{scalar}}]_{iJ} = \begin{cases} \frac{1}{\sigma_{iJ}} & \text{if } i \in Y, \quad J \in \bar{Y}, \\ 0 & \text{otherwise.} \end{cases} \quad (3.80)$$

Using the above result, we find

$$\text{Pf}B_n|_{\text{scalar}} = \det\left(\frac{1}{\sigma_{iJ}}\right) \quad \text{where } i \in Y, \quad J \in \bar{Y}. \quad (3.81)$$

Comparing (3.74) with (3.75), we deduce that the even-point integrand should be given by

$$\mathcal{J}_{n\text{ even}}(\alpha) = \text{PT}(\alpha) \text{Pf}' A_n \frac{\text{Pf } B_n|_{\text{scalar}}}{J_F}. \quad (3.82)$$

It is easy to prove that $\text{Pf } B_n|_{\text{scalar}}$ and J_F are actually identical. In particular, one can see that they, as rational functions, have the same zeros and poles. So we obtain the desired result, $\mathcal{J}_{n\text{ even}}(\alpha) = \text{PT}(\alpha) \text{Pf}' A_n$.

3.4 $\mathcal{N} = (1, 1)$ Super Yang–Mills: Odd Multiplicity

This section presents the formula for $\mathcal{N} = (1, 1)$ SYM amplitudes with odd multiplicity. This case is considerably subtler than the case of even n . It is perhaps the most novel aspect of the present work. Nevertheless, we will show that it can be written in a form entirely analogous to the even-point case:

$$\boxed{\mathcal{A}_{n\text{ odd}}^{\mathcal{N}=(1,1)\text{ SYM}}(\alpha) = \int d\mu_{n\text{ odd}}^{6\text{D}} \text{PT}(\alpha) \left(\text{Pf}' \widehat{A}_n \int d\widehat{\Omega}_F^{(1,1)} \right)}. \quad (3.83)$$

The following subsections describe the different ingredients in this expression.

Section 3.4 starts by presenting the form of the rational maps for n odd and studying the corresponding redundancies that enter in the integration measure. The explicit form of $d\mu_{n\text{ odd}}^{6\text{D}}$, given in (3.102), is deduced by considering a soft limit of an amplitude with n even. In particular, we deduce the existence of an emergent shift invariance acting on the rational maps. The discussion of how this new invariance interacts with the groups $\text{SL}(2, \mathbb{C})_\sigma$ and $\text{SL}(2, \mathbb{C})_\rho$ is relegated to Appendix B.1. Appendix B.2 presents the detailed derivation of the form of the maps, as well as the measure, from the soft limit of the even-point formula (3.56).

Section 3.4 discusses the form of the integrand for odd n , which can also be derived by carefully examining the soft limit. The fermionic integration measure $d\widehat{\Omega}_F^{(1,1)}$ is given explicitly in (3.121). We show that the odd- n analog of the A_n matrix is an antisymmetric $(n+1) \times (n+1)$ matrix, which is denoted \widehat{A}_n . It is constructed from $(n+1)$ momenta: the original n momenta of external particles and an additional special null vector, p_\star^{AB} , defined through an arbitrarily chosen puncture σ_\star . The formula for the matrix \widehat{A}_n is given in (3.157), and p_\star^{AB} in (3.158).

In Section 3.4 we describe consistency checks of (3.83). This includes a comparison with the CHY formula in the bosonic sector, as was done for n even

in 3.3. We also present a computation of the three-point superamplitude [121] directly from the connected formula.

Rational Maps and the Measure

Let us consider the definition of the scattering maps in 6D for the odd-point case $n = 2m + 1$:

$$p_i^{AB} = \frac{p^{AB}(\sigma_i)}{\prod_{j \neq i} \sigma_{ij}}. \quad (3.84)$$

This formula implies the scattering equations if $p^{AB}(z)$ is a polynomial of degree $n - 2 = 2m - 1$ such that the vector $p^{AB}(z)$ is massless for any value of z . The latter is realized by requiring

$$p^{AB}(z) = \langle \rho^A(z) \rho^B(z) \rangle = \rho^{A,+}(z) \rho^{B,-}(z) - \rho^{A,-}(z) \rho^{B,+}(z), \quad (3.85)$$

as in the case of even n . The polynomials $\rho^{A,+}(z)$ and $\rho^{A,-}(z)$ should have the same degree, since we want to maintain $\text{SL}(2, \mathbb{C})_\rho$ symmetry. This is achieved by choosing $\deg \rho^{A,a}(z) = m$. However, this produces an undesired term of degree $2m = n - 1$ in $p^{AB}(z)$. This term can be made to vanish by requiring that the coefficient of z^m in $\rho^{A,a}(z)$ takes the special form

$$\rho_m^{A,a} = \omega^A \xi^a, \quad (3.86)$$

since then $\langle \rho_m^A \rho_m^B \rangle = 0$. This is the first new feature we encounter for odd n . The maps for $n = 2m + 1$ then become

$$\rho^{A,a}(z) = \sum_{k=0}^{m-1} \rho_k^{A,a} z^k + \omega^A \xi^a z^m, \quad (3.87)$$

$$\tilde{\rho}_A^{\hat{a}}(z) = \sum_{k=0}^{m-1} \tilde{\rho}_{A k}^{\hat{a}} z^k + \tilde{\omega}_A \tilde{\xi}^{\hat{a}} z^m. \quad (3.88)$$

Note that the spinor ξ^a , which we also write as $|\xi\rangle$, involves a projective scale that can be absorbed into ω^A , which is invariant under $\text{SL}(2, \mathbb{C})_\rho$. In other words, ξ^a are homogeneous coordinates on \mathbb{CP}^1 . For instance, this freedom can be used to set

$$|\xi\rangle = \begin{pmatrix} 1 \\ \xi \end{pmatrix}. \quad (3.89)$$

In the following we use the symbol ξ to denote both the two-component spinor and its only independent component.

After plugging this form of the (chiral) maps into equations (3.84) we find the expected $(n - 3)!$ solutions. This is consistent since, as we show in Appendix B.2, this version of the maps can be obtained directly from a soft limit of the even multiplicity ones. However, a counting argument quickly leads to the fact that we must fix an extra component of the maps when solving the equations: There are $5n - 6$ independent equations for $5n + 1$ variables, which implies the existence of seven redundancies. Six of them are of course the $\text{SL}(2, \mathbb{C})$'s present in the even case, but there is an emergent redundancy that we call *T-shift* symmetry. It is the subject of the next section.

Action of the T-Shift

Consider the following transformation on the polynomials

$$\rho^A(z) \rightarrow \hat{\rho}^A(z) = (\mathbb{I} + zT)\rho^A(z). \quad (3.90)$$

Here T is a 2×2 matrix labeled by little-group indices. In order to preserve the bosonic delta functions, Δ_B , we require that for any value of z and for any polynomial $\rho^A(z)$:

$$\begin{aligned} p^{AB}(z) &= \hat{p}^{AB}(z) \\ &= \langle (\mathbb{I} + zT)\rho^A(z) (\mathbb{I} + zT)\rho^B(z) \rangle \\ &= \langle \rho^A(z) \rho^B(z) \rangle + z \langle (T\rho^A(z) \rho^B(z)) + (\rho^A(z) T\rho^B(z)) \rangle + z^2 \langle T\rho^A(z) T\rho^B(z) \rangle. \end{aligned} \quad (3.91)$$

Thus we obtain the following conditions

$$T^\top \epsilon + \epsilon T = 0, \quad T^\top \epsilon T = 0, \quad (3.92)$$

where T^\top is the transpose of T and ϵ is the 2×2 antisymmetric matrix. The first condition is equivalent to

$$\text{Tr } T = 0, \quad (3.93)$$

which implies that $T^2 \propto \mathbb{I}$. The second condition then fixes

$$T^2 = 0. \quad (3.94)$$

What is the meaning of the conditions (3.93) and (3.94)? They guarantee that the transformation (3.90) is a z -dependent $\text{SL}(2, \mathbb{C})_\rho$ transformation, hence preserving the polynomial map $p^{AB}(z)$. In other words, (3.93) and (3.94) are equivalent to

$$\det(\mathbb{I} + zT) = 1 \quad \text{for any } z. \quad (3.95)$$

We discuss such transformations in more generality in the next sections. For now, let us further impose that T preserves the degree of the maps, i.e., $\deg \hat{\rho}^{A,a}(z) = \deg \rho^{A,a}(z) = m$, that is

$$T_b^a \rho_m^{A,b} = 0, \quad (3.96)$$

where $\rho_m^{A,a}$ is the top coefficient. This means that the kernel of T consists of the four spinors $\rho_m^{A,a}$ with $A = 1, 2, 3, 4$. In general this would force the 2×2 matrix T to vanish. However, for an odd number of particles

$$\rho_m^{A,a} = \omega^A \xi^a \quad \implies \quad T_b^a \xi^b = 0. \quad (3.97)$$

These two equations, together with condition (3.93), fix three of the four components of T . It is easy to see that the solution is

$$T = \alpha |\xi\rangle \langle \xi|, \quad (3.98)$$

where $\alpha \in \mathbb{C}$ is a complex scale. Therefore we have found a redundancy on the coefficients of the maps given by the transformation (3.90). This is an inherent consequence of the description of the moduli space in terms of the polynomials (3.87). In fact, in Appendix B.1 we show how T is necessary from a purely group-theoretic point of view, when regarding the equivalent maps as representations of a bigger group, identified as $\text{SL}(2, \mathbb{C}) \times \mathbb{C}^2$. Finally, in Appendix B.2 we show how the soft limit of the even-multiplicity maps gives another interpretation of T that is reminiscent of the little group of the soft particle.

Let us close this part of the section by noting that T produces the following shift on the top component of the polynomial:

$$\hat{\rho}_m^{A,a} = \rho_m^{A,a} + T \rho_{m-1}^{A,a} = \omega^A \xi^a + \alpha \langle \xi | \rho_{m-1}^A \rangle \xi^a, \quad (3.99)$$

or equivalently,

$$\hat{\omega}^A = \omega^A + \alpha \langle \xi | \rho_{m-1}^A \rangle, \quad (3.100)$$

which will be useful in the next section.

Measure

Let us introduce the measure for $n = 2m + 1$, which can be obtained from the soft limit of the measure for $n = 2m + 2$. This leads to the correct

choice of integration variables, and the integral localizes on the solutions of the scattering equations. Specifically, we consider an amplitude for $n + 1 = 2m + 2$ particles, the last one of which is chosen to be a gluon. In the soft limit of the gluon momentum, i.e., $p_{2m+2} = \tau \hat{p}_{2m+2}$ and $\tau \rightarrow 0$, the even-point measure takes the form

$$\int d\mu_{2m+2}^{6D} = \delta(p_{n+1}^2) \int d\mu_{2m+1}^{6D} \frac{1}{2\pi i} \oint_{|\hat{E}_{n+1}|=\epsilon} \frac{d\sigma_{n+1}}{E_{n+1}} + O(\tau^0), \quad (3.101)$$

where the odd-point measure is given by:

$$d\mu_{2m+1}^{6D} = \frac{\left(\prod_{i=1}^n d\sigma_i \prod_{k=0}^{m-1} d^8 \rho_k \right) d^4 \omega \langle \xi d\xi \rangle}{\text{vol}(\text{SL}(2, \mathbb{C})_\sigma, \text{SL}(2, \mathbb{C})_\rho, \text{T})} \frac{1}{V_n^2} \prod_{i=1}^n \delta^6 \left(p_i^{AB} - \frac{p^{AB}(\sigma_i)}{\prod_{j \neq i} \sigma_{ij}} \right). \quad (3.102)$$

This is derived in detail in Appendix B.2. The volume factor here implies modding out by the action of the two $\text{SL}(2, \mathbb{C})$ groups, as well as the T-shift. Furthermore,

$$E_{n+1} = \tau \hat{E}_{n+1} = \tau \sum_{i=1}^n \frac{\hat{p}_{n+1} \cdot p_i}{\sigma_{n+1,i}} = 0 \quad (3.103)$$

corresponds to the scattering equation for the soft particle. The factor of τ in E_{n+1} makes the first term in the expansion of the $(n + 1)$ -particle measure singular as $\tau \rightarrow 0$. As we explain below, the measure given here for $n = 2m + 1$ has the correct $\text{SL}(2, \mathbb{C})_\sigma$ scaling, which is degree $4n$.

Let us now proceed to the explicit computation of the measure. Note that the redundancies can be used to fix seven of the $5n + 1$ variables, leaving $5n - 6$ integrations. This precisely matches the number of bosonic delta functions, which can be counted in the same way as in the even-point case. Therefore, as before, all the integration variables are localized by the delta functions. In order to carry out the computations, one needs use the seven symmetry generators to fix seven coordinates and obtain the corresponding Jacobian. The order in which this is done is also important, since T does not commute with the other generators. In order to make contact with the even-point counterpart, let us first fix the T-shift symmetry. Because T merely generates a shift in the coefficients of the polynomial, it can be seen that the measure in (3.102) is invariant. Now, let us regard the symmetry parameter α as one of the integration variables in favor of fixing one of the four components ω^A . For instance, one can choose ω^1 as fixed, and then integrate over the parameters

$\{\alpha, \omega^2, \omega^3, \omega^4\}$. It can be checked from (3.100) that this change of variables induces the Jacobian

$$d^4\hat{\omega} = \langle \xi \rho_{m-1}^1 \rangle d\alpha d\omega^2 d\omega^3 d\omega^4. \quad (3.104)$$

The other ingredients in the measure are invariant under this transformation, i.e.,

$$\Delta_B(\hat{\rho}, \sigma) = \Delta_B(\rho, \sigma), \quad (3.105)$$

$$\prod_{k=0}^{m-1} d^8 \hat{\rho}_k = \prod_{k=0}^{m-1} d^8 \rho_k. \quad (3.106)$$

The dependence on α can then be dropped, with the corresponding integration formally canceling the volume factor for the T-shift in the denominator of (3.102). The measure in this partially-fixed form is now

$$d\mu_{2m+1}^{6D} = \frac{(\prod_{i=1}^n d\sigma_i \prod_{k=0}^{m-1} d^8 \rho_k) d^3\omega \langle \xi \rho_{m-1}^1 \rangle \langle \xi d\xi \rangle}{\text{vol}(\text{SL}(2, \mathbb{C})_\sigma \times \text{SL}(2, \mathbb{C})_\rho)} \frac{1}{V_n^2} \prod_{i=1}^n \delta^6 \left(p_i^{AB} - \frac{p^{AB}(\sigma_i)}{\prod_{j \neq i} \sigma_{ij}} \right). \quad (3.107)$$

Note that the factor $d^3\omega \langle \xi \rho_{m-1}^1 \rangle \langle \xi d\xi \rangle$ is invariant under the projective scaling of ξ_α . By construction, it is also invariant under the action of the T shift, implying that ω^1 may be set to any value. However, after making these choices Lorentz invariance is no longer manifest.

Let us show explicitly how this measure has the correct $\text{SL}(2, \mathbb{C})_\sigma$ -scaling under the transformation $\sigma \rightarrow t\sigma$ together with the scaling of the coefficients in the maps,

$$\rho_k^{Aa} \rightarrow t^{m-k} \rho_k^{Aa}. \quad (3.108)$$

In particular, this implies that $\rho_m^{Aa} = \omega^A \xi^a$ is invariant. As is apparent from (3.90), the parameter α carries $\text{SL}(2, \mathbb{C})_\sigma$ -scaling -1 , as does the T volume $\langle \xi \rho_{m-1}^1 \rangle$ using (3.108). Since the projective scaling of ξ is completely independent from the $\text{SL}(2, \mathbb{C})_\sigma$ transformation, none of the components ξ^a and ω^A transform. Now, we find

$$\prod_{k=0}^{m-1} d^8 \rho_k \rightarrow t^{n^2-1} \prod_{k=0}^{m-1} d^8 \rho_k, \quad (3.109)$$

$$\frac{1}{V_n^2} \prod_{i=1}^n d\sigma_i \rightarrow t^{4n-n^2} \frac{1}{V_n^2} \prod_{i=1}^n d\sigma_i, \quad (3.110)$$

$$\langle \xi \rho_{m-1}^1 \rangle \langle \xi d\xi \rangle d^3\omega \rightarrow t \langle \xi \rho_{m-1}^1 \rangle \langle \xi d\xi \rangle d^3\omega, \quad (3.111)$$

leading to the scaling weight of $4n$ for the full measure as required.

Having carried out these checks, we are now in position to give the final form of the measure for $n = 2m + 1$ in the same way as explained earlier for even n . For this, we eliminate the remaining $\text{SL}(2, \mathbb{C})_\sigma \times \text{SL}(2, \mathbb{C})_\rho$ symmetry by performing the standard fixing of $\sigma_1, \sigma_2, \sigma_3$ and $\rho_0^{1,+}, \rho_0^{1,-}, \rho_0^{2,+}$. Note that we fixed the lowest coefficients ρ_0^{Aa} , because they are not affected by the T-shift. Otherwise, this would interfere with the T-shift. Finally, we extract the mass shell and momentum conservation delta functions as in (3.45). This leads to

$$d\mu_{2m+1}^{6D} = \frac{J_\rho J_\sigma}{V_n^2} \left(\prod_{i=4}^n d\sigma_i \right) d\rho_0^{2,-} d^2 \rho_0^3 d^2 \rho_0^4 \left(\prod_{k=1}^{m-1} d^8 \rho_k \right) d^3 \omega d\xi \langle \xi \rho_{d-1}^1 \rangle \hat{\Delta}_B, \quad (3.112)$$

where the Jacobians are given in (3.44), and $\hat{\Delta}_B$ is given in (3.46).

Transformations of the Maps

Having checked the scaling of the measure, here we consider other $\text{SL}(2, \mathbb{C})_\sigma$ transformations, as we will see that they lead to other interesting new features of the odd-point rational maps. In particular, let us consider the inversion $\sigma_i \rightarrow -1/\sigma_i$.³ Under this inversion, the rational map transforms as,

$$\frac{\langle \rho^A(\sigma_i) \rho^B(\sigma_i) \rangle}{\prod_{j \neq i} \sigma_{ij}} \rightarrow \frac{\langle \rho'^A(\sigma_i) \rho'^B(\sigma_i) \rangle}{(\prod_{j=1}^n \sigma_j^{-1}) (\prod_{j \neq i} \sigma_{ij})}, \quad (3.113)$$

and the new object $\rho'^A(\sigma_i)$ entering the map is given by

$$\rho'^A(\sigma_i) = (-1)^m \sum_{k=0}^m (-1)^k \rho_{k,a}^A \sigma_i^{m-k-\frac{1}{2}}. \quad (3.114)$$

Note that this is actually not a polynomial due to the fact that n is odd. To keep the rational-map constraints unchanged, we require that the coefficients transform as

$$\rho_{k,a}^A \rightarrow \rho'_{k,a}{}^A = (-1)^k \rho_{m-k,a}^A. \quad (3.115)$$

Then, up to an overall factor, the transformation exchanges the degree- k coefficient with the degree $m - k$ coefficient just like in the case of even n . What is different from the even-point case is the non-polynomial property of $\rho'^A(\sigma_i)$.

³The minus sign is for convenience only. Sign reversal is already established as a consequence of the scaling symmetry.

Therefore, inversion turns the polynomial map into a non-polynomial one of the following form

$$\rho'_a{}^A(z) = \sum_{k=0}^m \rho'_{k,a}{}^A z^{k-\frac{1}{2}}. \quad (3.116)$$

Now the lowest-degree coefficient, $\rho'_{0,a}{}^A$, which is proportional to the highest coefficient of the original map, has the special factorized form

$$\rho'_{0,a}{}^A = \omega^A \xi_a, \quad (3.117)$$

where we have used (3.86). Therefore the product $p^{AB}(z) = \langle \rho^A(z) \rho^B(z) \rangle$ remains a degree- $(n-2)$ polynomial.

Although we only use polynomial maps throughout the chapter, it is worth mentioning that the above non-polynomial form of the maps could be used equally well. This discussion makes it clear that for odd multiplicity a general $\text{SL}(2, \mathbb{C})_\sigma$ transformation can take the original polynomial maps to a more complicated-looking, but equivalent, version of maps. This is a consequence of the fact that the seven generators of $\text{SL}(2, \mathbb{C})_\sigma$, $\text{SL}(2, \mathbb{C})_\rho$, T do not close into a group, as can already be seen from the fact that

$$\text{vol}(\text{SL}(2, \mathbb{C})_\sigma, \text{SL}(2, \mathbb{C})_\rho, T) \quad (3.118)$$

carries weight -1 under scaling of $\text{SL}(2, \mathbb{C})_\sigma$. Compositions of the action of these seven generators on the maps lead to the general transformations of the form

$$\rho^{A,a}(z) \rightarrow (e^{\mathcal{T}(z)})_b^a \rho'^{A,b}(z), \quad (3.119)$$

where $\mathcal{T}_b^a(z)$ is a traceless 2×2 matrix depending on z .

It is interesting to study the subalgebra that preserves the form of the polynomial maps, which for even multiplicity is just $\text{SL}(2, \mathbb{C})_\sigma \times \text{SL}(2, \mathbb{C})_\rho$. In Appendix B.1 we obtain the corresponding algebra for odd multiplicity: We first show that the generators of $\text{SL}(2, \mathbb{C})_\sigma$ and $\text{SL}(2, \mathbb{C})_\rho$ do not commute in general and that a subset of these recombines into the algebra $\text{SL}(2, \mathbb{C}) \ltimes \mathbb{C}^2$. This includes inversion and T-shift, but it requires a partially fixed $\text{SL}(2, \mathbb{C})_\rho$ frame.

Integrand from Soft Limits

Here we apply the soft limit to the even-point integrand in order to obtain the odd-point version, with the soft factor included. The answer is composed of

two pieces:

$$\mathcal{I}_{\text{odd}}^{\mathcal{N}=(1,1) \text{ SYM}} = \int d\widehat{\Omega}_F^{(1,1)} \times \mathcal{J}_{\text{odd}}. \quad (3.120)$$

The fermionic measure $d\widehat{\Omega}_F^{(1,1)}$ can be obtained in a way similar to the bosonic one, and we relegate its derivation to Appendix B.2. The result is

$$d\widehat{\Omega}_F^{(1,1)} = V_n dg d\tilde{g} \prod_{k=0}^{m-1} d^2\chi_k d^2\tilde{\chi}_k \prod_{i=1}^n \delta^4\left(q_i^A - \frac{\langle \rho^A(\sigma_i) \chi(\sigma_i) \rangle}{\prod_{j \neq i} \sigma_{ij}}\right) \delta^4\left(\tilde{q}_{i,A} - \frac{[\tilde{\rho}_A(\sigma_i) \tilde{\chi}(\sigma_i)]}{\prod_{j \neq i} \sigma_{ij}}\right). \quad (3.121)$$

The fermionic maps are constructed such that $\langle \rho(z) \chi(z) \rangle$ and its conjugate are polynomials of degree $n - 2$, and take a form similar to the bosonic map in (3.87). Specifically,

$$\chi^a(z) = \sum_{k=0}^{m-1} \chi_k^a z^k + g \xi^a z^m, \quad (3.122)$$

$$\tilde{\chi}^{\hat{a}}(z) = \sum_{k=0}^{m-1} \tilde{\chi}_k^{\hat{a}} z^k + \tilde{g} \tilde{\xi}^{\hat{a}} z^m, \quad (3.123)$$

where the χ 's and $\tilde{\chi}$'s, as well as g and \tilde{g} , are Grassmann coefficients. Note that the same spinors ξ^a and $\tilde{\xi}^{\hat{a}}$ appear in the coefficients of z^m for both the bosonic maps and the fermionic maps. This form ensures the coefficient of z^{2m} in the product of maps vanishes, so that the product has the desired degree, $2m - 1 = n - 2$, for an odd number of particles.

With this parametrization of the maps, the first check is to show that the construction has the right Grassmann degree. As in the case of the even n , we need to remove the fermionic “wave functions” $\prod_{i=1}^n \delta^2(\tilde{\lambda}_{i,A,\hat{a}} q_i^A) \delta^2(\lambda_{i,b}^B \tilde{q}_B)$. This leaves an integrand with Grassmann degree of $4n$, as required. Having established the Grassmann degree of the integrand, let us next count the number of fermionic integrations. There are $4m$ χ and $\tilde{\chi}$ integrals and two g and \tilde{g} integrals, giving a total of $4m + 2 = 2n$ integrations. The final amplitude thus has Grassmann degree $2n$. More precisely, just as for even n , it has degree n in both the η 's and the $\tilde{\eta}$'s, which is what we expect for the superamplitudes of 6D $\mathcal{N} = (1, 1)$ SYM in the representation (3.48).

The factor \mathcal{J}_{odd} , which is purely bosonic, contains a contour integral in σ_{n+1} that emerges from the soft limit of the measure (3.101). Therefore, it encodes all of the dependence on the soft particle. Using the identity permutation \mathbb{I}_n

and setting $\sigma_{n+1} = z$ for convenience, we show in Appendix B.2 that for a soft gluon

$$S^{a\hat{a}} \mathcal{J}_{\text{odd}} = \text{PT}(\mathbb{I}_n) \frac{\sigma_{1n}}{2\pi i} \oint_{|\hat{\mathcal{E}}_{n+1}|=\varepsilon} \frac{dz}{\mathcal{E}_{n+1}} \times \frac{\text{Pf}' A_{n+1}}{(z - \sigma_1)(z - \sigma_n)} \frac{x^a}{\langle \xi \Xi \rangle} \frac{\tilde{x}^{\hat{a}}}{[\tilde{\xi} \tilde{\Xi}]}. \quad (3.124)$$

Let us explain the various terms appearing in this formula. First, the vanishing of $\mathcal{E}_{n+1} = \tau \hat{\mathcal{E}}_{n+1} = p(z) \cdot p_{n+1}$ is the rescaled scattering equation for the soft $(n+1)$ th particle (on the support of the hard scattering equations), such that $\mathcal{E}_{n+1} = E_{n+1} \prod_{i=1}^n (z - \sigma_i)$. In terms of the 6D spinor-helicity formalism, Weinberg's soft factor for a gluon is given by

$$S^{a\hat{a}} = \frac{[\tilde{\lambda}_{n+1}^{\hat{a}} | p_1 \tilde{p}_n | \lambda_{n+1}^a \rangle}{s_{n+1,1} s_{n,n+1}} = \frac{\tilde{\lambda}_{n+1,A}^{\hat{a}} p_1^{AB} \tilde{p}_{n,BC} \lambda_{n+1}^{a,C}}{s_{n+1,1} s_{n,n+1}}. \quad (3.125)$$

The reduced Pfaffian can be expanded as

$$\text{Pf}' A_{n+1} = \frac{(-1)^{n+1}}{\sigma_{1n}} \sum_{i=2}^{n-1} (-1)^i \frac{p_{n+1} \cdot p_i}{z - \sigma_i} \text{Pf} A_{n+1}^{[1,i,n,n+1]}, \quad (3.126)$$

where $A_{n+1}^{[1,i,n,n+1]}$ denotes the matrix A_{n+1} with rows and columns 1, i , n , $n+1$ removed. This odd-point integrand by construction does not depend on τ , the scaling parameter introduced to define the soft limit. It is also independent of the choice of polarization (a, \hat{a}) and the direction of the soft momentum $p_{n+1} = \tau \hat{p}_{n+1}$. Recall that $\xi^a = (1, \xi)$ is determined from the hard scattering maps, while $\Xi^a = (\Xi^+, \Xi^-)$ and $x^a = (x, -1)$ are given by the following linear equations (for $z = \sigma_{n+1}$):

$$\langle \Xi \rho^A(z) \rangle = \langle x \lambda_{n+1}^A \rangle, \quad [\tilde{\Xi} \tilde{\rho}^A(z)] = [\tilde{x} \tilde{\lambda}_{n+1}^A]. \quad (3.127)$$

Introducing a reference spinor r^A and contracting the first of the preceding two equations with $\epsilon_{ABCD} \lambda_{n+1}^{B,a} \rho^{C,b}(z) r^D$, we obtain

$$x^a \langle \rho^b(z) | \tilde{p}_{n+1} | r \rangle = \Xi^b \langle \lambda_{n+1}^a | \tilde{p}(z) | r \rangle. \quad (3.128)$$

This can be used to make the z -dependence explicit in the integrand. Contracting with ξ_b and repeating these steps for the anti-chiral piece gives

$$\frac{x^a}{\langle \xi \Xi \rangle} \frac{\tilde{x}^{\hat{a}}}{[\tilde{\xi} \tilde{\Xi}]} = \frac{\langle \lambda_{n+1}^a | \tilde{p}(z) | r \rangle [\tilde{r} | p(z) | \tilde{\lambda}_{n+1}^{\hat{a}}]}{\xi^b \langle \rho_b(z) | \tilde{p}_{n+1} | r \rangle [\tilde{r} | p_{n+1} | \tilde{\rho}_{\hat{b}}(z) | \tilde{\xi}^{\hat{b}}]}, \quad (3.129)$$

where $|r\rangle$ and $[\tilde{r}]$ are independent reference spinors. Hence

$$S^{a\hat{a}} \mathcal{J}_{\text{odd}} = \text{PT}(\mathbb{I}_n) \frac{\sigma_{1n}}{2\pi i} \oint_{|\hat{\mathcal{E}}_{n+1}|=\varepsilon} \frac{dz}{\mathcal{E}_{n+1}} \times \frac{\text{Pf}' A_{n+1}}{(z - \sigma_1)(z - \sigma_n)} \frac{\langle \lambda_{n+1}^a | \tilde{p}(z) | r \rangle [\tilde{r} | p(z) | \tilde{\lambda}_{n+1}^{\hat{a}}]}{\xi^b \langle \rho_b(z) | \tilde{p}_{n+1} | r \rangle [\tilde{r} | p_{n+1} | \tilde{\rho}_b(z)] \xi^{\hat{b}}}. \quad (3.130)$$

In Section 3.4 we evaluate this integral via contour deformation. However, let us point out here the difficulties arising when trying to evaluate this integral. For a given solution of the hard punctures $\{\sigma_i\}_{i=1}^n$ the scattering equation $\hat{\mathcal{E}}_{n+1} = 0$ is a polynomial equation of degree $n - 2$ in z , which in general does not have closed-form solutions. In the CHY formalism the soft limit can be evaluated by deforming the contour and enclosing instead the hard punctures at $z = \sigma_i$. This is because the CHY integrand can be decomposed into Parke–Taylor factors, which altogether yield $1/z^2$ as the fall off at infinity. The argument can be straightforwardly repeated for the Witten–RSV formula in four dimensions, as we outline in Appendix B.2. In the case of (3.130) we find the leading behavior at infinity to be exactly $1/z^2$. However, the new contour will also enclose the poles associated to the brackets in the denominator, which are given by the solutions of a polynomial equation of degree $(n - 3)/2$. Since these contributions to the integral also turn out to be cumbersome to evaluate, in the next section we introduce a novel contour deformation that allows us to evaluate the integral without the need to compute these individual contributions.

Contour Deformation

The soft factor $S^{a\hat{a}}$, given by (3.125), is still contained in the integrand \mathcal{J}_{odd} and introduces an apparent dependence on the soft momentum. In order to extract it and evaluate the contour integral at the same time, we perform a complex shift of the soft momentum p_{n+1} . More specifically, for a given solution of the hard data $\{\sigma_i, \rho, \tilde{\rho}\}$, we perform a holomorphic shift in $|\lambda_{n+1}\rangle$ and use it to extract the odd-point integrand as a residue.

First, consider a reference null six-vector $Q = |q_a\rangle\langle q^a|$. (The Lorentz indices are implicit.) Using the little-group symmetry, the spinors can be adjusted such that

$$\langle \rho_a(\sigma_n) | \tilde{q}_b] = m \epsilon_{ab}, \quad (3.131)$$

together with $\langle q_a | \tilde{q}_b] = 0$. Here $m^2 = 2p(\sigma_n) \cdot Q$ is a mass scale that drops out at the end of the computation, so we set $m = 1$ for convenience. Note

that $\tilde{q}_{b,A}$ transforms under the antifundamental representation of the Lorentz group, $SU^*(4)$, but under the *chiral* $SL(2, \mathbb{C})_\rho$. Now consider a shift described by a complex variable w :

$$|\lambda_{n+1}^a\rangle \rightarrow |\lambda_w^a\rangle = |\rho_n^a\rangle + w |q^a\rangle \quad (3.132)$$

$$[\tilde{\lambda}_{n+1}^\dagger] \rightarrow [\tilde{\lambda}_w^\dagger] = [\tilde{\rho}_n] + w C^a [\tilde{q}_a], \quad (3.133)$$

where $|\rho_n^a\rangle^A$ is shorthand for $\rho^{A,a}(\sigma_n)$, while

$$[\tilde{\rho}_n]_A = [\tilde{\xi} \tilde{\rho}_A(\sigma_n)], \quad (3.134)$$

and the index A has been suppressed in the preceding equations. Without loss of generality, we may make the deformation for a specific choice of the polarization, which we have chosen to be $\hat{a} = \hat{+}$ in the second line. The only requirement for $[\tilde{\lambda}_{n+1}^\dagger]$ is that

$$0 = \langle \lambda_{n+1}^a | \tilde{\lambda}_{n+1}^\dagger \rangle = \langle \lambda_w^a | \tilde{\lambda}_w^\dagger \rangle = \langle \rho_n^a | \tilde{q}_b \rangle C^b + \langle q^a | \tilde{\rho}_n \rangle, \quad a = +, -, \quad (3.135)$$

and using (3.131) this implies $C^a = \langle q^a | \tilde{\rho}_n \rangle$.

The shifted soft factor that we utilize is

$$S_w^{a\hat{+}} = \frac{\langle \lambda_w^a | \tilde{p}_n p_1 | \tilde{\lambda}_w^\dagger \rangle}{s_{w,1} s_{w,n}}, \quad (3.136)$$

which has a simple pole at $w = 0$. After a short computation one can show that

$$\frac{1}{2\pi i} \oint_{|w|=\varepsilon} dw S_w^{a\hat{+}} = \frac{C^a}{2\pi i} \oint_{|w|=\varepsilon} \frac{dw}{w} = C^a. \quad (3.137)$$

Thus, the odd-point integrand can be recast in the form

$$\mathcal{J}_{\text{odd}} = \text{PT}(\mathbb{I}_n) \times \frac{1}{2\pi i C^a} \oint_{|w|=\varepsilon} dw I_w^a, \quad (3.138)$$

with

$$I_w^a = \frac{1}{2\pi i} \oint_{|p(z) \cdot p_w|=\varepsilon} \frac{dz}{p(z) \cdot p_w} \times \frac{\sigma_{1n} \text{Pf}' A_{n+1}}{(z - \sigma_1)(z - \sigma_n)} \frac{x^a}{\langle \xi \Xi \rangle} \frac{\tilde{x}^\dagger}{[\tilde{\xi} \tilde{\Xi}]}. \quad (3.139)$$

As $w \rightarrow 0$, the soft momentum $p_w \rightarrow p(\sigma_n)$, and hence we expect $z \rightarrow \sigma_n$. In fact, we claim that this solution is the only one contributing to the singularity

in w . Therefore we may redefine the contour as enclosing only the pole at σ_n , and

$$I_w^a = \frac{1}{2\pi i} \oint_{|z-\sigma_n|=\varepsilon} \frac{dz}{p(z) \cdot p_w} \times \frac{\sigma_{1n} \text{Pf}' A_{n+1}}{(z-\sigma_1)(z-\sigma_n)} \frac{x^a}{\langle \xi \Xi \rangle} \frac{\tilde{x}^\dagger}{[\tilde{\xi} \tilde{\Xi}]} \quad (3.140)$$

$$= \frac{\text{Pf}' A_{n+1}|_{z=\sigma_n}}{p(\sigma_n) \cdot p_w} \frac{\langle \lambda_w^a | \tilde{p}(\sigma_n) | r \rangle [\tilde{r} | p(\sigma_n) | \tilde{\lambda}_w]}{\langle \rho_n | \tilde{p}_w | r \rangle [\tilde{r} | p_w | \tilde{\rho}_n]}. \quad (3.141)$$

One can show that:

$$p(\sigma_n) \cdot p_w = \frac{w^2}{2}, \quad (3.142)$$

$$\text{Pf}' A_{n+1}|_{z=\sigma_n} = \frac{\omega}{2} \frac{1}{\sigma_{n1}} \sum_{i=2}^{n-1} (-1)^i \frac{\langle q^a | \tilde{p}_i | \rho_{n,a} \rangle}{\sigma_{ni}} \text{Pf} A_{n+1}^{[1,i,n,n+1]} + \mathcal{O}(w^2), \quad (3.143)$$

where we have used the identity

$$\sum_{i=2}^{n-1} (-1)^i \frac{p_n \cdot p_i}{\sigma_{ni}} \text{Pf} A_{n+1}^{[1,i,n,n+1]} = 0. \quad (3.144)$$

We also have that

$$\frac{[\tilde{r} | p(\sigma_n) | \tilde{\lambda}_w]}{[\tilde{r} | p_w | \tilde{\rho}_n]} = \frac{w [\tilde{r} | \rho_{n,a} \rangle \langle \rho_n^a | \tilde{q}_b \rangle C^b}{w [\tilde{r} | \rho_{n,b} \rangle C^b} + \mathcal{O}(w) = 1 + \mathcal{O}(w). \quad (3.145)$$

Note that for the chiral piece we can set $|r\rangle$ such that $\tilde{p}(\sigma_n)|r\rangle = |\tilde{\rho}_n\rangle$. Then

$$\frac{\langle \lambda_w^a | \tilde{p}(\sigma_n) | r \rangle}{\langle \rho_n | \tilde{p}_w | r \rangle} = \frac{w \langle q^a | \tilde{\rho}_n \rangle}{w \epsilon_{ABCD} \xi^c \rho_{n,c}^A \rho_{n,b}^B q^{C,b} r^D} + \mathcal{O}(w), \quad (3.146)$$

where the contraction in the denominator evaluates to

$$\epsilon_{ABCD} \xi^c \rho_{n,c}^A \rho_{n,b}^B q^{C,b} r^D = \langle q | \tilde{p}(\sigma_n) | r \rangle = \langle q | \tilde{\rho}_n \rangle, \quad (3.147)$$

with $|q\rangle^A := \xi^a q_a^A$. Hence we obtain

$$\lim_{w \rightarrow 0} \frac{\langle \lambda_w^a | \tilde{p}(\sigma_n) | r \rangle}{\langle \rho_n | \tilde{p}_w | r \rangle} = \frac{C^a}{\langle q | \tilde{\rho}_n \rangle}. \quad (3.148)$$

Putting everything together we find

$$\begin{aligned} \mathcal{J}_{\text{odd}} &= \text{PT}(\mathbb{I}_n) \times \frac{1}{2\pi i C^a} \oint_{|w|=\varepsilon} \frac{dw}{w} \frac{C^a}{\sigma_{n1}} \sum_{i=2}^{n-1} (-1)^i \frac{\langle q^a | \tilde{p}_i | \rho_{n,a} \rangle}{\sigma_{ni} \langle q | \tilde{\rho}_n \rangle} \text{Pf} A_{n+1}^{[1,i,n,n+1]} \\ &= \text{PT}(\mathbb{I}_n) \times \frac{\langle q^a | \tilde{X}_{(1,n)} | \rho_{n,a} \rangle}{\langle q | \tilde{\rho}_n \rangle}, \end{aligned} \quad (3.149)$$

where for convenience we have defined the null vector

$$X_{(1,n)}^{AB} := \frac{1}{\sigma_{n1}} \sum_{i=2}^{n-1} (-1)^i \frac{p_i^{AB}}{\sigma_{ni}} \text{Pf} A_{n+1}^{[1,i,n,n+1]} = \frac{1}{2} \epsilon^{ABCD} \tilde{X}_{(1,n),CD}. \quad (3.150)$$

Despite using the notation $\text{Pf} A_{n+1}^{[1,i,n,n+1]}$, this Pfaffian is completely independent of the soft momentum and the associated puncture. As anticipated, the expression is independent of the scale of q , so we can remove the normalization condition $2p(\sigma_n) \cdot Q = 1$, turning $|q^a\rangle$ into a completely arbitrary spinor. Expanding the numerator of (3.149) in a basis given by $\{\xi, \zeta\}$, where ζ is a reference spinor such that $\langle \xi \zeta \rangle = 1$, we find:

$$\mathcal{J}_{\text{odd}} = \text{PT}(\mathbb{I}_n) \times \frac{\langle q | \tilde{X}_{(1,n)} | \pi_n \rangle - \langle w | \tilde{X}_{(1,n)} | \rho_n \rangle}{\langle q | \tilde{\rho}_n \rangle}, \quad (3.151)$$

where

$$|\pi_n\rangle^A = \langle \zeta | \rho^A(\sigma_n) \rangle \quad (3.152)$$

is the conjugate component of $|\rho_n\rangle$. Also,

$$|w\rangle^A = \langle \zeta | q^A \rangle. \quad (3.153)$$

In particular, the fact that the integrand is independent of w implies the non-trivial identity:

$$\tilde{X}_{(1,n)} |\rho_n\rangle = 0, \quad (3.154)$$

which yields the following form of the integrand

$$\mathcal{J}_{\text{odd}} = \text{PT}(\mathbb{I}_n) \times \frac{\langle q | \tilde{X}_{(1,n)} | \pi_n \rangle}{\langle q | \tilde{\rho}_n \rangle}. \quad (3.155)$$

Using (3.154) this expression can be recast in a non-chiral form. Let us introduce another reference spinor $|\tilde{q}\rangle$ and consider

$$\mathcal{J}_{\text{odd}} = \text{PT}(\mathbb{I}_n) \times \frac{\langle q | \tilde{X}_{(1,n)} p(\sigma_n) | \tilde{q} \rangle}{\langle q | \tilde{\rho}_n \rangle \langle \rho_n | \tilde{q} \rangle}. \quad (3.156)$$

Note that $\tilde{p}(\sigma_n)_{AB} X_{(1,n)}^{BC} = -\tilde{X}_{(1,n),AB} p(\sigma_n)^{BC}$. Finally, using the definition of $X_{(1,n)}$ in (3.150) we recognize that the second factor in (3.156) is in fact a reduced Pfaffian of an antisymmetric $(n+1) \times (n+1)$ matrix constructed out of A_n with an additional column and row (labeled by \star) attached. We call this

matrix \widehat{A}_n . Restoring the original integration variables, its entries are given by:

$$[\widehat{A}_n]_{ij} = \begin{cases} \frac{p_i \cdot p_j}{\sigma_{ij}} & \text{if } i \neq j, \\ 0 & \text{if } i = j, \end{cases} \quad \text{for } i, j = 1, 2, \dots, n, \star, \quad (3.157)$$

where

$$p_\star^{AB} = \frac{2 q^{[A} p^{B]C}(\sigma_\star) \tilde{q}_C}{q^D [\tilde{\rho}_D(\sigma_\star) \tilde{\xi}] \langle \rho^E(\sigma_\star) \xi \rangle \tilde{q}_E} \quad (3.158)$$

is a reference null vector entering the final row and column, q and \tilde{q} are arbitrary spinors, and σ_\star is a reference puncture that can be set to one of the punctures associated to removed rows and columns. In fact, we have numerical evidence that σ_\star can be chosen completely arbitrarily without changing the result. Here, $q^{[A} p^{B]C}$ denotes the antisymmetrization $q^A p^{BC} - q^B p^{AC}$. The reduced Pfaffian is then defined analogously to (3.58), with the restriction that the starred column and row are not removed. Independence of the choice of removed columns and rows follows from the analogous statement for n even. It is straightforward to confirm that $\text{Pf}' \widehat{A}_n$ transforms as a quarter-integrand in the $\text{SL}(2, \mathbb{C})_\rho$ -frame studied in Appendix B.1, and that its mass dimension is $n-2$, as required. This completes the derivation of the odd-point formula (3.83). The reasoning was complicated, but the result is as simple as could be hoped for.

Consistency Checks

We have checked numerically that the new formula (3.83) correctly reproduces the 6D SYM amplitudes of gluons and scalars directly computed from Feynman diagrams, up to $n = 7$. In this subsection we perform additional consistency checks of the formula. We begin by re-deriving the odd-point integrand \mathcal{I}_{odd} by comparing it with the corresponding CHY expression for a particular bosonic sector following a similar argument used earlier for the case of even n . We will then show analytically that the formula leads to the correct three-point super-amplitude of 6D SYM. It is worth noting that the three-point amplitudes in 6D YM are rather subtle due to the special kinematics first explained in [43]. As we will see, our formula gives a natural parametrization of the special three-point kinematics.

Comparison with CHY

This section presents an alternative derivation of the integrand of the odd-point amplitudes. The method we will use here is similar to the one for the even-point case given in Section 3.3. It is based on comparison to known results of the CHY formulation of YM amplitudes in general spacetime dimensions. This method of derivation is independent of and very different from the soft-theorem derivation presented in the previous sections. Therefore it constitutes an additional consistency check.

Let us begin with the general form of the odd-point amplitudes of 6D $\mathcal{N} = (1, 1)$ SYM,

$$\mathcal{A}^{\mathcal{N}=(1,1)\text{SYM}_n} = \int d\mu_n^{6\text{D}} d\widehat{\Omega}_F^{(1,1)} \times \mathcal{J}_{n\text{odd}}, \quad (3.159)$$

for $n = 2m + 1$. Recall that the bosonic measure $d\mu_n^{6\text{D}}$ is defined in (3.102), and the fermionic measure $d\widehat{\Omega}_F^{(1,1)}$ is given in (3.121), which is the part that is more relevant to the discussion here. The goal is to determine the integrand $\mathcal{J}_{n\text{odd}}$. As mentioned above, we will follow the same procedure as in the case of even n , namely comparison of our formula with the CHY formulation of amplitudes for adjoint scalars and gluons. To do so, we consider a particular component of the amplitude. Due to the fact that n is odd and the scalars have to appear in pairs, it is not possible to choose all the particles to be scalars. The most convenient choice of the component amplitudes one with $n-1$ scalars and one gluon. Concretely, in the same notation as before, we choose to consider

$$\mathcal{A}_n(\phi_1^{1\hat{1}}, \dots, \phi_m^{1\hat{1}}, \phi_{m+1}^{2\hat{2}}, \dots, \phi_{2m}^{2\hat{2}}, A_n^{a\hat{a}}), \quad (3.160)$$

where $A_n^{a\hat{a}}$ is a gluon.

As in Section 3.3, we integrate out the fermionic variables so as to extract the desired component amplitude. The computation is similar to the one for even n , but slightly more complicated due to the appearance of $A_n^{a\hat{a}}$ in the middle term of the superfield. Projecting to this component amplitude, we obtain

$$\int d\Omega_F^{(1,1)} \implies V_n J_w \int \prod_{k=0}^{m-1} d^2\chi_k d^2\tilde{\chi}_k dg d\tilde{g} d\eta_n^\alpha d\tilde{\eta}_n^{\hat{\alpha}} \Delta_F^{\text{proj}} \tilde{\Delta}_F^{\text{proj}}. \quad (3.161)$$

The factor $J_w = \prod_{i=1}^n \frac{1}{(p_i^{13})^2}$ arises from extracting the fermionic wave func-

tions. The fermionic delta functions are given by

$$\Delta_F^{\text{proj}} = \prod_{A=1,3} \delta \left(q_n^A - \frac{\langle \rho^A(\sigma_n) \chi(\sigma_n) \rangle}{\prod_{j \neq n} \sigma_{nj}} \right) \prod_{i \in Y} \delta \left(\frac{\langle \rho^A(\sigma_i) \chi(\sigma_i) \rangle}{\prod_{j \neq i} \sigma_{ij}} \right) \prod_{i \in \bar{Y}} p_i^{13} \quad (3.162)$$

$$\tilde{\Delta}_F^{\text{proj}} = \prod_{A=2,4} \delta \left(\tilde{q}_{nA} - \frac{[\tilde{\rho}_A(\sigma_n) \tilde{\chi}(\sigma_n)]}{\prod_{j \neq n} \sigma_{nj}} \right) \prod_{i \in Y} \delta \left(\frac{[\tilde{\rho}_A(\sigma_i) \tilde{\chi}(\sigma_i)]}{\prod_{j \neq i} \sigma_{ij}} \right) \prod_{i \in \bar{Y}} p_i^{13} \quad (3.163)$$

with $Y := \{1, \dots, m\}$ and $\bar{Y} := \{m+1, \dots, n-1\}$. Compared to the even-particle case, we have an additional contribution coming from the gluon $A_n^{a\hat{a}}$. Performing the fermionic integrations leads to the final result,

$$d\widehat{\Omega}_F^{(1,1)} \implies (J_F)_{a\hat{a}} = \frac{\lambda_{n,a}^{[A} \langle \rho^B \rangle(\sigma_n) \xi \rangle \tilde{\lambda}_{n,\hat{a},[C} [\tilde{\rho}_D](\sigma_n) \tilde{\xi}]}{p_n^{AB} p_{n,CD}} \frac{V_n}{\prod_{j \neq n} \sigma_{nj}^2} \prod_{i \in Y, J \in \bar{Y}} \frac{1}{\sigma_{iJ}^2}, \quad (3.164)$$

where the square brackets denote anti-symmetrization on indices A, B and C, D . Note that although the formula for $(J_F)_{a\hat{a}}$ exhibits explicit Lorentz indices A, B and C, D , it is actually independent of the choice of these indices. Therefore, we have only made the dependence on the little-group indices a and \hat{a} explicit in $(J_F)_{a\hat{a}}$. They appear because the component amplitude contains a gluon $A_n^{a\hat{a}}$.

Having extracted the component amplitude that we want, we can compare it to the corresponding result from the CHY formulation. From the comparison, we find that the odd-point integrand is given by

$$\mathcal{J}_{n\text{odd}}(\alpha) = \frac{\text{Pf}'(\Psi_{\text{project}})_{a\hat{a}}}{(J_F)_{a\hat{a}}} \times \text{PT}(\alpha). \quad (3.165)$$

This ratio should be scalar, independent of the choice of the little-group indices a and \hat{a} . As in the case of n even, $\text{Pf}'\Psi_{\text{project}}$ is defined by the usual $\text{Pf}'\Psi$, projected to the component amplitude under consideration. In the present case this means that the dot products of a pair of polarization vectors for scalars particles are the same as before, namely $\varepsilon_i \cdot \varepsilon_I = 1$ if $i \in Y$ and $I \in \bar{Y}$, and otherwise they vanish. Furthermore $\varepsilon_i \cdot \varepsilon_n = 0$, and $p_i \cdot \varepsilon_j = 0$ if $j \neq n$. Using these rules, the original reduced Pfaffian $\text{Pf}'\Psi$ simplifies to

$$\text{Pf}'(\Psi_{\text{project}})_{a\hat{a}} = \det(\Delta_m) \sum_{i=1}^{n-2} (-1)^i \frac{p_i \cdot (\varepsilon_n)_{a\hat{a}}}{\sigma_{in}} \text{Pf} A_n^{[i, n-1, n]}, \quad (3.166)$$

where the $m \times m$ matrix Δ_m has entries given by $\frac{1}{\sigma_{iI}}$ for $i \in Y$ and $I \in \bar{Y}$.

The ratio entering the integrand $\mathcal{J}_{n\text{ odd}}$ in (3.165) can be dramatically simplified. To demonstrate this, note that as $\mathcal{J}_{n\text{ odd}}(\alpha)$ is a scalar, the following two tensors are proportional,

$$\lambda_{n,a}^A \langle \rho^B \rangle (\sigma_n) \xi \rangle \tilde{\lambda}_{n,\hat{a},[C} [\tilde{\rho}_D] (\sigma_n) \tilde{\xi}] \times R = p_n^{AB} p_{n,CD} \sum_{i=1}^{n-2} (-1)^i \frac{p_i \cdot (\varepsilon_n)_{a\hat{a}}}{\sigma_{in}} \text{Pf}A_n^{[i,n-1,n]}, \quad (3.167)$$

where the proportionality factor R is a scalar. After multiplying both sides of this equation with $\lambda_n^{A,a} \tilde{\lambda}_{n,C}^{\hat{a}}$ and contracting indices a and \hat{a} , we obtain

$$\begin{aligned} \langle \rho^A (\sigma_n) \xi \rangle [\tilde{\rho}_C (\sigma_n) \tilde{\xi}] \times R &= \sum_{i=1}^{n-2} (-1)^i \frac{\lambda_n^{A,a} p_i \cdot (\varepsilon_n)_{a\hat{a}} \tilde{\lambda}_{n,C}^{\hat{a}}}{\sigma_{in}} \text{Pf}A_n^{[i,n-1,n]} \\ &= \sum_{i=1}^{n-2} \frac{(-1)^i p_n^{AB} p_{i,BD} \varrho^{DE} p_{n,EC}}{\sigma_{in} \varrho \cdot p_n} \text{Pf}A_n^{[i,n-1,n]}, \end{aligned} \quad (3.168)$$

where in the last line we used the spinor form of the polarization vector $(\varepsilon_n)_{a\hat{a}}$ [43], with ϱ a reference vector. Collecting everything and plugging R back into the integrand, we arrive at:

$$\mathcal{J}_{n\text{ odd}}(\alpha) = \frac{\text{PT}(\alpha)}{\sigma_{n-1,n}} \sum_{i=1}^{n-2} \frac{(-1)^i p^{AB}(\sigma_n) p_{i,BD} \varrho^{DE} p_{n,EC}}{\sigma_{in} \varrho \cdot p_n \rho_n^A \tilde{\rho}_{n,C}} \text{Pf}A_n^{[i,n-1,n]}, \quad (3.169)$$

where we have also simplified the σ -dependent part, and defined

$$\rho_n^A := \langle \rho^A (\sigma_n) \xi \rangle, \quad \tilde{\rho}_{n,C} := [\tilde{\rho}_C (\sigma_n) \tilde{\xi}], \quad (3.170)$$

as in the previous subsection. Furthermore, using the identity

$$\sum_{i=1}^{n-2} (-1)^i \frac{p_i \cdot p_n}{\sigma_{in}} \text{Pf}A_n^{[i,n-1,n]} = 0, \quad (3.171)$$

the summation in the expression of $\mathcal{J}_{n\text{ odd}}(\alpha)$ can be further simplified, leading to the final form of the integrand:

$$\mathcal{J}_{n\text{ odd}}(\alpha) = \frac{\text{PT}(\alpha)}{\sigma_{n-1,n}} \sum_{i=1}^{n-2} (-1)^i \frac{p^{AB}(\sigma_n) p_{i,BC}}{\sigma_{in} \rho_n^A \tilde{\rho}_{n,C}} \text{Pf}A_n^{[i,n-1,n]}. \quad (3.172)$$

This result is actually a Lorentz scalar, as it should be, even though it appears to depend on the explicit Lorentz spinor indices A and C . The above expression agrees with (3.156) after contraction with reference spinors in the numerator and denominator and choosing $\sigma_\star = \sigma_n$. In the derivation here, we have chosen particles n as well as $n-1$ to be special. However, the final result should be independent of such a choice, and therefore we have a complete agreement with (3.156), the result obtained by using the soft theorem.

Three-point Amplitude

Here we derive analytically the three-point amplitude from our odd- n formula. As explained in [43], the three-point amplitude requires additional considerations such as an adequate parametrization of its special kinematics. Here we find that our formula naturally leads to such a parametrization together with the correct supersymmetric expression. Since the result, which is quite subtle, exists in the literature [121], it is nice to see that our formula reproduces the known result. It turns out that it is more convenient to use the linearized constraints introduced in (3.47). So we start with the following integral representation of the superamplitude:

$$\mathcal{A}_3^{\mathcal{N}=(1,1) \text{ SYM}}(123) = \int d\mu_3^{6\text{D}} \frac{\mathcal{J}_3}{(V_3)^3} \int d^2\chi_0 d^2\tilde{\chi}_0 dg d\tilde{g} \prod_{i=1}^3 \delta^2(\eta_i^b M_{i,b}^a - \chi^a(\sigma_i)) \delta^2(\tilde{\eta}_i^{\hat{b}} \tilde{M}_{i,\hat{b}}^{\hat{a}} - \tilde{\chi}^{\hat{a}}(\sigma_i)). \quad (3.173)$$

The fermionic delta functions in the above formula are the fermionic versions of the linear constraints, and we will discuss the n -point version of these constraints in Section 3.5. For now we take this as a given, and write the degree 1 three-point maps as:

$$\begin{aligned} \rho^{A,a}(z) &= \rho_0^{A,a} + \omega^A \xi^a z, \\ \chi^a(z) &= \chi_0^a + g \xi^a z, \end{aligned} \quad (3.174)$$

together with their conjugates $\tilde{\rho}_{A\hat{a}}(z)$ and $\tilde{\chi}_{\hat{a}}(z)$. Imposing the orthogonality condition $\rho^{A,a}(z)\tilde{\rho}_{A,\hat{a}}(z) = 0$ we find:

$$\begin{aligned} \rho_0^{A,a} \tilde{\rho}_{0,A,\hat{a}} &= 0, \\ \rho_0^{A,a} \tilde{\omega}_A \tilde{\xi}_{\hat{a}} + \xi^a \omega^A \tilde{\rho}_{0,A,\hat{a}} &= 0, \\ \omega^A \tilde{\omega}_A &= 0. \end{aligned} \quad (3.175)$$

The solution to the middle constraint is given by

$$\begin{aligned} \rho_0^{A,a} \tilde{\omega}_A &= t \xi^a, \\ \omega^A \tilde{\rho}_{0,A,\hat{a}} &= -t \tilde{\xi}_{\hat{a}}, \end{aligned} \quad (3.176)$$

for some scale t . Recall that the top component of each map, i.e., $\xi^a \omega^A$ and its conjugate, carries a $\text{GL}(1, \mathbb{C})$ freedom which we previously used to fix $\xi^+ = 1$. For reasons that will become apparent soon, here it is more convenient to use this scaling to fix $t = V_3$. Using this and the previous equations we find the following relation:

$$\rho^{A,a}(\sigma_i) \tilde{\rho}_{A,\hat{a}}(\sigma_j) = V_3 \xi^a \tilde{\xi}_{\hat{a}} \sigma_{ij}. \quad (3.177)$$

Let us now evaluate the integrand in the representation of (3.155) and (3.150):

$$\begin{aligned}
\mathcal{J}_3 &= \frac{1}{(V_3)^2 \sigma_{13}} \times \frac{\langle q | \tilde{p}(\sigma_1) | \pi_3 \rangle}{\langle q | \tilde{\rho}_3 \rangle} \\
&= \frac{1}{(V_3)^2 \sigma_{13}} \frac{q^A \tilde{\rho}_{A,\hat{a}}(\sigma_1) \tilde{\rho}_{\hat{B}}^{\hat{a}}(\sigma_1) \rho_a^B(\sigma_3) \zeta^a}{q^A \tilde{\rho}_{0,A}^{\hat{a}} \tilde{\xi}_{\hat{a}}} \\
&= 1/V_3,
\end{aligned} \tag{3.178}$$

where we used $\tilde{X}_{(1,3)} = -\frac{\tilde{p}(\sigma_1)}{V_3 \sigma_{13}}$, $\text{Pf} A_4^{[1,2,3,4]} = 1$, $\langle \xi \zeta \rangle = 1$ and $q^A \tilde{\rho}_A^{\hat{a}}(\sigma) \tilde{\xi}_{\hat{a}} = q^A \tilde{\rho}_{0,A}^{\hat{a}} \tilde{\xi}_{\hat{a}}$. For three points, the $\text{SL}(2, \mathbb{C})_\sigma$ symmetry completely fixes all three σ 's, and we have,

$$\int d\mu_3^{\text{CHY}} = (V_3)^2. \tag{3.179}$$

Plugging this into (3.173) we are left with

$$\mathcal{A}_3^{\mathcal{N}=(1,1) \text{ SYM}}(123) = F_3^{(1,0)} F_3^{(0,1)}, \quad F_3^{(1,0)} = \frac{1}{V_3} \int d\chi_0^+ d\chi_0^- dg \prod_{i=1}^3 \delta^2(\eta_i^b M_{i,b}^a - \chi^a(\sigma_i)), \tag{3.180}$$

together with its conjugate $F_3^{(0,1)}$. We find that now the three-point amplitude only involves fermionic integrals and factorizes into chiral and antichiral pieces. However, this form is not completely satisfactory as it still carries redundancies. In order to match this expression with the known ones [43, 114], we note that (3.177) can be inverted as follows: Pick three labels $\{i, j, k\} = \{1, 2, 3\}$ for the external particles, then

$$\langle \lambda_i^a | \tilde{\lambda}_j^{\hat{a}} \rangle = V_3 \frac{M_{i,b}^a \xi^b \tilde{M}_{j\hat{b}}^{\hat{a}} \tilde{\xi}^{\hat{b}}}{|M_i| |\tilde{M}_j|} \sigma_{ij} = \epsilon_{ijk} (M_{i,b}^a \xi^b) (\tilde{M}_{j,\hat{b}}^{\hat{a}} \tilde{\xi}^{\hat{b}}), \tag{3.181}$$

where ϵ_{ijk} is the sign of the permutation (ijk) , as usual. This allows us to read off the variables defined in [43] for the special case of three-point kinematics. Since $\det \langle \lambda_i^a | \tilde{\lambda}_j^{\hat{a}} \rangle = 0$,

$$u_i^a = M_{i,b}^a \xi^b, \quad \tilde{u}_i^{\hat{a}} = \tilde{M}_{i,\hat{b}}^{\hat{a}} \tilde{\xi}^{\hat{b}}. \tag{3.182}$$

It is easy to check that they satisfy $u_i^a \lambda_{i,a}^A = u_j^a \lambda_{j,a}^A$ for any i, j . Their duals, defined as

$$w_i^a = \frac{M_{i,b}^a \zeta^b}{\sigma_{ij} \sigma_{ik}}, \quad \tilde{w}_i^{\hat{a}} = \frac{\tilde{M}_{i,\hat{b}}^{\hat{a}} \tilde{\zeta}^{\hat{b}}}{\sigma_{ij} \sigma_{ik}}, \tag{3.183}$$

satisfy $\langle u_i w_i \rangle = [\tilde{u}_i \tilde{w}_i] = 1$. Since the maps are constructed such that momentum conservation is guaranteed, the condition imposed in [43],

$$\sum_{i=1}^3 \omega_i^a \lambda_{i,a}^A = \zeta^a \sum_{i=1}^3 \frac{\rho_a^A(\sigma_i)}{|M_i|} = 0, \tag{3.184}$$

is also satisfied by virtue of the residue theorem. Furthermore, note that there are scaling and shifting redundancies in the definition of $u_i, \tilde{u}_i, w_i, \tilde{w}_i$ [43]. In particular, these variables are defined up to a rescaling,

$$u_i \rightarrow \alpha u_i, \quad \tilde{u}_i \rightarrow \alpha^{-1} \tilde{u}_i, \quad w_i \rightarrow \alpha^{-1} w_i, \quad \tilde{w}_i \rightarrow \alpha \tilde{w}_i, \quad (3.185)$$

which is a reflection of scaling redundancy of ξ and ζ . Additionally, there is a shift redundancy in w_i ,

$$w_i \rightarrow w_i + b_i u_i, \quad (3.186)$$

with $\sum_{i=1}^3 b_i = 0$ corresponds to the redundancy $\zeta \rightarrow \zeta + b \xi$ in the defining condition $\langle \zeta \xi \rangle = 1$. Let us now fix this $\text{SL}(2, \mathbb{C})$ redundancy by setting $\xi = (1, 0)$ and $\zeta = (0, 1)$. Then

$$M_i = \begin{pmatrix} u_i^+ & u_i^- \\ \sigma_{ij} \sigma_{ik} w_i^+ & \sigma_{ij} \sigma_{ik} w_i^- \end{pmatrix}, \quad (3.187)$$

and similarly for the conjugate. We will now focus on the chiral piece F_3 . Following [121], we define $\mathbf{w}_i = w_i^a \eta_{i,a}$ and $\mathbf{u}_i = u_i^a \eta_{i,a}$. Then we evaluate the fermionic integrals as follows

$$\begin{aligned} F_3^{(1,0)} &= \frac{1}{V_3} \int d\chi_0^+ d\chi_0^- dg \prod_{i=1}^3 \delta(\sigma_{ij} \sigma_{ik} \mathbf{w}_i - \chi_0^+ - g \sigma_i) \delta(\mathbf{u}_i - \chi_0^-) \\ &= \frac{1}{V_3} (\mathbf{u}_1 - \mathbf{u}_2)(\mathbf{u}_1 - \mathbf{u}_3) \int d\chi_0^+ dg \prod_{i=1}^3 \delta(\sigma_{i,i+1} \sigma_{i,i+2} \mathbf{w}_i - \chi_0^+ - g \sigma_i) \\ &= (\mathbf{u}_1 \mathbf{u}_2 + \mathbf{u}_2 \mathbf{u}_3 + \mathbf{u}_3 \mathbf{u}_1)(\mathbf{w}_1 + \mathbf{w}_2 + \mathbf{w}_3), \end{aligned} \quad (3.188)$$

where we have omitted the notation “ δ ” for fermionic delta functions. The final result is in precise agreement with the three-point superamplitude given, e.g., in [114]. For example, the three-gluon amplitude is:

$$\mathcal{A}_3(A_1^{a\hat{a}}, A_2^{b\hat{b}}, A_3^{c\hat{c}}) = (u_1^a u_2^b w_3^c + u_1^a w_2^b u_3^c + w_1^a u_2^b u_3^c) \left(\tilde{u}_1^{\hat{a}} \tilde{u}_2^{\hat{b}} \tilde{w}_3^{\hat{c}} + \tilde{u}_1^{\hat{a}} \tilde{w}_2^{\hat{b}} \tilde{u}_3^{\hat{c}} + \tilde{w}_1^{\hat{a}} \tilde{u}_2^{\hat{b}} \tilde{u}_3^{\hat{c}} \right). \quad (3.189)$$

3.5 Linear Form of the Maps

In this section, we present an alternative version of the connected formula for tree-level scattering amplitudes in 6D $\mathcal{N} = (1, 1)$ SYM. We make use of “linear” constraints involving λ_a^A and η_a directly, instead of the quadratic combinations $p^{AB} = \langle \lambda^A \lambda^B \rangle$ and $q^A = \langle \lambda^A \eta \rangle$. This form of the constraints is a natural generalization of the 4D Witten–RSV formula, in the form of (3.24).

We have previously presented the linear constraints in (3.47). However, our conventions in this section differ from the previous formula by the change of variables $W_i = M_i^{-1}$. Since the M_i 's are 2×2 matrices, the two formulations differ by where W_i appears in the constraints as well as an overall Jacobian. For certain computations such as the soft limits, it may be preferable to use the previous version of the constraints.

One way in which the linear constraints differ from the quadratic constraints is that the on-shell conditions are no longer built in. Instead, they are enforced by the introduction of spinor-helicity variables. Another feature of the linear form is that it makes manifest more of the symmetries, including the $SU(2) \times SU(2)$ R symmetry. We will also give evidence that this representation may be a step towards a Grassmannian formulation of 6D theories [150].

As in the previous formulation of 6D theories, there are additional subtleties when the number of particles n is odd. As before, the maps appropriate for odd n require the T symmetry, which acts as a redundancy of these maps. SYM amplitudes follow by pairing these constraints with the integrands found previously.

Using the linear constraints for even- and odd-point SYM amplitudes, in Section 3.5 we obtain a version of these constraints that is even closer to the original Witten–RSV form. In the case of 4D, this version is sometimes known as the *Veronese embedding* [151]. This is achieved by evaluating the integral over the original rational maps $\rho_a^A(z)$, $\chi_a(z)$, $\tilde{\chi}_a(z)$, leaving an integral over only the punctures and the W_i variables. This allows one to view the linear constraints as those for a symplectic (or Lagrangian) Grassmannian acting on a vector built from the external kinematic data.

As an application of this formulation, we also present an alternative version of the tree-level amplitudes of the abelian $(2, 0)$ M5-brane theory. Since this theory does not have odd-point amplitudes, it is not a focus of the present work. Still, the linear version of the tree amplitudes of this theory have some advantages compared to the formula presented in Chapter 2.

Linear Even-Point Measure

The linear form of the 6D even-point measure is obtained by introducing an integration over $GL(2)$ matrices $(W_i)_a^b$ associated to each particle (or punc-

ture):

$$\begin{aligned} \int d\mu_n^{\text{6D}} &= \int \frac{\prod_{i=1}^n d\sigma_i \prod_{k=0}^m d^8 \rho_k}{\text{vol}(\text{SL}(2, \mathbb{C})_\sigma \times \text{SL}(2, \mathbb{C})_\rho)} \frac{1}{V_n^2} \prod_{i=1}^n \delta^6 \left(p_i^{AB} - \frac{\langle \rho^A(\sigma_i) \rho^B(\sigma_i) \rangle}{\prod_{j \neq i} \sigma_{ij}} \right) \\ &= \left(\prod_{i=1}^n \delta(p_i^2) \right) \int \frac{\prod_{i=1}^n \prod_{k=0}^m d^8 \rho_k}{\text{vol}(\text{SL}(2, \mathbb{C})_\sigma \times \text{SL}(2, \mathbb{C})_\rho)} \mathcal{W}(\lambda, \rho, \sigma), \end{aligned} \quad (3.190)$$

where

$$\mathcal{W}(\lambda, \rho, \sigma) = \prod_{i=1}^n \int d^4 W_i \delta^8(\lambda_{ia}^A - (W_i)_a^b \rho_b^A(\sigma_i)) \delta \left(|W_i| - \frac{1}{\prod_{j \neq i} \sigma_{ij}} \right) \quad (3.191)$$

and $|W_i| = \det W_i$. The total number of delta functions exceeds the number of integrations by $n + 6$, accounting for the mass-shell and momentum-conservation delta functions. This step introduces $4n$ integrals in addition to the previous $5n - 6$ that were previously present after accounting for the $\text{SL}(2, \mathbb{C})_\sigma \times \text{SL}(2, \mathbb{C})_\rho$ symmetry. It allowed us to extract the n mass-shell constraints $\delta(p_i^2)$.

Before proceeding, let us comment on the $\text{SL}(2, \mathbb{C})$ indices of the matrix $(W_i)_a^b$. Throughout this work, we have used the Latin indices $a = +, -$ to denote both the ‘‘global’’ $\text{SL}(2, \mathbb{C})_\rho$ indices as well as the little-group indices of the external particles. The latter was not visible when all the external data entered the formulas through the little-group invariant combinations p_i^{AB} , q_i^A , and \tilde{q}_{iA} . In passing to the linear form, we have introduced one matrix $(W_i)_a^b$ *per particle*. We should view the upper index as global, because it contracts with the maps, whereas the lower index must transform under the little group of the i th external particle in order for the delta functions to be little-group invariant. So each W_i transforms as a bi-fundamental under the global $\text{SL}(2, \mathbb{C})_\rho$ and the i th $\text{SL}(2, \mathbb{C})$ little group. (The corresponding feature was also present in 4D when the t_i and \tilde{t}_i variables were introduced.) More explicitly, it is sometimes useful to solve for them in favor of the maps as follows: If we pick $\{A, B\} \subset \{1, 2, 3, 4\}$, then

$$p_i^{AB} W_{i,b}^a = \frac{\rho^{[A,a}(\sigma_i) \lambda_{i,b}^{B]}}{\prod_{j \neq i} \sigma_{ij}}, \quad (3.192)$$

the above solution also makes clear the difference between these two $\text{SL}(2, \mathbb{C})$ indices. Despite this subtlety, we have elected not to use different notations for the different kinds of the $\text{SL}(2, \mathbb{C})$ indices, though it is always easy to distinguish them based on the context.

The passage to linear constraints works analogously for the fermionic delta functions. The relevant identity is now:

$$\begin{aligned}\Delta_F &= \prod_{i=1}^n \delta^4 \left(q_i^A - \frac{\langle \rho^A(\sigma_i) \chi(\sigma_i) \rangle}{\prod_{j \neq i} \sigma_{ij}} \right) \\ &= \prod_{i=1}^n \delta^2 \left(\tilde{\lambda}_{iA\hat{a}} q_i^A \right) \delta^2 \left(\eta_i^a - (W_i)_b^a \chi^b(\sigma_i) \right),\end{aligned}\quad (3.193)$$

$$\begin{aligned}\tilde{\Delta}_F &= \prod_{i=1}^n \delta^4 \left(\tilde{q}_{i,A} - \frac{[\tilde{\rho}_A(\sigma_i) \tilde{\chi}(\sigma_i)]}{\prod_{j \neq i} \sigma_{ij}} \right) \\ &= \prod_{i=1}^n \delta^2 \left(\lambda_{i\hat{a}}^A \tilde{q}_{iA} \right) \delta^2 \left(\tilde{\eta}_i^{\hat{a}} - (\tilde{W}_i)_{\hat{b}}^{\hat{a}} \tilde{\chi}^{\hat{b}}(\sigma_i) \right).\end{aligned}\quad (3.194)$$

These formulas are only valid on the support of the bosonic delta functions. Just like $\tilde{\rho}_k$, the conjugate set of matrices, \tilde{W}_i , are not integrated over. Rather, they are solved for by the conjugate set of constraints, as in (3.63). As before, this form allows us to explicitly extract the super-wave-function factors leaving linear fermionic delta functions in the η and $\tilde{\eta}$ variables.

For the case of 6D $\mathcal{N} = (1, 1)$ SYM with n even, the right-hand integrand, which is the Parke–Taylor factor, does not depend on this change of variables. So we can now assemble the even-point integrand, which in terms of the usual maps,

$$\chi^a(z) = \sum_{k=0}^m \chi_k^a z^k, \quad \tilde{\chi}^{\hat{a}}(z) = \sum_{k=0}^m \tilde{\chi}_k^{\hat{a}} z^k, \quad (3.195)$$

is given by

$$\mathcal{I}_n^{\mathcal{N}=(1,1)\text{ SYM}} = \text{PT}(\alpha) \left(V_n \text{Pf}' A_n \int \left(\prod_{k=0}^m d^2 \chi_k d^2 \tilde{\chi}_k \right) \Delta_F \tilde{\Delta}_F \right). \quad (3.196)$$

Removing the mass-shell delta functions, the explicit formula for the linear form of the even-point scattering amplitudes of 6D $\mathcal{N} = (1, 1)$ SYM is

$$\begin{aligned}\mathcal{A}_n^{\mathcal{N}=(1,1)\text{ SYM}}(\alpha) &= \int \frac{\prod_{i=1}^n d\sigma_i \prod_{k=0}^m d^8 \rho_k d^2 \chi_k d^2 \tilde{\chi}_k}{\text{vol}(\text{SL}(2, \mathbb{C})_\sigma \times \text{SL}(2, \mathbb{C})_\rho)} \text{PT}(\alpha) \mathcal{W}(\lambda, \rho, \sigma) \\ &\times V_n \text{Pf}' A_n \prod_{i=1}^n \delta^2 \left(\eta_i^a - (W_i)_b^a \chi^b(\sigma_i) \right) \delta^2 \left(\tilde{\eta}_i^{\hat{a}} - (\tilde{W}_i)_{\hat{b}}^{\hat{a}} \tilde{\chi}^{\hat{b}}(\sigma_i) \right).\end{aligned}\quad (3.197)$$

So far we have used the fact that the kinematic data associated to a given particle in 6D can be encoded in two pairs of spinors, $\lambda_{i\hat{a}}^A$ and $\tilde{\lambda}_A^{i\hat{a}}$. However,

using the overall scaling it is also possible to associate the chiral part, λ_{ia}^A , with a line in \mathbb{CP}^3 and two points on it, where the two components, $a = \pm$, label the points. The linear formula implements the transformation from one description to the other. $\rho_a^A(\sigma_i)$ can be taken to define a line in \mathbb{CP}^3 , while each row of the 2×2 matrix W_i can be interpreted as defining the homogeneous coordinates for two points on this line. We believe that this new viewpoint would be useful in writing formulas in the 6D version of twistor space.

An added benefit of the linear form is that it makes parts of the non-linearly realized R symmetry generators manifest, as we mentioned previously. Recalling (3.52), the generators are quadratic in the $\eta_i, \tilde{\eta}_i$ variables and their derivatives. In particular, let us consider the generators $R^+ = \sum_{i=1}^n \eta_{i,a} \eta_i^a$ and $\tilde{R}^+ = \sum_{i=1}^n \tilde{\eta}_{i,\hat{a}} \tilde{\eta}_i^{\hat{a}}$. One may verify that these are symmetry generators by first noting that under the support of the delta functions

$$\eta_{ia} = (W_i)_{ab} \chi^b(\sigma_i), \quad \tilde{\eta}_{i\hat{a}} = (\tilde{W}_i)_{\hat{a}\hat{b}} \tilde{\chi}^{\hat{b}}(\sigma_i). \quad (3.198)$$

Similar to how one constructs the momenta p_i^{AB} from antisymmetric combinations of the analogous bosonic delta functions for λ_{ia}^A , we can construct the combinations:

$$R^+ = \sum_{i=1}^n \langle \eta_i \eta_i \rangle = \sum_{i=1}^n (W_i)_{ab} (W_i)_c^a \chi^b(\sigma_i) \chi^c(\sigma_i) = \sum_{i=1}^n |W_i| \chi_b(\sigma_i) \chi^b(\sigma_i), \quad (3.199)$$

and similarly for \tilde{R}^+ . Under the support of the bosonic delta functions the determinant $|W_i|$ can be replaced by $(\prod_{j \neq i} \sigma_{ij})^{-1}$, whereas $\chi_b(\sigma_i) \chi^b(\sigma_i)$ is a polynomial of degree $n-2$ in σ_i . Using the identity

$$\sum_{i=1}^n \frac{\sigma_i^k}{\prod_{j \neq i} \sigma_{ij}} = 0, \quad \text{for } k = 0, 1, \dots, n-2, \quad (3.200)$$

which can be understood as a consequence of a residue theorem, we find that $R^+ = 0$. This means that the amplitude is supported on configurations such that $\sum_i \eta_{ia} \eta_i^a = 0$ and $\sum_i \tilde{\eta}_{i\hat{a}} \tilde{\eta}_i^{\hat{a}} = 0$, which proves the conservation of this R charge. The vanishing of the final R symmetry generators, R^- and \tilde{R}^- , which are second derivative operators, is still not made manifest in this formulation, but it is not hard to prove. For example, a Grassmann Fourier transform interchanges the role of η and $\partial/\partial\eta$.

As a final application, we apply the formalism of linear constraints to the tree amplitudes of a single M5-brane in 11D Minkowski spacetime. This provides

an example of a 6D theory with $(2, 0)$ supersymmetry; the amplitudes in the rational maps formalism are given by the result of Chapter 2:

$$\mathcal{A}_n^{\text{M5-brane}} = \int \frac{\prod_{i=1}^n d\sigma_i \prod_{k=0}^m d^8 \rho_k d^4 \chi_k}{\text{vol}(\text{SL}(2, \mathbb{C})_\sigma \times \text{SL}(2, \mathbb{C})_\rho)} \Delta_B \Delta_F \frac{(\text{Pf}' A_n)^3}{V_n}, \quad (3.201)$$

where

$$\Delta_B = \prod_{i=1}^n \delta^6 \left(p_i^{AB} - \frac{\langle \rho^A(\sigma_i) \rho^B(\sigma_i) \rangle}{\prod_{j \neq i} \sigma_{ij}} \right), \quad (3.202)$$

$$\Delta_F = \prod_{i=1}^n \delta^8 \left(q_i^{AI} - \frac{\langle \rho^A(\sigma_i) \chi^I(\sigma_i) \rangle}{\prod_{j \neq i} \sigma_{ij}} \right), \quad (3.203)$$

and $I = 1, 2$ denotes the two chiral supercharges.

Since this theory has only even-point amplitudes, we do not need the machinery of odd-point rational maps in this case. Introducing the W_i variables, the bosonic measure is identical to that of SYM. The fermionic delta functions with $\mathcal{N} = (2, 0)$ supersymmetry become:

$$\Delta_F = \prod_{i=1}^n \delta^4(\tilde{\lambda}_{iA\hat{a}} q_i^{AI}) \delta^4(\eta_i^{aI} - (W_i)_b^a \chi^{bI}(\sigma_i)), \quad (3.204)$$

so the amplitudes have the representation:

$$\begin{aligned} \mathcal{A}_n^{\text{M5-brane}} &= \int \frac{\prod_{i=1}^n d\sigma_i \prod_{k=0}^m d^8 \rho_k d^4 \chi_k}{\text{vol}(\text{SL}(2, \mathbb{C})_\sigma \times \text{SL}(2, \mathbb{C})_\rho)} \mathcal{W}(\lambda, \rho, \sigma) \\ &\quad \times (\text{Pf}' A_n)^3 V_n \prod_{i=1}^n \delta^4(\eta_i^{aI} - (W_i)_b^a \chi^{bI}(\sigma_i)). \end{aligned} \quad (3.205)$$

It is worth noting that for chiral $\mathcal{N} = (2, 0)$ supersymmetry there is no need to introduce $\tilde{\rho}$, \widetilde{W}_i , or $\tilde{\chi}$. In some sense, the 6D chiral theories appear more natural than their non-chiral counterparts. This theory has $\text{USp}(4)$ R symmetry, which can be verified in the linear formulation by the technique described above.

By the same reasoning, the D5-brane formula which has $\mathcal{N} = (1, 1)$ supersymmetry, can be recast in a similar form with the same fermionic delta functions as in (3.197)

Linear Odd-Point Measure

To complete the discussion for the $\mathcal{N} = (1, 1)$ SYM odd-point measure and integrand in this formalism, we introduce the parametrization of the odd-point

maps described in Section 3.4. As before, we define

$$\rho_a^A(z) = \sum_{k=0}^{m-1} \rho_{a,k}^A z^k + \omega^A \xi_a z^m, \quad (3.206)$$

$$\tilde{\rho}_A^{\hat{a}}(z) = \sum_{k=0}^{m-1} \tilde{\rho}_{A,k}^{\hat{a}} z^k + \tilde{\omega}_A \tilde{\xi}^{\hat{a}} z^m, \quad (3.207)$$

and similarly for the fermionic partners, where $m = (n - 1)/2$. In the case where we used constraints for $p^{AB}(z)$, the introduction of this parametrization of the maps included a new redundancy. This was because the polynomial $\langle \rho^A(z) \rho^B(z) \rangle$ has a shift symmetry of the form $\rho^A(z) \rightarrow \hat{\rho}^A(z) = (\mathbb{I} + zT) \rho^A(z)$, where $T_b^a = \alpha \xi^a \xi_b$ and α is a parameter. The invariance of the product is still required in the linear formalism, and there must be a redundancy that reduces the number of components of ω^A and ξ_a . As before, the integrations over the moduli and the Riemann sphere are completely localized by the bosonic delta functions, which requires five independent components.

We will find that the appropriate choice is to keep the general action of the T-shift on $\rho_a^A(\sigma_i)$ but now allowing the W_i to transform at the same time. The linear constraint $\delta^8(\lambda_{ia}^A - (W_i)_a^b \rho_b^A(\sigma_i))$ is left invariant under the T-shift, which now explicitly depends on each puncture σ_i :

$$\rho_b^A(\sigma_i) \rightarrow \rho_b^A(\sigma_i) + \alpha \sigma_i \xi^c \xi_b \rho_c^A(\sigma_i) \quad (3.208)$$

$$(W_i)_a^b \rightarrow (W_i)_a^b - \alpha \sigma_i \xi^b \xi_c (W_i)_a^c, \quad (3.209)$$

or more abstractly,

$$\rho^A(\sigma_i) \rightarrow (\mathbb{I} + \sigma_i T) \rho^A(\sigma_i) \quad (3.210)$$

$$(W_i)_a \rightarrow (\mathbb{I} - \sigma_i T^\top) (W_i)_a. \quad (3.211)$$

These transformations leave the product invariant by virtue of (3.92). Recall that the lower index a on $(W_i)_a^b$ is the little-group index for the i th particle, and it does not participate in the shift.

With the maps and redundancy more or less the same as in Section 3.4, we may now write down the measure associated to the linear constraints for odd

n , which takes a similar form as the even-point one:

$$\begin{aligned} \int d\mu_{n\text{ odd}}^{6\text{D}} &= \int \frac{(\prod_{i=1}^n d\sigma_i \prod_{k=0}^{m-1} d^8 \rho_k) d^4 \omega \langle \xi d\xi \rangle}{\text{vol}(\text{SL}(2, \mathbb{C})_\sigma, \text{SL}(2, \mathbb{C})_\rho, \mathbb{T})} \frac{1}{V_n^2} \prod_{i=1}^n \delta^6 \left(p_i^{AB} - \frac{p^{AB}(\sigma_i)}{\prod_{j \neq i} \sigma_{ij}} \right) \\ &= \left(\prod_{i=1}^n \delta(p_i^2) \right) \int \frac{(\prod_{i=1}^n d\sigma_i \prod_{k=0}^{m-1} d^8 \rho_k) d^4 \omega \langle \xi d\xi \rangle}{\text{vol}(\text{SL}(2, \mathbb{C})_\sigma, \text{SL}(2, \mathbb{C})_\rho, \mathbb{T})} \mathcal{W}(\lambda, \rho, \sigma). \end{aligned} \quad (3.212)$$

We are free to fix the scaling and T-shift symmetry of this measure exactly as before, so all Jacobians will be the same as in previous sections. Therefore in terms of the linear maps, the superamplitudes of 6D $\mathcal{N} = (1, 1)$ SYM can be expressed as

$$\begin{aligned} \mathcal{A}_{n\text{ odd}}^{\mathcal{N}=(1,1)\text{ SYM}}(\alpha) &= \int \frac{(\prod_{i=1}^n d\sigma_i \prod_{k=0}^{m-1} d^8 \rho_k) d^4 \omega \langle \xi d\xi \rangle}{\text{vol}(\text{SL}(2, \mathbb{C})_\sigma, \text{SL}(2, \mathbb{C})_\rho, \mathbb{T})} \mathcal{W}(\lambda, \rho, \sigma) \text{PT}(\alpha) \text{Pf} \hat{A}_n \\ &\quad \times V_n \int \prod_{k=0}^{m-1} d^2 \chi_k d^2 \tilde{\chi}_k dg d\tilde{g} \prod_{i=1}^n \delta^2(\eta_i^a - (W_i)_b^a \chi^b(\sigma_i)) \delta^2(\tilde{\eta}_i^{\hat{a}} - (\tilde{W}_i)_{\hat{b}}^{\hat{a}} \tilde{\chi}^{\hat{b}}(\sigma_i)), \end{aligned} \quad (3.213)$$

where, as before, the fermionic maps for n odd are defined to be

$$\chi^a(z) = \sum_{k=0}^{m-1} \chi_k^a z^k + g \xi^a z^m, \quad (3.214)$$

$$\tilde{\chi}^{\hat{a}}(z) = \sum_{k=0}^{m-1} \tilde{\chi}_k^{\hat{a}} z^k + \tilde{g} \tilde{\xi}^{\hat{a}} z^m. \quad (3.215)$$

Veronese Maps and Symplectic Grassmannian

The preceding results can be brought even closer to the original Witten–RSV formulation by integrating out the moduli $\rho_{a,k}^A$ of the maps, which leaves an integral over only the σ_i and the W_i . This will allow us to show that these constraints apply to the elements of a *symplectic* Grassmannian. Let us begin with the even- n case and recast the bosonic measure:

$$\begin{aligned} \int d\mu_{n\text{ even}}^{6\text{D}} &= \int \frac{(\prod_{i=1}^n d\sigma_i d^4 W_i) \prod_{k=0}^m d^8 \rho_k}{\text{vol}(\text{SL}(2, \mathbb{C})_\sigma \times \text{SL}(2, \mathbb{C})_\rho)} \prod_{i=1}^n \delta^8(\lambda_{ia}^A - (W_i)_a^b \rho_b^A(\sigma_i)) \delta\left(|W_i| - \frac{1}{\prod_{j \neq i} \sigma_{ij}}\right) \\ &= \int \frac{\prod_{i=1}^n d\sigma_i d^4 W_i}{\text{vol}(\text{SL}(2, \mathbb{C})_\sigma \times \text{SL}(2, \mathbb{C})_W)} \prod_{k=0}^m \delta^8\left(\sum_{i=1}^n (W_i)_a^b \sigma_i^k \lambda_{ib}^A\right) \prod_{i=1}^n \delta\left(|W_i| - \frac{1}{\prod_{j \neq i} \sigma_{ij}}\right). \end{aligned} \quad (3.216)$$

This result can be obtained by using the following identity for each of the eight components separately [55, 152, 127],

$$\prod_{k=0}^m \delta \left(\sum_{i=1}^n \sigma_i^k X_i \right) = V_n \int \left(\prod_{k=0}^m d\rho_k \right) \prod_{i=1}^n \delta \left(\rho(\sigma_i) - X_i \prod_{j \neq i} \sigma_{ij} \right), \quad (3.217)$$

where $\rho(z) = \sum_{k=0}^m \rho_k z^k$ denotes any component of the polynomial map. Starting with (3.193), one can obtain a similar result for the fermions. Specifically,

$$\int \left(\prod_{k=0}^m d^2 \chi_k \right) \prod_{i=1}^n \delta^2 \left(\eta_{i,a} - (W_i)_a^b \chi_b(\sigma_i) \right) = \prod_{k=0}^m \delta^2 \left(\sum_{i=1}^n (W_i)_a^b \sigma_i^k \eta_{i,b} \right). \quad (3.218)$$

We now note that $(W_i)_a^b \sigma_i^k$ forms an $n \times 2n$ matrix:

$$C_{a,k;i,b} = (W_i)_a^b \sigma_i^k, \quad (3.219)$$

where we group the index k with the global $\text{SL}(2, \mathbb{C})$ index a and the index i with the i th little-group $\text{SL}(2, \mathbb{C})$ index b . Interestingly, under the constraints $|W_i| - \frac{1}{\prod_{j \neq i} \sigma_{ij}} = 0$, the matrix C formed in this way is symplectic satisfying

$$C \cdot \Omega \cdot C^T = 0, \quad (3.220)$$

which follows from the application of the identity (3.200) to each block matrix of the product. Here Ω is a symplectic metric: an anti-symmetric $2n \times 2n$ matrix with non-zero entries at $\Omega_{i,i+1} = -\Omega_{i+1,i} = 1$. Therefore C is a symplectic Grassmannian, which was mentioned in [150] for its possible applications to scattering amplitudes. Here we construct the symplectic Grassmannian explicitly in the spirit of the Veronese maps as discussed in [151] to relate Witten–RSV formulas with Grassmannian formulations for 4D $\mathcal{N} = 4$ SYM [153]. Using the $n \times 2n$ matrix C , one may rewrite the constraints nicely as

$$\sum_{i=1}^n (W_i)_a^b \sigma_i^k \lambda_{ib}^A := (C \cdot \Omega \cdot \Lambda)_a^A = 0, \quad (3.221)$$

where $\Lambda^A = \lambda_{i,b}^A$ is a $2n$ -dimensional vector. The fermionic constraints take a similar form with the same Grassmannian. Geometrically, this is a 6D version of the orthogonality conditions of the 4D Grassmannian described in [154].

Similarly, when $n = 2m + 1$ is odd, the identity (3.217) leads to

$$\begin{aligned}
\int d\mu_n^{6D} &= \int \frac{\prod_{i=1}^n d\sigma_i d^4 W_i (\prod_{k=0}^{m-1} d^8 \rho_k) d^4 \omega \langle \xi d\xi \rangle}{\text{vol}(\text{SL}(2, \mathbb{C})_\sigma, \text{SL}(2, \mathbb{C})_\rho, T)} \prod_{i=1}^n \delta^8(\lambda_{ia}^A - (W_i)_a^b \rho_b^A(\sigma_i)) \delta\left(|W_i| - \frac{1}{\prod_{j \neq i} \sigma_{ij}}\right) \\
&= \int \frac{(\prod_{i=1}^n d\sigma_i d^4 W_i) \langle \xi d\xi \rangle}{\text{vol}(\text{SL}(2, \mathbb{C})_\sigma, \text{SL}(2, \mathbb{C})_W, T)} \prod_{k=0}^{m-1} \delta^8\left(\sum_{i=1}^n (W_i)_a^b \sigma_i^k \lambda_{ib}^A\right) \\
&\quad \times \delta^4\left(\sum_{i=1}^n \xi^a (W_i)_a^b \sigma_i^m \lambda_{ib}^A\right) \prod_{i=1}^n \delta\left(|W_i| - \frac{1}{\prod_{j \neq i} \sigma_{ij}}\right).
\end{aligned} \tag{3.222}$$

For odd n , the form of the Grassmannian constraints is unmodified except for the highest degree, σ_i^m . The highest-degree terms must be modified so that the number of constraints decreases by 5 when passing from even to odd, which is the case for this expression. Note that we have integrated out the Lorentz spinor ω^A but not the global little-group spinor ξ^a . One of the $\text{SL}(2, \mathbb{C})_\rho$ generators can be used to fix the only independent component in ξ^a , making it effectively arbitrary. This nontrivial relation leaves only four independent constraints for the highest-degree part of the Grassmannian.

For odd n , this Veronese form also has the T-shift symmetry inherited from that of the W_i 's, as shown in (3.209). The T-shift acts on the Grassmannian as

$$(W_i)_a^b \sigma_i^k = C_{a,k;i,b} \rightarrow C_{a,k;i,b} - \alpha \xi_a \xi^c C_{c,k+1;i,b}, \quad k = 0, \dots, m-1, \tag{3.223}$$

$$\xi^a (W_i)_a^b \sigma_i^m = \xi^a C_{a,m;i,b} \rightarrow \xi^a C_{a,m;i,b}. \tag{3.224}$$

The term of highest degree is invariant under the shift due to $\langle \xi \xi \rangle = 0$. This shift can be interpreted as a special kind of row operation on the Grassmannian in which the rows of degree k are translated by the rows of degree $k+1$ with the exception of the highest-degree rows.

One must now fix the various redundancies of this description. In the end the number of integrals should equal the number of constraints after gauge fixing. There are $5n$ integrals before fixing the two $\text{SL}(2, \mathbb{C})$'s and $5n - 6$ after fixing them. These choices can be used to fix three of the punctures σ_i as well as two values of a W_i and one component of ξ_a . Finally, the T-shift can be used to fix the last value of the chosen W_i .

The fermionic delta functions satisfy a similar identity,

$$\int dg \prod_{k=0}^{m-1} d^2 \chi_k \prod_{i=1}^n \delta^2 (\eta_{i,a} - (W_i)_a^b \chi_b(\sigma_i)) = \delta \left(\sum_{i=1}^n \xi^a (W_i)_a^b \sigma_i^m \eta_{i,b} \right) \prod_{k=0}^{m-1} \delta^2 \left(\sum_{i=1}^n (W_i)_a^b \sigma_i^k \eta_{i,b} \right). \quad (3.225)$$

Now $(W_i)_a^b \sigma_i^k$ with $k = 0, 1, \dots, m-1$ combines with $\xi^a (W_i)_a^b \sigma_i^m$ to form an $n \times 2n$ symplectic matrix acting on the vector of external Grassmann variables, entirely analogous to the constraints for the external spinors.

Using these relations, it is then straightforward to rewrite all of the superamplitudes given in previous sections in terms of the Veronese maps. In the case of 6D $\mathcal{N} = (1, 1)$ SYM and odd n , in the integrand, the term $\text{Pf}' \widehat{A}_n$ contains a special ‘‘momentum’’ vector, which we recall here:

$$p_\star^{AB} = \frac{2 q^{[A} p^{B]C}(\sigma_\star) \tilde{q}_C}{q^D [\tilde{\rho}_D(\sigma_\star) \tilde{\xi}] \langle \rho^E(\sigma_\star) \xi \rangle \tilde{q}_E}. \quad (3.226)$$

This shows that p_\star^{AB} is in general a function of the moduli $\rho_{a,k}^A$ and $\tilde{\rho}_{A,k}^{\hat{a}}$. Therefore, when we integrate out the moduli and express the amplitudes in the Veronese form, we should solve for $\rho_{a,k}^A$ and $\tilde{\rho}_{A,k}^{\hat{a}}$ in terms of the W_i 's and \widetilde{W}_i 's, as well as the σ_i 's. If we choose σ_\star to be one of the σ_i 's, then it is trivial to express p_\star^{AB} in terms of W_i and σ_i by using the relation,

$$\rho_a^A(\sigma_i) = (M_i)_a^b \lambda_{i,b}^A, \quad (3.227)$$

and a similar relation for $\tilde{\rho}_A^{\hat{a}}(\sigma_i)$, and recalling that $M_i = W_i^{-1}$. If, instead, we choose σ_\star to be arbitrary, $\rho_a^A(\sigma_\star)$ can also be determined in terms of M_i and σ_i using the above relation (3.227), since $\rho_a^A(z)$ is a degree $m = \frac{n-1}{2}$ polynomial, and there are n such relations.

3.6 Various Theories in $D \leq 6$ and $\mathcal{N} = 4$ SYM on the Coulomb Branch

This section describes some interesting applications and consistency checks of the 6D SYM formulas that we have obtained. We start by writing down a formula for 6D $\mathcal{N} = (2, 2)$ supergravity amplitudes in Section 3.6, which follows from the double copy of the formula of 6D $\mathcal{N} = (1, 1)$ SYM studied in previous sections. Then in Section 3.6 we consider mixed amplitudes by coupling the 6D $\mathcal{N} = (1, 1)$ SYM with a single D5-brane. We will also study the dimensional reduction of these theories. We begin with the reduction to

five dimensions in Section 3.6, followed by $\mathcal{N} = 4$ SYM on the Coulomb branch in Section 3.6. We obtain new connected formulas for all tree-level scattering amplitudes of these theories. In Section 3.6 we study dimensional reduction to 4D $\mathcal{N} = 4$ SYM at the origin of the moduli space.

$\mathcal{N} = (2, 2)$ Supergravity in Six Dimensions

In this section we consider the tree amplitudes of $\mathcal{N} = (2, 2)$ supergravity in 6D. Even though 6D $\mathcal{N} = (2, 2)$ SUGRA is nonrenormalizable, it has a well-known UV completion. This completion is given by Type IIB superstring theory compactified on T^4 or (equivalently) M theory compactified on T^5 . In either case, the theory has an $E_{5,5}(\mathbb{Z}) = \text{SO}(5, 5; \mathbb{Z})$ U-duality group. This is a discrete global symmetry. (It is believed that string theory does not give rise to continuous global symmetries [155].) The low-energy effective description of this theory, which is the 6D supergravity theory under consideration here, extends this symmetry to the continuous non-compact global symmetry $\text{Spin}(5, 5)$. However, much of this symmetry is non-perturbative, and only the compact subgroup $\text{Spin}(5) \times \text{Spin}(5)$ is realized as a symmetry of the supergravity tree-level scattering amplitudes. (Recall that $\text{Spin}(5) = \text{USp}(4)$.) This symmetry is the relevant R symmetry group. This is called an R symmetry group because particles with different spins belong to different representations of this group even though they form an irreducible supermultiplet. The UV complete theory and its low-energy supergravity effective description are both maximally supersymmetric. This means that there are 32 local supersymmetries, gauged by the gravitino fields. It also implies that the supergravity theory has a 6D Minkowski-space solution that has 32 unbroken global supersymmetries. When we discuss scattering amplitudes, this is the background geometry under consideration. If we further reduce to four dimensions, we get $\mathcal{N} = 8$ supergravity, which has nonperturbative $E_{7(7)}$ symmetry. Again, only the compact subgroup, which is $\text{SU}(8)$ in this case, is the R symmetry of the tree amplitudes.

The 6D $\mathcal{N} = (2, 2)$ supergravity multiplet contains 128 bosonic and 128 fermionic degrees of freedom, which can be elegantly combined into a scalar superparticle by introducing eight Grassmann coordinates in a manner that will be described below. This multiplet contains six different spins, i.e., little-group representations, which we will now enumerate. They are characterized by their $\text{SU}(2) \times \text{SU}(2)$ little-group representations and their $\text{USp}(4) \times \text{USp}(4)$ R sym-

metry representations. The graviton transforms as $(\mathbf{3}, \mathbf{3}; \mathbf{1}, \mathbf{1})$ under these four groups. Similarly, the eight gravitinos belong to $(\mathbf{3}, \mathbf{2}; \mathbf{1}, \mathbf{4}) + (\mathbf{2}, \mathbf{3}; \mathbf{4}, \mathbf{1})$. Also, the ten two-form particles belong to $(\mathbf{3}, \mathbf{1}; \mathbf{1}, \mathbf{5}) + (\mathbf{1}, \mathbf{3}; \mathbf{5}, \mathbf{1})$. The 16 vector particles belong to $(\mathbf{2}, \mathbf{2}; \mathbf{4}, \mathbf{4})$, the spinors belong to $(\mathbf{2}, \mathbf{1}; \mathbf{4}, \mathbf{5}) + (\mathbf{1}, \mathbf{2}; \mathbf{5}, \mathbf{4})$, and the scalars belong $(\mathbf{1}, \mathbf{1}; \mathbf{5}, \mathbf{5})$. As in the case of the SYM theory, the amplitudes will be presented in a form that makes the helicity properties of the particles straightforward to read off, but only a subgroup of the R symmetry will be manifest. With some effort, one can prove that the entire $\text{USp}(4) \times \text{USp}(4)$ R symmetry is actually realized. Even though this is a non-chiral (left-right symmetric) theory, corresponding left- and right-handed particles have their R symmetry factors interchanged. So this interchange should be understood to be part of the definition of the reflection symmetry.

The on-shell superfield description of the supergravity multiplet, analogous to the one for the SYM multiplet in (3.48), utilizes eight Grassmann coordinates denoted $\eta^{I,a}$ and $\tilde{\eta}^{\hat{I},\hat{a}}$. It contains 128 bosonic and 128 fermionic modes with the spectrum enumerated above. It has the schematic form

$$\Phi(\eta) = \phi + \dots + \eta_a^I \eta_{b,I} \tilde{\eta}_{\hat{a}}^{\hat{I}} \tilde{\eta}_{\hat{b},\hat{I}} G^{ab;\hat{a}\hat{b}} + \dots + (\eta)^4 (\tilde{\eta})^4 \bar{\phi}. \quad (3.228)$$

Note that $I = 1, 2$ and $\hat{I} = \hat{1}, \hat{2}$ label components of an $\text{SU}(2) \times \text{SU}(2)$ subgroup of the R symmetry group. Only this subgroup of the $\text{USp}(4) \times \text{USp}(4)$ R symmetry is manifest in this formulation. The on-shell field $G^{ab;\hat{a}\hat{b}}$ in the middle of the on-shell superfield is the 6D graviton. We have only displayed this field and two of the 25 scalar fields.

The supergravity superamplitudes have total symmetry in the n scattered particles. This is to be contrasted with the cyclic symmetry of the color-stripped SYM amplitudes. For instance, the four-point superamplitude is given by

$$M_4^{\mathcal{N}=(2,2) \text{ SUGRA}} = \delta^6 \left(\sum_{i=1}^4 p_i^{AB} \right) \frac{\delta^8 \left(\sum_{i=1}^4 q_i^{A,I} \right) \delta^8 \left(\sum_{i=1}^4 \tilde{q}_{i,\hat{A}}^{\hat{I}} \right)}{s_{12} s_{23} s_{13}}, \quad (3.229)$$

which has manifest permutation symmetry. Here the supercharges are defined as $q_i^{A,I} = \lambda_{i,a}^A \eta_i^{I,a}$, and $\tilde{q}_{i,\hat{A}}^{\hat{I}} = \tilde{\lambda}_{i,\hat{A},\hat{a}} \tilde{\eta}_i^{\hat{I},\hat{a}}$. As in the case of the SYM theory, these are half of the supercharges, and the other half involve η derivatives. Conservation of these additional supercharges automatically follows from the first set together with the R symmetry.

Thanks to the separation of the $\mathcal{N} = (1, 1)$ SYM formulas into the measure, left- and right-integrands, the formulas for $\mathcal{N} = (2, 2)$ SUGRA amplitudes follow from the standard KLT argument [40] in the context of CHY formulations [59]. One replaces the Parke–Taylor factor with a second copy of the remaining half-integrand. The resulting connected formula for amplitudes of all multiplicities can be written in a compact form:

$$\boxed{\mathcal{M}_n^{\mathcal{N}=(2,2) \text{ SUGRA}} = \int d\mu_n^{6\text{D}} (\text{Pf}' A_n)^2 \int d\Omega_F^{(2,2)}.} \quad (3.230)$$

Here the fermionic measure $d\Omega_F^{(2,2)}$ that implements the 6D $\mathcal{N} = (2, 2)$ supersymmetry is the double copy of the $\mathcal{N} = (1, 1)$ version $d\Omega_F^{(1,1)}$, with

$$\chi_k^a \rightarrow \chi_k^{Ia}, \quad \tilde{\chi}_k^{\hat{a}} \rightarrow \tilde{\chi}_k^{\hat{I}\hat{a}}, \quad g \rightarrow g^I, \quad \tilde{g} \rightarrow \tilde{g}^{\hat{I}}. \quad (3.231)$$

Here $I = 1, 2$ and $\hat{I} = 1, 2$ are the $\text{SU}(2) \times \text{SU}(2)$ R symmetry indices. Explicitly, the measure is defined as

$$d\Omega_F^{(2,2)} = V_n^2 \left(\prod_{k=0}^m d^4\chi_k d^4\tilde{\chi}_k \right) \Delta_F^{(8)} \tilde{\Delta}_F^{(8)}, \quad (3.232)$$

for even $n = 2m + 2$, and

$$d\hat{\Omega}_F^{(2,2)} = V_n^2 d^2g d^2\tilde{g} \left(\prod_{k=0}^{m-1} d^4\chi_k d^4\tilde{\chi}_k \right) \Delta_F^{(8)} \tilde{\Delta}_F^{(8)}, \quad (3.233)$$

for odd $n = 2m + 1$. The fermionic delta functions are also a double copy of the $\mathcal{N} = (1, 1)$ ones, and they are given by

$$\Delta_F^{(8)} = \prod_{i=1}^n \delta^8 \left(q_i^{I,A} - \frac{\rho_a^A(\sigma_i) \chi^{I,a}(\sigma_i)}{\prod_{j \neq i} \sigma_{ij}} \right), \quad (3.234)$$

$$\tilde{\Delta}_F^{(8)} = \prod_{i=1}^n \delta^8 \left(\tilde{q}_{i,A}^{\hat{I}} - \frac{\tilde{\rho}_{A,\hat{a}}(\sigma_i) \tilde{\chi}^{\hat{I},\hat{a}}(\sigma_i)}{\prod_{j \neq i} \sigma_{ij}} \right). \quad (3.235)$$

Finally, it is understood that the reduced Pfaffian in the integrand refers to the matrix A_n in (3.57) for the even-point case and the hatted matrix \hat{A}_n in (3.157) for the odd-point case.

$\mathcal{N} = (1, 1)$ Super Yang–Mills Coupled to D5-branes

Since we now have connected formulas for the scattering amplitudes in the effective field theories of the D5-brane and $\mathcal{N} = (1, 1)$ SYM in 6D, we can

consider mixed amplitudes involving both kinds of particles. It was proposed in [106] that these types of amplitudes admit a simple CHY formula, which interpolates between the Parke–Taylor factor $\text{PT}(\alpha)$ for the non-abelian theory and $(\text{Pf}' A_n)^2$ for the abelian one. Such a construction was used in [106] to write down amplitudes coupling Non-linear Sigma Model (NLSM) pions to bi-adjoint scalars, as well as their supersymmetrization in 4D involving Volkov–Akulov theory (effective theory on a D3-brane) [100, 101] and $\mathcal{N} = 4$ SYM. Related models were later written down in the context of string-theory amplitudes [156]. These mixed amplitudes are also parts of the unifying relations for scattering amplitudes [157, 158]. In all of the above cases, the connected formula selects preferred couplings between the two theories. They were identified in [159, 160] in the case of the NLSM coupled to bi-adjoint scalar theory.

Following the same approach allows us to write down a formula coupling the D5-brane effective theory to 6D SYM:

$$\boxed{\mathcal{A}_n^{\text{D5-brane} \oplus \text{SYM}}(\alpha) = \int d\mu_n^{6\text{D}} \left(\text{PT}(\alpha) (\text{Pf} A_{\bar{\alpha}})^2 \right) \left(\text{Pf}' A_n \int d\Omega_{\text{F}}^{(1,1)} \right)}, \quad (3.236)$$

where α represents the states of SYM, which are color ordered, and the complement, $\bar{\alpha}$, represents states of the abelian D5-brane theory. We have also used the fact that the D5-brane theory and 6D SYM have identical supermultiplets and the same supersymmetry. Here the right-integrand, which is common between the two theories, remains unchanged. Of course, whenever the total number of particles n is odd, one should make use of the odd-multiplicity counterparts of the reduced Pfaffian and the bosonic and fermionic measures. In the left-integrand we have a Parke–Taylor factor constructed out of only the SYM states that enter the color ordering α . The D5-brane states belonging to $\bar{\alpha}$ do not have color labels, and hence they appear in the formula through the permutation-invariant Pfaffian. The matrix $A_{\bar{\alpha}}$ is an $|\bar{\alpha}| \times |\bar{\alpha}|$ minor of $\begin{bmatrix} p_i \cdot p_j \\ \sigma_{ij} \end{bmatrix}$ with columns and rows labeled by the D5-brane states. This implies that the above amplitude is non-vanishing only if the number of D5-brane particles $|\bar{\alpha}|$ is even.

Note that whenever $|\alpha| = 2$, i.e., only two states are SYM particles, the left integrand reduces to the square of a reduced Pfaffian, and the amplitude is equal to the D5-brane amplitude, though two particles carry color labels.

Hence the first non-trivial amplitude in this mixed theory arises for $n = 5$:

$$\mathcal{A}_5^{\text{D5-brane} \oplus \text{SYM}}(345) = \frac{1}{4} s_{12} \left(s_{23} \mathcal{A}_5^{\mathcal{N}=(1,1) \text{ SYM}}(12345) - s_{24} \mathcal{A}_5^{\mathcal{N}=(1,1) \text{ SYM}}(12435) \right). \quad (3.237)$$

Here we used KLT to rewrite (3.236) in terms of the NLSM $\oplus \phi^3$ amplitudes from [106] and 6D $\mathcal{N} = (1, 1)$ SYM ones, and presented the final result in terms of the SYM amplitudes. Symmetry in labels 1, 2 and antisymmetry with respect to 3, 4, 5 of the right-hand side follows from the BCJ relations [161]. Expressions for 5-point SYM amplitudes can be found in [121].

The construction of these mixed amplitudes uniquely defines nontrivial interactions between the two sectors, as the amplitude given above illustrates. It is a curious fact that these interactions have not yet been explored from a Lagrangian point of view. There are indications that the interactions implied by these amplitude constructions may have better soft behavior than any other possible interactions. This warrants further exploration.

5D SYM and SUGRA

Let us now consider 5D SYM and SUGRA with maximal supersymmetry. The spin of a massless particle in 5D is given by a $\text{Spin}(3) = \text{SU}(2)$ little-group representation. The appropriate spinor-helicity formalism can be conveniently obtained from the 6D one, with additional constraints, see for instance [162]. Concretely, a 5D massless momentum can be expressed

$$p^{AB} = \lambda_a^A \lambda_b^B \epsilon^{ab}. \quad (3.238)$$

This is identical to the 6D formula, but now there is only one kind of λ_a^A due to the fact that the little-group consists of a single $\text{SU}(2)$, which can be identified with the diagonal subgroup of the $\text{SU}(2) \times \text{SU}(2)$ little group in 6D. Of course, one still has to impose a further condition to restrict the momentum to 5D. The additional constraint that achieves this is

$$\Omega_{AB} \lambda_a^A \lambda_b^B \epsilon^{ab} = 0. \quad (3.239)$$

Here Ω_{AB} is the anti-symmetric invariant tensor of $\text{Spin}(4, 1)$, which is a non-compact version of $\text{USp}(4)$. Here we choose $\Omega_{13} = \Omega_{24} = 1$, and the other components of Ω_{AB} vanish for $A < B$. Note that the antisymmetry of Ω_{AB} implies that $\Omega_{AB} \lambda_a^A \lambda_b^B = c \epsilon_{ab}$. Therefore (3.239) actually implies that $\Omega_{AB} \lambda_a^A \lambda_b^B = 0$ for all $a, b = 1, 2$. This fact will be useful later.

Having set up the kinematics, we are now ready to present the formulas for the scattering amplitudes of 5D theories. Let us begin with 5D maximal SYM theory. This theory has $\text{Spin}(5) = \text{USp}(4)$ R symmetry. The spectrum of an on-shell supermultiplet consists of a vector that transforms as $(\mathbf{3}, \mathbf{1})$, spinors $(\mathbf{2}, \mathbf{4})$, and scalars $(\mathbf{1}, \mathbf{5})$. The bold-face integers label little-group and R symmetry representations. The on-shell superfield of the theory can be expressed,

$$\Phi(\eta) = \phi + \eta_a^I \psi_I^a + \epsilon_{IJ} \eta_a^I \eta_b^J A^{ab} + \epsilon^{ab} \eta_a^I \eta_b^J \phi_{IJ} + (\eta^3)_a^I (\bar{\psi})_I^a + (\eta^4) \bar{\phi}. \quad (3.240)$$

The index $I = 1, 2$ labels a doublet of an $\text{SU}(2)$ subgroup of the R symmetry group, whereas the entire little-group properties are manifest. This superfield is the dimensional reduction of the 6D on-shell superfield (3.48) obtained by removing all hats from 6D little-group indices. This works because the 5D $\text{SU}(2)$ little group corresponds to the diagonal subgroup of the 6D $\text{SU}(2) \times \text{SU}(2)$ little group. One consequence of this is that the 6D gluon reduces to the 5D gluon with three degrees of freedom and a scalar. Similarly, 5D amplitudes can be obtained directly from the 6D ones by making the substitution

$$\tilde{\lambda}_A^{\hat{a}} \rightarrow \Omega_{AB} \lambda^{aB}. \quad (3.241)$$

A 6D Lorentz contraction, such as $V^A \tilde{V}_A$, now is realized by the use of Ω_{AB} , namely $V^A \tilde{V}_A \rightarrow \Omega_{AB} V^A V^B$. For instance, the four-gluon amplitude is given by

$$\mathcal{A}_4(A_{a_1 b_1}, A_{a_2 b_2}, A_{a_3 b_3}, A_{a_4 b_4}) = \delta^5 \left(\sum_{i=1}^4 p_i^{AB} \right) \frac{\langle 1_{a_1} 2_{b_1} 3_{c_1} 4_{d_1} \rangle \langle 1_{a_2} 2_{b_2} 3_{c_2} 4_{d_2} \rangle}{s_{12} s_{23}} + \text{sym.}, \quad (3.242)$$

where the symmetrization is over the little-group indices of each gluon.

This procedure gives the following color-ordered tree-level superamplitudes for 5D maximal SYM:

$$\boxed{\mathcal{A}_n^{5\text{D SYM}}(\alpha) = \int d\mu_n^{5\text{D}} \text{PT}(\alpha) \left(\text{Pf} A_n \int d\Omega_F^{(8)} \right)}. \quad (3.243)$$

Here the 5D measure is defined as

$$\int d\mu_n^{5\text{D even}} = \int \frac{\prod_{i=1}^n d\sigma_i \prod_{k=0}^m d^8 \rho_k}{\text{vol}(\text{SL}(2, \mathbb{C})_\sigma \times \text{SL}(2, \mathbb{C})_\rho)} \frac{1}{V_n^2} \Delta_B^{5D}, \quad (3.244)$$

for even n , and

$$\int d\mu_{n,\text{odd}}^{5\text{D}} = \int \frac{\left(\prod_{i=1}^n d\sigma_i \prod_{k=0}^{m-1} d^8\rho_k\right) d^4\omega \langle \xi d\xi \rangle}{\text{vol}(\text{SL}(2, \mathbb{C})_\sigma, \text{SL}(2, \mathbb{C})_\rho, \text{T})} \frac{1}{V_n^2} \Delta_B^{5\text{D}}, \quad (3.245)$$

for odd n . The 5D delta-function constraints $\Delta_B^{5\text{D}}$ will be defined later. We see that the integration variables and symmetry groups are identical to those of 6D, and the same for the maps,

$$\rho_a^A(z) = \sum_{k=0}^m \rho_{ak}^A z^k, \quad \chi_a(z) = \sum_{k=0}^m \chi_{ak} z^k \quad (3.246)$$

and similarly for conjugate ones. Here $m = \frac{n}{2} - 1$ or $m = \frac{n-1}{2}$ depending on whether n is even or odd, and the highest coefficients factorize if n is odd, namely $\rho_{am}^A = \omega^A \xi_a$, $\chi_{am} = g \xi_a$ for $n = 2m + 1$.

Let us now examine the 5D delta-function constraints $\Delta_B^{5\text{D}}$. We propose that the 5D conditions for the rational maps are given by

$$\Delta_B^{5\text{D}} = \prod_{i=1}^n \delta^6 \left(p_i^{AB} - \frac{\langle \rho^A(\sigma_i) \rho^B(\sigma_i) \rangle}{\prod_{j \neq i} \sigma_{ij}} \right) \prod_{j=1}^{n-1} \delta \left(\frac{\Omega_{AB} \langle \rho^A(\sigma_j) \rho^B(\sigma_j) \rangle}{\prod_{l \neq j} \sigma_{jl}} \right), \quad (3.247)$$

where the first part is identical to the 6D version, and the second part imposes additional constraints to incorporate the 5D kinematic constraints (3.239). The constraints should only be imposed for $(n-1)$ particles, because the remaining one is then automatically satisfied due to momentum conservation. As in the case of 6D, momentum conservation and on-shell conditions are built into (3.247), so to compute the usual scattering amplitudes we should pull out the corresponding delta functions,

$$\Delta_B^{5\text{D}} = \delta^5 \left(\sum_{i=1}^n p_i^{AB} \right) \left(\prod_{i=1}^n \delta(p_i^2) \delta(\Omega_{AB} p_i^{AB}) \right) \hat{\Delta}_B^{5\text{D}}. \quad (3.248)$$

Note that besides the usual on-shell conditions $p_i^2 = 0$, there are additional conditions $\Omega_{AB} p_i^{AB} = 0$ that one has to extract. 5D momentum conservation is now implemented by restricting, for instance, the Lorentz indices in the δ^5 -function to be $\{A, B\} \neq \{2, 4\}$. Then the remaining constraints $\hat{\Delta}_B^{5\text{D}}$ are given by

$$\begin{aligned} \hat{\Delta}_B^{5\text{D}} &= \prod_{j=1}^{n-1} \delta \left(\frac{\Omega_{AB} \langle \rho^A(\sigma_j) \rho^B(\sigma_j) \rangle}{\prod_{l \neq j} \sigma_{jl}} \right) \prod_{i=1}^{n-2} \delta^4 \left(p_i^{AB} - \frac{\langle \rho^A(\sigma_i) \rho^B(\sigma_i) \rangle}{\prod_{j \neq i} \sigma_{ij}} \right) \\ &\times \delta^3 \left(p_n^{AB} - \frac{\langle \rho^A(\sigma_n) \rho^B(\sigma_n) \rangle}{\prod_{j \neq n} \sigma_{nj}} \right) \prod_{i=1}^n p_i^{12} \left(\frac{p_{n-1}^{14}}{p_{n-1}^{12}} - \frac{p_n^{14}}{p_n^{12}} \right), \end{aligned} \quad (3.249)$$

where the δ^4 -function has $\{A, B\} = \{1, 2\}, \{1, 3\}, \{1, 4\}, \{2, 3\}$, and the δ^3 -function has $\{A, B\} = \{1, 2\}, \{1, 3\}, \{1, 4\}$. Of course, the final result is independent of the choices we make here. Altogether the number of independent of delta functions is $5n - 6$, which matches with the number of integration variables (after modding out the symmetry factors). It is also straightforward to check that the formula has the correct power counting for the scattering amplitudes of 5D SYM. Finally, we remark that just like the rational maps in 6D, the 5D rational constraints also incorporate all $(n - 3)!$ solutions because of the non-trivial summation over the little-group indices.

The reduction of supersymmetry to lower dimensions is straightforward, and therefore the 5D fermionic measure, $d\Omega_F^{(8)}$, is almost identical to the 6D version, except that the fermionic maps $\chi^a(\sigma_i)$ and $\tilde{\chi}^{\hat{a}}(\sigma_i)$ now combine into $\chi^{Ia}(\sigma_i)$ (with $I = 1, 2$), just as the η 's and $\tilde{\eta}$'s combined to give η^I , as we discussed previously. The corresponding 5D fermionic delta functions are therefore given by

$$\Delta_F^{(8)} = \prod_{i=1}^n \delta^8 \left(q_i^{AI} - \frac{\langle \rho^A(\sigma_i) \chi^I(\sigma_i) \rangle}{\prod_{j \neq i} \sigma_{ij}} \right), \quad (3.250)$$

whereas the fermionic on-shell conditions that have to be taken out for computing scattering amplitudes become,

$$\prod_{i=1}^n \delta^4 \left(\Omega_{AB} \lambda_{a,i}^A q_i^{BI} \right). \quad (3.251)$$

As usual, these constraints allow one to introduce the Grassmann coordinates η_{ia}^I by writing the supercharges in the form $\lambda\eta$. Furthermore, the meaning of the factor denoted $\text{Pf}'A_n$ in (3.243) takes a different form depending on whether the number of particles is even or odd. Recall that if n is even, $\text{Pf}'A_n$ is defined in (3.58), whereas for odd n , it is given in (3.157). For both cases, the reduction to 5D is straightforward using (3.241) and the discussion following it. We have carried out various checks of this formula by comparing it with explicit component amplitudes from Feynman diagrams; these analytically agree for $n = 3, 4$, and numerically agree up to $n = 8$.

Next, we present the formula for the tree-level amplitudes of 5D maximal supergravity, which can be obtained either by a double copy of the 5D SYM formula or by a direct reduction of the 6D SUGRA formula. Either procedure

gives the result

$$\boxed{\mathcal{M}_n^{5\text{D SUGRA}} = \int d\mu_n^{5\text{D}} (\text{Pf}' A_n)^2 \int d\Omega_F^{(16)},} \quad (3.252)$$

with the fermionic measures and delta-functions all doubled up,

$$\Delta_F^{(16)} = \prod_{i=1}^n \delta^{16} \left(q_i^{AI} - \frac{\langle \rho^A(\sigma_i) \chi^I(\sigma_i) \rangle}{\prod_{j \neq i} \sigma_{ij}} \right), \quad (3.253)$$

where now $I = 1, 2, 3, 4$. This makes an $SU(4)$ subgroup of the $USp(8)$ R symmetry manifest. Again, the details of the formula depend on whether n is even or odd.

Finally, it is worth mentioning that there are analogous formulas for the super-amplitudes of the world-volume theory of a D4-brane, which are nonzero only when n is even. These can be obtained either as the dimensional reduction of a D5-brane world-volume theory or of an M5-brane world-volume theory. Using the 5D measures, the probe D4-brane amplitudes can be expressed as

$$\mathcal{A}_n^{\text{D4-brane}} = \int d\mu_n^{5\text{D}} (\text{Pf}' A_n)^2 \left(\text{Pf}' A_n \int d\Omega_F^{(8)} \right), \quad (3.254)$$

where the number of particles, n , is always taken to be even.

$\mathcal{N} = 4$ SYM on the Coulomb Branch

A further application of our 6D formulas involves the embedding of 4D *massive* kinematics into the 6D massless kinematics. In this approach, we view some components of the 6D spinors as 4D masses [122, 138]. In the case of 6D $\mathcal{N} = (1, 1)$ SYM, this procedure allows us to obtain amplitudes for 4D $\mathcal{N} = 4$ SYM on the Coulomb branch.

4D Massive Amplitudes from 6D Massless Ones

Four-dimensional $\mathcal{N} = 4$ SYM on the Coulomb branch can be achieved by giving vevs to scalar fields of the theory. For instance, in the simplest case,

$$\langle (\phi^{12})_J^I \rangle = \langle (\phi^{34})_J^I \rangle = v \delta_J^I, \quad (3.255)$$

other scalars have zero vev. Here “12” and “34” are $SU(4)$ R symmetry indices, whereas I, J are color indices for the gauge group $U(M)$. So the vev spontaneously breaks the gauge group from $U(M+N)$ to $U(N) \times U(M)$, and

the off-diagonal gauge bosons, which are bifundamentals of $U(N) \times U(M)$, denoted W and \overline{W} , gain mass. In the simple example, given above, all of the masses are equal, with $m = g_{\text{YM}} v$. One can consider more general situations with different masses, as our formulas will describe. There have been many interesting studies of $\mathcal{N} = 4$ SYM on the Coulomb branch in the context of scattering amplitudes. For instance, the masses introduced by moving onto the Coulomb branch can be used as IR regulators [163, 164, 165]; one can also study the low-energy effective action by integrating out the masses, which has led to interesting supersymmetric non-renormalization theorems [116, 117]. The subject we are interested in here is to study the tree-level massive amplitudes of $\mathcal{N} = 4$ SYM on the Coulomb branch [166, 167].

One can obtain 4D massive amplitudes from 6D massless ones via dimensional reduction. As discussed in [122], 4D massive kinematics can be parametrized by choosing the 6D spinor-helicity coordinates to take the special form

$$\lambda_a^A = \begin{pmatrix} -\kappa\mu_\alpha & \lambda_\alpha \\ \tilde{\lambda}^{\dot{\alpha}} & \tilde{\kappa}\tilde{\mu}^{\dot{\alpha}} \end{pmatrix}, \quad \tilde{\lambda}_{A\hat{a}} = \begin{pmatrix} \kappa'\mu^\alpha & \lambda^\alpha \\ -\tilde{\lambda}_{\dot{\alpha}} & \tilde{\kappa}'\tilde{\mu}_{\dot{\alpha}} \end{pmatrix}, \quad (3.256)$$

where

$$\kappa = \frac{M}{\langle\lambda\mu\rangle}, \quad \tilde{\kappa} = \frac{\widetilde{M}}{[\lambda\mu]}, \quad \kappa' = \frac{\widetilde{M}}{\langle\lambda\mu\rangle}, \quad \tilde{\kappa}' = \frac{M}{[\lambda\mu]}, \quad (3.257)$$

and $M\widetilde{M} = m^2$ is the mass squared. As usual, the indices α and $\dot{\alpha}$ label spinor representations of the 4D Lorentz group $SL(2, \mathbb{C})$. With this setup, a 4D massive momentum is given by

$$p_{\alpha\dot{\alpha}} = \lambda_\alpha \tilde{\lambda}_{\dot{\alpha}} + \rho \mu_\alpha \tilde{\mu}_{\dot{\alpha}}, \quad (3.258)$$

with $\rho = \kappa\tilde{\kappa} = \kappa'\tilde{\kappa}'$. We have decomposed a massive momentum into two light-like momenta, where $\mu_\alpha \tilde{\mu}_{\dot{\alpha}}$ can be considered a reference momentum.

$\mathcal{N} = 4$ SYM on the Coulomb branch can be viewed as a dimensional reduction of 6D $\mathcal{N} = (1, 1)$ SYM with massless particles. For instance, the four-point amplitude involving two massive conjugate W bosons and two massless gluons, $A(W_1^+, \overline{W}_2^-, g_3^-, g_4^-)$ can be obtained from the 6D pure gluon amplitude,

$$A_4^{6\text{D YM}}(A_1^{+\hat{+}}, A_2^{-\hat{-}}, A_3^{-\hat{-}}, A_4^{-\hat{-}}) = \frac{\langle 1^+ 2^- 3^- 4^- \rangle [1^{\hat{+}} 2^{\hat{-}} 3^{\hat{-}} 4^{\hat{-}}]}{s_{12} s_{23}}. \quad (3.259)$$

Plugging in the massive spinors (3.256), and using the identity,

$$\langle 1_+ 2_- 3_- 4_- \rangle = -\tilde{\kappa}_2 [1\mu] \langle 34 \rangle, \quad [1_{\hat{+}} 2_{\hat{-}} 3_{\hat{-}} 4_{\hat{-}}] = -\tilde{\kappa}'_2 [1\mu] \langle 34 \rangle, \quad (3.260)$$

as well as the definition of κ in (3.257), the result can be expressed as,

$$A_4^{6D}(W_1^+, \overline{W}_2^-, g_3^-, g_4^-) = \frac{m^2[1\mu]^2\langle 34 \rangle^2}{[2\mu]^2 s_{12}(s_{23} - m^2)}, \quad (3.261)$$

which agrees with the result in [166].

Alternatively, one can choose a different way of parameterizing 4D massive kinematics,

$$\lambda_a^A = \begin{pmatrix} \lambda_{\alpha,1} & \lambda_{\alpha,2} \\ \tilde{\lambda}_{\dot{\alpha},1} & \tilde{\lambda}_{\dot{\alpha},2} \end{pmatrix}, \quad \tilde{\lambda}_{A\hat{a}} = \begin{pmatrix} \lambda_1^\alpha & \lambda_2^\alpha \\ \tilde{\lambda}_{\dot{\alpha},1} & \tilde{\lambda}_{\dot{\alpha},2} \end{pmatrix}, \quad (3.262)$$

where we split the Lorentz indices $A \Rightarrow \{\alpha, \dot{\alpha}\}$, and 1 and 2 are little-group indices of massive particles in 4D. The momentum and mass are given by

$$p_{\alpha,\dot{\alpha}} = \lambda_{\alpha,a} \tilde{\lambda}_{\dot{\alpha},b} \epsilon^{ab}, \quad \lambda_{\alpha,a} \lambda_{\beta,b} \epsilon^{ab} = M \epsilon_{\alpha\beta}, \quad \tilde{\lambda}_{\dot{\alpha},a} \tilde{\lambda}_{\dot{\beta},b} \epsilon^{ab} = M \epsilon_{\dot{\alpha}\dot{\beta}}, \quad (3.263)$$

with $M^2 = m^2$. The advantage of this setup is that it makes the massive 4D little group $\text{Spin}(3) = \text{SU}(2)$ manifest. In fact, it actually leads to the massive spinor-helicity formalism of the recent work [144], which one can refer to for further details. In this formalism, for instance,

$$A_4^{6D}(W_1^{ab}, \overline{W}_2^{cd}, g_3^-, g_4^-) = \frac{([1_a 2_c][1_b 2_d])\langle 34 \rangle^2}{s_{12}(s_{23} - m^2)} + \text{sym}, \quad (3.264)$$

and

$$A_4^{6D}(W_1^{ab}, \overline{W}_2^{cd}, g_3^+, g_4^-) = \frac{(\langle 1_a 4 \rangle [2_c 3] - \langle 2_c 4 \rangle [1_a 3])(\langle 1_b 4 \rangle [2_d 3] - \langle 2_d 4 \rangle [1_b 3])}{s_{12}(s_{23} - m^2)} + \text{sym}, \quad (3.265)$$

where a, b and c, d are $\text{SU}(2)$ little-group indices of the massive particles $W_1^{ab} = W_1^{ba}$ and $\overline{W}_2^{cd} = \overline{W}_2^{dc}$, respectively. The notation “+sym” means that one should symmetrize on the little-group indices of each massive W boson. Here we have also defined

$$[1_a 2_b] = \tilde{\lambda}_{1,\dot{\alpha},a} \tilde{\lambda}_{2,\dot{\beta},b} \epsilon^{\dot{\alpha}\dot{\beta}}, \quad \langle 1_a 2_b \rangle = \lambda_{1,\alpha,a} \lambda_{2,\beta,b} \epsilon^{\alpha\beta}, \quad (3.266)$$

for massive spinors. Note if $a \neq b$, they vanish in the massless limit which sets $\lambda_{\dot{\alpha},+} = \tilde{\lambda}_{\dot{\alpha},-} = 0$. While if $a = b$, they reduce to the usual spinor brackets for 4D massless particles. Clearly, this formalism is very convenient for massive amplitudes, as was emphasized in [144].

Massive SUSY

Amplitudes for 4D $\mathcal{N} = 4$ SYM on the Coulomb branch can be constructed using the massive spinor-helicity formalism. Recall that the 16 supercharges of a particle in 6D (1, 1) SYM can be expressed in the form

$$q^A = \lambda_a^A \eta^a, \quad \bar{q}^A = \lambda_a^A \frac{\partial}{\partial \eta_a}, \quad (3.267)$$

$$\tilde{q}_A = \tilde{\lambda}_{A\hat{a}} \tilde{\eta}^{\hat{a}}, \quad \bar{\tilde{q}}_A = \tilde{\lambda}_{A\hat{a}} \frac{\partial}{\partial \tilde{\eta}_{\hat{a}}}. \quad (3.268)$$

The reduction to the supercharges of a 4D massive particle can be obtained using (3.262),

$$q^{I\alpha} = \lambda_-^\alpha \eta_+^I - \lambda_+^\alpha \eta_-^I, \quad \bar{q}^{I\dot{\alpha}} = \tilde{\lambda}_+^{\dot{\alpha}} \frac{\partial}{\partial \eta_+^I} + \tilde{\lambda}_-^{\dot{\alpha}} \frac{\partial}{\partial \eta_-^I}, \quad (3.269)$$

$$\tilde{q}_\alpha^I = \lambda_{\alpha-} \frac{\partial}{\partial \eta_-^I} + \lambda_{\alpha+} \frac{\partial}{\partial \eta_+^I}, \quad \bar{\tilde{q}}_{\dot{\alpha}} = \tilde{\lambda}_{\dot{\alpha}+} \eta_-^I - \tilde{\lambda}_{\dot{\alpha}-} \eta_+^I, \quad (3.270)$$

where we have identified $\{\eta, \tilde{\eta}\}$ as η^I with $I = 1, 2$. Their anti-commutation relations are

$$\{q^{I\alpha}, \tilde{q}^{J\beta}\} = M \varepsilon^{IJ} \varepsilon^{\alpha\beta}, \quad \{\bar{q}^{I\dot{\alpha}}, \bar{\tilde{q}}^{J\dot{\beta}}\} = M \varepsilon^{IJ} \varepsilon^{\alpha\beta}, \quad (3.271)$$

$$\{q^{I\alpha}, \bar{q}^{J\dot{\alpha}}\} = \varepsilon^{IJ} p^{\alpha\dot{\alpha}}, \quad \{\tilde{q}^{I\alpha}, \bar{\tilde{q}}^{J\dot{\beta}}\} = -\varepsilon^{IJ} p^{\alpha\dot{\alpha}}. \quad (3.272)$$

The central charge Z satisfies $Z^2 = M^2 = m^2$, which reflects the fact that the W 's of $\mathcal{N} = 4$ SYM on the Coulomb branch are BPS. To reduce to the massless case, one sets $\lambda_+^\alpha = \tilde{\lambda}_{\dot{\alpha}-} = 0$ and identifies $\lambda_+^\alpha = \lambda^\alpha$ and $\tilde{\lambda}_{\dot{\alpha}-} = \tilde{\lambda}_{\dot{\alpha}}$. That is, of course, the familiar (super) spinor-helicity formalism for $\mathcal{N} = 4$ SYM at the origin of moduli space. With the introduction of supersymmetry, a massive supermultiplet of $\mathcal{N} = 4$ SYM on the Coulomb branch can be neatly written as

$$\Phi(\eta) = \phi + \eta_a^I \psi_I^a + \epsilon_{ab} \eta^{Ia} \eta^{Jb} \phi_{IJ} + \epsilon_{IJ} \eta_a^I \eta_b^J A^{ab} + (\eta)^2 \eta_a^J \bar{\psi}_J^a + (\eta)^4 \bar{\phi}, \quad (3.273)$$

which contains one vector, four fermions, and five scalars. One scalar has been eaten by the vector, compared to the massless case with six scalars.

We can also express the massive amplitudes supersymmetrically. For instance, the superamplitude for the four-point amplitude with a pair of conjugate W -bosons, considered previously, can be written as

$$A_4 = \frac{\delta_F^4 \tilde{\delta}_F^4}{s_{12}(s_{23} - m^2)}, \quad (3.274)$$

with the fermionic delta-functions given by

$$\delta_F^4 = \delta^4(\lambda_{1a}^\alpha \eta_1^{Ia} + \lambda_{2a}^\alpha \eta_2^{Ia} + \lambda_3^\alpha \eta_3^{I,-} + \lambda_4^\alpha \eta_4^{I,-}), \quad (3.275)$$

$$\tilde{\delta}_F^4 = \delta^4(\tilde{\lambda}_{1a}^{\dot{\alpha}} \eta_1^{Ia} + \tilde{\lambda}_{2a}^{\dot{\alpha}} \eta_2^{Ia} + \tilde{\lambda}_3^{\dot{\alpha}} \eta_3^{I,+} + \tilde{\lambda}_4^{\dot{\alpha}} \eta_4^{I,+}). \quad (3.276)$$

These delta functions make the conservation of eight supercharges manifest.

Massive Amplitudes on the Coulomb Branch of $\mathcal{N} = 4$ SYM

Having set up the 4D massive kinematics and supersymmetry, we are ready to write down a general Witten–RSV formula for 4D scattering amplitudes of $\mathcal{N} = 4$ SYM on the Coulomb branch by a simple dimensional reduction of 6D massless $\mathcal{N} = (1, 1)$ SYM. The formula is

$$\boxed{\mathcal{A}_n^{\mathcal{N}=4 \text{ SYM CB}}(\alpha) = \int d\mu_n^{\text{CB}} \text{PT}(\alpha) \left(\text{Pf}' A_n \int d\Omega_F^{(4), \text{CB}} \right)}. \quad (3.277)$$

The measure $d\mu_n^{\text{CB}}$ is obtained directly from the 6D massless one with the following replacement of the bosonic delta functions:

$$\Delta_B \rightarrow \prod_{i=1}^n \delta^4 \left(p_i^{\alpha\dot{\alpha}} - \frac{\langle \rho^\alpha(\sigma_i) \tilde{\rho}^{\dot{\alpha}}(\sigma_i) \rangle}{\prod_{j \neq i} \sigma_{ij}} \right) \delta \left(M_i - \frac{\langle \rho^1(\sigma_i) \rho^2(\sigma_i) \rangle}{\prod_{j \neq i} \sigma_{ij}} \right) \delta \left(\tilde{M}_i - \frac{\langle \tilde{\rho}^1(\sigma_i) \tilde{\rho}^2(\sigma_i) \rangle}{\prod_{j \neq i} \sigma_{ij}} \right), \quad (3.278)$$

and using massive kinematics of (3.262), we set $\tilde{M}_i = M_i$ for $i = 1, 2, \dots, n-1$, where $M_i^2 = m_i^2$ is the mass squared of the i th particle ($\tilde{M}_n = M_n$ is a consequence of 6D momentum conservation). The mass m_i^2 , is m_W^2 or 0, as appropriate, for the simple symmetry breaking pattern described previously. Similarly, for the fermionic part

$$\Delta_F \rightarrow \prod_{i=1}^n \delta^4 \left(q_i^{\alpha, I} - \frac{\langle \rho^\alpha(\sigma_i) \chi^I(\sigma_i) \rangle}{\prod_{j \neq i} \sigma_{ij}} \right), \quad \tilde{\Delta}_F \rightarrow \prod_{i=1}^n \delta^4 \left(\tilde{q}_i^{\dot{\alpha}, I} - \frac{\langle \tilde{\rho}^{\dot{\alpha}}(\sigma_i) \chi^I(\sigma_i) \rangle}{\prod_{j \neq i} \sigma_{ij}} \right), \quad (3.279)$$

where the supercharges $q_i^{\alpha, I}$ and $\tilde{q}_i^{\dot{\alpha}, I}$ are defined in the previous section.

The polynomial maps are defined as usual,

$$\rho_a^\alpha(z) = \sum_{k=0}^m \rho_{k,a}^\alpha z^k, \quad \tilde{\rho}_a^{\dot{\alpha}}(z) = \sum_{k=0}^m \tilde{\rho}_{k,a}^{\dot{\alpha}} z^k, \quad \chi_a^I(z) = \sum_{k=0}^m \chi_{k,a}^I z^k. \quad (3.280)$$

They can be understood as a reduction from the 6D maps,

$$\rho_a^A(z) = \begin{pmatrix} \rho_{\alpha,1}(z) & \rho_{\alpha,2}(z) \\ \tilde{\rho}_{\dot{\alpha},1}(z) & \tilde{\rho}_{\dot{\alpha},2}(z) \end{pmatrix}, \quad \tilde{\rho}_{A\hat{a}}(z) = \begin{pmatrix} \rho_1^\alpha(z) & \rho_2^\alpha(z) \\ \tilde{\rho}_{\dot{\alpha},1}(z) & \tilde{\rho}_{\dot{\alpha},2}(z) \end{pmatrix}. \quad (3.281)$$

Again, we have to treat amplitudes with n even and n odd differently. So $n = 2m + 2$ or $n = 2m + 1$ if n is even or odd, and the highest coefficients in the maps take the factorized form if n is odd.

The factor $\text{Pf} A_n$ in the integrand is defined differently depending on whether n is even or odd, but they are straightforward reductions from 6D ones. For instance, we find that the odd-point Pfaffian can be constructed with the additional vector

$$p_*^{\alpha\dot{\alpha}} = \frac{2r^\alpha \tilde{\rho}_a^{\dot{\alpha}}(\sigma_*) \langle \rho^a(\sigma_*), r \rangle}{(\xi_b \langle \rho^b(\sigma_*), r \rangle)^2}, \quad m_* = 0. \quad (3.282)$$

This is obtained from (3.158) by splitting the 6D spinor index A into 4D ones $\alpha, \dot{\alpha}$ according to (3.281), and choosing the reference spinors as $q^A = (r_\alpha; 0)$, $\tilde{q}_A = (r^\alpha; 0)$. The same manipulations are required for the description of the n scattered particles, according to (3.262).

If the amplitudes involve massless external particles, we set $m_i = 0$ for them. The massive particle masses should satisfy the conservation constraint $\sum_i m_i = 0$, which is imposed by the rational maps automatically. Note that it is necessary to keep track of the signs of masses, even though the inertial mass is always $|m|$. This would be the only condition for a general 4D theory obtained by dimensional reduction. Specifying the particular Coulomb branch of $\mathcal{N} = 4$ SYM requires that we impose further conditions. In the simplest cases, where all of the massive particles have the same mass, we have $m_i^2 = m_W^2$ for all i , but all the W bosons have mass m_W , whereas all the \overline{W} 's have mass $-m_W$. More generally, different masses can be assigned to different massive particles, but if we assign m as the mass of a W boson, then we should then assign $-m$ to the corresponding conjugate \overline{W} boson. Therefore $\sum_i m_i = 0$ is satisfied in pairs. Finally, due to the color structure, a W boson and its conjugate \overline{W} boson should appear in adjacent pairs with gluons sandwiched in between. For instance, there are nontrivial amplitudes of the type $A_n(W_1, g_2, \dots, g_{i-1}, \overline{W}_i, \tilde{g}_{i+1}, \dots, g_n)$, with gluons g and \tilde{g} belonging to the gauge groups $U(N)$ and $U(M)$, respectively.

We checked that the formula produces correct four-point amplitudes in previous section. It also gives correct five- and six-point ones such as

$$\begin{aligned} A_5(g_1^+, g_2^+, g_3^+, W_4^{ab}, \overline{W}_5^{cd}) &= \frac{\langle 4_a 5_c \rangle \langle 4_b 5_d \rangle [1|p_5(p_1 + p_2)|3]}{\langle 12 \rangle \langle 23 \rangle (s_{51} - m^2)(s_{34} - m^2)} + \text{sym}, \quad (3.283) \\ A_6(g_1^+, g_2^+, g_3^+, g_4^+, W_5^{ab}, \overline{W}_6^{cd}) &= \frac{\langle 5_a 6_c \rangle \langle 5_b 6_d \rangle [1|p_6(p_1 + p_2)(p_3 + p_4)p_5|4]}{\langle 12 \rangle \langle 23 \rangle \langle 34 \rangle (s_{61} - m^2)(s_{612} - m^2)(s_{45} - m^2)} + \text{sym}, \end{aligned}$$

or SU(4) R symmetry-violating amplitudes that vanish in the massless limit, such as

$$A_5(\phi_1^{34}, \phi_2^{34}, \phi_3^{34}, W_4^{ab}, \overline{W}_5^{cd}) = -\frac{m \langle 4_a 5_c \rangle [4_b 5_d]}{(s_{51} - m^2)(s_{34} - m^2)} + \text{sym}, \quad (3.284)$$

$$A_6(\phi_1^{34}, \phi_2^{34}, \phi_3^{34}, \phi_4^{34}, W_5^{ab}, \overline{W}_6^{cd}) = -\frac{m^2 \langle 5_a 6_c \rangle [5_b 6_d]}{(s_{61} - m^2)(s_{612} - m^2)(s_{45} - m^2)} + \text{sym}. \quad (3.285)$$

When restricted to W bosons with helicity ± 1 , they are all in agreement with the results in [166], but now in a form with manifest SU(2) little-group symmetry for the massive particles. One can also consider cases in which the massive particles are not adjacent, for instance

$$A_4(W_1^{ab}, g_2^+, \overline{W}_3^{cd}, \tilde{g}_4^+) = \frac{\langle 1_a 3_c \rangle \langle 1_b 3_d \rangle [24]^2}{(s_{12} - m^2)(s_{23} - m^2)} + \text{sym}, \quad (3.286)$$

$$A_4(W_1^{ab}, g_2^-, \overline{W}_3^{cd}, \tilde{g}_4^+) = \frac{(\langle 1_a 2 \rangle [3_c 4] - \langle 3_c 2 \rangle [1_a 4])(\langle 1_b 2 \rangle [3_d 4] - \langle 3_d 2 \rangle [1_b 4])}{(s_{12} - m^2)(s_{23} - m^2)} + \text{sym}. \quad (3.287)$$

Reduction to Four Dimensions: Special Sectors

One can further reduce our 6D formulas down to 4D massless kinematics. It is interesting that 4D kinematics induces a separation into sectors, as reviewed in Section 3.2, whereas there is no natural separation into sectors in higher dimensions. In fact, one of the motivations for developing formulas in 6D is to unify all of the 4D sectors. Here we will explain how to naturally obtain the integrand of 4D theories from 6D via dimensional reduction in the middle ($d = \tilde{d}$) and “next to middle” ($d = \tilde{d} \pm 1$) sectors for even and odd multiplicity, respectively. However, the emergence of the other sectors is more difficult to see via dimensional reduction, even though all sectors are present. We will comment on this at the end of this subsection.

For the first case, it was already argued in Chapter 2 that the 6D measure for rational maps reduces to the corresponding 4D measure provided the maps behave regularly under the dimensional reduction, i.e., they reduce to the ones appearing in the Witten–RSV formula. After reviewing the reduction for n even, we will generalize the argument to odd n for the near-to-middle sectors, i.e., $d = \tilde{d} \pm 1$.⁴

⁴One can input kinematics $\{p_i^\mu\}$ in $D = 4 + \epsilon$ dimensions and study the behavior of the 6D maps as $\epsilon \rightarrow 0$. We find that when the solution corresponds to the aforementioned sectors the maps are regular. This implies that the measure is finite and reproduces the CHY measure of Section 3.2, valid for both 6D and 4D. For other sectors, the maps become divergent and additional care is needed to define the limit of the measure.

Let us first consider the even-point case, $n = 2m + 2$. For the solutions corresponding to the middle sector $d = \tilde{d} = m$, the maps behave as follows:

$$\rho_a^A(z) \rightarrow \begin{pmatrix} 0 & \rho_\alpha(z) \\ \tilde{\rho}^{\hat{\alpha}}(z) & 0 \end{pmatrix}, \quad \tilde{\rho}_{A\hat{a}}(z) \rightarrow \begin{pmatrix} 0 & \rho^\alpha(z) \\ \tilde{\rho}_{\hat{\alpha}}(z) & 0 \end{pmatrix}, \quad (3.288)$$

where $\deg \rho_\alpha(z) = \deg \tilde{\rho}_{\hat{\alpha}}(z) = d$. Here we have used the 4D embedding described in [43], with the analogous behavior for the kinematic data λ_a^A and $\tilde{\lambda}_{A\hat{a}}$. This corresponds to setting $p_i^{AB} = 0$ for $\{A, B\} = \{1, 2\}, \{3, 4\}$. Note further that the action of the subgroup $\text{GL}(1, \mathbb{C}) \subset \text{SL}(2, \mathbb{C}) \times \text{SL}(2, \mathbb{C})$ is manifest and given by $\rho_-^A \rightarrow \ell \rho_-^A$, $\rho_+^A \rightarrow \frac{1}{\ell} \rho_+^A$, etc. Consider now the fermionic piece of the SYM integrand in (3.56):

$$V_n \int \prod_{k=0}^d d^2 \chi_k d^2 \tilde{\chi}_k \prod_{i=1}^n \delta^4 \left(q_i^A - \frac{\rho_a^A(\sigma_i) \chi^a(\sigma_i)}{\prod_{j \neq i} \sigma_{ij}} \right) \delta^4 \left(\tilde{q}_{i,A} - \frac{\tilde{\rho}_{A,\hat{a}}(\sigma_i) \tilde{\chi}^{\hat{a}}(\sigma_i)}{\prod_{j \neq i} \sigma_{ij}} \right). \quad (3.289)$$

Under the embedding (3.288) this becomes

$$V_n \int \prod_{k=0}^d d\chi_k^+ d\chi_k^- d\tilde{\chi}_k^- d\tilde{\chi}_k^+ \times \prod_{i=1}^n \delta^2 \left(q_{i\alpha}^1 - \frac{\rho_\alpha(\sigma_i) \chi^-(\sigma_i)}{\prod_{j \neq i} \sigma_{ij}} \right) \delta^2 \left(\tilde{q}_i^{\hat{\alpha}1} - \frac{\tilde{\rho}^{\hat{\alpha}}(\sigma_i) \chi^+(\sigma_i)}{\prod_{j \neq i} \sigma_{ij}} \right) \\ \times \delta^2 \left(\tilde{q}_{i\hat{\alpha}}^2 - \frac{\tilde{\rho}_{\hat{\alpha}}(\sigma_i) \tilde{\chi}_-(\sigma_i)}{\prod_{j \neq i} \sigma_{ij}} \right) \delta^2 \left(q_i^{\alpha 2} - \frac{\rho^\alpha(\sigma_i) \tilde{\chi}_+(\sigma_i)}{\prod_{j \neq i} \sigma_{ij}} \right), \quad (3.290)$$

where we have labeled $q^A = (q_\alpha^1; \tilde{q}^{\hat{\alpha}1})$ and $\tilde{q}_A = (\tilde{q}_{\hat{\alpha}}^2; q^{\alpha 2})$. We can now identify the 4D fermionic degrees of freedom as

$$\tilde{\chi}^{\hat{I}} = (\chi^-, \tilde{\chi}_+), \quad \chi^I = (\chi^+, \tilde{\chi}_-), \quad (3.291)$$

with $I = 1, 2$ and $\hat{I} = 1, 2$ transforming under the manifest $\text{SU}(2) \times \text{SU}(2) \subset \text{SU}(4)$ R symmetry group in 4D. Hence, the fermionic piece is

$$\int d\Omega_F = V_n \int \prod_{k=0}^d d^2 \chi_k^I d^2 \tilde{\chi}_k^{\hat{I}} \times \prod_{i=1}^n \delta^4 \left(q_i^{\alpha \hat{I}} - \frac{\rho^\alpha(\sigma_i) \tilde{\chi}^{\hat{I}}(\sigma_i)}{\prod_{j \neq i} \sigma_{ij}} \right) \delta^4 \left(\tilde{q}_i^{\hat{\alpha} I} - \frac{\tilde{\rho}^{\hat{\alpha}}(\sigma_i) \chi^I(\sigma_i)}{\prod_{j \neq i} \sigma_{ij}} \right). \quad (3.292)$$

The remaining part of the even-multiplicity integrand is trivially reduced to four dimensions, since the matrix $[A_n]_{ij} = \frac{p_i \cdot p_j}{\sigma_{ij}}$ is not sensitive to any specific dimension. Alternatively, it can be seen that under the embedding (3.288) and the support of the bosonic delta functions

$$V_n \text{Pf} A_n \rightarrow R^d(\rho) R^{\tilde{d}}(\tilde{\rho}). \quad (3.293)$$

Let us now derive the analogous statement for $n = 2m + 1$. We assume $\tilde{d} = d - 1$ (with the case $\tilde{d} = d + 1$ being completely analogous). The embedding (3.288) can then be obtained by fixing the components $\xi = \tilde{\xi} = (1, 0)$ and $\zeta = \tilde{\zeta} = (0, 1)$ for the odd-point maps (recall that we defined $\{\xi, \zeta\}$ as an $\text{SL}(2, \mathbb{C})_\rho$ basis). For the fermionic part we again introduce two polynomials $\chi^I(\sigma)$ and $\tilde{\chi}^{\tilde{I}}(\sigma)$ of degrees d and \tilde{d} . The top components of the polynomial χ^I can be identified as

$$(\chi_d^1, \chi_d^2) = (\chi_d^+, \tilde{\chi}_-) = (g, \tilde{g}) \quad (3.294)$$

according to (3.122) and (3.123). The bosonic part of the integrand becomes

$$\text{Pf}' \hat{A}_n = \frac{1}{\sigma_{n1}} \sum_{i=2}^{n-1} \frac{(-1)^i}{\sigma_{ni}} \frac{[q|P(\sigma_i)|\tilde{\rho}_{\hat{a}}(\sigma_n)]\zeta^{\delta\hat{a}}}{[q|\rho_a(\sigma_n)]\xi^a} \text{Pf} A^{[1in]} \quad (3.295)$$

$$= \frac{1}{\sigma_{n1}} \sum_{i=2}^{n-1} \frac{(-1)^i}{\sigma_{ni}} \frac{[qi]\langle i\rho(\sigma_n)\rangle}{[q\tilde{\rho}(\sigma_n)]} \text{Pf} A^{[1,i,n]}. \quad (3.296)$$

We have checked numerically up to $n = 7$ that this expression coincides with $V_n^{-1} R^d(\rho) R^{\tilde{d}}(\tilde{\rho})$ for $\tilde{d} = d - 1$ on the support of the 4D equations (3.18). Hence for this sector ($d = \tilde{d}$ for even n or $d = \tilde{d} \pm 1$ for odd n) the integrand can be recast into the non-chiral form of the Witten–RSV formula, and the amplitude is given by [56]:

$$\begin{aligned} \mathcal{A}_{n,d}^{\mathcal{N}=4 \text{ SYM}} &= \int \mu_{n,d}^{\text{4D}} R^d(\rho) R^{\tilde{d}}(\tilde{\rho}) \int \prod_{k=0}^d d^2 \chi_k^I \prod_{k=0}^{\tilde{d}} d^2 \tilde{\chi}_k^{\tilde{I}} \\ &\times \prod_{i=1}^n \delta^4 \left(q_i^{\alpha\hat{I}} - \frac{\rho^\alpha(\sigma_i) \tilde{\chi}^{\hat{I}}(\sigma_i)}{\prod_{j \neq i} \sigma_{ij}} \right) \delta^4 \left(\tilde{q}_i^{\dot{\alpha}\hat{I}} - \frac{\tilde{\rho}^{\dot{\alpha}}(\sigma_i) \chi^{\hat{I}}(\sigma_i)}{\prod_{j \neq i} \sigma_{ij}} \right). \end{aligned} \quad (3.297)$$

Let us finally comment on other sectors. First of all, given the fact that the 6D rational maps contain all $(n - 3)!$ solutions, it is clear that all the sectors are there. One can see it by considering completely integrating out all the moduli ρ 's, then reducing the 6D formulas to 4D will not be different from the dimensional reduction of the original CHY formulations. However, from the procedure outlined above, it is subtle to see how other sectors emerge directly by dimensional reduction. As we will discuss in Section 3.7, this subtlety is closely related to the fact that both $\text{Pf}' A_n$ (for even n) and $\text{Pf}' \hat{A}_n$ (for odd n) vanish for the kinematics of the non-middle sectors (for even n) and the non next-to-middle sectors (for odd n).

3.7 Conclusion and Discussion

In this chapter we presented new connected formulas for tree-level scattering amplitudes of 6D $\mathcal{N} = (1, 1)$ SYM theory as well as for $\mathcal{N} = (2, 2)$ SUGRA via the KLT double-copy procedure. Due to the peculiar properties of 6D spinor-helicity variables, scattering amplitudes of even and odd number of particles must be treated differently. In the case of even multiplicity, our formulas are direct extensions of the results for the world-volume theory of a probe D5-brane which were introduced in Chapter 2. By considering a soft limit of the even-point formulas we obtained the rational maps and the integrands for odd multiplicity, with many interesting features and novelties. In particular, a new redundancy, which we call T-shift symmetry, emerges for the odd-point worldsheet formulas. Interestingly, the T shift intertwines with the original Möbius $SL(2, \mathbb{C})_\sigma$ and $SL(2, \mathbb{C})_\rho$ redundancies. Another new feature is the generalized Pfaffian $\text{Pf}' \widehat{A}_n$ in the integrand. Besides the original n punctures, it contains an additional reference puncture, which can be set to an arbitrary value. Associated to the new puncture there is a special “momentum” vector. The special vector is used to increase the size of the original matrix A_n to $(n+1) \times (n+1)$ such that it has a non-vanishing reduced Pfaffian for odd n . Moreover, since the special null vector p_\star has zero mass dimension, $\text{Pf}' \widehat{A}_n$ has the correct mass dimension for Yang–Mills amplitudes. It would be of great interest to better understand the physical origin of the additional puncture and the additional special vector. One clear future direction is to obtain an ambitwistor model that realizes all of these new features of the odd-multiplicity connected formulas. This was undertaken in a slightly different formalism in [168], which has the advantage of treating even and odd point amplitudes on an equal footing at the cost of reintroducing polarization information.

We also presented the 6D formulas in alternative forms, with constraints linearly in terms of the 6D external helicity spinors. They are a direct analog of the Witten–RSV formulations for 4D $\mathcal{N} = 4$ SYM. By integrating out the moduli of maps, the linear maps can be further recast into a form with a symplectic Grassmannian structure. The symplectic Grassmannian is realized in terms of 6D version of the Veronese maps.

Having obtained formulas for 6D theories, we also considered their dimensional reduction to 5D and 4D leading to various new connected formulas. By reducing to 5D for massless kinematics and utilizing the 5D spinor-helicity

formalism, we obtained new formulas for 5D SYM and SUGRA theories. Reduction to 4D reproduced the original Witten–RSV formula for $\mathcal{N} = 4$ SYM in 4D for the middle helicity sector for even n and the next-to-middle sector for odd n . The appearance of other disconnected sectors for 4D kinematics is rather subtle, and we leave it for future investigations. On the other hand, it is very nice that reduction to 4D massive kinematics turns out to be more straightforward without such subtleties. By doing so, we deduced a connected formula for massive amplitudes of 4D $\mathcal{N} = 4$ SYM on the Coulomb branch.

Another natural future application of our 6D formulas would be to use the procedure of forward limits in [169, 65] to obtain the one-loop integrand of 4D $\mathcal{N} = 4$ SYM. Since now we have manifestly supersymmetric formulas for amplitudes in 5D and 6D, we are in a good position to apply the forward limit procedure of [65] supersymmetrically. This procedure might lead to an analog of the Witten–RSV formulas at loop level, which might be genuinely different from previous formulations [63, 64, 65, 66, 67]. We leave this as a future research direction.

Even though 6D $\mathcal{N} = (1, 1)$ SYM is not a conformal theory, its planar scattering amplitudes enjoy a dual conformal symmetry [140] just like $\mathcal{N} = 4$ SYM in 4D [170, 171]. Such hidden symmetries are often obscured in traditional ways of representing the amplitudes (such as Feynman diagrams), and become more transparent in modern formulations, such as the Grassmannian [154, 150], as shown in [172]. It would be of interest to investigate whether our 6D $\mathcal{N} = (1, 1)$ SYM formulas, especially the version in terms of the Veronese maps or its ultimate symplectic Grassmannian form, can make dual conformal symmetry manifest.

Having succeeded in using the spinor-helicity formalism to study supersymmetric theories in 6D, it is tempting to try to carry out analogous constructions in even higher dimensions where supersymmetric theories still exist, such as ten or eleven. The main challenge is that in $D > 6$ one has to impose non-linear constraints on the spinors. Not long after the 6D spinor-helicity formalism was developed, a proposal for a 10D version was introduced [173], also see recent work [174, 175] for 10D and 11D theories. It would be interesting to pursue this line of research further.

Finally, there are two issues that are very natural open questions and deserve a detailed discussion. The first has to do with a mysterious but natural object

that has 6D $\mathcal{N} = (2, 0)$ symmetry and a non-abelian structure similar to that of Yang–Mills. The second is related to the mathematical characterization of the moduli space of maps from $\mathbb{C}\mathbb{P}^1$ to the null-cone in six dimensions.

Non-abelian $\mathcal{N} = (2, 0)$ Formula

As discussed in Section 3.3, the 6D $\mathcal{N} = (1, 1)$ non-abelian SYM amplitudes for even n can be obtained from those of the D5-brane theory by replacing $(\text{Pf} A_n)^2$ with the Parke–Taylor factor $\text{PT}(\alpha)$. It is natural to ask what happens if we apply the same replacement to the M5-brane formula which was central to the discussion of Chapter 2, at least for an even number n of particles. This procedure leads to a formula with a non-abelian structure and $\mathcal{N} = (2, 0)$ supersymmetry,

$$\begin{aligned} \mathcal{A}_n^{\mathcal{N}=(2,0)}(\alpha) &= \int \frac{\prod_{i=1}^n d\sigma_i \prod_{k=0}^m d^8 \rho_k d^4 \chi_k}{\text{vol}(\text{SL}(2, \mathbb{C})_\sigma \times \text{SL}(2, \mathbb{C})_\rho)} \prod_{i=1}^n \delta^6 \left(p_i^{AB} - \frac{\langle \rho^A(\sigma_i) \rho^B(\sigma_i) \rangle}{\prod_{j \neq i} \sigma_{ij}} \right) \\ &\quad \times \delta^8 \left(q_i^{AI} - \frac{\langle \rho^A(\sigma_i) \chi^I(\sigma_i) \rangle}{\prod_{j \neq i} \sigma_{ij}} \right) \frac{\text{Pf} A_n}{V_n} \text{PT}(\alpha). \end{aligned} \quad (3.298)$$

One would be tempted to speculate that these new formulas compute some observable in the mysterious $\mathcal{N} = (2, 0)$ theory that arises in the world-volume of multiple coincident M5-branes. Of course, this would be too naive based on what it is currently known about the $\mathcal{N} = (2, 0)$ theory; simple dimensional arguments suggest that the $\mathcal{N} = (2, 0)$ theory does not have a perturbative parameter and hence a perturbative S matrix. Moreover, explicit no-go results have been obtained preventing the existence of three-particle amplitudes with all the necessary symmetries [113, 114].

Here we take the viewpoint that since (3.298) is well defined as an integral, i.e., it has all correct redundancies, $\text{SL}(2, \mathbb{C})_\sigma \times \text{SL}(2, \mathbb{C})_\rho$, it is worth exploring in its own right. Moreover, the new non-abelian $\mathcal{N} = (2, 0)$ formulas can be combined with non-abelian $\mathcal{N} = (0, 2)$ formulas using the KLT procedure in order to compute $\mathcal{N} = (2, 2)$ supergravity amplitudes. Given that the non-abelian $\mathcal{N} = (2, 0)$ formulas are purely chiral, they have some computational advantages over their $\mathcal{N} = (1, 1)$ Yang–Mills cousins, which are traditionally used in KLT.

A natural step in the study of any connected formula based on rational maps is to consider its behavior under factorization. Any physical amplitude must satisfy locality and unitarity: a tree-level amplitude should only have simple

poles when non-overlapping Mandelstam variables approach to zero, and the corresponding residues should be products of lower-point ones.

Let us investigate these physical properties of the non-abelian $\mathcal{N} = (2, 0)$ formula. Already for $n = 4$ we find a peculiar behavior under factorization. As we discussed in Section 3.3, the net effect of changing from $(\text{Pf } A_4)^2$ to the Parke–Taylor factor $\text{PT}(1234)$ is to introduce an additional factor of $1/(s_{12} s_{23})$. Therefore, for $n = 4$ the non-abelian $(2, 0)$ formula gives [142]:

$$\mathcal{A}_4^{\mathcal{N}=(2,0)}(1234) = \delta^6 \left(\sum_{i=1}^4 p^{AB} \right) \frac{\delta^8(\sum_{i=1}^4 q_i^{A,I})}{s_{12} s_{23}}, \quad (3.299)$$

which is related to that of 6D $\mathcal{N} = (1, 1)$ SYM by a simple change to the fermionic delta functions. Comparing with the four-point amplitude of the theory of a probe M5-brane, the new feature is that $\mathcal{A}_4^{\mathcal{N}=(2,0)}(1234)$ has simple poles at $s_{12} \rightarrow 0$ and $s_{23} \rightarrow 0$, and the question is what the corresponding residues are. In order to explore the singularity in the s_{12} -channel, let us define the following two objects at $s_{12} = 0$:

$$x_{23} = w_2^a \langle 2_a | 3_b \rangle \tilde{u}_3^b, \quad \tilde{x}_{23} = \tilde{w}_2^{\hat{a}} [2_{\hat{a}} | 3_b \rangle u_3^b. \quad (3.300)$$

It is easy to check that $s_{23} = x_{23} \tilde{x}_{23}$. One can then show that the residue is given by

$$\lim_{s_{12} \rightarrow 0} s_{12} \mathcal{A}_4^{\mathcal{N}=(2,0)}(1234) = \delta^6 \left(\sum_{i=1}^4 p_i^{AB} \right) \frac{x_{23}^2}{s_{23}} \int d^4 \eta_P^I F_3^{(2,0)}(1, 2, P) F_3^{(2,0)}(-P, 3, 4), \quad (3.301)$$

where $F_3^{(2,0)}$ is obtained from $\mathcal{A}_3^{\mathcal{N}=(1,1) \text{ SYM}}$ by the replacement of fermionic delta functions (3.188) to make it $\mathcal{N} = (2, 0)$ supersymmetric. Note that the left-hand side still diverges as $s_{23} \rightarrow 0$. These three-point objects, $F_3^{(2,0)}$, are ambiguous since they are not invariant under α -scaling of (3.185) as we discussed in Section 3.4, which is a redundancy of the three-particle special kinematics [113, 114]. However, equation (3.301) is well-defined, because the prefactor on the right-hand side precisely cancels out the ambiguity. Moreover, the scaling acts by sending $x_{23} \rightarrow \alpha x_{23}$, $\tilde{x}_{23} \rightarrow \alpha^{-1} \tilde{x}_{23}$, so it is clear that there is a choice of $\alpha = \alpha(w_2, \tilde{u}_3)$ that sets $x_{23}^2 = s_{23}$. For this choice the four-particle residue can in fact be written as a product of the three-point objects $F_3^{(2,0)}$ summed over internal states. Note, however, that the two $F_3^{(2,0)}$ factors cannot be regarded as independent amplitudes, i.e., they are non-local, since

they are defined only in the frame $\frac{x_{23}^2}{s_{23}} = 1$, which in turn depends on all four particles involved. A similar decomposition can be achieved by implementing an unfixed α -scale, but using the shift redundancy (3.186), $w_i \rightarrow w_i + b_i u_i$, to set

$$w_2^a \langle 2_a | 3_b \rangle \tilde{w}_3^{\hat{b}} + w_1^a \langle 1_a | 3_b \rangle \tilde{w}_3^{\hat{b}} = 0. \quad (3.302)$$

In this frame we find $\frac{x_{23}^2}{s_{23}} = [\tilde{u}_P \tilde{u}_{-P}] \langle w_P w_{-P} \rangle$, and we can write⁵

$$\lim_{s_{12} \rightarrow 0} s_{12} \mathcal{A}_4^{\mathcal{N}=(2,0)}(1234) = \delta^6 \left(\sum_{i=1}^4 p_i^{AB} \right) \int d^4 \eta_P^I F_3^{a\hat{a}}(1, 2, P) F_{3,a\hat{a}}(-P, 3, 4), \quad (3.303)$$

with

$$F_3^{a\hat{a}}(1, 2, P) := F_3^{(2,0)}(1, 2, P) w_P^a \tilde{u}_P^{\hat{a}}, \quad (3.304)$$

which now resembles the three-particle amplitude of higher spin states with $\mathcal{N} = (2, 0)$ supersymmetry, as described in [114]. Non-locality is now present because the objects are not b -shift invariant. In fact, the defining frame given by (3.302) again depends on the kinematics of all the particles involved. We hence recognize two different “frames” in which the residue of $\mathcal{A}_4^{\mathcal{N}=(2,0)}(1234)$ is given by a sum over exchanges between three-point $\mathcal{N} = (2, 0)$ objects.

Since the residue is not given by local quantities, we expect that the non-abelian $\mathcal{N} = (2, 0)$ formulas give rise to a generalization of physical scattering amplitudes whose meaning might be interesting to explore. Note that the same computation for the 6D $\mathcal{N} = (1, 1)$ SYM theory yields no prefactor, and therefore the residue of a four-point amplitude is precisely a product of two three-point amplitudes summed over the exchange of all allowed on-shell states in the theory, as required by unitarity.

We have further checked that the naive non-abelian $(2, 0)$ integral formula for odd multiplicity does not have the required $(\text{SL}(2, \mathbb{C})_\sigma, \text{SL}(2, \mathbb{C})_\rho, T)$ redundancies anymore, i.e., it depends on the “fixing” of σ 's and ρ 's. In the case of three particles this is a reflection of the α -scaling ambiguity and is again in agreement with the analysis of [113, 114].

Along the same line of thought, one may further construct 6D $\mathcal{N} = (4, 0)$ “supergravity” formulas by the double copy of two non-abelian $\mathcal{N} = (2, 0)$ formulas discussed previously and $\mathcal{N} = (3, 1)$ “supergravity” formulas by the double copy of the non-abelian $\mathcal{N} = (2, 0)$ formulas with $\mathcal{N} = (1, 1)$ SYM. The

⁵We thank Yu-tin Huang for this observation.

possible existence of a 6D $\mathcal{N} = (4, 0)$ theory and its relation to supergravity theories have been discussed in [176]; also see the recent works [177, 178] on constructing the actions of 6D free theories with $\mathcal{N} = (4, 0)$ or $\mathcal{N} = (3, 1)$ supersymmetry.⁶ These constructions clearly will lead to well-defined integral formulas as far as the $\text{SL}(2, \mathbb{C})_\sigma \times \text{SL}(2, \mathbb{C})_\rho$ redundancies are concerned. For instance, the four-point formulas should be given by (3.229), but with a change of the fermionic delta functions in the numerator such that they implement $\mathcal{N} = (4, 0)$ or $\mathcal{N} = (3, 1)$ supersymmetry. However, as we can see already at four points, the formulas contain kinematics poles, and the residues do not have clear physical interpretations, just like the $\mathcal{N} = (2, 0)$ non-abelian formulas above.

It is worth mentioning that, even though all these formulas are pathological in 6D, upon dimensional reduction to lower dimensions the non-abelian $\mathcal{N} = (2, 0)$ formulas or the $\mathcal{N} = (4, 0)$ and $\mathcal{N} = (3, 1)$ “supergravity” formulas actually behave as well as 6D $\mathcal{N} = (1, 1)$ SYM or 6D $\mathcal{N} = (2, 2)$ supergravity. In fact, they give the same results. This phenomenon has already been observed for branes, where the $\mathcal{N} = (2, 0)$ M5-brane formulas and the $\mathcal{N} = (1, 1)$ D5-brane formulas both reduce to the same D4-brane amplitudes in 5D.

Degenerate Kinematics in 6D

The last topic we address has to do with a very important assumption made in the construction of our formulas. Up to this point we have been using maps of degree $n - 2$ from \mathbb{CP}^1 into the null cone defined by

$$p^{AB}(z) = \langle \rho^A(z) \rho^B(z) \rangle = \rho^{A,+}(z) \rho^{B,-}(z) - \rho^{A,-}(z) \rho^{B,+}(z), \quad (3.305)$$

with $\rho^{A,+}(z)$ and $\rho^{A,-}(z)$ both polynomials of degree $(n - 2)/2$ for even n and $(n - 1)/2$ for odd n . The assumption made so far is that these maps are sufficient to cover the entire relevant moduli space for the computation of Yang–Mills amplitudes. In particular, a natural question is what happens when $d_+ = \deg \rho^{A,+}(z)$ and $d_- = \deg \rho^{A,-}(z)$ are allowed to be distinct and whether such maps are needed to cover regions of the moduli space when the external kinematics takes special values.

Let us start the discussion with n even. Considering maps of general degrees d_+ and d_- , subject to the constraint $d_+ + d_- = n - 2$, we may require $\Delta :=$

⁶The double copy of the $(2, 0)$ spectrum to produce the $(4, 0)$ one was discussed in [179], and more recently in [180].

$d_+ - d_- \geq 0$ without loss of generality. While for generic kinematics $\Delta = 0$ maps exist for all $(n - 3)!$ solutions of the scattering equations, we find that there are codimension one or higher subspaces for which some solutions escape the “coordinate patch” covered by $\Delta = 0$ maps.

There are three matrices that control all connected formulas presented in this work. They are K_n , A_n and Φ_n . The first and the last one only appeared implicitly. For reader’s convenience we list below the definition of all three even though A_n has been previously defined:

$$(K_n)_{ij} = \begin{cases} p_i \cdot p_j & i \neq j, \\ 0 & i = j, \end{cases} \quad (A_n)_{ij} = \begin{cases} \frac{p_i \cdot p_j}{\sigma_{ij}} & i \neq j, \\ 0 & i = j, \end{cases} \quad (\Phi_n)_{ij} = \begin{cases} \frac{p_i \cdot p_j}{\sigma_{ij}^2}, & i \neq j, \\ -\sum_{k \neq i} \frac{p_i \cdot p_k}{\sigma_{ik}^2} & i = j. \end{cases}$$

The physical meaning of the first one is clear: It is the matrix of kinematic invariants. The second is the familiar A_n matrix whose reduced Pfaffian enters in all the formulas we have presented. Finally, Φ_n is the Jacobian matrix of the scattering equations.

In dimensions $D \geq n - 1$ the number of independent Mandelstam invariants is $n(n - 3)/2$, and therefore the matrix K_n has rank $n - 1$. When $D < n - 1$ the space of Mandelstam invariants has the lower dimension $(D - 1)n - D(D + 1)/2$, and therefore the matrix K_n has a lower rank. This is easy to understand as the momentum vectors in $p_i \cdot p_j$ start to satisfy linear dependencies. In general, if the dimension is D , then so is the rank of the K_n matrix. The rank of K_n is therefore a measure of the minimal spacetime dimension where a given set of kinematic invariants $p_i \cdot p_j$ can be realized as physical momentum vectors. By contrast, in general the matrices A_n and Φ_n have ranks $n - 2$ and $n - 3$, respectively, for any spacetime dimension D .

At this point we have numerical evidence up to $n = 10$ to support the following picture: There exist subspaces in the space of 6D kinematic invariants where some solutions to the scattering equations lower the rank of A_n while keeping the rank of K_n and Φ_n the same as is expected for generic kinematics.

Since A_n is antisymmetric, its rank decreases by multiples of two. Moreover, we find that when the rank has decreased by $2r$, i.e., its new rank is $n - 2(r + 1)$, the maps that cover such solutions of the scattering equations are those for which $\Delta = 2r$. From the definition $\Delta = d_+ - d_-$ it is clear that the maps needed to cover these new regions are of degree $d_+ = n/2 + (r - 1)$ and $d_- = n/2 - (r + 1)$.

The extreme case $r = n/2 - 2$, i.e., when $d_- = 1$, is never reached while keeping the rank of K_n equal to six. In fact, it is only when the rank of K_n becomes four that such maps are needed. Note that decreasing the rank of K_n to four implies that such kinematic points can be realized by momenta embedded in 4D spacetime. In 4D it is well-known that the solutions to the scattering equations split into sectors, as discussed in Section 3.2, and maps of different degrees are needed to cover all solutions.

For odd n the preceding statement needs to be refined. To see why, recall that in Section 3.4 we introduced the notion of z -dependent $\mathrm{SL}(2, \mathbb{C})$ transformations (3.119). In particular, for $d_+ = \Delta + d_-$ one has the following redundancy of the maps:

$$\rho^{A,+}(z) \rightarrow \rho^{A,+}(z) + u(z)\rho^{A,-}(z), \quad (3.306)$$

where $\deg u(z) = \Delta$. This is an intrinsic redundancy of each sector, since the maps (and hence the matrix A_{ij}) are invariant under such transformation. However, when $d_+ < \Delta + d_-$ this transformation will “shift” between sectors, leading to maps that satisfy $d_+ = \Delta + d_-$, but are equivalent to those with lower degree. We see that these points of the moduli space should be modded out in order to define sector decomposition. The way to recognize them is to notice that when $d_+ < \Delta + d_-$ the transformation (3.306) will determine coefficients of $\rho^+(z)$ in terms of those of $\rho^-(z)$. Hence, for n even, the natural way of modding out such cases is to consider the moduli space with completely independent coefficients of $\rho^+(z)$ and $\rho^-(z)$, which is what we did so far. For n odd, this is not the case since in general the top coefficients of $\rho^+(z)$ and $\rho^-(z)$ are related, i.e., $\rho_{d_+}^+ = \xi \rho_{d_-}^-$. A natural choice is then to set $\xi = 0$, which effectively removes linear dependences within coefficients. Hence we define the $\Delta = 1$ sector as the one with $d_+ = d_- + 1$ and all the coefficients being independent. The transformations (3.306) are now the standard $\mathrm{SL}(2, \mathbb{C})_\rho$ shift and the T shift, which we leave as the redundancies of the sector. We further note that since the degree of the map $p^{AB}(z) = \rho_+^A(z)\rho_-^B(z)$ is odd, for even $\Delta = d_+ - d_-$ there will be trivial linear relations among coefficients. This motivates us to label the sectors as

$$\Delta = d_+ - d_- = 2r + 1. \quad (3.307)$$

The maps that we have used so far correspond to $r = 0$. We find that for $r > 0$ it is the odd-point analog of the reduced Pfaffian, $\mathrm{Pf}' \widehat{A}_n$, defined in Section 3.4, that vanishes for the troublesome solutions supported by these maps.

Finally, we comment that, even though integrands of all the theories we consider in this chapter contain $\text{Pf}A_n$ or $\text{Pf}\widehat{A}_n$, the full integrand does not necessarily vanish for the missing solutions in the degenerate kinematics sector (as we approach it via analytic continuation). In fact, depending on the projected components of the supermultiplet, the fermionic integrations may generate singularities for these solutions such that they contribute finitely. This can happen in all the theories considered so far except in the case of M5 brane and D-branes, where there are enough powers of $\text{Pf}A_n$ to generate a zero for the degenerate solutions. These facts can also be seen by considering purely bosonic amplitudes and directly using CHY formulas. This means that at degenerate kinematic points there are solutions to the scattering equations that require maps with $|\Delta| > 0$. However, this is of course not a problem for our formulas: As we mentioned earlier the degenerate regions of kinematic space are of codimension one or higher, so we can define the amplitudes by analytic continuation of the $\Delta = 0$ formulas. In practice, the integral over the maps moduli space can be first performed in a generic configuration close to the degenerate kinematics, after which the degenerate configuration can be easily reached. We leave a complete exploration of the moduli space of maps for all values of Δ , together with the related topic of 4D dimensional reduction, for future research.

HALF MAXIMAL CHIRAL SUPERGRAVITY: 6D (2, 0) SUPERGRAVITY AND THE K3 MODULI SPACE

4.1 Introduction

As we have described throughout this thesis [1, 2], scattering amplitudes of supersymmetric theories in higher dimensions can be described by a six-dimensional rational map formalism in the spirit of [46, 55, 56]. So far, compact formulas have been found for tree-level amplitudes of a wide range of interesting theories, including maximally supersymmetric gauge theories and supergravity in diverse dimensions, as well as the world-volume theories of probe D-branes and the M5-brane in flat space. In the case of the M5-brane (the subject of Chapter 2), which contains a chiral tensor field, the formalism circumvents a common difficulty in formulating a covariant action principle due to the self-duality constraint.

In this chapter, we continue to explore the utility of the 6D rational maps and spinor-helicity formalism and present the tree-level S matrix for the theory of 6D (2, 0) supergravity. This chiral theory arises as the low-energy limit of Type IIB string theory compactified on a K3 surface [37] and is particularly interesting because it describes the interaction of self-dual tensors and gravitons. This is also the first example we consider with less than maximal supersymmetry, and it is particularly interesting because of the *chiral supersymmetry*.

As before, to describe massless scattering in 6D, it is convenient to introduce spinor-helicity variables [43] with the sometimes convenient notation,

$$p_i^{AB} = \lambda_{i,a}^A \lambda_{i,b}^B \epsilon^{ab} := \langle \lambda_i^A \lambda_i^B \rangle. \quad (4.1)$$

Here, and throughout, $i = 1, \dots, n$ labels the n particles, $A = 1, 2, 3, 4$ is a spinor index of the $Spin(5, 1)$ Lorentz group, and $a = 1, 2$ is a left-handed index of the $SU(2)_L \times SU(2)_R$ massless little group. This is the only non-trivial little-group information that enters for chiral (2, 0) supersymmetry—the (2, 0) supergravity multiplet and a number of (2, 0) tensor multiplets, which contain a chiral tensor. The tensor multiplets transform as singlets of $SU(2)_R$, whereas the gravity multiplet is a triplet; later we will introduce the doublet index \hat{a} for $SU(2)_R$.

We also introduce a flavor index f_i with $i = 1, \dots, 21$ to label the 21 tensor multiplets; this is the number that arises in 6D from compactification of the NS and R fields of Type IIB superstring theory on a K3 surface. It is also the unique number for which the gravitational anomalies cancel. This fact is well known and has been discussed from several points of view, but here we comment that this anomaly cancellation has also been studied from the amplitude point of view where one uses four-point amplitudes and unitarity [181].

In addition to consistent anomaly cancellation, the geometry of K3 determines the scalar moduli space of (2,0) supergravity. We will soon rediscover this moduli space through soft theorems, and we briefly review the standard description [182]. The Hodge numbers of a manifold X are the dimensions of the Dolbeault cohomology groups, $h^{p,q}(X) = \dim(H^{p,q}(X))$. The K3 surface is known to have $h^{1,0} = h^{0,1} = 0$, $h^{2,0} = h^{0,2} = 1$, and $h^{1,1} = 20$. Importantly, this surface has a globally defined holomorphic 2-form which can be integrated over integral 2-cycles to construct periods. Integral 2-cycles are classified by $H_2(\text{K3}, \mathbb{Z})$. One can show from the second Betti numbers above, this homology group is isomorphic to \mathbb{Z}^{22} . The space of holomorphic 2-cycles has a natural inner product given by their intersection number, and this inner product defines a Lorentzian lattice. K3 has 3 anti-self dual 2-cycles and 19 self-dual 2-cycles, and the lattice has signature (3, 19).

Using this information, one can construct the moduli space of complex structures and, additionally, the moduli space of Einstein metrics for K3. The moduli space of metrics (roughly the scalar manifold from the 10D graviton) turns out to be

$$\mathcal{M}_g = O(3, 19; \mathbb{Z}) \backslash O(3, 19) / (O(3) \times O(19)) \times \mathbb{R}_+ \quad (4.2)$$

A choice of complex structure determines a plane in $\mathbb{R}^{3,19}$ with respect to the Lorentzian lattice. The factor of \mathbb{R}_+ is the volume modulus. The dimension of this coset is 58, and these are parametrized by scalar fields.

In addition to the information from the graviton, we also need to include the NS-NS 2-form wrapped on K3 which gives 22 additional scalars. So now locally, the moduli space is given by

$$\mathcal{M}_{NS} = O(3, 19) / (O(3) \times O(19)) \times \mathbb{R}^{22} \times \mathbb{R}_+ \simeq O(4, 20) / (O(4) \times O(20)) \quad (4.3)$$

which is now parametrized by 80 scalars. Globally we must divide by the action of the appropriate discrete group.

For Type IIB compactified on K3 the remaining scalar moduli are 1 from the dilaton and 24 from the RR fields. This gives 105 total scalars, the same number found in 21 tensor multiplets. The moduli space is finally:

$$\mathcal{M}_{(2,0)} = O(5, 21; \mathbb{Z}) \backslash O(5, 21) / (O(5) \times O(21)) \quad (4.4)$$

Actually, we will mostly consider $SO(5, 21; \mathbb{Z}) \backslash SO(5, 21) / (SO(5) \times SO(21))$ as the additional information cannot be seen at tree level. Additionally, in the field theory limit, the discrete group is not visible and we are left with the smooth coset space for the scalars. This coset can be understood as the spontaneous breaking of the noncompact group with the scalar fields as the massless Goldstone bosons. The unbroken compact subgroup $SO(5) \times SO(21)$ can be interpreted as the $USp(4)$ R-symmetry group required by 6D (2, 0) supersymmetry times a global flavor group for the tensor multiplets.

We assume that we are at generic points of the moduli space, where perturbative amplitudes are well-defined. The moduli space has singularities at fixed points of the $SO(5, 21; \mathbb{Z})$ duality group, which are the global identifications described above. At such fixed points one or more tensor multiplets are replaced by non-Lagrangian (2, 0) CFTs [37], and a perturbative analysis is no longer possible, as we have addressed in the discussion of Chapter 3. Therefore, the amplitudes presented in this chapter are applicable at generic points in the moduli space where we can treat the tensor multiplets as abelian. We consider the leading couplings in derivative order, and not the (2, 0) higher derivative corrections central to Chapter 2; this theory interacts via graviton exchange.

So far, we have abstractly introduced the moduli space of (2, 0) supergravity. The local part of this moduli space is present in the classical theory, and it can be extracted directly from the S-matrix by studying soft limits [183]. We derive new soft theorems from the formula we construct, which describe precisely the moduli space of 6D (2, 0) supergravity, which finally is the coset,

$$\mathcal{M}_{\text{Sugra}} = \frac{SO(5, 21)}{SO(5) \times SO(21)}. \quad (4.5)$$

We now turn to the construction of the amplitudes of this theory, which will follow our usual rational maps or twistor-string-like formalism. Before discussing this, it is worth mentioning that the four-point amplitudes of (2, 0)

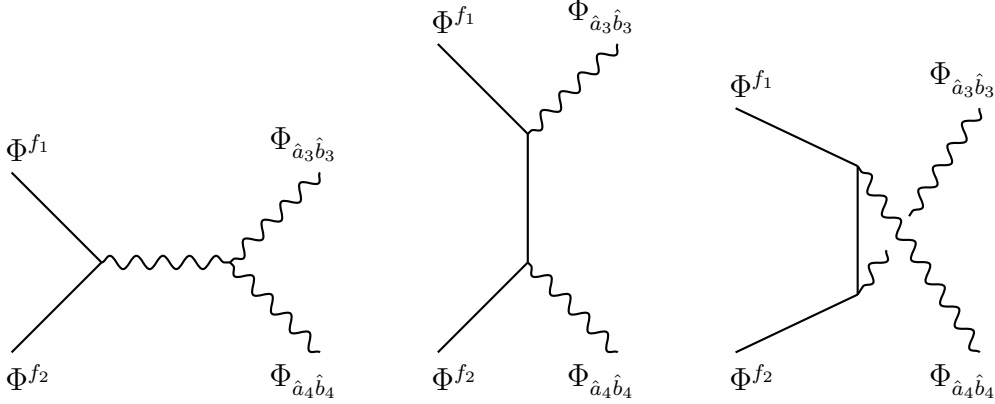


Figure 4.1: On-shell diagrams contributing to the 2-supergraviton, 2-tensor supermultiplet amplitude in Eq. (4.8). Wavy lines denote a propagating $(2, 0)$ supergravity multiplet, and straight lines denote tensor supermultiplets with $SO(21)$ flavor symmetry. Vertices represent the 3-point amplitudes, and *not* the 3-point couplings in the Lagrangian. At tree level, the amplitude is fixed by these pole diagrams.

supergravity are relatively simple, and some may be found in the literature, e.g. [184]. We use the notation $A_{n_1, n_2}^{(2,0)}$ to denote an amplitude with n_1 supergravitons $\Phi_{\hat{a}\hat{b}}$ and n_2 tensor supermultiplets Φ^f transforming as $SO(21)$ fundamentals. Then the four point amplitudes are,

$$A_{4,0}^{(2,0)} = \delta^8(Q) \left(\frac{[1_{\hat{a}_1} 2_{\hat{a}_2} 3_{\hat{a}_3} 4_{\hat{a}_4}][1_{\hat{b}_1} 2_{\hat{b}_2} 3_{\hat{b}_3} 4_{\hat{b}_4}]}{s_{12} s_{23} s_{31}} \right) + \text{sym}, \quad (4.6)$$

$$A_{0,4}^{(2,0)} = \delta^8(Q) \left(\frac{\delta^{f_1 f_2} \delta^{f_3 f_4}}{s_{12}} + \frac{\delta^{f_1 f_3} \delta^{f_2 f_4}}{s_{13}} + \frac{\delta^{f_2 f_3} \delta^{f_1 f_4}}{s_{23}} \right), \quad (4.7)$$

$$A_{2,2}^{(2,0)} = \delta^8(Q) \left(\delta^{f_1 f_2} \frac{[1_{\hat{a}_1} 2_{\hat{a}_2} 3_{\hat{a}_3} 4_{\hat{a}_4}][1_{\hat{b}_1} 2_{\hat{b}_2} 3_{\hat{b}_3} 4_{\hat{b}_4}]}{s_{12} s_{23} s_{31}} \right) + \text{sym}. \quad (4.8)$$

We symmetrize \hat{a}_i, \hat{b}_i for the external graviton multiplets, and $[1_{\hat{a}_1} 2_{\hat{a}_2} 3_{\hat{a}_3} 4_{\hat{a}_4}] = \epsilon_{ABCD} \tilde{\lambda}_{1\hat{a}_1}^A \tilde{\lambda}_{2\hat{a}_2}^B \tilde{\lambda}_{3\hat{a}_3}^C \tilde{\lambda}_{4\hat{a}_4}^D$, and $\delta^8(Q) = \delta^8(\sum_{i=1}^4 \lambda_{i,a}^A \eta_i^{Ia})$. The third of these amplitudes is represented by the on-shell diagrams of Fig (4.1).

As usual, in the rational-map formulation, amplitudes for n particles are expressed as integrals over the moduli space of rational maps from the n -punctured Riemann sphere to the space of spinor-helicity variables. In general, as in the previous chapters the amplitudes take the form [58, 1, 2],

$$A_n^{6D} = \int d\mu_n^{6D} \mathcal{I}_L \mathcal{I}_R, \quad (4.9)$$

where $d\mu_n^{6D}$ is the measure encoding the 6D kinematics and the product $\mathcal{I}_L \mathcal{I}_R$ is the integrand that contains the dynamical information of the theories, including supersymmetry. The measure is given by

$$d\mu_n^{6D} = \frac{\prod_{i=1}^n d\sigma_i \prod_{k=0}^m d^8 \rho_k}{\text{vol}(\text{SL}(2, \mathbb{C})_\sigma \times \text{SL}(2, \mathbb{C})_\rho)} \frac{1}{V_n^2} \prod_{i=1}^n E_i^{6D}, \quad (4.10)$$

and $n = 2m + 2$ (we will discuss $n = 2m + 1$ later). The coordinates σ_i label the n punctures, and $V_n = \prod_{i < j} \sigma_{ij}$, with $\sigma_{ij} = \sigma_i - \sigma_j$. They are determined up to an overall $\text{SL}(2, \mathbb{C})_\sigma$ Möbius group transformation, whose “volume” is divided out in a standard way. The 6D scattering equations are given by

$$E_i^{6D} = \delta^6 \left(p_i^{AB} - \frac{\langle \rho^A(\sigma_i) \rho^B(\sigma_i) \rangle}{\prod_{j \neq i} \sigma_{ij}} \right). \quad (4.11)$$

These maps are given by degree- m polynomials $\rho_a^A(\sigma) = \sum_{k=0}^m \rho_{a,k}^A \sigma^k$, which are determined up to an overall $\text{SL}(2, \mathbb{C})_\rho$ transformation, whose volume is divided out. This group is a complexification of $SU(2)_L$.

It is straightforward to see that (4.11) implies the on-shell conditions $p_i^2 = 0$ and momentum conservation. Furthermore as we have discussed, this construction implies that the integrals are completely localized on the $(n - 3)!$ solutions, which are equivalent to those of the general dimensional scattering equations [58], which we introduced in Chapter 1.3:

$$\sum_{i \neq j} \frac{p_i \cdot p_j}{\sigma_{ij}} = 0, \quad \text{for all } j. \quad (4.12)$$

As we have already seen, unlike the general-dimensional scattering equations, the use of the spinor-helicity coordinates and 6D scattering equations allows us to make supersymmetry manifest. Much of our discussion of the kinematics and supersymmetry will be identical to previous chapters.

Now consider $n = 2m + 1$, for which we have [2],

$$d\mu_n^{6D} = \frac{(\prod_{i=1}^n d\sigma_i \prod_{k=0}^{m-1} d^8 \rho_k) d^4 \omega \langle \xi d\xi \rangle}{\text{vol}(\text{SL}(2, \mathbb{C})_\sigma, \text{SL}(2, \mathbb{C})_\rho, T)} \frac{1}{V_n^2} \prod_{i=1}^n E_i^{6D}. \quad (4.13)$$

The polynomials $\rho_a^A(\sigma)$ now are given by

$$\rho_a^A(\sigma) = \sum_{k=0}^{m-1} \rho_{a,k}^A \sigma^k + \omega^A \xi_a \sigma^m, \quad (4.14)$$

and there is a shift symmetry $T(\alpha)$ acting on ω^A : $\omega^A \rightarrow \omega^A + \alpha \langle \xi \rho_{m-1}^A \rangle$, which we also have to mod out.

Here we review the integrand factors for 6D (2, 2) supergravity, since they will be relevant. For (2, 2) supergravity, we have,

$$\mathcal{I}_L = \det' S_n, \quad \mathcal{I}_R = \Omega_F^{(2,2)}, \quad (4.15)$$

where S_n is a $n \times n$ anti-symmetric matrix, with entries: $[S_n]_{ij} = \frac{p_i \cdot p_j}{\sigma_{ij}}$. This matrix has rank $(n-2)$, and the reduced Pfaffian and determinant are defined as

$$\text{Pf}' S_n = \frac{(-1)^{i+j}}{\sigma_{ij}} \text{Pf} S_{ij}^{ij}, \quad \det' S_n = (\text{Pf}' S_n)^2. \quad (4.16)$$

Here S_{ij}^{ij} means that the i -th and j -th rows and columns of S_n are removed, and the result is i, j independent [125]. $\Omega_F^{(2,2)}$ is a fermionic function of Grassmann coordinates $\eta_i^{Ia}, \tilde{\eta}_i^{\hat{I}\hat{a}}$, which we use to package the supermultiplet of on-shell states into the superfield,

$$\begin{aligned} \Phi^{(2,2)}(\eta, \tilde{\eta}) &= \phi' + \dots + \eta_a^I \eta_{I,b} B^{ab} + \tilde{\eta}^{\hat{I},\hat{a}} \tilde{\eta}_{\hat{I},\hat{b}} B_{\hat{a}\hat{b}} \\ &+ \dots + \eta_a^I \eta_{I,b} \tilde{\eta}_{\hat{a}}^{\hat{I}} \tilde{\eta}_{\hat{I},\hat{b}} G^{ab\hat{a}\hat{b}} + \dots + (\eta)^4 (\tilde{\eta})^4 \bar{\phi}', \end{aligned} \quad (4.17)$$

where B^{ab} and $B_{\hat{a}\hat{b}}$ are self-dual and anti self-dual two forms, and $G^{ab\hat{a}\hat{b}}$ is the graviton. Here $I, \hat{I} = 1, 2$ are the R-symmetry indices corresponding to a $SU(2) \times SU(2)$ subgroup of the full $USp(4) \times USp(4)$ R-symmetry. This information can be summarized by saying the particles transform in the representations $(\mathbf{3}, \mathbf{3}; \mathbf{1}, \mathbf{1}) \oplus (\mathbf{3}, \mathbf{2}; \mathbf{1}, \mathbf{4}) \oplus (\mathbf{2}, \mathbf{3}; \mathbf{4}, \mathbf{1}) \oplus (\mathbf{3}, \mathbf{1}; \mathbf{1}, \mathbf{5}) \oplus (\mathbf{1}, \mathbf{3}; \mathbf{5}, \mathbf{1}) \oplus (\mathbf{2}, \mathbf{2}; \mathbf{4}, \mathbf{4}) \oplus (\mathbf{2}, \mathbf{1}; \mathbf{4}, \mathbf{5}) \oplus (\mathbf{1}, \mathbf{2}; \mathbf{5}, \mathbf{4}) \oplus (\mathbf{1}, \mathbf{1}; \mathbf{5}, \mathbf{5})$. The fermionic function $\Omega_F^{(2,2)}$ imposes the conservation of supercharge, which may be viewed as a double copy: $\Omega_F^{(2,2)} = \Omega_F^{(2,0)} \Omega_F^{(0,2)}$, and $\Omega_F^{(2,0)}$ is given by

$$\Omega_F^{(2,0)} = V_n \prod_{k=0}^m \delta^4 \left(\sum_{i=1}^n C_{a,k;i,b} \eta_i^{Ib} \right). \quad (4.18)$$

The $n \times 2n$ matrices $C_{a,k;i,b} = (W_i)_a^b \sigma_i^k$ and $(W_i)_a^b$ can be expressed in terms of $\rho_a^A(\sigma_i)$ via

$$p_i^{AB} W_{i,b}^a = \frac{\rho^{[A,a}(\sigma_i) \lambda_{i,b}^{B]}}{\prod_{j \neq i} \sigma_{ij}}, \quad (4.19)$$

which is independent of A, B , and satisfies $\det W_i = \prod_{j \neq i} \sigma_{ij}^{-1}$. The matrix $C_{a,k;i,b}$ is a symplectic Grassmannian which was used in [2] and Chapter 3 as an

alternative way to impose the 6D scattering equations. $\Omega_F^{(0,2)}$ is the conjugate of $\Omega_F^{(2,0)}$, and the definition is identical, with the understanding that we use the right-handed variables, such as $\tilde{\eta}_{\hat{a}}^{\hat{I}}, \tilde{\lambda}_{\hat{A}\hat{a}}, \tilde{\rho}_{\hat{A}\hat{a}}, \tilde{\xi}_{\hat{a}}, (\tilde{W}_i)_{\hat{a}}^{\hat{b}}$, etc.

For $n = 2m + 1$, the integrands take a slightly different form. For the fermionic part, we have

$$\Omega_F^{(2,0)} = V_n \prod_{k=0}^{m-1} \delta^4 \left(\sum_{i=1}^n C_{a,k;i,b} \eta_i^{Ib} \right) \delta^2 \left(\sum_{i=1}^n \xi^a C_{a,m;i,b} \eta_i^{Ib} \right). \quad (4.20)$$

whereas the $n \times n$ matrix S_n is modified to an $(n+1) \times (n+1)$ matrix, which we denote \hat{S} . \hat{S}_n is defined in the same way as S_n , but with $i, j = 1, \dots, n, \star$. Here σ_\star is a reference puncture, and p_\star is given by

$$p_\star^{AB} = \frac{2 q^{[A} p^{B]C}(\sigma_\star) \tilde{q}_C}{q^D [\tilde{\rho}_D(\sigma_\star) \tilde{\xi}] \langle \rho^E(\sigma_\star) \xi \rangle \tilde{q}_E}, \quad (4.21)$$

where q and \tilde{q} are arbitrary spinors.

4.2 6D (2, 0) Supergravity

The 6D (2, 0) supergravity theory contains 21 tensor multiplets and the graviton multiplet. The superfield of the tensor multiplet is a singlet of the little group,

$$\Phi(\eta) = \phi + \dots + \eta_a^I \eta_{I,b} B^{ab} + \dots + (\eta)^4 \bar{\phi}, \quad (4.22)$$

where $a, b = 1, 2$ are the $SU(2)_L$ little-group indices. The graviton multiplet transforms as a $(\mathbf{1}, \mathbf{3})$ of the little group, so the superfield carries explicit $SU(2)_R$ indices,

$$\Phi_{\hat{a}\hat{b}}(\eta) = B_{\hat{a}\hat{b}} + \dots + \eta_a^I \eta_{I,b} G_{\hat{a}\hat{b}}^{ab} + \dots + (\eta)^4 \bar{B}_{\hat{a}\hat{b}}, \quad (4.23)$$

and $\Phi_{\hat{a}\hat{b}}(\eta) = \Phi_{\hat{b}\hat{a}}(\eta)$. We see that both the tensor multiplet and graviton multiplet can be obtained from the 6D (2, 2) superfield in (4.17) via SUSY reductions [185]¹,

$$\begin{aligned} \Phi(\eta) &= \int d\tilde{\eta}_{\hat{a}}^{\hat{I}} d\tilde{\eta}_{\hat{I}}^{\hat{a}} \Phi^{(2,2)}(\eta, \tilde{\eta})|_{\tilde{\eta} \rightarrow 0}, \\ \Phi_{\hat{a}\hat{b}}(\eta) &= \int d\tilde{\eta}_{\hat{a}}^{\hat{I}} d\tilde{\eta}_{\hat{I}\hat{b}} \Phi^{(2,2)}(\eta, \tilde{\eta})|_{\tilde{\eta} \rightarrow 0}. \end{aligned} \quad (4.24)$$

¹For the superfield of the tensor, $\Phi(\eta)$, one may choose different I, J ; however, only the case of $I = 1, J = 2$ leads to non-vanishing results when we integrate away $\tilde{\eta}$'s from the amplitudes of (2, 2) supergravity.

These integrals have the effect of projecting onto the right-handed $USp(4)$ R-symmetry singlet sector, which reduces $(2, 2) \rightarrow (2, 0)$. Using the reduction, the amplitudes of $(2, 0)$ supergravity with n_1 supergravity multiplets and n_2 tensor multiplets of the same flavor ($n_1 + n_2 = n$) can be obtained from the $(2, 2)$ supergravity amplitude via

$$A_{n_1, n_2}^{(2,0)} = \int \prod_{i \in n_1} d\tilde{\eta}_{i, \hat{a}_i}^{\hat{I}} d\tilde{\eta}_{i, \hat{b}_i} d\tilde{\eta}_{j, \hat{a}_j}^{\hat{J}} d\tilde{\eta}_{j, \hat{b}_j} A_n^{(2,2)}(\eta, \tilde{\eta}). \quad (4.25)$$

Note $A_n^{(2,2)}(\eta, \tilde{\eta}) \sim \eta^{2n} \tilde{\eta}^{2n}$, so the integration removes all $\tilde{\eta}$'s. The fermionic integral can be performed using (4.15), and (4.18) (or (4.20) for odd n), and we obtain

$$A_{n_1, n_2}^{(2,0)} = \int d\mu_n^{6D} \tilde{M}_{\hat{a}\hat{b}}^{n_1 n_2} V_n \det' S_n \Omega_F^{(2,0)}, \quad (4.26)$$

where $\tilde{M}_{\hat{a}\hat{b}}^{n_1 n_2}$, which we will define shortly, is obtained by integrating out $\Omega_F^{(0,2)}$.

We begin with n even, as the odd- n case works in a similar fashion. Introducing the $n \times n$ matrix

$$\tilde{M}_{\hat{a}_1 \dots \hat{a}_n} = \begin{pmatrix} \tilde{C}_{\hat{1},0;1,\hat{a}_1} & \tilde{C}_{\hat{1},0;2,\hat{a}_2} & \cdots & \tilde{C}_{\hat{1},0;n,\hat{a}_n} \\ \vdots & \vdots & \cdots & \vdots \\ \tilde{C}_{\hat{1},m;1,\hat{a}_1} & \tilde{C}_{\hat{1},m;2,\hat{a}_2} & \cdots & \tilde{C}_{\hat{1},m;n,\hat{a}_n} \\ \tilde{C}_{\hat{2},0;1,\hat{a}_1} & \tilde{C}_{\hat{2},0;2,\hat{a}_2} & \cdots & \tilde{C}_{\hat{2},0;n,\hat{a}_n} \\ \vdots & \vdots & \cdots & \vdots \\ \tilde{C}_{\hat{2},m;1,\hat{a}_1} & \tilde{C}_{\hat{2},m;2,\hat{a}_2} & \cdots & \tilde{C}_{\hat{2},m;n,\hat{a}_n} \end{pmatrix}, \quad (4.27)$$

then $\tilde{M}_{\hat{a}\hat{b}}^{n_1 n_2}$ is given by

$$\tilde{M}_{\hat{a}\hat{b}}^{n_1 n_2} = \det \tilde{M}_{\hat{a}_1 \dots \hat{a}_n} \det \tilde{M}_{\hat{b}_1 \dots \hat{b}_n}. \quad (4.28)$$

Note that here \hat{a} and \hat{b} denote sets of indices. The indices \hat{a}_i, \hat{b}_i are contracted if $i \in n_2$, whereas for $j \in n_1$ we symmetrize \hat{a}_j, \hat{b}_j . This corresponds to constructing little-group singlets for tensor multiplets and triplets for graviton multiplets. After the contraction and symmetrization, the result of (4.28) simplifies drastically²

$$\tilde{M}_{\hat{a}\hat{b}}^{n_1 n_2} \rightarrow \frac{\text{Pf } X_{n_2}}{V_{n_2}} \tilde{M}_{\hat{a}\hat{b}}^{n_1 0}, \quad (4.29)$$

²The identity may be understood by studying the zeros and singularities on both sides of the equation, we have also checked it explicitly up to $n = 12$.

where X_{n_2} is a $n_2 \times n_2$ anti-symmetric matrix given by

$$[X_{n_2}]_{ij} = \begin{cases} \frac{1}{\sigma_{ij}} & \text{if } i \neq j \\ 0 & \text{if } i = j, \end{cases} \quad (4.30)$$

and $\tilde{M}_{\hat{a}\hat{b}}^{n_1 0}$ contains only the graviton multiplets. Let's remark that the simplification (4.29) (especially the appearance of $\text{Pf}X_{n_2}$) will be crucial for the generalization to amplitudes with multiple tensor flavors which is more interesting and relevant for type IIB on K3.

At this point in the analysis, we have obtained the tree-level amplitudes of 6D (2, 0) supergravity with a single flavor of tensor multiplets:

$$A_{n_1, n_2}^{(2,0)} = \int d\mu_n^{6D} \frac{\text{Pf}X_{n_2}}{V_{n_2}} \tilde{M}_{\hat{a}\hat{b}}^{n_1 0} V_n \det' S_n \Omega_F^{(2,0)}. \quad (4.31)$$

The factor $\text{Pf}X_{n_2}$ requires the non-vanishing amplitudes to contain an even number n_2 of tensor multiplets, as expected. For odd n , the matrix $\tilde{M}_{\hat{a}_1 \dots \hat{a}_n}$ is given by

$$\tilde{M}_{\hat{a}_1 \dots \hat{a}_n} = \begin{pmatrix} \tilde{\xi}^{\hat{b}} \tilde{C}_{\hat{b}, m; 1, \hat{a}_1} & \tilde{\xi}^{\hat{b}} \tilde{C}_{\hat{b}, m; 2, \hat{a}_2} & \cdots & \tilde{\xi}^{\hat{b}} \tilde{C}_{\hat{b}, m; n, \hat{a}_n} \\ \tilde{C}_{\hat{1}, 0; 1, \hat{a}_1} & \tilde{C}_{\hat{1}, 0; 2, \hat{a}_2} & \cdots & \tilde{C}_{\hat{1}, 0; n, \hat{a}_n} \\ \vdots & \vdots & \cdots & \vdots \\ \tilde{C}_{\hat{1}, m-1; 1, \hat{a}_1} & \tilde{C}_{\hat{1}, m-1; 2, \hat{a}_2} & \cdots & \tilde{C}_{\hat{1}, m-1; n, \hat{a}_n} \\ \tilde{C}_{\hat{2}, 0; 1, \hat{a}_1} & \tilde{C}_{\hat{2}, 0; 2, \hat{a}_2} & \cdots & \tilde{C}_{\hat{2}, 0; n, \hat{a}_n} \\ \vdots & \vdots & \cdots & \vdots \\ \tilde{C}_{\hat{2}, m-1; 1, \hat{a}_1} & \tilde{C}_{\hat{2}, m-1; 2, \hat{a}_2} & \cdots & \tilde{C}_{\hat{2}, m-1; n, \hat{a}_n} \end{pmatrix} \quad (4.32)$$

recall $\tilde{\xi}^{\hat{b}}$ is the right-hand version of ξ^b in (4.14). Then the amplitudes take the same form

$$A_{n_1, n_2}^{(2,0)} = \int d\mu_n^{6D} \frac{\text{Pf}X_{n_2}}{V_{n_2}} \tilde{M}_{\hat{a}\hat{b}}^{n_1 0} V_n \det' \hat{S}_n \Omega_F^{(2,0)}. \quad (4.33)$$

Multi-flavor tensor multiplets

As we have emphasized, the identity (4.29) is crucial for the generalization to multiple tensor flavors, which is required for the 6D (2, 0) supergravity. Indeed, the formula takes a form similar to that of an Einstein–Maxwell theory worked out by Cachazo, He and Yuan [125], especially the object $\text{Pf}X_{n_2}$. In that case, in passing from single- $U(1)$ photons to multiple- $U(1)$ ones, one simply replaces

the matrix X_n by \mathcal{X}_n [125],

$$[\mathcal{X}_n]_{ij} = \begin{cases} \frac{\delta_{f_i f_j}}{\sigma_{ij}} & \text{if } i \neq j \\ 0 & \text{if } i = j \end{cases} \quad (4.34)$$

which allows the introduction of multiple distinct flavors: namely, f_i, f_j are flavor indices, and $\delta_{f_i f_j} = 1$ if particles i, j are of the same flavor, otherwise $\delta_{f_i f_j} = 0$. Inspired by this result, we are led to a proposal for the complete tree-level S-matrix of 6D (2, 0) supergravity with multiple flavors of tensor multiplets:

$$A_{n_1, n_2}^{(2,0)} = \int d\mu_n^{6D} \frac{\text{Pf } \mathcal{X}_{n_2}}{V_{n_2}} \tilde{M}_{\hat{a}\hat{b}}^{n_1 0} V_n \det' S_n \Omega_F^{(2,0)}. \quad (4.35)$$

Again, the 6D scattering equations and integrands take different forms depending on whether n is even or odd. As we have emphasized, the artificial difference between the formulas of even- and odd-point amplitudes is due to the peculiar property of the 6D scattering equations in the rational map form, and not specific to chiral (2, 0) supergravity. Since n_2 is necessarily even, this is equivalent to distinguishing whether n_1 is even or odd.

Equation (4.35) is our main result, which is a localized integral formula that describes all tree-level superamplitudes of abelian tensor multiplets (with multiple flavors) coupled to gravity multiplets. We can verify that it has all the correct properties. For instance, due to the fact that all the building blocks of the formula come from either 6D (2, 2) supergravity or Einstein–Maxwell theory, they all behave properly in the factorization limits, and transform correctly under the symmetries: $\text{SL}(2, \mathbb{C})_\sigma$, $\text{SL}(2, \mathbb{C})_\rho$, etc. Also, as we will show later, when reduced to 4D the proposed formula produces (supersymmetric) Einstein–Maxwell amplitudes, which is another consistency check. Finally, it is straightforward to check that the formula gives correct low-point amplitudes, Eq. (4.8).

4.3 The K3 Moduli Space from Soft Limits

Type IIB string theory compactified on K3 has a well-studied moduli space as we have discussed in the introduction of this chapter. The moduli space is,

$$\mathcal{M}_{(2,0)} = SO(5, 21; \mathbb{Z}) \backslash SO(5, 21) / (SO(5) \times SO(21)). \quad (4.36)$$

The discrete group is invisible in the supergravity approximation, so we concern ourselves with the local form of the moduli space of the supergravity

theory, namely $\frac{SO(5,21)}{SO(5) \times SO(21)}$. It has dimension of 105, which corresponds precisely to the 105 scalars in the 21 tensor multiplets. These scalars are Goldstone bosons of the breaking of $SO(5, 21)$ to $SO(5) \times SO(21)$, which are the R-symmetry and flavor symmetry, respectively. Therefore, the scalars obey soft theorems, which are the tools to explore the structure of the moduli space directly from the S matrix [183].

We find that the amplitudes behave like pion amplitudes with ‘‘Adler’s zero’’ [186] in the single soft limit. Indeed, for $p_1 \rightarrow 0$, we find,

$$A_n(\phi_1^{f_1}, 2, \dots, n) \rightarrow \mathcal{O}(p_1), \quad (4.37)$$

and the same for other scalars in the tensor multiplets. The commutator algebra of the coset space may be explored by considering double soft limits for scalars. Physically, the process of taking two particles to be soft is ambiguous. If a global symmetry G is spontaneously broken to a subgroup H with unbroken generators R and Goldstone bosons ϕ , the double soft limit of two such ϕ leads to a momentum dependent H rotation acting on the remaining $n - 2$ hard particles.

The situation for half maximal supergravities is somewhat more complicated than the maximal case because we have Goldstones corresponding to both flavor and R symmetries which are here both denoted with R and distinguished by the indices they carry. Beginning with the flavor symmetry, we find for $p_1, p_2 \rightarrow 0$ simultaneously

$$A_n(\phi_1^{f_1}, \bar{\phi}_2^{f_2}, \dots) \rightarrow \frac{1}{2} \sum_{i=3}^n \frac{p_i \cdot (p_1 - p_2)}{p_i \cdot (p_1 + p_2)} R_i^{f_1 f_2} A_{n-2}, \quad (4.38)$$

where f_i ’s are flavor indices, and $R_i^{f_1 f_2}$ is a generator of the unbroken $SO(21)$, which may be viewed as the result of the commutator of two broken generators. $R_i^{f_1 f_2}$ acts on superfields (4.24) as

$$\begin{aligned} R_i^{f_1 f_2} \Phi_i^{f_2} &= \Phi_i^{f_1}, & R_i^{f_1 f_2} \Phi_i^{f_1} &= -\Phi_i^{f_2}, \\ R_i^{f_1 f_2} \Phi_i^{f_3} &= 0, & R_i^{f_1 f_2} \Phi_{i, \hat{a}\hat{b}} &= 0, \end{aligned} \quad (4.39)$$

where $f_3 \neq f_1, f_2$. Therefore, the generator exchanges tensor multiplets of flavor f_1 with ones of f_2 , and sends all others and the graviton multiplet to 0.

To study the $SO(5)$ R-symmetry generators we take soft limits of two scalars which do not form a R-symmetry singlet. For instance

$$A_n(\bar{\phi}_1, \phi_2^{IJ}, \dots) \rightarrow \frac{1}{2} \sum_{i=3}^n \frac{p_i \cdot (p_1 - p_2)}{p_i \cdot (p_1 + p_2)} R_i^{IJ} A_{n-2}, \quad (4.40)$$

with $R_i^{IJ} = \eta_{i,a}^I \eta_i^{J,a}$. Similarly, other choices of soft scalars lead to the remaining R-symmetry generators:

$$R_{i,IJ} = \frac{\partial}{\partial \eta_{i,a}^I} \frac{\partial}{\partial \eta_i^{J,a}}, \quad R_{i,J}^I = \eta_{i,a}^I \frac{\partial}{\partial \eta_i^{J,a}}. \quad (4.41)$$

Finally, we consider the cases where soft scalars carry different flavors and do not form an R-symmetry singlet. This actually leads to new soft theorems:

$$\boxed{A_n(\bar{\phi}_1^{f_1}, \phi_2^{f_2, IJ}, \dots) \rightarrow \sum_{i=3}^n \frac{p_1 \cdot p_2}{p_i \cdot (p_1 + p_2)} R_i^{f_1 f_2} R_i^{IJ} A_{n-2}} \quad (4.42)$$

and similarly for other R-symmetry generators. The results of the soft limits now contain both flavor and R-symmetry generators, reflecting the direct product structure in $\frac{SO(5,21)}{SO(5) \times SO(21)}$. This is a new phenomenon that is not present in pure maximal supergravity [183, 187].

The above soft theorems may be obtained by analyzing how the integrand and the scattering equations behave in the limits. For instance, the vanishing of the amplitudes in the single-soft limits is due to

$$\int d\mu_n^{6D} \sim \mathcal{O}(p_1^{-1}), \quad \det' S_n \sim \mathcal{O}(p_1^2), \quad (4.43)$$

and the rest remains finite. The double-soft theorems require more careful analysis along the lines of, e.g. [188]. The structures of double-soft theorems, however, are already indicated by knowing the four-point amplitudes given in (4.8), since important contributions are diagrams with a four-point amplitude on one side such that the propagator becomes singular in the limit. For the study of the moduli space, the scalars we choose do not form a singlet, therefore the most singular diagrams with a three-point amplitude on one side are not allowed. If instead the two scalars do form a singlet, then such diagrams dominate and contain a propagating soft graviton. The soft theorem for such a pair of scalars is simply given by Weinberg's soft graviton theorem attached with the three-point amplitude, which we have also checked using our formula. Finally, we have also checked the soft theorems explicitly using our formula (4.35) for various examples.

4.4 4D $\mathcal{N} = 4$ Einstein–Maxwell Theory

One can dimensionally reduce 6D (2, 0) supergravity to obtain 4D $\mathcal{N} = 4$ Einstein–Maxwell theory. The tree-level amplitudes of this theory capture the leading low-energy behavior of Type IIB (or Type IIA) superstring theory on $K3 \times T^2$.

The reduction to 4D can be obtained by decomposing the 6D spinor as $A \rightarrow \alpha = 1, 2, \dot{\alpha} = 3, 4$. The compact momenta are $P_i^{\alpha\beta} = P_i^{\dot{\alpha}\dot{\beta}} = 0$; this is implemented by $\lambda_a^A \rightarrow \lambda_+^\alpha = 0$ and $\lambda_-^{\dot{\alpha}} = 0$.

The 6D tensor superfield becomes an $\mathcal{N} = 4$ vector multiplet in 4D, in a non-chiral form [138, 1],

$$\begin{aligned} \Phi(\eta_a) \rightarrow V_{\mathcal{N}=4}(\eta_+, \eta_-) &= \phi + \eta_-^{\hat{I}} \psi_{\hat{I}}^- + \dots \\ &+ (\eta_+)^2 A^+ + (\eta_-)^2 A^- + \dots + (\eta_+)^2 (\eta_-)^2 \bar{\phi}. \end{aligned} \quad (4.44)$$

Dimensional reduction of $\Phi^{\hat{a}\hat{b}}(\eta)$ is analogous. It separates into 3 cases, where $\Phi^{\hat{+}\hat{+}} \rightarrow V_{\mathcal{N}=4}(\eta_+, \eta_-)$, and $\Phi^{\hat{+}\hat{-}}, \Phi^{\hat{-}\hat{-}}$ become a pair of positive and negative-helicity graviton multiplets

$$\begin{aligned} \Phi^{\hat{+}\hat{+}}(\eta_a) \rightarrow \mathcal{G}_{\mathcal{N}=4}^+(\eta_+, \eta_-) &= A^+ + \eta_-^{\hat{I}} \psi_{\hat{I}}^{-+} + \dots \\ &+ (\eta_+)^2 G^{++} + (\eta_-)^2 \phi + \dots + (\eta_+)^2 (\eta_-)^2 \bar{A}^+, \end{aligned} \quad (4.45)$$

$$\begin{aligned} \Phi^{\hat{-}\hat{-}}(\eta_a) \rightarrow \mathcal{G}_{\mathcal{N}=4}^-(\eta_+, \eta_-) &= \bar{A}^- + \eta_-^{\hat{I}} \Psi_{\hat{I}}^{-} + \dots \\ &+ (\eta_-)^2 G^{--} + (\eta_+)^2 \bar{\phi} + \dots + (\eta_+)^2 (\eta_-)^2 A^-. \end{aligned} \quad (4.46)$$

We see the on-shell spectrum of the 4D supergravity theory consists of the \mathcal{G}^+ and \mathcal{G}^- superfields coupled to 22 $\mathcal{N} = 4$ Maxwell multiplets.

We are now ready to perform the dimensional reduction on (4.35). First, the 6D measure reduces to

$$d\mu^{4D} = \frac{\prod_{i=1}^n d\sigma_i \prod_{k=0}^d d^2 \rho_k \prod_{k=0}^{\tilde{d}} d^2 \tilde{\rho}_k}{\text{vol}(\text{SL}(2, \mathbb{C})_\sigma \times \text{GL}(1, \mathbb{C}))} \frac{1}{R(\rho)R(\tilde{\rho})} \prod_{i=1}^n E_i^{4D}$$

where $R(\rho), R(\tilde{\rho})$ are the resultants of the polynomials

$$\rho^\alpha(\sigma) = \sum_{k=0}^d \rho_k^\alpha \sigma^k, \quad \tilde{\rho}^{\dot{\alpha}}(\sigma) = \sum_{k=0}^{\tilde{d}} \tilde{\rho}_k^{\dot{\alpha}} \sigma^k, \quad (4.47)$$

with $d + \tilde{d} = n - 2$, and the 4D scattering equations are given by

$$E_i^{4D} = \delta^4 \left(p_i^{\alpha\dot{\alpha}} - \frac{\rho^\alpha(\sigma_i) \tilde{\rho}^{\dot{\alpha}}(\sigma_i)}{\prod_{j \neq i} \sigma_{ij}} \right). \quad (4.48)$$

The 2×2 matrix $(\tilde{W}_i)_{ab}$ reduces to

$$(\tilde{W}_i)_{\hat{+}\hat{+}} = (\tilde{W}_i)_{\hat{-}\hat{-}} = 0, \quad (\tilde{W}_i)_{\hat{+}\hat{-}} = t_i, \quad (\tilde{W}_i)_{\hat{-}\hat{+}} = \tilde{t}_i. \quad (4.49)$$

with $t_i = \frac{\lambda_i^\alpha}{\rho^\alpha(\sigma_i)}$, $\tilde{t}_i = \frac{\tilde{\lambda}_i^{\dot{\alpha}}}{\tilde{\rho}^{\dot{\alpha}}(\sigma_i)}$ (independent of $\alpha, \dot{\alpha}$), and $t_i \tilde{t}_i = \prod_{j \neq i} \frac{1}{\sigma_{ij}}$. As for the integrand, the parts that reduce to 4D non-trivially are

$$\tilde{M}_{\hat{a}\hat{b}}^{n_1} \rightarrow \tilde{T}_{\hat{a}\hat{b}}^{n_1}, \quad \det' S_n \rightarrow R^2(\rho) R^2(\tilde{\rho}) V_n^{-2}. \quad (4.50)$$

Assume we have m_1 \mathcal{G}^+ superparticles and m_2 \mathcal{G}^- , with $m_1 + m_2 = n_1$ ³, we find \tilde{T}^{n_1} is given by

$$\tilde{T}^{n_1} = T_+^{m_1} T_-^{m_2} = \left(V_{m_1}^2 \prod_{i \in m_1} t_i^2 \right) \left(V_{m_2}^2 \prod_{j \in m_2} \tilde{t}_j^2 \right), \quad (4.51)$$

where $V_{m_1} = \prod_{i < j} \sigma_{ij}$ for $i, j \in m_1$, and similarly for V_{m_2} . We therefore obtain a general formula for the amplitudes of 4D $\mathcal{N} = 4$ Einstein-Maxwell theory:

$$A_n^{\mathcal{N}=4} = \int d\mu^{4D} \frac{\text{Pf } \mathcal{X}_{n_2}}{V_{n_2} V_n} T_+^{m_1} T_-^{m_2} R^2(\rho) R^2(\tilde{\rho}) \Omega_F^{\mathcal{N}=4}, \quad (4.52)$$

where $\Omega_F^{\mathcal{N}=4}$ implements the 4D $\mathcal{N} = 4$ supersymmetry, arising as the reduction of $\Omega_F^{(2,0)}$,

$$\Omega_F^{\mathcal{N}=4} = \prod_{k=0}^d \delta^2 \left(\sum_{i=1}^n t_i \sigma_i^k \eta_{i+}^I \right) \prod_{k=0}^{\tilde{d}} \delta^2 \left(\sum_{i=1}^n \tilde{t}_i \sigma_i^k \eta_{i-}^I \right). \quad (4.53)$$

The formula should be understood as summing over d, \tilde{d} obeying $d + \tilde{d} = n - 2$. However, it is clear from the superfields that we should require

$$d = \frac{n_2}{2} + m_1 - 1, \quad \tilde{d} = \frac{n_2}{2} + m_2 - 1, \quad (4.54)$$

recall n_2 is even. Therefore, for a given number of photon and graviton multiplets, the summation over sectors becomes a sum over different m_1, m_2 . We have checked (4.52) against many explicit amplitudes, and also verified that the integrand is identical to that of [125] for certain component amplitudes.

4.5 Discussion and Conclusion

We have presented a formula for the tree-level S matrix of 6D (2, 0) supergravity. The formula for single-flavor tensor multiplets is constructed via a SUSY

³We do not consider $\Phi^{\hat{+}\hat{-}}$ here since they are identical to the vector which we have already included, as shown in (4.45).

reduction of the one for $(2, 2)$ supergravity. We observed important simplifications in deriving the formula, particularly the appearance of the object $\text{Pf} X_n$, crucially for the generalization to 21 flavors required for $(2, 0)$ supergravity. By studying soft limits of the formula, we were able to explore the moduli space of the theory. Via dimensional reduction, we also deduced a new formula for amplitudes of 4D $\mathcal{N} = 4$ Einstein-Maxwell. Since 6D $(2, 0)$ supergravity has a UV completion as a string theory, it would be of interest to extend our formula to include α' corrections, perhaps along the lines of [189]. Also recent papers [168, 137] introduce an alternative form of the scattering equations that treats even and odd points equally, but uses a different formalism for supersymmetry. It will be interesting to study our formula into this formalism.

Our results provide an S matrix confirmation of various properties of $(2, 0)$ supergravity and the dimensionally reduced theory as predicted by string dualities. While the 10D theory has a dilaton that sets the coupling, in 6D this scalar is one of the 105 moduli fields, and appears equally with the other 104 scalars. If one considers the compactification on $K3 \times T^2$, standard U-dualities imply equivalence to the Type IIA superstring theory on the same geometry or the heterotic string theory compactified to 4D on a torus. The formulas discussed in this chapter apply to all these cases, at least at generic points of the moduli space.

PROJECTIVE CURVES AND P -ADIC ADS/CFT**5.1 Introduction**

In this chapter, we propose a version of the AdS/CFT correspondence now known as *p -adic AdS/CFT*. This is a somewhat unusual generalization of the AdS₃/CFT₂ correspondence based on the relationship between complex projective geometry, algebraic curves, and hyperbolic 3-manifolds. An introduction to these ideas is given in Sec. 1.4.

The bulk geometries relevant to the AdS₃/CFT₂ correspondence are well understood. The most well-known black hole solution is that of Bañados, Teitelboim, and Zanelli [73]; this solution was generalized to a family of higher-genus Euclidean black holes by Krasnov [72]. These solutions can be understood in general using the technique of *Schottky uniformization*, which presents a higher-genus black hole as the quotient of empty AdS₃ by a particular discrete subgroup of its isometries.

In [190], a holographic correspondence was established for these three-dimensional geometries. This correspondence expresses the conformal two point correlation function on the conformal boundary at infinity (a Riemann surface X_Γ of genus g) in terms of geodesic lengths in the bulk space (a hyperbolic handlebody \mathcal{H}_Γ of genus g). The formula relating the boundary theory to gravity in the bulk is based on Manin's result [191] on the Arakelov Green's function.

However, we consider AdS₃/CFT₂ not merely because it is a simple setting for holography. For us, the crucial property of conformal field theory in two dimensions is its strong ties to algebraic geometry. These occur because every compact Riemann surface is a projective algebraic curve, so that many of the analytic concepts that arise in physics can (in two-dimensional contexts) be reformulated in purely algebraic terms. Once a concept can be formulated algebraically, it has many natural generalizations, obtained by changing the field of numbers one is considering. For instance, given a Riemann surface as the zero locus of a polynomial equation with rational coefficients, one can ask for the set of solutions over \mathbb{C} , over \mathbb{R} , over more exotic fields like the p -adics, or even over the integers.

In p -adic AdS/CFT, the complex field is replaced by the field of p -adic numbers. The p -adics are metrically complete, but have a totally disconnected topology and there is a sense in which they are a discrete space. This has a dramatic effect on the boundary geometry, which loses the smooth structure which seems essential for two-dimensional conformal field theory. Despite this, essential and basic features of AdS/CFT, such as bulk isometries and boundary conformal symmetry (which are destroyed by a naive discretization), have analogs and can be fully understood in this p -adic setting. This is in contrast to other discrete models of holography, including most tensor network models.

The aforementioned holographic formula—and the whole geometric setting of the correspondence, consisting of the Euclidean hyperbolic space AdS_3 , its conformal boundary $\mathbb{P}^1(\mathbb{C})$, and quotients by actions of Schottky groups $\Gamma \subset \text{PSL}(2, \mathbb{C})$ —has a natural analog in which the field is the p -adic numbers \mathbb{Q}_p . The bulk space becomes the Bruhat–Tits tree of \mathbb{Q}_p , which is a manifestly discrete infinite graph of uniform valence. Its conformal boundary at infinity is $\mathbb{P}^1(\mathbb{Q}_p)$, which can be thought of as the spacetime for an unusual class of CFTs. Black hole solutions are understood to be quotients of this geometry by p -adic Schottky groups $\Gamma \subset \text{PGL}(2, \mathbb{Q}_p)$; these are known as *Mumford curves* in the mathematics literature. We will give what we hope are intuitive introductions to these possibly unfamiliar concepts in the bulk of the chapter, with additional important ideas in Chapter 6.

Conformal field theory on p -adic spacetime has previously been developed, for the most part, in the context of the p -adic string theory (see the discussion in Sec. 1.2, and also for instance, [83] and references therein), but has also been considered abstractly [192]. However, our perspective on the subject will be somewhat different: rather than using the p -adics as a worldsheet to construct real-space string amplitudes, our goal in this chapter is to further develop the original holographic correspondence of [190] for the higher-genus black holes, informed by recent developments in the understanding of the AdS/CFT correspondence. We will emphasize the large extent to which algebraic structure allows familiar ideas, concepts, and arguments from ordinary $\text{AdS}_3/\text{CFT}_2$ can be carried over—in many cases line by line—to the p -adic setting. In addition to the holographic formulas of Manin and Marcolli, the standard semiclassical holographic analysis of scalar fields propagating without backreaction in anti-de Sitter space applies almost without alteration to the Bruhat–Tits tree. We

discuss this in detail in Sec. 5.3.

In some cases, intuitions about how holography works in the Archimedean case are supported even more sharply over the p -adics. For example, one normally thinks of the holographic direction as corresponding to a renormalization-group scale. Over the p -adics, as shown in Sec. 5.3, boundary modes contribute to the reconstruction of bulk functions only up to a height determined by their wavelength, and reconstruct precisely to zero above this height in the tree.

Finally, on an even more speculative note, it is natural to wonder if the study of p -adic models of holography can be used to learn about the real case. So-called “adelic formulas” relate quantities defined over the various places (finite and infinite) of \mathbb{Q} ; it was suggested in [193] that fundamental physics should be adelic in nature, with product formulas that relate the Archimedean side of physics to a product of the contributions of all the p -adic counterparts. This program is still incomplete in p -adic AdS/CFT, but it provides a physical and mathematical reason to study these systems.

5.2 Review of Necessary Ideas

Basics of p -adic numbers

We begin with a lightning review of elementary properties of the p -adic fields. Our treatment here is far from complete; for a more comprehensive exposition, the reader is referred to [194], or to another of the many books that treat p -adic techniques.

When one constructs the continuum of the real numbers from the rationals, one completes with respect to a metric: the distance between two points $x, y \in \mathbb{Q}$ is

$$d(x, y) = |x - y|_\infty, \quad (5.1)$$

where $|\cdot|_\infty$ is the usual absolute value. There are Cauchy sequences of rational numbers for which successive terms become arbitrarily close together, but the sequence does not approach any limiting rational number. The real numbers “fill in the gaps,” such that every Cauchy sequence of rational numbers converges to a real limit by construction. That property is known as metric completeness.

The p -adic fields \mathbb{Q}_p are completions of \mathbb{Q} with respect to its other norms;

these are defined by

$$\text{ord}_p(x) = n \text{ when } x = p^n(a/b) \text{ with } a, b \perp p; \quad (5.2)$$

$$|x|_p = p^{-\text{ord}_p(x)}. \quad (5.3)$$

By a theorem of Ostrowski, every norm on \mathbb{Q} is equivalent to one of the p -adic norms or the usual (∞ -adic) norm. It is common to refer to the different possible completions as the different “places” of \mathbb{Q} .

A number is p -adically small when it is divisible by a large power of p ; one can think of the elements of \mathbb{Q}_p as consisting of decimal numbers written in base p , which can extend infinitely far *left* (just as real numbers can be thought of as ordinary decimals extending infinitely far *right*). \mathbb{Q}_p is uncountable and locally compact with respect to the topology defined by its metric; as usual, a basis for this topology is the set of open balls,

$$B_\epsilon(x) = \{y \in \mathbb{Q}_p : |x - y|_p < \epsilon\}. \quad (5.4)$$

The ring of integers \mathbb{Z}_p of \mathbb{Q}_p is also the unit ball about the origin:

$$\mathbb{Z}_p = \{x \in \mathbb{Q}_p : |x|_p \leq 1\}. \quad (5.5)$$

It can be described as the inverse limit of the system of base- p decimals with no fractional part and finite (but increasingly many) digits:

$$\mathbb{Z}_p = \varprojlim (\cdots \rightarrow \mathbb{Z}/p^{n+1}\mathbb{Z} \rightarrow \mathbb{Z}/p^n\mathbb{Z} \rightarrow \mathbb{Z}/p^{n-1}\mathbb{Z} \rightarrow \cdots). \quad (5.6)$$

\mathbb{Z}_p is a discrete valuation ring; its unique maximal ideal is $\mathfrak{m} = p\mathbb{Z}_p$, and the quotient of \mathbb{Z}_p by \mathfrak{m} is the finite field \mathbb{F}_p . In general, for any finite extension of \mathbb{Q}_p , the quotient of its ring of integers by its maximal ideal is a finite field \mathbb{F}_{p^n} ; we give more detail about this case in Sec. 5.5.

The Bruhat–Tits tree and its symmetries

In this section, we will describe the Bruhat–Tits Tree T_p and its symmetries. It should be thought of as a hyperbolic (though discrete) bulk space with conformal boundary $\mathbb{P}^1(\mathbb{Q}_p)$. Since these trees are a crucial part of this chapter and may be unfamiliar to the reader, our treatment is informal, and aims to build intuition. Out of necessity, our discussion is also brief; for a more complete treatment, the reader may consult notes by Casselman [195] for constructions and properties related to the tree, or [82] for analysis on the tree and connections to the p -adic string.

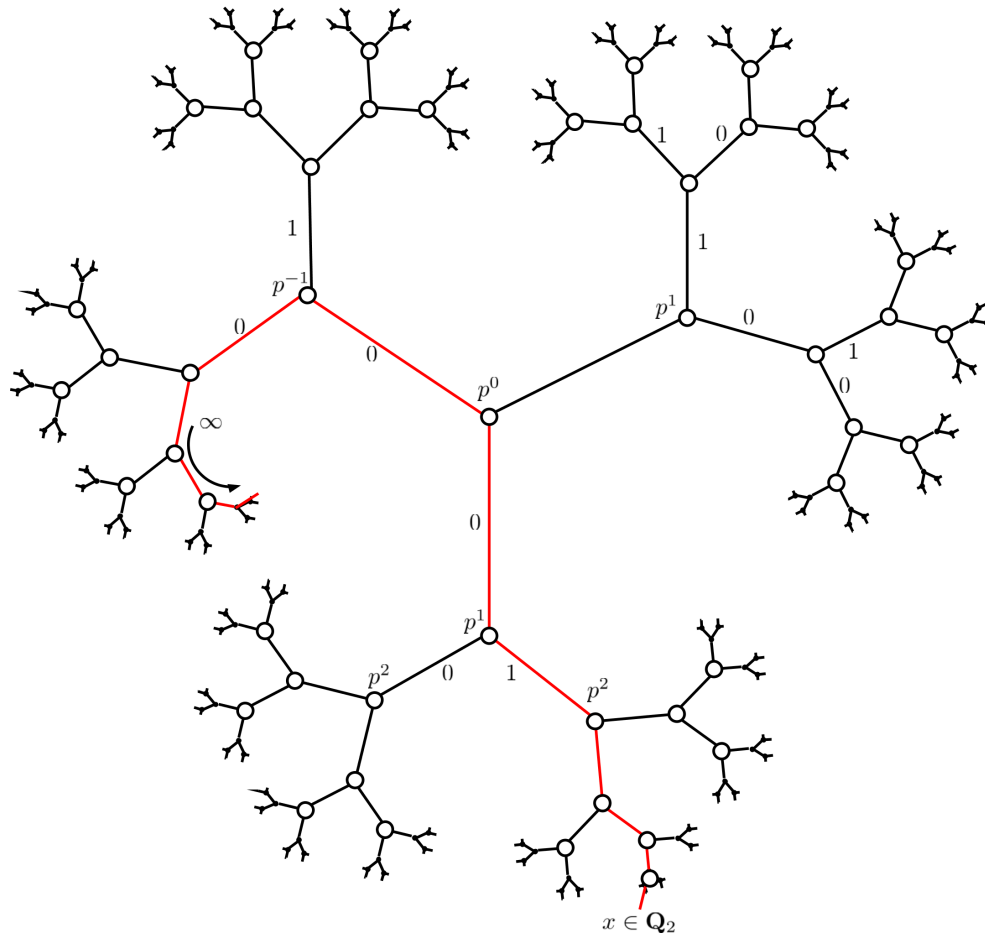


Figure 5.1: The standard representation of the Bruhat–Tits tree. The point at infinity and the center are arbitrary as the tree is homogeneous. Geodesics such as the highlighted one are infinite paths through the tree from ∞ to the boundary which uniquely specify elements of \mathbb{Q}_p . This path as a series specifies the digits of the decimal expansion of $x \in \mathbb{Q}_2$ in this example. At the n th vertex, we choose either 0 or 1 corresponding to the value of x_n in the p^n th term of x . Negative powers of p correspond to larger p -adic norms as we move towards the point ∞ .

We begin with a description of the boundary and its symmetries, which are completely analogous to the global conformal transformations of $\mathbb{P}^1(\mathbb{C})$. We then turn our attention to the bulk space T_p , focusing on its construction as a coset space and the action of $\text{PGL}(2, \mathbb{Q}_p)$ on the vertices. Despite the fractal topology of the p -adic numbers, we will find (perhaps surprisingly) that many formulas from the real or complex cases are related to their p -adic counterparts by the rule $|\cdot|_\infty \rightarrow |\cdot|_p$.

Conformal group of $\mathbb{P}^1(\mathbb{Q}_p)$

The global conformal group on the boundary is $\mathrm{SL}(2, \mathbb{Q}_p)$, which consists of matrices of the form

$$A = \begin{pmatrix} a & b \\ c & d \end{pmatrix}, \text{ with } a, b, c, d \in \mathbb{Q}_p, \quad ad - bc = 1. \quad (5.7)$$

This acts on points $x \in \mathbb{P}^1(\mathbb{Q}_p)$ by fractional linear transformations,

$$x \rightarrow \frac{ax + b}{cx + d}. \quad (5.8)$$

It can be checked that matrix multiplication corresponds to composition of such maps, so that the group action is well-defined. This is analogous to the $\mathrm{SL}(2, \mathbb{C})$ action on the Riemann sphere $\mathbb{P}^1(\mathbb{C})$. (We will sometimes also refer to $\mathrm{PGL}(2, \mathbb{Q}_p)$; the two differ only in minor details.)

The existence of a local conformal algebra for \mathbb{Q}_p , in analogy with the Virasoro symmetry in two-dimensional conformal field theory or general holomorphic mappings of $\mathbb{P}^1(\mathbb{C})$, is a subtle question. It is difficult to find definitions of a p -adic derivative or an infinitesimal transformation that are satisfactory for this purpose. In particular, since the “well-behaved” complex-valued functions on \mathbb{Q}_p are in some sense locally constant, there are no interesting derivations that act on the space of fields [192]. In this chapter, we will concern ourselves only with global symmetries, which can still be used to constrain the properties of p -adic conformal field theories. We speculate about the possibility of enhanced conformal symmetry in Sec. 5.5.

The determinant condition implies that there are three free p -adic numbers which specify an element of $\mathrm{SL}(2, \mathbb{Q}_p)$. A convenient way to decompose a general $\mathrm{SL}(2, \mathbb{Q}_p)$ transformation is to view it as the product of a special conformal transformation, a rotation, a dilatation, and a translation:

$$\begin{pmatrix} p^m a & b \\ c & p^{-m} a^{-1} (1 + bc) \end{pmatrix} = \begin{pmatrix} 1 & 0 \\ cp^{-m} a^{-1} & 1 \end{pmatrix} \begin{pmatrix} a & 0 \\ 0 & a^{-1} \end{pmatrix} \begin{pmatrix} p^m & 0 \\ 0 & p^{-m} \end{pmatrix} \begin{pmatrix} 1 & bp^{-m} a^{-1} \\ 0 & 1 \end{pmatrix}, \quad (5.9)$$

where $a, b, c \in \mathbb{Q}_p$ and $|a|_p = 1$. One can verify that the product is an arbitrary element of $\mathrm{SL}(2, \mathbb{Q}_p)$, where the determinant condition has been used to eliminate the d parameter. This represents a translation by $bp^{-m} a^{-1}$, a dilatation by p^{2m} , a rotation by a^2 , and a special conformal translation by $cp^{-m} a^{-1}$. We

have separated the diagonal subgroup into multiplication by elements of the unit circle, $a \in \mathbb{U}_p \subset \mathbb{Z}_p$, which do not change the p -adic norm (and thus are “rotations” in a p -adic sense), and multiplication by powers of p which scale the p -adic norm (and so correspond to dilatations). Representations of the multiplicative group of unit p -adics provide an analog of the spin quantum number; we discuss this further in Sec. 5.3. It is worth stressing that these transformations are finite, and so we are characterizing the symmetry group rather than the algebra.

As is often the case in real conformal field theories, we can focus on the dilation subgroup. A diagonal matrix in $\text{SL}(2, \mathbb{Q}_p)$ and its action on the coordinate is

$$\begin{pmatrix} \alpha & 0 \\ 0 & \alpha^{-1} \end{pmatrix}, \quad x \rightarrow x' = \alpha^2 x. \quad (5.10)$$

This has the effect of changing the p -adic norm by

$$|x'|_p = |\alpha|_p^2 |x|_p. \quad (5.11)$$

So if $|\alpha|_p \neq 1$, this will scale the size of coordinate. This parallels the complex case in which a dilatation changes the complex norm by $|z'| = |\alpha|^2 |z|$. It will turn out to be the case that 2-point functions of spinless operators in p -adic conformal field theory will depend only on the p -adic norm of their separation. Schematically,

$$\langle \phi(x)\phi(y) \rangle \approx \frac{1}{|x-y|_p^{2\Delta}}. \quad (5.12)$$

Dilations will thus affect correlation functions of the p -adic conformal field theory exactly as in the complex case.

$\text{PGL}(2, \mathbb{Q}_p)$ action on the tree T_p

We have seen that fractional linear transformations of the boundary coordinate work as in the real case. The action of the symmetry on the bulk space T_p is slightly more complicated to describe. Were we working in the Archimedean theory, we would identify $\text{PSL}(2, \mathbb{R})$ as the isometry group of the hyperbolic upper half space $\mathbb{H} = \text{SL}(2, \mathbb{R})/\text{SO}(2)$. Here $\text{SO}(2)$ is a maximal compact subgroup. Similarly, in the context of $\text{AdS}_{2+1}/\text{CFT}_2$, we can think of the hyperbolic upper-half 3-space as a quotient space of the isometry group by its maximal compact subgroup: $\mathbf{H}^3 = \text{SL}(2, \mathbb{C})/\text{SU}(2)$.

Following this intuition, we define the *Bruhat–Tits tree* to be the quotient of the p -adic conformal group by its maximal compact subgroup:

$$T_p = \mathrm{PGL}(2, \mathbb{Q}_p) / \mathrm{PGL}(2, \mathbb{Z}_p). \quad (5.13)$$

In contrast with the Archimedean examples, T_p is a discrete space: it is a homogeneous infinite tree, with vertices of valence $p+1$, whose boundary can be identified with the p -adic projective line. We expect isometries to correspond to rigid transformations of the vertices. Formally, the tree represents the incidence relations of equivalence classes of lattices in $\mathbb{Q}_p \times \mathbb{Q}_p$. As outlined in the appendix of [83], the group $\mathrm{PGL}(2, \mathbb{Q}_p)$ acts by matrix multiplication on the lattice basis vectors and takes one between equivalence classes. These transformations are translations and rotations of the points in the tree; they preserve distances, which are measured in the tree by just counting the number of edges along a given path. Since any two vertices in a connected tree are joined by exactly one path, this is well-defined; all paths are geodesics.

A standard way of representing T_p is depicted in Fig. 5.1 for the case $p = 2$. This is a regular tree with $p + 1$ legs at each vertex; the exponential growth in the number of vertices with distance from a base point reflects the “hyperbolic” nature of distance in the tree. Since paths are unique, there is a one-to-one correspondence between infinite paths in the tree starting at ∞ and elements of \mathbb{Q}_p . (This can be viewed like a p -adic version of stereographic projection.)

The choice of the apparent center and geodesic corresponding to infinity are arbitrary. Just as in the Archimedean case, we must fix three boundary points to identify a p -adic coordinate on the projective line, corresponding to 0, 1, and ∞ . Once these arbitrary choices are made, the geodesics joining them form a Y in the bulk, whose center is taken to be the centerpoint of the tree. We can then understand the geodesic connecting ∞ to x as labeling the unique p -adic decimal expansion for $x = p^\gamma(x_0 + x_1p + x_2p^2 + \dots)$, where each of the x_n take values in $0, 1, \dots, p - 1$ corresponding to the p possible choices to make at each vertex. Each vertex of the tree is naturally marked with a copy of the finite field \mathbb{F}_p , identified with one “digit” of a p -adic number.

Viewing the tree as the space of p -adic decimal expansions may in some ways be more useful than the definition in terms of equivalence classes of lattices. Geometrically moving closer or further from the boundary corresponds to higher or lower precision of p -adic decimal expansions. Even with no reference to

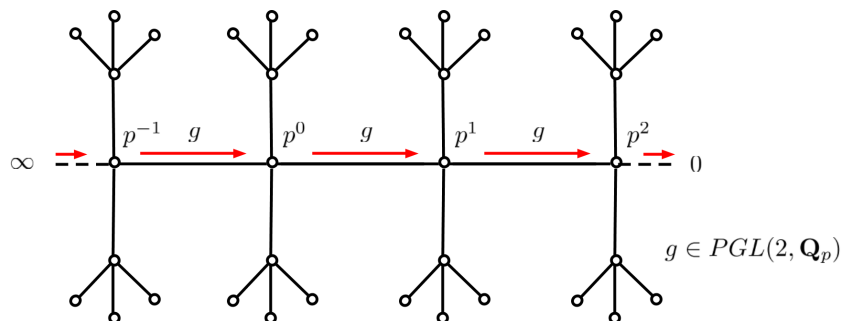


Figure 5.2: An alternative representation of the Bruhat–Tits Tree (for $p = 3$) in which we have unfolded the tree along the 0 geodesic. The action of elements of $\mathrm{PGL}(2, \mathbb{Q}_p)$ acts by translating the entire tree along different possible geodesics. In this example we translate along the 0 geodesic, which can be thought of as multiplication of each term in a p -adic decimal expansion by p . This map has two fixed points at 0 and ∞ . In this “unfolded” form, a point in $\mathbb{P}^1(\mathbb{Q}_p)$ is specified by a geodesic that runs from ∞ and follows the 0 geodesic until some level in the tree where it leaves the 0 geodesic towards the boundary. The p -adic norm is simply p to the inverse power of the point where it leaves the 0 geodesic (so leaving “sooner” leads to a larger norm, and later to a smaller norm).

quantum mechanics or gravity, we see some hint of holography and renormalization in the tree— a spatial direction in the bulk parameterizes a scale or precision of boundary quantities. This is explored more fully in Sec. 5.3.

We now illustrate some examples of $\mathrm{PGL}(2, \mathbb{Q}_p)$ transformations on the tree. First note that the choice of the center node is arbitrary. We can take this point to be the equivalence class of unit lattices modulo scalar multiplication. One can show that this equivalence class (or the node it corresponds to) is invariant under the $\mathrm{PGL}(2, \mathbb{Z}_p)$ subgroup, so these transformations leave the center fixed and rotate the branches of the tree about this point.

More interesting is a generator such as

$$g = \begin{pmatrix} p & 0 \\ 0 & 1 \end{pmatrix} \in \mathrm{PGL}(2, \mathbb{Q}_p). \quad (5.14)$$

This transformation (and others in $\mathrm{PGL}(2, \mathbb{Q}_p)$) act by translating the entire tree along a given geodesic (one can see this either from the lattice incidence relations, or from translating or shifting the p -adic decimal series expansion). This is illustrated in Fig. 5.2. We can think of these transformations as the lattice analogs of translations and dilatations of the real hyperbolic plane.

Integration measures on p -adic spaces

Just as is the case for \mathbb{C} , there are two natural measures on \mathbb{Q}_p (or more properly, on the projective line over \mathbb{Q}_p); they can be understood intuitively by thinking of \mathbb{Q}_p as the boundary of T_p . The first is the Haar measure $d\mu$, which exists for all locally compact topological groups. With respect to either measure, the size of the set of p -adic integers is taken to be 1:

$$\mu(\mathbb{Z}_p) = 1. \quad (5.15)$$

The Haar measure is then fixed by multiplicativity and translation invariance; any open ball has measure equal to the p -adic norm of its radius. It is helpful to think of \mathbb{Q}_p as being “flat” when considered with this measure.

The other measure, the Patterson-Sullivan measure, is the p -adic analog of the Fubini-Study metric on $\mathbb{P}^1(\mathbb{C})$. It is most easily defined with reference to the tree, in which we fix a basepoint C (to be thought of as the unique meeting point of the geodesics joining 0, 1, and ∞ when a coordinate is chosen on the boundary). Recall that the open balls in \mathbb{Q}_p correspond to the endpoints of branches of the tree below a vertex v . In the Patterson-Sullivan measure,

$$d\mu_0(B_v) = p^{-d(C,v)}. \quad (5.16)$$

The two measures are related by

$$\begin{aligned} d\mu_0(x) &= d\mu(x), & |x|_p &\leq 1; \\ d\mu_0(x) &= \frac{d\mu(x)}{|x|_p^2}, & |x|_p &> 1. \end{aligned} \quad (5.17)$$

(Later on, we will at times use the familiar notation dx to refer to the Haar measure.) The most intuitive way to picture the Patterson-Sullivan measure is to imagine the tree pointing “radially outward” from its centerpoint. It is then easy to understand the transformation rule (5.17); it says that when all geodesics point downward from infinity and the boundary is “flat” at the lower end of the picture, points far from zero (outside \mathbb{Z}_p) can only be reached by geodesics that travel upward from C before turning back down towards the boundary.

Schottky uniformization of Riemann surfaces

In this section, we review Schottky uniformization, which allows one to think of a higher-genus Riemann surface as a quotient of the projective line by a particular discrete subgroup of its Möbius transformations.

A Schottky group of rank $g \geq 1$ is a discrete subgroup of $\mathrm{PSL}(2, \mathbb{C})$ which is purely loxodromic and isomorphic to a free group on g generators. The group $\mathrm{PSL}(2, \mathbb{C})$ acts on $\mathbb{P}^1(\mathbb{C})$ by fractional linear transformations,

$$\gamma = \begin{pmatrix} a & b \\ c & d \end{pmatrix} : z \mapsto \frac{az + b}{cz + d}.$$

The loxodromic condition means that each nontrivial element $\gamma \in \Gamma \setminus \{1\}$ has two distinct fixed points z_γ^\pm (one attractive and one repelling) in $\mathbb{P}^1(\mathbb{C})$. The closure in $\mathbb{P}^1(\mathbb{C})$ of the set of all fixed points of elements in Γ is the limit set Λ_Γ of Γ , the set of all limit points of the action of Γ on $\mathbb{P}^1(\mathbb{C})$. In the case $g = 1$ the limit set consists of two points, which we can choose to identify with $\{0, \infty\}$, while for $g > 1$ the set Λ_Γ is a Cantor set of Hausdorff dimension $0 \leq \dim_H(\Lambda_\Gamma) < 2$. The Hausdorff dimension is also the exponent of convergence of the Poincaré series of the Schottky group: $\sum_{\gamma \in \Gamma} |\gamma'|^s$ converges for $s > \dim_H(\Lambda_\Gamma)$, [196].

It is well known that any compact smooth Riemann surface X admits a Schottky uniformization, namely $X = \Omega_\Gamma/\Gamma$, where $\Gamma \subset \mathrm{PSL}(2, \mathbb{C})$ is a Schottky group of rank equal to the genus $g = g(X)$ of the Riemann surface, and $\Omega_\Gamma = \mathbb{P}^1(\mathbb{C}) \setminus \Lambda_\Gamma$ is the *domain of discontinuity* of the action of Γ on $\mathbb{P}^1(\mathbb{C})$. There is a well known relation between Schottky and Fuchsian uniformizations of compact Riemann surfaces of genus $g \geq 2$, see [197].

A *marking* of a rank g Schottky group $\Gamma \subset \mathrm{PSL}(2, \mathbb{C})$ is a choice of a set of generators $\{\gamma_1, \dots, \gamma_g\}$ of Γ and a set of $2g$ open connected regions D_i in $\mathbb{P}^1(\mathbb{C})$, with $C_i = \partial D_i$ the boundary Jordan curves homeomorphic to S^1 , with the following properties:

1. the closures of the D_i are pairwise disjoint
2. $\gamma_i(C_i) \subset C_{g+i}$
3. $\gamma_i(D_i) \subset \mathbb{P}^1(\mathbb{C}) \setminus D_{g+i}$.

The marking is *classical* if all the C_i are circles. (All Schottky groups admit a marking, but not all admit a classical marking.) A fundamental domain F_Γ for the action of the Schottky group Γ on the domain of discontinuity $\Omega_\Gamma \subset \mathbb{P}^1(\mathbb{C})$ can be constructed by taking

$$F_\Gamma = \mathbb{P}^1(\mathbb{C}) \setminus \cup_{i=1}^g (D_i \cup \bar{D}_{g+i}).$$

This satisfies $\cup_{\gamma \in \Gamma} \gamma(F_\Gamma) = \Omega_\Gamma$. In the case of genus $g = 1$, with $\Gamma = q^{\mathbb{Z}}$, for some $q \in \mathbb{C}$ with $|q| > 1$, the region F_Γ constructed in this way is an annulus A_q , with D_1 the unit disk in \mathbb{C} and D_2 the disk around ∞ given by complement in $\mathbb{P}^1(\mathbb{C})$ of the disk centered at zero of radius $|q|$, so that $q^{\mathbb{Z}}A_q = \mathbb{C}^* = \mathbb{P}^1(\mathbb{C}) \setminus \{0, \infty\} = \Omega_{q^{\mathbb{Z}}}$. The resulting quotient $E_q = \mathbb{C}^*/q^{\mathbb{Z}}$ is the Tate uniformization of elliptic curves.

Hyperbolic handlebodies and higher genus black holes

The action of $\mathrm{PSL}(2, \mathbb{C})$ by fractional linear transformations on $\mathbb{P}^1(\mathbb{C})$ extends to an action by isometries on the real 3-dimensional hyperbolic space \mathbf{H}^3 , with $\mathbb{P}^1(\mathbb{C})$ its conformal boundary at infinity. In coordinates $(z, y) \in \mathbb{C} \times \mathbb{R}_+^*$ in \mathbf{H}^3 , the action of $\mathrm{PSL}(2, \mathbb{C})$ by isometries of the hyperbolic metric is given by

$$\gamma = \begin{pmatrix} a & b \\ c & d \end{pmatrix} : (z, y) \mapsto \left(\frac{(az + b)\overline{(cz + d)} + a\bar{c}y^2}{|cz + d|^2 + |c|^2y^2}, \frac{y}{|cz + d|^2 + |c|^2y^2} \right).$$

Given a rank g Schottky group $\Gamma \subset \mathrm{PSL}(2, \mathbb{C})$, we can consider its action on the conformally compactified hyperbolic 3-space $\overline{\mathbf{H}^3} = \mathbf{H}^3 \cup \mathbb{P}^1(\mathbb{C})$. The only limit points of the action are on the limit set Λ_Γ that is contained in the conformal boundary $\mathbb{P}^1(\mathbb{C})$, hence a domain of discontinuity for this action is given by

$$\mathbf{H}^3 \cup \Omega_\Gamma \subset \overline{\mathbf{H}^3} = \mathbf{H}^3 \cup \mathbb{P}^1(\mathbb{C}).$$

The quotient of \mathbf{H}^3 by this action is a 3-dimensional hyperbolic handlebody of genus g

$$\mathcal{H}_\Gamma = \mathbf{H}^3/\Gamma,$$

with conformal boundary at infinity given by the Riemann surface $X_\Gamma = \Omega_\Gamma/\Gamma$,

$$\overline{\mathcal{H}_\Gamma} = \mathcal{H}_\Gamma \cup X_\Gamma = (\mathbf{H}^3 \cup \Omega_\Gamma)/\Gamma.$$

Given a marking of a rank g Schottky group Γ (for simplicity we will assume the marking is classical), let D_i be the discs in $\mathbb{P}^1(\mathbb{C})$ of the marking, and let \mathcal{D}_i denote the geodesic domes in \mathbf{H}^3 with boundary $C_i = \partial D_i$, namely the \mathcal{D}_i are the open regions of $\overline{\mathbf{H}^3}$ with boundary $S_i \cup D_i$, where the S_i are totally geodesic surfaces in \mathbf{H}^3 with boundary C_i that project to D_i on the conformal boundary. Then a fundamental domain for the action of Γ on $\mathbf{H}^3 \cup \Omega_\Gamma$ is given by

$$\mathcal{F}_\Gamma = F_\Gamma \cup (\mathbf{H}^3 \setminus \cup_{i=1}^g (\mathcal{D}_i \cup \bar{\mathcal{D}}_{g+i})).$$

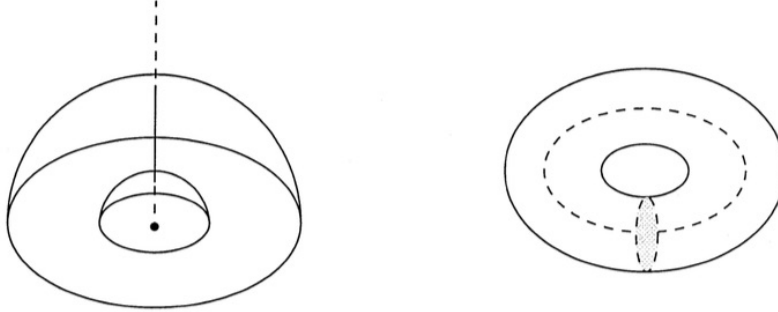


Figure 5.3: A helpful figure reproduced from 1.4. The Fundamental domain and quotient for the Euclidean BTZ black hole. Compare with the p -adic BTZ geometry, shown in Figure 5.7.

The boundary curves C_i for $i = 1, \dots, g$ provide a collection of A -cycles, that give half of the generators of the homology of the Riemann surface X_Γ : the generators that become trivial in the homology of the handlebody $\bar{\mathcal{H}}_\Gamma$. The union of fundamental domains $\gamma(\mathcal{F}_\Gamma)$ for $\gamma \in \Gamma$ can be visualized as in Fig. 5.4.

In the case of genus $g = 1$ with $\Gamma = q^{\mathbb{Z}}$, acting on \mathbf{H}^3 by

$$\begin{pmatrix} q^{1/2} & 0 \\ 0 & q^{-1/2} \end{pmatrix} (z, y) = (qz, |q|y),$$

with limit set $\{0, \infty\}$ the fundamental domain \mathcal{F}_Γ consists of the space in the upper half space \mathbf{H}^3 contained in between the two spherical domes of radius 1 and $|q| > 1$. The generator q of the group acts on the geodesic with endpoints 0 and ∞ as a translation by $\log |q|$. The quotient $\mathbf{H}^3/q^{\mathbb{Z}}$ is a hyperbolic solid torus, with the Tate uniformized elliptic curve $E_q = \mathbb{C}^*/q^{\mathbb{Z}}$ as its conformal boundary at infinity, and with a unique closed geodesic of length $\log q$. It is well known (see [198, 199, 190]) that the genus one handlebodies $\mathcal{H}_{q^{\mathbb{Z}}}$ are the Euclidean BTZ black holes [73], where the cases with $q \in \mathbb{C} \setminus \mathbb{R}$ correspond to spinning black holes. The geodesic length $\log |q|$ is the area of the event horizon, hence proportional to the black hole entropy.

The case of higher genus hyperbolic handlebodies correspond to generalizations of the BTZ black hole to the higher genus asymptotically AdS_3 black holes considered in [72] and [190].

In these more general higher genus black holes, because of the very different nature of the limit set (a fractal Cantor set instead of two points) the structure of the black hole event horizon is significantly more complicated. In the Eu-

clidean BTZ black hole, the only infinite geodesic that remains confined into a compact region inside the hyperbolic solid torus \mathcal{H}_{qz} for both $t \rightarrow \pm\infty$ is the unique closed geodesic (the image in the quotient of the geodesic in \mathbf{H}^3 given by the vertical line with endpoints 0 and ∞). On the other hand, in the higher genus cases, the geodesics in the hyperbolic handlebody $\mathcal{H}_\Gamma = \mathbf{H}^3/\Gamma$ can be classified as:

1. *Closed geodesics*: these are the images in the quotient \mathcal{H}_Γ of geodesics in \mathbf{H}^3 with endpoints $\{z_\gamma^+, z_\gamma^-\}$, the attractive and repelling fixed points of some element $\gamma \in \Gamma$.
2. *Bounded geodesics*: these images in the quotient \mathcal{H}_Γ of geodesics in \mathbf{H}^3 with endpoints on Λ_Γ . If the endpoints are not a pair of fixed points of the same element of Γ the geodesic in the quotient is not closed, but it remains forever confined within a compact region inside \mathcal{H}_Γ , the *convex core* \mathcal{C}_Γ .
3. *Unbounded geodesics*: these are images in the quotient \mathcal{H}_Γ of geodesics in \mathbf{H}^3 with at least one of the two endpoints in Ω_Γ . These are geodesics in \mathcal{H}_Γ that wander off (in at least one time direction $t \rightarrow \infty$ or $t \rightarrow -\infty$) towards the conformal boundary X_Γ at infinity and eventually leave every compact region in \mathcal{H}_Γ .

The convex core $\mathcal{C}_\Gamma \subset \mathcal{H}_\Gamma$ is the quotient by Γ of the geodesic hull in \mathbf{H}^3 of the limit set Λ_Γ . It is a compact region of finite hyperbolic volume in \mathcal{H}_Γ , and it is a deformation retract of \mathcal{H}_Γ . A natural replacement for the event horizon of the BTZ black hole in these higher genus cases can be identified in terms of the convex core \mathcal{C}_Γ , where we think of \mathcal{C}_Γ as the region from which geodesic trajectories cannot escape and must remain forever confined. The complement $\mathcal{H}_\Gamma \setminus \mathcal{C}_\Gamma$ is homeomorphic to $\partial\mathcal{C}_\Gamma \times \mathbb{R}_+$. The boundary $\partial\mathcal{C}_\Gamma$ is the event horizon of the higher genus black hole, with the black hole entropy proportional to the area of $\partial\mathcal{C}_\Gamma$.

In [200] and [191], Manin proposed to interpret the tangle of bounded geodesics inside the hyperbolic handlebody \mathcal{H}_Γ as a model for the missing “closed fiber at infinity” in Arakelov geometry. This interpretation was based on the calculation of the Arakelov Green function [191], and the analogy with the theory of Mumford curves [75] and the computations of [201] for p -adic Schottky

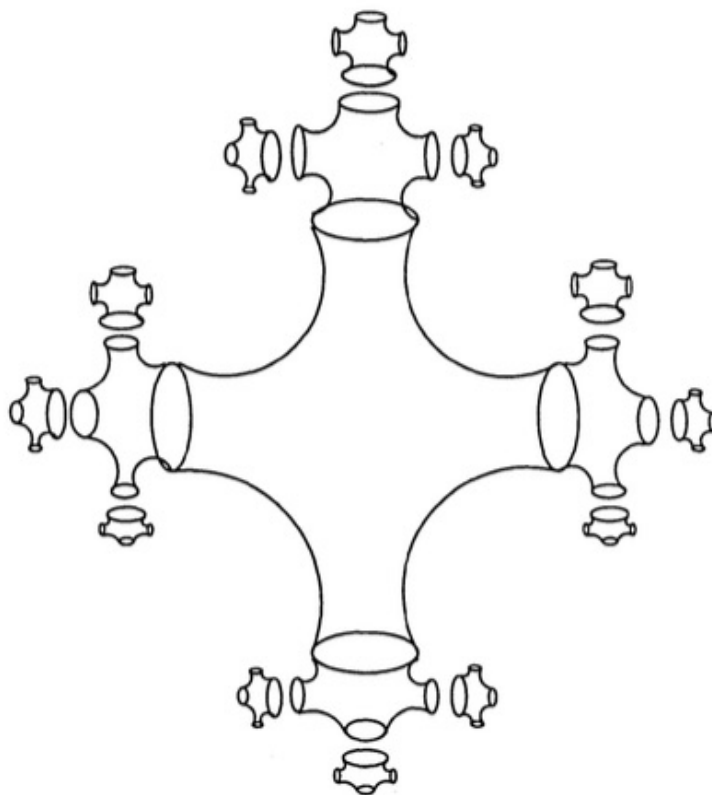


Figure 5.4: Fundamental domains for the action of Γ on \mathbf{H}^3 .

groups. The results of [191] and their holographic interpretation in [190], as well as the parallel theory of Mumford curves and periods of p -adic Schottky groups, will form the basis for our development of a p -adic and adelic form of the $\text{AdS}_{+1}/\text{CFT}$ correspondence. The interpretation of the tangle of bounded geodesics in \mathcal{H}_Γ as “closed fiber at infinity” of Arakelov geometry was further enriched with a cohomological interpretation in [202] (see also [203], [204] for the p -adic counterpart).

Bruhat–Tits trees, p -adic Schottky groups, and Mumford curves

The theory of Schottky uniformization of Riemann surfaces as conformal boundaries of hyperbolic handlebodies has a non-Archimedean parallel in the theory of Mumford curves, uniformized by p -adic Schottky groups, seen as the boundary at infinity of a quotient of a Bruhat–Tits tree.

Some basic facts regarding the geometry of the Bruhat–Tits tree T_p of \mathbb{Q}_p have been recalled in Sec. 5.2. More generally, the geometry we consider

here applies to any finite extension \mathbf{k} of the p -adic field \mathbb{Q}_p . By identifying $(\mathcal{O}_{\mathbb{Q}_p}/\mathfrak{m}^r) \otimes \mathcal{O}_{\mathbf{k}} = \mathcal{O}_{\mathbf{k}}/\mathfrak{m}^{re_{\mathbf{k}}}$, where $e_{\mathbf{k}}$ is the ramification index of \mathbf{k} over \mathbb{Q}_p , we see that the Bruhat–Tits tree $T_{\mathbf{k}}$ for a finite extension \mathbf{k} of \mathbb{Q}_p is obtained from the Bruhat–Tits tree of \mathbb{Q}_p by adding $e_{\mathbf{k}} - 1$ new vertices in each edge of $T_{\mathbb{Q}_p}$ and increasing the valence of all vertices to $p^f + 1$, where $f = [\mathbf{k} : \mathbb{Q}_p]/e_{\mathbf{k}}$, the degree of the extension normalized by the ramification index.

Let $\mathcal{O}_{\mathbf{k}}$ denote the ring of integers of \mathbf{k} and $\mathfrak{m} \subset \mathcal{O}_{\mathbf{k}}$ the maximal ideal, so that the residue field $\mathcal{O}_{\mathbf{k}}/\mathfrak{m} = \mathbb{F}_q$ is a finite field with $q = p^r$ for some $r \in \mathbb{N}$. The set of vertices $V(T_{\mathbf{k}})$ of the Bruhat–Tits tree $T_{\mathbf{k}}$ of \mathbf{k} is the set of equivalence classes of free rank two $\mathcal{O}_{\mathbf{k}}$ -modules, under the equivalence $M_1 \sim M_2$ if $M_1 = \lambda M_2$, for some $\lambda \in \mathbf{k}^*$. For a pair of such modules with $M_2 \subset M_1$, one can define a distance function $d(M_1, M_2) = |l - k|$, where $M_1/M_2 = \mathcal{O}_{\mathbf{k}}/\mathfrak{m}^l \oplus \mathcal{O}_{\mathbf{k}}/\mathfrak{m}^k$. This distance is independent of representatives in the equivalence relation. There is an edge in $E(T_{\mathbf{k}})$ connecting two vertices in $V(T_{\mathbf{k}})$ whenever the corresponding classes of modules have distance one. The resulting tree $T_{\mathbf{k}}$ is an infinite homogeneous tree with vertices of valence $q + 1$, where $q = \#\mathcal{O}_{\mathbf{k}}/\mathfrak{m}$ is the cardinality of the residue field. The boundary at infinity of the Bruhat–Tits tree is identified with $\mathbb{P}^1(\mathbf{k})$. One can think of the Bruhat–Tits tree as a network, with a copy of the finite field \mathbb{F}_q (or better of the projective line $\mathbb{P}^1(\mathbb{F}_q)$) associated to each vertex.

The reader should beware that there is an unavoidable clash of notation: q is the standard notation for the modular parameter of an elliptic curve, but is also used to denote a prime power $q = p^r$ in the context of finite fields or extensions of the p -adics. While both uses will be made in this chapter, particularly in this section and in Sec. 5.5, we prefer not to deviate from standard usage; it should be apparent from context which is intended, and hopefully no confusion should arise.

There is an action of $\mathrm{PGL}(2, \mathbf{k})$ on the set of vertices $V(T_{\mathbf{k}})$ that preserves the distance, hence it acts as isometries of the tree $T_{\mathbf{k}}$. A p -adic Schottky group is a purely loxodromic finitely generated torsion free subgroup of $\mathrm{PGL}(2, \mathbf{k})$. The Schottky group Γ is isomorphic to a free group on g -generators, with g the rank of Γ .

In this p -adic setting the loxodromic condition means that every nontrivial element γ in Γ has two fixed points z_{γ}^{\pm} on the boundary $\mathbb{P}^1(\mathbf{k})$. Equivalently, an element γ is loxodromic if the two eigenvalues have different p -adic valuation.

The closure of the set of fixed points z_γ^\pm , or equivalently the set of accumulation points of the action of Γ on $T_{\mathbf{k}} \cup \mathbb{P}^1(\mathbf{k})$ is the limit set Λ_Γ of the Schottky group Γ . The complement $\mathbb{P}^1(\mathbf{k}) \setminus \Lambda_\Gamma = \Omega_\Gamma(\mathbf{k})$ is the domain of discontinuity of the action of Γ on the boundary.

There is a unique geodesic ℓ_γ in $T_{\mathbf{k}}$ with endpoints $\{z_\gamma^-, z_\gamma^+\}$, the *axis* of a loxodromic element γ . The subgroup $\gamma^{\mathbb{Z}}$ acts on $T_{\mathbf{k}}$ by translations along ℓ_γ . There is a smallest subtree $T_\Gamma \subset T_{\mathbf{k}}$ that contains all the axes ℓ_γ of all the nontrivial elements $\gamma \in \Gamma$. The boundary at infinity of the subtree T_Γ is the limit set Λ_Γ . T_Γ is the non-Archimedean analog of the geodesic hull of the limit set of a Schottky group in \mathbf{H}^3 .

The quotient $X_\Gamma(\mathbf{k}) = \Omega_\Gamma(\mathbf{k})/\Gamma$ is a Mumford curve with its p -adic Schottky uniformization, [75]. The quotient $T_{\mathbf{k}}/\Gamma$ consists of a finite graph T_Γ/Γ with infinite trees appended at the vertices of T_Γ/Γ , so that the boundary at infinity of the graph $T_{\mathbf{k}}/\Gamma$ is the Mumford curve $X_\Gamma(\mathbf{k})$. The finite graph $G_{\mathbf{k}} = T_\Gamma/\Gamma$ is the dual graph of the special fiber X_q (a curve over \mathbb{F}_q which consists of a collection of $\mathbb{P}^1(\mathbb{F}_q)$ at each vertex of $G_{\mathbf{k}}$, connected along the edges). A family of finite graphs $G_{\mathbf{k},n}$, for $n \in \mathbb{N}$, is obtained by considering neighborhoods $T_{\Gamma,n}$ of T_Γ inside $T_{\mathbf{k}}$ consisting of T_Γ together with all vertices in $T_{\mathbf{k}}$ that are at a distance at most n from some vertex in T_Γ and the edges between them (these trees are preserved by the action of Γ), and taking the quotients $G_{\mathbf{k},n} = T_{\Gamma,n}/\Gamma$. The endpoints (valence one vertices) in $G_{\mathbf{k},n}$ correspond to the \mathbb{F}_{q^n} points in the special fiber, $X_q(\mathbb{F}_{q^n})$, see [200]. One sees in this way, geometrically, how the \mathbf{k} -points in the Mumford curve $X_\Gamma(\mathbf{k})$ are obtained as limits, going along the infinite ends of the graph $T_{\mathbf{k}}/\Gamma$, which correspond to successively considering points of X_q over field extensions \mathbb{F}_{q^n} . Conversely, one can view the process of going into the tree from its boundary $X_\Gamma(\mathbf{k})$ towards the graph $G_{\mathbf{k}}$ in the middle of $T_{\mathbf{k}}/\Gamma$ as applying reductions to \mathbb{F}_{q^n} . We will see later in the chapter how this process should be thought of physically as a form of renormalization. The finite graph $G_{\mathbf{k}} = T_\Gamma/\Gamma$ is the non-Archimedean analog of the convex core \mathcal{C}_Γ of the hyperbolic handlebody \mathcal{H}_Γ , while the infinite graph $T_{\mathbf{k}}/\Gamma$ is the non-Archimedean analog of \mathcal{H}_Γ itself, with the Mumford curve $X_\Gamma(\mathbf{k})$ replacing the Riemann surface $X_\Gamma = X_\Gamma(\mathbb{C})$ as the conformal boundary at infinity of $T_{\mathbf{k}}/\Gamma$. Geodesics in the bulk space $T_{\mathbf{k}}/\Gamma$ correspond to images in the quotient of infinite paths without backtracking in the tree $T_{\mathbf{k}}$, with endpoints at infinity on $\mathbb{P}^1(\mathbf{k})$. Again, one can subdivide these in several cases. When the endpoints

are the attractive and repelling fixed points z_γ^\pm of some element $\gamma \in \Gamma$, the path in $T_{\mathbf{k}}/\Gamma$ is a closed loop in the finite graph $G_{\mathbf{k}}$. If the endpoints are both in Λ_Γ but not the fixed points of the same group element, then the geodesic is a finite path in $G_{\mathbf{k}}$ that is not a closed loop (but which winds around several closed loops in $G_{\mathbf{k}}$ without a fixed periodicity). If at least one of the endpoints is in $\Omega_\Gamma(\mathbf{k})$ then the path in $T_{\mathbf{k}}/\Gamma$ eventually (for either $t \rightarrow +\infty$ or $t \rightarrow -\infty$) leaves the finite graph $G_{\mathbf{k}}$ and wanders off along one of the attached infinite trees towards the boundary $X_\Gamma(\mathbf{k})$ at infinity. We still refer to these cases as closed, bounded, and unbounded geodesics, as in the Archimedean case.

5.3 p -adic CFT and Holography for Scalar Fields

In this section, we discuss field theories defined on p -adic spacetimes: either in the bulk of the tree T_p (or possibly a quotient by a Schottky group) or on a p -adic algebraic curve at the boundary. We will find evidence for a rich holographic structure strongly reminiscent of ordinary AdS/CFT. The conformal theory on the fractal p -adic boundary is analogous to 1+1 dimensional field theory with a p -adic global conformal group; our principle example is the p -adic free boson which permits a Lagrangian description. In the bulk, semi-classical massive scalar fields defined on the lattice model naturally couple to operators on the conformal boundary in a way that allows for precise holographic reconstruction. One can also interpret the radial direction in the tree as a renormalization scale. These observations unite discrete analogs of AdS geometry, conformal symmetry, and renormalization in a holographic way.

Generalities of p -adic CFT, free bosons, and mode expansions

While non-Archimedean conformal field theory has been considered in the literature from several different perspectives [192, 83, 81], it remains much less well-studied than ordinary two-dimensional CFT. Melzer [192] defines these theories in general by the existence of an operator product algebra, where all operators in the theory are primaries with the familiar transformation law under the global conformal group $\mathrm{SL}(2, \mathbb{Q}_p)$. Descendants are absent in Melzer's formulation because there is no analog of the derivative operators ∂ and $\bar{\partial}$ acting on complex-valued functions over \mathbb{Q}_p [192], and (correspondingly) no local conformal algebra.

In this formulation, the correlation function between two primary fields $\phi_m(x)$ and $\phi_n(y)$ inserted at points x and y and having scaling dimensions Δ_n is given

(after normalization) by

$$\langle \phi_m(x) \phi_n(y) \rangle = \frac{\delta_{m,n}}{|x - y|_p^{2\Delta_n}}. \quad (5.18)$$

(We will understand this formula holographically in what follows.) As in the Archimedean case, as we take the points x and y to be close together (p -adically), we wish to expand the product as a sum of local field insertions: the operator product expansion. For two such primaries $\phi_m(x)$ and $\phi_n(y)$, there exists an $\epsilon > 0$ such that for $|x - y|_p < \epsilon$, the correlation function (perhaps with other primaries $\phi_{n_i}(x_i)$ inserted) is given by the expansion:

$$\langle \phi_m(x) \phi_n(y) \phi_{n_1}(x_1) \dots \phi_{n_i}(x_i) \rangle = \sum_r \tilde{C}_{mn}^r(x, y) \langle \phi_r(y) \phi_{n_1}(x_1) \dots \phi_{n_i}(x_i) \rangle, \quad (5.19)$$

where the sum runs over all primaries in the theory, and $\tilde{C}_{mn}^r(x, y)$ are real valued. This relation should hold whenever $|x - y|_p$ is smaller than the distances to the x_i 's. Invariance under $SL(2, \mathbb{Q}_p)$ implies

$$\tilde{C}_{mn}^r(x, y) = C_{mn}^r |x - y|_p^{\Delta_r - \Delta_m - \Delta_n} \quad (5.20)$$

with constant OPE coefficients C_{mn}^r .

Theories defined in this way enjoy a number of special properties not true of their Archimedean counterparts. They are automatically unitary since they possess no descendant fields. Additionally, because \mathbb{Q}_p is an *ultrametric* field, all triangles are isosceles: for $x, y, z \in \mathbb{Q}_p$, from the p -adic norm we have

$$\text{If } |x - y|_p \neq |y - z|_p, \text{ then } |x - z|_p = \max\{|x - y|_p, |y - z|_p\}. \quad (5.21)$$

This fundamental property of the p -adic numbers implies that the three- and four-point functions are *exactly* determined by the conformal weights and OPE coefficients. In the case of the four-point function, after an $SL(2, \mathbb{Q}_p)$ transformation which maps three points to 0, 1, and ∞ , the only free parameter (the cross ratio of the original points) must be contained in a ball in the neighborhood of one of the other points. Since the OPE is exact in each neighborhood, one can compute the three possible cases and determine the full four-point function.

In fact, all higher-point functions are constrained by global conformal symmetry alone; by contrast, the spectrum of OPE coefficients is less constrained than

in familiar CFTs. A consistent model can be constructed using the structure constants of any unital commutative algebra, subject to one simple condition. These features may be of interest in the study of conformal field theory and conformal blocks, but we do not pursue that direction here; the interested reader is referred to [192].

Let us now step back and consider the p -adic theory from the perspective of quantizing a classical field theory described by a Lagrangian. Many familiar objects from the study of quantum fields over normal (Archimedean) spacetime have direct analogs in the p -adic setting. For example, one frequently makes use of the idea of a *mode expansion* of a field on flat spacetime in terms of a special class of basis functions, the plane waves:

$$\phi(x) = \int_{\mathbb{R}} dx e^{ikx} \tilde{\phi}(k). \quad (5.22)$$

The functions e^{ikx} are eigenfunctions of momentum, or equivalently of translations. Mathematically, we can think of these as *additive characters* of \mathbb{R} : they are group homomorphisms $\chi : \mathbb{R} \rightarrow \mathbb{C}$, such that $\chi(x + y) = \chi(x)\chi(y)$.

The additive characters of the fields \mathbb{Q}_p are also known: they take the form [77]

$$\chi_k(x) = e^{2\pi i \{kx\}}. \quad (5.23)$$

Here $k, x \in \mathbb{Q}_p$, and the normalization factor 2π is included for convenience (in keeping with the typical math conventions for Fourier transforms). The symbol $\{\cdot\} : \mathbb{Q}_p \rightarrow \mathbb{Q}$ denotes the *fractional part* of the p -adic number.¹ It is defined by truncating the decimal expansion to negative powers of the prime:

$$\left\{ \sum_{k=m}^{\infty} a_k p^k \right\} = \sum_{k=m}^{-1} a_k p^k, \quad (5.24)$$

where the right-hand side is interpreted as an ordinary rational number, understood to be zero when the range of the sum is empty (m is non-negative). Since a p -adic number and its fractional part differ (at least in a formal sense) by an integer, it makes sense that the complex exponential (5.23) should depend only on the fractional part of kx . (However, care should be taken: in general, it is not true for rational x that $e^{2\pi i x} = e^{2\pi i \{x\}_p}$! For instance, $0.1 = 1/10$ is a 3-adic integer.)

¹As with other notations referring to the p -adics, we will sometimes use the subscript $\{\cdot\}_p$ when it is necessary for emphasis or to refer to a specific choice of prime.

A wide class of scalar fields on \mathbb{Q}_p can be expanded in a basis of the additive characters, just like a mode expansion in the Archimedean setting:

$$\phi(x) = \int d\mu(k) e^{2\pi i\{kx\}} \tilde{\phi}(k). \quad (5.25)$$

Here $d\mu(k)$ is the Haar measure on \mathbb{Q}_p . The theory of the p -adic Fourier transform is developed in more detail in Appendix C.1.

Our principal example (and also by far the most well-studied instance) of a p -adic conformal field theory is the free boson: a single (real or complex) scalar field on $\mathbb{P}^1(\mathbb{Q}_p)$ or another p -adic Riemann surface, with a massless quadratic action. This theory was of interest in the context of p -adic string theory, in which the worldsheet is a p -adic space, but the target space (and hence all physically observable quantities) are ordinary. Many results were derived in that literature, including the well-known Freund–Olson–Witten tachyon scattering amplitudes [205, 18, 19].

Our interpretation of the system in question will be somewhat different, as we will emphasize the holographic nature of the interplay between field theory defined on a Riemann surface (algebraic curve) and the study of its hyperbolic filling, a quotient of the Bruhat–Tits tree. (In the p -adic string literature, it was common to view the tree as playing the role of the “interior” of the worldsheet.) Many of our results will parallel aspects of the p -adic string, but we will view this theory as a CFT on $\mathbb{P}^1(\mathbb{Q}_p)$ without any reference to a target space.

The p -adic free boson is considered here because it permits a Lagrangian description in terms of the nonlocal Vladimirov derivative, $\partial_{(p)}$, which acts on complex- or real-valued fields of a p -adic coordinate. This derivative is defined by

$$\partial_{(p)}^n f(x) = \int_{\mathbb{Q}_p} \frac{f(x') - f(x)}{|x' - x|_p^{n+1}} dx'. \quad (5.26)$$

In the p -adic string literature, $\partial_{(p)}$ is also known as a normal derivative, for reasons that will become clear in the following sections. Intuitively, the formula is similar to Cauchy’s representation of the n -th derivative of a function by a contour integral. A more detailed explanation of its properties is given in Appendix C.2. While the parameter n is often taken to be an integer, it may in principle assume any real value.

One can arrive at the following action either by “integrating out” the interior of the string worldsheet T_p as done in [82], or by hypothesis as the minimal “quadratic” action of a scalar over a p -adic coordinate [79]. The action for a single scalar is (setting the overall coupling to 1) [206, 207, 208]:

$$S_p[\phi] = - \int_{\mathbb{Q}_p} \phi(x) \partial_{(p)} \phi(x) dx. \quad (5.27)$$

where $\partial_{(p)} \phi(x)$ is the first Vladimirov derivative of the field ϕ . We take $\phi(x)$ to be a scalar representation of the conformal group (see [209] for discussion of representations of $\mathrm{SL}(2, \mathbb{Q}_p)$.) Under an element

$$g = \begin{pmatrix} a & b \\ c & d \end{pmatrix}$$

of the conformal group, where $a, b, c, d \in \mathbb{Q}_p$ and $ad - bc = 1$, quantities in the above expression transform as

$$\begin{aligned} x &\rightarrow \frac{ax + b}{cx + d}, & x' &\rightarrow \frac{ax' + b}{cx' + d}, \\ dx &\rightarrow \frac{dx}{|cx + d|_p^2}, & dx' &\rightarrow \frac{dx'}{|cx' + d|_p^2}, \\ |x' - x|_p^{-2} &\rightarrow |(cx' + d)(cx + d)|_p^2 |x' - x|_p^{-2}. \end{aligned}$$

As in [192], a field $\phi_n(x)$ having conformal dimension Δ_n transforms as

$$\phi_n(x) \rightarrow \phi'_n \left(\frac{ax + b}{cx + d} \right) = |cx + d|_p^{-2\Delta_n} \phi_n(x) \quad (5.28)$$

under the p -adic conformal group. For the free boson $\phi(x)$, we claim $\Delta = 0$. With this one can see the derivative $\partial_{(p)} \phi(x)$ carries a weight $|cx + d|_p^{-2}$ and thus is a field of dimension 1. It should now be clear that the action $S_p[\phi]$ is invariant under the global conformal group.

Given the action $S_p[\phi]$, we can define the partition function in the usual way by integrating over configurations with measure $\mathcal{D}\phi$. As in the case of the p -adic string, because ϕ is a complex (and not p -adic) valued field, this integration measure is exactly the one that appears in ordinary field theory:

$$Z_p = \int \mathcal{D}\phi e^{-S_p[\phi]}. \quad (5.29)$$

As many authors have noted [206, 207, 210], this action and the partition function actually describe a free theory. This means the saddle point approximation to the partition function is exact, and it can be computed by Gaussian

integration exactly as in the case of a real free field. Of more interest in the present discussion is the two point function. To do this we introduce sources $J(x)$ to define the generating function:

$$Z_p[J] = \int \mathcal{D}\phi \exp \left\{ \left(-S_p[\phi] + \int_{\mathbb{Q}_p} J(x')\phi(x')dx' \right) \right\}. \quad (5.30)$$

The sources for the 2-point function or propagator take the form of p -adic delta functions at the insertion points x, y are $J(x) = \delta(x' - x) + \delta(x' - y)$. Just as in the real case, we vary with respect to $\phi(x)$ and find the classical solution which extremizes the above action. This is the Green's function for the Vladimirov derivative $G(x - y)$, satisfying

$$\partial_{(p)}G(x - y) = -\delta(x - y). \quad (5.31)$$

To solve for $G(x-y) = \langle 0|\phi(x)\phi(y)|0\rangle$, we apply the p -adic Fourier transform to both sides using techniques from Appendix C.1. In Fourier space the derivative brings down one power of the momentum and the delta function becomes an additive character:

$$\tilde{G}(k) = -\frac{\chi(ky)}{|k|_p}. \quad (5.32)$$

The 2-point function in position space can be obtained by inverse Fourier transform (with $u = x - y$):

$$G(x - y) = -\int_{\mathbb{Q}_p} \frac{\chi(k(y - x))}{|k|_p} dk \quad (5.33)$$

$$= -\int_{\mathbb{Q}_p} \frac{\chi(ku)}{|k|_p} dk. \quad (5.34)$$

This integral is divergent as $k \rightarrow 0$. We compute two similar integrals in Appendix C.2, where the apparent divergence is canceled by the numerator. Unlike in those examples, this integral really does diverge logarithmically, just as the 2-point function of a dimension 0 operator in 2d conformal field theory has a log-divergence. Proceeding as in that case, we introduce a regulator to extract the finite part by computing

$$\lim_{\alpha \rightarrow 0} \int_{\mathbb{Q}_p} \chi(ku)|k|_p^{\alpha-1} dk. \quad (5.35)$$

This appears in the second integral computed in the appendix; in terms of the p -adic gamma function $\Gamma_p(x)$ it is:

$$\lim_{\alpha \rightarrow 0} \int_{\mathbb{Q}_p} \chi(ku)|k|_p^{\alpha-1} dk = \lim_{\alpha \rightarrow 0} \Gamma_p(\alpha)|u|_p^{-\alpha}. \quad (5.36)$$

As $\alpha \rightarrow 0$ the gamma function has a simple pole and the norm has a log piece:

$$\lim_{\alpha \rightarrow 0} \Gamma_p(\alpha) \approx \frac{p-1}{p \ln p} \frac{1}{\alpha} \quad (5.37)$$

$$\lim_{\alpha \rightarrow 0} |u|_p^{-\alpha} \approx 1 - \alpha \ln |u|_p. \quad (5.38)$$

Finally we restore $u = x - y$ and find the 2-point function up to normalization is:

$$\langle 0 | \phi(x) \phi(y) | 0 \rangle \sim \ln \left| \frac{x-y}{a} \right|_p, \quad a \rightarrow 0. \quad (5.39)$$

This is exactly analogous to the correlator for the ordinary free boson in two dimensions.

The Laplacian and harmonic functions on T_p

In addition to boundary scalar fields, we will be interested in scalar fields in the “bulk,” i.e., defined on the Bruhat–Tits tree. Such a field is a real- or complex-valued function on the set of vertices. We will also consider fields that are functions on the set of edges; as we will discuss later, such functions will be analogous to higher-form fields or metric degrees of freedom in the bulk. For now we mention them for completeness and to fix some standard notation. For more information about fields in the tree, the reader can consult [82] and references given therein.

We think of the tree as the 1-skeleton of a simplicial complex, and make use of standard notations and ideas from algebraic topology. The two types of fields mentioned above are just 0- and 1-cochains; we will refer to the space of such objects as $C^*(T_p)$, where $*$ = 0 or 1.

If an orientation is chosen on the edges of the tree, the boundary operator acts on its edges by $\partial e = t_e - s_e$, where s and t are the source and target maps. The corresponding coboundary operator acts on fields according to the rule

$$d : C^0(T_p) \rightarrow C^1(T_p), \quad (d\phi)(e) = \phi(t_e) - \phi(s_e). \quad (5.40)$$

The formal adjoint of this operator is

$$d^\dagger : C^1(T_p) \rightarrow C^0(T_p), \quad (d^\dagger\psi)(v) = \sum_e \pm\psi(e), \quad (5.41)$$

where the sum is over the $p + 1$ edges adjacent to vertex v , with positive sign when v is the source and negative sign when it is the target of e . Whether or not

d^\dagger is actually an adjoint to d depends on the class of functions being considered; the L^2 inner product must be well-defined, and boundary conditions at infinity must be chosen to avoid the appearance of a boundary term.

Upon taking the anticommutator $\{d, d^\dagger\}$, we obtain an operator of degree zero, which is the proper analog of the Laplacian. We will most often use its action on the 0-cochains, which can be represented by the formula

$$\Delta\phi(v) = \sum_{d(v,v')=1} \phi(v') - (p+1)\phi(v). \quad (5.42)$$

This is sometimes written using the notation $\Delta_p = t_p - (p+1)$, where t_p is the Hecke operator on the tree. The analogous formula for 1-cochains is

$$\Delta\psi(e) = \sum_{e'} \pm\psi(e') - 2\psi(e), \quad (5.43)$$

where the sum goes over the $2p$ edges adjacent to e at either side. Unlike for the vertices, there is a dependence on the choice of orientation here: an edge in the sum (5.43) enters with positive sign when it points in the “same direction” as e , i.e., points out from t_e or into s_e . Edges enter with negative sign when the opposite is true. In the standard picture of the tree with ∞ at the top and all finite points of \mathbb{Q}_p at the bottom, oriented vertically, we therefore have exactly one negative term in (5.43), corresponding to the unique edge above e . Notice that, for general p , the Laplacian acting on edges (unlike on vertices) will not have a zero mode; this makes sense, since the tree is a contractible space. The exception is $p = 2$, for which the standard choice of vertical orientations defines a Laplacian which annihilates constant functions of the edges. (Of course, the $p = 2$ tree is still contractible.)

Action functional and equation of motion for scalar fields

Equipped with these ingredients, it is now straightforward to write down action functionals and equations of motion for free scalar fields. The massless quadratic action is

$$S[\phi] = \sum_e |d\phi(e)|^2. \quad (5.44)$$

In what follows, we will study properties of solutions to the “wave equation” $\Delta\phi = 0$, and its massive generalization $(\Delta - m^2)\phi = 0$, on the tree. These have been considered in [82].

There is a family of basic solutions to the Laplace equation, labeled by a choice of a boundary point x and an arbitrary complex number κ . The idea is as follows: Given an arbitrary vertex v in the bulk of the tree, a unique geodesic (indeed, a unique path) connects it to x . As such, exactly one of its $p+1$ neighbors will be closer (by one step) to x , and the other p will be farther by one step. Therefore, the function

$$\varepsilon_{\kappa,x}(v) = p^{-\kappa d(x,v)} \quad (5.45)$$

will be an eigenfunction of the Hecke operator, with eigenvalue $(p^\kappa + p^{1-\kappa})$.

The catch in this is that the distance $d(x, v)$ is infinite everywhere in the bulk. We need to regularize it by choosing a centerpoint C in the tree, and declaring that $d(x, C) = 0$. (This just scales the eigenfunction (5.45) by an infinite constant factor). Then $d(x, v) \rightarrow -\infty$ as $v \rightarrow x$, but we have a well-defined solution to the Laplace equation everywhere in the tree. These solutions are analogous to plane waves; the solution varies as the exponent of the (regularized) distance to a boundary point, which in the normal Archimedean case is just the quantity $\mathbf{k} \cdot \mathbf{r}$.

The corresponding eigenvalue of the Laplacian is

$$\Delta \varepsilon_{\kappa,x} = m_\kappa^2 \varepsilon_{\kappa,x} = [(p^\kappa + p^{1-\kappa}) - (p+1)] \varepsilon_{\kappa,x}. \quad (5.46)$$

It is therefore immediate that the harmonic functions on the tree (solutions to the massless wave equation) are those with $\kappa = 0$ or 1 ; $\kappa = 0$ is the zero mode consisting of constant functions, whereas $\kappa = 1$ is the nontrivial zero mode. The eigenvalues (5.46) are invariant under the replacement $\kappa \rightarrow 1 - \kappa$, due to the inversion symmetry of the boundary theory.

If we are considering a real scalar field, we must be able to write a basis of real solutions. Of course, when κ is real, we will always be able to do this. More generally, if $\kappa = \kappa_0 + i\gamma$, our solutions look like

$$\varepsilon \sim p^{-\kappa_0 d} e^{-i\gamma \ln(p) d}, \quad p^{(1-\kappa_0)d} e^{i\gamma \ln(p) d}. \quad (5.47)$$

Thus, to construct a basis of real solutions, the following possibilities can occur:

- $\kappa = 1/2$. In this case, there is no restriction on γ , and the solutions look like cosines and sines of $\gamma \ln(p) d(x, v)$, modulated by $p^{d(x,v)/2}$.

- $\kappa > 1/2$.² In this case, the amplitude parts of the two solutions are linearly independent, and so $\exp(i\gamma \ln(p) d)$ must be real. Since d is an integer, the choices are $\gamma \ln(p) = 0$ or $\pi \pmod{2\pi}$.

While it would be interesting to consider solutions with nonzero γ , we will consider only the one-parameter family of solutions with real κ in the sequel. The parameter m_κ^2 then attains its minimum value for $\kappa = 1/2$. Considering only solutions of this plane-wave form, we therefore have a bound

$$m_\kappa^2 \geq -(\sqrt{p} - 1)^2. \quad (5.48)$$

Note that we could also rewrite (5.46) in the form

$$m_\kappa^2 = -(p+1) + 2\sqrt{p} \cosh \left[\left(\kappa - \frac{1}{2} \right) \ln p \right]. \quad (5.49)$$

Bulk reconstruction and holography

It is clear from the definition that, when the real part of κ is positive, the plane wave solution (5.45) tends to zero everywhere on the boundary, except at the point x (where it tends to infinity). So we can think of it as representing the solution to the Laplace equation (taking $\kappa = 1$) in the bulk, with specified Dirichlet-type boundary conditions that look like a delta function centered at x . By linearity, we can therefore reconstruct the solution to more general Dirichlet problems by superposition: if the boundary value is to be a certain function $\phi_0(x)$ on $\partial T_p = \mathbb{P}^1(\mathbb{Q}_p)$, then the required bulk harmonic function is

$$\phi(v) = \frac{p}{p+1} \int d\mu_0(x) \phi_0(x) \varepsilon_{1,x}(v). \quad (5.50)$$

Here $d\mu_0(x)$ is the Patterson-Sullivan measure on $\mathbb{P}^1(\mathbb{Q}_p)$. The normalization factor can be fixed by taking the boundary value to be the characteristic function of any p -adic open ball in the boundary.

We can perform the analogous calculation for massive fields as well, but the sense in which $\phi(v)$ will approach $\phi_0(x)$ as $x \rightarrow v$ will be more subtle (since the equation of motion will have no constant mode). Using notation from [82], let $\delta(a \rightarrow b, c \rightarrow d)$ be the overlap (with sign) of the two indicated oriented paths in the tree, and let

$$\langle v, x \rangle = \delta(C \rightarrow v, C \rightarrow x) + \delta(v \rightarrow x, C \rightarrow v). \quad (5.51)$$

²Due to the $\kappa \mapsto 1 - \kappa$ symmetry, such a choice is always possible.

This expression makes sense for any bulk vertex v ; x may be either a boundary or a bulk point. Note that $\langle z, x \rangle$ is just the negative of the “regularized distance” occurring in our previous discussion.

We would like to compute the bulk solution to the massive equation of motion obtained by integrating our primitive solution (5.45) over its boundary argument, weighted by a boundary function. As a simple choice of boundary function, pick the characteristic function of the p -adic open ball below a vertex w in the tree:

$$\phi_w(v) = \int_{\partial B_w} d\mu_0(x) p^{\kappa\langle v, x \rangle}. \quad (5.52)$$

The integral is straightforward to calculate. There are two cases:

$v \notin B_w$ Here, the integrand is constant, and is just equal to $p^{\kappa\langle v, w \rangle}$. The measure of the set over which the integral is performed is $\mu_0(\partial B_w) = p^{-d(C, w)}$, so that the final result is

$$\phi_w(v) = p^{\kappa\langle v, w \rangle - d(C, w)}. \quad (5.53)$$

Note that, if v moves towards the boundary along a branch of the tree, $\langle v, w \rangle$ differs from $-d(C, v)$ by a constant, so that the solution scales as $p^{-\kappa d(C, z)}$.

$v \in B_w$ There are now two cases to consider: $x \in B_v$ or $x \notin B_v$. In the first scenario, the integrand is again constant; its value is $p^{\kappa d(C, v)}$, and the measure is $\mu_0(B_v) = p^{-d(C, v)}$.

In the second scenario, the geodesic $x \rightarrow C$ will meet the geodesic $v \rightarrow C$ at a distance h above v ; by assumption, $1 \leq h \leq d(v, w)$. For each value of h , the integrand takes the constant value $p^{\kappa(d(C, v) - 2h)}$, and the measure of the corresponding set is

$$\mu(h) = \frac{p-1}{p} p^{-d(C, v) + h}. \quad (5.54)$$

The factor $(p-1)/p$ enters because $p-1$ of the p vertices one step below the meeting vertex correspond to meeting height h (one of

them is closer to v). Putting the pieces together, the result is

$$\begin{aligned}\phi_w(v) &= p^{(\kappa-1)d(C,v)} \left(1 + \frac{p-1}{p} \sum_{h=1}^{d(w,v)} (p^{1-2\kappa})^h \right) \\ &= \left(\frac{p^{-2\kappa} - 1}{p^{1-2\kappa} - 1} \right) p^{(\kappa-1)d(C,v)} + \frac{p-1}{p} \left(\frac{p^{(2\kappa-1)d(C,w)}}{p^{2\kappa-1} - 1} \right) p^{-\kappa d(C,v)}.\end{aligned}\tag{5.55}$$

The reader can check that we recover the correct answer in the massless case, $\kappa \rightarrow 1$. Furthermore, our result is a superposition of the asymptotic behavior of the two eigenfunctions corresponding to the mass determined by our original choice of κ . To resolve the ambiguity, we will choose $\kappa > 1/2$.

At this point, we have accumulated enough understanding of scalar fields on the tree to point out how the simplest version of holography will work: namely, classical scalar fields in a non-dynamical AdS background, neglecting backreaction and metric degrees of freedom. In the Archimedean case, this version of holography was neatly formulated by Witten [69] in terms of a few simple key facts. First, the coupling between bulk scalar fields and boundary operators must relate the asymptotics (and hence the mass) of the bulk fields to the conformal dimension of the corresponding boundary operators; massless bulk scalars should couple to marginal operators in the boundary CFT. Second, the crucial fact that allows the correspondence to work is the existence of a unique solution to the generalized Dirichlet problem for the bulk equations of motion with specified boundary conditions.

Luckily, as we have now shown, all of the important features of the problem persist in the p -adic setting, and Witten's analysis can be carried over to the tree. In particular, we make his holographic ansatz:

$$\left\langle \int_{\mathbb{P}^1(\mathbb{Q}_p)} d\mu_0 \phi_0 \mathcal{O} \right\rangle_{\text{CFT}} = e^{-I_{\text{bulk}}[\phi]},\tag{5.56}$$

where the bulk field ϕ is the unique classical solution extending the boundary condition ϕ_0 , and \mathcal{O} is a boundary operator to which the bulk field couples (and not an integer ring). In the massless case, where one literally has $\phi_0(x) = \lim_{v \rightarrow x} \phi(z)$, \mathcal{O} is an exactly marginal operator in the CFT.

Given our result (5.55), it is simple to write down the correctly normalized bulk-reconstruction formula for massive fields:

$$\begin{aligned}\phi(v) &= \frac{p^{1-2\kappa} - 1}{p^{-2\kappa} - 1} \int d\mu_0(x) \phi_0(x) p^{\kappa\langle v, x \rangle}, \\ \phi(v) &\sim p^{(\kappa-1)d(C,v)} \phi_0(x) \text{ as } v \rightarrow x.\end{aligned}\tag{5.57}$$

When the point v approaches the boundary, the exponent in the kernel becomes

$$\langle v, x \rangle = -d(C, v) + 2 \operatorname{ord}_p(x - y),\tag{5.58}$$

where y is any boundary point below v . (5.57) then becomes

$$\phi(v) = \left(\frac{p^{1-2\kappa} - 1}{p^{-2\kappa} - 1} \right) p^{-\kappa d(C,v)} \int d\mu(x) \frac{\phi_0(x)}{|x - y|_p^{2\kappa}}.\tag{5.59}$$

We can now understand why the Vladimirov derivative is a “normal” derivative on the boundary; it measures the rate of change in the holographic direction of the reconstructed bulk function. In particular, we have that

$$\begin{aligned}\lim_{v \rightarrow y} (\phi(v) - \phi(y)) p^{\kappa d(C,v)} &= \left(\frac{p^{1-2\kappa} - 1}{p^{-2\kappa} - 1} \right) \int d\mu(x) \frac{\phi_0(x) - \phi_0(y)}{|x - y|_p^{2\kappa}} \\ &= \left(\frac{p^{1-2\kappa} - 1}{p^{-2\kappa} - 1} \right) \partial_{(p)}^{2\kappa-1} \phi(y).\end{aligned}\tag{5.60}$$

An argument precisely akin to Zabrodin’s demonstration [82] that the bulk action may be written (upon integrating out the interior) as a boundary integral of the nonlocal Vladimirov action shows that we can write $I_{\text{bulk}}[\phi]$ in exactly this form. This demonstrates, exactly as in Witten’s Archimedean analysis, that a massive field ϕ corresponds to a boundary operator of conformal dimension κ , where $\kappa > 1/2$ is the larger of the two values that correspond to the correct bulk mass. Moreover, the boundary two-point function is proportional to $|x - y|_p^{-2\kappa}$, as expected.

Scale dependence in bulk reconstruction of boundary modes

Let us consider how the mode expansion of a boundary scalar field interacts with the reconstruction of the corresponding bulk harmonic function. We will be interested in developing the interpretation of the extra, holographic direction as a renormalization scale in our p -adic context. The idea that moving upward in the tree corresponds to destroying information or coarse-graining is

already suggested by the identification of the cone above \mathbb{Z}_p (or more generally any branch of the tree) with the inverse limit

$$\mathbb{Z}_p = \varprojlim \mathbb{Z}/p^n\mathbb{Z}, \quad (5.61)$$

where the set of vertices at depth n corresponds to the elements of $\mathbb{Z}/p^n\mathbb{Z}$, and the maps of the inverse system are the obvious quotient maps corresponding to the unique way to move upwards in the tree. A nice intuitive picture to keep in mind is that p -adic integers can be thought of as represented on an odometer with infinitely many \mathbb{F}_p -valued digits extending to the left. $\mathbb{Z}/p^n\mathbb{Z}$ is then the quotient ring obtained by forgetting all but n digits, so that there is integer overflow; the maps of the inverse system just forget successively more odometer rings. Since digits farther left are smaller in the p -adic sense, we can think of this as doing arithmetic with finite (but increasing) precision. The parallel to the operation of coarse-graining is apparent; however, we will be able to make it more precise in what follows.

Let's consider a boundary field that is just given by an additive character (plane wave), $\phi_0(x) \sim \exp(2\pi i\{kx\}_p)$. Just as in the complex case, a plane wave in a given coordinate system will not define a solution of fixed wavelength everywhere on $\mathbb{P}^1(\mathbb{C})$; the coordinate transformation (stereographic projection) will mean that the wavelength tends to zero as one moves away from the origin, and the function will become singular at infinity. Therefore, we should instead consider a boundary function of *wavepacket* type, that looks like a plane wave, but supported only in a neighborhood of the origin.

A nice choice to make in the p -adic setting is to take the boundary function to be

$$\phi_0(x) = e^{2\pi i\{kx\}} \cdot \Theta(x, \mathbb{Z}_p), \quad (5.62)$$

where $\Theta(x, S)$ is the characteristic function of the set $S \subset \mathbb{Q}_p$. The transformation (5.17) is actually trivial inside \mathbb{Z}_p , so no distortion of the wavepacket occurs at all (unlike for a similar setup in \mathbb{C}). Of course, we ought to take $|k|_p > 1$, so that $\{kx\}$ is not constant over the whole of \mathbb{Z}_p .

Given this choice of boundary function, the corresponding solution to the bulk equations of motion can be reconstructed using the integral kernel (5.50):

$$\phi(v) = \frac{p}{p+1} \int_{\mathbb{Z}_p} d\mu(x) e^{2\pi i\{kx\}} p^{-d_C(x,v)}. \quad (5.63)$$

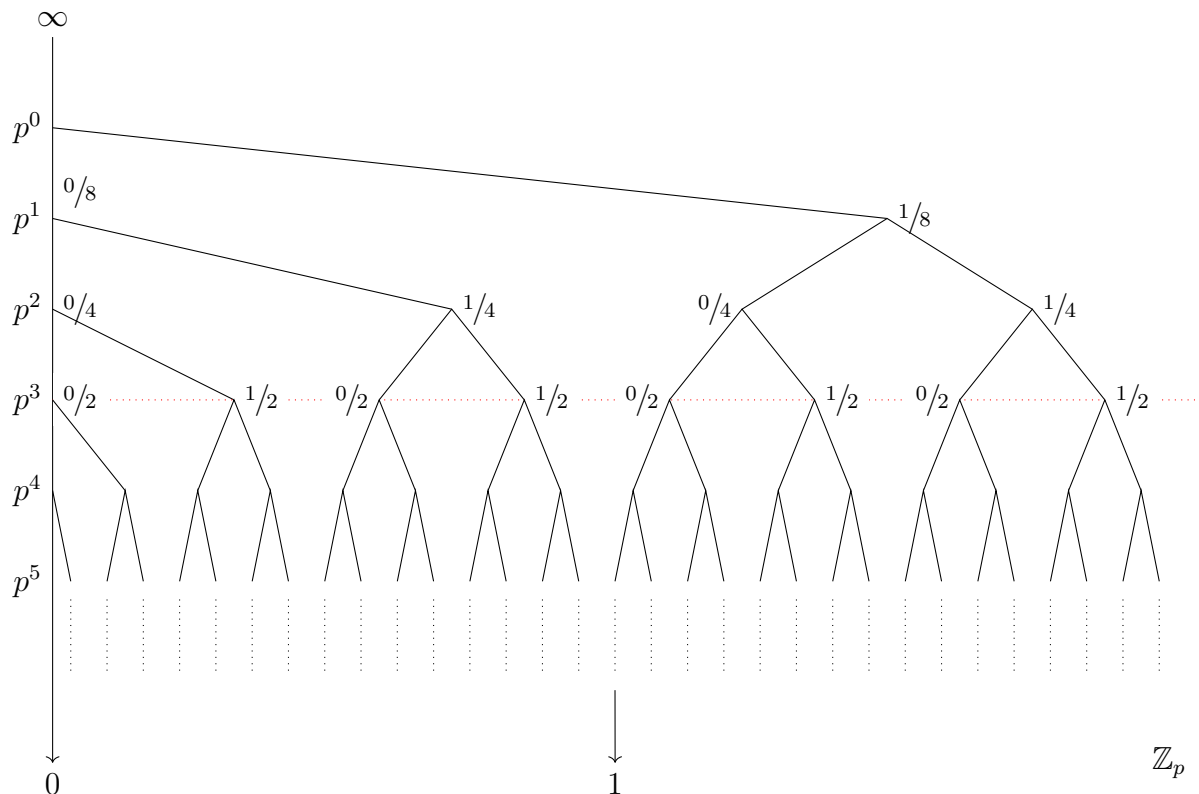


Figure 5.5: A drawing of \mathbb{Z}_p ($p = 2$ for simplicity). Here $k = p^{-4}$. The marked fractions at vertices indicate contributions to $\{kx\}$, which are summed along the geodesic ending at x .

Recall that $d_C(x, v)$ is the distance from v to x , regularized to be zero at the centerpoint $v = C$ of the tree. We will calculate this integral when v is inside the branch of the tree above \mathbb{Z}_p .

Proposition 1. *Let v be a vertex in the branch above \mathbb{Z}_p , at a depth ℓ (i.e., since $v \in \mathbb{Z}_p$, distance from the centerpoint) such that $0 \leq \ell < -\text{ord}_p(k) - 2$. Then the reconstructed bulk function $\phi(v)$ is zero.*

Proof. The claim relies on the simple fact that the sum of all p -th roots of unity is zero. Since v is above the red line in Fig. (5.5) (at depth equal to $-\text{ord}_p(k) - 1$), both terms in the integrand are locally constant below the line, and the integral may be evaluated as a sum along the vertices at the height of the red line. Furthermore, the factor $p^{-d_C(v, x)}$ is constant for each of the p vertices on the line that descend from the same ancestor. Since the measure of each branch is equal, the integral is proportional to the sum of all p -th roots of unity, and hence to zero. Notice that this also demonstrates that

the reconstructed bulk function is zero everywhere *outside* \mathbb{Z}_p : it is zero at the central vertex, and zero on the boundary of the open ball complementary to \mathbb{Z}_p . \square

Even without calculating the explicit form of the bulk function for vertices below the screening height, this simple argument already allows us to make our physical point: in p -adic holography, the qualitative features of ordinary AdS/CFT persist in a setting where the bulk geometry is discrete, and in some cases are even sharpened. For instance, we have shown explicitly that modes for which $|k|_p$ is large (i.e. the short-wavelength behavior of the boundary conditions) must drop out of the reconstructed bulk field, making exactly zero contribution to it above a height in the tree precisely determined by $|k|_p$. The usual intuition that moving into the bulk along the holographic direction corresponds to integrating out UV modes is thus neatly confirmed.

The explicit form of the reconstructed bulk function at vertices below the screening height is easy to calculate, but less central to our discussion; we leave the computation as an exercise for the reader.

The possibility of higher-spin fields

We now wish to propose an analog of higher-spin fields that could be defined in the p -adic case. While we will motivate our proposal here, we do not investigate any properties of p -adic CFT with fields other than scalars. For work along this direction describing fermions, see [6, 91].

We proceed by analogy with two-dimensional CFT, in which the conformal dimension and spin together describe a character of the multiplicative group \mathbb{C}^\times :

$$\phi(re^{i\theta} \cdot z) = r^\Delta e^{is\theta} \phi(z). \quad (5.64)$$

The group $\mathbb{C}^\times \simeq \mathbb{R}_{>0}^\times \times \Upsilon(1)$; the conformal dimension determines a character of the first factor, and the spin a character of the second, which can be thought of as scale transformations and rotations of the coordinate, respectively. The existence of the logarithm function means that we can think of the multiplicative group \mathbb{R}_+ as isomorphic to the additive group \mathbb{R} .

The structure of the group of units of any local field is understood (see [211] for details). In particular, for the field \mathbb{Q}_p , the result is that

$$\mathbb{Q}_p^\times \simeq p^\mathbb{Z} \times \mathbb{F}_p^\times \times U^{(1)}, \quad (5.65)$$

where $U^{(1)}$ is the group of “principal units” of the form $1 + p \cdot a$, with $a \in \mathbb{Z}_p$. This decomposition just reflects the structure of the p -adic decimal expansion: since the p -adic norm is multiplicative, any number $x \neq 0$ can be written in the form

$$x = p^{\text{ord}_p(x)} (x_0 + x_1 p + \dots), \quad (5.66)$$

where $x_0 \neq 0$ (so that $x \in \mathbb{F}_p^\times \simeq C_{p-1}$) and the other x_i may be any digits chosen from \mathbb{F}_p . Dividing through by x_0 , one gets

$$x = p^{\text{ord}_p(x)} \cdot x_0 \left(1 + \sum_{i \geq 1} \tilde{x}_i p^i \right), \quad (5.67)$$

where $\tilde{x}_i = x_i/x_0$, and the factor in parentheses is a principal unit. A character of \mathbb{Q}_p^\times is therefore a triple of characters, one for each factor in (5.65). The first factor, as in the normal case, corresponds to the scaling dimension of the field; the last two factors are therefore analogous to the spin. Obviously, the second factor corresponds to a $\mathbb{Z}/(p-1)\mathbb{Z}$ phase. It is also known [211] that the set of characters of $U^{(1)}$ is countable and discrete.

In fact, we can naively understand a broader class of the characters of $\mathbb{Z}_p^\times = \mathbb{F}_p^\times \times U^{(1)}$. Recall the description of \mathbb{Z}_p as the inverse limit of its finite truncations:

$$\mathbb{Z}_p = \varprojlim \mathbb{Z}/p^n \mathbb{Z}. \quad (5.68)$$

Since this is an inverse limit of rings, there are therefore projection maps between the respective multiplicative groups:

$$\mathbb{Z}_p^\times \rightarrow (\mathbb{Z}/p^n \mathbb{Z})^\times \simeq C_{p^{n-1}(p-1)}. \quad (5.69)$$

Therefore, any multiplicative character of a cyclic group $C_{p^{n-1}(p-1)}$ (i.e., any finite root of unity of order $p^{n-1}(p-1)$, for arbitrary n) will give a character of $(\mathbb{Z}/p^n \mathbb{Z})^\times$, which will in turn pull back to define a multiplicative character of the spin part of \mathbb{Q}_p^\times . Spin in the p -adic case is therefore both similar to and interestingly different from ordinary two-dimensional CFT.

5.4 Entanglement Entropy

In real $\text{AdS}_3/\text{CFT}_2$, the Ryu-Takayangi formula [92] relates the entanglement entropy in a 2D CFT for a single interval to the length of a minimal geodesic in the dual bulk spacetime. Thus, it is interesting to evaluate if such a proposal holds true in p -adic AdS/CFT . The entanglement entropy in quantum

field theories is a notoriously difficult and subtle quantity to compute, and much effort has been expended in developing a toolbox of techniques that provide exact results. One of the first systems in which the computation became tractable was two-dimensional conformal field theory, and in particular the theory of free bosons. Since we are primarily considering the free boson in our discussion of this section, one might hope that the same techniques can be applied in the p -adic case. Real and p -adic field theories have many similarities, and there is a very natural guess for what the p -adic single interval entanglement entropy should be.

However, it seems different methods might be required for a microscopic derivation. In this section, we will demonstrate the standard techniques, illustrate the subtle issues that arise, and justify our conjecture for the entanglement entropy in what follows. An alternative proposal is advocated in Chapter 6 of this thesis. In this chapter, we will propose a tensor network model of p -adic AdS/CFT involving large but finite-dimensional local Hilbert spaces. In this model, the (finite-dimensional) density matrices are analytically calculable, and we obtain p -adic or non-Archimedean analogs of various entanglement quantities. All of these quantities have a very natural interpretation in terms of discrete bulk geometries, providing strong evidence that p -adic entropies may have holographic properties similar to their real counterparts. We save the bulk of the discussion of the model and those issues for Chapter 6, and reserve this section as a brief appetizer and motivation for that model.

As in the real case, we expect the entanglement entropy to have UV divergences. These are normally thought of as localized to the “boundary” of the region under consideration. Care must be used in defining what we mean by interval and boundary; the p -adic numbers have no ordering, and every element of an open set is equally (or equally not) a boundary element.

Whenever possible, we must think in terms of open sets. Over the reals, the open sets are intervals with measure or length given by the norm of the separation distance of the endpoints; as the reader will recall, p -adic open sets are perhaps best visualized using the Bruhat–Tits tree. Once a center C of the tree is picked, we can pick any other vertex v and consider the cone of points below v extending out towards the boundary, which is an open neighborhood in $\mathbb{P}^1(\mathbb{Q}_p)$. A perhaps surprising fact which follows from the definition of the p -adic norm $|x - y|_p$ ($x, y \in \mathbb{P}^1(\mathbb{Q}_p)$) is that it is related to the height of the

cone required to connect x to y (see Fig. 5.6).

Following standard arguments, say of [212, 213], we can pick the boundary cone below the point v to be called the region V . The total Hilbert space on \mathbb{Q}_p splits into Hilbert spaces on V and its complement, $\mathcal{H} = \mathcal{H}_V \otimes \mathcal{H}_{-V}$. The entanglement entropy defined by $S(V) = -\text{Tr}(\rho_V \log \rho_V)$ and by construction satisfies $S(V) = S(-V)$. As there are an infinite number of points $x_i \in V \in \mathbb{P}^1(\mathbb{Q}_p)$, there is an unbounded number of local degrees of freedom $\phi(x_i)$ as is typical of quantum field theory. In the continuum case this implies logarithmic divergences from modes in V entangled with those in $-V$, and we expect the same to be true in the p -adic case.

In the works of Cardy and Calabrese [214, 215], the entanglement entropy for intervals in $1+1$ -dimensional conformal field theories are explicitly calculated. The p -adic field theories considered here are exactly analogous to the two-dimensional free boson; in both, the scalar $\phi(x)$ has conformal dimension zero and (as we have shown above) a logarithmically divergent propagator. We wish to understand how much of their calculation can be duplicated in the p -adic case. These authors generally follow a series of steps beginning with the replica trick, which is the observation that n powers of the reduced density matrix ρ_V can be computed by evaluating the partition function on a Riemann surface obtained by gluing n copies of the theory together along the interval V . The entanglement entropy follows from analytic continuation of these results in n , followed by the limit $n \rightarrow 1$, according to the formula

$$\text{Tr}(\rho_V^n) = \frac{Z_n(V)}{Z_1^n}, \quad S_V = -\lim_{n \rightarrow 1} \frac{\partial}{\partial n} \frac{Z_n(V)}{Z_1^n}, \quad (5.70)$$

where $Z_n(V)$ is the n -sheeted partition function and Z_1 is the partition function of 1 sheet with no gluing, which is required for normalization.

In $1+1$ dimensions, the n -sheeted partition function can be viewed as a Riemann surface, and the holomorphic properties of this surface make the calculation tractable. In particular, if the interval has the boundary points x and y , the complicated world sheet topology can be mapped to the target space by defining multi-valued *twist fields* $\Phi_n(x), \Phi_n(y)$ on the plane whose boundary conditions implement the n -sheeted surface. One can find that $\text{Tr}(\rho_V^n)$ behaves exactly like the n^{th} power of a two point function of the twist fields, once their

conformal dimension has been determined using Ward identities:

$$\mathrm{Tr}(\rho_V^n) \sim \langle 0 | \Phi_n(x) \Phi_n(y) | 0 \rangle^n \sim \left(\frac{x-y}{\epsilon} \right)^{-\frac{c}{6}(n-\frac{1}{n})} \quad (5.71)$$

where c is the central charge and ϵ is a normalization constant from Z_1 . When $n = 1$ exactly, the twist fields have scaling dimension 0 and the above correlator no longer makes sense. Instead, taking the limit as $n \rightarrow 1$, the linear term is $-n \frac{c}{3} \ln \left(\frac{x-y}{\epsilon} \right)$. Taking the derivative gives the famous universal formula for the entanglement entropy [216].

The difficulty in performing the same calculation over the p -adics consists in fixing the dimensions of the twist operators. These operators can be defined just as in the normal case; after all, all that they do is implement certain boundary conditions at branch points on the fields in a theory of n free bosons. However, the usual arguments that fix their dimension rely on the existence of a uniformizing transformation $z \mapsto z^n$ that describes the relevant n -sheeted branched cover of \mathbb{P}^1 by \mathbb{P}^1 ; the Schwarzian of this holomorphic (but not Möbius) transformation then appears as the conformal dimension. The argument using the OPE with the stress tensor is identical in content. Both cases rely on the existence of holomorphic (but not fractional-linear) transformations, and a measure—the Schwarzian or conformal anomaly—of their “failure” to be Möbius.

In the p -adic case, this is related to the question of local conformal transformations; it has been suggested [192] that no such symmetries exist. Moreover, since \mathbb{Q}_p is not algebraically closed, a transformation like $z \mapsto z^n$ need not even be onto. Nevertheless, we can still define the twist operators, and we suppose that they transform as primaries with some conformal dimensions Δ_n . Their two-point function then gives the density matrix. This function is:

$$\langle 0 | \Phi_n^{(p)}(x) \Phi_n^{(p)}(y) | 0 \rangle^n \sim \left| \frac{x-y}{\epsilon} \right|_p^{-2n\Delta_n} \quad (5.72)$$

where Δ_n are the model-dependent (and unknown) conformal dimensions. Inserting this ansatz into $-\lim_{n \rightarrow 1} \frac{\partial}{\partial n} \mathrm{Tr}(\rho_V^n)$ and taking the limit $n \rightarrow 1$, $\Delta_n \rightarrow 0$ gives:

$$\left(2n \frac{\partial \Delta_n}{\partial n} \Big|_{n=0} \right) \ln \left| \frac{x-y}{\epsilon} \right|_p. \quad (5.73)$$

While this is not a proof, it provides some evidence for the expected logarithmic scaling of the entropy. We expect that the dimensions $\Delta_n \rightarrow 0$ as $n \rightarrow 1$,

since, of course, the twist operator on one sheet is just the identity. If we could fix the conformal dimension without using the conformal anomaly, this calculation would fix not only the logarithmic form of the answer, but also the coefficient that plays the role of the central charge. It may be possible to do this by examining the path integral with twist-operator insertions directly. As we have said, we propose an alternate model in Chapter 6 in which these entropies can be computed microscopically using tensor network techniques. A discussion of these results is found in Sec. 6.3.

Ryu–Takayanagi formula

Let us take as given the conjecture from the previous section that the entanglement entropy of a region in the boundary CFT should be computed as the logarithm of its p -adic size. We take our interval to be the smallest p -adic open ball which contains points x and y . This interval has size $|x - y|_p$. To understand the Ryu–Takayanagi formula, it remains to compute the length of the unique geodesic connecting x to y . The tree geometry for this setup is depicted in Fig. 5.6. Since there are an infinite number of steps required to reach the boundary, the geodesic length is formally infinite, just as in the real case. We regulate this by cutting off the tree at some finite tree distance a from the center C , which can be thought of as $\text{ord}_p(\epsilon)$ for some small p -adic number ϵ . We will then take this minimum number $\epsilon \rightarrow 0$ (p -adically). This limit will push the cutoff in the tree to infinite distance from C .

A $SL(2, \mathbb{Q}_p)$ transformation can always be used to move the points x and y to the \mathbb{Z}_p part of the tree first to simplify the argument. Then introducing the distance cutoff a effectively truncates the decimal expansions of x and y to the first a decimal places. In the case where $|x - y|_p = 1$, the geodesic connecting the two points passes through C and has length $2a$. If $|x - y|_p < 1$, the geodesic is shorter by a factor of $2d$, where $|x - y|_p = p^{-d}$. Roughly speaking, as can be seen in Fig. 5.6, smaller boundary regions are subtended by shorter geodesics in the tree.

We see that the cut-off-dependent distance is

$$d(x, y)_a = 2a + \frac{2}{\ln p} \ln |x - y|_p. \quad (5.74)$$

We would like to take $a \rightarrow \infty$. Up to the factor of $\ln p$, we can define a to be the logarithm of a p -adic cutoff ϵ such that $a \rightarrow \infty$ as $\epsilon \rightarrow 0$. Using this

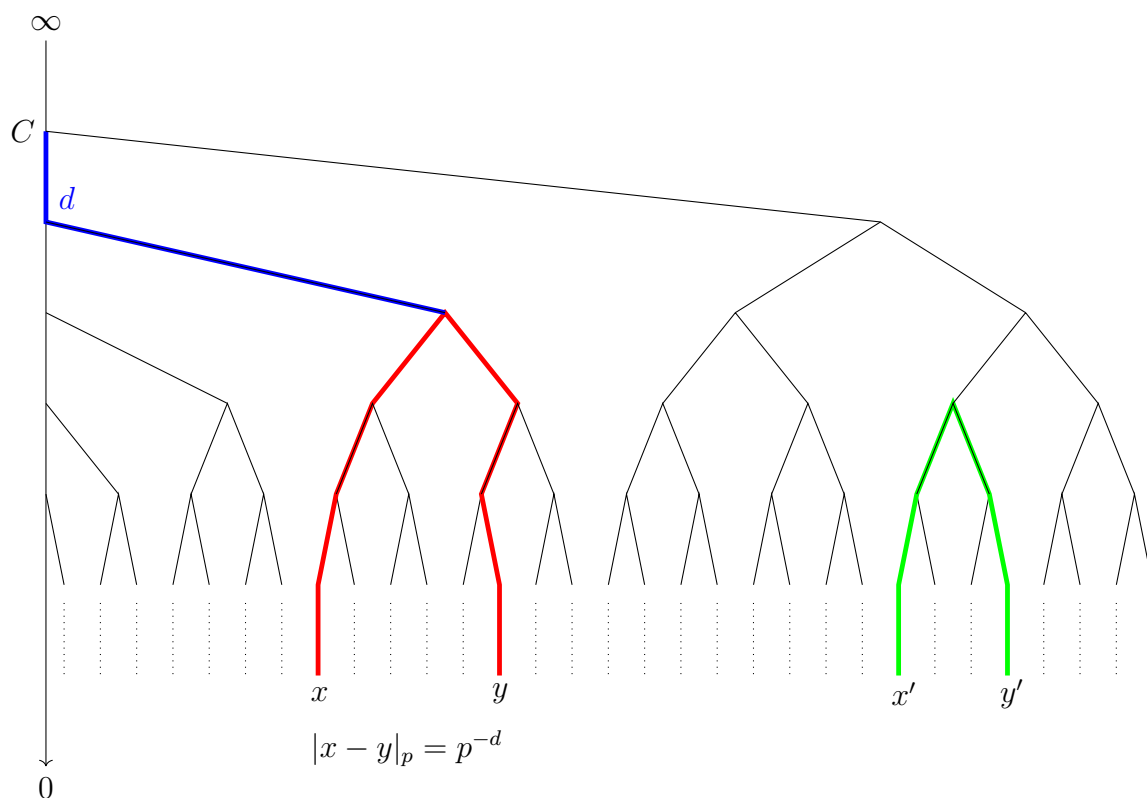


Figure 5.6: Boundary-anchored geodesics in T_p have a natural interpretation in terms of the p -adic norm. Once the arbitrary position of the center C is fixed, the norm of open sets in \mathbb{Q}_p is given by p^{-d} , where d is the integer number of steps from C required before the path to the endpoints splits. In this example, $|x - y|_p$ is described by the red geodesic and the value is p^{-2} . The set corresponding to the green geodesic has a smaller norm by a factor of p because the vertex is 1 step further down the tree. As in the case of real AdS, the length of the geodesic is formally infinite because an infinite number of steps is required to reach the boundary. One may introduce a cutoff corresponding to truncation of the tree at a fixed distance, then take the limit as this cutoff goes to zero. It should be apparent that the (formally infinite) red geodesic is longer than the green one by two steps. Up to constant factors, the length of any boundary-anchored geodesic is an infinite term minus d . This explains the logarithmically divergent scaling of geodesic length with p -adic norm.

definition, we find the length of a boundary-anchored geodesic to be

$$d(x, y) = \lim_{\epsilon \rightarrow 0} \frac{2}{\ln p} \ln \left| \frac{x - y}{\epsilon} \right|_p. \quad (5.75)$$

Up to the overall factor in front (which presumably depended on our choice of the length of each leg of the tree), we see the geodesic length is logarithmically divergent in interval size.

5.5 p -adic Bulk Geometry: Schottky Uniformization and Non-Archimedean Black Holes

Holography for Euclidean higher-genus black holes

The first explicit form of AdS/CFT correspondence for the asymptotically AdS₃ higher genus black holes, in the Euclidean signature, was obtained in [190], where the computation of the Arakelov Green function of [191] is shown to be a form of the holographic correspondence for these black holes, where the two-point correlation function for a field theory on the conformal boundary X_Γ is written in terms of gravity in the bulk \mathcal{H}_Γ , as a combination of lengths of geodesics.

At the heart of Manin's holographic formula lies a simple identity relating conformal geometry on $\mathbb{P}^1(\mathbb{C})$ and hyperbolic geometry on \mathbf{H}^3 , namely the fact that the cross ratio of four points on the boundary $\mathbb{P}^1(\mathbb{C})$ can be written as the length of an arc of geodesic in the bulk \mathbf{H}^3 . More precisely, consider the two point correlation function $g(A, B)$ on $\mathbb{P}^1(\mathbb{C})$. This is defined by considering, for a divisor $A = \sum_x m_x x$, the Green function of the Laplacian

$$\partial\bar{\partial}g_A = \pi i(\text{deg}(A)d\mu - \delta_A),$$

with δ_A the delta current associated to the divisor, $\delta_A(\varphi) = \sum_x m_x \varphi(x)$, and $d\mu$ a positive real-analytic 2-form. The Green function g_A has the property that $g_A - m_x \log |z|$ is real analytic for z a local coordinate near x , and is normalized by $\int g_A d\mu = 0$. For two divisors A, B , with A as above and $B = \sum_y n_y y$ the two point function is given by $g(A, B) = \sum_y n_y g_A(y)$. For degree zero divisors it is independent of the form $d\mu$ and is a conformal invariant. If w_A is a meromorphic function on $\mathbb{P}^1(\mathbb{C})$ with $\text{Div}(w_A) = A$, and C_B is a 1-chain with boundary B , the two point function satisfies

$$g(A, B) = \text{Re} \int_{C_B} \frac{dw_A}{w_A}.$$

For (a, b, c, d) a quadruple of points in $\mathbb{P}^1(\mathbb{C})$, the cross ratio $\langle a, b, c, d \rangle$ satisfies

$$\langle a, b, c, d \rangle = \frac{w_{(a)-(b)}(c)}{w_{(a)-(b)}(d)},$$

where $(a) - (b)$ is the degree zero divisor on $\mathbb{P}^1(\mathbb{C})$ determined by the points a, b , and the two point function is

$$g((a) - (b), (c) - (d)) = \log \frac{|w_{(a)-(b)}(c)|}{|w_{(a)-(b)}(d)|}.$$

Given two points a, b in $\mathbb{P}^1(\mathbb{C})$, let $\ell_{\{a,b\}}$ denote the unique geodesics in \mathbf{H}^3 with endpoints a and b . Also given a geodesic ℓ in \mathbf{H}^3 and a point $c \in \mathbb{P}^1(\mathbb{C})$ we write $c * \ell$ for the point of intersection between ℓ and the unique geodesic with an endpoint at c and intersecting ℓ orthogonally. We also write $\lambda(x, y)$ for the oriented distance of the geodesic arc in \mathbf{H}^3 connecting two given points x, y on an oriented geodesic. Then the basic holographic formula identifies the two point function with the geodesic length

$$g((a) - (b), (c) - (d)) = -\lambda(a * \ell_{\{c,d\}}, b * \ell_{\{c,d\}}).$$

One can also express the argument of the cross ratio in terms of angles between bulk geodesics (see [191, 190]). This basic formula relating the two point correlation function on the boundary to the geodesic lengths in the bulk is adapted to the higher genus cases by a suitable procedure of averaging over the action of the group that provides an explicit construction of a basis of meromorphic differentials on the Riemann surface X_Γ in terms of cross ratios on $\mathbb{P}^1(\mathbb{C})$. A basis of holomorphic differentials on X_Γ , with

$$\int_{A_k} \omega_{\gamma_j} = 2\pi i \delta_{jk}, \quad \int_{B_k} \omega_{\gamma_j} = \tau_{jk}$$

the period matrix, is given by

$$\omega_{\gamma_i} = \sum_{h \in S(\gamma_i)} d_z \log \langle z_h^+, z_h^-, z, z_0 \rangle,$$

for $z, z_0 \in \Omega_\Gamma$, with $S(\gamma)$ the conjugacy class of γ in Γ . The series converges absolutely when $\dim_H(\Lambda_\Gamma) < 1$. Meromorphic differentials associated to a divisor $A = (a) - (b)$ are similarly obtained as averages over the group action

$$\nu_{(a)-(b)} = \sum_{\gamma \in \Gamma} d_z \log \langle a, b, \gamma z, \gamma z_0 \rangle$$

and the Green function is computed as a combination $\nu_{(a)-(b)} - \sum_j X_j(a, b)\omega_{\gamma_j}$ with the coefficients $X_j(a, b)$ so that the B_k -periods vanish. Since in the resulting formula each crossed ratio term is expressible in terms of the length of an arc of geodesic in the bulk, the entire Green function is expressible in terms of gravity in the bulk space. We refer the reader to [190] and to [217] for a more detailed discussion and the resulting explicit formula of the holographic correspondence for arbitrary genus.

Holography on p -adic higher genus black holes

In the special case of a genus-one curve, the relevant Schottky group is isomorphic to $q^{\mathbb{Z}}$, for some $q \in \mathbf{k}^*$, and the limit set consists of two points, which we can identify with 0 and ∞ in $\mathbb{P}^1(\mathbf{k})$. The generator of the group acts on the geodesic in $T_{\mathbf{k}}$ with endpoints 0 and ∞ as a translation by some length $n = \log|q| = v_{\mathbf{m}}(q)$, the valuation. The finite graph $G_{\mathbf{k}}$ is then a polygon with n edges, and the graph $T_{\mathbf{k}}/\Gamma$ consists of this polygon with infinite trees attached to the vertices. The boundary at infinity of $T_{\mathbf{k}}/\Gamma$ is a Mumford curve $X_{\Gamma}(\mathbf{k})$ of genus one with its p -adic Tate uniformization. The graph $T_{\mathbf{k}}/\Gamma$ is the p -adic BTZ black hole, with the central polygon $G_{\mathbf{k}}$ as the event horizon. The area of the black hole and its entropy are computed by the length of the polygon (see Fig. 5.7).

The higher genus cases are p -adic versions of the higher genus black holes discussed above, with the finite graph $G_{\mathbf{k}}$ as event horizon, and its geodesic length proportional to the black hole entropy.

Given a set of generators $\{\gamma_1, \dots, \gamma_g\}$ of a p -adic Schottky group, let n_{γ_i} be the translation lengths that describe the action of each generator γ_i on its axis ℓ_{γ_i} . More precisely, if an element γ is conjugate in $\mathrm{PGL}(2, \mathbf{k})$ to an element of the form

$$\begin{pmatrix} q & 0 \\ 0 & 1 \end{pmatrix},$$

then the translation length is $n_{\gamma} = v_{\mathbf{m}}(q) = \mathrm{ord}_{\mathbf{k}}(q)$, the order (valuation) of q . The translation lengths $\{n_{\gamma_i}\}$ are the Schottky invariants of the p -adic Schottky group Γ . It is shown in [218] that the Schottky invariants can be computed as a spectral flow.

The Drinfeld–Manin holographic formula of [201] for p -adic black holes of arbitrary genus is completely analogous to its Archimedean counterpart of

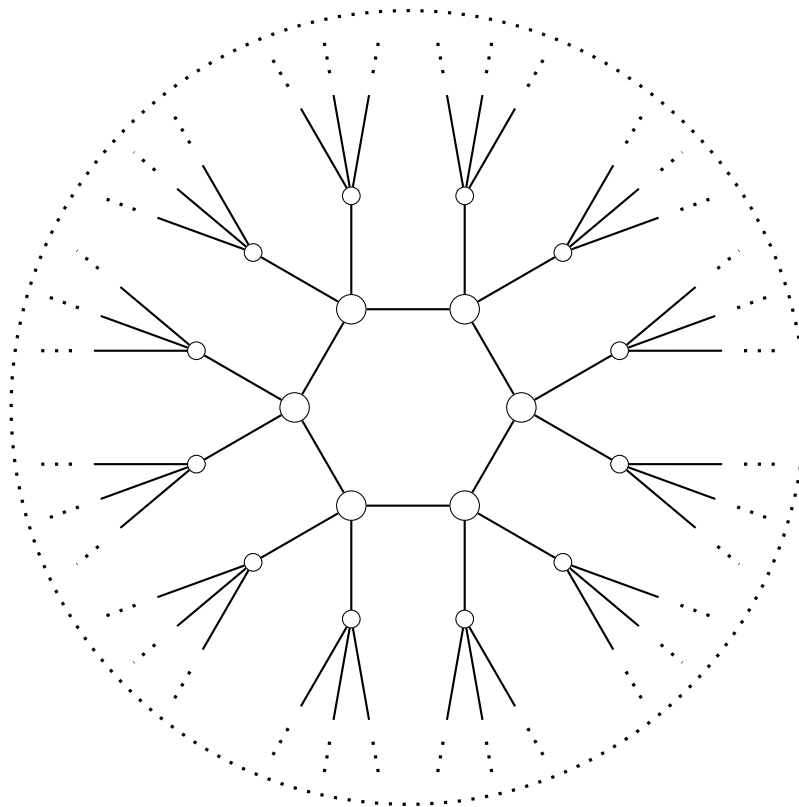


Figure 5.7: The p -adic BTZ black hole, reproduced from 1.4. (As pictured, $p = 3$).

[191]. There is a good notion of \mathbf{k} -divisor on $\mathbb{P}^1(\mathbf{k})$, as a function $\mathbb{P}^1(\bar{\mathbf{k}}) \rightarrow \mathbb{Z}$, with $z \mapsto m_z$, with the properties that $m_{z_1} = m_{z_2}$ if z_1 and z_2 are conjugate over \mathbf{k} ; that all points z with $m_z \neq 0$ lie in the set of points of \mathbb{P}^1 over a finite extension of \mathbf{k} ; and that the set of points with $m_z \neq 0$ has no accumulation point. As before we write such a divisor as $A = \sum_z m_z z$. Given a Γ -invariant divisor A of degree zero, there exists a meromorphic function on $\Omega_\Gamma(\mathbf{k})$ with divisor A . It is given by a Weierstrass product

$$W_{A,z_0} = \prod_{\gamma \in \Gamma} \frac{w_A(\gamma z)}{w_A(\gamma z_0)},$$

where $w_A(z)$ is a \mathbf{k} -rational function on $\mathbb{P}^1(\mathbf{k})$ with divisor A . The convergence of this product is discussed in Proposition 1 of [201]: the non-Archimedean nature of the field \mathbf{k} implies that the product converges for all $z \in \Omega_\Gamma \setminus \cup_\gamma \gamma(\text{supp}(A))$. The function W_{A,z_0} is a p -adic automorphic function (see [219]) with $W_{A,z_0}(\gamma z) = \mu_A(\gamma) W_{A,z_0}(z)$, with $\mu_A(\gamma) \in \mathbf{k}^*$, multiplicative in A and γ . One obtains a basis of Γ -invariant holomorphic differentials on $X_\Gamma(\mathbf{k})$ by taking

$$\omega_{\gamma_i} = d \log W_{(\gamma_i^{-1})z_0, z_1},$$

where

$$W_{(\gamma-1)z_0, z_1}(z) = \prod_{h \in C(\gamma)} \frac{w_{hz_\gamma^+ - hz_\gamma^-}(z)}{w_{hz_\gamma^+ - hz_\gamma^-}(z_0)},$$

for $C(g)$ a set of representatives of $\Gamma/\gamma^{\mathbb{Z}}$.

It is shown in [201] that the order of the cross ratio on $\mathbb{P}^1(\mathbf{k})$ is given by

$$\text{ord}_{\mathbf{k}} \frac{w_A(z_1)}{w_A(z_2)} = \#\{\ell_{z_1, z_2}, \ell_{a_1, a_2}\},$$

for $A = a_1 - a_2$ and $\ell_{x,y}$ the geodesic in the Bruhat–Tits tree with endpoints $x, y \in \mathbb{P}^1(\mathbf{k})$, with $\#\{\ell_{z_1, z_2}, \ell_{a_1, a_2}\}$ the number of edges in common to the two geodesics in $T_{\mathbf{k}}$. This is the basic p -adic holographic formula relating boundary two point function to gravity in the bulk.

A difference with respect to the Archimedean case is that, over \mathbb{C} , both the absolute value and the argument of the cross ratio have an interpretation in terms of geodesics, with the absolute value expressed in terms of lengths of geodesic arcs and the argument in terms of angles between geodesics, as recalled above. In the p -adic case, however, it is only the valuation of the two point correlation function that has an interpretation in terms of geodesic lengths in the Bruhat–Tits tree. The reason behind this discrepancy between the Archimedean and non-Archimedean cases lies in the fact that the Bruhat–Tits tree $T_{\mathbf{k}}$ is the correct analog of the hyperbolic handlebody \mathbf{H}^3 only for what concerns the part of the holographic correspondence that involves the absolute value (respectively, the p -adic valuation) of the boundary two point function. There is a more refined p -adic space, which maps surjectively to the Bruhat–Tits tree, which captures the complete structure of the p -adic automorphic forms for the action of a p -adic Schottky group Γ : Drinfeld’s p -adic upper half plane, see Chapter I of [220]. Given \mathbf{k} as above, let \mathbb{C}_p denote the completion of the algebraic closure of \mathbf{k} . Drinfeld’s p -adic upper half plane is defined as $\mathbf{H}_{\mathbf{k}} = \mathbb{P}^1(\mathbb{C}_p) \setminus \mathbb{P}^1(\mathbf{k})$. One can view this as an analog of the upper and lower half planes in the complex case, with $\mathbf{H}^+ \cup \mathbf{H}^- = \mathbb{P}^1(\mathbb{C}) \setminus \mathbb{P}^1(\mathbb{R})$. There is a surjection $\lambda : \mathbf{H}_{\mathbf{k}} \rightarrow T_{\mathbf{k}}$, defined in terms of the valuation, from Drinfeld’s p -adic upper half plane $\mathbf{H}_{\mathbf{k}}$ to the Bruhat–Tits tree $T_{\mathbf{k}}$. For vertices $v, w \in V(T_{\mathbf{k}})$ connected by an edge $e \in E(T_{\mathbf{k}})$, the preimages $\lambda^{-1}(v)$ and $\lambda^{-1}(w)$ are open subsets of $\lambda^{-1}(e)$, as illustrated in Fig. 5.8. The map $\lambda : \mathbf{H}_{\mathbf{k}} \rightarrow T_{\mathbf{k}}$ is equivariant with respect to the natural actions of $\text{PGL}(2, \mathbf{k})$ on $\mathbf{H}_{\mathbf{k}}$ and on $T_{\mathbf{k}}$. In particular, given a p -adic Schottky group $\Gamma \subset \text{PGL}(2, \mathbf{k})$, we can

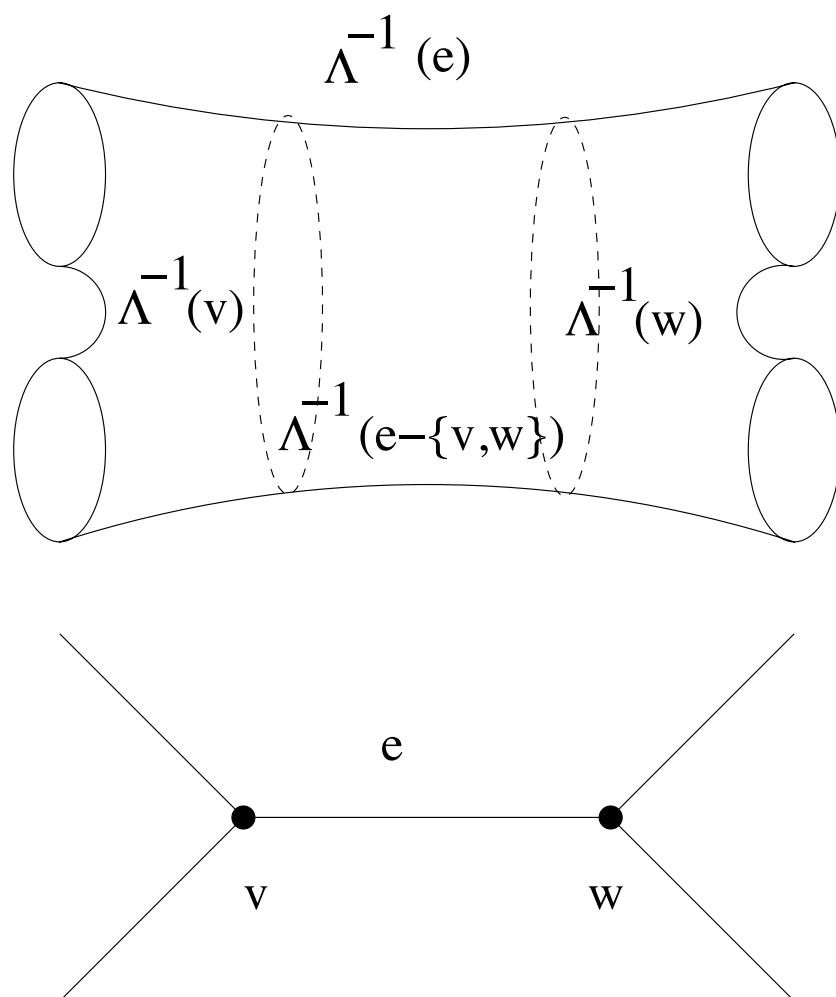


Figure 5.8: Drinfeld’s p -adic upper half plane and the Bruhat–Tits tree.

consider the quotients $\tilde{\mathcal{H}}_\Gamma = \mathbf{H}_k/\Gamma$ and $\mathcal{H}_\Gamma = T_k/\Gamma$ and the induced projection $\lambda : \tilde{\mathcal{H}}_\Gamma \rightarrow \mathcal{H}_\Gamma$. Both quotients have conformal boundary at infinity given by the Mumford curve $X_\Gamma = \Omega_\Gamma(\mathbf{k})/\Gamma$, with $\Omega_\Gamma(\mathbf{k}) = \mathbb{P}^1(\mathbf{k}) \setminus \Lambda_\Gamma$, the domain of discontinuity of the action of Γ on $\mathbb{P}^1(\mathbf{k}) = \partial\mathbf{H}_k = \partial T_k$. One can view the relation between \mathbf{H}_k and T_k illustrated in Fig. 5.8, and the corresponding relation between $\tilde{\mathcal{H}}_\Gamma$ and \mathcal{H}_Γ , by thinking of $\tilde{\mathcal{H}}_\Gamma$ as a “thickening” of the graph \mathcal{H}_Γ , just as in the Euclidean case one can view the union of the fundamental domains of the action of Γ on \mathbf{H}^3 , as illustrated in Fig. 5.4, as a thickening of the Cayley graph (tree) of the Schottky group Γ , embedded in \mathbf{H}^3 .

Thus, when considering the non-Archimedean holographic correspondence and p -adic black holes of arbitrary genus, one can choose to work with either \mathcal{H}_Γ

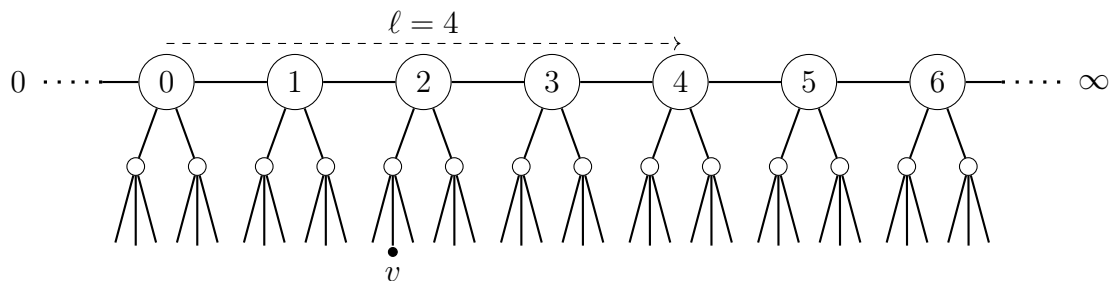


Figure 5.9: The action of a rank-one Schottky group (translation by ℓ along a fixed geodesic) on the Bruhat–Tits tree. As pictured, $n = h = 2$.

or with $\tilde{\mathcal{H}}_\Gamma$ as the bulk space, the first based on Bruhat–Tits trees and the second (more refined) based on Drinfeld’s p -adic upper half spaces. In this chapter we will be focusing on those aspects of the non-Archimedean AdS/CFT correspondence that are captured by the Bruhat–Tits tree, while a more refined form of non-Archimedean holography, based on Drinfeld’s p -adic upper half planes, is an interesting possible generalization.

Scalars on higher-genus backgrounds: sample calculation

In light of this discussion of higher-genus holography in the p -adic case, it is easy to understand how to generalize the arguments and calculations we discussed for scalar fields in Sec. 5.3 to the BTZ black hole, or to higher-genus hyperbolic handlebodies, the p -adic analogs of Krasnov’s Euclidean black holes. One can simply think of the higher-genus geometry as arising from the quotient of the tree T_p (and its boundary $\mathbb{P}^1(\mathbb{Q}_p)$) by the action of a rank- g Schottky group. Any quantity that can then be made equivariant under the action of the Schottky group will then descend naturally to the higher-genus setting.

As a simple example, it is easy to construct the genus-1 analog of our basic Green’s function (5.45), using the method of images. We perform this calculation in the following paragraphs. The result makes it easy to perform the reconstruction of bulk solutions to the equations of motion in a BTZ background, with specified boundary conditions at infinity along the genus-1 conformal boundary.

Without loss of generality, we can label the distance along the geodesic which is translated by the chosen Schottky generator by integers, and imagine that the source is attached at a boundary point x connected to the vertex 0. The bulk vertex v at which we want to evaluate the Green’s function will be attached

to vertex n ($0 \leq n < \ell$), at a depth h from the central geodesic. The quantity to be calculated is simply

$$\varepsilon_{\kappa,x}^{(g=1)}(v) = \sum_{g \in \mathbb{Z}} p^{\kappa \langle v, gx \rangle}, \quad (5.76)$$

where the sum ranges over the images of x under the Schottky group. We take the integrand to be normalized to 1 at the vertex where the branch containing x meets the central geodesic. The cases $n = 0$ and $n \neq 0$ are different, and we will treat them separately.

$n = 0$: In this case, the sum becomes

$$\begin{aligned} \varepsilon_{\kappa,x}(v) &= p^{\kappa \langle v, x \rangle} + 2 \sum_{m>0} (p^{-\kappa \ell})^m \\ &= p^{\kappa \langle v, x \rangle} + \frac{2p^{-\kappa h}}{p^{\kappa \ell} - 1}. \end{aligned} \quad (5.77)$$

$n \neq 0$: In this case, the sum becomes

$$\begin{aligned} \varepsilon_{\kappa,x}(v) &= \sum_{m \leq 0} p^{\kappa(-n-h-|m|\ell)} + \sum_{m > 0} p^{\kappa(n-h-m\ell)} \\ &= p^{-\kappa h} \left(\frac{p^{\kappa(\ell-n)} + p^{\kappa n}}{p^{\kappa \ell} - 1} \right). \end{aligned} \quad (5.78)$$

In both cases, the result has the expected boundary behavior: it falls off asymptotically as $p^{-\kappa h}$ when v approaches any boundary point other than x itself.

5.6 Conclusion

In this chapter we have proposed an algebraically motivated way to discretize the AdS/CFT correspondence. The procedure of replacing real or complex spacetimes by \mathbb{Q}_p introduces a nontrivial discrete bulk and boundary structure while still preserving many desirable features of the correspondence. The boundary conformal field theory lives on an algebraic curve in both the ordinary and non-Archimedean examples; the $\mathbb{P}^1(\mathbb{Q}_p)$ theory naturally enjoys the p -adic analog of the familiar global conformal symmetry, $\mathrm{PGL}(2, \mathbb{Q}_p)$. This same group comprises the isometries of the lattice bulk spacetime $T_p = \mathrm{PGL}(2, \mathbb{Q}_p) / \mathrm{PGL}(2, \mathbb{Z}_p)$, a maximally symmetric coset space analogous to Euclidean AdS.

In analogy with the BTZ black hole and higher genus examples in AdS_3 , higher genus bulk spaces in the p -adic case are obtained by Schottky uniformization. One takes quotients of the geometry by p -adic Schottky groups $\Gamma \subset \text{PGL}(2, \mathbb{Q}_p)$, producing Mumford curves at the boundary. These curves holographically correspond to bulk geometries consisting of discrete black holes, which appear automatically and do not need to be put in by hand.

We then turned our attention to continuous Hilbert spaces of scalar fields in the tree. In the semiclassical analysis, massless and massive scalar solutions to the lattice model couple naturally to CFT operators at the boundary, just as in the Archimedean case. We identified boundary/bulk propagators in the discrete analog of empty AdS, as well as in the p -adic BTZ black hole; the method of images can be used to generalize these results to arbitrary higher-genus bulk backgrounds. We are led to believe that the semiclassical physics of the bulk “gravity” theory is dual to an exotic conformal field theory living on the fractal p -adic boundary. At the present time, little is known about these p -adic conformal field theories outside of p -adic string theory; we hope the connection to holography may draw attention to this area. Viewed as a renormalization scale, we have shown that moving up the tree corresponds to exact course graining of boundary mode expansions. The intimate relation between conformal symmetry, AdS geometry, and renormalization still holds in this entirely discrete setting.

We also suggest that the entanglement entropy of regions of the field theory is computed by the unique geodesic lengths in the bulk space. While as of yet we have no formal proof in the free-boson field theory, a number of arguments have been presented which support this conjecture. Chapter 6 is concerned with a concrete p -adic tensor network model in which it is possible to compute the entanglement entropy exactly and match it to the RT formula.

While we have established some essential features of p -adic holography, ranging from algebraic curves to tensor networks and from bulk/boundary propagators and renormalization scales to entanglement, much about these exotic systems remains to be understood. We propose a number of ideas to be explored in future work.

One major ingredient missing from our story is a proper description of (and quantization of) the gravitational degrees of freedom. The bulk geometries (with or without black holes in the interior) can loosely be described as p -adic

discretizations of asymptotically AdS spacetimes. One way to add dynamical metric degrees of freedom without spoiling the asymptotic behavior might be to make the edge lengths of the Bruhat–Tits tree dynamical. This essential idea was the subject of [7], which proposes an edge length model with some features of dilaton gravity.

From the point of view of the p -adic CFT, one might ask for more interesting examples than the free boson. We have already offered some speculations about higher spin fields based on representation theory of the p -adic conformal group, and subsequent work [6, 91] has demonstrated the existence of interesting p -adic fermion theories. Additionally, the models we have studied so far do not appear to have extended conformal symmetry or a central charge. These important ingredients of 1+1 dimensional CFT's might appear with the more careful inclusion of finite extensions of \mathbb{Q}_p . These finite extensions might also be linked to the passage to Lorentzian signature. Finally, it remains to be seen how much can be learned about real AdS/CFT from studying these systems adelically over every prime.

NON-ARCHIMEDEAN HOLOGRAPHIC ENTROPY AND TENSOR NETWORKS

6.1 Introduction

In Chapter 5, we introduced a discretized version of the AdS/CFT correspondence by defining lattice field theory models based on the p -adic numbers, \mathbb{Q}_p . On the CFT side, we took the ‘spacetime’ to be the p -adic projective line, $\mathbb{P}^1(\mathbb{Q}_p)$. This forms a continuum with respect to the p -adic norm and has discrete versions of conformal transformations. Correlation functions of local operators have power law behavior, and the conformal field theories are relatively simple due to the lack of CFT descendants. On the bulk side is the Bruhat–Tits tree of $\mathrm{SL}(2, \mathbb{Q}_p)$, an infinite tree of uniform valence whose boundary is the p -adic projective line. Scalar field dynamics on this tree compute the CFT correlators.

The purpose of this chapter is to focus on the tensor network approach to holography, and in particular on holographic states generated by networks of perfect tensors as in [99]. Like the Bruhat–Tits tree, tensor networks are generally discrete and provide simplified models to study bulk and boundary entanglement properties. In fact one is tempted to view the Bruhat–Tits tree itself as a tensor network [87, 221], or closely related to a tensor network [4]; however these models were unsuccessful in reproducing the RT formula or various expected entropy inequalities in the p -adic setting, so the question of whether entanglement entropy results familiar from the usual real holography hold over the p -adics has remained open.

In this chapter, we present a simple model of holographic quantum error correction in the p -adic setting based on the existence of an infinite class of perfect tensors which can be used to build networks associated with the bulk geometry; either the Bruhat–Tits tree or its black hole variant. The tensor networks we use are closely related to those of [99] based on hyperbolic tessellations; in the simplest case of vacuum AdS this is described by the Schläfli symbol $\{m, n\}$ and the associated tensor network $\{n, m\}$. Heuristically, in our model we study the limit in which the Schläfli symbols of the associated bulk geometry and the

dual tensor network tend to $\{\infty, p+1\}$ and $\{p+1, \infty\}$, respectively. The subtleties associated with the p -adic interpretation of such tensor networks built from perfect tensors of rank tending to infinity are discussed at length in this chapter. We emphasize, however, that the genus 1 black hole tensor networks we consider are fundamentally different from those proposed in [99], and are instead obtained via a physically well-motivated quotient procedure.

This model addresses a number of shortcomings of previous approaches to tensor network holography and allows for the explicit analytic computation of holographic states, density matrices, and entropies. While this model is discrete and preserves a (finite) group of conformal symmetries at finite cutoff, we see a full restoration of conformal symmetry as the cutoff is taken to zero, in the form of the p -adic fractional linear transformations $\text{PGL}(2, \mathbb{Q}_p)$, which we interpret as the conformal group acting on a spatial region of the boundary. This group acts by isometries on the Bruhat–Tits tree, thought of as the analog of a time slice of AdS_3 . The tensor network inherits the symmetries, and is essentially related to minimal geodesics of the Bruhat–Tits tree. Additionally, while the network is defined and manipulated in the bulk space, all quantities we compute can ultimately be defined or described in terms of purely boundary data such as configurations of points and sets on $\mathbb{P}^1(\mathbb{Q}_p)$ or the genus one curve.

Given a choice of prime number p and choice of bulk IR cut off, there is essentially a single network defined for each bulk space which generates a highly entangled state of boundary qudits, interpreted as the analog of a vacuum state of a boundary conformal field theory. Equipped with the p -adic analogs of various quantities and the knowledge of how to manipulate perfect tensors, we are able to explicitly compute non-Archimedean entanglement entropies for connected and disconnected intervals; the results are dual to minimal surfaces in the bulk, as expected from the Ryu–Takayanagi formula. We also compute the black hole entropy and find that it is proportional to the perimeter of the p -adic BTZ black hole, as expected according to the Bekenstein–Hawking formula, and verify the RT formula, which equates the von Neumann entropy of reduced density matrices obtained from mixed states on the boundary to the lengths of minimal geodesics in the p -adic black hole background homologous to boundary regions. We also give a holographic derivation of subadditivity, strong subadditivity, and the monogamy of mutual information in the p -adic setting. In the limit of an infinite network, all of these results can be phrased

in terms of conformally invariant information on the boundary, where the ultrametric geometry plays an essential simplifying role. Another interesting feature is our use of graphical tools to perform bulk computations; essentially all entropy quantities can be obtained by geometric operations such as cutting, gluing, and tracing the discrete vertices and bonds of the network. Among other things, this leads to the interpretation of a thermal density as being dual to a two-sided AdS black hole obtained by gluing two bulk regions together.

We construct the network of perfect tensors associated to the Bruhat–Tits tree as follows. Rather than placing the tensors at the nodes of the Bruhat–Tits tree as previously suggested, we identify two explicit conditions for the construction of an appropriate “dual graph” on which the tensor network lives. While this at first appears to require an embedding of a non-Archimedean bulk space into an ordinary Archimedean plane, we argue that the results are independent of the embedding. The two main conditions required for the construction of the tensor network are that the sets of edges of the Bruhat–Tits tree and its dual graph are in one-to-one correspondence, with an edge of the dual graph cutting exactly one edge of the Bruhat–Tits tree and that the arrangements of dual graph edges around each vertex of the Bruhat–Tits tree form “plaquettes,” i.e., admit a cyclic ordering. Any construction of a dual graph that satisfies these properties can be used for the purpose of von Neumann entropy computations.

In trying to capture holographic states, perfect tensors have appeared as a convenient way of generating maximally entangled states. We offer a refined point of view on perfect tensors, which was already partially outlined in [4] and [221]. Starting with classical error-correcting codes in the form of Reed–Solomon codes built over projective lines over finite fields [222], one may upgrade these to quantum codes by applying the CRSS algorithm [223], which we show can be generalized to directly obtain perfect tensors from certain self-orthogonal codes. These self-orthogonal codes are Lagrangian subspaces of symplectic vector spaces over finite fields; they can thus be thought of as analogous to semiclassical states, and the theory of the Heisenberg group over finite fields can be used to quantize them, replacing the equations defining the Lagrangian by operator equations (or eigenvalue problems) and producing the corresponding quantum codes.

This chapter is somewhat extensive, with many interdependent parts. It is

helpful now to give a concise summary of the main results presented in this chapter, followed by a more detailed organization. While Chapter 5 of this thesis serves as motivation for this chapter, we have chosen to keep the presentation self contained due to ease of notation and conventions. There will naturally be some overlap with previous sections. Additionally, some of the main mathematical results which appeared in the original paper [5] have been omitted. We focus on the basic physical setup of the tensor network model based on our theme of projective geometry. We direct an interested reader to the paper for rigorous proofs of some statements and more details on the formalism.

Summary of the main results

We show that for static holographic states built through a network of perfect tensors dual to the p -adic Bruhat–Tits tree (both when the boundary is the “infinite line” \mathbb{Q}_p and when it is the projective line $\mathbb{P}^1(\mathbb{Q}_p)$), the bipartite entanglement entropy of a single connected interval as well as disconnected intervals obeys a Ryu–Takayanagi like formula. The perfect tensors may be viewed as built via the CRSS algorithm from algebro-geometric codes on projective lines over finite fields. The construction of the codes is not crucial to our setup, but their existence and error correcting properties guarantee our results. The entanglement is computed by constructing the holographic state, tracing out regions of the tensor network, and explicitly computing the reduced density matrices and the von Neumann entropy, which is expressed in terms of (regularized) lengths of minimal geodesics in the bulk Bruhat–Tits tree. We also prove subadditivity, strong subadditivity and monogamy of mutual information in this setup.

We then construct p -adic BTZ black holes as quotients of the Bruhat–Tits tree by a rank-one Schottky group with boundary a Mumford–Tate elliptic curve, and demonstrate that the construction of the tensor network adapts naturally to this case. Essentially the tensor network is obtained as a quotient of the genus 0 tensor network, paralleling the quotient construction of the geometry. Instead of a pure state at the boundary one has in this case a vertex behind the horizon that needs to be traced out, which results in a thermal density matrix with a Bekenstein–Hawking entropy measured in terms of the length of the horizon (the polygon in the quotient of the Bruhat–Tits tree). This density matrix can be seen to be dual to a bulk geometry with two

asymptotic regions connected by the analog of a two-sided black hole, with the entropy given by the number of tensor bonds suspended between the two sides. We also prove that the entanglement entropy satisfies an analog of the Ryu–Takayanagi formula in this geometry in terms of the minimal length of homologous geodesics in the black hole background.

Organization of this Chapter

In Section 6.2 we review some basic background material that we will be using throughout the chapter, extending the discussion of Chapter 5. Section 6.2 gives the minimal background on the geometry of the p -adic Bruhat–Tits trees, which serve as our bulk spaces in the rest of the chapter. A discussion of quotients of Bruhat–Tits trees by p -adic Schottky groups is given later, in Section 6.4. In Section 6.2 we briefly review networks of perfect tensors and maximally entangled states. Section 6.2 recalls several facts about classical and quantum codes that we will be using in the rest of the chapter, with particular focus on the CRSS algorithm that promotes classical to quantum error correcting codes, which we describe in terms of Heisenberg group representations. We review in particular the classical algebro-geometric codes associated to the projective line over a finite field (the Reed–Solomon codes), and we show that they can be used to construct, through the CRSS algorithm, quantum codes given by perfect tensors. An explicit example is illustrated in Appendix D.1.

In Section 6.3 we present the main results on our construction of a quantum error-correcting tensor network, built using perfect tensors, associated to the p -adic Bruhat–Tits trees via a “dual graph” construction, and we establish the p -adic analog of the Ryu–Takayanagi formula. Section 6.3 describes the construction of the “dual graph” tensor network associated to the p -adic Bruhat–Tits trees by identifying two axiomatic properties that characterize the network in relation to the tree. As discussed more in detail in Section 6.6, different choices satisfying these properties are possible, which can be characterized in terms of different choices of embeddings. For the purpose of the entanglement entropy computation any such choice of a “dual graph” will achieve the desired result. We also describe the perfect tensors associated to the nodes of the dual graph for a finite cutoff of the infinite Bruhat–Tits tree, the number of dangling (uncontracted) legs at the vertices and the resulting boundary wavefunction. The rank of the perfect tensors is related to the cutoff

on the tree and goes to infinity in the limit of the infinite tree. In Section 6.3 we summarize the main technical results in the genus 0 background, that the dual graph tensor network satisfies a Ryu–Takayanagi like formula, where instead of “intervals” we specify the boundary datum in terms of configurations of points (though we still use the terminology “connected interval” or “disconnected interval”). We show that the von Neumann entropy computation matches what is expected for CFT_2 and that it is naturally expressed in terms of the p -adic norm, which leads to the expected bulk interpretation (consistent with the minimal cut rule obeyed by perfect tensor networks [99]) as the length of the minimal geodesic joining the entangling surfaces determined by the chosen configuration of boundary points. We also comment on the disconnected interval (four points) entropy case, the dependence of the mutual information on the cross-ratio and entropy inequalities such as subadditivity, strong subadditivity and monogamy of mutual information, where the ultrametric property plays a direct, simplifying role, the details of which are found in Sections 6.5–6.5.

Section 6.4 deals with the p -adic BTZ black hole, described in terms of Mumford–Tate elliptic curves as boundary and with bulk space a quotient of the p -adic Bruhat–Tits tree by a rank one Schottky group. In Section 6.4 we review the p -adic geometry of Mumford curves of genus one and the associated bulk spaces, comparing it with the case of complex elliptic curves with Tate uniformization by the multiplicative group. We also explain how to adapt our construction of the tensor network as dual graph of the Bruhat–Tits tree to a network similarly dual to the homologically non-trivial quotient of the Bruhat–Tits tree in the genus one case. In particular, the tensor network obtained in this way has a vertex beyond the black hole horizon that does not correspond to boundary degrees of freedom. In Section 6.4 we come to our main results in the BTZ black hole case. Computing on the tensor network the thermal entropy of the boundary density matrix obtained by tracing out this special vertex gives the black hole horizon perimeter, which can be seen as a Bekenstein–Hawking formula for the p -adic BTZ black hole. In Section 6.4 we discuss the Ryu–Takayanagi formula in genus one backgrounds, with the boundary entanglement entropy of a single interval corresponding to the length of a minimal geodesic in the bulk black hole geometry. Unlike the genus zero case, the entropy of a boundary region and its complement are not necessarily the same, corresponding to the fact that the boundary state is no longer pure, and in

the bulk geometry a geodesic may wrap around the loop of the quotient graph (the black hole horizon).

Section 6.5 contains all the detailed explicit computations used in Section 6.3 and Section 6.4 for obtaining the von Neumann entropy via the density matrices determined by the tensor network. Section 6.5 illustrates the rules for the computation of states and reduced density matrices from perfect tensors, and the graphical calculus used to keep track of contractions, and a convenient representation of the resulting density matrices in block-diagonal form. We describe how to obtain the reduced density matrices corresponding to tracing out regions determined by sets of vertices of the tensor network, and we compute the associated von Neumann entropy. In Section 6.5 we discuss the computation of the inner product of the holographic state with itself. The computation method is described in terms of certain graphical contraction rules (“splits”), decomposing the network into disjoint simple curves; each resulting closed cycle then determines an overall multiplicative factor. Section 6.5 then contains the computation of the norm of the holographic state obtained from our tensor network dual to the Bruhat–Tits tree, with an assigned cutoff on the infinite tree. This depends on different types of vertices (in terms of number of dangling legs) and the corresponding multiplicities and the application of the “splits and cycles” method. In Section 6.5 we then show how a Ryu–Takayanagi like formula is obeyed exactly in the single connected interval (“two point”) case. The entanglement of a boundary region with its complement is computed by computing the density matrix of the full holographic state produced by the tensor network and then computing a partial trace using the computational techniques developed in the previous subsections. The result is then compared with the (regulated) geodesic length in the bulk Bruhat–Tits tree.

The disconnected interval case (in particular the “four point” case) is discussed in Section 6.5 in terms of overlapping or non-overlapping geodesics in the bulk, depending on the sign of the logarithm of the cross-ratio, and the corresponding properties of the mutual information. We show subadditivity (both Araki–Lieb inequality as well as non-negativity of mutual information) and give the exact dependence of mutual information on the cross-ratio constructed from the boundary points. We show that a Ryu–Takayanagi like formula is satisfied exactly for disconnected intervals, and in Section 6.5 we proceed to prove

strong subadditivity and monogamy of mutual information. In fact, we show that in this tensor network mutual information is exactly extensive.

Section 6.5 contains the computation of the black hole entropy as well as the Ryu–Takayanagi formula for the minimal geodesics in the black hole background. Using tools from the previous sections, the norm of the black hole boundary state is computed in terms of types of vertices and multiplicities, and the density matrix and corresponding von Neumann entropy is determined. This entropy is seen to be proportional to the length of the horizon or the length of the minimal geodesic homologous to the boundary interval, where the homologous condition, an important feature of the RT formula, is obeyed automatically by the tensor network.

Section 6.6 further discusses some of the geometric aspects of our tensor network construction. In Section 6.6 we discuss more in detail the symmetry properties of the tensor networks with respect to the global symmetries of the Bruhat–Tits tree, showing how the properties needed for the construction of a suitable “dual graph” reduce the symmetries and obtaining in this way a characterization of all the possible choices of dual graph. We also discuss the construction of measures on the Mumford–Tate curve induced from the Patterson–Sullivan measure on the p -adic projective line.

Finally, a list of possible further directions of investigation and open questions is given in Section 6.7.

6.2 Background

The Bruhat–Tits tree as a p -adic bulk space

Let us briefly recall the setup of p -adic AdS/CFT which was discussed in Chapter 5. We review this here from a somewhat different viewpoint and establish the notation and the physical interpretation to be used in this chapter. Readers familiar with the construction of the previous chapter may wish to skip ahead.

In the simplest formulation, the bulk geometry is described by an infinite $(p + 1)$ -regular graph (without cycles), called the Bruhat–Tits tree, and its asymptotic boundary is given by the projective line over the p -adic numbers, $\mathbb{P}^1(\mathbb{Q}_p)$. (For an introduction to the theory of p -adic numbers, see [194, 224]; a shorter discussion in the physics literature can be found in e.g. [83].) The Bruhat–Tits tree \mathcal{T}_p is a discrete, maximally symmetric space of constant neg-

ative curvature, which plays the role of (Euclidean) AdS space. One can study perturbative bulk dynamics on the tree by considering lattice actions defined on its nodes (or bonds) [84, 4, 7]. A central result of these works is that semi-classical dynamics of these lattice models in the bulk \mathcal{T}_p compute correlation functions in a dual conformal field theory defined on $\mathbb{P}^1(\mathbb{Q}_p)$.

In the following, we will view the Bruhat–Tits tree as a constant-time spatial slice of a higher-dimensional p -adic analog of Lorentzian AdS space. To make the analogy with the real setup more concrete, we view the Bruhat–Tits tree as the p -adic analog of the Poincaré disk (or equivalently the hyperbolic plane \mathbb{H}^2), arising as a constant-time slice of an appropriate higher-dimensional building describing (p -adic) Lorentzian AdS_3 .¹ This analogy is motivated by the fact that the real hyperbolic plane \mathbb{H}^2 is a symmetric, homogeneous space of constant negative curvature, and arises algebraically as the quotient space $\mathbb{H}^2 = \text{SL}(2, \mathbb{R})/\text{SO}(2, \mathbb{R})$, where $\text{SL}(2, \mathbb{R})$ is the isometry group of \mathbb{H}^2 and $\text{SO}(2, \mathbb{R})$ is its maximal compact subgroup. Similarly, the Bruhat–Tits tree is a symmetric, homogeneous space which can be viewed as the quotient $\mathcal{T}_p = \text{PGL}(2, \mathbb{Q}_p)/\text{PGL}(2, \mathbb{Z}_p)$. Here, the group $\text{PGL}(2, \mathbb{Q}_p)$ acts on \mathcal{T}_p by isometries, and $\text{PGL}(2, \mathbb{Z}_p)$ is its maximal compact subgroup. However, while the hyperbolic plane is a two-dimensional manifold, the Bruhat–Tits tree is described by a discrete (but infinite) collection of points (as seen later in figure 6.3). In Section 6.3, we use the “dual” of this discrete tree to define a tensor network, and the entanglement properties of the boundary state are described geometrically in terms of the Bruhat–Tits tree.

We now describe the action of $G = \text{PGL}(2, \mathbb{Q}_p)$ on the Bruhat–Tits tree in more detail. Let $H = \text{PGL}(2, \mathbb{Z}_p) < G$ denote a maximal compact subgroup. Choose representatives $g_i \in G$ of the left cosets of H . In other words, $G = \bigcup_{i=0}^{\infty} g_i H$, where the cosets $g_i H, g_j H$ are pairwise disjoint for $i \neq j$. The cosets $g_i H$ are in bijective correspondence with the equivalence classes of \mathbb{Z}_p -lattices in $\mathbb{Q}_p \times \mathbb{Q}_p$, as well as with the nodes on the Bruhat–Tits tree (see e.g. [83]). The group G has a natural action on equivalence classes of lattices (r, s) by

¹In this chapter we remain agnostic about the appropriate higher dimensional origins of the Bruhat–Tits tree (such as hyperbolic buildings), and will only be interested in studying entanglement entropy in the static (time symmetric) case.

matrix multiplication:

$$g \cdot (r, s) \equiv g \cdot \left\{ \begin{pmatrix} ar_1 + bs_1 \\ ar_2 + bs_2 \end{pmatrix} : a, b \in \mathbb{Z}_p \right\} = \begin{pmatrix} A & B \\ C & D \end{pmatrix} \left\{ \begin{pmatrix} ar_1 + bs_1 \\ ar_2 + bs_2 \end{pmatrix} : a, b \in \mathbb{Z}_p \right\}, \quad (6.1)$$

for $r = (r_1, r_2)^T, s = (s_1, s_2)^T \in \mathbb{Q}_p \times \mathbb{Q}_p, g \in G$.

Equivalently, G acts on the space of cosets G/H , by the rule $g_i H \mapsto gg_i H$. Each equivalence class (or equivalently, coset) is stabilized by a conjugate of H ; the coset $g_i H$ is stabilized by $g_i H g_i^{-1} < G$. Either of these descriptions gives the action of G on the nodes of \mathcal{T}_p .

Two nodes on the tree are defined to be adjacent when the relation

$$p\Lambda \subset \Lambda' \subset \Lambda \quad (6.2)$$

holds between the corresponding \mathbb{Z}_p -lattices Λ and Λ' . This relation is reflexive, so that the previous inclusion holds if and only if $p\Lambda' \subset \Lambda \subset \Lambda'$. The action of the group G on the nodes of the Bruhat–Tits tree preserves these incidence relations. In other words, the group G acts by isometries of the Bruhat–Tits tree, preserving the graph distance between any pair of nodes. Intuitively, G acts by translations and rotations on the (infinite) nodes of the tree in analogy to the ordinary isometries of AdS; additionally for any given vertex we may find a stabilizer subgroup, which is always a conjugate of $H = \text{PGL}(2, \mathbb{Z}_p)$, which rotates the entire tree around this point.

As is well known in AdS/CFT, the isometry group of the bulk acts as conformal transformations on the boundary. In p -adic AdS/CFT, we have $\partial\mathcal{T}_p = \mathbb{P}^1(\mathbb{Q}_p)$, with G acting as fractional linear transformations:

$$\mathbb{P}^1(\mathbb{Q}_p) \ni z \mapsto g \cdot z = \frac{Az + B}{Cz + D} \quad g = \begin{pmatrix} A & B \\ C & D \end{pmatrix} \in G = \text{PGL}(2, \mathbb{Q}_p). \quad (6.3)$$

These are interpreted as the global (p -adic) conformal transformations acting on the dual theory defined on the boundary $\partial\mathcal{T}_p$.

In analogy with static AdS₃, it is possible to obtain black hole like bulk geometries algebraically. One may quotient the Bruhat–Tits tree by an abelian discrete subgroup $\Gamma \in \text{PGL}(2, \mathbb{Q}_p)$ to obtain an analog of the BTZ black hole. The bulk and boundary properties of this construction are explored in Section 6.4, where we will describe why this is a good model of a p -adic black hole geometry and compute the entropy via the tensor network proposed in this work.

Tensor networks

In the recent literature, there has been much interest in so-called *tensor network* models, which describe a state or family of states in a Hilbert space that is the tensor product of many qubits or local Hilbert spaces of fixed rank. Such states are built by considering concatenations of many tensors, each operating on a finite number of qubits in the manner of a quantum circuit. Early proposals [225, 226] showed that such setups could be used to construct states whose entanglement structure mimics that of the vacuum state of a conformal field theory [227, 228, 229]. Subsequently, it was proposed [230, 231] that the geometry of the tensor network could be thought of as a discrete analogue of an AdS bulk space, and various models have been developed to try and exhibit this correspondence more precisely [99, 232, 98, 233, 234, 235].

In particular, in the proposal of [99], tensor networks were associated to uniform tilings of hyperbolic two-dimensional space by k -gons, by placing a tensor with m indices on each polygon and contracting indices across each adjacent face. The residual $m - k$ indices represent “logical” inputs in the bulk. (Of course, $m \geq k$; equality is not necessary, but $2m - k$ should not be too large. Furthermore, m is taken to be even. See [99] for a discussion of the precise conditions.) Using this construction, analogues of the Ryu–Takayanagi formula for the entanglement entropy were proved.

This formula follows from a key property of the m -index tensors that are used on each plaquette:

Definition 1. Let $T \in V^{\otimes m}$ be an m -index tensor, where each index labels an identical tensor factor or “qubit” $V \cong \mathbb{C}^q$. V is equipped with a Hilbert space structure, so that we can raise and lower indices using the metric. Let $I \subseteq M = \{1, \dots, m\}$ be any subset of the index set, and J its complement; without loss of generality, we can take $\#I \leq \#J$. T is said to be *perfect* if, for every such bipartition of the indices,

$$T_I^J : V^I \rightarrow V^J \tag{6.4}$$

is an isometric map of Hilbert spaces. Here we are using the notation that T_I^J means T with the indices in the set I lowered, and those in the set J raised. (In particular, T_I^J is injective, so that one can think of the condition as asking that T have the largest possible rank for any such tensor decomposition.)

The parity of m is not important to the above definition, but the applications in [99] make use of perfect tensors for which m is even. It is then shown that requiring T_I^J to define a unitary map for every bipartition with $\#I = \#J$ is sufficient to imply perfection in the sense of definition 1.

The connection to maximally entangled states should hopefully be apparent: Recall that a state is said to be maximally entangled between two subsystems if the reduced density matrix, obtained by tracing out one subsystem, is “as mixed as possible.” At the level of density matrices, this means “proportional to the identity matrix” (recall that pure states correspond one-to-one to density matrices of rank one). So, for a state defined by a perfect tensor, we can write

$$\rho = |\alpha|^2 T_M T^M, \quad (6.5)$$

where α is a normalization constant required so that ρ has unit trace (equivalently, so that the state $T_M \in V^{\otimes m}$ is normalized). Note that no Einstein summation convention applies; M denotes a set of indices, rather than an index. To reduce the density matrix, though, we *do* contract along the indices in the set J :

$$(\rho_{\text{red}})_I^I = |\alpha|^2 T_I^J \circ T_J^I. \quad (6.6)$$

In the case that m is even and $\#I = \#J$, this shows that ρ_{red} is the composition of two unitary maps; as a consequence, it is full-rank. Indeed, by unitarity, the two maps T_I^J and T_J^I are inverses of one another, so that the reduced density matrix is proportional to the identity. From the condition of unit trace, it follows that the normalization constant must be taken to be

$$|\alpha|^2 = p^{-m/2}. \quad (6.7)$$

For more details on computations with perfect tensors, look forward to Section 6.5.

Classical and quantum codes

There are many close relations between perfect tensors, maximally entangled states, and quantum error-correcting codes. We have outlined some of the connections between the first two ideas above; in this subsection, we will discuss the third, which will give us a way to produce examples of perfect tensors. The key construction will be the CRSS algorithm [223], which produces quantum error-correcting codes from a particular class of classical codes. In turn, the

CRSS algorithm makes use of a particular complete set of matrices acting on qubits, which come from the theory of Heisenberg groups; these groups generalize the familiar theory of the canonical commutation relations to variables which are discrete (\mathbb{F}_q -valued) rather than continuous. As such, the CRSS procedure can be seen as perfectly analogous to canonical quantization problems of a familiar sort. This interpretation is not necessary to understand the holographic tensor networks proposed later, but we will make heavy use of the existence of an infinite class of such tensors.

Heisenberg groups

The simplest example of a finite Heisenberg group can be presented as follows:

$$G = \langle X, Z, c : ZX = cXZ, X^p = Z^p = 1, c \text{ central} \rangle. \quad (6.8)$$

(It follows from these relations that $c^p = 1$ as well.) The center of the group is a copy of \mathbb{F}_p , generated by c , and the quotient by the center is also abelian, so that the group fits into a short exact sequence

$$0 \rightarrow \mathbb{F}_p \rightarrow G \rightarrow \mathbb{F}_p^2 \rightarrow 0 \quad (6.9)$$

exhibiting it as a central extension of one abelian group by another. Despite this, G itself is nonabelian.

Representations of this group are also easy to understand; each representation can be restricted to $Z(G) = \mathbb{F}_p$, and defines a character χ of that group, called the central character. In the case at hand, a central character is just a choice of p -th root of unity, corresponding to $\chi(c)$.

Given a choice of representation, a corresponding representation can be constructed on the vector space $\mathcal{H} = \mathbb{C}^p$. In a particular basis, the generators of V act according to the rule

$$X |a\rangle = |a+1\rangle, \quad Z |a\rangle = \chi(c)^a |a\rangle. \quad (6.10)$$

For a nontrivial central character, this representation is irreducible. An analogue of the Stone–von Neumann theorem shows that this is in fact the unique irreducible representation with central character χ . Furthermore, the representation matrices form an additive basis (over \mathbb{C}) for the matrix algebra $M_{p \times p}(\mathbb{C})$.

On the other hand, when the central character is trivial, any representation factors through the quotient map to \mathbb{F}_p^2 ; since that (additive) group is abelian, there are p^2 different one-dimensional representations. As such, we have understood the complete representation theory of G . A quick check reveals that we have found the whole character table: there are $(p - 1)$ nontrivial central characters, each with a representation of dimension p , together with p^2 abelian representations. This makes a total of $p^2 + p - 1$ irreps, which corresponds to the number of conjugacy classes: these are the powers of c , together with the nonzero powers $X^i Z^j$. One can also double-check that

$$\sum_{\rho} (\dim \rho)^2 = (p - 1)p^2 + p^2 = p^3 = \#G. \quad (6.11)$$

This simple example already contains most of the structural features, and motivates the following definition. In what follows, k will be an arbitrary field, though the cases that will be relevant will be when k is locally compact (i.e., k is a local field or a finite field). In fact, we will only really consider the cases where $k = \mathbb{R}$ or \mathbb{F}_q , although some amount of the discussion even continues to make sense over an arbitrary commutative ring, for instance \mathbb{Z} .

Definition 2. Let V be a symplectic vector space over k , with symplectic form ω . The *Heisenberg group* associated to this data, denoted $\text{Heis}(V)$, is the central extension of the additive abelian group V by the cocycle

$$\omega : V^2 \rightarrow k. \quad (6.12)$$

Note that, since $\text{Heis}(V, \omega)$ is a central extension, there is a natural short exact sequence of abelian groups

$$0 \rightarrow k \rightarrow \text{Heis}(V) \rightarrow V \rightarrow 0, \quad (6.13)$$

generalizing the sequence (6.9). Furthermore, the image of k is the center of the group. Our previous example arises in the case $k = \mathbb{F}_p$, $V = \mathbb{F}_p^2$, and ω the standard Darboux symplectic form on a two-dimensional vector space.

In speaking of ω as a group cocycle, we are thinking of the inhomogeneous group cochains of $(V, +)$. The cocycle condition is obeyed because

$$\begin{aligned} d\omega(u, v, w) &\doteq \omega(v, w) - \omega(u + v, w) + \omega(u, v + w) - \omega(u, v) \\ &= 0. \end{aligned} \quad (6.14)$$

An analogue of the Stone–von Neumann theorem also holds in this more general case, so that $\text{Heis}(V)$ admits a unique irreducible representation for any choice of central character. We will discuss this theorem further below. Furthermore, just as in our example above, it is true for more general Heisenberg groups that the representation matrices form an additive basis for $M_{p^n \times p^n}(\mathbb{C})$, where $n = \dim(V)/2$.

An explicit construction of that unique irreducible representation can be given as follows. Let $\mathcal{H} = \text{Fun}(\mathbb{F}_q, \mathbb{C}) \cong \mathbb{C}^q$ be the Hilbert space of a single q -ary qubit. An orthonormal basis of \mathcal{H} is labeled by states $|a\rangle$ where $a \in \mathbb{F}_q$. Quantum error-correcting spaces are subspaces of $\mathcal{H}^{\otimes n}$ which are error-correcting for a certain number of qubits. All errors can be constructed from the error operators $E = E_1 \otimes \cdots \otimes E_n$ which are the representation matrices of the Heisenberg group. Each of the E_i can be thought of as a particular combination of bit-flip and phase-flip operators, which we now describe.

Define the $p \times p$ matrices

$$T = \begin{pmatrix} 0 & 1 & 0 & \cdots & 0 \\ 0 & 0 & 1 & \cdots & 0 \\ \vdots & & & \ddots & \vdots \\ 0 & 0 & 0 & \cdots & 1 \\ 1 & 0 & 0 & \cdots & 0 \end{pmatrix} \quad R = \begin{pmatrix} 1 & & & & \\ & \xi & & & \\ & & \xi^2 & & \\ & & & \ddots & \\ & & & & \xi^{p-1} \end{pmatrix}, \quad (6.15)$$

where $\xi = e^{2\pi i/p}$ is a (nontrivial) p -th root of unity. If $q = p$, ξ is precisely a choice of central character, and it is easy to check that these matrices define the representation of the simplest Heisenberg group (6.8) with that central character. However, in the case $q = p^r$, we must do slightly more work.

Let $\{\gamma_j : 1 \leq j \leq r\}$ be a basis of \mathbb{F}_q as an \mathbb{F}_p -vector space; see e.g. (6.24). Then we can write $a = \sum_{j=1}^r a_j \gamma_j$ for any $a \in \mathbb{F}_q$, where $a_i \in \mathbb{F}_p$. This also defines a tensor product basis in $\mathcal{H} = \text{Fun}(\mathbb{F}_q, \mathbb{C})$, such that $|a\rangle = |a_1\rangle \otimes \cdots \otimes |a_r\rangle$ when a is decomposed as a direct sum, as above. Then the error operators act on individual copies of \mathbb{C}^p as follows:

$$T^{b_j} |a_j\rangle = |a_j + b_j\rangle \quad R^{b_j} |a_j\rangle = \xi^{\text{Tr}(a_j b_j)} |a_j\rangle \quad a_j, b_j \in \mathbb{F}_p. \quad (6.16)$$

Here, the trace function $\text{Tr}_{q:p} : \mathbb{F}_q \rightarrow \mathbb{F}_p$ (with $q = p^r$) is defined as

$$\text{Tr}_{q:p}(a) = \sum_{i=0}^{r-1} a^{p^i} \quad a \in \mathbb{F}_q. \quad (6.17)$$

It is easy to see that this is precisely the trace of the endomorphism of \mathbb{F}_q that is multiplication by the element a , regarded as an $n \times n$ matrix over \mathbb{F}_p .

It is now simple to define the bit- and phase-flip operators acting on single q -ary qubits; they are the $q \times q$ matrices

$$T_b = T^{b_1} \otimes \cdots \otimes T^{b_r} \quad R_b = R^{b_1} \otimes \cdots \otimes R^{b_r}. \quad (6.18)$$

These operators act on a single q -ary qubit via

$$T_b|a\rangle = |a + b\rangle \quad R_b|a\rangle = \xi^{\text{Tr}(\langle a, b \rangle)}|a\rangle, \quad (6.19)$$

where $a = \sum_{j=1}^r a_j \gamma_j \in \mathbb{F}_q$, and

$$|a\rangle = \otimes_{j=1}^r |a_j\rangle. \quad (6.20)$$

As emphasized above, the operators $T_a R_b$ form an orthonormal basis for $M_{q \times q}(\mathbb{C})$ under the inner product $\langle A, B \rangle = q^{-1} \text{Tr}(A^\dagger B)$, and thus generate all possible errors on \mathcal{H} . We can further construct error operators which act on $\mathcal{H}^{\otimes n}$ as follows. Given $a = (a_1, \dots, a_n), b = (b_1, \dots, b_n) \in \mathbb{F}_q^n$, define

$$E_{a,b} = T_a R_b = (T_{a_1} \otimes \cdots \otimes T_{a_n})(R_{b_1} \otimes \cdots \otimes R_{b_n}). \quad (6.21)$$

It is straightforward to check that $E_{a,b}^p = 1$, and that they obey the following commutation and composition laws:

$$E_{a,b} E_{a',b'} = \xi^{\langle a, b' \rangle - \langle a', b \rangle} E_{a',b'} E_{a,b} \quad E_{a,b} E_{a',b'} = \xi^{-\langle b, a' \rangle} E_{a+a', b+b'}. \quad (6.22)$$

Here, we have made use of an \mathbb{F}_p -valued pairing,

$$\langle a, b \rangle = \sum_{i=1}^n \langle a_i, b_i \rangle = \sum_{i=1}^n \sum_{j=1}^r a_{i,j} b_{i,j} \quad a, b \in \mathbb{F}_q^n, \quad (6.23)$$

where the elements $a_i, b_i \in \mathbb{F}_q$ are expanded in terms of an \mathbb{F}_p -basis as

$$a_i = \sum_{j=1}^r \gamma_j a_{i,j} \quad b_i = \sum_{j=1}^r \gamma_j b_{i,j} \quad a_{i,j}, b_{i,j} \in \mathbb{F}_p. \quad (6.24)$$

(6.21) therefore produces the explicit representation matrices of the Heisenberg group of \mathbb{F}_q^{2n} , corresponding to a particular (nontrivial) choice of central character.

Classical algebrogeometric codes

In this section, we give a few general remarks about classical codes over finite fields. The next section will review the CRSS algorithm, which associates a quantum error-correcting code to each such self-orthogonal classical code. Placing the two together, one can demonstrate that perfect tensors with arbitrarily many indices can be constructed, which we will require for the models of Section 6.3; an additional ingredient is an appropriate family of classical codes, an example of which is given in appendix D.1.

A (classical) *linear code* is nothing more than a linear subspace of a vector space over a finite field. In a basis, it is defined by an injective map

$$i : \mathbb{F}_q^k \hookrightarrow \mathbb{F}_q^n, \quad (6.25)$$

which can be thought of as encoding k bits of information (each bit being of size q) into n bits of information.

The *Hamming weight* is defined to be the function

$$\text{wt} : \mathbb{F}_q^n \rightarrow \mathbb{N}, \quad c \mapsto \#\{i : c_i \neq 0\}. \quad (6.26)$$

Note that this is a basis-dependent definition! The *minimum weight* of a code is simply the minimum Hamming weight of all nonzero elements of the code subspace; one often uses the notation “[n, k, d] $_q$ code” to speak of a code with the given parameters. We may sometimes omit the weight parameter d from this list; no confusion should arise.

Equipping \mathbb{F}_q^n with an inner product or more generally a bilinear form, one can classify codes according to the properties of the code subspace. In particular, a code is said to be *self-orthogonal* when the code subspace is isotropic with respect to the bilinear form, i.e., contained in its orthogonal complement: $\text{im}(i) \subseteq \text{im}(i)^\perp$.²

The CRSS algorithm produces a quantum error-correcting code from classical self-orthogonal codes associated to symplectic vector spaces over finite fields. Such codes are generally of the form $[2n, \ell]_q$, where $\ell \leq n$ is the dimension of the isotropic subspace, and the inner product on \mathbb{F}_q^{2n} may, without loss of generality, be taken to have the standard Darboux form. We review the

² The superscript $^\perp$ denotes the dual (orthogonal) code. The dual code is defined as follows: If C is a classical code over \mathbb{F}_q of size n , then $C^\perp = \{v \in \mathbb{F}_q^n : a * v = 0 \forall a \in C\}$.

construction in the following subsection. For certain choices of the code parameters, CRSS quantum codes may then be used in turn to produce perfect tensors.

Let us also remark that isotropic subspaces in symplectic vector spaces may be constructed from other types of classical codes. For example, let D be a classical self-orthogonal $[n, k, d]_{q^2}$ code over \mathbb{F}_{q^2} , where the self-orthogonality is established with respect to the Hermitian inner product

$$v * w = \sum_{i=1}^n v_i w_i^q \quad v, w \in \mathbb{F}_{q^2}^n. \quad (6.27)$$

By Theorem 4 of [236], there exists a classical code C of length $2n$ and size $2k$ over \mathbb{F}_q which is self-orthogonal with respect to the inner product,

$$(a, b) * (a', b') = \text{Tr}(\langle a, b' \rangle_* - \langle a', b \rangle_*) \quad (a, b), (a', b') \in \mathbb{F}_q^{2n}, \quad (6.28)$$

where the Euclidean inner product $\langle \cdot, \cdot \rangle_*$ is defined to be

$$\langle a, b \rangle_* = \sum_{i=1}^n a_i b_i \quad a, b \in \mathbb{F}_q^n \quad a_i, b_i \in \mathbb{F}_q. \quad (6.29)$$

This is of course precisely the standard Darboux symplectic form on \mathbb{F}_q^{2n} .

The inner product given in (6.28) has an equivalent description in terms of the inner product of (6.23), as follows (see [236]):

$$(a, b) * (a', b') = \langle a, \varphi(b') \rangle - \langle a', \varphi(b) \rangle, \quad (6.30)$$

where³

$$\varphi(a) = (\varphi(a_1), \dots, \varphi(a_n)) \quad a \in \mathbb{F}_q^n \quad a_i \in \mathbb{F}_q, \quad (6.31)$$

and the action of φ on elements of \mathbb{F}_q is given by matrix multiplication, where φ acts as an $r \times r$ matrix M on the elements of \mathbb{F}_q , with

$$M_{ij} = \text{Tr}(\gamma_i \gamma_j) \quad i, j = 1, \dots, r. \quad (6.32)$$

CRSS algorithm

We briefly review the CRSS algorithm [223], which produces a quantum error-correcting code from an appropriately chosen classical code. We emphasize

³More generally, φ is an automorphism of the vector space \mathbb{F}_p^r , but for convenience we will restrict our focus to the particular choice of φ described here.

the perspective that CRSS is intimately related to the formalism of canonical quantization, albeit for Heisenberg groups over \mathbb{F}_p rather than \mathbb{R} . For further discussion, the reader is referred to [221, 223, 237].

As mentioned above, the CRSS algorithm starts with a symplectic vector space V of dimension $2n$ over a finite field. We let $\mathcal{H}(V)$ denote the “quantization” of this symplectic space, i.e., the unique irreducible representation of $\text{Heis}(V)$ with central character χ . In fact, by results of [238], there is a canonical model for $\mathcal{H}(V)$ (we review and extend these results in the original work [5]). Now, $\mathcal{H}(V)$ is isomorphic to the tensor product of n p -dimensional Hilbert spaces, one for each “qubit” or discrete degree of freedom. Such a tensor product decomposition corresponds to a choice of Darboux basis for V , which splits it as the direct sum of standard two-dimensional symplectic spaces. As noted above, the representation matrices of $\text{Heis}(V)$ additively span the space $\text{End}(\mathcal{H}(V))$ of all operators over \mathbb{C} .

Now, consider any maximal isotropic subspace L of V ; every such subspace defines a maximal abelian subgroup of $\text{Heis}(V)$. Mutually diagonalizing the action of the operators representing L splits \mathcal{H} as a direct sum of one-dimensional eigenspaces.

Then, consider a (necessarily isotropic) subspace $C \subset L$, whose dimension is $i < n$. C is to be thought of as the classical code subspace. The mutual eigenspaces of the abelian group associated to C define a decomposition of \mathcal{H} into $\#C = q^i$ eigenspaces, each of dimension q^{n-i} . Each of these is further split as a sum of one-dimensional eigenspaces of L . Now, one can define the quantum code space to be the invariant subspace of C , $\mathcal{H}(V)^C$, which is a Hilbert space of $(n - i)$ qubits, isomorphic to $(\mathbb{C}^q)^{\otimes(n-i)}$. (One could equivalently have chosen any of the joint eigenspaces of C .) Choosing an identification of this space with a standard set of $n - i$ qubits gives an encoding of $n - i$ qubits to n qubits; the “code words” can be thought of as the natural basis in the code space consisting of eigenspaces of L .

To think of the code as a perfect tensor, we’d like to view the isometric injection of the $(n - i)$ -qubit code space into the n -qubit encoding space as arising from a partitioning of the indices of a $(2n - i)$ -index tensor. In other words, we should consider the larger space consisting of $(n - i)$ degrees of freedom to be encoded, together with n degrees of freedom for the encoding space. Note that the number of indices of the perfect tensor will be even precisely

when $i = \dim C$ is even, as is the case for the codes of the previous section. The error-correction properties of such a code are discussed in [223]; we note that quantization of a self-orthogonal $[2n, 2k]_q$ code, such as those discussed above, produces a quantum code with parameters $\llbracket n, n - 2k, d_Q \rrbracket_q$. That is, one encodes $n - 2k$ qubits in n qubits in a manner that protects against d_Q errors, where $d_Q = \min\{\text{wt}(a, b) : (a, b) \in C^\perp \setminus C\}$. In order to produce a perfect tensor, we will need $d_Q = n - k$.

In appendix D.1 we consider an explicit example of a particular classical code, one of the Reed–Solomon codes, and construct the associated quantum Reed–Solomon code. The classical Reed–Solomon codes have parameters $[n, k, n - k + 1]_q$, and are constructed using a set of points $X \subseteq \mathbb{P}^1(\mathbb{F}_q)$ with $|X| = n \leq q + 1$, and homogeneous polynomials $f \in \mathbb{F}_q[u, v]$ where $x = [u : v] \in X$. For an input k -tuple of q -ary bits, $a = (a_0, \dots, a_{k-1}) \in \mathbb{F}_q^k$, the homogeneous polynomial is chosen to be

$$f_a(u, v) = \sum_{i=0}^{k-1} a_i u^i v^{k-1-i}, \quad (6.33)$$

and the resulting code takes the form

$$C = \{(f_a(u_1, v_1), \dots, f_a(u_n, v_n)) : a \in \mathbb{F}_q^k, [u_i : v_i] \in X\}. \quad (6.34)$$

This family of Reed–Solomon codes can be used to construct quantum error-correcting Reed–Solomon codes $\llbracket n, n - 2k, k + 1 \rrbracket_q$ [221]. The case of perfect tensors is obtained by setting $n = q$ and $k + 1 = n - k$, which leads to a $\llbracket q, 1, (q + 1)/2 \rrbracket_q$ code describing perfect tensors with $q + 1$ indices and bond dimension q , where we can take the prime q to be large as required for our later applications. In this chapter we will consider precisely this code to construct holographic tensor networks; however our results are applicable more generally to tensor networks built out of any error-correcting code with the “perfectness” property in definition 1.

The reader will have noticed that we have chosen to emphasize the perspective of canonical quantization in our exposition of the CRSS algorithm. In the original publication [5], we offer an elegant natural generalization of the CRSS algorithm that produces perfect tensors *directly*, without any intermediate reference to the theory of quantum codes. This construction also gives a physical interpretation of the perfect-tensor condition. More generally, we offer a proof that the perfect tensor condition is, in a suitable sense, “generic” within the CRSS construction of quantum codes.

Notational remark: In this section, as well as in appendix D.1, we set $q = p^r$ where p is a prime and r is a positive integer. Later in Section 6.3 onward, we will reserve the letter p to parametrize the bulk geometry of the Bruhat–Tits tree of valence $p + 1$, and will set up on this geometry the quantum Reed–Solomon code $[[r, 1, (r + 1)/2]]_r$ where r will be an independent prime number. It is also worth emphasizing that, in addition to being a prime power, q will be used for the parameter of a multiplicative normalization of an elliptic curve (i.e. a representation as $\mathbb{C}^\times/q^\mathbb{Z}$, or $\mathbb{Q}_p^\times/q^\mathbb{Z}$ in the p -adic case). Both notations are standard, but the context should always be sufficient to determine which usage is intended.

6.3 Entanglement in p -adic AdS/CFT

In this section we build on section 6.2 to initiate the study of holographic entanglement entropy in p -adic AdS/CFT, via a quantum error-correcting tensor network construction built using perfect tensors. We begin by discussing the framework for the vacuum (p -adic) AdS geometry, culminating in the verification of a Ryu–Takayanagi like formula in this purely p -adic setting, and in the next section proceed to discuss entanglement in a genus 1 (p -adic) black hole geometry.

The dual graph tensor network

The states we want to focus on in this chapter are a subset of all possible states which can be constructed using contractions of perfect tensors, each of which can be referred to as a “tensor network”. The basic idea of this construction involves the contraction of many tensors in a “bulk” space to produce a complicated entangled state at the boundary of the network. One may interpret this boundary state as an analog of the ground state of a boundary conformal field theory, and there are many proposals in the literature on how this may be realized. The details of the particular tensor network proposed here are along the lines of [99] and are important to the overall conclusions and generalizations. We will see the tensor network is closely associated with p -adic AdS/CFT.

To construct a holographic state $|\psi\rangle$ in the boundary Hilbert space, we consider a tensor network given by what we call the “dual graph” of the holographically dual bulk geometry. For instance, if the boundary is $\mathbb{P}^1(\mathbb{Q}_p)$, then we consider the “dual graph” of the Bruhat–Tits tree in the bulk. If we are interested

in states dual to the p -adic analog of the BTZ black hole, we must consider the corresponding “dual graph” of the genus 1 Schottky uniformization of the Bruhat–Tits tree. In this section we focus on the tensor network associated with the Bruhat–Tits tree (which as mentioned in Section 6.2 is to be thought of as the p -adic analog of a time slice of vacuum AdS₃). In the following, the introduction of this dual graph to the Bruhat–Tits tree may at first sight appear to be an additional structure beyond what is needed to study bulk dynamics p -adic AdS/CFT, but it will turn out to be crucial to our investigation of the relationship between bulk geometries and boundary entanglement.

We recall from Section 6.2 that every edge on the Bruhat–Tits tree can be uniquely specified by specifying its two end-points (either as a pair of adjacent lattice equivalence classes or as a pair of cosets) and for every node on the Bruhat–Tits tree, there are $p + 1$ edges incident on it. We define the dual graph as follows:

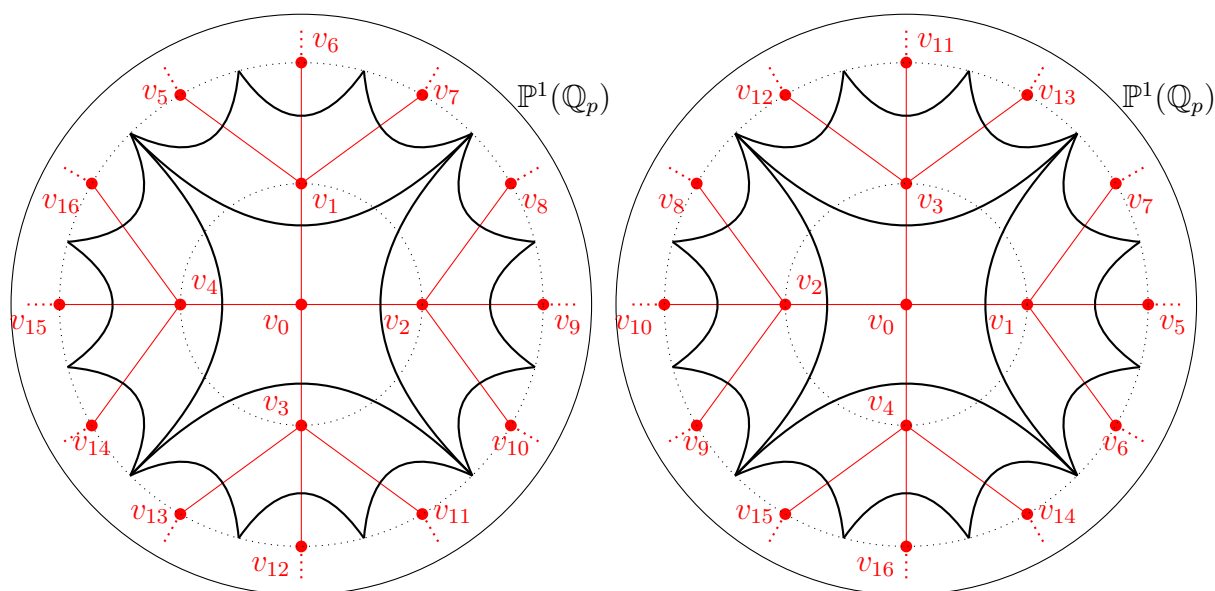
Definition 3. A *dual graph* of the Bruhat–Tits tree is a graph which satisfies the following two properties:⁴

- There exists a bijective correspondence between bonds on the dual graph and edges on the Bruhat–Tits tree. (Both “edge” and “bond” refer to the same object in graph theory – links between nodes on the graph, but for clarity we reserve the term “edge” for the Bruhat–Tits tree and “bond” for the dual graph.) Consequently, each bond on the dual graph is identified by specifying the corresponding edge on the Bruhat–Tits tree.
- The incidence relations of the set of bonds in bijective correspondence with those edges on the Bruhat–Tits tree incident at a particular node, are such that they form a cycle graph. We refer to such cycle graphs as “plaquettes”. Thus there is a bijective correspondence between nodes on the Bruhat–Tits tree and plaquettes on the dual graph.

In fact, the dual graph in the p -adic black hole geometry also satisfies the same properties.

⁴These properties are motivated from the “minimum cut rule” which provides a discrete analog of the Ryu–Takayanagi formula for connected regions in networks of perfect tensors [99]; however we do not assume this in the following. In fact in our setup the “minimum cut rule” applies more generally, for instance in the evaluation of the bipartite entanglement of a disconnected region as discussed in Section 6.5.

Any valid dual graph must satisfy the definition above; however, the definition does not uniquely specify a particular dual graph. By construction, a $\mathrm{PGL}(2, \mathbb{Q}_p)$ transformation acts simultaneously on both the Bruhat–Tits tree and its dual graph as an isometry. The choice of picking a particular valid dual graph (which corresponds to making a particular choice on the connectivity of the plaquettes at each node) corresponds to a choice of “planar embedding” of the Bruhat–Tits tree as we explain in Section 6.6. See figure 6.1 for an example. The construction of the dual graph may appear sensitive to the existence and choice of a planar embedding of the Bruhat–Tits tree. However, we show that physical quantities do not depend on this choice. Additionally, in the original publication [5], we offer a rigorous proof of this fact and explain this construction entirely in the context of the p -adic Drinfeld upper half plane without assuming an embedding in the ordinary (real) upper half plane.



(a) A choice of a planar embedding for the dual graph

(b) A different planar embedding for the dual graph

Figure 6.1: A finite part of the infinite Bruhat–Tits tree is shown in red, with the nodes labeled v_i . The graphical representation of the dual graph for the finite red subgraph is shown in black. The Bruhat–Tits tree in (b) is obtained by acting on the Bruhat–Tits tree in (a) with a $\mathrm{PGL}(2, \mathbb{Q}_p)$ transformation fixing the vertex v_0 . Equivalently, the dual graphs in (a) and (b) correspond to two different choices of incidence relations for bonds on the dual graph, subject to the two requirements mentioned in definition 3. In the infinite graph limit, the geometry of the Bruhat–Tits tree is represented by the Schläfli symbol $\{\infty, p + 1\}$, while the dual graph is given by the Schläfli symbol $\{p + 1, \infty\}$.

The dual graph will describe a tensor network. Each node on the dual graph will represent a rank- $(r+1)$ perfect tensor for some chosen r , with the bonds on the dual graph specifying how tensor indices are contracted among themselves. In this chapter we restrict ourselves to the study of the so-called holographic states rather than holographic codes [99]. Thus there are no “bulk logical inputs” in our setup. Interestingly, the Bruhat–Tits tree and (any choice of) its dual graph may be obtained as the asymptotic limit of the simplest holographic states considered in [99] – where the geometry is described by a regular hyperbolic tiling using q -gons with $p+1$ q -gons incident at each vertex (which is represented by the Schläfli symbol $\{q, p+1\}$) and the corresponding perfect tensor network with Schläfli symbol $\{p+1, q\}$ – in the limit $q \rightarrow \infty$. Viewed as such a limit, we observe that in fact all nodes of the dual graph tensor network may be interpreted as having been “pushed to the boundary” leaving no “bulk nodes” on the tensor network (see figure 6.2b for an example with a finite tree).⁵ As mentioned in Section 6.2 the perfect tensors themselves originate from quantum Reed-Solomon codes, particularly the $[[r, 1, (r+1)/2]]_r$ -code, where r is prime, although in the following the only thing we will explicitly use is the perfectness property of the quantum code and the fact that the tensors have rank and bond dimension r . Depending on the chosen rank of the perfect tensor, there will be a varying number of free (uncontracted or “dangling”) legs at each node on the dual graph. (We have suppressed such “dangling” legs in figure 6.1.) As with other tensor network models, we interpret the “boundary wavefunction” as a complicated entangled state in the tensor product Hilbert space of these dangling legs.

In practice, we always work with a boundary UV cutoff, so that we only consider finite graphs in the bulk. Thus in constructing a dual graph tensor network which describes a holographic state, in addition to the prime p (which parametrizes the bulk geometry \mathcal{T}_p), we need to specify two other integral parameters: the UV “cut-off parameter” Λ and the rank of the perfect tensors $(r+1)$.

Definition 4. The *cut-off parameter* Λ is defined to be one-half the length of the longest geodesic on the radially truncated (i.e. cut-off) Bruhat–Tits tree.

⁵Since we restrict our attention in this chapter to only holographic states [99], the results do not depend on this curious feature of the p -adic tensor network. Thus we do not comment further on the physical interpretation of this observation.

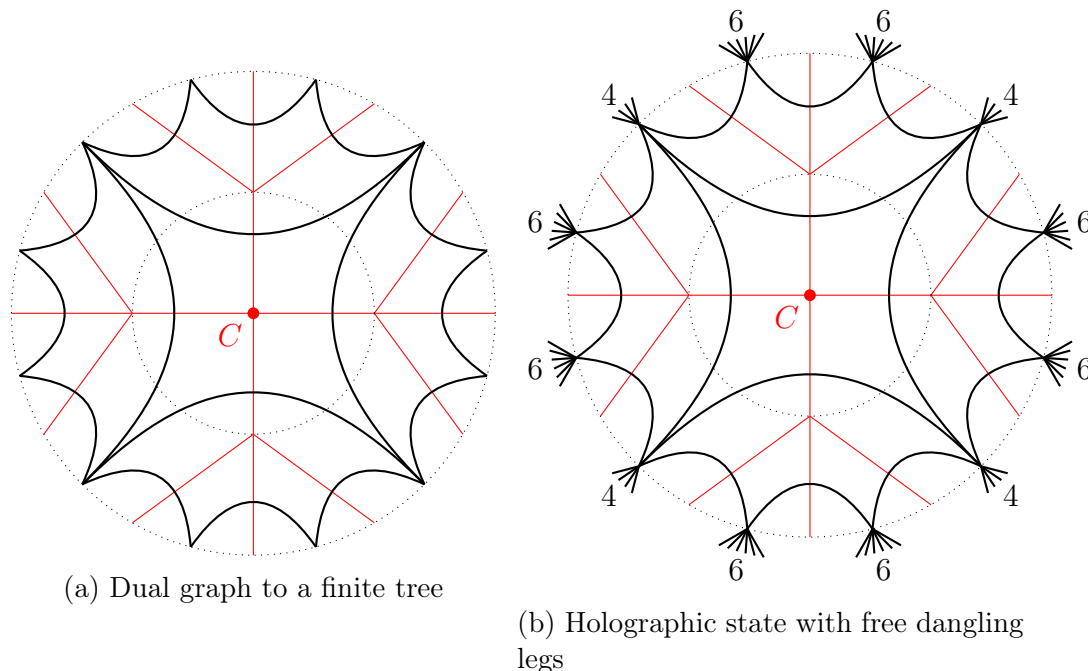


Figure 6.2: The construction of the holographic tensor network for the cutoff Bruhat–Tits tree. In this example, we have used perfect tensors of rank eight. The construction shown here corresponds to the parameters $p = 3$, $\Lambda = 2$, and $r = 7$. Hereafter we will suppress showing the free uncontracted/dangling legs displayed in (b).

See figure 6.2. Eventually, we will take the number of tensors and r to be large; the resulting boundary holographic states will have entanglement properties which are geometrized by this bulk network.

Cutting off ordinary (real) or p -adic AdS at a finite radius provides an IR regulator from the bulk point of view, as the length of boundary anchored geodesics formally diverges for an infinite tree. In the usual picture, this IR regulator of minimal surfaces is dual to the UV cut-off of the conformal field theory; in this model it is the finiteness of the number of boundary tensors. For each choice of p and Λ , the endpoints of the cut-off (truncated) Bruhat-Tits tree form the space $\mathbb{P}^1(\mathbb{Z}/p^\Lambda\mathbb{Z})$,⁶ and the tensor network is the dual graph to the tree of this space. As we remove the cutoff, the boundary approaches $\mathbb{P}^1(\mathbb{Q}_p)$,

⁶As usual, points in $\mathbb{P}^1(\mathbb{Z}/p^\Lambda\mathbb{Z})$ are obtained by considering pairs in the ring $\mathbb{Z}/p^\Lambda\mathbb{Z}$ modulo scaling. For $\Lambda > 1$, this is not a field and there are zero divisors without multiplicative inverses. When forming the projective line, one finds there are multiple “points at infinity” beyond the usual inverse of 0. Perhaps surprisingly, the set of base points and points at infinity are in one to one correspondence with the boundary of the tree cut off at finite distance.

and we will show that various quantities such as the length of geodesics and the entanglement entropy will have logarithmic UV divergences as expected in a two-dimensional quantum field theory.

Further, we impose a constraint on the rank $(r+1)$. We require $(r+1)/2 \geq 2\Lambda$. Thus in the limit $\Lambda \rightarrow \infty$, the rank of the perfect tensor also goes to infinity. This means considering limits, in the appropriate sense, of density matrices of increasing ranks. This limiting procedure can be made precise in the setting of AF-algebras and states, but it is somewhat outside the scope of this thesis. A detailed conceptual and technical analysis of such a limit is given in the original publication [5].

If for a chosen vertex v on the dual graph, the number of contracted legs of the tensor is denoted v_c , while the number of uncontracted legs is denoted v_d , then for cut-off Λ , all vertices on the dual graph tensor network satisfy $2\Lambda \geq v_c$. Since $v_c + v_d = r+1$, the requirement above implies $v_c \leq v_d$ at all vertices of the tensor network. Thus this condition ensures that the number of free dangling legs at any vertex on the dual graph is greater than or equal to the number of contractions at the vertex. This requirement may seem arbitrary, but plays an important role in our setup. Without this constraint the minimal cut rule obeyed by perfect tensors may lead to the cuts being made at the uncontracted dangling legs of the tensor network rather than along the contractions in the bulk of the network, which will be necessary for recovering the appropriate RT surface.

The holographic state so constructed is a pure state which is a ground state of the dual toy model CFT. We show that the dual graph tensor network satisfies a Ryu–Takayanagi like formula and is independent of the choice of the planar embedding. We will prove this in general for the bipartite entanglement of “connected” and “disconnected regions” (which we will be define more precisely shortly). In this section, we restrict to discussing the results; all detailed computations can be found in Section 6.5.

Entanglement in genus zero p -adic background

The p -adic numbers have a totally disconnected topology, so that open balls (in fact, all balls are clopen, i.e. closed and open) are either fully disjoint or contained one inside another. Clopen balls are defined as $\mathcal{B}_v(x) \equiv \{y \in \mathbb{Q}_p : |x - y|_p \leq p^v\}$ for any integer v . The set of non-zero p -adic numbers

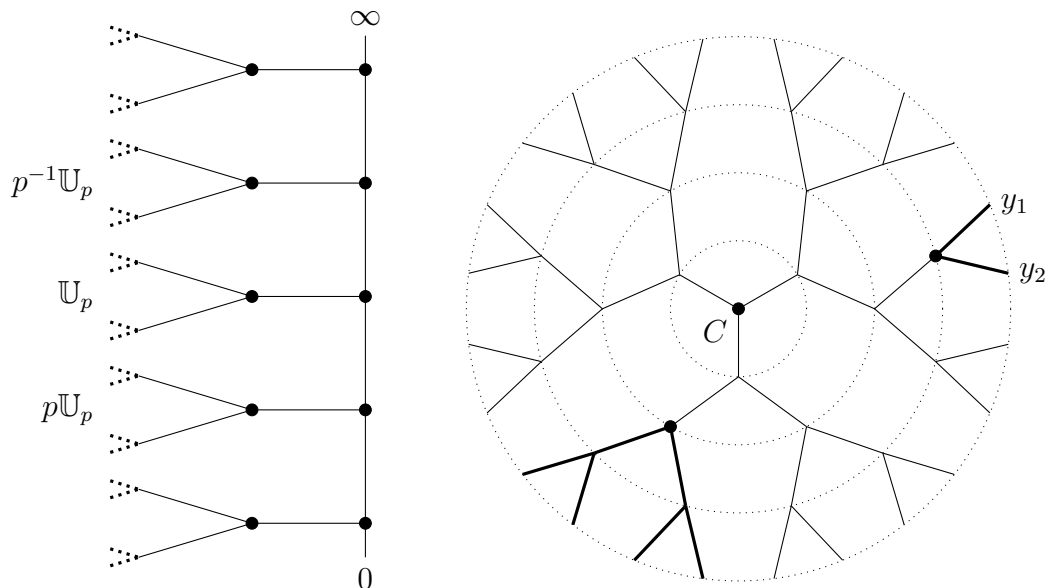
(a) The multiplicative group \mathbb{Q}_p^\times .(b) Clopen balls in $\mathbb{P}^1(\mathbb{Q}_p)$.

Figure 6.3: Two pictures of the Bruhat–Tits tree for $P^1(\mathbb{Q}_2)$, emphasizing either the action of the multiplicative group \mathbb{Q}_2^\times or the Patterson–Sullivan measure.

itself can be written as the disjoint union of the clopen balls $\mathbb{Q}_p \setminus \{0\} = \bigcup_{m=-\infty}^{\infty} p^m \mathbb{U}_p$, where $\mathbb{U}_p = \mathbb{Z}_p \setminus p\mathbb{Z}_p = \{x \in \mathbb{Q}_p : |x|_p = 1\}$. Thus although p -adic numbers are not ordered, they admit a partial sense of ordering with respect to the p -adic norm. This partial ordering is captured by the Bruhat–Tits tree. Using conformal transformation, set any two points on the projective line $\mathbb{P}^1(\mathbb{Q}_p)$, the boundary of the Bruhat–Tits tree, to 0 and ∞ . Then the particular clopen balls of $\mathbb{Q}_p^\times = \mathbb{Q}_p \setminus \{0\}$ of the form $p^m \mathbb{U}_p$ arrange themselves as shown in figure 6.3a. In the Poincaré disk picture, any clopen ball of $\mathbb{P}^1(\mathbb{Q}_p)$ can be obtained by cutting the Bruhat–Tits tree along one of its edges – the terminus of the disconnected branches of the tree represent the (mutually complimentary) clopen sets whose union is the whole of $\mathbb{P}^1(\mathbb{Q}_p)$ (see figure 6.3b). More general clopen sets are obtained as finite union of balls.

Now recall from standard results in holography that in a CFT_2 , the entanglement of a connected region A with its complement on a one-dimensional spatial slice admits an interpretation as the length of the minimal geodesic(s) in AdS_3 homologous to the region A , i.e. one minimizes over the length of the geodesic(s) such that there exists a bulk region r whose boundary is the union of the minimal geodesic(s) and the boundary region A . In this case the bound-

ary of A is simply a pair of points (which together comprise the “entangling surface”). This presents an obvious obstruction over the p -adic formulation, since \mathbb{Q}_p is not ordered, and it is clear one cannot define regions by specifying end points in \mathbb{Q}_p . How, then, is entanglement to be interpreted in a p -adic theory over one (spatial) dimension? There are at least two physically motivated points of view:

- One possibility is to study entanglement of clopen sets on the projective line with their complementary clopen sets. However, due to ultrametricity, every point in a clopen ball is the center of the ball. Thus the notion of “boundary” of the ball is ill-defined (more generally, the “boundary” of a clopen set is ill-defined), nor is there an analog of entangling surfaces. One can however specify the *smallest* clopen ball containing a given pair of points. The size of such a clopen ball is given by the Patterson-Sullivan measure [239, 240], and is directly related to the (regulated) length of the boundary-anchored bulk geodesic joining the given pair of points.
- A second related possibility, but closer in spirit to the real formalism, is to motivate entanglement directly in terms of the “entangling surface” on the spatial p -adic boundary, namely, in terms of pairs of points on the boundary $\mathbb{P}^1(\mathbb{Q}_p)$. We note that the (regulated) geodesic distance between any two chosen points on the boundary is invariant under any automorphism of the Bruhat–Tits tree, and thus is independent of the planar embedding, which is an essential feature of the setup. The freedom in the choice of planar embedding reflects the fact that p -adic numbers (living on the boundary of the Bruhat–Tits tree) do not form an ordered field and thus admit all possible planar embeddings equally.

We adopt the latter point of view here (although some aspects of the former point of view will also inevitably feature in our discussion of the p -adic results due to the inherent ultrametric nature of p -adic numbers), as it represents a generalization which is applicable to both the real and the p -adic formulations. We comment further on this point in Section 6.7.

We emphasize that the geometry, which is given by the Bruhat–Tits tree has a strong non-Archimedean flavor owing to the direct connection with p -adic num-

bers.⁷ The dual graph tensor network is however closer in spirit to the usual tensor networks framework over the reals. The network still encodes a maximally entangled ground state of the CFT, and the perfect tensors from which it is made provide the quantum-error correction properties. In this setup, we will compute entanglement in the usual way: by tracing out “boundary regions” of the tensor network, specified by sets of nodes on the dual graph (more precisely the collection of uncontracted tensor legs at those nodes), and then explicitly compute the reduced density matrix, and from it the von Neumann entropy. However, we will argue in the p -adic setting that the specification of intervals is not as fundamental as the specification of the entangling surfaces.

Regions in the bulk and boundary of tensor networks

In a static slice of the boundary theory, the standard way of specifying a connected region at the terminus of a holographic tensor network is by picking a pair of points on the spatial slice of the two-dimensional CFT. This naturally defines a pair of complimentary intervals at the boundary of the tensor network, and provides a factorization of the Hilbert space, $\mathcal{H} = \mathcal{H}_1 \otimes \mathcal{H}_2$, where \mathcal{H}_i are the Hilbert spaces associated with the individual regions. Starting with a pure state in \mathcal{H} given by the density matrix ρ , the bipartite von Neumann entropy of region 1 is computed by tracing out the states associated with \mathcal{H}_2 , producing the reduced density matrix $\rho_1 = \text{Tr}_{\mathcal{H}_2} \rho$. The von Neumann entropy, in this case called the entanglement entropy, is then given by $S_1 = -\text{Tr}(\rho_1 \log \rho_1)$.

However, the situation is different in the p -adic setting in an important way, namely the specification of intervals on the boundary. As mentioned above, the notion of an interval with end-points is ill-defined when the CFT lives on a (spatial) p -adic slice \mathbb{Q}_p (or the projective line over \mathbb{Q}_p); however one can *still* define a corresponding pair of complimentary connected regions at the boundary on the *tensor network*, separated by two boundary points as we now explain.

In our setup, the “connected region” of interest on the tensor network will be

⁷The non-Archimedean property of p -adic numbers is as follows: Given two p -adic numbers $a, b \in \mathbb{Q}_p$, such that $|a|_p < |b|_p$, then for all $n \in \mathbb{Z}$, $|na|_p < |b|_p$. We will also use the term “ultrametricity” in the context of the p -adic norm. Ultrametricity refers to the stronger form of the triangle inequality obeyed by the p -adic norm: Given $a, b \in \mathbb{Q}_p$, $|a + b|_p \leq \sup\{|a|_p, |b|_p\}$. The non-Archimedean property follows from ultrametricity.

specified by a set of nodes on the tensor network which lie “in between” the given boundary points x and y , which themselves lie at the terminus of the cutoff Bruhat–Tits tree. We will explain the terminology “in between” shortly, but essentially it corresponds to selecting a set of vertices at the boundary of the tensor network in between the chosen end points, in a given planar embedding. The exact region to be traced out will depend on the choice of planar embedding (i.e. the choice of the dual graph). See figure 6.4 for an example. The ambiguity in picking a region or its complement is fixed by assigning an orientation, such as an anti-clockwise orientation. We stress that we are not assuming any ordering of the p -adic numbers. Once a planar embedding is chosen, the region “in between” x and y is $\mathrm{PGL}(2, \mathbb{Q}_p)$ “covariant”, which follows from the transformation properties of the dual graph explained earlier.⁸ The final result for the von Neumann entropy for the connected region is independent of this choice of the planar embedding.

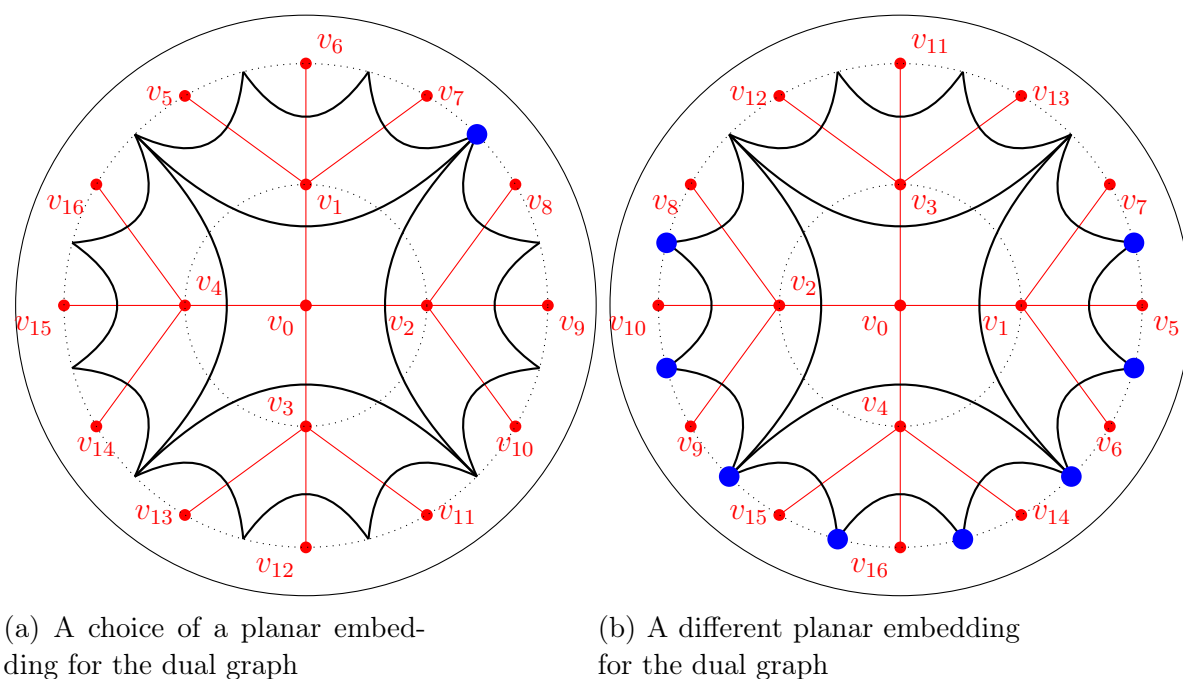


Figure 6.4: The region at the boundary of the dual graph “in between” boundary points v_8 and v_7 for two choices of planar embedding for the dual graph, depicted in blue.

Let us make this more precise.

⁸By covariance, we mean that the region is always given by the set of nodes on the tensor network “in between” the given boundary points. The boundary points will in general transform under $\mathrm{PGL}(2, \mathbb{Q}_p)$ to a new set of points, and accordingly, the region will transform to one between the transformed pair of points.

Definition 5. The *shortest bonds* on the tensor network comprise the subset of bonds (contractions) on the tensor network which are in bijective correspondence with the set of edges on the Bruhat–Tits tree situated at the cutoff boundary.

Definition 6. A *connected region* on the tensor network is defined to be a set of vertices on the tensor network which are “path-connected” to each other (by which we mean one can jump, solely via the shortest bonds on the tensor network, from any vertex in the set to any other without landing on a vertex which is not in the set). We define a *disconnected region* to be a region which is not connected.

We will also interchangeably mean the (connected or disconnected) region to stand for the uncontracted tensor legs situated at the vertices in the specified region.

As noted earlier, we specify the connected region (on the dual tensor network) by specifying two boundary points on the Bruhat–Tits tree and considering all vertices on the dual graph which lie “in between” the boundary points (after making a choice of orientation), which we now define.

Definition 7. Given two points x and y in ∂T_p and a choice of a planar embedding, we define the connected region on the tensor network *in between* x and y (up to a choice of orientation) as the set of nodes on the tensor network path-connected to each other via the “shortest bonds” starting at the “start bond” and ending at the “end bond”, without backtracking. The “start” and “end” bonds correspond to bonds on the tensor network dual to the cutoff edges on the Bruhat–Tits tree ending at x and y .

For instance, in figure 6.5a, the chosen connected region lies in between the boundary points x and y . By contrast, in figure 6.5b we show an example of a “disconnected region”, associated to a given set of *four* boundary points. The von Neumann entropy of the chosen region in such a case will depend on the von Neumann entropy of its disjoint connected parts and the mutual information shared between them. We will discuss the case of disconnected regions in more detail in Sections 6.5-6.5.

Looking ahead, we make two more definitions.

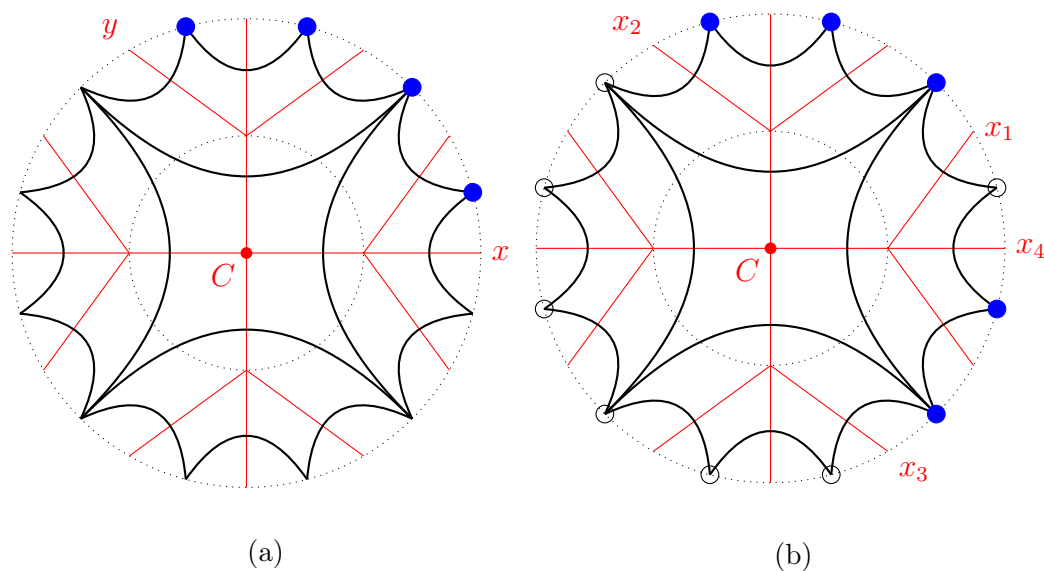


Figure 6.5: (a) The set of vertices on the dual graph marked in blue form a “connected region”. (b) The set of blue vertices form a “disconnected region” which can be specified by a set of four boundary points. Note that for the given set of boundary points and a chosen planar embedding, another choice of disconnected regions, shown in black circles, is possible.

Definition 8. Given a planar embedding (i.e. a choice of a dual graph tensor network) and a geodesic γ that separates the tensor network into two connected components, called *bulk regions* P and Q , the *boundary* of each bulk region is a collection of uncontracted tensor legs, which includes the tensor legs which were originally contracted across γ .

Definition 9. Given a boundary interval A specified by a set of nodes on the tensor network (where more precisely, by A we mean the collection of uncontracted tensor legs at the specified set of nodes), we say a geodesic γ is *homologous* to A if there exists a bulk region on the tensor network, part of whose boundary is given by (the full set of uncontracted tensor legs at) A while the remaining uncontracted legs forming the boundary of the bulk region are in bijective correspondence with the edges of the geodesic γ .

This definition applies to both connected and disconnected regions A , and has an obvious extension to the setting with multiple geodesics. This notion of homologous geodesics is a natural adaptation of the notion in continuum case to tensor networks, and makes a natural appearance in our tensor network setup.

Results

We now summarize the entanglement entropy results for the tensor network described above; the detailed calculations can be found in Sections 6.5–6.5. In the case of a connected region A , parametrized by the points $x, y \in \mathbb{Q}_p$ as described previously, we prove in Section 6.5 that the vacuum von Neumann entropy is given by

$$S(x, y) = (2 \log r) \log_p \left| \frac{x - y}{\epsilon} \right|_p, \quad (6.35)$$

where $\epsilon = p^\Lambda \in \mathbb{Q}_p$ is the UV cutoff, and the tensor network is built out of perfect tensors of rank $r + 1$. The overall factor of $\log r$ can be absorbed by taking a logarithm in base r when computing von Neumann entropy via $S = -\text{Tr} \rho \log \rho$. We use the notation $S(x, y)$ to emphasize that the entropy is independent of the choice of planar embedding and only a function of p -adic coordinates x and y . The p -adic norm $|\cdot|_p$ appears naturally in this tensor network setup, and the expression (6.35) makes sense in the limit $|\epsilon|_p \rightarrow 0$ when the finite cutoff tree approaches the infinite Bruhat–Tits tree.⁹ The quantity $|x - y|_p$ has a natural interpretation as the measure of the smallest clopen set in \mathbb{Q}_p containing both x and y and is the analog of the “length of an interval” over the reals. The result (6.35) is obtained by explicitly computing the reduced density matrix and diagonalizing it. The entanglement entropy obtained is in direct analogy with the corresponding classic result for the entanglement of a connected interval (of size $|x - y|$ over the real line) with its complement, on a static spatial slice of a massless CFT₂ with UV cutoff ϵ [216, 214].

The tensor network also affords a bulk interpretation for (6.35). We show in Section 6.5 that the von Neumann entropy $S(x, y)$ is precisely equal to the length of the minimal geodesic in the bulk homologous to the connected region A , consistent with the Ryu–Takayanagi formula. On a static slice of CFT₂, the minimal geodesic joins the end-points of A , given by the “entangling surfaces” $x, y \in \mathbb{Q}_p$. Indeed, we show that

$$S(x, y) = \frac{\text{length}(\gamma_{xy})}{\ell} \log r, \quad (6.36)$$

where γ_{xy} is the minimal geodesic on the cutoff Bruhat–Tits tree joining boundary points x and y , and ℓ , the length of each edge on the tree, is proportional

⁹For a finite tree bulk geometry, the expression (6.35) continues to make sense if one views the boundary points x, y , which are now elements of the ring $\mathbb{Z}/p^\Lambda \mathbb{Z}$, as p -adic numbers with a truncated power series expansion.

to the AdS radius. As remarked earlier, this result is consistent with the minimum-cut rule obeyed by networks of perfect tensors in the case of bipartite entropy of connected regions [99], although we do not assume it in our setup. Essentially, the dual graph tensor network proposed in this chapter has the property that the minimal number of tensor contractions on the tensor network which must be “cut” across to completely separate the connected region from the rest of the network, precisely equals the length of the minimal geodesic on the Bruhat–Tits tree. Indeed, we show in Section 6.5 that these cuts trace out precisely the path of the minimal geodesic joining the entangling surfaces.¹⁰

Moreover, we have the bulk formula

$$\text{length}(\gamma_{xy})/\ell = \delta(C \rightarrow x, C \rightarrow x) + \delta(C \rightarrow y, C \rightarrow y) - 2\delta(C \rightarrow x, C \rightarrow y), \quad (6.37)$$

where C is an arbitrary node on the Bruhat–Tits tree (or its boundary), and $\delta(\cdot, \cdot)$ is the signed-overlap between the two directed paths in its argument [82].¹¹ Equations (6.36)-(6.37) are applicable for connected regions in the genus 1 geometry as well, which is discussed in the next section.

We also show in Section 6.5 that the result (6.36)-(6.37) continues to apply to a (massless) CFT defined over a circle, more precisely the projective line $\mathbb{P}^1(\mathbb{Q}_p)$. Let’s first recall the result in the real case. Over the reals, the entropy formula

$$S(x, y) \propto \log \frac{L}{\epsilon}, \quad (6.38)$$

where $L = |x - y|$ is the size of the connected interval $A = [x, y]$ and ϵ the UV cutoff in the CFT, gets replaced by [214]

$$S(x, y) \propto \log \left(\frac{2R}{\epsilon} \sin \frac{L}{2R} \right), \quad (6.39)$$

where R , the IR cutoff parametrizing the total size of the spatial boundary, is the radius of the Poincaré disk, and $L = R|\arg x - \arg y|$ is the arc length

¹⁰In fact the geodesic is homologous to the specified region. This condition is especially important in black hole geometries where there can exist shorter geodesics not homologous to the given region. The tensor network always picks the one which is homologous. This will be discussed in more detail in the next section.

¹¹For example, the signed-overlap of a path with itself is simply the length of the path, while the signed-overlap with the same path but with opposite orientation is *negative* the total length of the path. The signed overlap vanishes for paths which do not share any edges.

of the interval with $x, y \in \mathbb{P}^1(\mathbb{R}) = S^1$. In the limit $L \ll R$, (6.39) reduces to (6.38).

When the spatial slice at the boundary is the projective line over \mathbb{Q}_p , the results in the p -adic tensor network setup continue to be analogous to the real case. The measure of the smallest clopen set in \mathbb{Q}_p containing $x, y \in \mathbb{Q}_p$, given by $|x - y|_p$ in (6.35) gets replaced by the Patterson-Sullivan measure of the smallest clopen set in $\mathbb{P}^1(\mathbb{Q}_p)$ containing $x, y \in \mathbb{P}^1(\mathbb{Q}_p)$ [239], so we have

$$S(x, y) = (2 \log r) \log_p \frac{|\mathfrak{B}(x, y)|_{\text{PS}}}{|\epsilon|_p}. \quad (6.40)$$

Explicitly, choosing C to be the radial center of the cutoff Bruhat–Tits tree in the Poincaré disk picture (recall figure 6.3b), the Patterson-Sullivan measure is given by $|\mathfrak{B}(x, y)|_{\text{PS}} \equiv p^{-d(C, \text{anc}(x, y))}$, where $d(\cdot, \cdot)$ is the graph distance between the nodes in its argument, and $\text{anc}(x, y)$ is the unique vertex on the Bruhat–Tits tree at which the geodesics from x, y and C simultaneously intersect.

When $d(C, \text{anc}(x, y)) \ll d(C, x) = d(C, y)$, the Patterson-Sullivan measure is approximated by $|x - y|_p$, thus recovering the formula (6.35) from (6.40).¹² Moreover, the Patterson-Sullivan measure rises, attains a maxima, and then falls as the boundary points x and y are moved away from each other, similar to the sine function in (6.39) which rises, reaches a maxima, and then falls as L is increased. This can be seen from the explicit form of the Patterson-Sullivan measure quoted above, by fixing one of the boundary points while moving the other “away” from it.¹³

We remark that as is clear from (6.35) and (6.40), the measure of the clopen set is more fundamental than the number of boundary vertices falling within a connected region in a chosen planar embedding. Fixing a planar embedding, a given pair of end-points x, y may simply contain “in between” themselves a single vertex on the tensor network but may still correspond to a clopen set with a larger measure than that of another pair of points which carry “in

¹²Here we are being loose about the distinction between $x \in \mathbb{P}^1(\mathbb{Q}_p)$ and $x \in \mathbb{Q}_p$. The precise statement is that when the radial center C is sent to a boundary point, say $\infty \in \mathbb{P}^1(\mathbb{Q}_p)$, the remaining boundary of the Bruhat–Tits tree is described precisely by the p -adic numbers \mathbb{Q}_p and in this case, the Patterson-Sullivan measure on $\mathbb{P}^1(\mathbb{Q}_p)$, $|\mathfrak{B}(x, y)|_{\text{PS}} = p^{-d(C, \text{anc}(x, y))}$ reduces exactly to the Haar measure on \mathbb{Q}_p , given by the p -adic norm $|x - y|_p$.

¹³The Patterson-Sullivan measure rises, attains a maximum, and then eventually falls in discrete steps in contrast to the smoothly varying sine function in (6.39), as one fixes one of the nodes but moves the other “away” in the sense of increasing the path length along the “shortest bonds” between the two nodes for a chosen orientation.

between” themselves a larger number of vertices. This essentially is due to the inherent ultrametric nature of the setup.

In Section 6.5 we extend the results for a single connected interval to the case of a disconnected interval. Instead of two boundary points specifying a single connected interval, we now have four boundary points parametrizing the disconnected case, with the full interval written as a union of its two connected components. We show that the entropy is independent of the planar embedding and obeys an RT-like formula exactly (see, for instance, the discussion around (6.104)). We also verify the non-negativity of mutual information as well as the Araki–Lieb inequality, and in fact in (6.103) write down an explicit expression for mutual information in terms of the conformal cross-ratio constructed from the boundary points. We then provide a dual bulk interpretation of mutual information in terms of the overlap of the minimal geodesics of the individual components. Finally, in Section 6.5 we give a simple holographic proof of strong subadditivity in the p -adic setting, demonstrating its relation to ultrametricity, and a proof for monogamy of mutual information. In fact, we find that mutual information is extensive, that is, the tripartite entropy is identically zero. We refer to these sections for more details.

6.4 p -adic BTZ Black Hole

In this section, we continue the study of the proposed tensor network in bulk geometries which can be considered the p -adic analog of black hole or thermal states. We will first summarize the construction of these p -adic geometries (\mathbb{Q}_p) in analogy with the complex case of Euclidean AdS₃ (\mathbb{C}) or a time slice of the Lorentzian counterpart. This *uniformization* procedure is an algebraic way to obtain black hole geometries from empty AdS, and there is a natural way to apply this construction to the perfect tensor network of the previous section. Instead of a pure state on the boundary in this toy model, one finds degrees of freedom behind the ‘horizon’ which must be traced out. The result is a thermal density matrix, and following [199] we interpret this as the thermal state at the conformal boundary with entropy analogous to the entropy first observed by Bekenstein and Hawking [241, 242]. In this discrete p -adic model, using computational tools described in the next section we find precise agreement between the perimeter of the black hole horizon and the thermal entropy of the boundary density matrix. We postpone the details of this calculation until Section 6.5, and here we will focus on the setup and results.

One can further study entanglement entropy in these genus 1 backgrounds by tracing out regions of qubits at the boundary. The resulting entanglement entropy has a dual interpretation in the bulk as the lengths of minimal geodesics homologous to the boundary intervals in the black hole background, the analog of the Ryu–Takayanagi formula in this geometry [92, 93]. In our model, the boundary anchored geodesics wrap non-trivially around the horizon to minimize the total length, and one might have expected this minimization property of tensor networks from the minimal cut rule of [99]; however we emphasize that the genus 1 tensor network is fundamentally different from the one considered in [99] and is obtained instead as a quotient of the genus 0 construction. We have verified this agreement between the boundary entropy and the bulk geodesic length by direct computation, and conjecture that this gives a holographic derivation of entanglement entropy in p -adic AdS/CFT in thermal backgrounds.

Genus 1 curves and Schottky uniformization

In analogy with the complex case of AdS₃/CFT₂ where the Bañados, Teitelboim, and Zanelli [73] (BTZ) black hole boundary in Euclidean signature is a T^2 , the boundary picture of these p -adic BTZ black holes can be understood as genus $g = 1$ curves over non-Archimedean fields. These curves were originally described in the classical work of Tate for $g = 1$ and Mumford for $g > 1$ [75], and while we focus on the genus 1 case we will often refer to the boundary curve as a Tate–Mumford curve. The applications of the boundary curve/bulk graph to p -adic AdS/CFT are described in Chapter 5 as well as [74]. The bulk spaces are then given by quotients of the p -adic Bruhat–Tits tree (the analog of empty AdS) by the action by isometries of a discrete group. For a general introduction to Mumford curves and their associated bulk spaces see [243, 244].

In the complex case of a torus boundary, a familiar realization is a uniformization of the elliptic curve $E(\mathbb{C})$ by the complex plane \mathbb{C} . If the modular parameter is τ with $\text{Im}(\tau) > 0$, one may construct a \mathbb{C} lattice $\Lambda = \mathbb{Z} \oplus \tau\mathbb{Z}$ and describe the curve as the quotient

$$T^2 \simeq E(\mathbb{C}) \simeq \mathbb{C}/\Lambda. \quad (6.41)$$

This is the familiar procedure of identifying opposite sides of a parallelogram. However, a direct p -adic analog using a lattice turns out to not be possible. An

alternative approach due to Tate is essentially to consider the exponentiated map. Defining the standard Fourier parameter $q = e^{2\pi i\tau}$ which satisfies $|q| < 1$ since $\text{Im}(\tau) > 0$, we may instead consider a quotient of the multiplicative group \mathbb{C}^\times :

$$T^2 \simeq E(\mathbb{C}) \simeq \mathbb{C}^\times / q^{\mathbb{Z}}, \quad (6.42)$$

where $q^{\mathbb{Z}}$ for the integers \mathbb{Z} form a discrete abelian group. This construction of the elliptic curve is an example of complex *Schottky uniformization* of genus 1 curves, which can be generalized to $g > 1$ curves and has a natural p -adic analog. Schottky uniformization is the uniformization of an elliptic curve by quotienting the projective line by a chosen discrete subgroup of its Möbius transformations. More precisely, we must first remove a certain limit set of the projective line where the Schottky group acts poorly; in the present $g = 1$ case these can be chosen to be the two points $\{0, \infty\}$, which explains the \mathbb{C}^\times used above. At higher genus the limit set is much more complicated, see Sections 5.2 and 5.5 for details.

At genus 1 we can be even more explicit. Recall in the complex case that Möbius transformations form the group $G = \text{PSL}(2, \mathbb{C})$ which acts on $\mathbb{P}^1(\mathbb{C})$ with complex coordinate z by fractional linear transformations,

$$g \in G = \begin{pmatrix} a & b \\ c & d \end{pmatrix} : z \mapsto \frac{az + b}{cz + d}. \quad (6.43)$$

Removing the aforementioned limit points, we may now pick a discrete subgroup $\Gamma \in \text{PSL}(2, \mathbb{C})$ with which to perform the quotient. For genus $g = 1$ with the abelian group $\Gamma = q^{\mathbb{Z}}$, a generator γ acts on the domain by

$$\gamma \in \Gamma = \begin{pmatrix} q^{1/2} & 0 \\ 0 & q^{-1/2} \end{pmatrix} : z \mapsto qz, \quad (6.44)$$

and we may obtain a torus by dividing by this action; explicitly points in the plane are identified under this scaling.

In Euclidean signature, this action uplifts to the 3-dimensional hyperbolic upper half plane which has the complex projective line as its boundary. Here we view $\text{PSL}(2, \mathbb{C})$ as the group of isometries of Euclidean AdS_3 with the scaling extending into the bulk direction. In the bulk, this Schottky generator q acts by scaling of geodesic surfaces, and in particular it acts on the unique geodesic connecting $\{0, \infty\}$ as translations by $\log q$. Taking a quotient of the

bulk by this action gives the Euclidean BTZ black hole, presented as a solid torus with the desired elliptic curve $E(\mathbb{C})$ at the conformal boundary. This was illustrated in the Chapter 5 in figure 5.3. (In fact, one may obtain a family of black hole and thermal AdS solutions by acting with modular transformations [199, 245].)

It is possible to repeat the above uniformization in Lorentzian AdS_3 . In this case, the isometry group is $SO(2, 2)$, the connected part of which is isomorphic to $(\text{SL}(2, \mathbb{R}) \times \text{SL}(2, \mathbb{R}))/\mathbb{Z}_2$ (in fact, there is a subtlety in the choice of covering group [246], which will not concern us here.) As before, quotienting with discrete abelian subgroups can be used to find BTZ black hole spacetimes in Lorentzian signature, possibly with angular momentum. In our case in analogy with genus 0, we would like to interpret the p -adic tensor network as describing a time slice of a static black hole. To this end, one may pick a discrete subgroup of the diagonal $\text{PSL}(2, \mathbb{R})$ acting on the $t = 0$ slice, which is now a copy of the upper half plane $\mathbb{H}^2 \sim \mathbb{R} \times \mathbb{R}^+$. For $q \in \mathbb{R}$, the Schottky group is again $\Gamma = q^{\mathbb{Z}}$ with matrix form (6.44), acting by fractional linear transformation, but now on \mathbb{H}^2 (rather than the complex boundary coordinate as in the Euclidean case.) The result of this quotient is the $t = 0$ slice of the non-rotating BTZ black hole in Lorentzian signature. In the bulk, this is two-sided and has one non-contractible cycle—the black hole horizon.

In the conventions of [247] with unit cosmological constant, this black hole with mass $M = r_+$ and angular momentum $J = 0$ is generated by the Schottky element

$$\gamma = \begin{pmatrix} e^{\pi r_+} & 0 \\ 0 & e^{-\pi r_+} \end{pmatrix}. \quad (6.45)$$

From this one may find the horizon perimeter and compute the Bekenstein-Hawking entropy. In these units it is simply $S_{BH} = 4\pi r_+ = 2 \log q$ in terms of the q parameter.

When moving from \mathbb{R} or \mathbb{C} to \mathbb{Q}_p , the topology and geometry of both the bulk and boundary change dramatically. The goal of the present work is not to define or classify the possible choices in this p -adic setting (which might involve even more exotic structures such as buildings), but rather to provide a discrete toy model of holography in which aspects of the bulk can be computed exactly. For this reason, in discussing genus 1 black holes we will assume the simplest interpretation of a static black hole where we work on a spatial slice;

this is the situation where our formulas have qualitative similarity to real AdS/CFT in 3-dimensions. There may be other interpretations of our results, and we will remain agnostic about more general signatures and situations such as rotating black holes.

We now proceed to describe the uniformization of the Tate-Mumford curve by the p -adic multiplicative group \mathbb{Q}_p^\times . This describes the boundary geometry for the black hole, and there is a natural extension to the bulk Bruhat-Tits tree. As explained above, we will not rely on a lattice, but rather identification of points under a Schottky generator; now a discrete subgroup of the p -adic conformal group. Mathematically, we will mimic the above construction with the substitutions $\mathrm{PSL}(2, \mathbb{R}) \rightarrow \mathrm{PGL}(2, \mathbb{Q}_p)$ along with the discrete Schottky generator $\Gamma \subset \mathrm{PGL}(2, \mathbb{Q}_p)$. Physically as we have explained, we interpret the result in the bulk as a time slice of a static black hole. Asymptotically, this geometry looks like the Bruhat-Tits tree, but the center contains a non-contractible cycle of integer length. In a different context, this uniformization was used in the context of open p -adic string theory to compute multi-loop amplitudes in [81], which viewed the Bruhat-Tits tree and its higher genus generalizations as worldsheets.

We seek a p -adic version of equation (6.42), which is the desired Tate-Mumford curve at the boundary. Beginning with the usual boundary $z \in \mathbb{P}^1(\mathbb{Q}_p)$, the Möbius transformations now form the group $\mathrm{PSL}(2, \mathbb{Q}_p)$ acting on z by fractional linear transformations, though below we will use $G = \mathrm{PGL}(2, \mathbb{Q}_p)$ which is the isometry group of the tree.¹⁴ We choose the abelian Schottky group $\Gamma = q^{\mathbb{Z}} \in \mathrm{PGL}(2, \mathbb{Q}_p)$, with $q \in \mathbb{Q}_p^\times$, $|q|_p < 1$. The PGL matrix which generates the Schottky group can be chosen to be

$$\gamma \in \Gamma = \begin{pmatrix} q & 0 \\ 0 & 1 \end{pmatrix} : z \mapsto qz. \quad (6.46)$$

Performing the quotient, which identifies p -adic numbers related by this scaling, we obtain a curve of genus 1 at the conformal boundary, which is the

¹⁴We have passed from the special linear group to the general linear group because this more properly accounts for the isometries of the Bruhat-Tits tree. One may see that the $\mathrm{SL}(2)$ matrix in (6.44) requires us to take a square root in \mathbb{C} ; this is in general not possible for $q \in \mathbb{Q}_p$ without extensions. Among other things, restricting to $\mathrm{SL}(2)$ thus excludes translations on the tree by non-square elements, while a $\mathrm{GL}(2)$ matrix allows one to act with isometries of this type.

elliptic curve uniformized by the p -adic multiplicative group:

$$E(\mathbb{Q}_p) \simeq \mathbb{Q}_p^\times / q^{\mathbb{Z}}. \quad (6.47)$$

This in principle completes the description of the boundary curve for the black hole geometry which might be interpreted as a thermal state of a conformal field theory at a fixed time slice. An important technical caveat is that not all elliptic curves over \mathbb{Q}_p can be uniformized in this way, only those with split multiplicative reduction. However, it is precisely these Tate-Mumford curves which have a natural extension to the Bruhat-Tits tree \mathcal{T}_p , so we will only consider these in this work.

The situation so far over the p -adics may be somewhat abstract, but a very intuitive picture resembling a black hole emerges when we consider the quotient of the Bruhat-Tits tree itself by the above Schottky generator. Algebraically, one again removes the boundary points $\{0, \infty\}$ of \mathcal{T}_p and identifies vertices and edges of the tree related by the action of the Schottky generator; we can express this as $(\mathcal{T}_p \setminus \{0, \infty\})/q^{\mathbb{Z}}$. In analogy with the real case, an explicit form of this generator is a $\mathrm{PGL}(2, \mathbb{Q}_p)$ element which translates along the $\{0, \infty\}$ by $\log_p |q|_p^{-1}$. Pictorially (and more formally), the geometry after the quotient is obtained by taking the entire tree and identifying points which are related by translation by $\mathrm{ord}_p(q) = \log_p |q|_p^{-1}$ steps along this main geodesic. The condition on the norm of q means this translation is always an integer number of steps, and the result is a central ring of length $\mathrm{ord}_p(q)$ with branches which asymptotically look like \mathcal{T}_p . It is a motivating result that the boundary of this ring geometry can be identified with the Tate-Mumford curve, and mathematically it is guaranteed by our uniformization procedure. This is was already illustrated in Chapter 5, but here we reproduce the figure 6.6, where by analogy with the real case we interpret this as a time slice of a static BTZ black hole.

Our final task of this section is to explain how to extend this p -adic uniformization to the tensor network living on the dual graph of the Bruhat-Tits tree. The most natural way to do this is to simply perform the identifications under the Schottky generator on both the tree and the dual graph simultaneously, and one can see graphically that this will introduce a special vertex behind the ‘horizon’. This vertex is most naturally traced out (as in a two-sided black hole geometry,) and we will later show by explicit computation that this

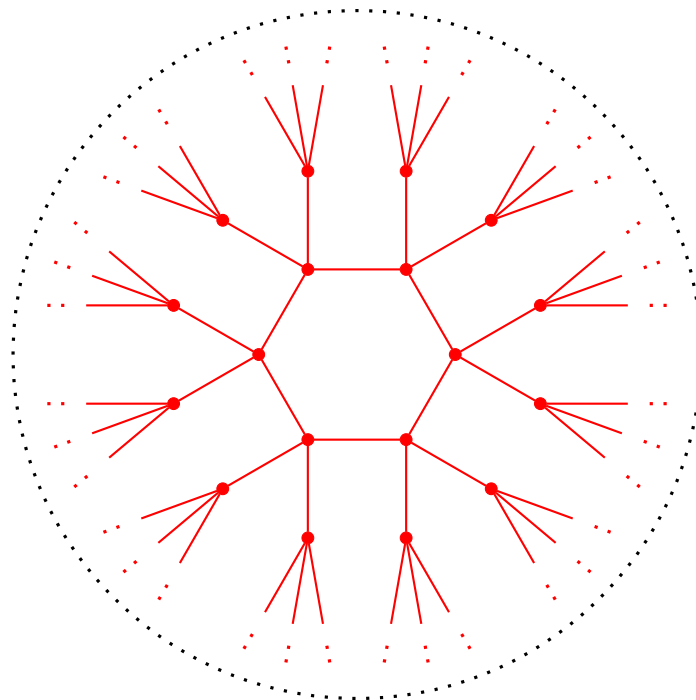


Figure 6.6: The p -adic BTZ black hole, obtained here for $p = 3$ by a quotient of the Bruhat–Tits tree by a Schottky generator with $\log_p |q|_p^{-1} = 6$. The geometry is locally indistinguishable from the Bruhat–Tits tree, but the presence of the horizon signifies the boundary interpretation will be very different. In the tensor network analysis we will find the boundary state of this geometry will have a thermal entropy proportional to $6 \log p$.

choice produces a mixed density matrix for the boundary state. The thermal entropy of this density matrix is proportional to the perimeter of the p -adic BTZ black hole, giving agreement with Bekenstein–Hawking formula up to an overall constant. In this toy model, the interpretation of these microstates are those legs (namely contracted bonds) of the tensor network which stretch across the horizon.

As usual, the identification and resulting BTZ black hole tensor network are best done with the aid of a figure. We first redraw the tree in a form that is ‘flattened out’ along the preferred $\{0 \rightarrow \infty\}$ geodesic, as shown in the top sub-figure of figure 6.7, where we have explicitly chosen $p = 3$ and $\log_p |q|_p^{-1} = 5$ as an example. While we can only display a small portion of the tree, one should think of this geodesic as stretching infinitely, with branches coming off and continuing to the conformal boundary. This is nothing but a relabeling of figure 6.2b, but we have now labeled a special vertex O on the tensor network which sits above the central geodesic as well as a special vertex a on the tree.

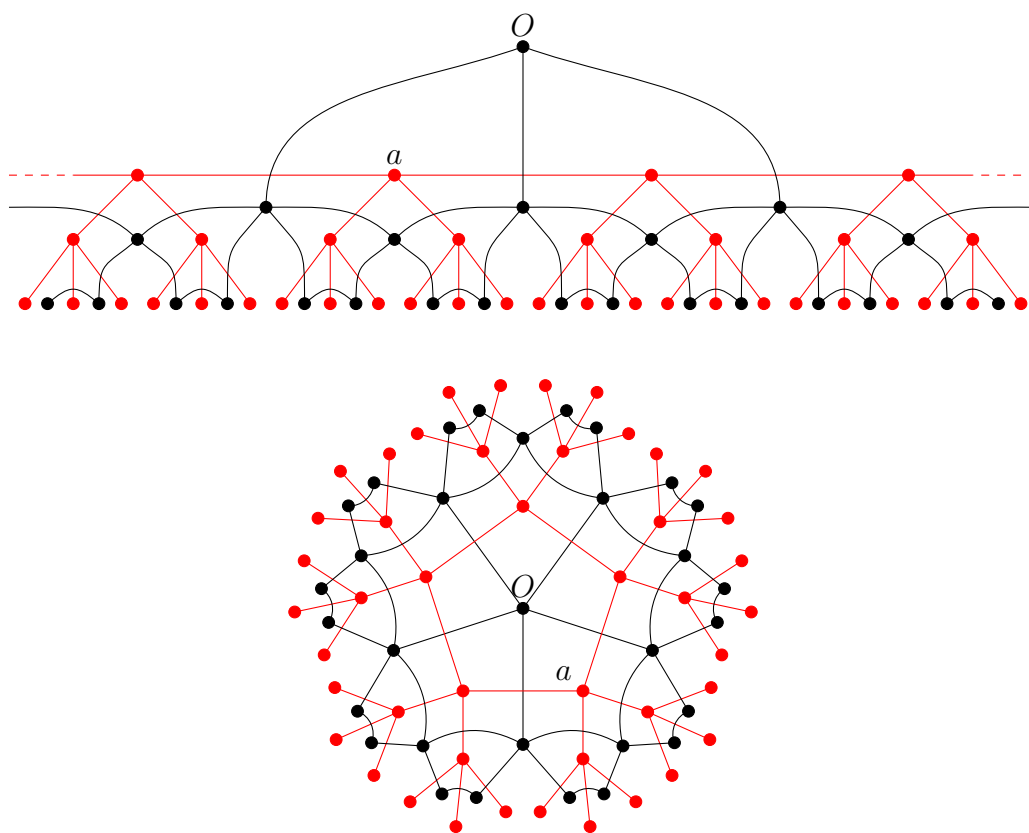


Figure 6.7: The quotient construction of the dual graph tensor network (in black). As pictured, $p = 3$ and $\text{ord}_p(q) = 5$.

After the quotient, O will be in the black hole interior and a will be identified with its image under $a \rightarrow a - \log_p |q|_p$. Recall also that all the vertices on this dual graph have dangling legs and represent degrees of freedom on the boundary, but we have not yet specified the rank of these tensors due to a subtlety explained below.

After taking the quotient, we can redraw the tree and its dual graph in a form that has rotational symmetry as seen in the second figure 6.7. The infinite geodesic has now become the central cycle or horizon of the black hole, and the genus 1 boundary is now the boundary of the infinite branches coming off of this cycle. The center point O , which before the quotient was just another vertex on the boundary, has now moved behind the horizon. The number of internal bonds connected to O is determined by the p -adic norm of our Schottky parameter q , which can be any integer greater than 1.

This is an intuitive picture of how one might make a black hole tensor network

state which agrees with our uniformization procedure for the tree. It is now necessary to explain both the subtleties of how the dual graph is defined as well as the cut-off prescription. Recall in the genus 0 picture, the bulk IR regulator Λ was defined as half the length of the longest geodesic- this meant truncating both the tree and the dual graph Λ steps from the central vertex in all directions. For the black hole case, we would like the analogous statement to be that we truncate the tree and network Λ steps from the horizon. However, in order to achieve this, we had to use a different cutoff before identifying points related by the Schottky group. This should be clear from examining the ‘flat’ picture of the tree, which for finite cut-off would not correspond to something radially symmetric. Conceptually, we could treat the genus 0 and genus 1 on an equal footing if we worked with the infinite tree and network and only apply the cut-off prescription after taking the quotient.

One can note that the two criterion expressed in Section 6.3 continue to hold in the black hole background; every edge of the tree has exactly one bond of the dual graph which “cuts” it, and every vertex of the tree is surrounded by a plaquette with $p + 1$ sides. These facts do not guarantee that the dual graph after taking the quotient is uniquely defined, but later we will discuss the boundary measure associated to the Mumford curve and the dual graph and find a canonical choice. Recall that in the genus 0 case, the non-uniqueness could be interpreted as the lack of ordering of p -adic numbers at the boundary.

A further technical point concerns black holes that are large compared to the cutoff scale. When working with the genus 0 network with a finite cutoff, we observed that our uniform use of a single kind of perfect tensor of rank $r + 1$ required certain conditions on the rank and the cutoff in order for the Ryu–Takayanagi formula to hold. Roughly speaking, the number of bulk contracted legs at any tensor could not exceed the number of boundary uncontracted legs. Increasing the cutoff thus meant increasing the rank, corresponding to a large number of UV degrees of freedom at the boundary. Similarly, the perimeter of the black hole horizon at genus 1 also constrains the minimum rank of the tensor, as now the center point may have a larger number of bulk bonds than other points in the network. This becomes an issue for black holes that are large compared to the cutoff, but using a sufficiently large rank perfect tensor will always produce the correct answers for the black hole entropy.

There is one final point to address, which is the curious case of a horizon with

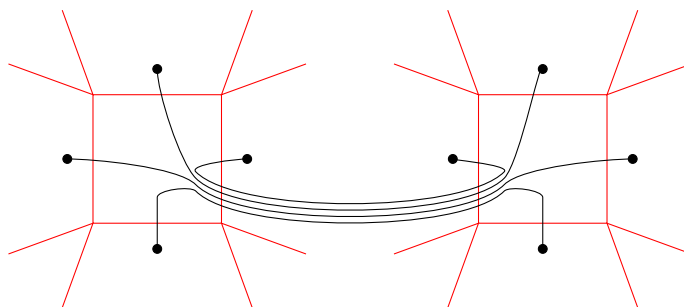


Figure 6.8: The genus 1 tensor network after tracing out the vertex behind the horizon. One should imagine the two sides corresponding to $|\psi\rangle$ and $\langle\psi|$, and the total state being the mixed density matrix which has von Neumann entropy proportional to the number of shared bonds. We postpone the explanation of the graphical rules and the computation of the entropy until Section 6.5, but the reader might be reminded of the 2-sided BTZ black hole.

length $\log_p |q|_p^{-1} = 1$. This is the minimal Tate-Mumford curve allowed by the uniformization; the corresponding quotient of the Bruhat-Tits tree contains a self-looping edge, and it correspondingly leads to a degenerate configuration of the network. One of the plaquettes of the dual graph network collapses. Nonetheless, the entropy computed from this degenerate network still leads to the expected result.

Black hole entropy

In the previous subsection, we described the construction of BTZ black holes in p -adic AdS/CFT via the algebraic process of Schottky uniformization. We also explained how this naturally extended to the dual graph tensor network, essentially by identifying all nodes and bonds related by a translation by the horizon length. The result is a graph with a cycle and a dual graph tensor network with many desirable properties; crucially there is one special vertex behind the horizon which cannot be identified with any boundary degrees of freedom. In this section, we present the results of a computation on the tensor network for the thermal entropy of the boundary density matrix obtained by tracing out this vertex, explained in more detail in Section 6.5. We find perfect agreement between the thermal entropy and the black hole horizon perimeter, as predicted by an analog of the Bekenstein-Hawking formula.

Tracing out the center vertex in our tensor network amounts to constructing a mixed density matrix reminiscent of a two-sided BTZ black hole. This is depicted in figure 6.8 and follows from our graphical rules for computing

density matrices from tensor networks, explained in Section 6.5. Defining the perimeter to be $\tau = \log_p |q|_p^{-1}$, we find by detailed computation the von Neumann entropy of the boundary state to be proportional to the perimeter, which is the same as the number of bonds stretched across the two sides. The result is surprisingly simple and analogous to the BTZ black hole entropy discussed in the previous section:

$$S_{\text{BH}} = \tau \log r . \quad (6.48)$$

Ryu–Takayanagi formula in the black hole background

Here we will briefly summarize our results which combine the main ideas of Sections 6.3 and 6.4. This involves computing the boundary von Neumann entropy of a single connected interval in the thermal background, holographically found to be dual to the length of a minimal geodesic in the black hole geometry homologous to the interval. This presents further computational challenges which are discussed in Section 6.5. As is often the case with quantities that can be computed in the dual picture, the bulk result is easier to state than derive, but we find agreement in all cases considered. A schematic depiction of the behavior of the minimal surface is shown later in figure 6.17. It is a surprising and nontrivial fact that the tensor network proposed here automatically captures the three topologically distinct cases for the surface. We take the success of this tensor network proposal as a conjecture for the entanglement entropy of a connected interval in p -adic field theory at finite temperature.

A key conceptual difference from the genus 0 Ryu–Takayanagi formula is that the entropy of a boundary region and its complement are not equal, since the holographic state generated by the network is no longer a pure state. The bulk interpretation of this is the presence of the black hole horizon which minimal surfaces may wrap around. Varying the (p -adic) size of the boundary region, a minimal geodesic might jump from crossing one side of the horizon to the other, and one observes this behavior in the boundary von Neumann entropy as well. This is a feature that is desirable in principle and in practice, though care must be taken in the precise definition of the boundary measure and dual graphs. We chose to parametrize the size of the boundary ‘intervals’ using the measure for the covering space (before taking the quotient), and this is explained in greater mathematical detail in Section 6.6. However, after making

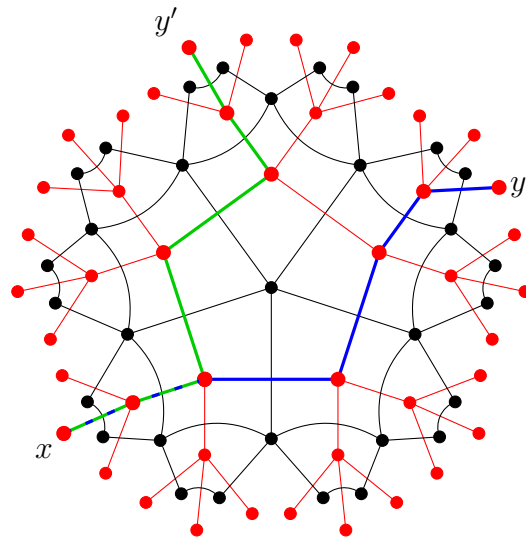


Figure 6.9: Geodesics in the BTZ black hole geometry. Moving y to y' leads to a “jump” of the minimal geodesic to a path wrapping the other side of the horizon.

a choice of a planar embedding for the tensor network, the intuitive picture of the genus 1 minimal geodesic behavior is easy to see in figure 6.9.

The structure of entanglement in this p -adic black hole setting has a particular novel feature not present in the usual picture of AdS_3 . In that case, small interval sizes or low temperatures will have entanglement entropy very nearly equal to the flat space result [214], which can be seen by Taylor expansion or noting the minimal surfaces do not approach the BTZ horizon. In contrast, for p -adic AdS/CFT the transition would seem to be much sharper. If one considers boundary regions that are small enough in the measure described above, one may see that the minimal geodesic never reaches the horizon, and the length and thus the entropy will be precisely equal to the genus 0 case. This is an interesting prediction for entanglement in thermal p -adic field theories, where the indication is that low enough temperatures have exactly zero effect on the short distance physics (rather than parametrically small effect.) This is ultimately due to the non-Archimedean or ultrametric nature of p -adic numbers.

The various features of the minimal geodesics in the black hole background can be described using a distance measure in the bulk. Given a planar embedding, the entropy of the connected region (x, y) is given by a minimal geodesic homologous to the given region (recall definition 9 of the homologous condition).

In the p -adic black hole background, given two boundary points, there are two possible boundary anchored geodesics to choose from, only one of which will be homologous to the given region. The geodesic homologous to the complementary region will be given by the other path. This can be unified together into the formula

$$S(x, y) = \frac{\text{length}(\gamma_{xy})}{\ell} \log r, \quad (6.49)$$

where

$$\text{length}(\gamma_{xy})/\ell = \delta(C \rightarrow x, C \rightarrow x) + \delta(C \rightarrow y, C \rightarrow y) - 2\delta(C \rightarrow x, C \rightarrow y). \quad (6.50)$$

Here ℓ is the constant length of each edge of the tree, and C is an arbitrary reference point on the genus 1 graph. Recall that $\delta(\cdot, \cdot)$ is an integer which counts the signed overlap between the two paths in its arguments. Equation (6.50) does not depend on the choice of C , but the two choices of paths for $C \rightarrow x$ (as well as $C \rightarrow y$) in (6.50) correspond in all to the two possible values of $S(x, y)$, corresponding to the interval (x, y) and its complement on the boundary (such that the geodesics are appropriately homologous). Define $\epsilon \in \mathbb{Q}_p$ to be the cutoff

$$\epsilon \equiv p^\Lambda, \quad (6.51)$$

which goes to zero p -adically, i.e. $|\epsilon|_p \rightarrow 0$ as $\Lambda \rightarrow \infty$. If $x, y \in E(\mathbb{Q}_p) \simeq \mathbb{Q}_p^\times / q^\mathbb{Z}$, then

$$\text{length}(\gamma_{xy})/\ell = 2 \log_p \frac{|\mathfrak{B}(\{x, y\})|_{g=1}}{|\epsilon|_p}, \quad (6.52)$$

where $|\mathfrak{B}(\{x, y\})|_{g=1}$ is the measure of the set containing $x, y \in E(\mathbb{Q}_p)$. On the covering space geometry, there are infinitely many sets which contain x and y because there is an infinite set of image points which correspond to these boundary points. From the point of view of the fundamental domain, there are two minimal sets which correspond to the two ways to wrap around the horizon. The measure above corresponds to choosing one of the two depending on which choice of minimal surface(s) is homologous to the boundary region. This measure is further explained in Section 6.6, and the explanation from tensor network contractions is outlined in Section 6.5. Here we comment that up to an overall constant factor, the entanglement entropy for the mixed states is equal to these geodesic lengths, and this is encapsulated by this measure. One can see this as a kind of prediction for the single interval entanglement entropies for thermal states in p -adic AdS/CFT.

6.5 Von Neumann Entropy and Inequalities

In this section we present the detailed computations leading to the results summarized in Sections 6.3 and 6.4, as well as proofs of various entropy inequalities in Sections 6.5-6.5.

Perfect tensors and density matrices

Before getting to calculations in the holographic setup, we point out some of the basic ingredients and properties which will be useful later using simpler toy examples. We focus on simple states (not necessarily holographic) constructed using rank- $(r+1)$ perfect tensors; the indices of such tensors will label bases of fixed finite-dimensional Hilbert spaces, which we interchangeably call “spins,” “qubits,” or “qudits.” For example, for $r = 3$, consider

$$|\psi\rangle = T_{abcd} |abcd\rangle \quad a, b, c, d \in \{0, 1, 2\}, \quad (6.53)$$

where repeated indices are summed over, and $|abcd\rangle = |a\rangle \otimes |b\rangle \otimes |c\rangle \otimes |d\rangle$ is a product state of four qutrits. T_{abcd} is the rank-4 perfect tensor, and we normalize it so that all its non-zero components are unity. Graphically, we may represent (6.53) as

$$|\psi\rangle = \begin{array}{c} b \\ | \\ \bullet \\ | \\ d \end{array} \begin{array}{c} c \text{---} \\ \text{---} \\ \text{---} \\ \text{---} \\ a \end{array} . \quad (6.54)$$

Since T is a perfect tensor, specifying half of its indices uniquely fixes the remaining half. For instance, we may choose

$$T_{0000} = T_{0111} = T_{0222} = T_{1012} = T_{1120} = T_{1201} = T_{2021} = T_{2210} = T_{2102} = 1, \quad (6.55)$$

with all other components vanishing. One may check that for any choice of two indices, there is a unique non-vanishing component of T , so the other two indices are also determined. The “perfectness property” is useful in writing out the full state $|\psi\rangle$ starting from (6.54). This $|\psi\rangle$ as constructed is a very special entangled superposition of 9 of the $3^4 = 81$ possible basis states. In this state, any choice of 2 spins are maximally entangled with the remaining two. This is a general feature of perfect states.

One can construct more complicated states by contracting multiple copies of the perfect tensor T in different ways. For example, the following graph

represents a new state,

$$|\psi'\rangle = \begin{array}{c} \diagup \quad \diagdown \\ \bullet \\ \diagdown \quad \diagup \\ \bullet \\ \text{---} \bullet \text{---} \bullet \text{---} \bullet \\ \bullet \\ \diagup \quad \diagdown \\ \bullet \\ \diagdown \quad \diagup \end{array} , \quad (6.56)$$

where we have suppressed the index labels. In (6.56) and future graphical representations, a shared edge between two vertices will denote that the corresponding index is to be summed over. Thus, explicitly, (6.56) represents the state

$$|\psi'\rangle = T_{a_0 b_0 c_0 d_0} T_{a_0 b_1 c_1 d_1} T_{b_0 b_2 c_2 d_2} T_{c_0 b_3 c_3 d_3} T_{d_0 b_4 c_4 d_4} |b_1 c_1 d_1 b_2 c_2 d_2 b_3 c_3 d_3 b_4 c_4 d_4\rangle . \quad (6.57)$$

In this example, the internal lines (denoted by indices with a 0 subscript) appear traced over in the tensors but do not label the basis of boundary states.

The (normalized) density matrix corresponding to the state $|\psi\rangle$ is given by

$$\rho = \frac{1}{\langle\psi|\psi\rangle} |\psi\rangle\langle\psi| . \quad (6.58)$$

For example, for the state in (6.53),

$$\rho = \frac{1}{9} T_{abcd} T_{a'b'c'd'} |abcd\rangle\langle a'b'c'd'| , \quad (6.59)$$

where we used

$$\langle\psi|\psi\rangle = T_{abcd} T_{abcd} = 9 , \quad (6.60)$$

which follows from the perfect tensor property of T and the fact that $a, b, c, d \in \{0, 1, 2\}$.

Just as states built from perfect tensor contractions had a convenient graphical representation, we will sometimes also write the density matrix in the same way. Because the density matrix is a product of the perfect state vector and the dual, graphically we can write (6.59) as

$$\rho = \frac{1}{9} \begin{array}{c} b \\ | \\ \bullet \\ | \\ d \end{array} \text{---} \begin{array}{c} a \\ | \\ \bullet \\ | \\ d \end{array} \begin{array}{c} c' \\ | \\ \bullet \\ | \\ d' \end{array} \text{---} \begin{array}{c} a' \\ | \\ \bullet \\ | \\ d' \end{array} , \quad (6.61)$$

with the understanding that (6.61) represents a density matrix, with the matrix elements given by specifying the external indices and performing the tensor contractions.

The normalization in (6.60) is a contraction on all indices, and we can represent this contraction by connecting the lines of (6.61), producing:

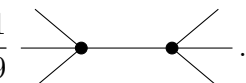
$$\langle \psi | \psi \rangle = \text{Diagram} . \quad (6.62)$$


This has no external legs, so it is a pure number. It evaluates to 9 as this is the number of non-vanishing components of T , equivalently the number of allowed assignments of the internal legs.

Taking partial traces leads to reduced density matrices. For example, for the ρ given in (6.59), if Tr_2 denotes tracing out the second factor of the direct product state $|\psi\rangle = |abcd\rangle$, then

$$\rho_1 \equiv Tr_2 \rho = \sum_{b''} \langle b'' | \rho | b'' \rangle = \frac{1}{9} T_{ab''cd} T_{a'b''c'd'} |acd\rangle \langle a'c'd'| . \quad (6.63)$$

Graphically, we represent this as

$$\rho_1 = \frac{1}{9} \text{Diagram} . \quad (6.64)$$



We have suppressed index labels on the graph. There is a slight abuse of notation by representing both states and reduced density matrices using the same kinds of pictures, even though the corresponding equations are unambiguous. We will be careful to distinguish between states and matrices in more complicated examples later; a rule of thumb is that the reduced density matrix is mirrored across the contracted lines.

The diagram in (6.64) is identical to that of a reduced density matrix where instead of the second factor, we traced out any of the other single qutrits in $|\psi\rangle = |abcd\rangle$. This follows from the permutation symmetry of the legs.

If instead we trace out two sites, say the first two, we obtain

$$\rho_2 \equiv Tr_{12} \rho = \sum_{a''b''} \langle a''b'' | \rho | a''b'' \rangle = \frac{1}{9} T_{a''b''cd} T_{a''b''c'd'} |cd\rangle \langle c'd'| . \quad (6.65)$$

Graphically, we write

$$\rho_2 = \frac{1}{9} \text{Diagram} . \quad (6.66)$$


Similarly, tracing out three sites leads to the following representation,

$$\rho_3 = \frac{1}{9} \text{---} \bullet \text{---} \text{---} \bullet \text{---} . \quad (6.67)$$

Explicitly evaluating expressions such as (6.63) and (6.65), and in fact the norm of a given state constructed out of perfect tensor contractions can become cumbersome for more complicated states. It would be useful to have a set of graphical rules which can be used to simplify and evaluate reduced density matrices without resorting to tedious (though straightforward) algebra. In the end, our goal is to evaluate the von Neumann entropy of the reduced density matrix $\rho_A = \text{Tr}_{A^c} \rho$,

$$S = -\text{Tr} \rho_A \log \rho_A, \quad (6.68)$$

which for pure ρ corresponds to a measure of quantum entanglement between the traced out region A^c and its complement $(A^c)^c = A$. With this in mind, we present some useful (diagrammatic) rules and techniques.

For two rank- $(r+1)$ perfect tensors T which have n_c indices contracted between them, with n_d free indices each, so that $n_c + n_d = r + 1$ we have

$$T_{a_1 \dots a_{n_d} b_1 \dots b_{n_c}} T_{a'_1 \dots a'_{n_d} b_1 \dots b_{n_c}} = \delta_{a_1 a'_1} \dots \delta_{a_{n_d} a'_{n_d}} \times r^{(n_c - n_d)/2} \quad n_c \geq n_d. \quad (6.69)$$

This easily follows from the “perfectness property” of perfect tensors and crucially assumes $n_c \geq n_d$. In this situation, we are tracing out at least half of the available indices on each tensor; once we have specified half the indices (for each term in the sum), the rest are uniquely determined. Tracing more than half the indices means we are performing a free sum on the remaining indices, this introduces the multiplicity given by $r^{(n_c - n_d)/2}$. In fact in (6.69), we need not have contracted precisely the final n_c indices, but some other subset of n_c indices to obtain the same form by symmetry. The Kronecker delta functions between “dangling” (uncontracted) indices in that case would still be between indices at matching positions.

Graphically, we write this contraction identity as

$$\begin{array}{c} a_1 \\ \vdots \\ a_{n_d} \end{array} \text{---} \bullet \text{---} \text{---} \bullet \text{---} \begin{array}{c} a'_1 \\ \vdots \\ a'_{n_d} \end{array} = \begin{array}{c} a_1 \text{---} a'_1 \\ \vdots \\ a_{n_d} \text{---} a'_{n_d} \end{array} \times \left(\bigcirc \right)^{(n_c - n_d)/2}, \quad (6.70)$$

which is valid whenever $n_c \geq n_d$. The horizontal line-segments correspond to the delta function factors in (6.69), with the understanding that precisely the free (dangling) indices at matching positions in the two tensors share a delta function. After doing the contraction, we see that we have “split” open the tensor to obtain the delta functions, and we refer to this operation as a “split”. The meaning of each disconnected loop represents a factor of r coming from the free sum. To see this, note that contracting a delta function δ_{ab} with another δ_{ab} results in

$$\delta_{ab}\delta_{ab} = \delta_{aa} = r, \quad (6.71)$$

which diagrammatically is represented as joining together the end-points of a line-segment, turning it into a (disconnected) loop. One checks that using rule (6.70), the inner product in (6.62) evaluates to $(\bigcirc)^2 = r^2 = 3^2$, which was the number of allowed terms in the free sum.

We may also interpret the l.h.s. of (6.70) as representing the partial trace of a pure (unnormalized) density matrix, leading to a diagonal reduced density matrix, as long as we remember to include appropriate ket and bra state factors in (6.69) when translating (6.70) back to equations. More precisely, starting with the pure (unnormalized) density matrix

$$\rho = T_{a_1 \dots a_{n_d} b_1 \dots b_{n_c}} T_{a'_1 \dots a'_{n_d} b'_1 \dots b'_{n_c}} |a_1 \dots a_{n_d} b_1 \dots b_{n_c}\rangle \langle a'_1 \dots a'_{n_d} b'_1 \dots b'_{n_c}|, \quad (6.72)$$

where $n_c + n_d = r + 1$, and tracing out, say, the final n_c sites (indices), one obtains a reduced density matrix ρ_r which is diagonal in the basis $\mathcal{B} = \{|a_1 \dots a_{n_d}\rangle : a_i = 0, 1, \dots, r - 1\}$:

$$\langle a_1 \dots a_{n_d} | \rho_r | a'_1 \dots a'_{n_d} \rangle = r^{(n_c - n_d)/2} \delta_{a_1 a'_1} \dots \delta_{a_{n_d} a'_{n_d}}, \quad (6.73)$$

as long as $n_c \geq n_d$ (this is the case where the sum over internal contracted lines fixes the values of the external legs.) Thus, ρ_r is a $r^{n_d} \times r^{n_d}$ diagonal density matrix. To start with a normalized ρ such that $\text{Tr } \rho = 1$, we normalize ρ in (6.72) by multiplying with an overall factor of $1/\langle \psi | \psi \rangle = r^{-(r+1)/2} = r^{-(n_c+n_d)/2}$. Then we see that the $\text{Tr } \rho_r = 1$ condition is satisfied automatically, and in fact ρ_r has r^{n_d} eigenvalues each equaling r^{-n_d} . The von Neumann entropy associated with ρ_r is then

$$S = -\text{Tr } \rho_r \log \rho_r = n_d \log r \quad (\text{perfect state with } n_c \geq n_d \text{ spins traced out}). \quad (6.74)$$

If $n_c < n_d$, then the reduced density matrix will no longer be diagonal in the previously chosen basis. In fact, since in this case $n_d > (r + 1)/2$, not all possible combinations for the string “ $a_1 \dots a_{n_d}$ ” are permissible anymore, as some combinations will lead to a vanishing tensor component $T_{a_1 \dots a_{n_d} b_1 \dots b_{n_c}}$. Thus the basis of states in which we may represent the reduced density matrix is no longer r^{n_d} -dimensional, but in fact an $r^{(r+1)/2}$ -dimensional subset $\mathcal{V} \subset \mathcal{B}$ (the exponent is $(r + 1)/2$ because that is precisely the maximum number of a_i indices one needs to specify before fully determining the tensor component $T_{a_1 \dots a_{n_d} b_1 \dots b_{n_c}}$ uniquely).

The reason that the reduced density matrix is not diagonal in \mathcal{V} is because in the l.h.s. of (6.69) (or (6.70)) knowledge about all the contracted indices no longer uniquely fixes the free dangling indices, since $n_c < (r + 1)/2$. In such cases, with an eye on computing the von Neumann entropy (6.68) – which comes down to finding the eigenvalues of the reduced density matrix – we use a convenient parametrization of \mathcal{V} in which the reduced density matrix assumes a Jordan block-diagonal form, with each diagonal block a matrix with all elements equal to 1.

To arrive at this convenient block diagonal form, enumerate the basis states $|a_1 \dots a_{n_d}\rangle$ such that the first $r^{(r+1)/2-n_c}$ states correspond to the set of $\{a_1, \dots, a_{n_d}\}$ such that given a particular numerical combination of the string “ $b_1 \dots b_{n_c}$ ”, the tensor $T_{a_1 \dots a_{n_d} b_1 \dots b_{n_c}}$ is non-zero. There are r^{n_c} distinct combinations possible for “ $b_1 \dots b_{n_c}$ ”, and for each single combination, the set of allowed $\{a_1, \dots, a_{n_d}\}$ such that $T_{a_1 \dots a_{n_d} b_1 \dots b_{n_c}}$ is non-zero has cardinality $r^{(r+1)/2-n_c}$. The next $r^{(r+1)/2-n_c}$ correspond to a different choice of “ $b_1 \dots b_{n_c}$ ”, and so on. In this way of enumerating the basis, the reduced density matrix assumes a block-diagonal form, with r^{n_c} blocks along the diagonal, each of size $r^{(r+1)/2-n_c} \times r^{(r+1)/2-n_c}$. Thus the total size of ρ_r is $r^{(r+1)/2} \times r^{(r+1)/2}$, as expected (since $\dim \mathcal{V} = r^{(r+1)/2}$).

So for $n_c < n_d$, by abuse of notation, we write graphically

$$\begin{array}{c} a_1 \\ \vdots \\ a_{n_d} \end{array} \begin{array}{c} \diagdown \\ \bullet \\ \diagup \end{array} \begin{array}{c} \text{---} \\ \text{---} \\ \text{---} \\ \text{---} \end{array} \begin{array}{c} \bullet \\ \bullet \\ \bullet \\ \bullet \end{array} \begin{array}{c} \diagup \\ \bullet \\ \diagdown \end{array} \begin{array}{c} a'_1 \\ \vdots \\ a'_{n_d} \end{array} = \begin{pmatrix} J_{r^{(r+1)/2-n_c}} & & \\ & \ddots & \\ & & J_{r^{(r+1)/2-n_c}} \end{pmatrix}_{r^{(r+1)/2} \times r^{(r+1)/2}} \quad n_c < n_d, \tag{6.75}$$

where J_n is the $n \times n$ matrix of all ones and all other entries are 0. We note that this argument holds regardless of precisely which n_c indices in (6.72) were

traced out. If we normalize ρ with an overall factor of $1/\langle\psi|\psi\rangle = r^{-(r+1)/2}$ so that $\text{Tr } \rho = 1$, the reduced density matrix will automatically have $\text{Tr } \rho_r = 1$. Further, it will have r^{n_c} non-zero eigenvalues, each equaling $\lambda_i = r^{-n_c}$ (this follows from a standard result on block diagonalization of these matrices.) From the eigenvalues, it follows that the von Neumann entropy of the (normalized) reduced density matrix will be

$$S = - \sum_i \lambda_i \log \lambda_i = n_c \log r \quad (\text{perfect state with } n_c < n_d \text{ spins traced out}). \quad (6.76)$$

Since n_c counts the number of contractions between the two copies of the state ψ in the reduced density matrix (and consequently the number of diagonal blocks in the matrix representation of ρ_r , which is r^{n_c}), we conclude in this case that for $n_c < n_d$, the von Neumann entropy is proportional to precisely the number of such contractions (more precisely, equal to the logarithm of the number of blocks in the Jordan block-diagonal matrix representation of ρ_r).

It is instructive to apply what we have learned so far to the previous examples of (6.63)-(6.67). We conclude that the latter two examples satisfy $n_c \geq n_d$ and the reduced density matrices have the explicit diagonal form $\rho_2 = \frac{1}{3^2} I_{3^2}$, $\rho_3 = \frac{1}{3} I_3$. The first example has $n_c < n_d$, and in an appropriate basis, $\rho_1 = \frac{1}{3^2} \text{diag}(J_3, J_3, J_3)$. Correspondingly, the von Neumann entropies are $S_2 = 2 \log 3$, $S_3 = \log 3$ and $S_1 = \log 3$, which is consistent with the expectation that the von Neumann entropy in tensor networks built out of perfect tensors is proportional to the minimal number of cuts needed to separate out the traced out part of the tensor network from the rest.

We have so far focused on the simplest explicit examples, but the reasoning we have used for the state given by (6.72) works for *any* state constructed out of any number of copies of the perfect tensor T of fixed rank- $(r + 1)$, with the proviso that we have already applied the rule (6.70) wherever possible to reduce the reduced density matrix to its “simplest” form. With even only a few tensors of modest rank, one can quickly construct enormous density matrices due to the doubly exponential power scaling of various quantities. However, armed with (6.70) and the properties of perfect tensors, it becomes possible to determine these density matrices analytically.

The dimension of the basis \mathcal{V} in more complicated examples will differ from the case of a single tensor determined above, but one can still parametrize

the basis such that the matrix representation of the reduced density matrix ρ_r (for $n_c < n_d$) is in Jordan form. The size of each diagonal block will also depend on the details of the original state ρ and the choice of n_c, n_d (even with $n_c + n_d$ no longer equaling $r + 1$), but the number of blocks will still equal r^{n_c} , where by definition, n_c is the number of contractions between the two copies of the state ψ in the “simplified” reduced density matrix as described in the previous paragraph. Thus the von Neumann entropy (for normalized states) will evaluate to $S = n_c \log r$ as long as $n_c < n_d$. As an example, if the reduced density matrix was obtained by tracing out the bottom three legs of the state in (6.56), we first apply rule (6.70) to replace the contraction of the form $\cdots \text{---} \bullet \text{---} \text{---} \bullet \text{---} \cdots$ by a single horizontal line (times a constant factor) to obtain the simplified reduced density matrix, which now has simply one contraction ($n_c = 1$) between the two copies of the state ψ . Thus $S = \log r$. This was also expected from the “minimal number of cuts” intuition, as we only needed one cut to separate the three sites to be traced out from the rest of the tensor network. We will return to similar calculations for holographic states next.

Efficient techniques: splits and cycles

Before discussing the partial trace of density matrices associated with the dual graph tensor network, let’s warm up with a simpler computation: the inner product of the holographic state with itself. As described in Section 6.3, a holographic state in the vacuum AdS cut-off tree geometry is specified by a prime p which labels the Bruhat–Tits tree \mathcal{T}_p , a prime r which relates to the rank of the perfect tensors forming the tensor network, and the bulk IR cut-off parameter Λ . In fact, before discussing this in full generality for any p, r and Λ , let’s work it out in the case of the state shown in figure 6.2b and in the process introduce some more useful tools and techniques (the state in figure 6.2b corresponds to the choice $p = 3, r = 7$, and $\Lambda = 2$).

Diagrammatically, computing $\langle \psi | \psi \rangle$, which is the same as contracting all free

dangling legs of ψ with another copy of ψ , is represented as

$$\langle \psi | \psi \rangle = \text{Diagram} \quad (6.77)$$

We have chosen to omit the lines representing contraction of dangling legs at the outermost vertices, but no confusion should arise. To evaluate the inner product, one must contract the dangling legs at *all* vertices. The contractions between the two copies of ψ , shown in blue in (6.77) to guide the eye, take precisely the form of the contraction rule (6.70). Note that the number of dangling legs at the vertices of $|\psi\rangle$, which we denoted v_d in Section 6.3, is now reinterpreted as the number of contractions n_c between pairs of vertices from the two copies of ψ . On the other hand, the number of contractions at a vertex within each $|\psi\rangle$, denoted v_c in Section 6.3, can be reinterpreted as the number of “dangling legs” n_d in each of the contractions between the two copies of ψ . Since $v_c \leq v_d$ at any vertex, which we recall follows from the requirement $(r + 1)/2 \geq 2\Lambda$, we now have $n_c \geq n_d$ for the contracted pair of vertices.

Thus we can apply rule (6.70). For example,

$$\text{Diagram} = \text{Diagram} \quad (6.78)$$

at each of the four pairs of vertex contractions between the dangling legs of vertices of ψ which originally had four dangling legs each. The second kind of

contraction between the two copies of ψ depicted in (6.77), which is between vertices carrying six dangling legs each, also admits a simplification. Since $n_c \geq n_d$ here as well, we may simplify this contraction using rule (6.70),

$$\text{Diagram} = \left(\text{Diagram} \right)^2 \times \text{Diagram} = r^2 \times \text{Diagram}. \quad (6.79)$$

The result of applying the contraction rule at all vertex contractions is,

$$\langle \psi | \psi \rangle = \text{Diagram} \quad (6.80)$$

We note the creation of new “cycles” (or disconnected loops) in (6.80). Each such cycle contributes a factor of r , as explained in (6.71). The factors of r^2 explicitly shown in (6.80) originate from the application of (6.79). One counts 16 new cycles and eight factors of r^2 , thus $\langle \psi | \psi \rangle = r^{16} \times (r^2)^8 = r^{32}$, where $r = 7$.¹⁵

Clearly this method is cumbersome to implement. We now propose a shorthand procedure which makes the computation of the norm much more efficient (see figure 6.10 for reference):

1. We start with the holographic state $|\psi\rangle$ depicted in figure 6.2b constructed from rank-8 tensors, but suppress drawing the dangling legs.

¹⁵The normalization, as well as several other quantities as computed by these kinds of diagrams, are reminiscent of similar calculations in topological quantum field theory. In that setting, for example, the norm of the state determined by a nullbordism of a particular manifold is computed by gluing two copies of the nullbordism along their common boundary, corresponding to the inner product in Hilbert space.

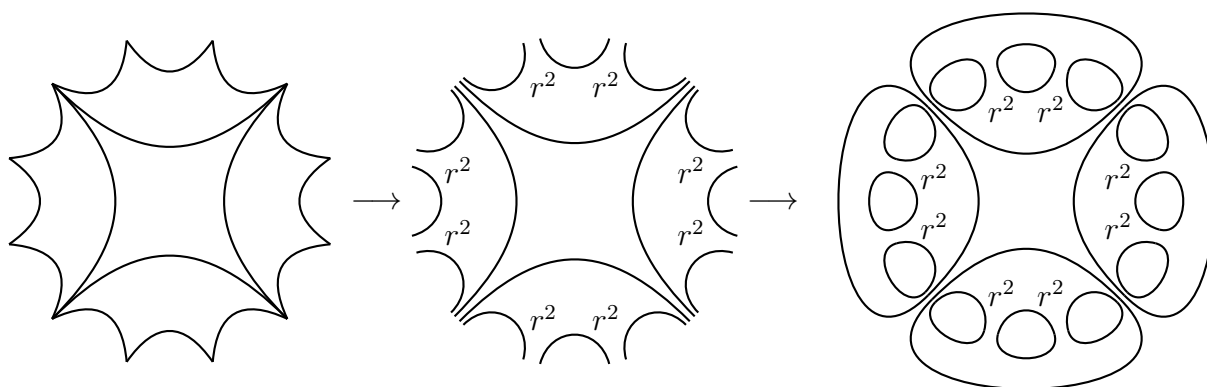


Figure 6.10: Computation of $\langle \psi | \psi \rangle$.

The number of dangling legs at each vertex can be reconstructed from the knowledge of the rank of the tensor.

2. **(Splits.)** We wish to contract all vertices of ψ with itself. Since the number of dangling legs at each vertex of ψ is greater than or equal to half the rank of the perfect tensor, we can apply the contraction rule (6.70) at each of the vertices. However, we draw just one-half, say the left half, of the entire diagram, and label the vertices with an appropriate power of r wherever the contraction rule (6.70) prescribes factors of r . In practice, as explained below (6.70), this comes down to “splitting” open each vertex of the tensor network as shown in the second step in figure 6.10, and assigning any prescribed powers of r at the corresponding vertex, coming from the application of the contraction rule (6.70). Such powers of r will be referred to as “splits”.
3. **(Cycles.)** Finally, we would like to count the number of new cycles created upon performing all the “splits” in step 2. Focusing on the left-half of the diagram in (6.80), it is clear that each disconnected bond (line-segment) in step 2 above will end up in a “cycle” (disconnected loop). So we simply join together the end-points of each line-segment creating as many cycles as disconnected line-segments.

Following this procedure to compute $\langle \psi | \psi \rangle$, as depicted in figure 6.10, we verify that we have created 16 new loops (coming from 16 cycles) and introduced 8

factors of r^2 as before, yielding $\langle \psi | \psi \rangle = r^{16} \times (r^2)^8 = r^{32}$.

Norm of a holographic state

In this subsection we work out the norm of a general holographic state dual to the $(p+1)$ -regular Bruhat–Tits tree geometry, with cutoff Λ and which is constructed as a dual graph tensor network made from perfect tensors of rank- $(r+1)$, where we assume $(r+1)/2 \geq 2\Lambda$. This ground state normalization is necessary for any computation involving the vacuum state or density matrix at the p -adic boundary. The black hole and more general backgrounds require an analogous normalization constant which will be determined later.

Let us begin by tabulating the “type” of vertices which make up the tensor network corresponding to a general holographic state. Two vertices are of the same “type” if the tensors at the respective vertices have the same number of legs (indices) contracted with other tensors. We refer to this number as v_c . Since the total number of legs (contracted and uncontracted) is constant (and equals $r+1$), vertices of the same type also have identical number of dangling (uncontracted) legs (which we refer to as v_d). Thus each type of vertex may appear with a non-trivial multiplicity in the holographic state. Some reflection immediately leads to the conclusion that for a fixed cutoff Λ , all vertices with the number of contracted legs v_c in the set $\{2, 4, \dots, 2\Lambda\}$ will appear in the tensor network. The multiplicity of each type of vertex is straightforward to work out thanks to the highly symmetric nature of the dual graph. We tabulate the results in Table 6.1. The multiplicities in the table add up to

v_c	v_d	multiplicity M
2Λ	$(r+1) - 2\Lambda$	$p+1$
$2\Lambda - 2$	$(r+1) - (2\Lambda - 2)$	$(p+1)(p^1 - p^0)$
$2\Lambda - 4$	$(r+1) - (2\Lambda - 4)$	$(p+1)(p^2 - p^1)$
\vdots	\vdots	\vdots
4	$(r+1) - 4$	$(p+1)(p^{\Lambda-2} - p^{\Lambda-3})$
2	$(r+1) - 2$	$(p+1)(p^{\Lambda-1} - p^{\Lambda-2})$

Table 6.1: Types of vertices in a general holographic state $|\psi\rangle$.

give $\sum_i M^{(i)} = (p+1)p^{\Lambda-1}$, where $M^{(i)}$ is the multiplicity of the vertex type i and we sum over all vertex types. This precisely equals the total number of vertices in the tensor network, and consequently the total number of vertices at the boundary of the (cutoff) Bruhat–Tits tree, which is $\mathbb{P}^1(\mathbb{Z}/p^\Lambda\mathbb{Z})$.

While computing the norm of $|\psi\rangle$, we argued that we may apply the contraction rule (6.70) at each vertex, where the role of v_d gets mapped to n_c , the number of legs contracted within each vertex pair coming from the two copies of ψ , while that of v_c is mapped to n_d , the number of “dangling” legs. We put dangling in quotes because in fact these legs are still contracted with other vertices within the *same* copy of ψ , but for the purposes of applying the contraction rule (6.70), we may treat them as dangling. We are able to apply (6.70) because $v_d \geq v_c \Rightarrow n_c \geq n_d$. As outlined in the previous subsection, we begin by performing “splits”. At each vertex, we pick up a factor of $r^{(n_c - n_d)/2} = r^{(v_d - v_c)/2}$ as prescribed by (6.70). Since each vertex type comes with a certain multiplicity, we really pick up a factor of $r^{M(v_d - v_c)/2}$ for each vertex *type*. Multiplying together factors from each vertex type, we obtain that “splitting” leads to an overall factor of $r^{N_{\text{splits}}}$, where

$$N_{\text{splits}} \equiv \sum_{\text{type } i} M^{(i)} \left(\frac{v_d^{(i)} - v_c^{(i)}}{2} \right) = \frac{p+1}{2(p-1)} (p^\Lambda(r-3) - p^{\Lambda-1}(r+1) + 4). \quad (6.81)$$

In the previous example, we specialized to $p = 3, \Lambda = 2, r = 7$, in which case $N_{\text{splits}} = \frac{4}{2 \cdot 2} (3^2 \cdot 4 - 3^1 \cdot 8 + 4) = 16$ as we found earlier.

After the “splitting” we proceed to counting the number of new cycles created. Each new cycle contributes a factor of r . Now the number of cycles is equal to the number of disconnected bonds obtained after the splitting. This number can be obtained by summing up the number of contracted legs v_c in a single copy of ψ at each vertex, and dividing by half to compensate for the overcounting. This gives,

$$N_{\text{cycles}} \equiv \frac{1}{2} \sum_{\text{type } i} M^{(i)} v_c^{(i)} = \frac{p+1}{p-1} (p^\Lambda - 1). \quad (6.82)$$

In our previous example, we had $N_{\text{cycles}} = \frac{4}{2} (3^2 - 1) = 16$, as expected.

Combining the results, we obtain

$$\log \langle \psi | \psi \rangle = (N_{\text{splits}} + N_{\text{cycles}}) \log r = \frac{p+1}{2(p-1)} (p^\Lambda(r-1) - p^{\Lambda-1}(r+1) + 2) \log r. \quad (6.83)$$

For $\Lambda \gg 1 \Rightarrow r \gg 1$ and fixed p , the norm takes the asymptotic form

$$\log \langle \psi | \psi \rangle \rightarrow \frac{p+1}{2} p^\Lambda r \log r. \quad (6.84)$$

Bipartite entanglement and the Ryu–Takayanagi formula

As explained in Section 6.3, fixing a planar embedding, two given boundary points x and y define a unique (up to the choice of the complimentary set which can be eliminated by specifying the orientation) connected interval on the tensor network, which we denote by A . Particularly, A is given as a set of nodes on the tensor network each of which has a number of contracted and uncontracted legs attached to it. Our goal is to compute the entanglement of A with its compliment $B = A^c$. We proceed by writing down the pure density matrix for the full holographic state $|\psi\rangle$,

$$\rho = \frac{1}{\langle\psi|\psi\rangle} |\psi\rangle\langle\psi|, \quad (6.85)$$

and computing the reduced density matrix obtained by tracing out the region B ,

$$\rho_A = \text{Tr}_B \rho = \frac{1}{\langle\psi|\psi\rangle} \text{Tr}_B |\psi\rangle\langle\psi|. \quad (6.86)$$

The trace over region B is performed exactly in the manner we described previously. Graphically, one may represent this trace by taking two copies of $|\psi\rangle$, then “gluing” the vertices along B . Just as in the computation of the normalization, this set of contractions implements the trace of the density matrix, now only over the qudits in B .

The first step is the application of the contraction rule (6.70) wherever possible to reduce the density matrix to its simplest form. At this point, like in the previous section, we parametrize the basis of states \mathcal{V} such that the reduced density matrix in this basis assumes a Jordan block-diagonal form with all diagonal blocks simply matrices of ones. Then the calculation of the von Neumann entropy reduces to the computation of the number of blocks, since as discussed earlier $S = \log N_{\text{blocks}}$.

We begin by simplifying the reduced density matrix using the contraction rule (6.70) at all vertices in B . Like in the previous subsection, we would like keep track of the number of splits and the number of new cycles generated in the process, as these factors not only affect the overall normalization of ρ_A but also dictate the form of the simplified reduced density matrix. We have

$$\begin{aligned} N_{\text{splits}} &= \sum_{v \in B} \frac{v_d - v_c}{2} \\ N_{\text{cycles}} &= \frac{1}{2} \left(\sum_{v \in B} v_c - C_{AB} \right), \end{aligned} \quad (6.87)$$

where C_{AB} is the number of tensor legs which extend between A and B (equivalently, the number of tensor leg contractions between vertices in A and B), and thus are precisely the number of contractions between the two copies of ψ in the diagrammatic representation of the reduced density matrix. For each of the C_{AB} tensor legs, we sum over the possible values in $0, 1, \dots, r-1$, giving $r^{C_{AB}}$ terms. In fact, from our discussion in the previous section, it follows that the number of blocks in the block-diagonal representation of ρ_A will be precisely $r^{C_{AB}}$, where each term of the internal sum implies a certain block of non-vanishing matrix elements.

With the choice of basis explained in the previous subsection, the density matrix becomes block diagonal with identical blocks of all 1's. The size of each block can be explicitly determined using the properties of perfect tensors, essentially by counting the number of allowed configurations of external legs for a given assignment of indices on the C_{AB} legs. This is always a power of r which can be determined in terms of other quantities by demanding the usual condition that the trace of the reduced density matrix is 1. If the size of each block is $r^\sigma \times r^\sigma$, then the total size of the density matrix is $r^{\sigma+C_{AB}} \times r^{\sigma+C_{AB}}$ (or equivalently $\dim \mathcal{V} = r^{\sigma+C_{AB}}$). Thus the explicit form of the reduced density matrix for any single interval can always be written as:

$$\rho_A = \frac{r^{N_{\text{splits}}+N_{\text{cycles}}}}{\langle \psi | \psi \rangle} \left(\begin{array}{ccc} \left[\begin{array}{ccc} 1 & \cdots & 1 \\ \vdots & \ddots & \vdots \\ 1 & \cdots & 1 \end{array} \right] & & \\ & \ddots & \\ & & r^\sigma \left[\begin{array}{ccc} 1 & \cdots & 1 \\ \vdots & \ddots & \vdots \\ 1 & \cdots & 1 \end{array} \right] \end{array} \right)_{r^{\sigma+C_{AB}} \times r^{\sigma+C_{AB}}} \quad (6.88)$$

where the number of blocks is $r^{C_{AB}}$. This is a generalization of the earlier examples, where the various parameters depend on Λ and the specific interval chosen.

Now we compute the trace

$$\text{Tr } \rho_A = \frac{r^{N_{\text{splits}}+N_{\text{cycles}}}}{\langle \psi | \psi \rangle} r^{\sigma+C_{AB}}, \quad (6.89)$$

and we recall that we computed the norm of the holographic state $|\psi\rangle$ in the previous subsection. However, for the purposes of simplifying the trace, we note that we can write the norm of ψ as an independent sum over vertices in A and B :

$$\log_r \langle \psi | \psi \rangle = \left(\sum_{v \in A} \frac{v_d - v_c}{2} + \sum_{v \in B} \frac{v_d - v_c}{2} \right) + \left(\frac{1}{2} \sum_{v \in A} v_c + \frac{1}{2} \sum_{v \in B} v_c \right). \quad (6.90)$$

where the first parenthesis corresponds to the total power of r originating from the contraction rule (6.70) upon “splitting” all vertices of ψ , while the second parenthesis counts the total number of new loops created after “splitting” all vertices of ψ . Combining all the results, we obtain an expression which only depends on quantities in region A and the number of bonds which connect A to B :

$$\log_r \text{Tr } \rho_A = - \sum_{v \in A} \frac{v_d}{2} + \sigma + \frac{C_{AB}}{2}. \quad (6.91)$$

For any (normalized) reduced density matrix, the trace is always unity, so the logarithm on the left hand side vanishes. This determines the size of the blocks in terms of other quantities which depend only on the chosen region to be traced out.

Returning back to the calculation of the von Neumann entropy, we have

$$S_A = C_{AB} \log r. \quad (6.92)$$

This follows by direct diagonalization of the block diagonal reduced density matrix, and gives an explicit connection between the von Neumann entropy and the number of tensor bonds extending between A and B . This kind of behavior for single intervals in perfect tensor networks was an attractive feature of [99], where a general argument was given for this behavior based on the properties of perfect tensors. We will explain in this section that the network proposed here for p -adic AdS/CFT gives analogous results for a broader class of physical situations such as black hole backgrounds and multiple intervals.

A key motivation for this specific (i.e. “dual graph”) tensor network is the relationship between S_A , thought of as the boundary entanglement entropy between A and B , and the bulk geometry of geodesics on the Bruhat-Tits tree. Recall that by construction, C_{AB} is the number of edges in the dual graph tensor network which originate from a vertex in A and end on a vertex outside A . For example, in the single interval example in figure 6.5, $C_{AB} = 4$,

where A is the connected region on the tensor network in between boundary points x and y . In other words, C_{AB} is the number of edges which start on a tensor network vertex belonging to the region A “in between” x and y , but end outside this region. In the case when the boundary is $\mathbb{P}^1(\mathbb{Q}_p)$ (although this argument also works when the boundary is the “infinite line” \mathbb{Q}_p) the outside of A is precisely the region “between” x and y which is *complementary* to A . Thus by construction, the edges on the tensor network constituting C_{AB} cut across those edges (geodesics) on the Bruhat–Tits tree which separate the boundary points x and y into two disconnected parts of the tree, if we imagine cutting the tree at precisely those edges (geodesics). In fact, on a tree geometry, there are precisely as many such edges as the length of the boundary anchored geodesic joining x and y (if we normalize the length of each edge to unity). Thus we conclude that

$$C_{AB} = \text{length}(\gamma_{xy})/\ell, \quad (6.93)$$

where γ_{xy} is the (regulated) geodesic on the Bruhat–Tits tree joining x to y and ℓ is the length of each edge on the tree. If the boundary is \mathbb{Q}_p so that $x, y \in \mathbb{Q}_p$, then

$$\begin{aligned} \text{length}(\gamma_{xy})/\ell &= d(C, x) + d(C, y) - 2d(C, \text{anc}(x, y)) \\ &= 2\Lambda + 2\log_p |x - y|_p \\ &= 2\log_p \left| \frac{x - y}{\epsilon} \right|_p \end{aligned} \quad (6.94)$$

where C is the any point on the Bruhat–Tits tree, $\text{anc}(x, y)$ is the unique vertex on the Bruhat–Tits tree where geodesics from C, x and y meet, and $d(\cdot, \cdot)$ measures the graph distance between two points. We have defined $\epsilon \in \mathbb{Q}_p$ to be the cutoff

$$\epsilon \equiv p^\Lambda, \quad (6.95)$$

which goes to zero p -adically, i.e. $|\epsilon|_p \rightarrow 0$ as $\Lambda \rightarrow \infty$. If $x, y \in \mathbb{P}^1(\mathbb{Q}_p)$, then

$$\begin{aligned} \text{length}(\gamma_{xy})/\ell &= d(C, x) + d(C, y) - 2d(C, \text{anc}(x, y)) \\ &= 2\log_p \frac{|\mathfrak{B}(x, y)|_{\text{PS}}}{|\epsilon|_p}, \end{aligned} \quad (6.96)$$

where we take C to be the “radial center” of the Bruhat–Tits tree (so that $d(C, x) = d(C, y) = \Lambda$), and as explained around (6.40), $|\mathfrak{B}(x, y)|_{\text{PS}}$ is the

Patterson-Sullivan measure of the smallest clopen ball in $\mathbb{P}^1(\mathbb{Q}_p)$ containing both x and y .¹⁶ As discussed in Section 6.3, equations (6.92)-(6.96) correspond to the p -adic analog of the RT formula.

We end this discussion by remarking that it is straightforward to see that the lengths in (6.96) and (6.94) can be re-expressed using the signed-overlap function $\delta(\cdot, \cdot)$ described in Section 6.3 (see (6.37)). This is more convenient because $\delta(\cdot, \cdot)$ admits a choice of alternate paths, which is important in the genus 1 case (see, for example, Sections 6.4 and 6.5) where there are always two choices.

Bipartite entanglement for a disconnected region and subadditivity

So far we have discussed bipartite entanglement entropy only in the case of a connected region, where we are given a pair of points on \mathbb{Q}_p (or $\mathbb{P}^1(\mathbb{Q}_p)$). We now extend the discussion to include the case of a “disconnected region” (recall definition 6).

To specify a disconnected region built from two connected subregions, we must specify a set of four distinct points on the projective line on which the spatial slice of the CFT resides, and which constitute the entangling surface. Given a set of four boundary points and a choice of planar embedding for the tensor network, there are two different choices for constructing a (complementary pair of) disconnected region on the tensor network, as previously illustrated in figure 6.5b. Each “path-disjoint” piece of a disconnected region is specified by the set of vertices at the boundary of the tensor network “in between” a chosen pair of boundary points, just like for connected regions in the previous subsection (recall definition 7 for the notion of “in between”). We define “path-disjoint” as follows:

Definition 10. Two regions (i.e. sets of vertices) on the dual graph tensor network are *path-disjoint* if they do not share any common vertices, *and* the tensors located on the vertices in one set are not contracted with the tensors in the other set via any of the “shortest bonds”.¹⁷

¹⁶In fact, we can interpret the “interval size” $|x - y|_p = |\mathfrak{B}(x, y)|_{\text{Haar}}$ in (6.94) as the Haar measure of the smallest clopen ball in \mathbb{Q}_p containing both x and y .

¹⁷Recall that the “shortest bonds” on the tensor network are the bonds in bijective correspondence with the UV edges (equivalently the boundary edges) of the cut off Bruhat–Tits tree (see definition 5). For a choice of planar embedding, the notion of “shortest bonds” is $\text{PGL}(2, \mathbb{Q}_p)$ invariant.

Particularly, we use the notation $A = (x, y)$ to specify the connected region A in the tensor network which corresponds to vertices on the network between boundary points x, y on the tree. The ordering inside the parenthesis is used to tell A apart from its complement. We will often use the convention that given a planar embedding, the region $A = (x, y)$ is given by the set of vertices “in between” x and y going counter-clockwise from x to y . Then the two choices for the complimentary pairs of path-disjoint subregions in figure 6.5b correspond to $A_1 = (x_1, x_2), A_2 = (x_3, x_4)$ and $A_3 = (x_4, x_1), A_4 = (x_2, x_3)$. The disconnected region $A = A_1 \cup A_2$ is the complement of $A^c = A_3 \cup A_4$. In vacuum, we expect $S(A) = S(A^c)$, and indeed this is borne out in our setup. A different choice of planar embedding will lead to a different pair of path-disjoint intervals $A_1 = (x_i, x_j), A_2 = (x_k, x_\ell)$ for distinct $i, j, k, \ell \in \{1, 2, 3, 4\}$; however the von Neumann entropy $S(A_1 A_2)$ will be independent of the choice of embedding, for the same reasons as in the case of the single-interval setup – in this case it will depend solely on the specified boundary points x_1, x_2, x_3, x_4 via a conformally invariant cross-ratio constructed from them. For this reason, we make the following definition:

Definition 11. We define the *bipartite entanglement entropy of a disconnected region* constructed using boundary points x_1, x_2, x_3 and x_4 , and denoted $S^{\text{disc.}}(x_1, x_2, x_3, x_4)$, as the von Neumann entropy of the union $A = A_1 \cup A_2$ of connected regions $A_1 = (x_i, x_j)$ and $A_2 = (x_k, x_\ell)$ in any chosen planar embedding, where the distinct indices $i, j, k, \ell \in \{1, 2, 3, 4\}$ are selected such that A_1 and A_2 are path-disjoint.

The calculation of bipartite entanglement in the case where $A = A_1 \cup A_2$ with A_1, A_2 appropriately chosen, proceeds almost identically to the single interval calculation described above. We begin by applying the contraction rule (6.70) on all vertices in $B = A^c$. In this case, after applying the diagrammatic methods from the previous subsection, two things may happen. Simplifying using the contraction rule, one either ends up with two disjoint pieces for the simplified form of the reduced density matrix (here by disjoint, we mean the diagrammatic representation of the reduced density matrix splits into two pieces which do not share *any* edges), or a single connected diagram. In either case, the bipartite entanglement for the disconnected region follows the Ryu–Takayanagi formula.

The case of the disjoint reduced density matrix is interpreted as a direct product reduced state, $\rho_A = \rho_{A_1} \otimes \rho_{A_2}$. Each of the disjoint reduced density matrix pieces can be evaluated using the method described in the previous subsection. This case is precisely when $S(A) = S(A_1 A_2) = S(A_1) + S(A_2)$, that is, A_1 and A_2 share no mutual information, defined to be

$$I(A_1 : A_2) \equiv S(A_1) + S(A_2) - S(A_1 A_2). \quad (6.97)$$

This general result follows from elementary results on diagonalization of tensor products of density matrices. We also write this in the alternate, more suitable notation

$$I(x_i, x_j, x_k, x_\ell) \equiv S(x_i, x_j) + S(x_k, x_\ell) - S^{\text{disc.}}(x_1, x_2, x_3, x_4), \quad (6.98)$$

where $i, j, k, \ell \in \{1, 2, 3, 4\}$ are distinct labels chosen so that (x_i, x_j) and (x_k, x_ℓ) are *any* connected subregions path-disjoint from each other, and $S^{\text{disc.}}(x_1, \dots, x_4)$ is the bipartite entanglement of the union $(x_i, x_j) \cup (x_k, x_\ell)$.¹⁸ This situation is depicted schematically in figure 6.11a.

In the other case, where we obtain a reduced density matrix given by a single diagram (as opposed to two disjoint diagrammatic pieces), we can again employ the method of the previous subsection to calculate the reduced density matrix as well as the entanglement entropy. In this case $S(A_1 A_2) \leq S(A_1) + S(A_2)$, i.e. the mutual information $I(A_1 : A_2)$ is non-negative. This situation is depicted schematically in figure 6.11b. In this case the entanglement entropy of the disconnected region $A = A_1 \cup A_2$, $S(A)$ is still given by the logarithm of the number of blocks in the Jordan block-diagonal representation of the reduced density matrix. Just like in the case of the single interval, the number of blocks is $r^{C_{AB}}$, where C_{AB} is the number of edges on the tensor network which originate on a vertex in $A = A_1 \cup A_2$ but end outside A (i.e. in $B = A^c$).

Let us now describe these cases in more detail. The two possible scenarios discussed above can be classified in terms of the entangling surface consisting the boundary points specifying the disconnected region A . If $A_1 = (x_1, x_2)$, and $A_2 = (x_3, x_4)$ are two path-disjoint intervals on the tensor network (with $x_i \neq x_j, \forall i, j$) with $A = A_1 \cup A_2$, then the sign of the logarithm of the cross-ratio

$$u(x_1, x_2, x_3, x_4) \equiv \left| \frac{x_{12}x_{34}}{x_{14}x_{23}} \right|_p, \quad (6.99)$$

¹⁸In fact as we stressed previously, $S^{\text{disc.}}(x_1, \dots, x_4)$ equals the bipartite entanglement of *any* disconnected region constructed from boundary points x_1, \dots, x_4 .

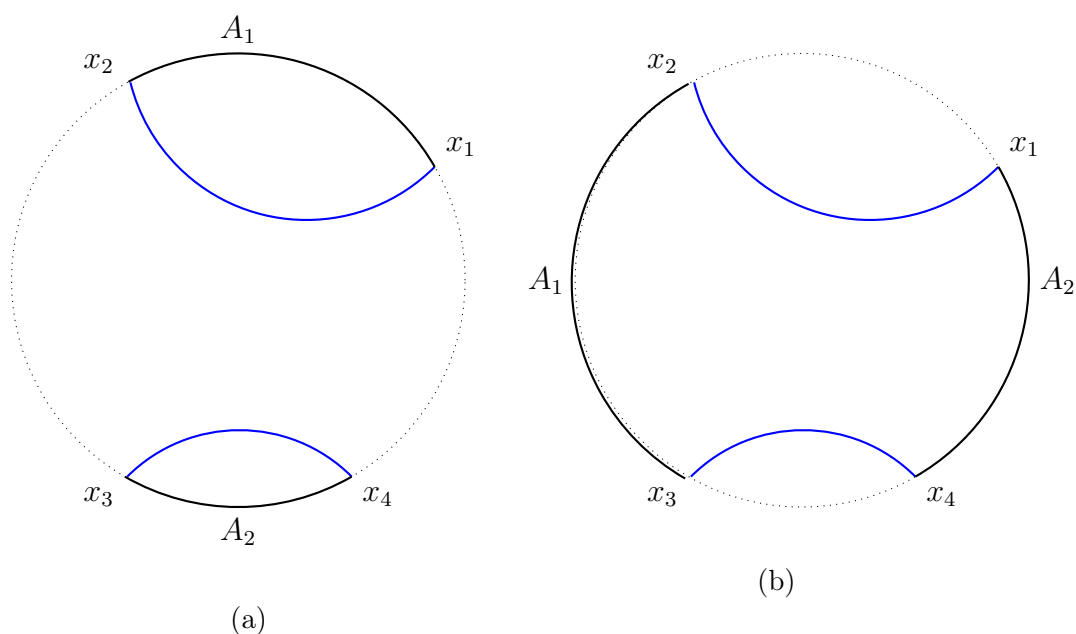


Figure 6.11: A schematic representation of the bipartite entanglement entropy calculation for the cases shown in figures 6.12 and 6.13b, here (a) and (b) respectively, to emphasize the parallel with the usual story over the reals. The disconnected region $A = A_1 \cup A_2$ is shown in black, while the minimal geodesics homologous to A is shown in blue.

dictates which of the scenarios depicted in figure 6.11 will occur.

If the logarithm is non-positive, then the pairwise boundary anchored geodesics between x_1 & x_2 and x_3 & x_4 do not overlap (i.e. they intersect at most at a single vertex) on the Bruhat–Tits tree, and in fact constitute the minimal surfaces homologous to A_1 and A_2 , respectively.¹⁹ Thus $S^{\text{disc.}}(x_1, x_2, x_3, x_4) = S(A_1 A_2) = S(A_1) + S(A_2)$.

Figure 6.12 shows an example of a disconnected region setup for $A_1 = (x_1, x_2)$, $A_2 = (x_3, x_4)$ with $u(x_1, x_2, x_3, x_4) < 1$.²⁰ As usual, the tensor network is shown in red with regions marked by blue vertices, while the Bruhat–Tits tree geometry is shown in black. Applying the contraction rule (6.70) to the trace out the complement of $A = A_1 \cup A_2$ in the state shown in the left subfigure “splits” open vertices on the tensor network marked in black (in the manner described in the previous subsections), while the dashed bonds on the tensor

¹⁹Recall definition 9 for the homologous condition.

²⁰In figure 6.12, $u(x_1, x_2, x_3, x_4) = p^{-1}$. See the discussion around (6.102) for the explanation.

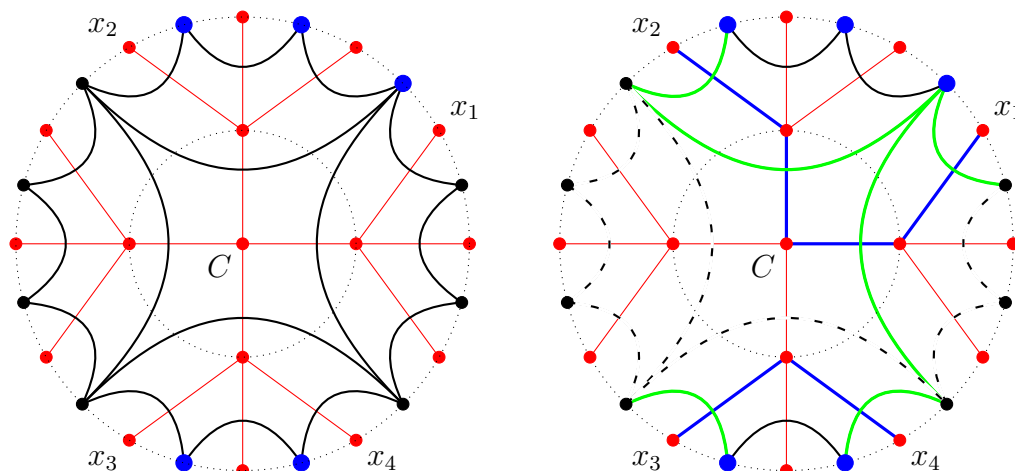


Figure 6.12: The setup for the bipartite entanglement calculation for a disconnected region, in the case when the cross-ratio $u(x_1, x_2, x_3, x_4)$ defined in (6.99) is strictly less than one. Left: The holographic state with the region marked in blue. Right: Computation of the reduced density matrix, and the depiction of the minimal surface homologous to the boundary region. See the main text for the detailed explanation of the figure.

network turn into “cycles”. The bonds marked in green connect vertices in A to vertices in the complement of A . The simplified reduced density matrix is given by the subdiagram containing blue vertices, along with black and green colored bonds, where we remember to “split open” all the black vertices so that all bonds originally coincident on such vertices no longer meet. Thus the reduced density matrix manifestly decomposes into two disjoint pieces, and can be written as the direct product of the density matrices for the individual sub-intervals. The number of green bonds in each individual piece correspond to the (base- r logarithm of the) number of blocks in the Jordan block form of the individual reduced density matrices. It is clear from counting the green bonds that $S^{\text{disc.}}(x_1, \dots, x_4) = S(A_1 A_2) = S(A_1) + S(A_2)$.²¹ The edges on the Bruhat–Tits tree corresponding to the green bonds are highlighted in blue. Together they correspond to the minimal length boundary-anchored geodesics homologous to A . Thus the RT formula is satisfied. Schematically, this case is the p -adic analog of the configuration depicted in figure 6.11a, where the minimal surface homologous to a disconnected region is the union of the min-

²¹Particularly, applying the methods from the previous subsection, we have $S(A_1) = 4$, $S(A_2) = 2$ and $S(A) = 6$, which can be confirmed visually in figure 6.12 by counting the length of the corresponding minimal geodesics homologous to various regions.

imal surfaces homologous to each disjoint piece of the region separately. Figure 6.13a shows the disconnected region setup for $A_1 = (x_1, x_2)$, $A_2 = (x_3, x_4)$ with $u(x_1, x_2, x_3, x_4) = 1$. The analysis in this case proceeds identically to the one above, so we do not repeat it here.

In figure 6.12, we could have considered the alternate choice of path-disjoint intervals, $A'_1 = (x_4, x_1)$ and $A'_2 = (x_2, x_3)$ with the full disconnected region given by $A' = A'_1 \cup A'_2$. Then the cross-ratio of interest (6.99) would become

$$u(x_4, x_1, x_2, x_3) = \left| \frac{x_{41}x_{23}}{x_{43}x_{12}} \right|_p = \frac{1}{u(x_1, x_2, x_3, x_4)} > 1. \quad (6.100)$$

We discuss this case in more detail next. Before proceeding, we note that in this case although the individual von Neumann entropies $S(A'_1)$ and $S(A'_2)$ will in general differ from $S(A_1)$ and $S(A_2)$, the von Neumann entropy of the union $S(A'_1 A'_2) = S(A_1 A_2) = S^{\text{disc.}}(x_1, \dots, x_4)$, and in fact the minimal surface homologous to $A'_1 \cup A'_2$ is the same as the minimal surface homologous to $A_1 \cup A_2$. Thus the bipartite von Neumann entropy is independent of the choice of choosing the disconnected region given a set of four boundary points.²² Moreover, it is independent of the choice of the planar embedding.

Let the logarithm of the cross-ratio $u(x_1, x_2, x_3, x_4)$ be positive; then the boundary anchored geodesics between x_1 & x_2 and between x_3 & x_4 overlap (i.e. share non-zero edges on the Bruhat–Tits tree). The bulk interpretation of mutual information $I(x_1, \dots, x_4) = I(A_1 : A_2)$ is that it is given precisely by (twice) the number of edges of overlap between the minimal geodesics homologous to A_1 and A_2 individually. Each such edge corresponds to a bond on the tensor network which extends from a node in A_1 to a node of A_2 , explaining why the combination $I(A_1 : A_2) = S(A_1) + S(A_2) - S(A_1 A_2)$ is given precisely by twice the number of such edges (up to an overall factor of $\log r$). From the boundary perspective, the mutual information between the path-disjoint intervals A_1, A_2 is given by

$$I(x_i, x_j, x_k, x_\ell) = I(A_1 : A_2) = (2 \log r) \log_p u(x_i, x_j, x_k, x_\ell), \quad (6.101)$$

provided $u(x_1, \dots, x_4) > 1$ (which is the same as $u(x_1, \dots, x_4) \geq p$ since the p -adic norm in (6.99) takes values in $p^{\mathbb{Z}}$), with $A_1 = (x_i, x_j)$, $A_2 = (x_k, x_\ell)$ where $i, j, k, \ell \in \{1, \dots, \}$ are distinct and chosen such that A_1, A_2 are path-disjoint.

²²The two choices are illustrated in figure 6.5b.

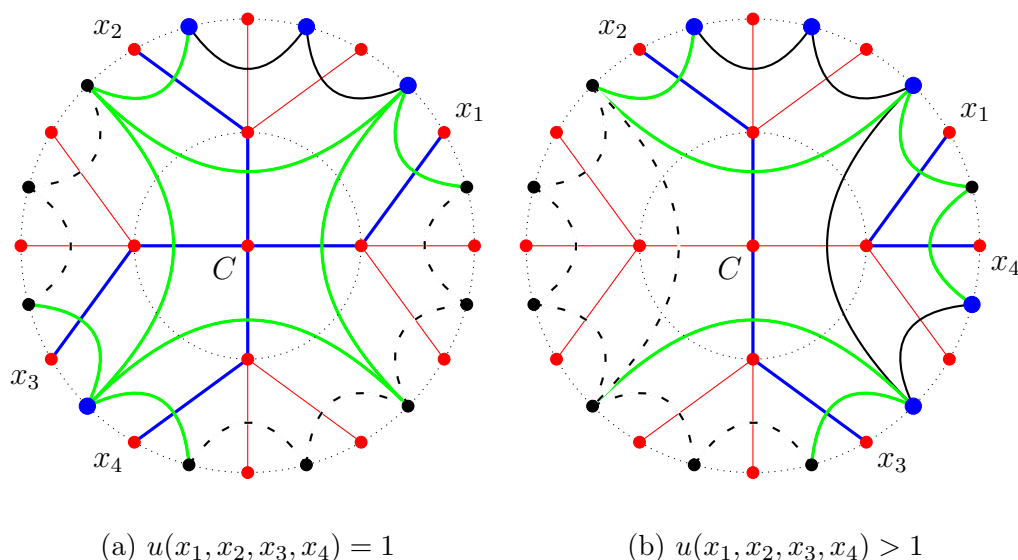


Figure 6.13: The case of a disconnected region with cross-ratio $u(x_1, x_2, x_3, x_4)$ defined in (6.99) greater than or equal to 1.

This result follows from a basic entry in the p -adic holographic dictionary between cross-ratios and graph distances on the Bruhat–Tits tree,

$$\left| \frac{(x-y)(z-w)}{(x-z)(y-w)} \right|_p = p^{-d(a,b)}, \quad (6.102)$$

where $x, y, z, w \in \mathbb{P}^1(\mathbb{Q}_p)$ such that the bulk geodesics joining x to z , and y to w intersect precisely along the path between the bulk points a and b on the Bruhat–Tits tree, and $d(a, b)$ is the graph distance between a and b .²³

This possibility is depicted in figure 6.13b. We consider the disjoint intervals $A_1 = (x_1, x_2)$ and $A_2 = (x_3, x_4)$ with $A = A_1 \cup A_2$ and $u(x_1, x_2, x_3, x_4) > 1$. Applying the contraction rule (6.70) to the trace out the complement of A in the state on the left “splits” open vertices marked in black, while the dashed bonds on the tensor network turn into cycles. Like for figure 6.12, the bonds marked in green connect vertices in A to vertices in the complement of A , and the simplified reduced density matrix is given by the subdiagram containing blue vertices, along with black and green bonds. Importantly, the reduced density matrix in this case does not split into individual disjoint pieces. The number of green bonds once again correspond to the (base- r logarithm of the) number of blocks in the Jordan block form of the reduced density matrix,

²³If the bulk geodesics do not intersect along a path on the tree, (6.102) can still be used after a simple relabelling of the boundary points.

and thus contribute to the von Neumann entropy as explained in Section 6.5. It is clear from counting the green bonds that $S^{\text{disc.}}(x_1, \dots, x_4) = S(A_1 A_2) < S(A_1) + S(A_2)$.²⁴ The excess on the r.h.s. (or equivalently the non-zero mutual information $I(A_1 : A_2)$) can precisely be accounted for by the existence of a black bond on the tensor network joining a vertex of A_1 with a vertex of A_2 . *This establishes the non-negativity of mutual information.* The edges on the Bruhat–Tits tree corresponding to the green bonds are highlighted in blue, and together they specify the minimal boundary-anchored geodesics homologous to the boundary region A . Thus once again the RT formula holds. This case is the p -adic analog of the situation in figure 6.11b, where the two regions share mutual information.

We note that while the sample computations presented above for the disconnected interval case considered specific examples (for a specific choice of cutoff and specific value of p), the lessons and results obtained here hold in full generality for arbitrarily chosen disconnected regions and arbitrary cutoffs for any prime p . In summary, from the boundary perspective, given path-disjoint regions $A_1 = (x_i, x_j)$ and $A_2 = (x_k, x_\ell)$ with $i, j, k, \ell \in \{1, 2, 3, 4\}$ distinct and A_1, A_2 path-disjoint, the sign of $\log u(x_i, x_j, x_k, x_\ell)$ fixes whether the mutual information $I(x_i, x_j, x_k, x_\ell) = I(A_1 : A_2)$ is positive or vanishing. Combining the cases described above, we write

$$\begin{aligned} I(x_i, x_j, x_k, x_\ell) &= (2 \log r) \max\{0, \log_p u(x_i, x_j, x_k, x_\ell)\} \\ &= (2 \log r) \gamma_p \left(\frac{x_{i\ell} x_{jk}}{x_{ij} x_{k\ell}} \right) \log_p \left| \frac{x_{ij} x_{k\ell}}{x_{i\ell} x_{jk}} \right|_p \\ &\geq 0, \end{aligned} \tag{6.103}$$

where $\gamma_p(x)$ is the characteristic function on \mathbb{Z}_p , that is $\gamma_p(x) = 1$ if $x \in \mathbb{Z}_p$ (equivalently $|x|_p \leq 1$), and zero otherwise, and we emphasize the non-negativity of mutual information in the final inequality. From the bulk perspective, mutual information equals twice the number of shared edges between the minimal surfaces homologous to the individual regions A_1 and A_2 (or equivalently twice the number of bonds in the tensor network which start in A_1 and end in A_2) up to an overall factor of $\log r$. The entropy of the disconnected region, $S(A)$ equals the entropy of any disconnected region built out of boundary points x_1, \dots, x_4 , thus we alternately denote the bipartite entropy

²⁴Particularly in figure 6.13b, $S(A_1) = 4, S(A_2) = 4$ and $S(A_1 A_2) = 6$.

as $S(x_1, \dots, x_4)$. Using the results from this and the previous subsections, we write

$$\begin{aligned}
& S^{\text{disc.}}(x_1, x_2, x_3, x_4) \\
&= S(x_i, x_j) + S(x_k, x_\ell) - I(x_i, x_j, x_k, x_\ell) \\
&= 2 \left(\log_p \frac{|\mathfrak{B}(x_i, x_j)|_{\text{PS}}}{|\epsilon|_p} + \log_p \frac{|\mathfrak{B}(x_k, x_\ell)|_{\text{PS}}}{|\epsilon|_p} - \gamma_p \left(\frac{x_{i\ell}x_{jk}}{x_{ij}x_{k\ell}} \right) \log_p \left| \frac{x_{ij}x_{k\ell}}{x_{i\ell}x_{jk}} \right|_p \right) \log r \\
&= (\delta(x_i \rightarrow x_j, x_i \rightarrow x_j) + \delta(x_k \rightarrow x_\ell, x_k \rightarrow x_\ell) - 2|\delta(x_i \rightarrow x_j, x_k \rightarrow x_\ell)|) \log r
\end{aligned} \tag{6.104}$$

where we used (6.92), (6.93), (6.96) and (6.37) for the first two terms in the last equality above,²⁵ while the third term in the last equality explicitly counts the number of shared edges between the minimal surfaces $x_i \rightarrow x_j$ and $x_k \rightarrow x_\ell$ (for regions A_1 and A_2 , respectively) which appear in the bulk interpretation of mutual information. Recall that the indices $i, j, k, \ell \in \{1, 2, 3, 4\}$ are chosen such that the subregions (x_i, x_j) and (x_k, x_ℓ) are path-disjoint. Thus, the three terms on the r.h.s. in the first equality of (6.104) depend on the initial choice of the dual graph tensor network (i.e. the choice of planar embedding). The second and third equalities show explicitly the functional form of the three terms, entirely in terms of the boundary coordinates (as well as the UV cut off). We now show that $S^{\text{disc.}}(x_1, x_2, x_3, x_4)$ as given by the particular combination in (6.104) is *independent* of the choice of a planar embedding.

Assume, without loss of generality, $u(x_1, x_2, x_3, x_4) \leq 1$ (the associated configuration on the Bruhat–Tits tree is shown in figure 6.14). (If not, we relabel the boundary points to ensure the inequality holds.) The choice of the path-disjoint intervals $A_1 = (x_i, x_j)$ and $A_2 = (x_k, x_\ell)$ depends on the choice of the planar embedding. Depending on the chosen planar embedding, there are in all three inequivalent possibilities:²⁶

- $x_i = x_1, x_j = x_2, x_k = x_3, x_\ell = x_4$, OR
- $x_i = x_1, x_j = x_3, x_k = x_2, x_\ell = x_4$, OR

²⁵Moreover, we made convenient choices for the arbitrary node C in (6.37) to obtain the simplified forms in (6.104).

²⁶Technically, one needs to be careful about the orientation of the interval to ensure there is no overlap, but we will assume proper orientations have already been chosen to ensure the subregions are path-disjoint. This simply amounts to being careful about the order of the boundary points in specifying the intervals A_1, A_2 ; however, the argument in the following is insensitive to this ordering as long as we assume the intervals are path-disjoint.

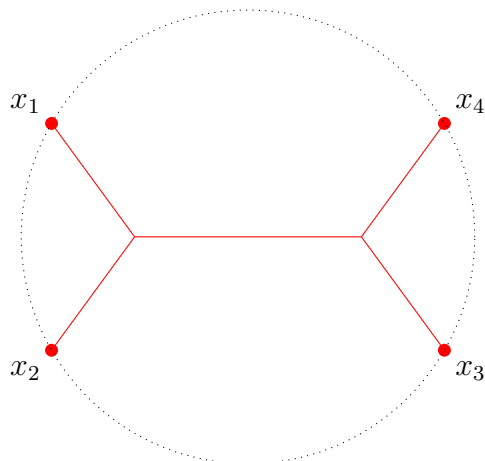


Figure 6.14: Boundary anchored bulk geodesics on the Bruhat–Tits tree and the boundary point configuration such that $u(x_1, x_2, x_3, x_4) \leq 1$.

- $x_i = x_1, x_j = x_4, x_k = x_2, x_\ell = x_3$.

In each of the three cases, the graph-theoretic quantity in the third line of (6.104) is easily computed to explicitly verify that $S^{\text{disc.}}(x_1, x_2, x_3, x_4)$ is identical in all cases, and in fact equals the *minimal* length of the geodesics homologous to the intervals A_1 and A_2 .²⁷ Thus the bipartite entanglement for a disconnected region is given exactly by the RT formula. The bipartite entanglement $S^{\text{disc.}}(x_1, \dots, x_4)$ as defined above is not only $\text{PGL}(2, \mathbb{Q}_p)$ invariant but also independent of the choice of planar embedding (equivalently the choice of a valid tensor network associated with the bulk geometry).

We are now in a position to show that the Araki–Lieb inequality [248] is satisfied as well. In our setup, this corresponds to showing that the inequality

$$S(x_1, x_2, x_3, x_4) \geq |S(x_i, x_j) - S(x_k, x_\ell)| \quad (6.105)$$

holds, where the various terms are defined below (6.98). Once again, without loss of generality, we assume the boundary point configuration of figure 6.14. As already discussed, in this case, $S(x_1, \dots, x_4)$ is proportional to the sum of the lengths of the unique geodesics joining x_1 to x_2 and x_3 to x_4 . On the other hand, the entropies of the path-disjoint intervals, $S(x_i, x_j)$ and $S(x_k, x_\ell)$ are

²⁷This observation is also illustrated in figure 6.11 where the two cases shown have the same minimal surface homologous to the disconnected regions.

proportional to lengths of the unique geodesics joining x_i to x_j and x_k to x_ℓ , respectively. Comparing lengths of geodesics in figure 6.14 it is immediately clear that for all possible choices of i, j, k, ℓ (subject to the requirements specified below (6.98)), the inequality (6.105) reduces to checking whether $a + b \geq |a - b|$ for positive real numbers a, b . This is clearly true, and thus establishes the Araki–Lieb inequality for path-disjoint intervals. The simplicity in comparison of lengths of geodesics such as the ones in figure 6.14 is a direct consequence of ultrametricity of the p -adic numbers (or equivalently, the simplifying tree structure of the bulk geometry).

Together, the Araki–Lieb inequality and the non-negativity of mutual information, which we have now established for path-disjoint intervals, are referred to as the subadditivity property of entropy. In the next subsection, we define path-adjointing intervals, and the proofs presented here extend easily to this case (we leave them as trivial exercises for the reader), thus establishing subadditivity in full generality in our setup.

More entropy inequalities: SSA and MMI

So far we have shown that the p -adic bipartite entropy satisfies an RT-like formula, as well as subadditivity of entropy. One should also expect strong subadditivity (SSA) and monogamy of mutual information (MMI) [249] to hold. Indeed in this section we establish these inequalities holographically.

Given three regions A_1, A_2 and A_3 , SSA is the statement that [250, 251]

$$S(A_1 A_2) + S(A_2 A_3) \geq S(A_1 A_2 A_3) + S(A_2), \quad (6.106)$$

or equivalently²⁸

$$S(A_1 A_2) + S(A_2 A_3) \geq S(A_1) + S(A_3). \quad (6.107)$$

In the previous subsection, we discussed the bipartite entropy of unions of path-disjoint regions. However, here we will focus on regions A_i such that in a given planar embedding, they are disjoint (i.e. they do not share any nodes on the tensor network) but are “adjointing”, that is they share end-points on the Bruhat–Tits tree. We refer to them as “path-adjointing” regions.

Definition 12. Given a planar embedding, two regions A_1 and A_2 are *path-adjointing* if they are disjoint as sets of nodes on the tensor network, but there

²⁸The inequality (6.107) can be obtained from (6.106) (and vice versa) by first purifying the system $\rho_{A_1 A_2 A_3}$ by formally adding a fourth region A_4 .

exists exactly one “shortest bond” on the network which contracts a vertex in A_1 with a vertex in A_2 .

A consequence of this definition is that if two regions are path-adjointing, then written as a set of nodes “in between” two boundary points, the two regions share a common boundary point. (This notion is also $\mathrm{PGL}(2, \mathbb{Q}_p)$ invariant.) The converse of this statement is not always true.

Given four boundary points x_1, \dots, x_4 and any choice of a planar embedding, we will assume that regions A_1 and A_2 are path-adjointing as well as A_2 and A_3 are path-adjointing.²⁹ Without loss of generality, we take $A_1 = (x_i, x_j)$, $A_2 = (x_j, x_k)$ and $A_3 = (x_k, x_\ell)$, where i, j, k, ℓ are distinct indices from the set $\{1, 2, 3, 4\}$ chosen such that A_1 and A_2 are path-adjointing, and similarly for A_2 and A_3 . This setup might be familiar to the reader from the holographic proof of strong subadditivity over the reals [97]. The proof presented here is similar in spirit but has a distinct p -adic flavor as will be apparent shortly.

Under the hypotheses of the previous paragraph, we can write

$$\begin{aligned} S(A_1) &= S(x_i, x_j) & S(A_2) &= S(x_j, x_k) & S(A_3) &= S(x_k, x_\ell) \\ S(A_1 A_2) &= S(x_i, x_k) & S(A_2 A_3) &= S(x_j, x_\ell) & S(A_1 A_2 A_3) &= S(x_i, x_\ell), \end{aligned} \tag{6.108}$$

where the two-point bipartite entropy $S(x, y)$ is the entropy of a connected region (x, y) , discussed previously in Section 6.3. Consequently all terms in (6.106) (and (6.107)) turn into bipartite entropies of connected regions. Thus to check SSA, we need to show

$$S(x_i, x_k) + S(x_j, x_\ell) \stackrel{!}{\geq} S(x_i, x_\ell) + S(x_j, x_k), \quad S(x_i, x_k) + S(x_j, x_\ell) \stackrel{!}{\geq} S(x_i, x_j) + S(x_k, x_\ell).$$

To be concrete, (without loss of generality) we label the given boundary points x_1, \dots, x_4 such that the pairwise boundary anchored bulk geodesics intersect as shown in figure 6.14. Now recall from Section 6.3 that in a genus zero background, $S(x, y)$ is given simply by the unique minimal geodesic joining boundary points x and y . Thus the inequalities in (6.109) turn into (trivial) statements about lengths of various boundary anchored geodesics in figure

²⁹In this chapter, we will not discuss the case where the regions A_1, A_2 and A_3 are path-disjoint from each other, although we expect SSA to hold here as well. This case requires an input data of six distinct boundary points. The notion of bipartite entropy presented in Section 6.5 given a set of four boundary points should generalize in a systematic way to the case of six (and higher) boundary points, but we leave this for future work.

6.14. Further they can be related them directly to the conformal cross-ratios as we now explain.

For example, suppose in a planar embedding we can choose $i = 1, j = 2, k = 3, \ell = 4$. Then it is clear from comparing lengths of minimal geodesics in figure 6.14 that the first inequality in (6.109) is saturated, while the second one is obeyed in the strict sense. In fact, the equality $S(x_1, x_3) + S(x_2, x_4) = S(x_1, x_4) + S(x_2, x_3)$ of the lengths of geodesics has the same content as the triviality of the cross-ratio, $u(x_1, x_3, x_2, x_4) = |(x_{13}x_{24})/(x_{14}x_{23})|_p = 1$. Similarly, the inequality $S(x_1, x_3) + S(x_2, x_4) > S(x_1, x_2) + S(x_3, x_4)$ has identical content as the inequality $u(x_1, x_2, x_4, x_3) = |(x_{12}x_{34})/(x_{13}x_{24})|_p < 1$.³⁰ The 23 other permutations of assignments for i, j, k, ℓ which could possibly be made over all possible planar embeddings admit identical analysis so we do not repeat it here. This confirms SSA.

To summarize, in each case one of the two inequalities in (6.109) is saturated,³¹ while the other remains an inequality.³² SSA is interpreted as an inequality between lengths of geodesics and admits a dual description in terms of boundary cross-ratios. From the boundary perspective, SSA (for path-adjointing regions) has the same content as the following statement about cross-ratios: Given four boundary points x_1, \dots, x_4 , up to a relabelling of coordinates one always has $|(x_{12}x_{34})/(x_{13}x_{24})|_p \leq 1$ with $|(x_{14}x_{23})/(x_{13}x_{24})|_p = 1$, which follows from the ultrametric nature of p -adic numbers.

Next let's turn to MMI (also referred to as the negativity of tripartite information) [249]. Given three disjoint intervals A, B and C (in our terminology in a given planar embedding, they can be either path-disjoint or path-adjointing or a mix of both such that no two intervals overlap), MMI is the following inequality obeyed by mutual information,

$$I(A : BC) \geq I(A : B) + I(A : C) \quad (6.109)$$

or equivalently

$$I(A : B : C) \equiv I(A : B) + I(A : C) - I(A : BC) \leq 0. \quad (6.110)$$

³⁰Refer to the discussion around (6.102).

³¹In the case of path-disjoint intervals A_1, A_2 and A_3 (see the comment in footnote 29), we do not expect such a saturation of one of the inequalities to hold in general.

³²The inequality is obeyed strictly unless the boundary points x_1, \dots, x_4 are such that the geodesics connecting them in the bulk meet at a single bulk point. This corresponds in figure 6.14 to the collapse of the internal bulk geodesic to a single point.

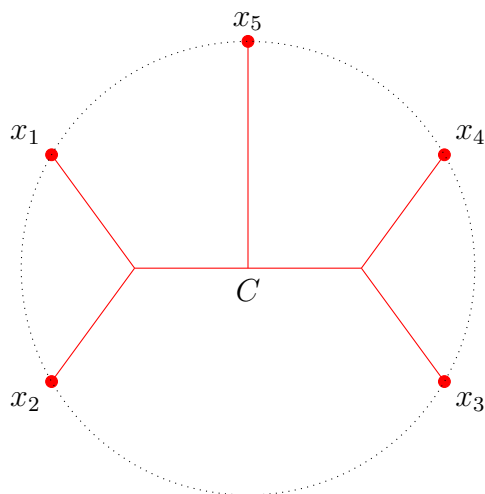


Figure 6.15: Boundary anchored bulk geodesics on the Bruhat–Tits tree and the boundary point configuration such that $u(x_1, x_2, x_4, x_5) \leq 1$ and $u(x_3, x_4, x_1, x_5) \leq 1$. Up to relabelling, this is the most general configuration of five boundary points at the terminus of the Bruhat–Tits tree.

Such an inequality does not hold in general for arbitrary quantum mechanical states, but is special to quantum states which admit a holographic dual. The inequality makes sense even for adjoining intervals since the divergences in the individual mutual information pieces cancel out among the various terms. We will now prove (6.109) holds in the p -adic tensor network setting for (connected) intervals A, B and C chosen in an arbitrary planar embedding such that they are either path-adjoining or path-disjoint but never overlapping. In fact, we show the inequality is always saturated. We will first prove this in the case these intervals are specified in terms of given set of *five* boundary points (see figure 6.15), and then extend this to full generality.

Fix a planar embedding. Let's first consider the case where B and C are chosen such that they are path-adjoining but $B \cup C$ is path-disjoint from A . There are then three inequivalent choices of intervals in figure 6.15.³³

- $A = (x_1, x_2), B = (x_3, x_4), C = (x_4, x_5)$, or
- $A = (x_5, x_1), B = (x_2, x_3), C = (x_3, x_4)$, or

³³We will suppress keeping track of orientation of intervals and simply assume the intervals are chosen with the correct orientation such that they are path-adjoining or path-disjoint as desired. Keeping track of orientations simply adds an extra layer of detail without changing the basic analysis.

- $A = (x_2, x_3), B = (x_4, x_5), C = (x_5, x_1)$.

In each of these cases, the mutual information measures $I(A : BC), I(A : B)$ and $I(A : C)$ take the form of $I(x_i, x_j, x_k, x_\ell)$ for appropriately chosen i, j, k, ℓ and can be determined simply by considering the overlap of minimal geodesics for given intervals A, B, C and $B \cup C$, as discussed in detail in Section 6.5. We immediately see that the inequality (6.109) is saturated in all three cases – in the first case each of the individual mutual information measures are identically zero, while in the second and third cases there is non-trivial overlap of minimal geodesics so not all I 's vanish.

The remaining cases involve choosing A, B and C such that A is path-adjointing to either B or C , where at the same time B and C may be path-adjointing or path-disjoint to each other. In all such cases, some of the mutual information measures will diverge, but the divergences still cancel out on both sides of (6.109). We leave it as a simple exercise to the reader to consider the finitely many inequivalent cases to consider and verify that in each case, (6.109) is satisfied, and in fact saturated. Thus we conclude that in the case of five points, (6.109) is saturated in the p -adic setting.

The restriction to five boundary points allowed us to prove (6.109) in the p -adic setting in almost full generality. The only case remaining is when the intervals A, B and C are pairwise path-disjoint, in which case we need six boundary points to specify the intervals. Once again there are a small number of cases to individually consider, with the analysis identical to the previously studied cases. We find (6.109) is saturated here as well. In all, we conclude in the p -adic tensor network considered in this chapter, $I(A : B : C) = 0$, that is

$$I(A : BC) = I(A : B) + I(A : C). \quad (6.111)$$

It is interesting to compare this observation with the result over real CFTs where it was shown that the inequality is saturated for a massless fermion in two dimensions (i.e. mutual information is exactly extensive), but not for instance for the massless scalar [249, 252, 253].

Black hole backgrounds

We now change gears and present some of the computational methods and results for black hole entropy and a Ryu–Takayanagi like formula for minimal

geodesics in the black hole background. This discussion is essentially an extension of Sections 6.4 and 6.4; we refer to these for the basic setup of the tensor network geometry. We will define the integer length of the horizon to be $\tau = \log_p |q|_p^{-1}$ with q our uniformizing parameter; we also assume a non-degenerate geometry so $\tau > 1$. As before, the cutoff is Λ (defined now from the horizon) and the rank is $r + 1$, where we assume $(r + 1)/2 \geq 2\Lambda + 1$ and $(r + 1)/2 \geq \tau$. The first condition ensures there are enough boundary dangling legs for minimal surfaces to extend into the bulk and the second condition ensures a similar property for the center vertex.

As in the genus 0 case, our first task is to calculate the norm of the black hole boundary state. This quantity is obtained by contracting all legs, including those at the center vertex behind the horizon. Denoting the boundary state of a black hole of size τ as $|\psi_\tau\rangle$, we may compute $\langle\psi_\tau|\psi_\tau\rangle$ graphically using techniques of the previous sections. This involves counting the number of each type of tensor, where again the type is the number of legs contracted with other tensors (in the network), v_c . The number of dangling legs is v_d , and $v_c + v_d = r + 1$ for every tensor.

In the black hole geometry, one can see all vertices with v_c in the set $\{2, 4, \dots, 2\Lambda, 2\Lambda + 1\}$ will appear, as well as the central vertex which always has $v_c = \tau$. The counting is similar to the genus 0 case, though all numbers explicitly depend on τ . The multiplicity of each type of vertex is found in Table 6.2, where we have singled out the center vertex multiplicity, even though it may coincide with one of the other types of tensors.

v_c	v_d	multiplicity M
τ	$(r + 1) - \tau$	1
$2\Lambda + 1$	$(r + 1) - (2\Lambda + 1)$	τ
2Λ	$(r + 1) - 2\Lambda$	$(p - 2)\tau$
$2\Lambda - 2$	$(r + 1) - (2\Lambda - 2)$	$(p - 1)(p^1 - p^0)\tau$
$2\Lambda - 4$	$(r + 1) - (2\Lambda - 4)$	$(p - 1)(p^2 - p^1)\tau$
\vdots	\vdots	\vdots
4	$(r + 1) - 4$	$(p - 1)(p^{\Lambda-2} - p^{\Lambda-3})\tau$
2	$(r + 1) - 2$	$(p - 1)(p^{\Lambda-1} - p^{\Lambda-2})\tau$

Table 6.2: Types of vertices in a black hole holographic state $|\psi_\tau\rangle$.

As in previous sections, we contract each vertex and obtain splits which contribute an overall factor of $r^{(v_d - v_c)/2}$ for each vertex as prescribed by (6.70).

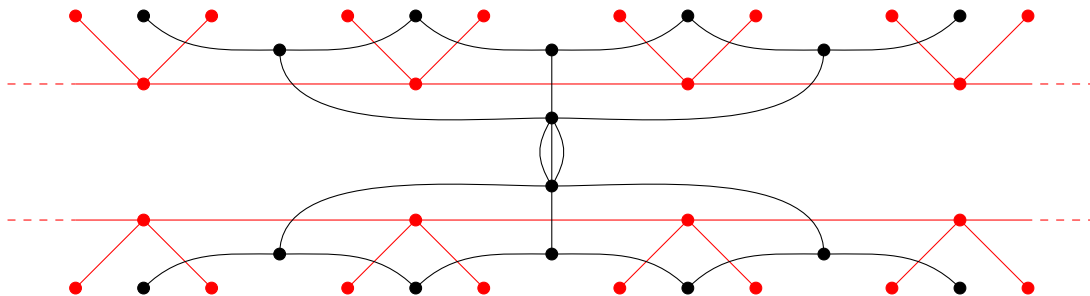


Figure 6.16: The density matrix associated to the thermal state on the boundary of a BTZ black hole tensor network.

After, splitting we must now count the number of new cycles created, where each new cycle contributes a factor of r . The number of cycles is the number of internal lines in the tensor network. These considerations mean that the norm of the state will go as a power of r , and we find:

$$\log \langle \psi_\tau | \psi_\tau \rangle = \frac{1}{2} \sum_{\text{type } i} \frac{M^{(i)} v_d^{(i)}}{2} \log r = \left(\frac{r+1}{2} + \frac{\tau}{2} p^{\Lambda-1} ((p-1)r - (p+1)) \right) \log r. \quad (6.112)$$

Having found the norm of the state, we may now compute the density matrix and entropy which comes from tracing out the central vertex behind the horizon, as shown in figure 6.16. The intuition is that these degrees of freedom cannot be associated to any boundary state, so we should trace them out of the Hilbert space. The result is a mixed density matrix describing only the boundary qudits. As we are only tracing out one vertex, the result is surprisingly simple and parallels the computation of the entanglement entropy at genus 0.

Applying our rule for tensor contractions to the center vertex as in figure 6.16, where the two sides denote $|\psi_\tau\rangle$ and $\langle\psi_\tau|$, we see that in general we have a mixed density matrix with τ bonds stretched across the two sides. This is somewhat reminiscent of a two-sided BTZ black hole, as depicted in figure 6.8. Based on the computation for the entanglement entropy, one would expect the thermodynamic entropy of this state to be proportional to τ , and this can be supported by explicit analytic computation.

Performing the split of the center vertex gives a factor of $r^{(v_d - v_c)/2} = r^{(r+1)/2 - \tau}$, and the general density matrix has a form similar to (6.88), with r^τ blocks of

all 1's of size r^σ :

$$\rho_{BH} = \frac{r^{\frac{(r+1)}{2} - \tau}}{\langle \psi_\tau | \psi_\tau \rangle} \left(\begin{array}{ccc} \left[\begin{array}{ccc} 1 & \cdots & 1 \\ \vdots & \ddots & \vdots \\ 1 & \cdots & 1 \end{array} \right]_{r^\sigma} & & \\ & \ddots & \\ & & \left[\begin{array}{ccc} 1 & \cdots & 1 \\ \vdots & \ddots & \vdots \\ 1 & \cdots & 1 \end{array} \right]_{r^\sigma} \end{array} \right)_{r^{\sigma+\tau} \times r^{\sigma+\tau}} \quad (6.113)$$

We may fix the value of σ by diagrammatic computation, but it is easier to simply impose the unit trace condition. Using the value of (6.112), we find σ is given by the second piece,

$$\sigma = \frac{\tau}{2} p^{\Lambda-1} ((p-1)r - (p+1)). \quad (6.114)$$

We now compute the von Neumann entropy of this state, which corresponds to the black hole entropy.

$$S_{BH} = -\text{Tr} \rho_{BH} \log \rho_{BH}, \quad (6.115)$$

where each block of ρ_{BH} may be diagonalized before taking the trace. This gives a sum of identical terms with the σ dependence cancelling,

$$S_{BH} = -\sum_{r^\tau} r^{-\tau} \log r^{-\tau}, \quad (6.116)$$

or the main result of this section,

$$S_{BH} = \tau \log r = (\log r) \log_p |q|_p^{-1}. \quad (6.117)$$

We see that the von Neumann entropy of the boundary state is large and directly proportional to the perimeter of the event horizon.

We now briefly discuss the entanglement entropy between an interval and its complement in the thermal background, dual to minimal geodesics in the black hole geometry. We have already explained the results of these computations in Section 6.4, which match the expectations of real AdS/CFT and the cut rule for perfect tensors. The computation of specific examples is straightforward

using the rules we have used throughout this section, but the general formula is cumbersome to present in detail, so we elect to explain the basic geometry and the result of the contractions.

Tracing out a boundary region in the black hole background is obtained by combining the two graphical rules for reduced density matrices so far. The mixed density matrix is constructed by gluing the state and its dual along the boundary interval to be traced out (implementing the partial trace), as well as along the center black hole vertex. Physically, these two gluings are two separate effects, but the resulting mixed state has an entropy which is sensitive both to the black hole horizon size and to the interval size. As before, we apply the rules of splits and cycles to the perfect tensors which are contracted, and from this point of view we treat the various contractions on equal footing to ultimately obtain the correct entropy. Several cases are possible, as the entanglement entropy of a region is no longer equal to that of the complement due to the presence of the black hole. There are essentially three possible cases which are schematically depicted in figure 6.17:

- Given a cutoff, if the region to be traced out is sufficiently small such that the entanglement wedge does not approach near the horizon of the black hole as in the first picture, the resulting entropy will be completely insensitive to the presence of the horizon. As in the genus 0 case, this entropy is proportional to the log of the interval size and can be graphically computed by counting the number of bonds shared across the traced-out region after performing all contractions. (These are exactly the bonds which cut the minimal surface on the genus 1 tree geometry.)
- For a larger region, the graphical rules imply that bonds crossing the horizon interfere with those for the traced-out region. The suspended bonds between the state and its dual now use up some of the bonds which were originally part of the horizon contraction. This is interpreted as the minimal surface wrapping around the horizon, and a computation reveals the entropy is given by exactly this length. This schematically looks like the middle figure.
- For a sufficiently large region, the available bonds inside the black hole become exhausted. The entanglement is now given by the number of remaining bonds across the state and the dual, which corresponds to a

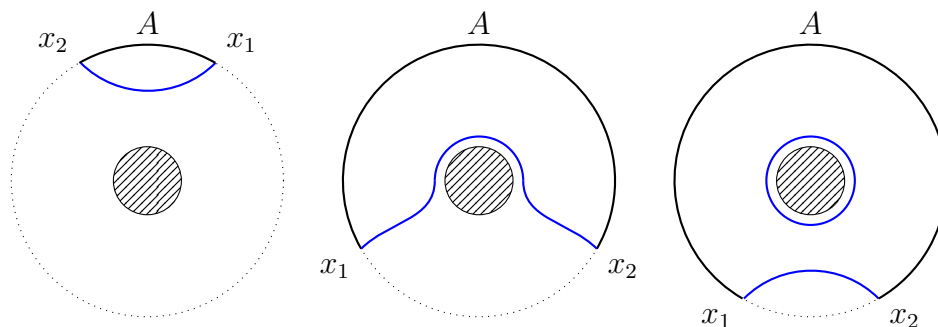


Figure 6.17: A schematic depiction of the three topologically distinct cases of minimal geodesics for a connected region A .

minimal surface which wraps the other side and includes the black hole; this is shown in the final figure. The entropy is given by the sum of the horizon area and the length of the minimal surface.

In each case the minimal geodesic is homologous to the boundary region as desired. From these basic geometric rules, the results of Section 6.4 follow, as one can see by direct though non-trivial calculation. The minimal surfaces we find closely resemble their Archimedean counterparts, but are distinctly discrete and ultrametric.

We take the success of this network as a prediction for entanglement in thermal p -adic AdS/CFT. We also suspect the methods we have described for single intervals in black hole backgrounds generalize, possibly to higher genus black holes and more intervals.

6.6 Geometric Properties of the Tensor Networks

Certain features of the tensor network we have introduced may appear to be ad hoc, such as the seemingly artificial choice of planar embedding and the choice of boundary measure.

Therefore, in this section we discuss in more detail some aspects of the geometry of the tensor networks introduced in this chapter. In particular we discuss more in detail the symmetries and the dependence in the choice of embedding. We also discuss measures on the p -adic Tate–Mumford curve induced by different restrictions of the Patterson–Sullivan measure on the projective line. Practical calculations have shown us that these issues do not appear to affect

the physical quantities we compute, and here we only touch on why this is the case.

Tensor networks: symmetries and embeddings

Recall from Section 6.2 that we can label the nodes on the Bruhat–Tits tree as cosets $G = \text{PGL}(2, \mathbb{Q}_p) = \bigcup_{i=1}^{\infty} g_i H$ where $H = \text{PGL}(2, \mathbb{Z}_p)$ and $g_i \in G$. Suppose we pick a particular planar embedding, or in other words, make a choice of all incidence relations among bonds on the dual graph consistent with definition 3. Further, focus on the particular bond in the dual graph specified by the corresponding edge between the nodes $g_1 H$ and $g_2 H$ on the Bruhat–Tits tree. Let it be incident with a bond in the dual graph corresponding to the edge between the nodes $g_3 H$ and $g_4 H$. After an isometric G transformation, suppose the nodes on the Bruhat–Tits tree go to the cosets $g'_1 H, g'_2 H, g'_3 H$ and $g'_4 H$ respectively. Then the G transformation sends the edge on the Bruhat–Tits tree between $g_1 H$ and $g_2 H$ to the edge between $g'_1 H$ and $g'_2 H$ (and similarly for the other edge). Correspondingly, the bonds on the dual graph transform as well, in such a way that all incidence relations are preserved on the dual graph. In other words, G acts as an isometry on the dual graph. The point of intersection of the two bonds on the dual graph before the G transformation was a node on the dual graph where the two bonds corresponding to cosets $g_1 H$ & $g_2 H$ and $g_3 H$ & $g_4 H$ met. After the transformation, the intersection node on the dual graph is mapped to the node which is the point of intersection of the bonds specified by the cosets $g'_1 H$ & $g'_2 H$ and $g'_3 H$ & $g'_4 H$ respectively.

Other choices for the dual graph can be obtained as follows. Starting with the Bruhat–Tits tree where the nodes are specified via the cosets $g_i H$ for $i = 0, 1, \dots, \infty$, we specialize to a particular planar embedding. Now we perform an isometric G transformation, which transforms $g_i H \rightarrow g'_i H$ for all i . The original dual graph incidence relations, given in terms of cosets $g_i H$ transform to the ones in terms of the transformed cosets $g'_i H$ as explained in the previous paragraph. However, we can construct a *different* dual graph, whose bond incidence relations are the original incidence relations (in terms of original labelling of the cosets $g_i H$) but the Bruhat–Tits tree nodes are given in terms of the transformed cosets $g'_i H$. (Here we are using the fact that $G = \bigcup_{i=1}^{\infty} g_i H = \bigcup_{i=0}^{\infty} g'_i H$.) From this we conclude there are at least as many possible dual graphs as elements of the isometry group G . In fact there exist more choices for the dual graph. One can act with any element of

the automorphism group of the Bruhat–Tits (which is still an isometry) and obtain a different planar embedding. All such planar embeddings are allowed but there is no preferred choice among them. For the purposes of computation, we usually picked a particular choice of a dual graph (i.e. a particular planar embedding); however, the final physical result of the computations was always independent of this choice as discussed in previous sections.

A measure on the Tate–Mumford curve

In the genus-zero case, the boundary $\mathbb{P}^1(\mathbb{K})$ of the Bruhat–Tits tree $T_{\mathbb{K}}$ is a finite extension \mathbb{K} of \mathbb{Q}_p carries a measure that is the Patterson–Sullivan measure for the action of $\mathrm{PGL}(2, \mathbb{K})$ on $T_{\mathbb{K}}$, which has the full boundary $\mathbb{P}^1(\mathbb{K})$ as limit set. It is known by the general construction of [254] that any Gromov-hyperbolic space with a proper discontinuous action of an isometry group determines a Patterson–Sullivan measure on the hyperbolic boundary, with support on the limit set of the group, and quasi conformal of dimension equal to the Hausdorff dimension of the limit set. In particular, in the case of a p -adic Schottky group Γ of rank at least two acting on the Bruhat–Tits tree and its boundary, one obtains in this way a Patterson–Sullivan measure supported on the limit set $\Lambda_{\Gamma} \subset \mathbb{P}^1(\mathbb{K})$ of the Schottky group. The properties of this Patterson–Sullivan measure are used to prove rigidity results for Mumford curves, [240]. However, notice that the Patterson–Sullivan measure lives on the limit set Λ_{Γ} , which is the complement of the boundary region that determines the Mumford curve $X_{\Gamma}(\mathbb{K}) = (\mathbb{P}^1(\mathbb{K}) \setminus \Lambda_{\Gamma})/\Gamma$. Thus, unlike the genus zero case, the natural construction of a Patterson–Sullivan measure does not produce a measure on the Mumford curve, but only a measure on the limit set. Moreover, in the particular case of genus one, even this measure on the limit set would be uninteresting, since in the genus one case the limit set only consists of two points (which we can always assume to be 0 and ∞), rather than a Cantor set type object as in the higher genus cases. One can also see that the other interesting group action that is present in the case of Mumford curves, namely the action of the automorphism group of the curve, also fails to give rise to an interesting Patterson–Sullivan measure (except in genus zero where the automorphism group of the projective line is $\mathrm{PGL}(2, \mathbb{K})$ and one obtains again the Patterson–Sullivan measure on $\mathbb{P}^1(\mathbb{K})$). Indeed, in the case with genus at least two the automorphism group $\mathrm{Aut}(X)$ of the Mumford curve X is a finite group hence the limit set is empty, hence we do not have a Patterson–Sullivan

measure supported on the Mumford curve X itself.

In the case of genus one (BTZ black hole) the automorphism group of the elliptic curve is a semidirect product of the elliptic curve E itself as a group (acting on itself by translations) by the automorphism group $Aut(E)$ of this group. In particular, the action on the Bruhat–Tits tree of arbitrary translations along the geodesic with endpoints $\{0, \infty\}$ induces automorphisms of the Mumford curve, which act on the infinite graph T/Γ and its boundary $\partial T/\Gamma = X_\Gamma$ as rotations of the central polygonal ring and of all the outgoing trees attached to it. The change of orientation that exchanges the endpoints $\{0, \infty\}$ also induces a self map of T/Γ and its boundary X_Γ . Again we do not obtain a non-trivial limit set on the boundary Mumford curve $X(\mathbb{K}) = (\mathbb{P}^1(\mathbb{K}) \setminus \{0, \infty\})/\Gamma$, hence we cannot just replace the Patterson–Sullivan measure on $\mathbb{P}^1(\mathbb{K})$ with a similar Patterson–Sullivan measure on the Mumford curves $X_\Gamma(\mathbb{K})$ of genus at least one.

However, for the genus one case of Tate–Mumford elliptic curves that we are mainly interested in here, it is possible to define a measure on $X_\Gamma(\mathbb{K})$ induced by the Patterson–Sullivan measure on $\mathbb{P}^1(\mathbb{K})$. Consider the geodesic $L_{\{0, \infty\}}$ in the Bruhat–Tits tree T that connects the fixed points $\{0, \infty\}$ of the Schottky group. Fix a fundamental domain \mathcal{F}_Γ of the action of the Schottky group $\Gamma \simeq \mathbb{Z}$ on T . The intersection $\mathcal{F}_\Gamma \cap L_{\{0, \infty\}}$ consists of a finite set of vertices in bijective correspondence with the vertices of the central polygon in the graph T/Γ .

There are then two main choices for how to construct a measure on $X_\Gamma(\mathbb{K})$ using the Patterson–Sullivan measure on $\mathbb{P}^1(\mathbb{K})$. The first choice generates a measure on $X_\Gamma(\mathbb{K})$ that is invariant under the automorphisms of X_Γ induced by arbitrary translations along $L_{\{0, \infty\}}$, while the second one does not have this invariant property.

For the first construction, fix a choice of a root vertex v_0 in the tree T contained in $\mathcal{F}_\Gamma \cap L_{\{0, \infty\}}$, and consider the tree T_0 stemming from v_0 with first edges the $q - 1$ directions at v_0 that are not along $L_{\{0, \infty\}}$. Let $\Omega_0(\mathbb{K}) \subset \mathbb{P}^1(\mathbb{K})$ be the boundary region $\Omega_0(\mathbb{K}) = \partial T_0$, endowed with the restriction $\mu_0 = \mu|_{\Omega_0}$ of the Patterson–Sullivan measure μ on $\mathbb{P}^1(\mathbb{K})$. Every other subtree of the Bruhat–Tits tree that has root vertex on $L_{\{0, \infty\}}$ and first edges not in the direction of $L_{\{0, \infty\}}$ is obtained from T_0 via the action of a translation along $L_{\{0, \infty\}}$. We can endow the boundary region of these trees with copies of the same measure μ_0 .

In this way we obtain a measure on $\mathbb{P}^1(\mathbb{K}) \setminus \{0, \infty\}$ that has infinite total mass and that is invariant under arbitrary translations along $L_{\{0, \infty\}}$. Since it is in particular invariant under the action of the rank one Schottky group Γ with limit set $\{0, \infty\}$ it descends to a measure on $X_\Gamma = (\mathbb{P}^1(\mathbb{K}) \setminus \{0, \infty\})/\Gamma$. This measure on X_Γ has finite total mass, since it consists of finitely many copies of μ_0 (one for each tree stemming from one of the vertices of the central polygon of T/Γ), hence we can normalize it to a probability measure on X_Γ which is invariant under the automorphisms induced by translations along $L_{\{0, \infty\}}$ and also by orientation reversal.

The second construction is similar, but instead of considering the tree T_0 stemming from the root vertex v_0 along the directions complementary to $L_{\{0, \infty\}}$, we consider now the forest $T_{\mathcal{F}}$ which is the disjoint union of the trees T_v stemming from the vertices in $\mathcal{F}_\Gamma \cap L_{\{0, \infty\}}$. We denote by $\Omega_{\mathcal{F}}$ the corresponding boundary region $\Omega_{\mathcal{F}} = \partial T_{\mathcal{F}} \subset \mathbb{P}^1(\mathbb{K})$. The normalized restriction $\mu_{\mathcal{F}}$ of the Patterson–Sullivan measure μ on $\mathbb{P}^1(\mathbb{K})$ to the region $\Omega_{\mathcal{F}}$ induces a Γ -invariant measure on $\mathbb{P}^1(\mathbb{K}) \setminus \{0, \infty\}$ of infinite total mass, and a probability measure on the quotient $X_\Gamma(\mathbb{K}) = (\mathbb{P}^1(\mathbb{K}) \setminus \{0, \infty\})/\Gamma$.

While the first construction gives a more “symmetric” measure on $X_\Gamma(\mathbb{K})$, the symmetry under arbitrary translations along $L_{\{0, \infty\}}$ has the disadvantage that the boundary measure no longer keeps track of geodesic paths along the central polygonal graph in T/Γ . The second measure instead is more useful for our purposes: while invariance under translations in Γ means that the measure descends to the quotient $X_\Gamma(\mathbb{K})$, hence it does not detect the number of times that a path in the bulk T/Γ wraps around the central polygon, it still does distinguish the number of polygon edges along the polygon modulo its total length.

6.7 Outlook

The study of holography over non-Archimedean fields such as the p -adics is still a very young area, and there is much more to be learned both from the study of models in the continuum and from the relation to tensor network constructions such as we have pursued here. In these paragraphs, we summarize a few questions and directions that seem worthy of further investigation.

One lesson of our computations is that, in this p -adic setting, it is more natural to think of the entropy as a function of boundary points and configurations

of points, rather than as a function of boundary regions (intervals). This is in spite of the fact that our computations always rely on a choice of region in the dual tensor network. Thus, our results are consistent with an interpretation in a continuum p -adic field theory, for example, in terms of correlation functions of twist operators (as used in real two-dimensional CFT computations by [216, 214]). This is also consistent with the physical intuition that the main contributions to entanglement entropy should arise from UV modes localized near the entangling surface. In our scenario, as in CFT_2 , the entangling surfaces are just points, and in particular live at the boundary of the Bruhat–Tits tree itself, rather than being associated to the dual tensor network. It would be interesting to find a calculational framework depending only on the positions of entangling surfaces that would work in parallel fashion in real and p -adic field theories.

One can interpret our results as giving predictions for entanglement entropies in certain continuum p -adic field theories, which we expect to be valid up to certain overall theory-dependent factors (such as the overall normalization). For pure states, these predictions include the connected interval (two point) entropy in (6.35) and (6.40), disconnected-interval (four point) entropy (6.104), and mutual information (6.103); when considering the thermal state dual to a p -adic BTZ black hole, we give the form of the connected interval result in (6.49) and (6.52). Furthermore, our proofs of entropy inequalities are evidence in support of such results—such as subadditivity and strong subadditivity—in continuum p -adic field theory. Extending these results to holographic codes [99] which include bulk logical inputs would be a natural next step.

It would also be interesting to investigate the recently conjectured duality between entanglement of purification and entanglement wedge cross-section [255, 256, 257] and its extensions [258, 259, 260, 261] in this setup, as well as other measures of entanglement for mixed states, such as entanglement negativity [262] and the conjectured bulk interpretation (see e.g. [263, 264, 265, 266]). The simplifying features of the tensor networks studied here provide an effective computational framework to explore such questions.

Along these lines, we have shown that many aspects of the bulk p -adic geometries closely parallel the situation in real AdS/CFT. Even so, it is comparably simpler to work with the discrete geometries, and this specific network pro-

vided a model in which we could efficiently compute many holographic entropy quantities. One might hope this trend will continue, and we expect that more complicated holographic quantities will be computationally easier to study in the p -adic setting. A major goal of this program is to reconstruct bulk quantities in smooth AdS from knowledge of the corresponding p -adic quantities for all p . We hope to return to the reconstruction of real AdS quantities from p -adic in future work.

Finally, generalizations of the BTZ black hole given by higher genus Mumford curves (quotients by higher rank Schottky groups) and higher dimensional models based on higher rank buildings may also exhibit more intricate relations between entanglement entropy on the boundary p -adic varieties and the geometry of the bulk regions, and may help identify a covariant generalization of the RT formula in the context of p -adic theories.

BIBLIOGRAPHY

- [1] Matthew Heydeman, John H. Schwarz, and Congkao Wen. “M5-Brane and D-Brane Scattering Amplitudes”. In: *JHEP* 12 (2017), p. 003. DOI: [10.1007/JHEP12\(2017\)003](https://doi.org/10.1007/JHEP12(2017)003). arXiv: [1710.02170](https://arxiv.org/abs/1710.02170) [[hep-th](#)].
- [2] Freddy Cachazo, Alfredo Guevara, Matthew Heydeman, Sebastian Mizera, John H. Schwarz, and Congkao Wen. “The S Matrix of 6D Super Yang-Mills and Maximal Supergravity from Rational Maps”. In: *JHEP* 09 (2018), p. 125. DOI: [10.1007/JHEP09\(2018\)125](https://doi.org/10.1007/JHEP09(2018)125). arXiv: [1805.11111](https://arxiv.org/abs/1805.11111) [[hep-th](#)].
- [3] Matthew Heydeman, John H. Schwarz, Congkao Wen, and Shun-Qing Zhang. “All Tree Amplitudes of 6D (2, 0) Supergravity: Interacting Tensor Multiplets and the $K3$ Moduli Space”. In: *Phys. Rev. Lett.* 122.11 (2019), p. 111604. DOI: [10.1103/PhysRevLett.122.111604](https://doi.org/10.1103/PhysRevLett.122.111604). arXiv: [1812.06111](https://arxiv.org/abs/1812.06111) [[hep-th](#)].
- [4] Matthew Heydeman, Matilde Marcolli, Ingmar Saberi, and Bogdan Stoica. “Tensor networks, p -adic fields, and algebraic curves: arithmetic and the $\text{AdS}_3/\text{CFT}_2$ correspondence”. In: *Adv. Theor. Math. Phys.* 22 (2018), pp. 93–176. DOI: [10.4310/ATMP.2018.v22.n1.a4](https://doi.org/10.4310/ATMP.2018.v22.n1.a4). arXiv: [1605.07639](https://arxiv.org/abs/1605.07639) [[hep-th](#)].
- [5] Matthew Heydeman, Matilde Marcolli, Sarthak Parikh, and Ingmar Saberi. “Nonarchimedean Holographic Entropy from Networks of Perfect Tensors”. In: (2018). arXiv: [1812.04057](https://arxiv.org/abs/1812.04057) [[hep-th](#)].
- [6] Steven S. Gubser, Matthew Heydeman, Christian Jepsen, Sarthak Parikh, Ingmar Saberi, Bogdan Stoica, and Brian Trundy. “Melonic theories over diverse number systems”. In: *Phys. Rev. D* 98.12 (2018), p. 126007. DOI: [10.1103/PhysRevD.98.126007](https://doi.org/10.1103/PhysRevD.98.126007). arXiv: [1707.01087](https://arxiv.org/abs/1707.01087) [[hep-th](#)].
- [7] Steven S. Gubser, Matthew Heydeman, Christian Jepsen, Matilde Marcolli, Sarthak Parikh, Ingmar Saberi, Bogdan Stoica, and Brian Trundy. “Edge length dynamics on graphs with applications to p -adic AdS/CFT ”. In: *JHEP* 06 (2017), p. 157. DOI: [10.1007/JHEP06\(2017\)157](https://doi.org/10.1007/JHEP06(2017)157). arXiv: [1612.09580](https://arxiv.org/abs/1612.09580) [[hep-th](#)].
- [8] Michael B. Green, J. H. Schwarz, and Edward Witten. *SUPERSTRING THEORY. VOL. 1: INTRODUCTION*. Cambridge Monographs on Mathematical Physics. 1988. ISBN: 9780521357524. URL: <http://www.cambridge.org/us/academic/subjects/physics/theoretical-physics-and-mathematical-physics/superstring-theory-volume-1>.
- [9] J. Polchinski. *String theory. Vol. 1: An introduction to the bosonic string*. Cambridge Monographs on Mathematical Physics. Cambridge

University Press, 2007. ISBN: 9780511252273, 9780521672276, 9780521633031.
DOI: [10.1017/CBO9780511816079](https://doi.org/10.1017/CBO9780511816079).

- [10] Joseph Polchinski. “Tasi lectures on D-branes”. In: *Fields, strings and duality. Proceedings, Summer School, Theoretical Advanced Study Institute in Elementary Particle Physics, TASI'96, Boulder, USA, June 2-28, 1996*. 1996, pp. 293–356. arXiv: [hep-th/9611050](https://arxiv.org/abs/hep-th/9611050) [[hep-th](#)].
- [11] K. Becker, M. Becker, and J. H. Schwarz. *String theory and M-theory: A modern introduction*. Cambridge University Press, 2006. ISBN: 9780511254864, 9780521860697.
- [12] Juan Martin Maldacena. “The Large N limit of superconformal field theories and supergravity”. In: *Int. J. Theor. Phys.* 38 (1999). [Adv. Theor. Math. Phys.2,231(1998)], pp. 1113–1133. DOI: [10.1023/A:1026654312961](https://doi.org/10.1023/A:1026654312961), [10.4310/ATMP.1998.v2.n2.a1](https://doi.org/10.4310/ATMP.1998.v2.n2.a1). arXiv: [hep-th/9711200](https://arxiv.org/abs/hep-th/9711200) [[hep-th](#)].
- [13] G. Veneziano. “Construction of a crossing - symmetric, Regge behaved amplitude for linearly rising trajectories”. In: *Nuovo Cim.* A57 (1968), pp. 190–197. DOI: [10.1007/BF02824451](https://doi.org/10.1007/BF02824451).
- [14] Leonard Susskind. “Dual symmetric theory of hadrons. 1.” In: *Nuovo Cim.* A69 (1970), pp. 457–496. DOI: [10.1007/BF02726485](https://doi.org/10.1007/BF02726485).
- [15] Y Nambu. “Quark model of the Veneziano amplitude”. In: (1970). URL: <https://cds.cern.ch/record/477520>.
- [16] Ziro Koba and Holger Bech Nielsen. “Manifestly crossing invariant parametrization of n meson amplitude”. In: *Nucl. Phys.* B12 (1969), pp. 517–536. DOI: [10.1016/0550-3213\(69\)90071-6](https://doi.org/10.1016/0550-3213(69)90071-6).
- [17] Z. Koba and Holger Bech Nielsen. “Reaction amplitude for n mesons: A Generalization of the Veneziano-Bardakci-Ruegg-Virasora model”. In: *Nucl. Phys.* B10 (1969), pp. 633–655. DOI: [10.1016/0550-3213\(69\)90331-9](https://doi.org/10.1016/0550-3213(69)90331-9).
- [18] Peter G. O. Freund and Edward Witten. “Adelic String Amplitudes”. In: *Phys. Lett.* B199 (1987), p. 191. DOI: [10.1016/0370-2693\(87\)91357-8](https://doi.org/10.1016/0370-2693(87)91357-8).
- [19] Lee Brekke, Peter G. O. Freund, Mark Olson, and Edward Witten. “Nonarchimedean String Dynamics”. In: *Nucl. Phys.* B302 (1988), pp. 365–402. DOI: [10.1016/0550-3213\(88\)90207-6](https://doi.org/10.1016/0550-3213(88)90207-6).
- [20] Joel Scherk and John H. Schwarz. “Dual Models for Nonhadrons”. In: *Nucl. Phys.* B81 (1974), pp. 118–144. DOI: [10.1016/0550-3213\(74\)90010-8](https://doi.org/10.1016/0550-3213(74)90010-8).
- [21] Pierre Ramond. “Dual Theory for Free Fermions”. In: *Phys. Rev.* D3 (1971), pp. 2415–2418. DOI: [10.1103/PhysRevD.3.2415](https://doi.org/10.1103/PhysRevD.3.2415).

- [22] P. Goddard, J. Goldstone, C. Rebbi, and Charles B. Thorn. “Quantum dynamics of a massless relativistic string”. In: *Nucl. Phys.* B56 (1973), pp. 109–135. DOI: [10.1016/0550-3213\(73\)90223-X](https://doi.org/10.1016/0550-3213(73)90223-X).
- [23] A. Neveu and J. H. Schwarz. “Factorizable dual model of pions”. In: *Nucl. Phys.* B31 (1971), pp. 86–112. DOI: [10.1016/0550-3213\(71\)90448-2](https://doi.org/10.1016/0550-3213(71)90448-2).
- [24] F. Gliozzi, Joel Scherk, and David I. Olive. “Supersymmetry, Supergravity Theories and the Dual Spinor Model”. In: *Nucl. Phys.* B122 (1977), pp. 253–290. DOI: [10.1016/0550-3213\(77\)90206-1](https://doi.org/10.1016/0550-3213(77)90206-1).
- [25] Michael B. Green and John H. Schwarz. “Supersymmetrical String Theories”. In: *Phys. Lett.* 109B (1982), pp. 444–448. DOI: [10.1016/0370-2693\(82\)91110-8](https://doi.org/10.1016/0370-2693(82)91110-8).
- [26] Alexander M. Polyakov. “Quantum Geometry of Bosonic Strings”. In: *Phys. Lett.* B103 (1981). [598(1981)], pp. 207–210. DOI: [10.1016/0370-2693\(81\)90743-7](https://doi.org/10.1016/0370-2693(81)90743-7).
- [27] Michael B. Green and John H. Schwarz. “Anomaly Cancellation in Supersymmetric D=10 Gauge Theory and Superstring Theory”. In: *Phys. Lett.* 149B (1984), pp. 117–122. DOI: [10.1016/0370-2693\(84\)91565-X](https://doi.org/10.1016/0370-2693(84)91565-X).
- [28] Lars Brink, John H. Schwarz, and Joel Scherk. “Supersymmetric Yang-Mills Theories”. In: *Nucl. Phys.* B121 (1977), pp. 77–92. DOI: [10.1016/0550-3213\(77\)90328-5](https://doi.org/10.1016/0550-3213(77)90328-5).
- [29] Joseph Polchinski. “Dirichlet Branes and Ramond-Ramond charges”. In: *Phys. Rev. Lett.* 75 (1995), pp. 4724–4727. DOI: [10.1103/PhysRevLett.75.4724](https://doi.org/10.1103/PhysRevLett.75.4724). arXiv: [hep-th/9510017](https://arxiv.org/abs/hep-th/9510017) [hep-th].
- [30] Arkady A. Tseytlin. “Born-Infeld action, supersymmetry and string theory”. In: (1999), pp. 417–452. DOI: [10.1142/9789812793850_0025](https://doi.org/10.1142/9789812793850_0025). arXiv: [hep-th/9908105](https://arxiv.org/abs/hep-th/9908105) [hep-th].
- [31] Mina Aganagic, Costin Popescu, and John H. Schwarz. “Gauge invariant and gauge fixed D-brane actions”. In: *Nucl. Phys.* B495 (1997), pp. 99–126. DOI: [10.1016/S0550-3213\(97\)00180-6](https://doi.org/10.1016/S0550-3213(97)00180-6). arXiv: [hep-th/9612080](https://arxiv.org/abs/hep-th/9612080) [hep-th].
- [32] Martin Cederwall, Alexander von Gussich, Bengt E. W. Nilsson, and Anders Westerberg. “The Dirichlet super three-brane in ten-dimensional type IIB supergravity”. In: *Nucl. Phys.* B490 (1997), pp. 163–178. DOI: [10.1016/S0550-3213\(97\)00071-0](https://doi.org/10.1016/S0550-3213(97)00071-0). arXiv: [hep-th/9610148](https://arxiv.org/abs/hep-th/9610148) [hep-th].
- [33] Mina Aganagic, Costin Popescu, and John H. Schwarz. “D-brane actions with local kappa symmetry”. In: *Phys. Lett.* B393 (1997), pp. 311–315. DOI: [10.1016/S0370-2693\(96\)01643-7](https://doi.org/10.1016/S0370-2693(96)01643-7). arXiv: [hep-th/9610249](https://arxiv.org/abs/hep-th/9610249) [hep-th].

- [34] Martin Cederwall, Alexander von Gussich, Bengt E. W. Nilsson, Per Sundell, and Anders Westerberg. “The Dirichlet super p-branes in ten-dimensional type IIA and IIB supergravity”. In: *Nucl. Phys.* B490 (1997), pp. 179–201. DOI: [10.1016/S0550-3213\(97\)00075-8](https://doi.org/10.1016/S0550-3213(97)00075-8). arXiv: [hep-th/9611159](https://arxiv.org/abs/hep-th/9611159) [hep-th].
- [35] E. Bergshoeff and P. K. Townsend. “Super D-branes”. In: *Nucl. Phys.* B490 (1997), pp. 145–162. DOI: [10.1016/S0550-3213\(97\)00072-2](https://doi.org/10.1016/S0550-3213(97)00072-2). arXiv: [hep-th/9611173](https://arxiv.org/abs/hep-th/9611173) [hep-th].
- [36] Edward Witten. “String theory dynamics in various dimensions”. In: *Nucl. Phys.* B443 (1995). [333(1995)], pp. 85–126. DOI: [10.1016/0550-3213\(95\)00158-0](https://doi.org/10.1016/0550-3213(95)00158-0). arXiv: [hep-th/9503124](https://arxiv.org/abs/hep-th/9503124) [hep-th].
- [37] Edward Witten. “Some comments on string dynamics”. In: *Future perspectives in string theory. Proceedings, Conference, Strings’95, Los Angeles, USA, March 13-18, 1995*. 1995, pp. 501–523. arXiv: [hep-th/9507121](https://arxiv.org/abs/hep-th/9507121) [hep-th].
- [38] E. Cremmer, B. Julia, and Joel Scherk. “Supergravity Theory in Eleven-Dimensions”. In: *Phys. Lett.* B76 (1978). [25(1978)], pp. 409–412. DOI: [10.1016/0370-2693\(78\)90894-8](https://doi.org/10.1016/0370-2693(78)90894-8).
- [39] Edward Witten. “Five-brane effective action in M theory”. In: *J. Geom. Phys.* 22 (1997), pp. 103–133. DOI: [10.1016/S0393-0440\(97\)80160-X](https://doi.org/10.1016/S0393-0440(97)80160-X). arXiv: [hep-th/9610234](https://arxiv.org/abs/hep-th/9610234) [hep-th].
- [40] H. Kawai, D. C. Lewellen, and S. H. H. Tye. “A Relation Between Tree Amplitudes of Closed and Open Strings”. In: *Nucl. Phys.* B269 (1986), pp. 1–23. DOI: [10.1016/0550-3213\(86\)90362-7](https://doi.org/10.1016/0550-3213(86)90362-7).
- [41] Henriette Elvang and Yu-tin Huang. “Scattering Amplitudes”. In: (2013). arXiv: [1308.1697](https://arxiv.org/abs/1308.1697) [hep-th].
- [42] R. Penrose. “Twistor algebra”. In: *J. Math. Phys.* 8 (1967), p. 345. DOI: [10.1063/1.1705200](https://doi.org/10.1063/1.1705200).
- [43] Clifford Cheung and Donal O’Connell. “Amplitudes and Spinor-Helicity in Six Dimensions”. In: *JHEP* 07 (2009), p. 075. DOI: [10.1088/1126-6708/2009/07/075](https://doi.org/10.1088/1126-6708/2009/07/075). arXiv: [0902.0981](https://arxiv.org/abs/0902.0981) [hep-th].
- [44] Stephen J. Parke and T. R. Taylor. “An Amplitude for n Gluon Scattering”. In: *Phys. Rev. Lett.* 56 (1986), p. 2459. DOI: [10.1103/PhysRevLett.56.2459](https://doi.org/10.1103/PhysRevLett.56.2459).
- [45] Frits A. Berends and W. T. Giele. “Recursive Calculations for Processes with n Gluons”. In: *Nucl. Phys.* B306 (1988), pp. 759–808. DOI: [10.1016/0550-3213\(88\)90442-7](https://doi.org/10.1016/0550-3213(88)90442-7).
- [46] Edward Witten. “Perturbative gauge theory as a string theory in twistor space”. In: *Commun. Math. Phys.* 252 (2004), pp. 189–258. DOI: [10.1007/s00220-004-1187-3](https://doi.org/10.1007/s00220-004-1187-3). arXiv: [hep-th/0312171](https://arxiv.org/abs/hep-th/0312171) [hep-th].

- [47] Freddy Cachazo and Peter Svrcek. “Lectures on twistor strings and perturbative Yang-Mills theory”. In: *PoS RTN2005* (2005), p. 004. DOI: [10.22323/1.019.0005](https://doi.org/10.22323/1.019.0005). arXiv: [hep-th/0504194](https://arxiv.org/abs/hep-th/0504194) [[hep-th](#)].
- [48] J. Wess and J. Bagger. *Supersymmetry and supergravity*. Princeton, NJ, USA: Princeton University Press, 1992. ISBN: 9780691025308.
- [49] V. P. Nair. “A Current Algebra for Some Gauge Theory Amplitudes”. In: *Phys. Lett.* B214 (1988), pp. 215–218. DOI: [10.1016/0370-2693\(88\)91471-2](https://doi.org/10.1016/0370-2693(88)91471-2).
- [50] Edward Witten. “An Interpretation of Classical Yang-Mills Theory”. In: *Phys. Lett.* 77B (1978), pp. 394–398. DOI: [10.1016/0370-2693\(78\)90585-3](https://doi.org/10.1016/0370-2693(78)90585-3).
- [51] Edward Witten. “Topological Sigma Models”. In: *Commun. Math. Phys.* 118 (1988), p. 411. DOI: [10.1007/BF01466725](https://doi.org/10.1007/BF01466725).
- [52] Edward Witten. “Chern-Simons gauge theory as a string theory”. In: *Prog. Math.* 133 (1995), pp. 637–678. arXiv: [hep-th/9207094](https://arxiv.org/abs/hep-th/9207094) [[hep-th](#)].
- [53] Marcel Vonk. “A Mini-course on topological strings”. In: (2005). arXiv: [hep-th/0504147](https://arxiv.org/abs/hep-th/0504147) [[hep-th](#)].
- [54] K. Hori, S. Katz, A. Klemm, R. Pandharipande, R. Thomas, C. Vafa, R. Vakil, and E. Zaslow. *Mirror symmetry*. Vol. 1. Clay mathematics monographs. Providence, USA: AMS, 2003. URL: <http://www.claymath.org/library/monographs/cmim01.pdf>.
- [55] Radu Roiban, Marcus Spradlin, and Anastasia Volovich. “On the tree level S matrix of Yang-Mills theory”. In: *Phys. Rev.* D70 (2004), p. 026009. DOI: [10.1103/PhysRevD.70.026009](https://doi.org/10.1103/PhysRevD.70.026009). arXiv: [hep-th/0403190](https://arxiv.org/abs/hep-th/0403190) [[hep-th](#)].
- [56] Freddy Cachazo, Song He, and Ellis Ye Yuan. “Scattering in Three Dimensions from Rational Maps”. In: *JHEP* 10 (2013), p. 141. DOI: [10.1007/JHEP10\(2013\)141](https://doi.org/10.1007/JHEP10(2013)141). arXiv: [1306.2962](https://arxiv.org/abs/1306.2962) [[hep-th](#)].
- [57] Freddy Cachazo, Song He, and Ellis Ye Yuan. “Scattering equations and Kawai-Lewellen-Tye orthogonality”. In: *Phys. Rev.* D90.6 (2014), p. 065001. DOI: [10.1103/PhysRevD.90.065001](https://doi.org/10.1103/PhysRevD.90.065001). arXiv: [1306.6575](https://arxiv.org/abs/1306.6575) [[hep-th](#)].
- [58] Freddy Cachazo, Song He, and Ellis Ye Yuan. “Scattering of Massless Particles in Arbitrary Dimensions”. In: *Phys. Rev. Lett.* 113.17 (2014), p. 171601. DOI: [10.1103/PhysRevLett.113.171601](https://doi.org/10.1103/PhysRevLett.113.171601). arXiv: [1307.2199](https://arxiv.org/abs/1307.2199) [[hep-th](#)].
- [59] Freddy Cachazo, Song He, and Ellis Ye Yuan. “Scattering of Massless Particles: Scalars, Gluons and Gravitons”. In: *JHEP* 07 (2014), p. 033. DOI: [10.1007/JHEP07\(2014\)033](https://doi.org/10.1007/JHEP07(2014)033). arXiv: [1309.0885](https://arxiv.org/abs/1309.0885) [[hep-th](#)].

- [60] Lionel Mason and David Skinner. “Ambitwistor strings and the scattering equations”. In: *JHEP* 07 (2014), p. 048. DOI: [10.1007/JHEP07\(2014\)048](https://doi.org/10.1007/JHEP07(2014)048). arXiv: [1311.2564](https://arxiv.org/abs/1311.2564) [hep-th].
- [61] Yvonne Geyer, Arthur E. Lipstein, and Lionel J. Mason. “Ambitwistor Strings in Four Dimensions”. In: *Phys. Rev. Lett.* 113.8 (2014), p. 081602. DOI: [10.1103/PhysRevLett.113.081602](https://doi.org/10.1103/PhysRevLett.113.081602). arXiv: [1404.6219](https://arxiv.org/abs/1404.6219) [hep-th].
- [62] Eduardo Casali, Yvonne Geyer, Lionel Mason, Ricardo Monteiro, and Kai A. Roehrig. “New Ambitwistor String Theories”. In: *JHEP* 11 (2015), p. 038. DOI: [10.1007/JHEP11\(2015\)038](https://doi.org/10.1007/JHEP11(2015)038). arXiv: [1506.08771](https://arxiv.org/abs/1506.08771) [hep-th].
- [63] Yvonne Geyer, Lionel Mason, Ricardo Monteiro, and Piotr Tourkine. “Loop Integrands for Scattering Amplitudes from the Riemann Sphere”. In: *Phys. Rev. Lett.* 115.12 (2015), p. 121603. DOI: [10.1103/PhysRevLett.115.121603](https://doi.org/10.1103/PhysRevLett.115.121603). arXiv: [1507.00321](https://arxiv.org/abs/1507.00321) [hep-th].
- [64] Yvonne Geyer, Lionel Mason, Ricardo Monteiro, and Piotr Tourkine. “One-loop amplitudes on the Riemann sphere”. In: *JHEP* 03 (2016), p. 114. DOI: [10.1007/JHEP03\(2016\)114](https://doi.org/10.1007/JHEP03(2016)114). arXiv: [1511.06315](https://arxiv.org/abs/1511.06315) [hep-th].
- [65] Freddy Cachazo, Song He, and Ellis Ye Yuan. “One-Loop Corrections from Higher Dimensional Tree Amplitudes”. In: *JHEP* 08 (2016), p. 008. DOI: [10.1007/JHEP08\(2016\)008](https://doi.org/10.1007/JHEP08(2016)008). arXiv: [1512.05001](https://arxiv.org/abs/1512.05001) [hep-th].
- [66] Yvonne Geyer, Lionel Mason, Ricardo Monteiro, and Piotr Tourkine. “Two-Loop Scattering Amplitudes from the Riemann Sphere”. In: *Phys. Rev. D* 94.12 (2016), p. 125029. DOI: [10.1103/PhysRevD.94.125029](https://doi.org/10.1103/PhysRevD.94.125029). arXiv: [1607.08887](https://arxiv.org/abs/1607.08887) [hep-th].
- [67] Yvonne Geyer and Ricardo Monteiro. “Two-Loop Scattering Amplitudes from Ambitwistor Strings: from Genus Two to the Nodal Riemann Sphere”. In: (2018). arXiv: [1805.05344](https://arxiv.org/abs/1805.05344) [hep-th].
- [68] Yvonne Geyer. “Ambitwistor Strings: Worldsheet Approaches to perturbative Quantum Field Theories”. PhD thesis. Oxford U., Inst. Math., 2016. arXiv: [1610.04525](https://arxiv.org/abs/1610.04525) [hep-th]. URL: <http://inspirehep.net/record/1492130/files/arXiv:1610.04525.pdf>.
- [69] Edward Witten. “Anti-de Sitter space and holography”. In: *Adv. Theor. Math. Phys.* 2 (1998), pp. 253–291. DOI: [10.4310/ATMP.1998.v2.n2.a2](https://doi.org/10.4310/ATMP.1998.v2.n2.a2). arXiv: [hep-th/9802150](https://arxiv.org/abs/hep-th/9802150) [hep-th].
- [70] S. S. Gubser, Igor R. Klebanov, and Alexander M. Polyakov. “Gauge theory correlators from noncritical string theory”. In: *Phys. Lett.* B428 (1998), pp. 105–114. DOI: [10.1016/S0370-2693\(98\)00377-3](https://doi.org/10.1016/S0370-2693(98)00377-3). arXiv: [hep-th/9802109](https://arxiv.org/abs/hep-th/9802109) [hep-th].

- [71] Ofer Aharony, Steven S. Gubser, Juan Martin Maldacena, Hiroshi Ooguri, and Yaron Oz. “Large N field theories, string theory and gravity”. In: *Phys. Rept.* 323 (2000), pp. 183–386. DOI: [10.1016/S0370-1573\(99\)00083-6](https://doi.org/10.1016/S0370-1573(99)00083-6). arXiv: [hep-th/9905111](https://arxiv.org/abs/hep-th/9905111) [[hep-th](#)].
- [72] Kirill Krasnov. “Holography and Riemann surfaces”. In: *Adv. Theor. Math. Phys.* 4 (2000), pp. 929–979. DOI: [10.4310/ATMP.2000.v4.n4.a5](https://doi.org/10.4310/ATMP.2000.v4.n4.a5). arXiv: [hep-th/0005106](https://arxiv.org/abs/hep-th/0005106) [[hep-th](#)].
- [73] Maximo Banados, Claudio Teitelboim, and Jorge Zanelli. “The Black hole in three-dimensional space-time”. In: *Phys. Rev. Lett.* 69 (1992), pp. 1849–1851. DOI: [10.1103/PhysRevLett.69.1849](https://doi.org/10.1103/PhysRevLett.69.1849). arXiv: [hep-th/9204099](https://arxiv.org/abs/hep-th/9204099) [[hep-th](#)].
- [74] Yuri I. Manin and Matilde Marcolli. “Holography principle and arithmetic of algebraic curves”. In: *Adv. Theor. Math. Phys.* 5 (2002), pp. 617–650. DOI: [10.4310/ATMP.2001.v5.n3.a6](https://doi.org/10.4310/ATMP.2001.v5.n3.a6). arXiv: [hep-th/0201036](https://arxiv.org/abs/hep-th/0201036) [[hep-th](#)].
- [75] David Mumford. “An analytic construction of degenerating curves over complete local rings”. In: *Compositio Math.* 24 (1972), pp. 129–174. ISSN: 0010-437X.
- [76] Francois Bruhat and Jacques Tits. “Groupes réductifs sur un corps local : I. Données radicielles valuées”. fr. In: *Publications Mathématiques de l’IHÉS* 41 (1972), pp. 5–251. DOI: [10.1007/BF02715544](https://doi.org/10.1007/BF02715544). URL: http://www.numdam.org/item/PMIHES_1972__41__5_0.
- [77] V. S. Vladimirov, I. V. Volovich, and E. I. Zelenov. *p-adic analysis and mathematical physics*. Vol. 1. Series on Soviet and East European Mathematics. World Scientific Publishing Co., Inc., River Edge, NJ, 1994, pp. xx+319. ISBN: 981-02-0880-4. DOI: [10.1142/1581](https://doi.org/10.1142/1581).
- [78] Andrei Khrennikov. *p-adic valued distributions in mathematical physics*. Vol. 309. Mathematics and its Applications. Kluwer Academic Publishers Group, Dordrecht, 1994, pp. xvi+264. ISBN: 0-7923-3172-9. DOI: [10.1007/978-94-015-8356-5](https://doi.org/10.1007/978-94-015-8356-5).
- [79] B. Dragovich, A. Yu. Khrennikov, S. V. Kozyrev, and I. V. Volovich. “On p-Adic Mathematical Physics”. In: *p-Adic Numbers Ultrametric Anal. Appl.* 1 (2009), pp. 1–17. DOI: [10.1134/S2070046609010014](https://doi.org/10.1134/S2070046609010014). arXiv: [0904.4205](https://arxiv.org/abs/0904.4205) [[math-ph](#)].
- [80] B. Dragovich, A. Yu. Khrennikov, S. V. Kozyrev, I. V. Volovich, and E. I. Zelenov. “p-Adic Mathematical Physics: The First 30 Years”. In: *Anal. Appl.* 9 (2017), pp. 87–121. DOI: [10.1134/S2070046617020017](https://doi.org/10.1134/S2070046617020017). arXiv: [1705.04758](https://arxiv.org/abs/1705.04758) [[math-ph](#)].
- [81] L. O. Chekhov, A. D. Mironov, and A. V. Zabrodin. “Multiloop Calculations in p-adic String Theory and Bruhat–Tits Trees”. In: *Commun. Math. Phys.* 125 (1989), p. 675. DOI: [10.1007/BF01228348](https://doi.org/10.1007/BF01228348).

- [82] A. V. Zabrodin. “Non-Archimedean strings and Bruhat-Tits trees”. In: *Comm. Math. Phys.* 123.3 (1989), pp. 463–483. ISSN: 0010-3616.
- [83] L. Brekke and P. G. O. Freund. “ p -adic numbers in physics”. In: *Phys. Rept.* 233 (1993), pp. 1–66. DOI: [10.1016/0370-1573\(93\)90043-D](https://doi.org/10.1016/0370-1573(93)90043-D).
- [84] Steven S. Gubser, Johannes Knaute, Sarthak Parikh, Andreas Samberg, and Przemek Witaszczyk. “ p -adic AdS/CFT”. In: *Commun. Math. Phys.* 352.3 (2017), pp. 1019–1059. DOI: [10.1007/s00220-016-2813-6](https://doi.org/10.1007/s00220-016-2813-6). arXiv: [1605.01061](https://arxiv.org/abs/1605.01061) [[hep-th](#)].
- [85] Steven S. Gubser, Christian Jepsen, Sarthak Parikh, and Brian Trundy. “ $O(N)$ and $O(N)$ and $O(N)$ ”. In: *JHEP* 11 (2017), p. 107. DOI: [10.1007/JHEP11\(2017\)107](https://doi.org/10.1007/JHEP11(2017)107). arXiv: [1703.04202](https://arxiv.org/abs/1703.04202) [[hep-th](#)].
- [86] Steven S. Gubser and Sarthak Parikh. “Geodesic bulk diagrams on the Bruhat–Tits tree”. In: *Phys. Rev. D* 96.6 (2017), p. 066024. DOI: [10.1103/PhysRevD.96.066024](https://doi.org/10.1103/PhysRevD.96.066024). arXiv: [1704.01149](https://arxiv.org/abs/1704.01149) [[hep-th](#)].
- [87] Arpan Bhattacharyya, Ling-Yan Hung, Yang Lei, and Wei Li. “Tensor network and (p -adic) AdS/CFT”. In: *JHEP* 01 (2018), p. 139. DOI: [10.1007/JHEP01\(2018\)139](https://doi.org/10.1007/JHEP01(2018)139). arXiv: [1703.05445](https://arxiv.org/abs/1703.05445) [[hep-th](#)].
- [88] Samrat Bhowmick and Koushik Ray. “Holography on local fields via Radon Transform”. In: *JHEP* 09 (2018), p. 126. DOI: [10.1007/JHEP09\(2018\)126](https://doi.org/10.1007/JHEP09(2018)126). arXiv: [1805.07189](https://arxiv.org/abs/1805.07189) [[hep-th](#)].
- [89] Feng Qu and Yi-hong Gao. “Scalar fields on p AdS”. In: *Phys. Lett. B* 786 (2018), pp. 165–170. DOI: [10.1016/j.physletb.2018.09.043](https://doi.org/10.1016/j.physletb.2018.09.043). arXiv: [1806.07035](https://arxiv.org/abs/1806.07035) [[hep-th](#)].
- [90] Christian Baadsgaard Jepsen and Sarthak Parikh. “ p -adic Mellin Amplitudes”. In: (2018). arXiv: [1808.08333](https://arxiv.org/abs/1808.08333) [[hep-th](#)].
- [91] Steven S. Gubser, Christian Jepsen, and Brian Trundy. “Spin in p -adic AdS/CFT”. In: (2018). arXiv: [1811.02538](https://arxiv.org/abs/1811.02538) [[hep-th](#)].
- [92] Shinsei Ryu and Tadashi Takayanagi. “Holographic derivation of entanglement entropy from AdS/CFT”. In: *Phys. Rev. Lett.* 96 (2006), p. 181602. DOI: [10.1103/PhysRevLett.96.181602](https://doi.org/10.1103/PhysRevLett.96.181602). arXiv: [hep-th/0603001](https://arxiv.org/abs/hep-th/0603001) [[hep-th](#)].
- [93] Shinsei Ryu and Tadashi Takayanagi. “Aspects of Holographic Entanglement Entropy”. In: *JHEP* 08 (2006), p. 045. DOI: [10.1088/1126-6708/2006/08/045](https://doi.org/10.1088/1126-6708/2006/08/045). arXiv: [hep-th/0605073](https://arxiv.org/abs/hep-th/0605073) [[hep-th](#)].
- [94] Thomas Faulkner, Aitor Lewkowycz, and Juan Maldacena. “Quantum corrections to holographic entanglement entropy”. In: *JHEP* 11 (2013), p. 074. DOI: [10.1007/JHEP11\(2013\)074](https://doi.org/10.1007/JHEP11(2013)074). arXiv: [1307.2892](https://arxiv.org/abs/1307.2892) [[hep-th](#)].

- [95] Veronika E. Hubeny, Mukund Rangamani, and Tadashi Takayanagi. “A Covariant holographic entanglement entropy proposal”. In: *JHEP* 07 (2007), p. 062. DOI: [10.1088/1126-6708/2007/07/062](https://doi.org/10.1088/1126-6708/2007/07/062). arXiv: [0705.0016](https://arxiv.org/abs/0705.0016) [hep-th].
- [96] Aron C. Wall. “Maximin Surfaces, and the Strong Subadditivity of the Covariant Holographic Entanglement Entropy”. In: *Class. Quant. Grav.* 31.22 (2014), p. 225007. DOI: [10.1088/0264-9381/31/22/225007](https://doi.org/10.1088/0264-9381/31/22/225007). arXiv: [1211.3494](https://arxiv.org/abs/1211.3494) [hep-th].
- [97] Matthew Headrick and Tadashi Takayanagi. “A Holographic proof of the strong subadditivity of entanglement entropy”. In: *Phys. Rev. D* 76 (2007), p. 106013. DOI: [10.1103/PhysRevD.76.106013](https://doi.org/10.1103/PhysRevD.76.106013). arXiv: [0704.3719](https://arxiv.org/abs/0704.3719) [hep-th].
- [98] Ahmed Almheiri, Xi Dong, and Daniel Harlow. “Bulk Locality and Quantum Error Correction in AdS/CFT”. In: *JHEP* 04 (2015), p. 163. DOI: [10.1007/JHEP04\(2015\)163](https://doi.org/10.1007/JHEP04(2015)163). arXiv: [1411.7041](https://arxiv.org/abs/1411.7041) [hep-th].
- [99] Fernando Pastawski, Beni Yoshida, Daniel Harlow, and John Preskill. “Holographic quantum error-correcting codes: Toy models for the bulk/boundary correspondence”. In: *JHEP* 06 (2015), p. 149. DOI: [10.1007/JHEP06\(2015\)149](https://doi.org/10.1007/JHEP06(2015)149). arXiv: [1503.06237](https://arxiv.org/abs/1503.06237) [hep-th].
- [100] D. V. Volkov and V. P. Akulov. “Is the Neutrino a Goldstone Particle?” In: *Phys. Lett.* 46B (1973), pp. 109–110. DOI: [10.1016/0370-2693\(73\)90490-5](https://doi.org/10.1016/0370-2693(73)90490-5).
- [101] Renata Kallosh. “Volkov-Akulov theory and D-branes”. In: (1997). [Lect. Notes Phys.509,49(1998)]. DOI: [10.1007/BFb0105228](https://doi.org/10.1007/BFb0105228). arXiv: [hep-th/9705118](https://arxiv.org/abs/hep-th/9705118) [hep-th].
- [102] A. A. Rosly and K. G. Selivanov. “Helicity conservation in Born-Infeld theory”. In: *Quarks. Proceedings, 12th International Seminar on High Energy Physics, Quarks'2002, Novgorod, Russia, June 1-7, 2002*. 2002. arXiv: [hep-th/0204229](https://arxiv.org/abs/hep-th/0204229) [hep-th]. URL: <http://quarks.inr.ac.ru/2002/proceedings/Field/F8.pdf>.
- [103] G. W. Gibbons and D. A. Rasheed. “Electric - magnetic duality rotations in nonlinear electrodynamics”. In: *Nucl. Phys.* B454 (1995), pp. 185–206. DOI: [10.1016/0550-3213\(95\)00409-L](https://doi.org/10.1016/0550-3213(95)00409-L). arXiv: [hep-th/9506035](https://arxiv.org/abs/hep-th/9506035) [hep-th].
- [104] Eric Bergshoeff, Frederik Coomans, Renata Kallosh, C. S. Shahbazi, and Antoine Van Proeyen. “Dirac-Born-Infeld-Volkov-Akulov and Deformation of Supersymmetry”. In: *JHEP* 08 (2013), p. 100. DOI: [10.1007/JHEP08\(2013\)100](https://doi.org/10.1007/JHEP08(2013)100). arXiv: [1303.5662](https://arxiv.org/abs/1303.5662) [hep-th].

- [105] Song He, Zhengwen Liu, and Jun-Bao Wu. “Scattering Equations, Twistor-string Formulas and Double-soft Limits in Four Dimensions”. In: *JHEP* 07 (2016), p. 060. DOI: [10.1007/JHEP07\(2016\)060](https://doi.org/10.1007/JHEP07(2016)060). arXiv: [1604.02834](https://arxiv.org/abs/1604.02834) [hep-th].
- [106] Freddy Cachazo, Peter Cha, and Sebastian Mizera. “Extensions of Theories from Soft Limits”. In: *JHEP* 06 (2016), p. 170. DOI: [10.1007/JHEP06\(2016\)170](https://doi.org/10.1007/JHEP06(2016)170). arXiv: [1604.03893](https://arxiv.org/abs/1604.03893) [hep-th].
- [107] Malcolm Perry and John H. Schwarz. “Interacting chiral gauge fields in six-dimensions and Born-Infeld theory”. In: *Nucl. Phys.* B489 (1997), pp. 47–64. DOI: [10.1016/S0550-3213\(97\)00040-0](https://doi.org/10.1016/S0550-3213(97)00040-0). arXiv: [hep-th/9611065](https://arxiv.org/abs/hep-th/9611065) [hep-th].
- [108] Mina Aganagic, Jaemo Park, Costin Popescu, and John H. Schwarz. “World volume action of the M theory five-brane”. In: *Nucl. Phys.* B496 (1997), pp. 191–214. DOI: [10.1016/S0550-3213\(97\)00227-7](https://doi.org/10.1016/S0550-3213(97)00227-7). arXiv: [hep-th/9701166](https://arxiv.org/abs/hep-th/9701166) [hep-th].
- [109] Paul S. Howe and E. Sezgin. “D = 11, p = 5”. In: *Phys. Lett.* B394 (1997), pp. 62–66. DOI: [10.1016/S0370-2693\(96\)01672-3](https://doi.org/10.1016/S0370-2693(96)01672-3). arXiv: [hep-th/9611008](https://arxiv.org/abs/hep-th/9611008) [hep-th].
- [110] Paolo Pasti, Dmitri P. Sorokin, and Mario Tonin. “Covariant action for a D = 11 five-brane with the chiral field”. In: *Phys. Lett.* B398 (1997), pp. 41–46. DOI: [10.1016/S0370-2693\(97\)00188-3](https://doi.org/10.1016/S0370-2693(97)00188-3). arXiv: [hep-th/9701037](https://arxiv.org/abs/hep-th/9701037) [hep-th].
- [111] Igor A. Bandos, Kurt Lechner, Alexei Nurmagambetov, Paolo Pasti, Dmitri P. Sorokin, and Mario Tonin. “Covariant action for the superfive-brane of M theory”. In: *Phys. Rev. Lett.* 78 (1997), pp. 4332–4334. DOI: [10.1103/PhysRevLett.78.4332](https://doi.org/10.1103/PhysRevLett.78.4332). arXiv: [hep-th/9701149](https://arxiv.org/abs/hep-th/9701149) [hep-th].
- [112] Paul S. Howe, E. Sezgin, and Peter C. West. “Covariant field equations of the M theory five-brane”. In: *Phys. Lett.* B399 (1997). [187(1997)], pp. 49–59. DOI: [10.1016/S0370-2693\(97\)00257-8](https://doi.org/10.1016/S0370-2693(97)00257-8). arXiv: [hep-th/9702008](https://arxiv.org/abs/hep-th/9702008) [hep-th].
- [113] Yu-tin Huang and Arthur E. Lipstein. “Amplitudes of 3D and 6D Maximal Superconformal Theories in Supertwistor Space”. In: *JHEP* 10 (2010), p. 007. DOI: [10.1007/JHEP10\(2010\)007](https://doi.org/10.1007/JHEP10(2010)007). arXiv: [1004.4735](https://arxiv.org/abs/1004.4735) [hep-th].
- [114] Bartłomiej Czech, Yu-tin Huang, and Moshe Rozali. “Chiral three-point interactions in 5 and 6 dimensions”. In: *JHEP* 10 (2012), p. 143. DOI: [10.1007/JHEP10\(2012\)143](https://doi.org/10.1007/JHEP10(2012)143). arXiv: [1110.2791](https://arxiv.org/abs/1110.2791) [hep-th].
- [115] Henriette Elvang, Daniel Z. Freedman, Ling-Yan Hung, Michael Kiermaier, Robert C. Myers, and Stefan Theisen. “On renormalization group flows and the a-theorem in 6d”. In: *JHEP* 10 (2012), p. 011. DOI: [10.1007/JHEP10\(2012\)011](https://doi.org/10.1007/JHEP10(2012)011). arXiv: [1205.3994](https://arxiv.org/abs/1205.3994) [hep-th].

- [116] Wei-Ming Chen, Yu-tin Huang, and Congkao Wen. “Exact coefficients for higher dimensional operators with sixteen supersymmetries”. In: *JHEP* 09 (2015), p. 098. DOI: [10.1007/JHEP09\(2015\)098](https://doi.org/10.1007/JHEP09(2015)098). arXiv: [1505.07093](https://arxiv.org/abs/1505.07093) [[hep-th](#)].
- [117] Massimo Bianchi, Andrea L. Guerrieri, Yu-tin Huang, Chao-Jung Lee, and Congkao Wen. “Exploring soft constraints on effective actions”. In: *JHEP* 10 (2016), p. 036. DOI: [10.1007/JHEP10\(2016\)036](https://doi.org/10.1007/JHEP10(2016)036). arXiv: [1605.08697](https://arxiv.org/abs/1605.08697) [[hep-th](#)].
- [118] Andrew Strominger. “Open p-branes”. In: *Phys. Lett.* B383 (1996). [,116(1995)], pp. 44–47. DOI: [10.1016/0370-2693\(96\)00712-5](https://doi.org/10.1016/0370-2693(96)00712-5). arXiv: [hep-th/9512059](https://arxiv.org/abs/hep-th/9512059) [[hep-th](#)].
- [119] Radu Roiban, Marcus Spradlin, and Anastasia Volovich. “A Googly amplitude from the B model in twistor space”. In: *JHEP* 04 (2004), p. 012. DOI: [10.1088/1126-6708/2004/04/012](https://doi.org/10.1088/1126-6708/2004/04/012). arXiv: [hep-th/0402016](https://arxiv.org/abs/hep-th/0402016) [[hep-th](#)].
- [120] Radu Roiban and Anastasia Volovich. “All conjugate-maximal-helicity-violating amplitudes from topological open string theory in twistor space”. In: *Phys. Rev. Lett.* 93 (2004), p. 131602. DOI: [10.1103/PhysRevLett.93.131602](https://doi.org/10.1103/PhysRevLett.93.131602). arXiv: [hep-th/0402121](https://arxiv.org/abs/hep-th/0402121) [[hep-th](#)].
- [121] Tristan Dennen, Yu-tin Huang, and Warren Siegel. “Supertwistor space for 6D maximal super Yang-Mills”. In: *JHEP* 04 (2010), p. 127. DOI: [10.1007/JHEP04\(2010\)127](https://doi.org/10.1007/JHEP04(2010)127). arXiv: [0910.2688](https://arxiv.org/abs/0910.2688) [[hep-th](#)].
- [122] Zvi Bern, John Joseph Carrasco, Tristan Dennen, Yu-tin Huang, and Harald Ita. “Generalized Unitarity and Six-Dimensional Helicity”. In: *Phys. Rev.* D83 (2011), p. 085022. DOI: [10.1103/PhysRevD.83.085022](https://doi.org/10.1103/PhysRevD.83.085022). arXiv: [1010.0494](https://arxiv.org/abs/1010.0494) [[hep-th](#)].
- [123] Andreas Brandhuber, Dimitrios Korres, Daniel Koschade, and Gabriele Travaglini. “One-loop Amplitudes in Six-Dimensional (1,1) Theories from Generalised Unitarity”. In: *JHEP* 02 (2011), p. 077. DOI: [10.1007/JHEP02\(2011\)077](https://doi.org/10.1007/JHEP02(2011)077). arXiv: [1010.1515](https://arxiv.org/abs/1010.1515) [[hep-th](#)].
- [124] Marcus Spradlin and Anastasia Volovich. “From Twistor String Theory To Recursion Relations”. In: *Phys. Rev.* D80 (2009), p. 085022. DOI: [10.1103/PhysRevD.80.085022](https://doi.org/10.1103/PhysRevD.80.085022). arXiv: [0909.0229](https://arxiv.org/abs/0909.0229) [[hep-th](#)].
- [125] Freddy Cachazo, Song He, and Ellis Ye Yuan. “Scattering Equations and Matrices: From Einstein To Yang-Mills, DBI and NLSM”. In: *JHEP* 07 (2015), p. 149. DOI: [10.1007/JHEP07\(2015\)149](https://doi.org/10.1007/JHEP07(2015)149). arXiv: [1412.3479](https://arxiv.org/abs/1412.3479) [[hep-th](#)].
- [126] Clifford Cheung, Karol Kampf, Jiri Novotny, Chia-Hsien Shen, and Jaroslav Trnka. “On-Shell Recursion Relations for Effective Field Theories”. In: *Phys. Rev. Lett.* 116.4 (2016), p. 041601. DOI: [10.1103/PhysRevLett.116.041601](https://doi.org/10.1103/PhysRevLett.116.041601). arXiv: [1509.03309](https://arxiv.org/abs/1509.03309) [[hep-th](#)].

- [127] Freddy Cachazo. “Resultants and Gravity Amplitudes”. In: (2013). arXiv: [1301.3970 \[hep-th\]](#).
- [128] Sergei Gukov, Lubos Motl, and Andrew Neitzke. “Equivalence of twistor prescriptions for superYang-Mills”. In: *Adv. Theor. Math. Phys.* 11.2 (2007), pp. 199–231. DOI: [10.4310/ATMP.2007.v11.n2.a1](#). arXiv: [hep-th/0404085 \[hep-th\]](#).
- [129] C. Vergu. “On the Factorisation of the Connected Prescription for Yang-Mills Amplitudes”. In: *Phys. Rev. D* 75 (2007), p. 025028. DOI: [10.1103/PhysRevD.75.025028](#). arXiv: [hep-th/0612250 \[hep-th\]](#).
- [130] Freddy Cachazo, Lionel Mason, and David Skinner. “Gravity in Twistor Space and its Grassmannian Formulation”. In: *SIGMA* 10 (2014), p. 051. DOI: [10.3842/SIGMA.2014.051](#). arXiv: [1207.4712 \[hep-th\]](#).
- [131] Andrea L. Guerrieri, Yu-tin Huang, Zhizhong Li, and Congkao Wen. “On the exactness of soft theorems”. In: *JHEP* 12 (2017), p. 052. DOI: [10.1007/JHEP12\(2017\)052](#). arXiv: [1705.10078 \[hep-th\]](#).
- [132] Clifford Cheung, Karol Kampf, Jiri Novotny, and Jaroslav Trnka. “Effective Field Theories from Soft Limits of Scattering Amplitudes”. In: *Phys. Rev. Lett.* 114.22 (2015), p. 221602. DOI: [10.1103/PhysRevLett.114.221602](#). arXiv: [1412.4095 \[hep-th\]](#).
- [133] Wei-Ming Chen, Yu-tin Huang, and Congkao Wen. “New Fermionic Soft Theorems for Supergravity Amplitudes”. In: *Phys. Rev. Lett.* 115.2 (2015), p. 021603. DOI: [10.1103/PhysRevLett.115.021603](#). arXiv: [1412.1809 \[hep-th\]](#).
- [134] Rutger Boels, Kasper J. Larsen, Niels A. Obers, and Marcel Vonk. “MHV, CSW and BCFW: Field theory structures in string theory amplitudes”. In: *JHEP* 11 (2008), p. 015. DOI: [10.1088/1126-6708/2008/11/015](#). arXiv: [0808.2598 \[hep-th\]](#).
- [135] Hui Luo and Congkao Wen. “Recursion relations from soft theorems”. In: *JHEP* 03 (2016), p. 088. DOI: [10.1007/JHEP03\(2016\)088](#). arXiv: [1512.06801 \[hep-th\]](#).
- [136] David Skinner. “Twistor Strings for N=8 Supergravity”. In: (2013). arXiv: [1301.0868 \[hep-th\]](#).
- [137] Yvonne Geyer and Lionel Mason. “The M-theory S-matrix”. In: (2019). arXiv: [1901.00134 \[hep-th\]](#).
- [138] Yu-tin Huang. “Non-Chiral S-Matrix of N=4 Super Yang-Mills”. In: (2011). arXiv: [1104.2021 \[hep-th\]](#).
- [139] J. M. Drummond. “Review of AdS/CFT Integrability, Chapter V.2: Dual Superconformal Symmetry”. In: *Lett. Math. Phys.* 99 (2012), pp. 481–505. DOI: [10.1007/s11005-011-0519-4](#). arXiv: [1012.4002 \[hep-th\]](#).

- [140] Tristan Dennen and Yu-tin Huang. “Dual Conformal Properties of Six-Dimensional Maximal Super Yang-Mills Amplitudes”. In: *JHEP* 01 (2011), p. 140. DOI: [10.1007/JHEP01\(2011\)140](https://doi.org/10.1007/JHEP01(2011)140). arXiv: [1010.5874](https://arxiv.org/abs/1010.5874) [hep-th].
- [141] Jan Plefka, Theodor Schuster, and Valentin Verschinin. “From Six to Four and More: Massless and Massive Maximal Super Yang-Mills Amplitudes in 6d and 4d and their Hidden Symmetries”. In: *JHEP* 01 (2015), p. 098. DOI: [10.1007/JHEP01\(2015\)098](https://doi.org/10.1007/JHEP01(2015)098). arXiv: [1405.7248](https://arxiv.org/abs/1405.7248) [hep-th].
- [142] Congkao Wen. *M5-brane and D-brane Scattering amplitudes*. Talk at the QCD Meets Gravity Workshop, Bhaumik Institute, UCLA, 2017.
- [143] Steven Weinberg. “Infrared photons and gravitons”. In: *Phys. Rev.* 140 (1965), B516–B524. DOI: [10.1103/PhysRev.140.B516](https://doi.org/10.1103/PhysRev.140.B516).
- [144] Nima Arkani-Hamed, Tzu-Chen Huang, and Yu-tin Huang. “Scattering Amplitudes For All Masses and Spins”. In: (2017). arXiv: [1709.04891](https://arxiv.org/abs/1709.04891) [hep-th].
- [145] Yong Zhang. “CHY formulae in 4d”. In: *JHEP* 07 (2017), p. 069. DOI: [10.1007/JHEP07\(2017\)069](https://doi.org/10.1007/JHEP07(2017)069). arXiv: [1610.05205](https://arxiv.org/abs/1610.05205) [hep-th].
- [146] I.M. Gelfand, M. Kapranov, and A. Zelevinsky. *Discriminants, Resultants, and Multidimensional Determinants*. Modern Birkhäuser Classics. Birkhäuser Boston, 2009. ISBN: 9780817647711. DOI: [10.1007/978-0-8176-4771-1](https://doi.org/10.1007/978-0-8176-4771-1).
- [147] Freddy Cachazo and Guojun Zhang. “Minimal Basis in Four Dimensions and Scalar Blocks”. In: (2016). arXiv: [1601.06305](https://arxiv.org/abs/1601.06305) [hep-th].
- [148] Freddy Cachazo and David Skinner. “Gravity from Rational Curves in Twistor Space”. In: *Phys. Rev. Lett.* 110.16 (2013), p. 161301. DOI: [10.1103/PhysRevLett.110.161301](https://doi.org/10.1103/PhysRevLett.110.161301). arXiv: [1207.0741](https://arxiv.org/abs/1207.0741) [hep-th].
- [149] Edward Witten. “New ‘gauge’ theories in six-dimensions”. In: *JHEP* 01 (1998). [Adv. Theor. Math. Phys.2,61(1998)], p. 001. DOI: [10.4310/ATMP.1998.v2.n1.a3](https://doi.org/10.4310/ATMP.1998.v2.n1.a3), [10.1088/1126-6708/1998/01/001](https://doi.org/10.1088/1126-6708/1998/01/001). arXiv: [hep-th/9710065](https://arxiv.org/abs/hep-th/9710065) [hep-th].
- [150] Nima Arkani-Hamed, Jacob L. Bourjaily, Freddy Cachazo, Alexander B. Goncharov, Alexander Postnikov, and Jaroslav Trnka. *Grassmannian Geometry of Scattering Amplitudes*. Cambridge University Press, 2016. ISBN: 9781107086586, 9781316572962. arXiv: [1212.5605](https://arxiv.org/abs/1212.5605) [hep-th]. URL: <http://inspirehep.net/record/1208741/files/arXiv:1212.5605.pdf>.

- [151] Nima Arkani-Hamed, Jacob Bourjaily, Freddy Cachazo, and Jaroslav Trnka. “Unification of Residues and Grassmannian Dualities”. In: *JHEP* 01 (2011), p. 049. DOI: [10.1007/JHEP01\(2011\)049](https://doi.org/10.1007/JHEP01(2011)049). arXiv: [0912.4912](https://arxiv.org/abs/0912.4912) [[hep-th](#)].
- [152] Edward Witten. “Parity invariance for strings in twistor space”. In: *Adv. Theor. Math. Phys.* 8.5 (2004), pp. 779–796. DOI: [10.4310/ATMP.2004.v8.n5.a1](https://doi.org/10.4310/ATMP.2004.v8.n5.a1). arXiv: [hep-th/0403199](https://arxiv.org/abs/hep-th/0403199) [[hep-th](#)].
- [153] Jacob L. Bourjaily, Jaroslav Trnka, Anastasia Volovich, and Congkao Wen. “The Grassmannian and the Twistor String: Connecting All Trees in N=4 SYM”. In: *JHEP* 01 (2011), p. 038. DOI: [10.1007/JHEP01\(2011\)038](https://doi.org/10.1007/JHEP01(2011)038). arXiv: [1006.1899](https://arxiv.org/abs/1006.1899) [[hep-th](#)].
- [154] Nima Arkani-Hamed, Freddy Cachazo, Clifford Cheung, and Jared Kaplan. “A Duality For The S Matrix”. In: *JHEP* 03 (2010), p. 020. DOI: [10.1007/JHEP03\(2010\)020](https://doi.org/10.1007/JHEP03(2010)020). arXiv: [0907.5418](https://arxiv.org/abs/0907.5418) [[hep-th](#)].
- [155] Tom Banks and Nathan Seiberg. “Symmetries and Strings in Field Theory and Gravity”. In: *Phys. Rev. D* 83 (2011), p. 084019. DOI: [10.1103/PhysRevD.83.084019](https://doi.org/10.1103/PhysRevD.83.084019). arXiv: [1011.5120](https://arxiv.org/abs/1011.5120) [[hep-th](#)].
- [156] John Joseph M. Carrasco, Carlos R. Mafra, and Oliver Schlotterer. “Semi-abelian Z-theory: NLSM+ ϕ^3 from the open string”. In: *JHEP* 08 (2017), p. 135. DOI: [10.1007/JHEP08\(2017\)135](https://doi.org/10.1007/JHEP08(2017)135). arXiv: [1612.06446](https://arxiv.org/abs/1612.06446) [[hep-th](#)].
- [157] Clifford Cheung, Chia-Hsien Shen, and Congkao Wen. “Unifying Relations for Scattering Amplitudes”. In: *JHEP* 02 (2018), p. 095. DOI: [10.1007/JHEP02\(2018\)095](https://doi.org/10.1007/JHEP02(2018)095). arXiv: [1705.03025](https://arxiv.org/abs/1705.03025) [[hep-th](#)].
- [158] Clifford Cheung, Grant N. Remmen, Chia-Hsien Shen, and Congkao Wen. “Pions as Gluons in Higher Dimensions”. In: *JHEP* 04 (2018), p. 129. DOI: [10.1007/JHEP04\(2018\)129](https://doi.org/10.1007/JHEP04(2018)129). arXiv: [1709.04932](https://arxiv.org/abs/1709.04932) [[hep-th](#)].
- [159] Clifford Cheung and Chia-Hsien Shen. “Symmetry for Flavor-Kinematics Duality from an Action”. In: *Phys. Rev. Lett.* 118.12 (2017), p. 121601. DOI: [10.1103/PhysRevLett.118.121601](https://doi.org/10.1103/PhysRevLett.118.121601). arXiv: [1612.00868](https://arxiv.org/abs/1612.00868) [[hep-th](#)].
- [160] Ian Low and Zhewei Yin. “Ward Identity and Scattering Amplitudes for Nonlinear Sigma Models”. In: *Phys. Rev. Lett.* 120.6 (2018), p. 061601. DOI: [10.1103/PhysRevLett.120.061601](https://doi.org/10.1103/PhysRevLett.120.061601). arXiv: [1709.08639](https://arxiv.org/abs/1709.08639) [[hep-th](#)].
- [161] Z. Bern, J. J. M. Carrasco, and Henrik Johansson. “New Relations for Gauge-Theory Amplitudes”. In: *Phys. Rev. D* 78 (2008), p. 085011. DOI: [10.1103/PhysRevD.78.085011](https://doi.org/10.1103/PhysRevD.78.085011). arXiv: [0805.3993](https://arxiv.org/abs/0805.3993) [[hep-ph](#)].
- [162] Yifan Wang and Xi Yin. “Supervertices and Non-renormalization Conditions in Maximal Supergravity Theories”. In: (2015). arXiv: [1505.05861](https://arxiv.org/abs/1505.05861) [[hep-th](#)].

- [163] Luis F. Alday, Johannes M. Henn, Jan Plefka, and Theodor Schuster. “Scattering into the fifth dimension of N=4 super Yang-Mills”. In: *JHEP* 01 (2010), p. 077. DOI: [10.1007/JHEP01\(2010\)077](https://doi.org/10.1007/JHEP01(2010)077). arXiv: [0908.0684](https://arxiv.org/abs/0908.0684) [[hep-th](#)].
- [164] Johannes M. Henn, Stephen G. Naculich, Howard J. Schnitzer, and Marcus Spradlin. “Higgs-regularized three-loop four-gluon amplitude in N=4 SYM: exponentiation and Regge limits”. In: *JHEP* 04 (2010), p. 038. DOI: [10.1007/JHEP04\(2010\)038](https://doi.org/10.1007/JHEP04(2010)038). arXiv: [1001.1358](https://arxiv.org/abs/1001.1358) [[hep-th](#)].
- [165] Johannes M. Henn, Stephen G. Naculich, Howard J. Schnitzer, and Marcus Spradlin. “More loops and legs in Higgs-regulated N=4 SYM amplitudes”. In: *JHEP* 08 (2010), p. 002. DOI: [10.1007/JHEP08\(2010\)002](https://doi.org/10.1007/JHEP08(2010)002). arXiv: [1004.5381](https://arxiv.org/abs/1004.5381) [[hep-th](#)].
- [166] Nathaniel Craig, Henriette Elvang, Michael Kiermaier, and Tracy Slatyer. “Massive amplitudes on the Coulomb branch of N=4 SYM”. In: *JHEP* 12 (2011), p. 097. DOI: [10.1007/JHEP12\(2011\)097](https://doi.org/10.1007/JHEP12(2011)097). arXiv: [1104.2050](https://arxiv.org/abs/1104.2050) [[hep-th](#)].
- [167] Aidan Herderschee, Seth Koren, and Timothy Trott. “Constructing $\mathcal{N} = 4$ Coulomb Branch Superamplitudes”. In: (2019). arXiv: [1902.07205](https://arxiv.org/abs/1902.07205) [[hep-th](#)].
- [168] Yvonne Geyer and Lionel Mason. “Polarized Scattering Equations for 6D Superamplitudes”. In: *Phys. Rev. Lett.* 122.10 (2019), p. 101601. DOI: [10.1103/PhysRevLett.122.101601](https://doi.org/10.1103/PhysRevLett.122.101601). arXiv: [1812.05548](https://arxiv.org/abs/1812.05548) [[hep-th](#)].
- [169] Song He and Ellis Ye Yuan. “One-loop Scattering Equations and Amplitudes from Forward Limit”. In: *Phys. Rev.* D92.10 (2015), p. 105004. DOI: [10.1103/PhysRevD.92.105004](https://doi.org/10.1103/PhysRevD.92.105004). arXiv: [1508.06027](https://arxiv.org/abs/1508.06027) [[hep-th](#)].
- [170] J. M. Drummond, J. Henn, V. A. Smirnov, and E. Sokatchev. “Magic identities for conformal four-point integrals”. In: *JHEP* 01 (2007), p. 064. DOI: [10.1088/1126-6708/2007/01/064](https://doi.org/10.1088/1126-6708/2007/01/064). arXiv: [hep-th/0607160](https://arxiv.org/abs/hep-th/0607160) [[hep-th](#)].
- [171] J. M. Drummond, J. Henn, G. P. Korchemsky, and E. Sokatchev. “Dual superconformal symmetry of scattering amplitudes in N=4 super-Yang-Mills theory”. In: *Nucl. Phys.* B828 (2010), pp. 317–374. DOI: [10.1016/j.nuclphysb.2009.11.022](https://doi.org/10.1016/j.nuclphysb.2009.11.022). arXiv: [0807.1095](https://arxiv.org/abs/0807.1095) [[hep-th](#)].
- [172] Nima Arkani-Hamed, Freddy Cachazo, and Clifford Cheung. “The Grassmannian Origin Of Dual Superconformal Invariance”. In: *JHEP* 03 (2010), p. 036. DOI: [10.1007/JHEP03\(2010\)036](https://doi.org/10.1007/JHEP03(2010)036). arXiv: [0909.0483](https://arxiv.org/abs/0909.0483) [[hep-th](#)].
- [173] Simon Caron-Huot and Donal O’Connell. “Spinor Helicity and Dual Conformal Symmetry in Ten Dimensions”. In: *JHEP* 08 (2011), p. 014. DOI: [10.1007/JHEP08\(2011\)014](https://doi.org/10.1007/JHEP08(2011)014). arXiv: [1010.5487](https://arxiv.org/abs/1010.5487) [[hep-th](#)].

- [174] Igor Bandos. “Britto-Cachazo-Feng-Witten–Type recurrent relations for tree amplitudes of $D = 11$ supergravity”. In: *Phys. Rev. Lett.* 118.3 (2017), p. 031601. DOI: [10.1103/PhysRevLett.118.031601](https://doi.org/10.1103/PhysRevLett.118.031601). arXiv: [1605.00036](https://arxiv.org/abs/1605.00036) [hep-th].
- [175] Igor Bandos. “Spinor frame formalism for amplitudes and constrained superamplitudes of 10D SYM and 11D supergravity”. In: (2017). arXiv: [1711.00914](https://arxiv.org/abs/1711.00914) [hep-th].
- [176] C. M. Hull. “Strongly coupled gravity and duality”. In: *Nucl. Phys.* B583 (2000), pp. 237–259. DOI: [10.1016/S0550-3213\(00\)00323-0](https://doi.org/10.1016/S0550-3213(00)00323-0). arXiv: [hep-th/0004195](https://arxiv.org/abs/hep-th/0004195) [hep-th].
- [177] Marc Henneaux, Victor Lekeu, and Amaury Leonard. “The action of the (free) $(4, 0)$ -theory”. In: *JHEP* 01 (2018), p. 114. DOI: [10.1007/JHEP01\(2018\)114](https://doi.org/10.1007/JHEP01(2018)114). arXiv: [1711.07448](https://arxiv.org/abs/1711.07448) [hep-th].
- [178] Marc Henneaux, Victor Lekeu, Javier Matulich, and Stefan Prohazka. “The Action of the (Free) $\mathcal{N} = (3, 1)$ Theory in Six Spacetime Dimensions”. In: (2018). arXiv: [1804.10125](https://arxiv.org/abs/1804.10125) [hep-th].
- [179] Marco Chiodaroli, Murat Gunaydin, and Radu Roiban. “Superconformal symmetry and maximal supergravity in various dimensions”. In: *JHEP* 03 (2012), p. 093. DOI: [10.1007/JHEP03\(2012\)093](https://doi.org/10.1007/JHEP03(2012)093). arXiv: [1108.3085](https://arxiv.org/abs/1108.3085) [hep-th].
- [180] L. Borsten. “ $D = 6$, $\mathcal{N} = (2, 0)$ and $\mathcal{N} = (4, 0)$ theories”. In: *Phys. Rev.* D97.6 (2018), p. 066014. DOI: [10.1103/PhysRevD.97.066014](https://doi.org/10.1103/PhysRevD.97.066014). arXiv: [1708.02573](https://arxiv.org/abs/1708.02573) [hep-th].
- [181] Wei-Ming Chen, Yu-tin Huang, and David A. McGady. “Anomalies without an action”. In: (2014). arXiv: [1402.7062](https://arxiv.org/abs/1402.7062) [hep-th].
- [182] Paul S. Aspinwall. “K3 surfaces and string duality”. In: *Differential geometry inspired by string theory*. [1(1996)]. 1996, pp. 421–540. arXiv: [hep-th/9611137](https://arxiv.org/abs/hep-th/9611137) [hep-th].
- [183] Nima Arkani-Hamed, Freddy Cachazo, and Jared Kaplan. “What is the Simplest Quantum Field Theory?” In: *JHEP* 09 (2010), p. 016. DOI: [10.1007/JHEP09\(2010\)016](https://doi.org/10.1007/JHEP09(2010)016). arXiv: [0808.1446](https://arxiv.org/abs/0808.1446) [hep-th].
- [184] Ying-Hsuan Lin, Shu-Heng Shao, Yifan Wang, and Xi Yin. “Supersymmetry Constraints and String Theory on K3”. In: *JHEP* 12 (2015), p. 142. DOI: [10.1007/JHEP12\(2015\)142](https://doi.org/10.1007/JHEP12(2015)142). arXiv: [1508.07305](https://arxiv.org/abs/1508.07305) [hep-th].
- [185] Henriette Elvang, Yu-tin Huang, and Cheng Peng. “On-shell superamplitudes in $N < 4$ SYM”. In: *JHEP* 09 (2011), p. 031. DOI: [10.1007/JHEP09\(2011\)031](https://doi.org/10.1007/JHEP09(2011)031). arXiv: [1102.4843](https://arxiv.org/abs/1102.4843) [hep-th].

- [186] Stephen L. Adler. “Consistency conditions on the strong interactions implied by a partially conserved axial vector current”. In: *Phys. Rev.* 137 (1965). [140(1964)], B1022–B1033. DOI: [10.1103/PhysRev.137.B1022](https://doi.org/10.1103/PhysRev.137.B1022).
- [187] Wei-Ming Chen, Yu-tin Huang, and Congkao Wen. “From U(1) to E8: soft theorems in supergravity amplitudes”. In: *JHEP* 03 (2015), p. 150. DOI: [10.1007/JHEP03\(2015\)150](https://doi.org/10.1007/JHEP03(2015)150). arXiv: [1412.1811](https://arxiv.org/abs/1412.1811) [[hep-th](#)].
- [188] Anastasia Volovich, Congkao Wen, and Michael Zlotnikov. “Double Soft Theorems in Gauge and String Theories”. In: *JHEP* 07 (2015), p. 095. DOI: [10.1007/JHEP07\(2015\)095](https://doi.org/10.1007/JHEP07(2015)095). arXiv: [1504.05559](https://arxiv.org/abs/1504.05559) [[hep-th](#)].
- [189] Sebastian Mizera and Guojun Zhang. “A String Deformation of the Parke-Taylor Factor”. In: *Phys. Rev. D* 96.6 (2017), p. 066016. DOI: [10.1103/PhysRevD.96.066016](https://doi.org/10.1103/PhysRevD.96.066016). arXiv: [1705.10323](https://arxiv.org/abs/1705.10323) [[hep-th](#)].
- [190] Yuri I. Manin and Matilde Marcolli. “Holography principle and arithmetic of algebraic curves”. In: *Adv. Theor. Math. Phys.* 5.3 (2001), pp. 617–650. ISSN: 1095-0761. DOI: [10.4310/ATMP.2001.v5.n3.a6](https://doi.org/10.4310/ATMP.2001.v5.n3.a6).
- [191] Yu. I. Manin. “Three-dimensional hyperbolic geometry as infinity-adic Arakelov geometry”. In: *Inventiones mathematicae* (1991), pp. 223–243. ISSN: 1432-1297. DOI: [10.1007/BF01245074](https://doi.org/10.1007/BF01245074). URL: <https://doi.org/10.1007/BF01245074>.
- [192] Ezer Melzer. “NONARCHIMEDEAN CONFORMAL FIELD THEORIES”. In: *Int. J. Mod. Phys. A* 4 (1989), p. 4877. DOI: [10.1142/S0217751X89002065](https://doi.org/10.1142/S0217751X89002065).
- [193] Yu. I. Manin. “Reflections on arithmetical physics”. In: *Conformal invariance and string theory (Poiana Brasov, 1987)*. Perspect. Phys. Academic Press, Boston, MA, 1989, pp. 293–303.
- [194] Neal Koblitz. “ p -adic numbers”. In: *p -adic Numbers, p -adic Analysis, and Zeta-Functions*. Springer, 1977, pp. 1–20.
- [195] Bill Casselman. “The Bruhat-Tits tree of $sl(2)$ ”. In: *Online lecture notes* (2014). URL: <https://pdfs.semanticscholar.org/3cc6/b53850a03003204f1225c780cf29ab625a6c.pdf>.
- [196] Rufus Bowen. “Hausdorff dimension of quasi-circles”. en. In: *Publications Mathématiques de l’IHÉS* 50 (1979), pp. 11–25. URL: http://www.numdam.org/item/PMIHES_1979__50__11_0.
- [197] P G Zograf and L A Takhtadzhyan. “On uniformization of Riemann surfaces and the Weil-Petersson metric on Teichmüller and Schottky spaces”. In: *Mathematics of the USSR-Sbornik* 60 (Oct. 2007), p. 297. DOI: [10.1070/SM1988v060n02ABEH003170](https://doi.org/10.1070/SM1988v060n02ABEH003170).

- [198] Danny Birmingham, Conall Kennedy, Siddhartha Sen, and Andy Wilkins. “Geometrical finiteness, holography, and the BTZ black hole”. In: *Phys. Rev. Lett.* 82 (1999), pp. 4164–4167. DOI: [10.1103/PhysRevLett.82.4164](https://doi.org/10.1103/PhysRevLett.82.4164). arXiv: [hep-th/9812206](https://arxiv.org/abs/hep-th/9812206) [hep-th].
- [199] Juan Martin Maldacena and Andrew Strominger. “AdS(3) black holes and a stringy exclusion principle”. In: *JHEP* 12 (1998), p. 005. DOI: [10.1088/1126-6708/1998/12/005](https://doi.org/10.1088/1126-6708/1998/12/005). arXiv: [hep-th/9804085](https://arxiv.org/abs/hep-th/9804085) [hep-th].
- [200] Yu I Manin. “Closed fibers at infinity in Arakelov’s geometry, preprint PAM-479”. In: *Center for Pure and Applied Mathematics, University of California Berkeley* (1989).
- [201] Yuri Manin and Vladimir Drinfeld. “Periods of p-adic Schottky groups”. In: *J. reine angew. Math* 262.263 (1973), pp. 239–247.
- [202] Caterina Consani and Matilde Marcolli. “Noncommutative geometry, dynamics, and infinity-adic Arakelov geometry”. In: *Selecta Mathematica* 10.2 (2004), p. 167.
- [203] Caterina Consani and Matilde Marcolli. “Spectral triples from Mumford curves”. In: *International Mathematics Research Notices* 2003.36 (2003), pp. 1945–1972.
- [204] Caterina Consani and Matilde Marcolli. “New perspectives in Arakelov geometry”. In: *Number Theory, in: CRM Proc. Lecture Notes*. Vol. 36. 2004, pp. 81–102.
- [205] Peter G.O. Freund and Mark Olson. “Non-archimedean strings”. In: *Physics Letters B* 199.2 (1987), pp. 186–190. ISSN: 0370-2693. DOI: [https://doi.org/10.1016/0370-2693\(87\)91356-6](https://doi.org/10.1016/0370-2693(87)91356-6). URL: <http://www.sciencedirect.com/science/article/pii/0370269387913566>.
- [206] B. L. Spokoiny. “Quantum Geometry of Nonarchimedean Particles and Strings”. In: *Phys. Lett.* B208 (1988), pp. 401–406. DOI: [10.1016/0370-2693\(88\)90637-5](https://doi.org/10.1016/0370-2693(88)90637-5).
- [207] Rui-bin Zhang. “Lagrangian Formulation of Open and Closed P-adic Strings”. In: *Phys. Lett.* B209 (1988), pp. 229–232. DOI: [10.1016/0370-2693\(88\)90937-9](https://doi.org/10.1016/0370-2693(88)90937-9).
- [208] Pascal Grange. “Deformation of p-adic string amplitudes in a magnetic field”. In: *Phys. Lett.* B616 (2005), pp. 135–140. DOI: [10.1016/j.physletb.2005.04.053](https://doi.org/10.1016/j.physletb.2005.04.053). arXiv: [hep-th/0409305](https://arxiv.org/abs/hep-th/0409305) [hep-th].
- [209] Paul J. Sally. “An Introduction to p-adic Fields, Harmonic Analysis and the Representation Theory of SL_2 ”. In: *Letters in Mathematical Physics* 46 (Jan. 1998), pp. 1–47. DOI: [10.1023/A:1007583108067](https://doi.org/10.1023/A:1007583108067).
- [210] G. Parisi. “ON P-ADIC FUNCTIONAL INTEGRALS”. In: *Mod. Phys. Lett.* A3 (1988), pp. 639–643. DOI: [10.1142/S0217732388000763](https://doi.org/10.1142/S0217732388000763).

- [211] Jurgen Neukirch. *Algebraic number theory*. Vol. 322. Springer Science & Business Media, 2013.
- [212] Mark Srednicki. “Entropy and area”. In: *Phys. Rev. Lett.* 71 (1993), pp. 666–669. DOI: [10.1103/PhysRevLett.71.666](https://doi.org/10.1103/PhysRevLett.71.666). arXiv: [hep-th/9303048](https://arxiv.org/abs/hep-th/9303048) [[hep-th](#)].
- [213] H. Casini and M. Huerta. “Universal terms for the entanglement entropy in 2+1 dimensions”. In: *Nucl. Phys.* B764 (2007), pp. 183–201. DOI: [10.1016/j.nuclphysb.2006.12.012](https://doi.org/10.1016/j.nuclphysb.2006.12.012). arXiv: [hep-th/0606256](https://arxiv.org/abs/hep-th/0606256) [[hep-th](#)].
- [214] Pasquale Calabrese and John L. Cardy. “Entanglement entropy and quantum field theory”. In: *J. Stat. Mech.* 0406 (2004), P06002. DOI: [10.1088/1742-5468/2004/06/P06002](https://doi.org/10.1088/1742-5468/2004/06/P06002). arXiv: [hep-th/0405152](https://arxiv.org/abs/hep-th/0405152) [[hep-th](#)].
- [215] Pasquale Calabrese and John Cardy. “Entanglement entropy and conformal field theory”. In: *J. Phys.* A42 (2009), p. 504005. DOI: [10.1088/1751-8113/42/50/504005](https://doi.org/10.1088/1751-8113/42/50/504005). arXiv: [0905.4013](https://arxiv.org/abs/0905.4013) [[cond-mat.stat-mech](#)].
- [216] Christoph Holzhey, Finn Larsen, and Frank Wilczek. “Geometric and renormalized entropy in conformal field theory”. In: *Nuclear Physics B* 424.3 (1994), pp. 443–467.
- [217] Matilde Marcolli and Jurij Ivanovic Manin. *Arithmetic noncommutative geometry*. Vol. 36. American Mathematical Soc., 2005.
- [218] Alan Carey, Matilde Marcolli, and Adam Rennie. “Modular index invariants of Mumford curves”. In: *arXiv preprint arXiv:0905.3157* (2009).
- [219] Yu I Manin. “p-Adic automorphic functions”. In: *Journal of Mathematical Sciences* 5.3 (1976), pp. 279–333.
- [220] J.-F. Boutot and H. Carayol. “Uniformisation p -adique des courbes de Shimura: les théorèmes de Cerednik et de Drinfel’d”. In: *Astérisque* 196-197 (1991). Courbes modulaires et courbes de Shimura (Orsay, 1987/1988), 7, 45–158 (1992). ISSN: 0303-1179.
- [221] Matilde Marcolli. “Holographic Codes on Bruhat–Tits buildings and Drinfeld Symmetric Spaces”. In: (2018). arXiv: [1801.09623](https://arxiv.org/abs/1801.09623) [[math-ph](#)].
- [222] Michael Tsfasman, Serge Vladuts, and Dmitry Nogin. *Algebraic geometric codes: basic notions*. Vol. 139. Mathematical Surveys and Monographs. American Mathematical Society, Providence, RI, 2007, pp. xx+338. ISBN: 978-0-8218-4306-2. DOI: [10.1090/surv/139](https://doi.org/10.1090/surv/139).
- [223] A. Robert Calderbank, Eric M. Rains, Peter W. Shor, and Neil J. A. Sloane. “Quantum error correction and orthogonal geometry”. In: *Phys. Rev. Lett.* 78.3 (1997), p. 405. DOI: [10.1103/PhysRevLett.78.405](https://doi.org/10.1103/PhysRevLett.78.405). arXiv: [quant-ph/9605005](https://arxiv.org/abs/quant-ph/9605005) [[quant-ph](#)].
- [224] Fernando Q Gouvea. *p-adic Numbers*. Springer, 1997, pp. 43–85.

- [225] G. Vidal. “Entanglement Renormalization”. In: *Phys. Rev. Lett.* 99.22 (2007), p. 220405. DOI: [10.1103/PhysRevLett.99.220405](https://doi.org/10.1103/PhysRevLett.99.220405). arXiv: [cond-mat/0512165](https://arxiv.org/abs/cond-mat/0512165) [cond-mat].
- [226] G. Evenbly and G. Vidal. “Class of Highly Entangled Many-Body States that can be Efficiently Simulated”. In: *Phys. Rev. Lett.* 112.24, 240502 (2014), p. 240502. DOI: [10.1103/PhysRevLett.112.240502](https://doi.org/10.1103/PhysRevLett.112.240502). arXiv: [1210.1895](https://arxiv.org/abs/1210.1895) [quant-ph].
- [227] G. Evenbly and G. Vidal. “Algorithms for entanglement renormalization”. In: *Phys. Rev.* B79.14 (2009), p. 144108. DOI: [10.1103/PhysRevB.79.144108](https://doi.org/10.1103/PhysRevB.79.144108). arXiv: [0707.1454](https://arxiv.org/abs/0707.1454) [cond-mat.str-el].
- [228] G. Evenbly and G. Vidal. “Entanglement Renormalization in Two Spatial Dimensions”. In: *Phys. Rev. Lett.* 102.18, 180406 (2009), p. 180406. DOI: [10.1103/PhysRevLett.102.180406](https://doi.org/10.1103/PhysRevLett.102.180406). arXiv: [0811.0879](https://arxiv.org/abs/0811.0879) [cond-mat.str-el].
- [229] G. Evenbly and G. Vidal. “Frustrated Antiferromagnets with Entanglement Renormalization: Ground State of the Spin-(1)/(2) Heisenberg Model on a Kagome Lattice”. In: *Phys. Rev. Lett.* 104.18, 187203 (2010), p. 187203. DOI: [10.1103/PhysRevLett.104.187203](https://doi.org/10.1103/PhysRevLett.104.187203). arXiv: [0904.3383](https://arxiv.org/abs/0904.3383) [cond-mat.str-el].
- [230] Brian Swingle. “Entanglement Renormalization and Holography”. In: *Phys. Rev.* D86 (2012), p. 065007. DOI: [10.1103/PhysRevD.86.065007](https://doi.org/10.1103/PhysRevD.86.065007). arXiv: [0905.1317](https://arxiv.org/abs/0905.1317) [cond-mat.str-el].
- [231] Brian Swingle. “Constructing holographic spacetimes using entanglement renormalization”. In: (2012). arXiv: [1209.3304](https://arxiv.org/abs/1209.3304) [hep-th].
- [232] Patrick Hayden, Sepehr Nezami, Xiao-Liang Qi, Nathaniel Thomas, Michael Walter, and Zhao Yang. “Holographic duality from random tensor networks”. In: *JHEP* 11 (2016), p. 009. DOI: [10.1007/JHEP11\(2016\)009](https://doi.org/10.1007/JHEP11(2016)009). arXiv: [1601.01694](https://arxiv.org/abs/1601.01694) [hep-th].
- [233] Daniel Harlow. “The Ryu–Takayanagi Formula from Quantum Error Correction”. In: *Commun. Math. Phys.* 354.3 (2017), pp. 865–912. DOI: [10.1007/s00220-017-2904-z](https://doi.org/10.1007/s00220-017-2904-z). arXiv: [1607.03901](https://arxiv.org/abs/1607.03901) [hep-th].
- [234] Daniel Harlow. “TASI Lectures on the Emergence of Bulk Physics in AdS/CFT”. In: *PoS TASI2017* (2018), p. 002. DOI: [10.22323/1.305.0002](https://doi.org/10.22323/1.305.0002). arXiv: [1802.01040](https://arxiv.org/abs/1802.01040) [hep-th].
- [235] Tobias J. Osborne and Deniz E. Stiegemann. “Dynamics for holographic codes”. In: (2017). arXiv: [1706.08823](https://arxiv.org/abs/1706.08823) [quant-ph].
- [236] A. Ashikhmin and E. Knill. “Nonbinary Quantum Stabilizer Codes”. In: *IEEE Trans. Inf. Theor.* 47.7 (2001), pp. 3065–3072. ISSN: 0018-9448. DOI: [10.1109/18.959288](https://doi.org/10.1109/18.959288). URL: <http://dx.doi.org/10.1109/18.959288>.

- [237] Markus Grassl, Thomas Beth, and Martin Rötteler. “On optimal quantum codes”. In: *International Journal of Quantum Information* 2.1 (2004), pp. 55–64. DOI: [10.1142/S0219749904000079](https://doi.org/10.1142/S0219749904000079). arXiv: [quant-ph/0312164](https://arxiv.org/abs/quant-ph/0312164).
- [238] Shamgar Gurevich and Ronny Hadani. “Quantization of symplectic vector spaces over finite fields”. In: *Journal of Symplectic Geometry* 7.4 (2009), pp. 475–502. DOI: [10.4310/JSG.2009.v7.n4.a4](https://doi.org/10.4310/JSG.2009.v7.n4.a4). arXiv: [0705.4556](https://arxiv.org/abs/0705.4556) [math.RT].
- [239] Dennis Sullivan. “The density at infinity of a discrete group of hyperbolic motions”. In: *Inst. Hautes Études Sci. Publ. Math.* 50 (1979), pp. 171–202. ISSN: 0073-8301. URL: http://www.numdam.org.clsproxy.library.caltech.edu/item?id=PMIHES_1979__50__171_0.
- [240] Gunther Cornelissen and Janne Kool. “Measure-theoretic rigidity for Mumford curves”. In: *Ergodic Theory and Dynamical Systems* 33.3 (2013), pp. 851–869. DOI: [10.1017/S0143385712000016](https://doi.org/10.1017/S0143385712000016).
- [241] Jacob D. Bekenstein. “Black holes and entropy”. In: *Phys. Rev.* D7 (1973), pp. 2333–2346. DOI: [10.1103/PhysRevD.7.2333](https://doi.org/10.1103/PhysRevD.7.2333).
- [242] S. W. Hawking. “Particle Creation by Black Holes”. In: *Commun. Math. Phys.* 43 (1975). [167(1975)], pp. 199–220. DOI: [10.1007/BF02345020](https://doi.org/10.1007/BF02345020), [10.1007/BF01608497](https://doi.org/10.1007/BF01608497).
- [243] Yu I Manin. “ p -adic automorphic functions”. In: *Journal of Soviet Mathematics* 5.3 (1976), pp. 279–333. DOI: [10.1007/BF01083779](https://doi.org/10.1007/BF01083779).
- [244] Lothar Gerritzen and Marius van der Put. *Schottky groups and Mumford curves*. Vol. 817. Lecture Notes in Mathematics. Springer, Berlin, 1980, pp. viii+317. ISBN: 3-540-10229-9.
- [245] Alexander Maloney and Edward Witten. “Quantum Gravity Partition Functions in Three Dimensions”. In: *JHEP* 02 (2010), p. 029. DOI: [10.1007/JHEP02\(2010\)029](https://doi.org/10.1007/JHEP02(2010)029). arXiv: [0712.0155](https://arxiv.org/abs/0712.0155) [hep-th].
- [246] Edward Witten. “Three-Dimensional Gravity Revisited”. In: (2007). arXiv: [0706.3359](https://arxiv.org/abs/0706.3359) [hep-th].
- [247] Steven Carlip. “The (2+1)-Dimensional black hole”. In: *Class. Quant. Grav.* 12 (1995), pp. 2853–2880. DOI: [10.1088/0264-9381/12/12/005](https://doi.org/10.1088/0264-9381/12/12/005). arXiv: [gr-qc/9506079](https://arxiv.org/abs/gr-qc/9506079) [gr-qc].
- [248] Huzihiro Araki and Elliott H. Lieb. “Entropy inequalities”. In: *Communications in Mathematical Physics* 18.2 (June 1970), pp. 160–170. ISSN: 1432-0916. DOI: [10.1007/BF01646092](https://doi.org/10.1007/BF01646092). URL: <https://doi.org/10.1007/BF01646092>.

- [249] Patrick Hayden, Matthew Headrick, and Alexander Maloney. “Holographic Mutual Information is Monogamous”. In: *Phys. Rev.* D87.4 (2013), p. 046003. DOI: [10.1103/PhysRevD.87.046003](https://doi.org/10.1103/PhysRevD.87.046003). arXiv: [1107.2940](https://arxiv.org/abs/1107.2940) [[hep-th](#)].
- [250] Elliott H. Lieb and Mary Beth Ruskai. “A Fundamental Property of Quantum-Mechanical Entropy”. In: *Phys. Rev. Lett.* 30 (1973), pp. 434–436. DOI: [10.1103/PhysRevLett.30.434](https://doi.org/10.1103/PhysRevLett.30.434).
- [251] E. H. Lieb and M. B. Ruskai. “Proof of the strong subadditivity of quantum-mechanical entropy”. In: *J. Math. Phys.* 14 (1973), pp. 1938–1941. DOI: [10.1063/1.1666274](https://doi.org/10.1063/1.1666274).
- [252] H. Casini and M. Huerta. “A Finite entanglement entropy and the c-theorem”. In: *Phys. Lett.* B600 (2004), pp. 142–150. DOI: [10.1016/j.physletb.2004.08.072](https://doi.org/10.1016/j.physletb.2004.08.072). arXiv: [hep-th/0405111](https://arxiv.org/abs/hep-th/0405111) [[hep-th](#)].
- [253] H. Casini, C. D. Fosco, and M. Huerta. “Entanglement and alpha entropies for a massive Dirac field in two dimensions”. In: *J. Stat. Mech.* 0507 (2005), P07007. DOI: [10.1088/1742-5468/2005/07/P07007](https://doi.org/10.1088/1742-5468/2005/07/P07007). arXiv: [cond-mat/0505563](https://arxiv.org/abs/cond-mat/0505563) [[cond-mat](#)].
- [254] Michel Coornaert. “Mesures de Patterson–Sullivan sur le bord d’un espace hyperbolique au sens de Gromov”. In: *Pacific J. Math.* 159.2 (1993), pp. 241–270. DOI: [10.2140/pjm.1993.159.241](https://doi.org/10.2140/pjm.1993.159.241).
- [255] Barbara M. Terhal, Michal Horodecki, Debbie W. Leung, and David P. DiVincenzo. “The entanglement of purification”. In: *Journal of Mathematical Physics* 43.9 (2002), pp. 4286–4298. DOI: [10.1063/1.1498001](https://doi.org/10.1063/1.1498001). arXiv: [quant-ph/0202044](https://arxiv.org/abs/quant-ph/0202044) [[quant-ph](#)]. URL: <https://doi.org/10.1063/1.1498001>.
- [256] Koji Umemoto and Tadashi Takayanagi. “Entanglement of purification through holographic duality”. In: *Nature Phys.* 14.6 (2018), pp. 573–577. DOI: [10.1038/s41567-018-0075-2](https://doi.org/10.1038/s41567-018-0075-2). arXiv: [1708.09393](https://arxiv.org/abs/1708.09393) [[hep-th](#)].
- [257] Phuc Nguyen, Trithip Devakul, Matthew G. Halbasch, Michael P. Zaletel, and Brian Swingle. “Entanglement of purification: from spin chains to holography”. In: *JHEP* 01 (2018), p. 098. DOI: [10.1007/JHEP01\(2018\)098](https://doi.org/10.1007/JHEP01(2018)098). arXiv: [1709.07424](https://arxiv.org/abs/1709.07424) [[hep-th](#)].
- [258] Ning Bao and Illan F. Halpern. “Holographic Inequalities and Entanglement of Purification”. In: *JHEP* 03 (2018), p. 006. DOI: [10.1007/JHEP03\(2018\)006](https://doi.org/10.1007/JHEP03(2018)006). arXiv: [1710.07643](https://arxiv.org/abs/1710.07643) [[hep-th](#)].
- [259] Ricardo Espíndola, Alberto Guijosa, and Juan F. Pedraza. “Entanglement Wedge Reconstruction and Entanglement of Purification”. In: *Eur. Phys. J.* C78.8 (2018), p. 646. DOI: [10.1140/epjc/s10052-018-6140-2](https://doi.org/10.1140/epjc/s10052-018-6140-2). arXiv: [1804.05855](https://arxiv.org/abs/1804.05855) [[hep-th](#)].

- [260] Ning Bao and Illan F. Halpern. “Conditional and Multipartite Entanglements of Purification and Holography”. In: (2018). arXiv: [1805.00476 \[hep-th\]](#).
- [261] Koji Umemoto and Yang Zhou. “Entanglement of Purification for Multipartite States and its Holographic Dual”. In: *JHEP* 10 (2018), p. 152. DOI: [10.1007/JHEP10\(2018\)152](#). arXiv: [1805.02625 \[hep-th\]](#).
- [262] Mukund Rangamani and Massimiliano Rota. “Comments on Entanglement Negativity in Holographic Field Theories”. In: *JHEP* 10 (2014), p. 060. DOI: [10.1007/JHEP10\(2014\)060](#). arXiv: [1406.6989 \[hep-th\]](#).
- [263] Pankaj Chaturvedi, Vinay Malvimat, and Gautam Sengupta. “Holographic Quantum Entanglement Negativity”. In: *JHEP* 05 (2018), p. 172. DOI: [10.1007/JHEP05\(2018\)172](#). arXiv: [1609.06609 \[hep-th\]](#).
- [264] Pankaj Chaturvedi, Vinay Malvimat, and Gautam Sengupta. “Entanglement negativity, Holography and Black holes”. In: *Eur. Phys. J. C* 78.6 (2018), p. 499. DOI: [10.1140/epjc/s10052-018-5969-8](#). arXiv: [1602.01147 \[hep-th\]](#).
- [265] Parul Jain, Vinay Malvimat, Sayid Mondal, and Gautam Sengupta. “Covariant Holographic Entanglement Negativity Conjecture for Adjacent Subsystems in AdS_3/CFT_2 ”. In: (2017). arXiv: [1710.06138 \[hep-th\]](#).
- [266] Jonah Kudler-Flam and Shinsei Ryu. “Entanglement negativity and minimal entanglement wedge cross sections in holographic theories”. In: (2018). arXiv: [1808.00446 \[hep-th\]](#).
- [267] A Kh Bikulov and AP Zubarev. “On one real basis for $L_2(Q_p)$ ”. In: *arXiv preprint arXiv:1504.03624* (2015).
- [268] Debashis Ghoshal and Teruhiko Kawano. “Towards p-Adic string in constant B-field”. In: *Nucl. Phys. B* 710 (2005), pp. 577–598. DOI: [10.1016/j.nuclphysb.2004.12.025](#). arXiv: [hep-th/0409311 \[hep-th\]](#).

APPENDICES FOR CHAPTER 2

A.1 Further Technical Details**D3 theory**

The goal here is to show that the n -particle amplitude \mathcal{A}_n in Eq. (2.53) contains the delta functions exhibited in the formula

$$\mathcal{A}_n = \left(\prod_{i=1}^n \delta(p_i^2) \delta^2(\langle \lambda_i q_i^I \rangle) \delta^2([\tilde{\lambda}_i \hat{q}_i^I]) \right) A_n, \quad (\text{A.1})$$

as well as additional momentum-conservation and supercharge-conservation delta functions, which are included in A_n . We also wish to compute the Jacobian J_B that arises from extracting the momentum-conservation and mass-shell delta functions from the bosonic delta functions,

$$\Delta_B = \prod_{i=1}^n \delta^4 \left(p_i^{\alpha\dot{\alpha}} - \frac{\rho^\alpha(\sigma_i) \tilde{\rho}^{\dot{\alpha}}(\sigma_i)}{P_i(\sigma)} \right), \quad (\text{A.2})$$

appearing in the formula for the D3 n -particle amplitude \mathcal{A}_n .

It is clear that these delta functions imply masslessness, since they constrain $p_i^{\alpha\dot{\alpha}}$ to take a factorized (rank one) form. It is less obvious that they imply momentum conservation. The delta functions imply that

$$\sum_{i=1}^n p_i^{\alpha\dot{\alpha}} = \sum_{i=1}^n \frac{1}{P_i(\sigma)} \sum_{m,m'=0}^d \rho_m^\alpha \tilde{\rho}_{m'}^{\dot{\alpha}} \sigma_i^{m+m'}. \quad (\text{A.3})$$

This will vanish provided that

$$\sum_{i=1}^n \frac{\sigma_i^m}{P_i(\sigma)} = 0 \quad \text{for } m = 0, 1, 2, \dots, n-2, \quad (\text{A.4})$$

since $2d = n - 2$. To prove that this is the case, let us introduce the Vandermonde determinant

$$V(\sigma) = \prod_{i>j} \sigma_{ij}. \quad (\text{A.5})$$

Recalling the definition $P_i(\sigma) = \prod_{j \neq i} \sigma_{ij}$, we note that

$$V_i(\sigma) = \frac{V(\sigma)}{P_i(\sigma)} = (-1)^i \prod_{j>k; j,k \neq i} \sigma_{jk}. \quad (\text{A.6})$$

Then, momentum conservation is a consequence of the following theorem:

$$W_m(\sigma) = \sum_{i=1}^n \sigma_i^m V_i(\sigma) = 0 \quad \text{for } m = 0, 1, \dots, n-2. \quad (\text{A.7})$$

This is proved by noting that W_m is a symmetric polynomial of the n σ variables whose degree does not exceed $n-2$ in any of them. Therefore, it vanishes if there are $n-1$ zeros in each of the coordinates. This is achieved if W_m vanishes when any pair of variables are equal. For example, when $\sigma_1 = \sigma_2$ only V_1 and V_2 are nonvanishing. But then $W_m(\sigma) = \sigma_1^m(V_1 + V_2)$. This vanishes because $V_1 + V_2 = 0$ when $\sigma_1 = \sigma_2$. This completes the proof of momentum conservation.

We have seen that $n+4$ of the $4n$ delta functions in Δ_B account for the mass-shell conditions and momentum conservation. The integrations over the ρ and $\tilde{\rho}$ coordinates use up $2n-1$ more of the delta functions, leaving $n-3$ to account for. The important fact is that the remaining delta functions lead to the scattering equations

$$E_i = \sum_{j \neq i} \frac{p_i \cdot p_j}{\sigma_{ij}} = 0, \quad i = 1, 2, \dots, n \quad (\text{A.8})$$

and the $n-3$ integrations over the σ coordinates imply that one should sum over the solutions of these equations. Only $n-3$ of the scattering equations are linearly independent, since the mass-shell and momentum-conservation conditions imply that

$$\sum_{i=1}^n E_i = \sum_{i=1}^n \sigma_i E_i = \sum_{i=1}^n \sigma_i^2 E_i = 0. \quad (\text{A.9})$$

Thus, there is just the right number of delta functions to account for the scattering equations. As discussed earlier, the scattering equations have $(n-3)!$ solutions, but only N_{dd} of them give nonzero contributions to the amplitudes. These are the ones that are helicity conserving, as required by the $U(1)$ R symmetry.

Let us now verify that the delta functions in Δ_B actually do imply the scattering equations. Substituting for $p_i \cdot p_j$ gives

$$E_i = \sum_{j \neq i} \sum_{mm'n'=0}^d \frac{\langle \rho_m \rho_n \rangle [\tilde{\rho}_{m'} \tilde{\rho}_{n'}] \sigma_i^{m+m'} \sigma_j^{n+n'}}{\sigma_{ij} P_i(\sigma) P_j(\sigma)} \quad (\text{A.10})$$

However, $\langle \rho_m \rho_n \rangle = -\langle \rho_n \rho_m \rangle$ and $\langle \tilde{\rho}_{m'} \tilde{\rho}_{n'} \rangle = -\langle \tilde{\rho}_{n'} \tilde{\rho}_{m'} \rangle$. Therefore we can replace $\sigma_i^m \sigma_j^n$ by

$$\frac{1}{2}(\sigma_i^m \sigma_j^n - \sigma_j^m \sigma_i^n) = \sigma_{ij} Q_{mn}(\sigma_i, \sigma_j) \quad (\text{A.11})$$

where Q_{mn} is a polynomial. It then follows that

$$E_i = \frac{1}{P_i(\sigma)} \sum_{j=1}^n \frac{\sigma_{ij} Q(\sigma_i, \sigma_j)}{P_j(\sigma)} \quad (\text{A.12})$$

where

$$Q(\sigma_i, \sigma_j) = \sum_{mmm'n'} \langle \rho_m \rho_n \rangle [\tilde{\rho}_{m'} \tilde{\rho}_{n'}] Q_{mn}(\sigma_i, \sigma_j) Q_{m'n'}(\sigma_i, \sigma_j). \quad (\text{A.13})$$

Since $\sigma_{ij} Q(\sigma_i, \sigma_j)$ is a polynomial function of σ_j of degree $n-3$, the scattering equations $E_i = 0$ follow as a consequence of Eq. (A.4).

The structure of the $4n$ delta functions in Δ_B ensures masslessness, momentum conservation, and the scattering equations, which is a total of $2n+1$ conditions. They can be expressed as delta functions and used to rewrite Δ_B as these $2n+1$ delta functions times $2n-1$ additional delta functions and a Jacobian factor, which will be described later. Given this, it is natural to examine next what can be learned from the structure of the $8n$ fermionic delta functions

$$\Delta_F(q, \rho, \chi) = \prod_{i=1}^n \delta^4 \left(q_i^{\alpha I} - \frac{\rho^\alpha(\sigma_i) \chi^I(\sigma_i)}{P_i(\sigma)} \right) \delta^4 \left(\hat{q}_i^{\dot{\alpha} \hat{I}} - \frac{\tilde{\rho}^{\dot{\alpha}}(\sigma_i) \tilde{\chi}^{\hat{I}}(\sigma_i)}{P_i(\sigma)} \right). \quad (\text{A.14})$$

First of all, the delta functions in Δ_F imply the conservation of eight supercharges:

$$\sum_{i=1}^n q_i^{\alpha I} = \sum_{i=1}^n \hat{q}_i^{\dot{\alpha} \hat{I}} = 0. \quad (\text{A.15})$$

This is proved by exactly the same reasoning that was used to establish momentum conservation earlier in this appendix. Note that these eight supercharges are mutually anticommuting, as are the other eight, but there are nonzero anticommutators between the two sets. The conservation of the second set of eight supercharges needs to be established separately.

Next we wish to account for the factors $\prod_i \delta^2(\langle \lambda_i q_i^I \rangle) \delta^2([\tilde{\lambda}_i \hat{q}_i^{\hat{I}}])$ in Eq. (A.1). The first set should derive from the first set of delta functions in Δ_F and the second set from the second factor (by identical reasoning). It is important that

the bosonic analysis has already been completed, so that masslessness, *i.e.*, the presence of the factors $\prod_i \delta(p_i^2)$, can be invoked to justify writing $p_i^{\alpha\dot{\alpha}} = \lambda_i^\alpha \tilde{\lambda}_i^{\dot{\alpha}}$. Therefore the fermionic delta functions imply that $\langle \lambda_i q_i^I \rangle = [\tilde{\lambda}_i \hat{q}_i^I] = 0$. These relations are implemented by the $4n$ fermionic delta functions exhibited in Eq. (A.1). They provide the justification for using the relations

$$q_i^{\alpha I} = \lambda_i^\alpha \eta_i^I \quad \text{and} \quad \hat{q}_i^{\dot{\alpha} I} = \tilde{\lambda}_i^{\dot{\alpha}} \hat{\eta}_i^I \quad (\text{A.16})$$

in the amplitude A_n .

Having established masslessness and momentum conservation, we can now write Δ_B as:

$$J_B \delta^4 \left(\sum_{i=1}^n p_i \right) \prod_{i=1}^n \delta(p_i^2) \prod_{i=1}^{n-2} \delta^3 \left(p_i^{\alpha\dot{\alpha}} - \frac{\rho^\alpha(\sigma_i) \tilde{\rho}^{\dot{\alpha}}(\sigma_i)}{P_i(\sigma)} \right) \delta^2 \left(p_n^{\alpha\dot{\alpha}} - \frac{\rho^\alpha(\sigma_n) \tilde{\rho}^{\dot{\alpha}}(\sigma_n)}{P_n(\sigma)} \right) \quad (\text{A.17})$$

where the three-dimensional delta functions can be chosen, for instance, to be $\{\alpha \dot{\alpha}\} = \{1\dot{1}\}, \{2\dot{1}\}, \{2\dot{2}\}$, and the two-dimensional delta function of particle n can be chosen to be $\{\alpha \dot{\alpha}\} = \{1\dot{1}\}, \{2\dot{1}\}$. For these choices, the Jacobian J_B is

$$J_B = \tilde{\lambda}_{n-1}^{\dot{1}} \tilde{\lambda}_n^{\dot{1}} \langle n-1 \ n \rangle \prod_{i=1}^{n-2} p_i^{2\dot{1}}. \quad (\text{A.18})$$

By the same kind of reasoning, the first set of fermionic delta functions in Δ_F can be recast in the form

$$J_F \delta^4 \left(\sum_{i=1}^n q_i^{\alpha I} \right) \prod_{i=1}^n \delta^2(\langle \lambda_i q_i^I \rangle) \prod_{i=1}^{n-2} \delta^2 \left(\lambda_i^1 \eta_i^I - \frac{\rho^1(\sigma_i) \chi^I(\sigma_i)}{P_i(\sigma)} \right), \quad (\text{A.19})$$

with J_F given by

$$J_F = \frac{1}{\langle n-1 \ n \rangle^2} \prod_{i=1}^{n-2} \left(\frac{1}{\lambda_i^1} \right)^2, \quad (\text{A.20})$$

and similarly for the second set of fermionic delta functions.

M5 theory

Let us now consider the 6D formula for the M5-theory amplitudes. Beginning with the bosonic delta functions, we can extract the mass-shell and momentum-conservation delta functions as follows

$$\begin{aligned} & \prod_{i=1}^n \delta^6 \left(p_i^{AB} - \frac{\rho_a^A(\sigma_i) \rho^{Ba}(\sigma_i)}{P_n(\sigma_i)} \right) = \delta^6 \left(\sum_{i=1}^n p_i \right) \prod_{i=1}^n \delta(p_i^2) \quad (\text{A.21}) \\ & \times J_B \prod_{i=1}^{n-2} \delta^5 \left(p_i^{AB} - \frac{\rho_a^A(\sigma_i) \rho^{Ba}(\sigma_i)}{P_i(\sigma)} \right) \delta^4 \left(p_n^{AB} - \frac{\rho_a^A(\sigma_n) \rho^{Ba}(\sigma_n)}{P_n(\sigma)} \right). \end{aligned}$$

If we choose the five-dimensional delta function with $\{A, B\} \neq \{3, 4\}$ and the four-dimensional one with $\{A, B\} \neq \{3, 4\}, \{1, 3\}$, J_B is given by

$$J_B = \prod_{i=1}^n p_i^{12} \left(\frac{p_{n-1}^{24}}{p_{n-1}^{12}} - \frac{p_n^{24}}{p_n^{12}} \right). \quad (\text{A.22})$$

Next, we proceed similarly for the fermionic delta functions. Extracting the fermionic “wave functions” and supercharge conservation from the fermionic delta functions gives

$$\begin{aligned} & \prod_{i=1}^n \delta^8 \left(q_i^{AI} - \frac{\rho_a^A(\sigma_i) \chi^{Ia}(\sigma_i)}{P_i(\sigma)} \right) = \delta^8 \left(\sum_{i=1}^n q_i^{AI} \right) \prod_{i=1}^n \delta^4(\hat{\lambda}_{iA\hat{a}} q_i^{AI}) \quad (\text{A.23}) \\ & \times J_F \prod_{i=1}^{n-2} \delta^2 \left(q_i^{1I} - \frac{\rho_a^1(\sigma_i) \chi^{Ia}(\sigma_i)}{P_i(\sigma)} \right) \delta^2 \left(q_i^{3I} - \frac{\rho_a^3(\sigma_i) \chi^{Ia}(\sigma_i)}{P_i(\sigma)} \right), \end{aligned}$$

with the Jacobian

$$J_F = \frac{1}{[\hat{\lambda}_{n-1\hat{a}} \hat{\lambda}_n^{\hat{a}} \hat{\lambda}_{n-1\hat{b}} \hat{\lambda}_n^{\hat{b}}]^2} \prod_{i=1}^{n-2} \left(\frac{1}{[\hat{\lambda}_i^2 \hat{\lambda}_i^4]} \right)^2, \quad (\text{A.24})$$

where $[\hat{\lambda}_i^2 \hat{\lambda}_i^4] = \varepsilon^{\hat{a}\hat{b}} \hat{\lambda}_{i\hat{a}}^2 \hat{\lambda}_{i\hat{b}}^4$.

A.2 R-Symmetry

D3 theory

Let us now verify the $SU(4)$ R symmetry of the D3 theory. (The $U(1)$ factor of the R symmetry was established in the main text.) As presented in Sect. 2.4, the formula for the amplitudes only makes an $SU(2) \times SU(2)$ subgroup manifest. However, as we saw in the case of the four-particle amplitude, the full $SU(4)$ symmetry can be made manifest by performing an appropriate Grassmann Fourier transform. For this purpose, it is useful to first recast the fermionic delta functions as follows

$$\begin{aligned} & \prod_{i=1}^n \delta^4 \left(q_i^{\alpha I} - \frac{\rho^\alpha(\sigma_i) \chi^I(\sigma_i)}{P_i(\sigma)} \right) = \\ & J_F \prod_{i=1}^n \left\{ \delta^2(\langle \lambda_i q_i^I \rangle) \delta^2 \left(\eta_i^I - \frac{\rho^1(\sigma_i) \chi^I(\sigma_i)}{\lambda_i^1 P_i(\sigma)} \right) \right\} \quad (\text{A.25}) \end{aligned}$$

and similarly for the \hat{q} and $\tilde{\lambda}$ sector. Here the explicit expression for the fermionic Jacobian J_F is not important for the following discussion.

Now let us consider the Grassmann Fourier transformation

$$I_F = \int \left(\prod_{m=0}^d d^2 \chi_m^I d^2 \hat{\chi}_m^I \right) \exp \left(\sum_{i=1}^n \hat{\eta}_i^I \zeta_{iI} \right) \\ \times \prod_{i=1}^n d^2 \hat{\eta}_i^I \delta^2(\eta_i^I - t_i \chi^I(\sigma_i)) \delta^2(\hat{\eta}_i^I - \tilde{t}_i \hat{\chi}^I(\sigma_i)), \quad (\text{A.26})$$

where we have Fourier transformed $\hat{\eta}_i^I$ and defined

$$t_i = \frac{\rho^1(\sigma_i)}{\lambda_i^1 P_i(\sigma)} \quad \text{and} \quad \tilde{t}_i = \frac{\tilde{\rho}^1(\sigma_i)}{\tilde{\lambda}_i^1 P_i(\sigma)}. \quad (\text{A.27})$$

Since the bosonic delta functions (not displayed in this Appendix) imply that

$$p_i^{1i} = \frac{\rho^1(\sigma_i) \tilde{\rho}^1(\sigma_i)}{P_i(\sigma)} = \lambda_i^1 \tilde{\lambda}_i^1, \quad (\text{A.28})$$

we have

$$t_i \tilde{t}_i = 1/P_i(\sigma). \quad (\text{A.29})$$

Integration over $d^2 \hat{\eta}_i^I$ gives

$$I_F = \int \left(\prod_{m=0}^d d^2 \chi_m^I d^2 \hat{\chi}_m^I \right) \exp \left(\sum_{i=1}^n \tilde{t}_i \hat{\chi}^I(\sigma_i) \zeta_{iI} \right) \prod_{i=1}^n \delta^2(\eta_i^I - t_i \chi^I(\sigma_i)), \quad (\text{A.30})$$

and further integration over $d^2 \hat{\chi}_m^I$ leads to

$$I_F = \prod_{m=0}^d \delta^2 \left(\sum_{i=1}^n \tilde{t}_i \zeta_{iI} \sigma_i^m \right) \int \prod_{m=0}^d d^2 \chi_m^I \prod_{i=1}^n \delta^2(\eta_i^I - t_i \chi^I(\sigma_i)). \quad (\text{A.31})$$

The final integration over $d^2 \chi_m^I$ involves n integrals of $2n$ delta functions, thereby leaving n delta functions. Using Eqs. (A.4) and (A.29), it is

$$\int \prod_{m=0}^d d^2 \chi_m^I \prod_{i=1}^n \delta^2(\eta_i^I - t_i \chi^I(\sigma_i)) = (V_n \prod_{i=1}^n \tilde{t}_i)^{-1} \prod_{m=0}^d \delta^2 \left(\sum_{i=1}^n \tilde{t}_i \eta_i^I \sigma_i^m \right), \quad (\text{A.32})$$

Renaming $\zeta_{i\hat{1}} = \eta_i^3$ and $\zeta_{i\hat{2}} = \eta_i^4$, as before, we now have a complete $SU(4)$ multiplet η_i^I with $I = 1, 2, 3, 4$, and

$$I_F \sim \prod_{m=0}^d \delta^4 \left(\sum_{i=1}^n \tilde{t}_i \eta_i^I \sigma_i^m \right), \quad (\text{A.33})$$

which is now manifestly $SU(4)$ invariant.

M5 theory

Next we wish to verify the $USp(4)$ R symmetry of the M5 theory. As in the case of 4D, it is useful to begin by decomposing the supercharge-conservation delta functions as follows

$$\begin{aligned} & \int \prod_{m=0}^d d^2 \chi_{m+}^I d^2 \chi_{m-}^I \prod_{i=1}^n \delta^8 \left(q_i^{AI} - \frac{\rho_a^A(\sigma_i) \chi^{Ia}(\sigma_i)}{P_i(\sigma)} \right) \\ &= J_F \prod_{i=1}^n \delta^4(\tilde{\lambda}_{iA\dot{a}} q_i^{AI}) \int \prod_{m=0}^d d^2 \chi_{m+}^I d^2 \chi_{m-}^I \\ & \quad \times \prod_{i=1}^n \delta^2 \left(q_i^{1I} - \frac{\rho_a^1(\sigma_i) \chi^{Ia}(\sigma_i)}{P_i(\sigma)} \right) \delta^2 \left(q_i^{3I} - \frac{\rho_a^3(\sigma_i) \chi^{Ia}(\sigma_i)}{P_i(\sigma)} \right) \end{aligned} \quad (\text{A.34})$$

where $d = \frac{n}{2} - 1$ and the Jacobian is given by

$$J_F = \prod_{i=1}^n \left(\frac{1}{\langle \tilde{\lambda}_i^2 \tilde{\lambda}_i^4 \rangle} \right)^2. \quad (\text{A.35})$$

Again the choice of singling out Lorentz indices 1, 3 is arbitrary. Ignore all the Jacobi, which are not relevant to the R symmetry, the integration over χ 's in the second line of Eq. (A.34) reduces to

$$\int \prod_{m=0}^d d^2 \chi_{m+}^I d^2 \chi_{m-}^I \prod_{i=1}^n \delta^2 \left(\eta_{i+}^I - \frac{\langle X_i^I \lambda_{i+} \rangle_{13}}{p_i^{13}} \right) \delta^2 \left(\eta_{i-}^I - \frac{\langle X_i^I \lambda_{i-} \rangle_{13}}{p_i^{13}} \right) \quad (\text{A.36})$$

where

$$\langle X_i^I \lambda_{ia} \rangle_{13} = X_i^{I3} \lambda_{ia}^1 - X_i^{I1} \lambda_{ia}^3, \quad (\text{A.37})$$

with

$$X_i^{I1} = \frac{\rho_a^1(\sigma_i) \chi^{Ia}(\sigma_i)}{P_i(\sigma)} \quad (\text{A.38})$$

and similarly for X_i^{I3} . Fourier transforming over η_{i-}^I now gives

$$\int \prod_{m=0}^d d^2 \chi_{m+}^I d^2 \chi_{m-}^I \exp \left(\sum_{i=1}^n \frac{\zeta_{iI} \langle X_i^I \lambda_{i-} \rangle_{13}}{p_i^{13}} \right) \prod_{i=1}^n \delta^2 \left(\eta_{i+}^I - \frac{\langle X_i^I \lambda_{i+} \rangle_{13}}{p_i^{13}} \right) \quad (\text{A.39})$$

The remaining $2n$ delta functions are exactly enough to integrate out the χ_+^I 's and χ_-^I 's. Explicitly, the delta functions lead to,

$$\eta_{i+}^I = \sum_{m=0}^d \kappa_{i,m,a}(\lambda_+) \chi_m^{Ia}, \quad (\text{A.40})$$

where the matrix κ is a square $n \times n$ matrix (with i running from 1 to n , and m, a together from 1 to n), and it is given by

$$\kappa_{i,m,a}(\lambda_+) = \frac{(\rho_a^1(\sigma_i)\lambda_{i+}^3 - \rho_a^3(\sigma_i)\lambda_{i+}^1)\sigma_i^m}{p_i^{13}P_i(\sigma)}. \quad (\text{A.41})$$

Solve χ_m^{Ia} in terms of η_{i+}^I using Eq. (A.40), and plug the result into the exponent (again ignoring the Jacobian, which is not relevant here), we arrive at

$$\exp\left(\sum_{i,j=1}^n \zeta_{iI} M_{ij} \eta_{j+}^I\right), \quad (\text{A.42})$$

with the matrix M_{ij} given by

$$M_{ij} = \sum_{m=0}^d \kappa_{i,m}^a(\lambda_-) \kappa_{j,m,a}^{-1}(\lambda_+). \quad (\text{A.43})$$

If the matrix M_{ij} is symmetric, then (as we showed for the case of $n = 4$ in Sect. 2.3), the expression has manifest R symmetry. We have checked explicitly that is indeed the case for $n = 6, 8$. We also note that the matrix M_{ij} has following property of converting λ_{j+}^A into λ_{j-}^A ,

$$\sum_j M_{ij} \lambda_{j+}^A = \lambda_{i-}^A. \quad (\text{A.44})$$

Multiplying λ_{i+}^B on both sides of the equation and summing over i gives

$$\sum_{i,j} \lambda_{i+}^B M_{ij} \lambda_{j+}^A = \sum_i \lambda_{i+}^B \lambda_{i-}^A. \quad (\text{A.45})$$

Due to momentum conservation, the right-hand side of this equation is symmetric in exchanging A and B , which is consistent with the fact that M_{ij} is symmetric. Curiously, the complete formula for the amplitude with manifest R symmetry is somewhat more complicated than the original one, which only makes a subgroup manifest.

APPENDICES FOR CHAPTER 3

B.1 Symmetry Algebra

This appendix examines the group of redundancies of the odd-point scattering maps that preserves their polynomial form. This consists of a five-dimensional subalgebra of the full Lie algebra. We will examine this five-dimensional algebra now, and leave the analysis of the full algebra for the future. More concretely, we first fix two generators of $\mathrm{SL}(2, \mathbb{C})_\rho$ corresponding to dilations and special conformal transformations in a suitable way, and then show that the algebra of residual symmetries corresponds to the semidirect product $\mathrm{SL}(2, \mathbb{C})_\sigma \ltimes \mathbb{C}^2$.

It is instructive to start by analyzing the even-point symmetry group $\mathrm{SL}(2, \mathbb{C})_\sigma \times \mathrm{SL}(2, \mathbb{C})_\rho$ in this setup. For $n = 2m + 2$ let us call the polynomials $\rho^{A,+}(z) = \varpi^A(z)$ and $\rho^{A,-}(z) = \vartheta^A(z)$, both of degree m . We consider transformations $(z, \sigma_i, \rho^{A,a}) \rightarrow (\hat{z}, \hat{\sigma}_i, \hat{\rho}^{A,a})$ such that

$$\frac{\hat{\varpi}^{[A}(\hat{z})\hat{\vartheta}^{B]}(\hat{z})}{\prod_{i=1}^n (\hat{z} - \hat{\sigma}_i)} d\hat{z} = \frac{\varpi^{[A}(z)\vartheta^{B]}(z)}{\prod_{i=1}^n (z - \sigma_i)} dz. \quad (\text{B.1})$$

This contains the $\mathrm{SL}(2, \mathbb{C})_\rho$ transformations, which can be defined as the stability subgroup satisfying $\hat{z} = z$. Among these, let us consider only the shift:¹

$$J = \begin{pmatrix} 0 & 1 \\ 0 & 0 \end{pmatrix} \in \mathrm{SL}(2, \mathbb{C})_\rho, \quad e^{\alpha J} : \quad \hat{\varpi}(z) = \varpi(z) + \alpha \vartheta(z), \quad \hat{\vartheta}(z) = \vartheta(z). \quad (\text{B.2})$$

The other two generators should be thought as fixed. For instance, consider the $\mathrm{SL}(2, \mathbb{C})_\sigma$ scaling $\hat{z} = e^\alpha z$. This induces the following transformation on the polynomials:

$$e^{\alpha \ell_0} : \quad \hat{\varpi}(z) = e^{p\alpha} \varpi(e^{-\alpha} z), \quad \hat{\vartheta}(z) = e^{q\alpha} \vartheta(e^{-\alpha} z), \quad (\text{B.3})$$

with $p + q = n - 1$. Since the generator of $\mathrm{SL}(2, \mathbb{C})_\rho$ scaling is fixed, so are the values of p and q , which will be determined below. Similarly, for the shift

¹In this section we will mostly suppress the $\mathrm{SU}^*(4)$ index, since it is not relevant to what follows.

$\hat{z} = z + \beta$ we find

$$e^{\beta\ell_{-1}} : \quad \hat{\varpi}(z) = \varpi(z - \beta), \quad \hat{\vartheta}(z) = \vartheta(z - \beta). \quad (\text{B.4})$$

The last generator is defined by $\ell_{+1} = \mathcal{I}\ell_{-1}\mathcal{I}$, where inversion \mathcal{I} acts in the following way. Consider the transformation $\hat{z} = -1/z$. The polynomials should then transform as

$$\mathcal{I} : \quad \hat{\varpi}(z) = z^m Y^{\frac{1}{2}} \varpi(-1/z), \quad \hat{\vartheta}(z) = z^m Y^{\frac{1}{2}} \vartheta(-1/z), \quad (\text{B.5})$$

where $Y = \prod_{i=1}^n \sigma_i$. It is straightforward to check that $\mathcal{I}^2 = (-1)^m \mathbf{1}$. The minus sign can be neglected since we are only interested in a representation of $\text{PSL}(2, \mathbb{C})_\sigma$, which corresponds to the Möbius transformations acting on the punctures, for which we have the \mathbb{Z}_2 identification $-1 \cong 1$. Let us consider the action of the following composition

$$\begin{aligned} \mathcal{I} e^{\alpha\ell_0} \mathcal{I}(\varpi(z)) &= \mathcal{I} e^{\alpha\ell_0} \left(z^m Y^{\frac{1}{2}}(\sigma_i) \varpi(-1/z) \right) \\ &= \mathcal{I} \left(e^{p\alpha} e^{-\alpha m} e^{-\frac{\alpha n}{2}} z^m Y^{\frac{1}{2}}(\sigma_i) \varpi(-e^\alpha/z) \right) \\ &\cong e^{p\alpha} e^{-\alpha m} e^{-\frac{\alpha n}{2}} \varpi(e^\alpha z), \end{aligned} \quad (\text{B.6})$$

where the symbol \cong indicates we have used the \mathbb{Z}_2 identification. Imposing $\mathcal{I}\ell_0\mathcal{I} = -\ell_0$ we find:

$$-p + m + \frac{2m + 2}{2} = p \quad \implies \quad p = q = m + \frac{1}{2}, \quad (\text{B.7})$$

which coincides with the choice of [1]. The analysis for $\vartheta(z)$ is identical. It then follows that

$$e^{\alpha J} e^{\beta\ell_0} \begin{pmatrix} \varpi(z) \\ \vartheta(z) \end{pmatrix} = e^{\beta\ell_0} e^{\alpha J} \begin{pmatrix} \varpi(z) \\ \vartheta(z) \end{pmatrix}, \quad (\text{B.8})$$

or equivalently, $[J, \ell_0] = 0$. We also have

$$\begin{aligned} \mathcal{I} e^{\alpha J} \mathcal{I}(\varpi(z)) &= \mathcal{I} \left[z^m Y^{\frac{1}{2}} (\varpi(-1/z) + \alpha\vartheta(-1/z)) \right] \\ &\cong \varpi(z) + \alpha\vartheta(z) \\ &= e^{\alpha J} \varpi(z), \end{aligned} \quad (\text{B.9})$$

which gives $\mathcal{I}J\mathcal{I} = J$ or $[\mathcal{I}, J] = 0$. This analysis is consistent with the fact that we are considering the subalgebra $\text{SL}(2, \mathbb{C})_\sigma \times J$ of the direct product $\text{SL}(2, \mathbb{C})_\sigma \times \text{SL}(2, \mathbb{C})_\rho$ and \mathcal{I} belongs to the first group.

Let us now examine how this situation changes when considering the odd-point maps with $n = 2m + 1$. Now, we fix the generators of $\mathrm{SL}(2, \mathbb{C})_\rho$ such that $\deg \varpi(z) = m$ and $\deg \vartheta(z) = m - 1$. Note that this is consistent with the fact that J is a residual symmetry. In fact, the actions of J , ℓ_0 and ℓ_{-1} are not modified, even though the values of p, q differ, as we will show below. The inversion \mathcal{I} now acts as

$$\mathcal{I} : \quad \hat{\varpi}(z) = z^m Y^{\frac{1}{2}} \varpi(-1/z), \quad \hat{\vartheta}(z) = z^{m-1} Y^{\frac{1}{2}} \vartheta(-1/z). \quad (\text{B.10})$$

Repeating the computation in (B.6) we find that

$$-p + m + \frac{2m + 1}{2} = p \quad \Longrightarrow \quad \begin{cases} p = m + \frac{1}{4}, \\ q = m - \frac{1}{4}. \end{cases} \quad (\text{B.11})$$

Furthermore, we have:

$$\begin{aligned} e^{\alpha J} e^{\beta \ell_0} \begin{pmatrix} \varpi(z) \\ \vartheta(z) \end{pmatrix} &= \begin{pmatrix} e^{(m+1/4)\beta} \varpi(e^{-\beta} z) + \alpha e^{(m-1/4)\beta} \vartheta(e^{-\beta} z) \\ e^{(m-1/4)\beta} \vartheta(e^{-\beta} z) \end{pmatrix} \\ &= \begin{pmatrix} e^{(m+1/4)\beta} (\varpi(e^{-\beta} z) + \tilde{\alpha} \vartheta(e^{-\beta} z)) \\ e^{(m-1/4)\beta} \vartheta(e^{-\beta} z) \end{pmatrix} \\ &= e^{\beta \ell_0} e^{\tilde{\alpha} J} \begin{pmatrix} \varpi(z) \\ \vartheta(z) \end{pmatrix}, \end{aligned} \quad (\text{B.12})$$

where $\tilde{\alpha} := \alpha e^{-\beta/2}$. This means that $[J, \ell_0] = -\frac{1}{2}J$.

In contrast to the case of even n , we have shown that for odd n the group structure is a semidirect extension of $\mathrm{SL}(2, \mathbb{C})_\sigma$ by an (Abelian) shift factor J . In other words, the Riemann sphere symmetry group $\mathrm{SL}(2, \mathbb{C})_\sigma$ and the group $\mathrm{SL}(2, \mathbb{C})_\rho$ are intertwined. Moreover, we will now show that the J extension of $\mathrm{SL}(2, \mathbb{C})_\sigma$ is not enough to achieve closure of the group. In fact, consider

$$\begin{aligned} \mathcal{I} e^{\alpha J} \mathcal{I}(\varpi(z)) &= \mathcal{I} \left[z^m Y^{\frac{1}{2}} \varpi(-1/z) + \alpha z^{m-1} Y^{\frac{1}{2}} \vartheta(-1/z) \right] \\ &= \mathcal{I} \left[z^m Y^{\frac{1}{2}} \varpi_{(\alpha)}(-1/z) \right] \\ &\cong \varpi_{(\alpha)}(z), \end{aligned} \quad (\text{B.13})$$

where we have defined the polynomial

$$\varpi_{(\alpha)}(z) := \varpi(z) - \alpha z \vartheta(z) = e^{\alpha T} \varpi(z). \quad (\text{B.14})$$

This shows that conjugating the shift J by an inversion leads to a new shift symmetry not present in the even- n case: $\mathcal{I}J\mathcal{I} = -T$. This precisely corresponds to the T-shift symmetry, introduced previously, acting on the fixed frame with $\xi = (1, 0)$. Conjugating the equation $[J, \ell_0] = -\frac{1}{2}J$ we find:

$$[T, \ell_0] = \frac{1}{2}T. \quad (\text{B.15})$$

Because J and T are Abelian shifts it follows that $[J, T] = 0$, i.e., they generate the translation group \mathbb{C}^2 and transform as a doublet under $\text{SL}(2, \mathbb{C})_\sigma$. The rest of the $\text{SL}(2, \mathbb{C})_\sigma \ltimes \mathbb{C}^2$ algebra is

$$[\ell_1, T] = [\ell_{-1}, J] = 0, \quad [\ell_{-1}, T] = -J, \quad [\ell_1, J] = T, \quad [\ell_i, \ell_j] = (i-j)\ell_{i+j}. \quad (\text{B.16})$$

More succinctly, if we define $(J, T) = (T_{-1/2}, T_{1/2})$, then we have $[T_r, T_s] = 0$ and

$$[\ell_i, T_r] = \left(\frac{i}{2} - r\right) T_{i+r}, \quad i = -1, 0, 1 \quad r = \pm 1/2, \quad (\text{B.17})$$

as well as

$$\mathcal{I}l_i\mathcal{I}^{-1} = -l_{-i} \quad i = -1, 0, 1 \quad \text{and} \quad \mathcal{I}T_r\mathcal{I}^{-1} = -T_{-r} \quad r = \pm 1/2. \quad (\text{B.18})$$

Finally, one can directly check that the remaining generators of $\text{SL}(2, \mathbb{C})_\rho$ do not preserve the polynomial form of the maps. Hence we claim that this is the maximal subalgebra associated to polynomial maps.

B.2 Details of the Soft-Limit Calculations

In this appendix we analyze the soft limit of the connected formula, treating the measure and the integrand separately. Because of its simplicity, we start in B.2 with the soft limit of the CHY measure and the deformation of the maps in 4D. In B.2 we turn to the even- n measure for 6D, where several new technical ingredients appear due to the $\text{SL}(2, \mathbb{C})$ little-group structure. This analysis allows us to recover the form of the odd-point maps and measure as well as the emergent symmetry T discussed in appendix A. In B.2 the odd-point integrand is derived from the even-point one for the case of $\mathcal{N} = (1, 1)$ SYM. Finally, in B.2 we obtain the even- n measure from the odd- n one, and use it to prove that the constraints have $(n - 3)!$ solutions.

Four dimensions

Let us illustrate the use of the soft limit by considering the simpler 4D case first. Here we will focus on the CHY measure in the Witten–RSV form and

show that it has the form given in (3.15). In particular, we consider the measure associated to the d th sector and show that in the soft limit, where $p_{n+1} = \tau \hat{p}_{n+1}$ with $\tau \rightarrow 0$, we have

$$\int d\mu_{n+1,d}^{4D} = \delta(p_{n+1}^2) \int d\mu_{n,d-1}^{4D} \frac{1}{2\pi i} \oint_{[\tilde{\lambda}_{n+1}, \tilde{\rho}(\sigma_{n+1})]=0} \frac{d\sigma_{n+1}}{E_{n+1}} + \text{conj.} + \mathcal{O}(\tau^0), \quad (\text{B.19})$$

where the scattering equation for the soft particle takes the form

$$E_{n+1} = \sum_{i=1}^n \frac{p_{n+1} \cdot p_i}{\sigma_{n+1,i}} = \frac{\langle \lambda_{n+1} \rho(\sigma_{n+1}) \rangle [\tilde{\lambda}_{n+1} \tilde{\rho}(\sigma_{n+1})]}{\prod_{i=1}^n \sigma_{n+1,i}} \quad (\text{B.20})$$

In (B.19) “conj.” means to consider the first term with the conjugated contour $[\tilde{\lambda}_{n+1} \tilde{\rho}(\sigma_{n+1})] \rightarrow \langle \lambda_{n+1} \rho(\sigma_{n+1}) \rangle$ as well as conjugated sector $d \rightarrow \tilde{d} = n - 2 - d$. By summing (B.19) over all sectors we obtain (3.15).

Let us now consider the soft limit of

$$\int d\mu_{n+1,d}^{4D} = \int \frac{\prod_{i=1}^{n+1} d\sigma_i \prod_{k=0}^d d^2\rho_k \prod_{k=0}^{\tilde{d}} d^2\tilde{\rho}_k}{\text{vol SL}(2, \mathbb{C}) \times \text{GL}(1, \mathbb{C})} \frac{1}{R^d(\rho) R^{\tilde{d}}(\tilde{\rho})} \prod_{i=1}^{n+1} \delta^4 \left(p_i^{\alpha\dot{\alpha}} - \frac{\rho^\alpha(\sigma_i) \tilde{\rho}^{\dot{\alpha}}(\sigma_i)}{\prod_{j \neq i}^{n+1} \sigma_{ij}} \right). \quad (\text{B.21})$$

The strategy is to first isolate the leading $1/\tau$ factor, which in this case comes from the resultants. As we will show, in the soft limit $R^d(\rho) R^{\tilde{d}}(\tilde{\rho}) \sim \tau$, which allows us to evaluate the rest of the measure for $\tau = 0$ (except for the factor $\delta(p_{n+1}^2)$). What makes the case of 4D simple is that $p_{n+1} \rightarrow 0$ has only two solutions: $\lambda_{n+1} \rightarrow 0$ or $\tilde{\lambda}_{n+1} \rightarrow 0$, which account for the two terms in (B.19). Choosing $\lambda_{n+1} \rightarrow 0$, the delta function for the last particle in (B.21) takes the form:

$$\begin{aligned} \delta^4 \left(p_{n+1}^{\alpha\dot{\alpha}} - \frac{\rho^\alpha(\sigma_{n+1}) \tilde{\rho}^{\dot{\alpha}}(\sigma_{n+1})}{\prod_{i=1}^n \sigma_{n+1,i}} \right) &\rightarrow \int dt d\tilde{t} \delta^2(\tilde{\lambda}_{n+1} - \tilde{t} \tilde{\rho}(\sigma_{n+1})) \delta^2(t \rho(\sigma_{n+1})) \delta \left(t \tilde{t} - \frac{1}{\prod_{i=1}^n \sigma_{n+1,i}} \right) \\ &= \left(\prod_{i=1}^n \sigma_{n+1,i} \right)^2 \int \tilde{t} d\tilde{t} \delta^2(\tilde{\lambda}_{n+1} - \tilde{t} \tilde{\rho}(\sigma_{n+1})) \delta^2(\rho(\sigma_{n+1})), \end{aligned} \quad (\text{B.22})$$

where we have used (3.24) and dropped the factor $\delta(p_{n+1}^2)$. If we now introduce a reference spinor $|q\rangle$, we can recast the result in the form

$$\begin{aligned} \left(\prod_{i=1}^n \sigma_{n+1,i} \right)^2 \int \tilde{t} d\tilde{t} \delta \left(\tilde{t} - \frac{[\tilde{\lambda}_{n+1} q]}{[\tilde{\rho}(\sigma_{n+1}) q]} \right) \delta \left([\tilde{\lambda}_{n+1} \tilde{\rho}(\sigma_{n+1})] \right) \delta^2(\rho(\sigma_{n+1})) \\ = \left(\prod_{i=1}^n \sigma_{n+1,i} \right) \frac{1}{t} \delta \left([\tilde{\lambda}_{n+1} \tilde{\rho}(\sigma_{n+1})] \right) \delta^2(\rho(\sigma_{n+1})), \end{aligned} \quad (\text{B.23})$$

where now

$$t = \frac{1}{\prod_{i=1}^n \sigma_{n+1,i}} \frac{[\tilde{\rho}(\sigma_{n+1}) q]}{[\tilde{\lambda}_{n+1} q]}. \quad (\text{B.24})$$

The first constraint is a polynomial equation of degree $n - d$ in σ_{n+1} , which we used for the contour in (B.19). To manipulate the second constraint let us reparametrize the polynomial as

$$\rho^\alpha(z) = \hat{\rho}^\alpha(z)(z - \sigma_{n+1}) + r^\alpha. \quad (\text{B.25})$$

Here $\hat{\rho}^\alpha(z) = \sum_{k=0}^{d-1} \hat{\rho}_k^\alpha z^k$ is a polynomial of degree $d - 1$, whose coefficients are shifted from those of $\rho^\alpha(z)$. Therefore the Jacobian is one, i.e.,

$$\prod_{k=0}^d d^2 \rho_k = d^2 r \prod_{k=0}^{d-1} d^2 \hat{\rho}_k \quad (\text{B.26})$$

Integration over r^α eliminates the second delta function in (B.23), since

$$\int d^2 r \delta^2(\rho(\sigma_{n+1})) = 1, \quad (\text{B.27})$$

setting $r = 0$, i.e., $\rho^\alpha(z) = \hat{\rho}^\alpha(z)(z - \sigma_{n+1})$. Putting everything together, (B.21) becomes

$$\begin{aligned} & \int \frac{\prod_i d\sigma_i \prod_{k=0}^{d-1} d^2 \hat{\rho}_k \prod_{k=0}^{\tilde{d}} d^2 \tilde{\rho}_k}{\text{vol SL}(2, \mathbb{C}) \times \text{GL}(1, \mathbb{C})} \prod_{i=1}^n \delta^4 \left(p_i^{\alpha\dot{\alpha}} - \frac{\hat{\rho}^\alpha(\sigma_i) \tilde{\rho}^{\dot{\alpha}}(\sigma_i)}{\prod_{j \neq i}^n \sigma_{ij}} \right) \\ & \times \frac{1}{2\pi i} \oint_{[\tilde{\lambda}_{n+1} \tilde{\rho}(\sigma_{n+1})]=0} \frac{d\sigma_{n+1}}{\left(\frac{[\tilde{\lambda}_{n+1} \tilde{\rho}(\sigma_{n+1})]}{\prod_{i=1}^n \sigma_{n+1,i}} \right)} \left(\frac{1}{t R^d(\rho) R^{\tilde{d}}(\tilde{\rho})} \right) + \mathcal{O}(\tau^0). \end{aligned} \quad (\text{B.28})$$

Note that in the bosonic delta functions the puncture σ_{n+1} has completely dropped thanks to the definition of $\hat{\rho}$. We will not prove it here, but using the definition (3.27) in terms of the matrices Φ_d and $\tilde{\Phi}_{\tilde{d}}$ one can show that in the soft limit the resultants behave as

$$t R^d(\rho) R^{\tilde{d}}(\tilde{\rho}) = \langle \lambda_{n+1} \rho(\sigma_{n+1}) \rangle R^{d-1}(\hat{\rho}) R^{\tilde{d}}(\tilde{\rho}) + \mathcal{O}(\tau^2) \quad (\text{B.29})$$

where $\lambda_{n+1} = \mathcal{O}(\tau)$ is responsible for the leading behavior, as anticipated. This concludes the proof of (B.19). The extension of this procedure to the integrand in (3.26), including the redefinition of the fermionic maps, is straightforward in 4D, but we do not present it here. After including the integrand one can deform the contour for σ_{n+1} such that it encloses two of the other punctures, i.e., at $\sigma_{n+1} = \sigma_i$. This leads to the soft limit of the $\mathcal{N} = 4$ SYM amplitude.

From even to odd multiplicity in 6D

Let us now consider the case of n odd in 6D. We show that the expression (3.102) can be obtained from the soft limit of the $n+1 = 2m+2$ measure after extracting the corresponding wave function and scattering equation. That is,

$$\int d\mu_{2m+2}^{6D} = \delta(p_{n+1}^2) \int d\mu_{2m+1}^{6D} \frac{1}{2\pi i} \oint_{|\hat{E}_{n+1}|=\varepsilon} \frac{d\sigma_{n+1}}{E_{n+1}} + \mathcal{O}(\tau^0), \quad (\text{B.30})$$

where

$$d\mu_{2m+1}^{6D} = \frac{(\prod_{i=1}^n d\sigma_i) (\prod_{k=0}^{m-1} d^8\rho_k) d^4\omega \langle \xi d\xi \rangle}{\text{vol}(\text{SL}(2, \mathbb{C})_\sigma, \text{SL}(2, \mathbb{C})_\rho, \mathbb{T})} \frac{1}{V_n^2} \Delta_B. \quad (\text{B.31})$$

The maps entering the bosonic delta functions Δ_B are defined in (3.45). As in 4D, the strategy is to first isolate the τ^{-1} piece and then manipulate the delta function for particle $n+1$ to get the corresponding scattering equation. In Section B.2 we achieve the first goal by proving that if $\hat{p}_{n+1}^{AB} = v^{[A}q^{B]}$ is the direction of the soft momentum, where $p_{n+1} = \tau \hat{p}_{n+1}$, then

$$\begin{aligned} \int d\mu_{2m+2}^{6D} &= \frac{1}{\tau} \delta(p_{n+1}^2) \int \frac{d\sigma_{n+1} (\prod_{i=1}^n d\sigma_i) (\prod_{k=0}^m d^8\rho_k)}{\text{vol}(\text{SL}(2, \mathbb{C})_\sigma \times \text{SL}(2, \mathbb{C})_\rho) V_n^2} \Delta_B^{(n)} \\ &\times \left(\prod_{i=1}^n \sigma_{n+1,i} \right) \int dx d^2\Xi \delta^8(\rho_a^A(\sigma_{n+1}) - \Xi_a(q^A + x v^A)) + \mathcal{O}(\tau^0). \end{aligned} \quad (\text{B.32})$$

Here $\Delta_B^{(n)}$ contains the bosonic delta functions for the n hard particles, but still depends on σ_{n+1} and the even-multiplicity maps. Since the leading power of τ has been extracted in this expression, the integral can be evaluated for $\tau = 0$. Note that this expression is invariant under little-group transformations of the soft particle. In fact, the $\text{SL}(2, \mathbb{C})_\rho$ transformation

$$q \rightarrow Dq + Bv \quad (\text{B.33})$$

$$v \rightarrow Cq + Av \quad (\text{B.34})$$

with $AD - BC = 1$ is equivalent to the following change of variables

$$x \rightarrow \hat{x} = \frac{Ax + B}{Cx + D}, \quad (\text{B.35})$$

$$\Xi_a \rightarrow \hat{\Xi}_a = \Xi_a(Cx + D), \quad (\text{B.36})$$

which leaves the measure invariant, i.e., $dx d^2\Xi = d\hat{x} d^2\hat{\Xi}$. The reason for introducing the variables x and Ξ will become clear in the following section. In Section B.2 we redefine the maps and isolate the scattering equation as a contour prescription for the puncture σ_{n+1} associated to the soft particle, leading to (B.30).

Derivation of (B.32)

We start with the following identity

$$\Delta_B^{(n+1)} = \Delta_B^{(n)} \delta(p_{n+1}^2) \int d^4 M |M|^3 \delta^8(\rho^{Aa}(\sigma_{n+1}) - M_b^a \lambda_n^{Ab}) \delta\left(|M| - \prod_{i=1}^n \sigma_{n+1,i}\right), \quad (\text{B.37})$$

where we have utilized the linear constraints in (3.47), and denoted $M = M_{n+1}$. Now, up to linear order in τ , the most general form of the soft momenta can be written as

$$\lambda_{n+1}^{Aa} = \beta^a v^A + \tau q^{Aa} \quad (\text{B.38})$$

which gives $p_{n+1}^{AB} = \tau v^{[A} q^{B]} + \mathcal{O}(\tau^2)$, once we set $q^A := \beta_a q^{Aa}$. Unlike 4D, where the soft condition $p_{n+1} \rightarrow 0$ has only two branches (the holomorphic and antiholomorphic soft limits,) here we have a family of solutions due to the less trivial $\text{SL}(2, \mathbb{C})$ structure. Let us now assume that as $\tau \rightarrow 0$ all the components of the maps $\rho^{Aa}(z)$ and the σ_i 's stay finite, as determined by the delta functions Δ_B , since they should be localized by the equations of the hard particles.

In the limit $\tau \rightarrow 0$, the matrix M has a singular piece:

$$M = \frac{\overline{M}}{\tau} + M_0 + \mathcal{O}(\tau^1). \quad (\text{B.39})$$

The strategy is to input this ansatz into the delta functions and evaluate the result power by power in τ leaving only four components of M to be integrated. That is, impose

$$\rho^{Ab}(\sigma_{n+1}) = \left(\frac{\overline{M}_a^b}{\tau} + M_{0,a}^b \right) (\beta^a v^A + \tau q^{Aa}) \quad (\text{B.40})$$

$$= \frac{\overline{M}_a^b \beta^a}{\tau} v^A + M_{0,a}^b \beta^a v^A + \overline{M}_a^b q^{Aa} + \mathcal{O}(\tau^1), \quad (\text{B.41})$$

$$\prod_{i=1}^n \sigma_{n+1,i} = |M| = \frac{1}{\tau^2} |\overline{M}| + \frac{\langle \overline{M}^+ M_0^- \rangle - \langle \overline{M}^- M_0^+ \rangle}{\tau} + |M_0|. \quad (\text{B.42})$$

Here \overline{M}^+ , \overline{M}^- , M_0^+ , M_0^- denote the respective columns of the matrices \overline{M} and M_0 . From the finiteness of the LHS of (B.41) and (B.42), we see that \overline{M} is degenerate and β is a null eigenvector, that is

$$\overline{M}_a^b = \Xi^b \beta_a. \quad (\text{B.43})$$

Equating terms at order τ^{-1} ,

$$0 = \langle \overline{M}^+ M_0^- \rangle - \langle \overline{M}^- M_0^+ \rangle = \langle \beta \Xi_a M_0^a \rangle \implies \Xi_a M_{0,b}^a \beta^b = 0. \quad (\text{B.44})$$

This result allows to introduce variables x and \bar{x} defined by

$$M_{0,b}^a \beta^b = x \Xi^a, \quad \Xi_a M_{0,b}^a = \bar{x} \beta_b. \quad (\text{B.45})$$

The general solution of these equations for M_0 can be expressed in the basis of spinors β and Ξ as

$$M_{0,b}^a = \frac{\bar{x} \beta^a \beta_b + x \Xi^a \Xi_b}{\langle \Xi \beta \rangle} + \gamma \Xi^a \beta_b, \quad (\text{B.46})$$

and thus

$$M_b^a = \frac{\bar{x} \beta^a \beta_b + x \Xi^a \Xi_b}{\langle \Xi \beta \rangle} + \left(\gamma + \frac{1}{\tau} \right) \Xi^a \beta_b. \quad (\text{B.47})$$

The component γ is a fixed constant, which can only be determined by considering subleading orders in τ . This is consistent since it only contributes to the result at order $O(\tau^1)$. In fact, choosing the change of variables $\{M_b^a\} \rightarrow \{x, \bar{x}, \Xi^+, \Xi^-\}$, we find

$$d^4 M = x \left(\frac{1 + \gamma \tau}{\tau} \right) dx d\bar{x} d^2 \Xi \sim \frac{x}{\tau} dx d\bar{x} d^2 \Xi. \quad (\text{B.48})$$

Having identified the singular dependence on τ , we can now select the leading pieces of the arguments inside the delta functions, yielding

$$\delta \left(|M| - \prod_{i=1}^n \sigma_{n+1,i} \right) = \delta \left(x \bar{x} - \prod_{i=1}^n \sigma_{n+1,i} \right), \quad (\text{B.49})$$

$$\delta^8 \left(\rho^{Ab}(\sigma_n) - M_a^b \lambda_n^{Aa} \right) = \delta^8 \left(\rho^{Ab}(\sigma_n) - \Xi^b (x v^A + q^A) \right). \quad (\text{B.50})$$

Integrating out \bar{x} , writing $V_{n+1}^2 = V_n^2 \prod_{i=1}^n \sigma_{i,n+1}^2$, and substituting in the identity (B.37), we finally arrive at the desired result (B.32).

Derivation of (B.30)

In this section we consider the expression (B.32) without the integration over Ξ^a , i.e., taking Ξ^a to be a fixed spinor. We will also introduce an auxiliary spinor ξ such that $\langle \Xi \xi \rangle = 1$. Note that ξ still has one free component, which we choose to be $\xi^+ = 1$. The integration over Ξ^a will be restored later.

We start by expanding the polynomial maps in basis vectors as

$$\rho^{A,a}(z) = \Xi^a \omega^A(z) + \xi^a \pi^A(z), \quad (\text{B.51})$$

the delta functions of (B.32) as

$$\delta^8(\rho^{Ab}(\sigma_{n+1}) - \Xi^b(xv^A + q^A)) = \delta^4(\pi^A(\sigma_{n+1})) \delta^4(\omega^A(\sigma_{n+1}) - xv^A - q^A), \quad (\text{B.52})$$

$$\Delta_B^{(n)} = \prod_{i=1}^n \delta^6 \left(p_i^{AB} - \frac{\omega^{[A}(\sigma_i) \pi^{B]}(\sigma_i)}{\prod_{j \neq i}^{n+1} \sigma_{ji}} \right), \quad (\text{B.53})$$

and the integration measure as

$$\prod_{k=0}^m d^8 \rho_k = \prod_{k=0}^m d^4 \omega_k d^4 \pi_k. \quad (\text{B.54})$$

As in 4D, we now parametrize $\pi^A(z) = (z - \sigma_{n+1}) \hat{\pi}^A(z) + r^A$, so that the first term vanishes at the last puncture. This change of variables gives,

$$\prod_{k=0}^m d^4 \pi_k = d^4 r \prod_{k=0}^{m-1} d^4 \hat{\pi}_k, \quad (\text{B.55})$$

$$\delta^4(\pi^A(\sigma_{n+1})) = \delta^4(r^A). \quad (\text{B.56})$$

On the support of the first delta function,

$$\Delta_B^{(n)} \Big|_{r^A=0} = \prod_{i=1}^n \delta^6 \left(p_i^{AB} - \frac{\omega^{[A}(\sigma_i) \hat{\pi}^{B]}(\sigma_i)}{\prod_{j \neq i}^n \sigma_{ij}} \right) =: \Delta_B^{(n)}(\omega, \hat{\pi}). \quad (\text{B.57})$$

Note that this result does not depend on σ_{n+1} .

The leading-order term in (B.32) can be rewritten in the form

$$\begin{aligned} & \frac{\delta(p_{n+1}^2)}{\tau} \int d^2 \Xi \int \frac{\prod_{k=0}^m d^4 \omega_k \prod_{k=0}^{m-1} d^4 \hat{\pi}_k \prod_{i=1}^n d\sigma_i}{\text{vol}(\text{SL}(2, \mathbb{C})_\sigma \times \text{SL}(2, \mathbb{C})_\rho) V_n^2} \times \Delta_B^{(n)}(\omega, \hat{\pi}) \\ & \times \int d\sigma_{n+1} dx \delta^4(\omega^A(\sigma_{n+1}) - xv^A - q^A) \left(\prod_{i=1}^n \sigma_{n+1,i} \right). \end{aligned} \quad (\text{B.58})$$

The integration over $\int d^2 \Xi$ has effectively dropped out of the integral. In principle we could use it to cancel two of the integrations over $\text{SL}(2, \mathbb{C})^2$ in the denominator. However, this would fix part of the $\text{SL}(2, \mathbb{C})^2$ invariance, which we want to be present in the odd version of the measure. Instead, let us

reintroduce the integration to get a manifestly symmetric answer. To achieve this we revert to the change of basis (B.51), i.e., for fixed $\{\Xi, \xi\}$ we define

$$\hat{\rho}^{A,a}(z) = \xi^a \omega^A(z) - \Xi^a \hat{\pi}^A(z). \quad (\text{B.59})$$

This transformation is defined coefficient by coefficient as an $\text{SL}(2, \mathbb{C})$ transformation except for the top one, which is not invertible. In fact,

$$d^4 \omega_m \prod_{k=0}^{m-1} d^4 \omega_k d^4 \hat{\pi}_k = d^4 \omega_m \prod_{k=0}^{m-1} d^8 \hat{\rho}_k \quad (\text{B.60})$$

and

$$\Delta_B^{(n)}(\omega, \hat{\pi}) = \Delta_B^{(n)}(\hat{\rho}) = \prod_{i=1}^n \delta^6 \left(p_i^{AB} - \frac{\langle \hat{\rho}^A(\sigma_i) \hat{\rho}^B(\sigma_i) \rangle}{\prod_{j \neq i}^n \sigma_{ij}} \right), \quad (\text{B.61})$$

where the highest coefficient of the map is given by

$$\hat{\rho}_m^{A,a} = \xi^a \omega_m^A = \begin{pmatrix} 1 \\ \xi \end{pmatrix} \omega_m^A, \quad (\text{B.62})$$

with $\Xi^+ \xi - \Xi^- = 1$. Noting that

$$\omega^A(\sigma_{n+1}) = \langle \Xi \hat{\rho}^A(\sigma_{n+1}) \rangle = \Xi^+ \hat{\rho}^{A,-}(\sigma_{n+1}) - \Xi^- \hat{\rho}^{A,+}(\sigma_{n+1}), \quad (\text{B.63})$$

the integral becomes

$$\frac{\delta(p_{n+1}^2)}{\tau} \int \frac{d^4 \omega_m \prod_{k=0}^{m-1} d^8 \hat{\rho}_k \prod_{i=1}^n d\sigma_i}{\text{vol}(\text{SL}(2, \mathbb{C})_\sigma \times \text{SL}(2, \mathbb{C})_\rho) V_n^2} \Delta_B^{(n)}(\hat{\rho}) \int d\sigma_{n+1} d^2 \Xi dx \delta^4(D^A) \left(\prod_{i=1}^n \sigma_{n+1,i} \right). \quad (\text{B.64})$$

where

$$D^A = \Xi^+ \hat{\rho}^{A,-}(\sigma_{n+1}) - \Xi^- \hat{\rho}^{A,+}(\sigma_{n+1}) - x v^A - q^A. \quad (\text{B.65})$$

Now we note that

$$\left(\prod_{i=1}^n \sigma_{n+1,i} \right) \int d^2 \Xi dx \delta^4(D^A) = \left(\prod_{i=1}^n \sigma_{n+1,i} \right) \delta(\langle \hat{\rho}^+(\sigma_{n+1}) \hat{\rho}^-(\sigma_{n+1}) v q \rangle) = \delta(\hat{E}_{n+1}). \quad (\text{B.66})$$

In the last line we recognize the scattering equation for the soft particle (in a form analogous to (B.20)), which we now implement as a contour integral for σ_{n+1} . This gives

$$\frac{\delta(p_{n+1}^2)}{\tau} \int \frac{d^4 \omega_m \prod_{k=0}^{m-1} d^8 \hat{\rho}_k \prod_{i=1}^n d\sigma_i}{\text{vol}(\text{SL}(2, \mathbb{C})_\sigma \times \text{SL}(2, \mathbb{C})_\rho) V_n^2} \frac{1}{2\pi i} \oint_{|\hat{E}_{n+1}|=\varepsilon} \frac{d\sigma_{n+1}}{\hat{E}_{n+1}} \Delta_B^{(n)}(\hat{\rho}). \quad (\text{B.67})$$

We have arrived at a compact expression. However, there is subtle but essential caveat. Recall that $\Delta_B^{(n)}(\hat{\rho})$ contains the variable $\xi = \frac{1+\Xi^-}{\Xi^+}$ in the top component of the polynomial, $\hat{\rho}_m$. This variable still depends on the soft puncture σ_{n+1} . In fact, it is implicitly defined through the relation

$$\langle \Xi \hat{\rho}^A(\sigma_{n+1}) \rangle = x v^A + q^A. \quad (\text{B.68})$$

In order to decouple ξ from this soft equation, we introduce a new redundancy that will enable us to turn ξ into an integration variable (which will be fixed by the hard data). Since v^A and q^A are only defined through $\hat{p}_{n+1}^{AB} = v^A q^B$, the formula must be invariant under $v \rightarrow \frac{v}{\alpha}$, $q \rightarrow \alpha q$. According to (B.68), such a transformation can be absorbed into a transformation of (Ξ^a, x, ξ) as follows:

$$x \rightarrow \frac{x}{\alpha^2}, \quad \Xi^a \rightarrow \frac{\Xi^a}{\alpha}, \quad \xi \rightarrow \xi + \frac{\alpha - 1}{\Xi^+} = \frac{\alpha + \Xi^-}{\Xi^+}. \quad (\text{B.69})$$

Since α is arbitrary, we add an additional integration in the form

$$1 = \frac{\int \frac{d\alpha}{\Xi^+}}{\text{vol}(\text{T})} = \frac{\int d\xi}{\text{vol}(\text{T})}, \quad (\text{B.70})$$

which should be regarded as a formal definition of the T-shift measure. Note that this is not $\text{SL}(2, \mathbb{C})^2$ covariant, signaling that the Jacobian is sensitive to the $\text{SL}(2, \mathbb{C})^2$ frame. Using this, we recast the formula as promised

$$\int d\mu_{2m+2}^{\text{CHY}} \rightarrow \delta(p_{n+1}^2) \int \frac{d\xi d^4\omega \prod_{k=0}^{m-1} d^8\hat{\rho}_k \prod_{i=1}^n d\sigma_i}{\text{vol}(\text{SL}(2, \mathbb{C})_\sigma, \text{SL}(2, \mathbb{C})_\rho, \text{T})} \frac{\Delta_B^{(n)}(\hat{\rho})}{V_n^2} \frac{1}{2\pi i} \oint_{|\hat{E}_{n+1}|=\varepsilon} \frac{d\sigma_{n+1}}{E_{n+1}}. \quad (\text{B.71})$$

Some comments are in order. We have used the little-group scaling of the soft particle to introduce a new redundancy in the hard equations. As the notation makes clear, this redundancy can be identified with the shift transformation explored in Section 3.4. Note that this symmetry was absent in (B.67), which can be regarded as a T-fixed version of the final measure. The reason is that while $\Delta_B^{(n)}(\hat{\rho})$ is invariant under the shift $\hat{\rho}(z) \rightarrow \hat{\rho}(z) + z\beta\xi\langle\xi, \hat{\rho}\rangle$, equation (B.68) is not, meaning that the shift parameter β can be determined in terms of v and q . By averaging over the little group, i.e., over different choices of v and q , we unfix this redundancy.

Integrand of $\mathcal{N} = (1, 1)$ SYM for odd multiplicity

Let us now apply the prescription given in the previous section, this time at the level of the $\mathcal{N} = (1, 1)$ integrand. For $n + 1 = 2m + 2$, this integrand can

be broken down as follows:

$$\begin{aligned}
\mathcal{I}_{2m+2} &= \text{PT}(\mathbb{I}_{n+1}) \text{Pf}' A_{n+1} V_{n+1} \int \prod_{k=0}^m d^2 \chi_k d^2 \tilde{\chi}_k \Delta_F^{(n+1)} \tilde{\Delta}_F^{(n+1)} \\
&= \delta^2 \left(Q_{n+1}^A \tilde{\lambda}_{n+1,A,\hat{a}} \right) \delta^2 \left(\lambda_{n+1,a}^A \tilde{Q}_{n+1,A} \right) V_n \text{PT}(\mathbb{I}_n) \text{Pf}' A_{n+1} \left(\prod_{i=1}^n \sigma_{n+1,i} \right) \frac{\sigma_{1n}}{\sigma_{1,n+1} \sigma_{n+1,n}} \\
&\times \int \prod_{k=0}^m d^2 \chi_k d^2 \tilde{\chi}_k \Delta_F^{(n)} \tilde{\Delta}_F^{(n)} \delta^2 \left(\eta_{n+1}^a - W_b^a \chi^b(\sigma_{n+1}) \right) \delta^2 \left(\tilde{\eta}_{n+1}^{\hat{a}} - \tilde{W}_{\hat{b}}^{\hat{a}} \tilde{\chi}^{\hat{b}}(\sigma_{n+1}) \right).
\end{aligned} \tag{B.72}$$

Here $W = W_{n+1} = M_{n+1}^{-1}$, as defined in Section 3.5. The fermionic delta functions are defined in (3.61), from which we have extracted the on-shell conditions of the soft particle (recall that $Q^A = \lambda_a^A \eta^a$, etc.). We will first project out the $(n+1)$ th gluon and then take the corresponding momentum to be soft. For a given polarization this will generate Weinberg's soft factor for the even point amplitude. In Section 3.4 we extract it to obtain the odd-point integrand.

A simple choice of polarization is $(a, \hat{a}) = (+, \hat{+})$, where the spinor in (B.38) and its conjugate are set to

$$\beta = \tilde{\beta} = \begin{pmatrix} 0 \\ 1 \end{pmatrix}. \tag{B.73}$$

We will proceed with this special choice, but the answer for a general polarization (a, \hat{a}) will be deduced at the end. For now, note that the soft factor (3.125) for this choice is

$$S^{+\hat{+}} = \frac{\tau^2 [\tilde{q}|p_1 \tilde{p}_n|q\rangle}{\tau^2 \hat{s}_{n+1,1} \hat{s}_{n+1,n}}, \tag{B.74}$$

where we have explicitly exhibited the powers of τ . Since they cancel, and the measure in (B.30) contributes a power of τ^{-1} , we expect the integrand to be of order τ^1 . In fact, the factor of τ comes from the expansion of the Pfaffian, i.e., $\text{Pf}' A_{n+1} = \tau \widehat{\text{Pf}} A_{n+1}$. Now, to extract the aforementioned polarization from

the amplitude we perform the following fermionic integration

$$\begin{aligned} \mathcal{I}_{2m+1}^{+\hat{+}} &:= \int d^4\eta_{n+1} d^4\tilde{\eta}_{n+1} \eta_{n+1}^1 \tilde{\eta}_{n+1}^1 \widehat{\mathcal{I}}_{2m+2} \\ &= \tau V_n \text{PT}(\mathbb{I}_n) \frac{\widehat{\text{Pf}}' A_{n+1}}{\prod_{i=1}^n \sigma_{n+1,i}} \frac{\sigma_{1n}}{\sigma_{1,n+1} \sigma_{n+1,n}} \\ &\quad \times \int \prod_{k=0}^m d^2\chi_k d^2\tilde{\chi}_k \Delta_F^{(n)} \tilde{\Delta}_F^{(n)} \delta\left(\overline{W}_a^+ \chi^a(\sigma_{n+1})\right) \delta\left(\widetilde{\overline{W}}_{\hat{a}}^{\hat{+}} \tilde{\chi}^{\hat{a}}(\sigma_{n+1})\right), \end{aligned} \quad (\text{B.75})$$

where $\widehat{\mathcal{I}}_{2m+2}$ corresponds to \mathcal{I}_{2m+2} stripped of its on-shell delta functions. We also have $W = \overline{W}/(\prod_{i=1}^n \sigma_{n+1,i})$ with

$$\overline{W}_b^a = \epsilon^{ac} \epsilon_{bd} M_c^d = \frac{\bar{x} \beta^a \beta_b + x \Xi^a \Xi_b}{\langle \Xi \beta \rangle} + \left(\gamma + \frac{1}{\tau} \right) \beta^a \Xi_b \quad (\text{B.76})$$

$$\Rightarrow \overline{W}_a^+ = \frac{x \Xi^+ \Xi_a}{\langle \Xi \beta \rangle} = x \Xi_a, \quad (\text{B.77})$$

using (B.47). Here we have implicitly followed all of the steps that were used in Section B.2 to simplify the form of the W variables in the soft limit. The antichiral piece works in the same way. Even though \widetilde{M} is not integrated, its behavior in the soft limit allows us to define the antichiral counterparts $\tilde{\Xi}$ and \tilde{x} :

$$\widetilde{\overline{W}}_{\hat{a}}^{\hat{+}} = \epsilon_{\hat{a}\hat{b}} \widetilde{M}_{\hat{b}}^{\hat{+}} = \tilde{x} \tilde{\Xi}_{\hat{a}}. \quad (\text{B.78})$$

In direct correspondence to the bosonic case of Section B.2, we have managed to make explicit the τ dependence in the integrand, and therefore we can evaluate the delta functions $\Delta_F^{(n)} \tilde{\Delta}_F^{(n)}$ for $\tau = 0$.

We follow now Section B.2, in which the basis element ξ was defined such that $\langle \xi \Xi \rangle = 1$ for a given Ξ^a . Then the polynomials are expanded as

$$\chi^a(z) = \xi^a l(z) + \Xi^a r(z) \quad (\text{B.79})$$

$$\tilde{\chi}^{\hat{a}}(z) = \tilde{\xi}^{\hat{a}} \tilde{l}(z) + \tilde{\Xi}^{\hat{a}} \tilde{r}(z), \quad (\text{B.80})$$

where $l(z)$ and $r(z)$ are degree- m polynomials with Grassmann coefficients. Dropping the powers of τ , we obtain

$$\begin{aligned} \mathcal{I}_{2m+1}^{+\hat{+}} &= V_n \text{PT}(\mathbb{I}_n) \frac{\widehat{\text{Pf}}' A}{\prod_{i=1}^n \sigma_{n+1,i}} \frac{\sigma_{1n}}{\sigma_{1,n+1} \sigma_{n+1,n}} \\ &\quad \times \int \prod_{k=0}^m dl_k dr_k d\tilde{l}_k d\tilde{r}_k \Delta_F^{(n)} \tilde{\Delta}_F^{(n)} \delta\left(l(\sigma_{n+1})\right) \delta\left(\tilde{l}(\sigma_{n+1})\right) x \tilde{x}. \end{aligned} \quad (\text{B.81})$$

All of the following expressions for the integrand should be thought as multiplied by the measure, as we continue to parallel the manipulations of Section B.2. Now we put $l(z) = (z - \sigma_{n+1})\hat{l}(z) + b$, and we note that the fermionic delta functions fix $b = 0$ in the same way as the bosonic delta functions fixed $r^A = 0$ in (B.56). Using (B.51) we have

$$\begin{aligned} \Delta_F^{(n)} &= \prod_{i=1}^n \delta^4 \left(Q_i^A - \frac{\omega^A(\sigma_i)l(\sigma_i) - \pi^A(\sigma_i)r(\sigma_i)}{\prod_{j \neq i}^{n+1} \sigma_{ij}} \right) \\ &= \prod_{i=1}^n \delta^4 \left(Q_i^A - \frac{\omega^A(\sigma_i)\hat{l}(\sigma_i) - \hat{\pi}^A(\sigma_i)r(\sigma_i)}{\prod_{j \neq i}^n \sigma_{ij}} \right) = \prod_{i=1}^n \delta^4 \left(Q_i^A - \frac{\langle \hat{\rho}^A(\sigma_i) \hat{\chi}(\sigma_i) \rangle}{\prod_{j \neq i}^n \sigma_{ij}} \right), \end{aligned} \quad (\text{B.82})$$

where we have defined

$$\hat{\chi}^a(z) = \xi^a r(z) - \Xi^a \hat{l}(z), \quad (\text{B.83})$$

and $\hat{\rho}^A(\sigma)$ is given by (B.59). The top component of this fermionic map is given by $\hat{\chi}_m^a = \xi^a r_m$. We identify $r_m = g$, hence agreeing with the fermionic maps introduced in Section 3.4. We now have

$$\mathcal{I}_{2m+1}^{+\hat{+}} = V_n \text{PT}(\mathbb{I}_n) \frac{\widehat{\text{Pf}}^A}{\prod_{i=1}^n \sigma_{n+1,i} \sigma_{1,n+1} \sigma_{n+1,n}} x \tilde{x} \int dg d\tilde{g} \prod_{k=0}^{m-1} d^2 \chi_k^a d^2 \tilde{\chi}_k^{\hat{a}} \Delta_F^{(n)} \tilde{\Delta}_F^{(n)}. \quad (\text{B.84})$$

Recall that at this stage the map component $\xi = \frac{1+\Xi^-}{\Xi^+}$ is determined implicitly by (B.68), which in turn depends on σ_{n+1} . Therefore the σ_{n+1} dependence cannot be isolated yet. The final step is to turn ξ into an extra variable, which is equivalent to unfixing the T-shift symmetry, as explained at the end of Section B.2. This is done by performing the transformation (B.69). However, as $\mathcal{I}_{2m+1}^{+\hat{+}}$ will be divided by $S^{+\hat{+}}$, given in (B.74), we also need to consider the scaling of the soft spinors $q \rightarrow q/\alpha$. Doing the corresponding scaling for the antichiral piece, $\tilde{q} \rightarrow \tilde{q}/\tilde{\alpha}$, we effectively promote ξ and $\tilde{\xi}$ into integration variables to be fixed by the bosonic equations. The relationship between the variables $\alpha, \tilde{\alpha}$ and the components $\xi, \tilde{\xi}$ can be read off from (B.69):

$$\alpha = \langle \Xi \xi \rangle, \quad \tilde{\alpha} = [\tilde{\Xi} \tilde{\xi}]. \quad (\text{B.85})$$

Including the scaling of the soft factor $S^{+\hat{+}} \rightarrow \alpha \tilde{\alpha} S^{+\hat{+}}$ and putting everything together, we find the following formula for the $\mathcal{N} = (1, 1)$ integrand:

$$\frac{1}{2\pi i} \oint_{|\hat{E}_{n+1}|=\varepsilon} \frac{d\sigma_{n+1}}{E_{n+1}} \frac{\mathcal{I}_{2m+1}^{+\hat{+}}}{S^{+\hat{+}}} = \mathcal{J}_{2m+1} \times \int d\hat{\Omega}_F^{(1,1)}. \quad (\text{B.86})$$

The Vandermonde factor V_n has been absorbed into the fermionic measure $d\widehat{\Omega}_F^{(1,1)}$, which is defined as:

$$d\widehat{\Omega}_F^{(1,1)} = V_n dg d\tilde{g} \prod_{k=0}^{m-1} d^2\chi_k d^2\tilde{\chi}_k \prod_{i=1}^n \delta^4\left(q_i^A - \frac{\langle \rho^A(\sigma_i) \chi(\sigma_i) \rangle}{\prod_{j \neq i} \sigma_{ij}}\right) \delta^4\left(\tilde{q}_{i,A} - \frac{[\tilde{\rho}_A(\sigma_i) \tilde{\chi}(\sigma_i)]}{\prod_{j \neq i} \sigma_{ij}}\right).$$

The bosonic part of the integrand \mathcal{J}_{2m+1} is given by

$$\mathcal{J}_{2m+1} = \text{PT}(\mathbb{I}_n) \frac{\sigma_{1n}}{2\pi i} \oint_{|\hat{E}_{n+1}|=\varepsilon} \frac{d\sigma_{n+1}}{E_{n+1}} \frac{1}{S^{+\dagger}} \frac{x \tilde{x}}{\langle \Xi \xi \rangle [\tilde{\Xi} \tilde{\xi}]} \frac{1}{\prod_{i=1}^n \sigma_{n+1,i}} \left(\frac{\text{Pf} \hat{A}}{\sigma_{1,n+1} \sigma_{n+1,n}} \right), \tag{B.87}$$

which encodes the complete σ_{n+1} and \hat{p}_{n+1} dependence. It is now straightforward to repeat these steps for other polarizations (a, \hat{a}) . In fact, from (B.76) we see that for the choice $a = -$, the τ^{-1} contribution will dominate, yielding no factor of x in the numerator. At the same time, the different τ dependence of this integrand will be compensated by the different τ behavior of the soft factor $S^{a\hat{a}}$. For a general polarization we have:

$$\frac{x \tilde{x}}{S^{+\dagger}} \rightarrow \frac{x^a \tilde{x}^{\hat{a}}}{S^{a\hat{a}}}, \tag{B.88}$$

where we have defined $x^a = (x, -1)$ and $\tilde{x}^{\hat{a}} = (\tilde{x}, -1)$. Setting $\sigma_{n+1} = z$ and removing the fermionic delta functions, the integrand becomes

$$\mathcal{J}_{2m+1} = \frac{1}{S^{a\hat{a}}} \text{PT}(\mathbb{I}_n) \frac{\sigma_{1n}}{2\pi i} \oint_{|\hat{E}_{n+1}|=\varepsilon} \frac{dz}{\mathcal{E}_{n+1}} \frac{\text{Pf} A_{n+1}}{(z - \sigma_1)(z - \sigma_n)} \frac{x^a}{\langle \xi \Xi \rangle} \frac{\tilde{x}^{\hat{a}}}{[\tilde{\xi} \tilde{\Xi}]}, \tag{B.89}$$

where $\mathcal{E}_{n+1} = \tau \hat{\mathcal{E}}_{n+1} = p(z) \cdot p_{n+1}$ is the scattering equation for the $(n + 1)$ th particle, valid on the support of the equations associated to hard particles. In this form the τ dependence cancels between the soft factor and the scattering equation. This form is taken as the starting point in Section 3.4.

From odd to even multiplicity and the number of solutions

Here we consider taking a soft limit of the odd-point measure. The goal is to prove that the relation

$$\int d\mu_{n+1}^{6D} = \delta(p_{n+1}^2) \int d\mu_n^{6D} \frac{1}{2\pi i} \oint_{|\hat{E}_{n+1}|=\varepsilon} \frac{d\sigma_{n+1}}{E_{n+1}} + \mathcal{O}(\tau^0), \tag{B.90}$$

holds for any n , whether it is even or odd. (The corresponding measures were defined in Sections 3.2 and 3.4). This result can be used to prove that the equations for the maps and the punctures of n particles have $(n - 3)!$ solutions,²

²This assumes generic kinematics in the sense of the discussion we give in Section 3.7.

as claimed in Section 3.2. Since we have already shown that integrating out the coefficients of the maps $\rho_k^{A,a}$ leaves delta functions localizing the σ_i 's, this implies that this measure should correspond to the CHY measure (3.13) up to a trivial Jacobian. Such a Jacobian must not carry a nontrivial $\text{SL}(2, \mathbb{C})$ weight or mass dimension. This has been checked numerically.

The reasoning used to find the number of solutions follows closely the inductive proof in [56]. For $n = 3$ one can analytically check that there is one solution for the moduli $\{\rho, \sigma\}$. We then assume that the lower-point measure $d\mu_n$ in (B.90) has support on exactly $(n - 3)!$ solutions. Then, we use the fact that in the soft limit $d\mu_{n+1}$ decouples into the lower-point measure and $\delta(E_{n+1})$. In the previous section we recognized E_{n+1} as the soft limit of the scattering equation for σ_{n+1} , which has been shown to yield $n - 2$ solutions for given hard data [56]. This can also be seen directly from (B.66). Since the number of solutions cannot change in the soft limit, we conclude that $d\mu_{n+1}$ has support on $(n - 2)!$ solutions, which completes the argument.

In order to show the validity of (B.90) for odd n we begin with the same identity used in the previous section for n odd:

$$\begin{aligned} \Delta_B^{(n+1)} &= \Delta_B^{(n)} \delta(p_{n+1}^2) \int d^4 M_{n+1} |M_{n+1}|^3 \\ &\quad \times \delta^8 \left(\rho^{A,a}(\sigma_{n+1}) - (M_{n+1})_b^a \lambda_{n+1}^{A,b} \right) \delta \left(|M_{n+1}| - \prod_{i=1}^n \sigma_{n+1 i} \right), \end{aligned} \quad (\text{B.91})$$

where we have used the odd-point parametrization of the rational maps,

$$\rho^{A,a}(z) = \sum_{k=0}^{m-1} \rho_k^{A,a} z^k + \omega'^A \xi'^a z^m, \quad (\text{B.92})$$

and $m = (n - 1)/2$. To avoid confusion we have labeled the highest-degree coefficient using primed variables. As before, we parametrize the $(n + 1)$ th soft particle for $\tau \rightarrow 0$ using a 6D spinor of the form $\lambda_{n+1}^{A,a} = \xi^a v^A + \tau q^{A,a}$, which gives $p_{n+1}^{AB} \sim O(\tau)$. We also define $q^{A,a} \xi_a = q^A$. For the odd-point parametrization of the maps, the symmetry group G includes the T-shift redundancy parametrized by the $\text{GL}(1, \mathbb{C})$ parameter α . $\rho(z)$ and M_i both transform under the T shift, as shown in (3.209) for $W_i = M_i^{-1}$.

Much of the soft-limit analysis for n odd is similar to the case of n even; the coefficients of the rational maps are fixed by the data of the hard particles

while M_{n+1} is allowed to have a singular piece in the soft limit. We may repeat the steps of Section B.2, inserting an ansatz for M_{n+1} and decomposing it in a basis of spinors Ξ^a and a modulus x . The dependence of the measure on the $(n+1)$ th particle can be written in the soft limit as

$$\frac{1}{\tau} \delta(p_{n+1}^2) \int \frac{\prod_{k=0}^{m-1} d^8 \rho_k d^4 \omega' \langle \xi' d\xi' \rangle d\sigma_{n+1} \prod_{i=1}^n \sigma_{n+1,i}}{\text{vol}(\text{SL}(2, \mathbb{C})_\sigma, \text{SL}(2, \mathbb{C})_\rho, \mathbb{T}) V_n^2} \Delta_B^{(n)} \\ \times \int dx d^2 \Xi \delta^8 (\rho^{A,a}(\sigma_{n+1}) - \Xi^a (q^A + xv^A)). \quad (\text{B.93})$$

After decomposing M_{n+1} in the soft limit as done here, the transformation rule for M_{n+1} becomes one for Ξ^a :

$$\delta \Xi^a = \alpha \sigma_{n+1} \xi'^a \langle \xi' \Xi \rangle. \quad (\text{B.94})$$

Having isolated the singular τ dependence in the soft limit, let us now examine the behavior of the even-point rational maps arising from the soft limit of odd-point amplitudes. At each point in the $d^2 \Xi$ integration, we expand the odd-point map in a special basis, the one determined by the two preferred spinors Ξ^a and ξ'^a . This basis is not orthonormal, and $\langle \Xi \xi' \rangle \neq 1$. Changing variables to (π^A, ω^A) spinor coordinates, the odd-point map ω'^A becomes the last component of the latter:

$$\rho^{A,a}(z) = \Xi^a \pi^A(z) + \xi'^a \omega^A(z), \quad (\text{B.95})$$

or more explicitly

$$\rho^{A,a}(z) = \Xi^a \sum_{k=0}^{m-1} \pi_k^A z^k + \xi'^a \left(\sum_{k=0}^{m-1} \omega_k^A z^k + \omega'^A z^m \right). \quad (\text{B.96})$$

By taking linear combinations of the eight-dimensional constraint equations for $\rho^{A,a}$, we arrive at a split form involving the basis:

$$\delta^8 (\rho^{A,a}(\sigma_{n+1}) - \Xi^a (q^A + xv^A)) = \frac{1}{\langle \Xi \xi' \rangle^4} \delta^4 (\omega^A(\sigma_{n+1})) \delta^4 (\pi^A(\sigma_{n+1}) - (q^A + xv^A)). \quad (\text{B.97})$$

Additionally, the remaining bosonic delta functions also change under this basis transformation:

$$\Delta_B^{(n)} = \prod_{i=1}^n \delta^6 \left(p_i^{AB} - \langle \Xi \xi' \rangle \frac{\pi^{[A}(\sigma_i) \omega^{B]}(\sigma_i)}{\prod_{j=1}^n \sigma_{n+1,j}} \right), \quad (\text{B.98})$$

along with the integration measure, which acquires a Jacobian

$$\left(\prod_{k=0}^{m-1} d^8 \rho_k \right) d^4 \omega' \rightarrow \langle \Xi \xi' \rangle^{4m} \left(\prod_{k=0}^{m-1} d^4 \pi_k d^4 \omega_k \right) d^4 \omega'. \quad (\text{B.99})$$

As in the case of taking a soft limit from even n to odd n , we may now use the delta functions to reduce the degree of the map. To see this, we parametrize the map evaluated at the $(n+1)$ th puncture as:

$$\omega^A(z) = (z - \sigma_{n+1}) \hat{\omega}^A(z) + r^A, \quad (\text{B.100})$$

$$\prod_{k=0}^{m-1} d^4 \omega_k d^4 \omega' \delta^4(\omega^A(\sigma_{n+1})) \rightarrow d^4 r^A \prod_{k=0}^{m-1} d^4 \hat{\omega}_k \delta^4(r^A). \quad (\text{B.101})$$

The r^A integrations are trivial, and now the ω' component has dropped out of the problem in favor of the $\hat{\omega}$ variables. This means we may now use the hatted variables in the remaining bosonic delta functions.

Having reduced the degree of the map, we may now switch back to the ρ variables through another change of basis:

$$\hat{\rho}^{A,a}(z) = \Xi^a \pi^A(z) + \xi'^a \hat{\omega}^A(z), \quad (\text{B.102})$$

$$\hat{\rho}^{A,a}(z) \Xi_a = \langle \Xi \xi' \rangle \hat{\omega}^A(z), \quad (\text{B.103})$$

$$\hat{\rho}^{A,a}(z) \xi'_a = \langle \xi' \Xi \rangle \pi^A(z). \quad (\text{B.104})$$

This has the effect of undoing several of the Jacobians acquired earlier, and the relevant piece of the measure and integrand becomes

$$\begin{aligned} & \frac{\prod_{i=1}^n \sigma_{n+1i}}{V_n^2} \int d\sigma_{n+1} \frac{\prod_{k=0}^{m-1} d^8 \hat{\rho}_k \langle \xi' d\xi' \rangle d^2 \Xi dx}{\text{vol}(\text{SL}(2, \mathbb{C})_\sigma, \text{SL}(2, \mathbb{C})_\rho, \mathbb{T})} \prod_{i=1}^n \delta^6 \left(p_i^{AB} - \frac{\langle \hat{\rho}^A(\sigma_i) \hat{\rho}^B(\sigma_i) \rangle}{\prod_{j=1}^n \sigma_{n+1j}} \right) \\ & \times \frac{1}{\langle \Xi \xi' \rangle^4} \delta^4 \left(\frac{\langle \hat{\rho}^A(\sigma_{n+1}) \xi' \rangle}{\langle \Xi \xi' \rangle} - q^A - xv^A \right). \quad (\text{B.105}) \end{aligned}$$

The freedom to projectively scale ξ' allows us to set the first component to 1 and define the second as ξ' so that $\langle \xi' d\xi' \rangle = d\xi'$. Now we may focus on the last piece, which can be written as

$$\prod_{i=1}^n \sigma_{n+1i} \int d\sigma_{n+1} d\xi' d^2 \Xi dx \delta^4(\hat{\rho}^{A,a}(\sigma_{n+1}) \xi'_a - \langle \Xi \xi' \rangle (q^A - xv^A)). \quad (\text{B.106})$$

There are now five integrations, four delta functions, and the T redundancy to cancel. The strategy is to isolate the scattering equation for the last particle,

integrate out the other delta functions, and cancel the T-shift symmetry. The scattering equation for the soft particle is supported on the solution of $E_{n+1} = \epsilon_{ABCD} \hat{\rho}^{A,+}(\sigma_{n+1}) \hat{\rho}^{B,-}(\sigma_{n+1}) v^C q^D = 0$. To get this, we first make the change of variables

$$\begin{aligned} \langle \xi' \Xi \rangle &= \Xi^- - \xi' \Xi^+ \rightarrow u, \\ x &\rightarrow \frac{x'}{u}, \\ d\xi' d\Xi^+ d\Xi^- dx &\rightarrow \frac{d\Xi^+}{u} d\xi' du dx', \\ \delta^4(\hat{\rho}^{A,a}(\sigma_{n+1}) \xi'_a - \langle \Xi \xi' \rangle (q^A - xv^A)) &\rightarrow \delta^4(\hat{\rho}^{A,+}(\sigma_{n+1}) \xi' - \hat{\rho}^{A,-}(\sigma_{n+1}) - uq^A - x'v^A). \end{aligned} \quad (\text{B.107})$$

Now we would like to evaluate the integrals over u , x' , and ξ' . As in the even-point case, we observe that these integrations give the scattering equation for the last particle after taking the appropriate linear combinations:

$$\begin{aligned} &\frac{\prod_{i=1}^n \sigma_{n+1i}}{\tau} \int d\sigma_{n+1} d\xi' du dx' \delta^4(\hat{\rho}^{A,+}(\sigma_{n+1}) \xi' - \hat{\rho}^{A,-}(\sigma_{n+1}) - uq^A - x'v^A) \\ &= \frac{\prod_{i=1}^n \sigma_{n+1i}}{\tau} \int d\sigma_{n+1} \delta(\epsilon_{ABCD} \hat{\rho}^{A,+}(\sigma_{n+1}) \hat{\rho}^{B,-}(\sigma_{n+1}) v^C q^D) = \int d\sigma_{n+1} \delta(E_{n+1}). \end{aligned} \quad (\text{B.108})$$

So we are left with

$$\begin{aligned} &\delta(p_{n+1}^2) V_n^{-2} \int \frac{\prod_{k=0}^{m-1} d^8 \hat{\rho}_k}{\text{vol}(\text{SL}(2, \mathbb{C})_\sigma, \text{SL}(2, \mathbb{C})_\rho, \text{T})} \frac{d\Xi^+}{u} \\ &\quad \times \prod_{i=1}^n \delta^6 \left(p_i^{AB} - \frac{\langle \hat{\rho}^A(\sigma_i) \hat{\rho}^B(\sigma_i) \rangle}{\prod_{j=1}^n \sigma_{n+1j}} \right) \int d\sigma_{n+1} \delta(E_{n+1}). \end{aligned} \quad (\text{B.109})$$

In this expression $u = \langle \xi' \Xi \rangle$ has a value determined by the constraints after doing the integral. Since T acts as a $\text{GL}(1, \mathbb{C})$ shift on the components of Ξ , we can absorb u and cancel the symmetry. The result is the expected measure for n even:

$$\int \frac{\prod_{i=1}^n d\sigma_i \prod_{k=0}^{m-1} d^8 \hat{\rho}_k}{\text{vol}(\text{SL}(2, \mathbb{C})_\sigma \times \text{SL}(2, \mathbb{C})_\rho)} \prod_{i=1}^n \delta^6 \left(p_i^{AB} - \frac{\langle \hat{\rho}^A(\sigma_i) \hat{\rho}^B(\sigma_i) \rangle}{\prod_{j=1}^n \sigma_{n+1j}} \right) \delta(p_{n+1}^2) V_n^{-2} \int d\sigma_{n+1} \delta(E_{n+1}). \quad (\text{B.110})$$

APPENDICES FOR CHAPTER 5

C.1 p -adic Integration

Here we review some aspects of p -adic integration, including basic properties and examples, the Fourier transform, and the p -adic gamma function Γ_p . A more comprehensive review is found in [83]. For formal proofs, as well as extensive integration tables, the reader may consult [77].

As already discussed, the unique additive Haar measure dx on \mathbb{Q}_p is normalized so that

$$\int_{\mathbb{Z}_p} dx = 1. \quad (\text{C.1})$$

To find the volume of the set B^r , which consists of $x \in \{\mathbb{Q}_p, |x|_p \leq p^r\}$, we may scale the measure and reduce this to the integral above on \mathbb{Z}_p as:

$$\int_{B^r} dx = p^r \int_{\mathbb{Z}_p} dx = p^r. \quad (\text{C.2})$$

As $r \rightarrow \infty$, the volume diverges as in the real case. Compactifying the point at infinity amounts to switching from the Haar measure to the Patterson-Sullivan measure $d\mu_0(x)$; these measures agree on \mathbb{Z}_p and differ in the complement by $d\mu_0(x) = dx/|x|_p^2$.

With this measure the volume is computed with a change of variables:

$$\int_{\mathbb{Q}_p} d\mu_0(x) = \int_{\mathbb{Z}_p} dx + \int_{\mathbb{Q}_p - \mathbb{Z}_p} |x|_p^{-2} dx \quad (\text{C.3})$$

$$= 1 + \frac{1}{p} \int_{\mathbb{Z}_p} du, \quad u = \frac{1}{px}, \quad du = \frac{p dx}{|x|_p^2} \quad (\text{C.4})$$

$$= \frac{p+1}{p}. \quad (\text{C.5})$$

A large class of elementary integrals may be evaluated using these methods; see the above references for complete details.

We now turn our attention to the p -adic Fourier transform of a function $f(x) : \mathbb{Q}_p \rightarrow \mathbb{C}$. As discussed in section 5.3, this involves integrating the function

against the additive character $\chi(x) = e^{2\pi i\{kx\}}$ over all \mathbb{Q}_p . This generates a new complex valued function in terms of the p -adic momentum $k \in \mathbb{Q}_p$:

$$\tilde{f}(k) = \int_{\mathbb{Q}_p} \chi(kx) f(x) dx, \quad (\text{C.6})$$

$$f(x) = \int_{\mathbb{Q}_p} \chi(-kx) \tilde{f}(k) dk. \quad (\text{C.7})$$

The analogy with the real Fourier transform should be clear. In practice evaluating this kind of integral often requires one to divide \mathbb{Q}_p into spheres consisting of points with $|x|_p = p^n$ and performing the integral on each sphere. This can be seen in the example:

$$\int_{B^r} \chi(kx) dx = \begin{cases} p^r, & |k|_p \leq p^{-r} \\ 0, & \text{otherwise.} \end{cases} \quad (\text{C.8})$$

As in the real case, one may find tables with numerous p -adic Fourier transforms of elementary functions in the literature.

The final integral expression is that of the Gelfand-Graev-Tate Γ function:

$$\Gamma_p(\alpha) = \int_{\mathbb{Q}_p} \chi(x) |x|_p^{\alpha-1} dx = \frac{1 - p^{s-1}}{1 - p^{-s}}. \quad (\text{C.9})$$

This function has some similar properties to the ordinary gamma function. It is fairly ubiquitous in certain p -adic integral calculations, and we refer the reader to literature on p -adic string theory for details.

C.2 p -adic Differentiation

As already discussed, complex fields living on the boundary $\mathbb{P}^1(\mathbb{Q}_p)$ are maps

$$f(x) : \mathbb{P}^1(\mathbb{Q}_p) \rightarrow \mathbb{C}. \quad (\text{C.10})$$

In the Archimedean case of 2d conformal field theory, we have $f(z, \bar{z}) : \mathbb{P}^1(\mathbb{C}) \rightarrow \mathbb{C}$ and it makes sense to define holomorphic and antiholomorphic derivatives $\frac{\partial f}{\partial z}$ and $\frac{\partial f}{\partial \bar{z}}$. In the p -adic case, analogous differentiation expressions no longer make sense as we would be dividing a complex number by a p -adic number and these fields have different topologies.

The only notion of derivative we may use is the *Vladimirov derivative* [77, 79], and it can be thought of as a nonlocal pseudo-differential operator. Roughly

speaking, this operation is the p -adic analog of Cauchy's Differentiation Formula in which the derivative of a function at a point is expressed as a weighted integral of the function over a curve. It is also known as a *normal derivative* [82] in the context of the p -adic string where it is interpreted as the derivative of the embedding coordinates X^μ normal to the boundary of the worldsheet. Because this operator is defined on \mathbb{Q}_p without any reference to an embedding or worldsheet, we opt to refer to it as a Vladimirov derivative. The n^{th} Vladimirov derivative is defined by

$$\partial_{(p)}^n f(x) = \int_{\mathbb{Q}_p} \frac{f(x') - f(x)}{|x' - x|_p^{n+1}} dx'. \quad (\text{C.11})$$

Some authors may choose a different normalization in front of this integral; usually in the form of p -adic gamma functions. At first sight the expression above may not resemble any familiar notions of differentiation. We may see this as a good notion for derivative in two ways; in the case of the p -adic string this expression is the limit of the normal derivative on T_p as we go to the boundary, as shown in [82]. We may also compute the Vladimirov derivative of some special p -adic functions and compare with the real case. This is done in the following section.

Examples

We wish to first compute the derivative of the additive character, $\chi(kx)$. This function is the p -adic analog of a plane wave with momentum k , so we expect it to be an eigenfunction of the derivative with eigenvalue related to k .

$$\partial_{(p)}^n \chi(kx) = \int_{\mathbb{Q}_p} \frac{\chi(kx') - \chi(kx)}{|x' - x|_p^{n+1}} dx'. \quad (\text{C.12})$$

Using the properties of the additive Haar measure of \mathbb{Q}_p , we can shift the integration measure,

$$y = k(x' - x), \quad dy = |k|_p dx' \quad (\text{C.13})$$

and simplify the integral

$$\int_{\mathbb{Q}_p} \frac{\chi(kx') - \chi(kx)}{|x' - x|_p^{n+1}} dx' \quad (\text{C.14})$$

$$= |k|_p^n \int_{\mathbb{Q}_p} \frac{\chi(y + kx) - \chi(kx)}{|y|_p^{n+1}} dy \quad (\text{C.15})$$

$$= |k|_p^n \chi(kx) \int_{\mathbb{Q}_p} \frac{\chi(y) - 1}{|y|_p^{n+1}} dy. \quad (\text{C.16})$$

Where we used the additive property of the character to extract the x dependence. The integral appears to diverge at $y \sim 0$; this divergence is actually canceled by the numerator and can be seen by introducing an infrared cutoff. Regularization of this integral is discussed in [267] and [268]. The result is

$$\int_{\mathbb{Q}_p} \frac{\chi(y) - 1}{|y|_p^{n+1}} dy = \frac{1 - p^{-n-1}}{1 - p^n} = \Gamma_p(-n), \quad (\text{C.17})$$

where we have used the definition of the p -adic gamma function in Eq. (C.9). So the end result is

$$\partial_{(p)}^n \chi(kx) = \Gamma_p(-n) |k|_p^n \chi(kx). \quad (\text{C.18})$$

Up to the factor of the gamma function (which could be absorbed into the normalization of the derivative,) we see the additive character $\chi(kx)$ is an eigenfunction of the Vladimirov derivative with the eigenvalue given by the p -adic norm of its “momentum.”

Another example we may wish to compute is the n^{th} derivative of $|x|_p^s$ for some $s \in \mathbb{C}$. This may be most easily be computed by Fourier transform and serves as an example of an alternative representation of the Vladimirov derivative:

$$\partial_{(p)}^n |x|_p^s = \int \chi(-kx) |k|_p^n \widetilde{|x|_p^s} dk \quad (\text{C.19})$$

where $\widetilde{|x|_p^s}$ is the p -adic Fourier transform of $|x|_p^s$, given in [207, 77]:

$$\widetilde{|x|_p^s} = \int \chi(kx) |x|_p^s dx = \Gamma_p(s+1) |k|_p^{-s-1} \quad (\text{C.20})$$

everywhere it is defined. Applying this formula twice to the derivative we wish to compute, we arrive at

$$\partial_{(p)}^n |x|_p^s = \Gamma_p(s+1) \Gamma_p(n-s) |x|_p^{s-n}, \quad (\text{C.21})$$

which should resemble the ordinary n^{th} derivative of a polynomial function.

APPENDICES FOR CHAPTER 6

D.1 The Three-Qudit Code

In this appendix, based on the discussion in section 6.2, we give an explicit example of a quantum Reed-Solomon code which has quantum error-correcting and ‘perfectness’ properties. We start with the classical Reed-Solomon code $[n, k, n - k + 1]_{q^2}$ (note the q^2 in the subscript) and choose parameters $n = q = 3$, $k = (q - 1)/2 = 1$, and $X = \mathbb{P}^1(\mathbb{F}_3) \setminus \{\infty\} = \{[1 : 0], [1 : 1], [1 : 2]\}$. The $[3, 1, 3]_{3^2}$ -code, which will serve as an example of a D -type code from section 6.2 (see discussion around (6.27)), takes the form $D = \{(f_a(1, 0), f_a(1, 1), f_a(1, 2)) : a = (a_0) \in \mathbb{F}_{3^2}, f_a \in \mathbb{F}_{3^2}[u, v]\}$. Since $k = 1$, the homogeneous polynomial takes a particularly simple form, $f_a(u, v) = a_0 \in \mathbb{F}_{3^2}$. Thus the $[3, 1, 3]_{3^2}$ -code becomes, $D = \{(a_0, a_0, a_0) : a_0 \in \mathbb{F}_{3^2}\}$.

It is easy to check that D is self-orthogonal with respect to the Hermitian inner product (6.27). Take $a = (a_0, a_0, a_0), b = (b_0, b_0, b_0) \in D$, where $a_0, b_0 \in \mathbb{F}_{3^2}$, then

$$a * b = 3a_0b_0^3 = 0. \quad (\text{D.1})$$

One can also check self-orthogonality by constructing the dual code D^\perp . It follows from the definition of the dual code in footnote 2 that if $b = (b_1, b_2, b_3) \in D^\perp$, then for all $a = (a_0, a_0, a_0) \in D$,

$$a * b = a_0(b_1^3 + b_2^3 + b_3^3) \stackrel{!}{=} 0. \quad (\text{D.2})$$

Since (D.2) must hold for all $a_0 \in \mathbb{F}_{3^2}$, we must have $b_1^3 + b_2^3 + b_3^3 = 0$. Writing $b_i = \sum_{j=1}^2 b_{i,j} \gamma_j$ where $b_{i,j} \in \mathbb{F}_3$ and $\{\gamma_1, \gamma_2\} = \{1, x\}$ form a basis for \mathbb{F}_{3^2} as an \mathbb{F}_3 -vector space, we have the result, $b_i^3 = b_{i,1} - b_{i,2}x$. So the condition of duality becomes

$$(b_{1,1} + b_{2,1} + b_{3,1}) - (b_{1,2} + b_{2,2} + b_{3,2})x = 0 \quad \Rightarrow \quad b_{1,j} = 2b_{2,j} + 2b_{3,j} \quad j = 1, 2, \quad (\text{D.3})$$

or, in other words, $D^\perp = \{(2b_2 + 2b_3, b_2, b_3) : b_2, b_3 \in \mathbb{F}_{3^2}\}$. One checks that $D \subset D^\perp$, thus D is self-orthogonal. While establishing self-orthogonality via the dual code may seem a bit roundabout, the construction of the dual code helps determine d_Q , the minimum distance of the quantum code. It is

straightforward to show that in this example, $d_Q = \min\{\text{wt}(v) : v \in D^\perp \setminus D\} = 2$.

Now consider the classical Reed–Solomon $[2n, 2k, 2n - 2k + 1]_q$ -code C , with $n = q = 3$ and $k = (q - 1)/2 = 1$ as before. The input 2-tuple now becomes $a = (a_0, b_0) \in \mathbb{F}_3^2$, and the code takes the form,

$$C = \left\{ \left((f_{a_0}(1, 0), f_{b_0}(1, 0)), (f_{a_0}(1, 1), f_{b_0}(1, 1)), (f_{a_0}(1, 2), f_{b_0}(1, 2)) \right) \right\} \quad (\text{D.4})$$

where $f_a[u, v] \in \mathbb{F}_3$ is the homogeneous polynomial given by (6.33). Like before, setting $k = 1$ leads to a significant simplification and results in $C = \left\{ \left((a_0, b_0), (a_0, b_0), (a_0, b_0) \right) : (a_0, b_0) \in \mathbb{F}_3^2 \right\}$.

To establish the self-orthogonality of C , we use the inner product given in (6.28) or equivalently (6.30). Given $(a, b) = \left((a_0, b_0), (a_0, b_0), (a_0, b_0) \right) \in C \subset \mathbb{F}_3^{2n}$ and similarly $(a', b') \in C$, using (6.28) we have

$$(a, b) * (a', b') = \text{Tr}(3a_0b'_0 - 3a'_0b_0) = 0, \quad (\text{D.5})$$

which tells us C is self-orthogonal.¹ Alternatively, we can use the inner product in (6.30). First note that since $q = 3$, the parameter $r = 1$ (recall that $q = p^r$), and consequently φ is the trivial identity automorphism. This is because $\varphi(a) = (\varphi(a_1), \varphi(a_2), \varphi(a_3))$ where $a \in \mathbb{F}_3^n$, but since $r = 1$, we have $\varphi(a_1) = a_1 \in \mathbb{F}_3$. Then, given $(a, b), (a', b') \in C$ as before and using (6.30) along with the fact that φ is the identity transformation, we have

$$(a, b) * (a', b') = \langle a, b' \rangle - \langle a', b \rangle = 3a_0b'_0 - 3a'_0b_0 = 0, \quad (\text{D.6})$$

which confirms self-orthogonality.

The trivial action of φ is due to the fact that we have chosen q to be a prime number, rather than a power of a prime. This makes the construction of the corresponding abelian subgroup especially simple: For every element $(a, b) \in C$ (where $a, b \in \mathbb{F}_3^n$), the corresponding group elements are given by $\xi^i E_{a,b}$ for $0 \leq i \leq 2$. The cardinality of C , $|C| = 9$ is small enough that we may explicitly list all its elements. They are

$$C = \left\{ \left((0, 0)^3, (0, 1)^3, (0, 2)^3, (1, 0)^3, (1, 1)^3, (1, 2)^3, (2, 0)^3, (2, 1)^3, (2, 2)^3 \right) \right\}, \quad (\text{D.7})$$

¹One can also construct C^\perp *a la* our construction of D^\perp outlined above, and verify self-orthogonality and check that $d_Q = \min\{\text{wt}(v, w) : (v, w) \in C^\perp \setminus C\} = 2$.

where $(i, j)^3 \equiv ((i, j), (i, j), (i, j)) \in \mathbb{F}_3^{2 \times 3}$. The operators in the corresponding subgroup are given by

$$\mathcal{S} = \{\xi^i E_{0^3, 0^3}, \xi^i E_{0^3, 1^3}, \xi^i E_{0^3, 2^3}, \xi^i E_{1^3, 0^3}, \xi^i E_{1^3, 1^3}, \xi^i E_{1^3, 2^3}, \xi^i E_{2^3, 0^3}, \xi^i E_{2^3, 1^3}, \xi^i E_{2^3, 2^3} : 0 \leq i \leq 2\}, \quad (\text{D.8})$$

where $j^3 \equiv (j, j, j) \in \mathbb{F}_3^3$. In constructing the simultaneous eigenspaces of these operators, we can ignore the overall scalar factors ξ^i in (D.8), since they come from the center of the Heisenberg group. Now using (6.21) we conclude that if $(a, b) \in C$, then $E_{a,b} = T_{a_0} R_{b_0} \otimes T_{a_0} R_{b_0} \otimes T_{a_0} R_{b_0}$. The matrices $T_{a_0} R_{b_0}$ where $a_0, b_0 \in \mathbb{F}_3$ are given by

$$\begin{aligned} T_0 R_0 &= \begin{pmatrix} 1 & & \\ & 1 & \\ & & 1 \end{pmatrix} & T_0 R_1 &= \begin{pmatrix} 1 & & \\ & \xi & \\ & & \xi^2 \end{pmatrix} & T_0 R_2 &= \begin{pmatrix} 1 & & \\ & \xi^2 & \\ & & \xi \end{pmatrix} \\ T_1 R_0 &= \begin{pmatrix} 0 & 1 & 0 \\ 0 & 0 & 1 \\ 1 & 0 & 0 \end{pmatrix} & T_1 R_1 &= \begin{pmatrix} 0 & \xi & 0 \\ 0 & 0 & \xi^2 \\ 1 & 0 & 0 \end{pmatrix} & T_1 R_2 &= \begin{pmatrix} 0 & \xi^2 & 0 \\ 0 & 0 & \xi \\ 1 & 0 & 0 \end{pmatrix} \\ T_2 R_0 &= \begin{pmatrix} 0 & 0 & 1 \\ 1 & 0 & 0 \\ 0 & 1 & 0 \end{pmatrix} & T_2 R_1 &= \begin{pmatrix} 0 & 0 & \xi^2 \\ 1 & 0 & 0 \\ 0 & \xi & 0 \end{pmatrix} & T_2 R_2 &= \begin{pmatrix} 0 & 0 & \xi \\ 1 & 0 & 0 \\ 0 & \xi^2 & 0 \end{pmatrix}. \end{aligned} \quad (\text{D.9})$$

Recalling that the orthonormal basis qubits $|a_0\rangle$ with $a_0 \in \mathbb{F}_3$ are given by

$$|0\rangle = \begin{pmatrix} 1 \\ 0 \\ 0 \end{pmatrix} \quad |1\rangle = \begin{pmatrix} 0 \\ 0 \\ 1 \end{pmatrix} \quad |2\rangle = \begin{pmatrix} 0 \\ 1 \\ 0 \end{pmatrix}, \quad (\text{D.10})$$

it is straightforward to check that the operators $E_{a,b}$ have the following common eigenvectors:

$$\begin{aligned} |A\rangle &= |000\rangle + |111\rangle + |222\rangle & |B\rangle &= |012\rangle + |120\rangle + |201\rangle & |C\rangle &= |021\rangle + |210\rangle + |102\rangle \\ |D\rangle &= |001\rangle + |112\rangle + |220\rangle & |E\rangle &= |010\rangle + |121\rangle + |202\rangle & |F\rangle &= |100\rangle + |211\rangle + |022\rangle \\ |G\rangle &= |002\rangle + |110\rangle + |221\rangle & |H\rangle &= |020\rangle + |101\rangle + |212\rangle & |I\rangle &= |200\rangle + |011\rangle + |122\rangle, \end{aligned} \quad (\text{D.11})$$

where $|ijk\rangle \equiv |i\rangle \otimes |j\rangle \otimes |k\rangle \in (\mathbb{C}^3)^{\otimes n}$. For completeness, we tabulate the

eigenvalues of each eigenvector under the operators $E_{a,b} \in \mathcal{S}$:

	$E_{0^3,0^3}$	$E_{0^3,1^3}$	$E_{0^3,2^3}$	$E_{1^3,0^3}$	$E_{1^3,1^3}$	$E_{1^3,2^3}$	$E_{2^3,0^3}$	$E_{2^3,1^3}$	$E_{2^3,2^3}$
$ A\rangle$	1	1	1	1	1	1	1	1	1
$ B\rangle$	1	1	1	1	1	1	1	1	1
$ C\rangle$	1	1	1	1	1	1	1	1	1
$ D\rangle$	1	ξ^2	ξ	1	ξ^2	ξ	1	ξ^2	ξ
$ E\rangle$	1	ξ^2	ξ	1	ξ^2	ξ	1	ξ^2	ξ
$ F\rangle$	1	ξ^2	ξ	1	ξ^2	ξ	1	ξ^2	ξ
$ G\rangle$	1	ξ	ξ^2	1	ξ	ξ^2	1	ξ	ξ^2
$ H\rangle$	1	ξ	ξ^2	1	ξ	ξ^2	1	ξ	ξ^2
$ I\rangle$	1	ξ	ξ^2	1	ξ	ξ^2	1	ξ	ξ^2

(D.12)

From this table, one can see that the invariant subspace of the abelian subgroup corresponding to C —which is the code subspace of the corresponding quantum CRSS code—is spanned by $|A\rangle$, $|B\rangle$, and $|C\rangle$. Other equivalent choices of code subspace are the other mutual eigenspaces of the operators in C , corresponding to $|D\rangle$, $|E\rangle$, and $|F\rangle$ or to $|G\rangle$, $|H\rangle$, and $|I\rangle$. The resulting quantum code is the quantum $[[3, 1, 2]]_3$ Reed–Solomon/three-qutrit code, corresponding to the simplest example of a four-index perfect tensor given in [99]; it maps basis states according to the rule

$$|0\rangle \mapsto \frac{1}{\sqrt{3}} |A\rangle, \quad |1\rangle \mapsto \frac{1}{\sqrt{3}} |B\rangle, \quad |2\rangle \mapsto \frac{1}{\sqrt{3}} |C\rangle. \quad (\text{D.13})$$

This page is intentionally left blank.